System Identification -

Data-Driven Modelling of Dynamic Systems

Paul M.J. Van den Hof

Lecture Notes

February 2020

Control Systems Group
Department of Electrical Engineering
Eindhoven University of Technology

TU/e Technische Universiteit
Eindhoven
University of Technology

Manuscript version: 1 February 2020

Address of the author:
Prof.dr.ir. Paul M.J. Van den Hof
Control Systems Group
Department of Electrical Engineering
P.O. Box 513, 5600 MB Eindhoven, The Netherlands
Tel. +31 40 2473839;
p.m.j.vandenhof@tue.nl
http://www.tue.nl/staff/p.m.j.vandenhof
http://www.pvandenhof.nl

Visiting address:
Building Flux, 5.134
De Zaale, Eindhoven, The Netherlands

Note

Contents

List of Symbols

$'$	Derivative with respect to θ
$\mathbb{C}$	Set of complex numbers
ε	One-step-ahead prediction error
e	White noise stochastic process
E	Expectation
$\bar{E}$	Generalized expectation of a quasi-stationary process
f_e	Probability density function of e
$\varphi(t)$	Regression vector
G_0	Data generating input-output system
$\mathcal{G}$	Set of input-output models
H_0	Noise shaping filter in data generating system
$\mathcal{M}$	Model set
$\mathbb{N}$	Set of natural numbers, 1, 2, $\cdots$
$\mathcal{N}$	Gaussian or normal distribution
N	Number of data
ω	Radial frequency
ω_s	Sampling (radial) frequency
Φ_u	(Auto-)spectral density of signal u
Φ_{yu}	Cross-spectral density of signals y and u
$\psi(t, \theta)$	Partial derivative of output predictor w.r.t. θ
$\mathbb{R}$	Set of real nunbers
$\Re\{\ \}, \Im\{\ \}$	Real and imaginary part
$R_u(\tau)$	Autocovariance function of u
$R_{yu}(\tau)$	Crosscovariance function of y and u
$\mathcal{S}$	Data generating system (G_0, H_0)
σ_e^2	Variance of white noise source e
θ	Parameter vector
$\hat{\theta}_N$	Estimated parameter based on N data
θ^*	Limiting parameter estimate $(N \to \infty)$
Θ	Domain of parameter vector
T_s	Sampling interval
u	Input signal
v	Output disturbance signal
$\bar{V}(\theta)$	Limiting quadratic cost function
y	Output signal
y^t	$\{y(s), s \leq t-1\}$
$\hat{y}(t|t-1)$	One-step-ahead output predictor
$\mathbb{Z}$	Set of integer numbers
Z^N	Set of input/output data $\{(y(t), u(t), t = 0, \cdots N-1\}$
$\star$	convolution
$(\cdot)^*$	complex conjugate

Chapter 1

Introduction

1.1 Model building

The construction and use of models is very common in almost all areas of science and technology. From econometricians to engineers and from sociologists to business managers, people deal with more or less formalized models of processes (mechanisms/phenomena) that occur in our physical reality. Whereas engineers for instance will model the behaviour of a specific material or mechanical construction, the econometrist will model the relation between several (macro)economic variables in our economy; the sociologist is modelling the behaviour and interrelation among collections of people, and the business manager will be most interested in handling simple models for the operation of his firm or for the process of decision-making that is most efficient in his situation. The widespread use of the notion of a model, makes it also extremely difficult to come up with a strict definition of what we mean when we use the word *model*. In different areas of science and technology, the notion will be interpreted and specified quite differently. On one point one might come to an agreement, being that when dealing with models one is working with abstractions from reality.

When taking a look at engineering models, there is still a huge variety of shapes and figures in which models are being represented. When looking at models for the behaviour of specific material under external forces, or at models for fluid dynamics of specific fluids under specific conditions, or at models for an industrial production process in some automated environment, the models are concerned with many different types of variables. In general, however, engineering models have one basic characteristic: they are concerned with relations between variables that are well-defined physical quantities, and moreover these quantities can very often be measured by some appropriate equipment. One can measure forces, accelerations, temperatures, flows, voltages, currents, pressures etcetera, and this possibility of measuring provides the engineer with important information in the process of constructing and of using models.

In systems and control engineering one is dealing with constructing models in the form of dynamical systems, and their consecutive use for different purposes, of which control design is of course an important one. When dealing with models in this area, one can distinguish between the following different types of models:

> *mental models.* These reflect the intuitive notion that people have of a system behaviour. Take e.g. the human operator that is able to control a complicated system

very well just by experience (captain of a huge tanker, people driving a car or bicycle, pilot steering a airplane).

software models. These reflect system descriptions that are contained in (extensive) software programs, possible including if-then rules, discrete-event types of mechanisms and look-up tables (schedule of a railway company).

graphical models. System descriptions in the form of (nonlinear) characteristics and graphs, Bode and Nyquist plots, impulse and step responses.

mathematical models. System descriptions in the form of mathematical relations as e.g. (partial) differential and difference equations, fuzzy type of models and neural networks.

In this book we will concentrate on models of the last two categories, and in particular on mathematical models, while the main emphasis will be on linear time-invariant models in the form of difference equations.

Model-based engineering is by far the dominant engineering paradigm to systematic design, operation and maintenance of engineering systems, and within the engineering field this is present in a wide variety of disciplines. In all those areas where dynamics plays a role, the system and control field has a growing role to play through its formalism of deriving and handling models of dynamical systems.

In this respect the particular characteristics of the systems and control field, contain:

- A framework for dynamic modelling that runs across many disciplines; mechanical engineering systems can be connected to electrical systems, to optical, flow or chemical systems. This is achieved by considering dynamic systems in a conceptual way, e.g. by causal input-output mappings (e.g. represented by transfer functions), that simply can be connected to each other.

- The understanding of interconnections of systems is a central topic in systems and control theory and has led to the important concept of feedback, which is considered as the crown-juwelry of the field.

- The ability to characterize and handle uncertainties and the ability to create techno-logical systems that are robust, i.e that can operate under uncertain circumstances and in uncertain environments. In this respect note that the accuracy with which a laser spot is positioned on the information track of a DVD-player, largely out-reaches the tolerance in the specifications of the several mechanical parts of which the equipment is produced. This is only possible on the basis of accurate sensing (measurements) and on-line (feedback) control.

Within the area of systems and control engineering, one will generally deal with models of dynamic systems, having different purposes in mind. You could speak about "Model-Based X" where "X" stands for several options:

System (re)design. Knowledge about the (dynamic/static) behaviour of a system can be used for design optimization. If a mechanical (robot) structure appears to be too flexible, it can be redesigned to be more stiff. If an industrial production process is hardly controllable, it can probably be redesigned to improve on controllability and, consequently, on achieved performance.

Control design. The design of a feedforward and/or feedback control system that achieves stabilization, disturbance rejection, tracking of reference trajectories etc.; in other words a control system that improves or optimizes the performance/efficiency of a dynamical system.

Prediction. Prediction of future behaviour of particular variables, as e.g. the weather, usage of water and electricity, etc.

Simulation. Testing of system behaviour under different input scenarios, training of operators that have to manually perform a control or surveillance task and/or need to be able to accurately respond to emergency situations, etc.

Estimation. Reconstruction/estimation of signals that are not directly measurable; reconstructing the state of a system.

Diagnosis. Fault detection as e.g. locating a leak in a long-distance gas pipeline or detecting sensor failures on the basis of indirect measurements.

Having illustrated the several options for "Model-Based X", we still have not said anything about the way in which models are constructed.

In engineering systems the dynamical systems mostly concern dynamical relationships between physical quantities. This implies that one can often use the basic laws of physics (first principles) to arrive at a model of the system. In this case the laws of physics are the main source for the model to be constructed. Complementary to this, measurement data of the input and output variables of the system, can contain all relevant information of the underlying system dynamics. So, rather than building models in theory, information from experimental data can be an effective approach to building models of the actual and emerging behaviour of dynamical systems. This leads us to an area which has become known as *system identification.*

1.2   System identification - data-driven modelling

In general there are two ways of arriving at models of physical processes c.q. engineering systems.

- First principles modelling (sometimes called physical modelling).
  Physical knowledge about the process, in the form of first principles relations, is employed in order to arrive at a model that will generally consist of a multitude of differential/partial differential/algebraic relations between physical quantities. The construction of the model is based on presumed knowledge about the physics that governs the system. The first principles relations concern e.g. the laws of conservation of energy and mass and Newton's law of movement.

- Data-driven modelling, or system identification. Measurements of several variables of the process are taken and a model is constructed by identifying a model that matches the dynamics that underlies the measured data as well as possible.

In many situations the first approach is followed, e.g. in chemical process industry, but also in mechanical type of systems. Here we generally have good knowledge about the

basic principles that govern the system behaviour. This, however, notwithstanding the fact that in many situations physical modelling is not the only approach that we have to take into our luggage in order to arrive at highly accurate models. Even in physical modelling we generally will need numerical values of (physical) coefficients that have to be substituted in the model relations. Exact values of masses, stiffnesses, material properties, properties of chemical reactions, or other (presumed) constants need to be known. And not only the direct relation between input variables (causes) and output variables (effects) is of importance here. Our dynamical system will practically never perform as a perfect set of deterministic equations; in real-life the system variables will be subject to all kinds of disturbances that influence the input-output relations within a dynamical system. For arriving at accurate models, and for their appropriate use, not only the direct input/output relation is of importance but one also needs to quantify what kind of disturbances act on the system. These disturbances will limit the validity of deterministic models in any type of application.

Generally one can say that for accurate modelling of systems the handling and analysis of real-life measurements is very important.

What are specific situations in which first principles modelling alone has its limitations:

- First principles modelling is impossible. This happens e.g. in the situation that we simply have no first principles relations available to construct our model. Consider e.g. econometric modelling, modelling of human behaviour.

- First principles models are too complex. Modelling huge chemical plants will most often lead to huge models, that in order to be complete, require such a high level of complexity (high number of equations) that the model becomes intractable for particular applications.

- First principles models are unreliable. This can happen e.g. if the first principles relations do not describe the behaviour of the system in enough detail. This does not imply that the resulting models are bad, they may just not be accurate enough for the application that one has in mind.

- One may need real data experiments to validate models that are being constructed on first principles. Even if the models are accurate, the model designer may want to get serious confidence in his model, by confronting it with real measurement data (validation).

In the situations sketched above, experimental data of the process can be used in order to arrive at an appropriate model. The situation that a model is identified purely on the basis of data, and without taking particular account of the physical structure, is referred to as *black box* identification. This in contrast with the *white box* approach, that is taken in the case of pure physical modelling.

Some examples of processes are given for which physical modelling does not suffice to construct models that are suitable for the desired application. In all examples the intended application of the models is to use them as a basis for model-based control design.

Example 1.2.1 *Glass tube production process.* The industrial process under consideration is a glass tube manufacturing process, schematically depicted in Figure 1.1[1]. By direct

---

[1]This picture is made available by H. Falkus, Department of Electrical Engineering, Eindhoven University of Technology.
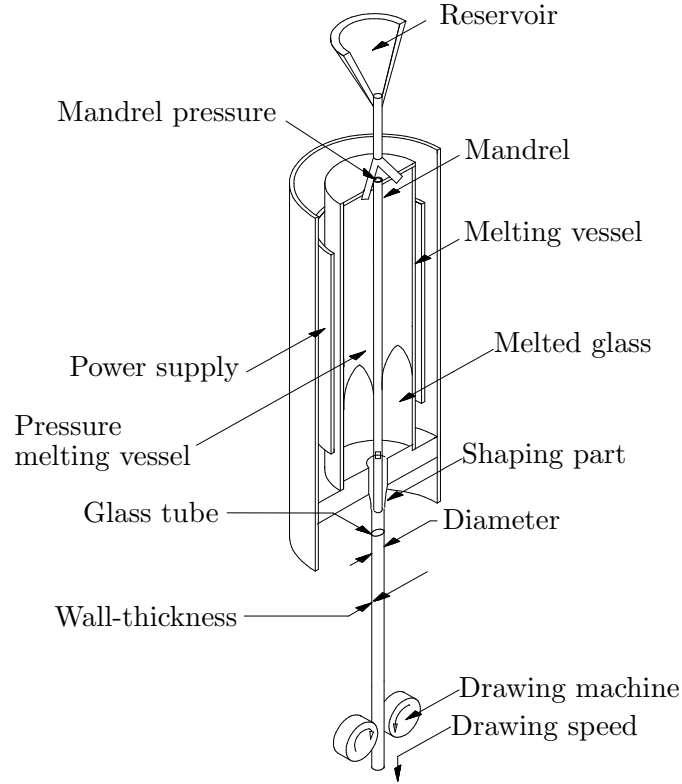
Figure 1.1: Schematic overview of the glass tube manufacturing process

electric heating, quartz sand is melted and flows down through a ring-shaped hole along the accurately positioned mandrel. Under pressure, gas is led through the hollow mandrel. The glass tube is pulled down due to gravity and supported by a drawing machine.

Shaping of the tube takes place at, and just below the end of the mandrel. The longitudinal shape of the tube is characterized by two important dimensions, which are taken as most important output variables to be controlled: tube diameter and tube wall-thickness. The purpose of this process is to produce glass tubes with a prespecified tube diameter and wall-thickness with high accuracy, i.e. allowing only small variations around the prespecified nominal values.

Both output variables are influenced by many process conditions such as:

- mandrel gas pressure,

- drawing speed,

- power applied to the furnace (temperature of the glass),

- melting vessel pressure,

- composition of raw materials.

Some of these have a small bandwidth (power and composition of raw materials), minorly influence the glass quality (composition of raw materials), or have extremely large delay

times involved (power, melting vessel pressure and composition of raw materials). Therefore these are not well suited for control of the tube dimensions.

Shaping of the glass tube clearly is a multivariable process with a high degree of interaction. Increase of the mandrel pressure results in an increase of the tube diameter and a decrease of the tube wall-thickness. Increase of the drawing speed causes a decrease of both diameter and wall-thickness. A physical model of this shaping part can be obtained by deriving the physical laws of the shaping process, describing the shaping of the tube in detail and over the full range of possible operating points, determined by various values of tube diameter and wall-thickness. However, this physical model is very complex and has physical parameters included with numerical values that are unknown for the different operating points. Besides, for complete modelling of this process by physical laws, there is simply not enough knowledge available of all physical details that play a role in this shaping process. Therefore one has to rely on experimental data to arrive at an appropriate description of the dynamic behaviour of this process.

In terms of a block diagram, the considered process is reflected in Figure 1.2.
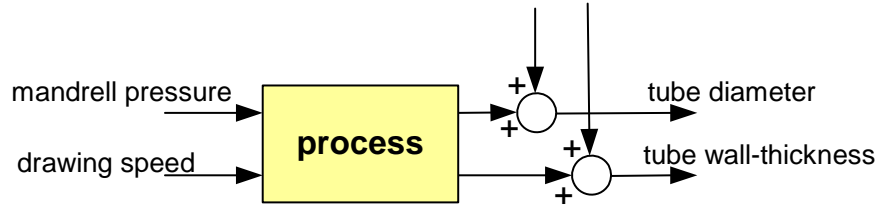
Figure 1.2: Block diagram of glass-tube production process.

Here two input variables are considered, being the mandrel pressure and the drawing speed; there are also two output variables, being the wall diameter and thickness, and two disturbance signals that act on the output variables reflecting all kinds of disturbances that act upon the system. These disturbances incorporate not only the measurement disturbances, but also several aspects of the system that are simply discarded when using only the two input variables as the source of explaining the two output variables of the process.

Example 1.2.2 *Compact-Disc player.*

The pick-up mechanism of a compact-disc player is a very nice example of a small-size high-tech engineering system. A schematic picture of the CD-mechanism is given in Figure 1.3. An actuator has to position a laser spot on the right position of a rotating disc. To this end a mechanical arm can move in the radial direction over the disc. The laser beam is reflected and an optical sensor is able to read out the digital information concerning the pits in the tracks of the compact-disc, see Figure 1.4.
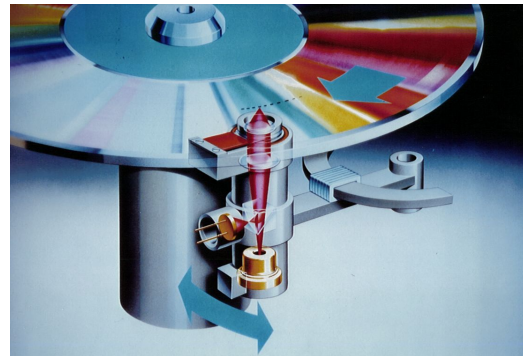
A current signal moves the actuator to a specific radial position. The actual position of the actuator, however, is not measured, and neither is the radial setpoint. The variable
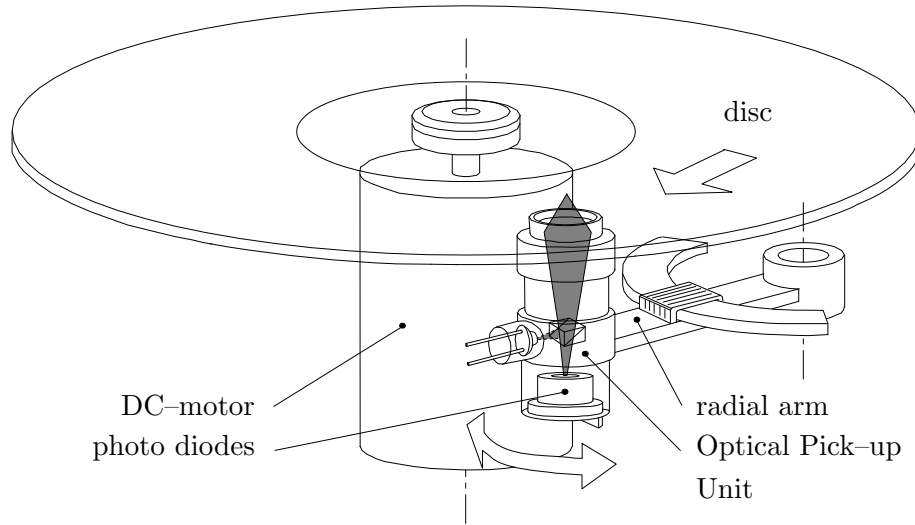
Figure 1.3: Schematic view of a CD mechanism
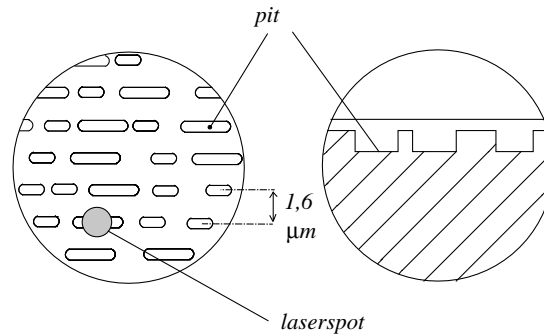
Figure 1.4: Schematic depiction (enlarged) of an audio disk surface. For DVD and Blu-Ray the track width reduces to 0.74 and 0.32 μm.

that is externally available is the radial error signal, indicating whether the laser spot is covering a track correctly. This error signal is processed by an optical measurement unit and converted into a current signal.

In considering the dynamical properties of this system, one has to realize what kind of effects play a role. The process as indicated in the block diagram 1.5 contains dynamic properties of both the actuator and of the whole mechanical structure on which the actuator is mounted. Note that because of the high-precision that is required in the motion control of this mechanism, the dynamical properties of the environment play an important role. The radial distance between two different tracks is $1.6\mu m$, and the required accuracy of the positioning control is $0.1\mu m$. The importance of the dynamic properties of the mechanical structure on which the pick-up mechanism is mounted, is reflected in the fact that each separate CD-player shows different dynamic behaviour in the form of different location of resonant modes.
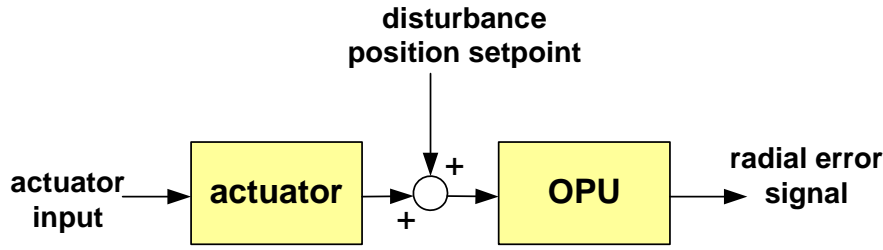
Figure 1.5: Block diagram of radial system of CD-mechanism; OPU = optical pick-up unit.
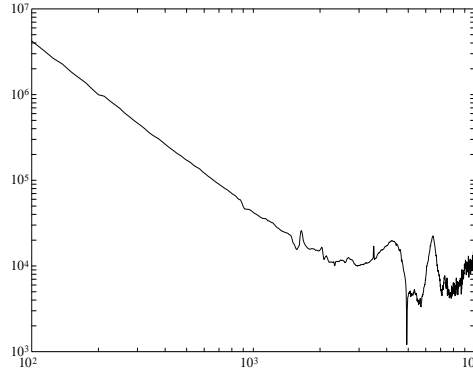
Figure 1.6: Measured frequency response (amplitude Bode plot) of the radial positioning mechanism in a CD player optical pick-up unit. Frequency axis is in [Hz].

Using physical models for characterizing the dynamic behaviour of this system shows severe problems, due to the extremely high accuracy of modelling that is required, and due to the influential role of the (mechanical) environment. Identifying dynamic models on the basis of measurement data can lead to models having the accuracy that is required for this high-performance control problem. An typical example of a measured amplitude Bode plot (frequency response) of the radial positioning mechanism in a CD-player is depicted in Figure 1.6. It matches the frequency response of a double integrator (transfer from force to position) with on top of that high order flexibilities in the construction, which appear at higher frequencies.

The two processes considered are two examples of situations in which identification of models from measurement data contributes essentially to the construction of accurate models. A (partial) combination of physical modelling and black box modelling is also possible, and in fact also quite appealing. This approach is often denoted by the term *grey box* modelling. In this case physical quantities are identified from data, but the basic model structure is directed by the first principles relations of the process. One of the properties of black box models is that they can provide a compact system description without making explicit statements concerning every single physical subsystem. The system is considered as one unity that exhibits itself though its external variables (input and output quantities).

As mentioned before, in system identification we consider the dynamical system to be modelled to exhibit itself through its external (measurable) variables as its input and output

signals. Let's take a look at the different signals that we can distinguish:

- Measurable output signals. These are measurable signals that can be considered as "consequences" or responses of the system behaviour; they can not be manipulated directly by the experimentor.

- Measurable input signals. These are measurable control signals that act as a "cause" of the system response. Generally they can be manipulated to a certain extent. If they can not be manipulated they are sometimes considered as (measurable) disturbance signals.

- Non-measurable disturbances. These reflect non-measurable disturbances that act on the system. These disturbances can not be manipulated nor influenced.

It is not very simple to formally define what we mean by "the system" or "the model". Actually what we call a system or a model is determined by a number of (external) variables or signals that exhibit a specific relation with each other. How we will deal with systems and models in a more formal way will be specified in a later stage.

1.3   The identification procedure

In this section we will give some attention to the main aspects that are involved in identification of dynamical models from measurement data.

First we briefly sketch a simple paradigm for the identification of a parametric model.

Consider the situation as depicted in the block diagram in Figure 1.7. Here u and y reflect the input and output signal, respectively. Signal v acts as a nonmeasurable disturbance on the output. S is the system to be modelled. $M(\theta)$ reflects a parametrized set of models, where the parameter θ can range over a parameter set $\Theta \subset \mathbb{R}^d$. For each $\theta_1 \in \Theta$, $M(\theta_1)$ is a model that relates input and output signals to each other.

However, when confronting a model $M(\theta_1)$ with measurement data (y, u), the model relations will generally not be satisfied exactly, as noise influences on the data will circumvent this to happen. This implies that when confronting a model with measurement data, an error or *residual signal* will result. This is reflected in Figure 1.7 by the residual signal $\varepsilon(\theta)$. In a general identification problem one can consider the following principal choices to be made:

- *Experiment.* Measurements of input and output signals have to be gathered, leading to a data set $\{y(t), u(t)\}_{t=1,\cdots,N}$. When designing an experiment, the characteristics of the input signal u have to be chosen so as to excite the relevant dynamics in the system S in order to get information on these relevant dynamics reflected in the measured output signal.

- *Model set.* Every model in the set can e.g. be represented by a difference equation

$$y(t) + a_1 y(t-1) + a_2 y(t-2) = b_1 u(t-1) + b_2 u(t-2) + \varepsilon(t) \qquad (1.1)$$

  with $t = 1, 2, \cdots$, and where the parameter vector $\theta \in \mathbb{R}^4$ is composed as $\theta = (a_1 \ a_2 \ b_1 \ b_2)^T$. After having specified the number of parameters (and thus the order of the difference equation), a model set is obtained by varying θ over a parameter set $\Theta \subset \mathbb{R}^4$.

- *Identification criterion.* Given measurement data $\{y(t), u(t)\}_{t=1,\cdots,N}$, each model (and therefore each parameter $\theta \in \Theta$) will generate a residual signal

$$\varepsilon(t,\theta) = y(t) + a_1 y(t-1) + a_2 y(t-2) - b_1 u(t-1) - b_2 u(t-2) \qquad (1.2)$$

which is now dependent on the parameter θ.
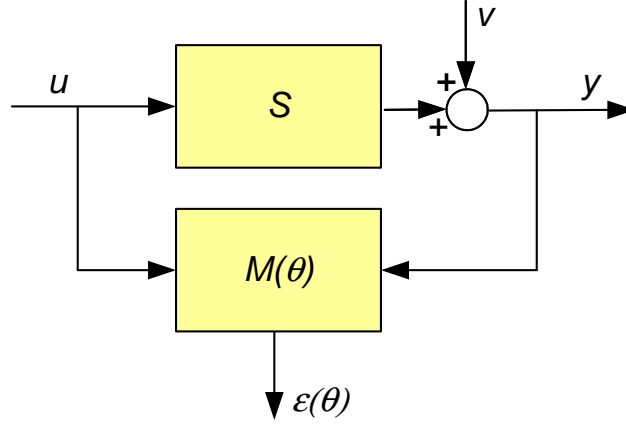
Figure 1.7: A simple paradigm for system identification.

This residual signal $\varepsilon(t,\theta)$ can be used as a basis for constructing the identified model(s), and this can be done in several different ways:

The most standard and classical way is to construct a cost function, which is minimized over θ. The most popular choice is a least-squares criterion:

$$V_N(\theta) = \frac{1}{N} \sum_{t=1}^{N} \varepsilon^2(t,\theta)$$

and a parameter estimate is constructed by finding that value of θ that minimizes $V_N(\theta)$. This is written as:

$$\hat{\theta}_N = \arg\min_{\theta \in \Theta} V_N(\theta) \qquad (1.3)$$

meaning that $\hat{\theta}_N$ is that value of θ that minimizes the sum-of-squares criterion.

However there are many alternatives to this approach, considering different types of identification criteria. In an instrumental variable (IV) criterion one selects the estimated parameter $\hat{\theta}_N$ so as to make $\varepsilon(t,\hat{\theta}_N)$ uncorrelated to some external (instrumental) signal, and in the approach of so-called *set membership identification*, the identification criterion delivers a set of estimated parameters $\hat{\theta}_N$ that satisfy $|\varepsilon(t,\hat{\theta}_N)| < c$ for some prechosen level c.

This general paradigm shows that we consider models in two different ways.
For identification purposes we consider a model as a mapping from measured data to some kind of residual signal, i.e. a mapping from (y, u) to ε. On the other hand, if we consider a model as an abstraction of the data generating system, we interpret it as a mapping from

input and disturbance signals to the output, i.e. a mapping from (u, v) to y. This duality is reflected in the block diagrams as depicted in Figure 1.8, and will play an important role in the sequel of this course.
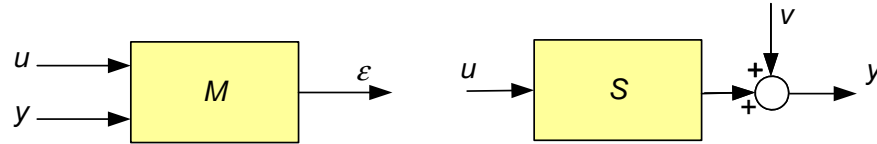
Figure 1.8: Two appearances of models; (a) model for identification, (b) model as reflection of the data generating system.

The different aspects that are crucial in any identification procedure are reflected in a scheme in Figure 1.9, which is due to Ljung (1987).
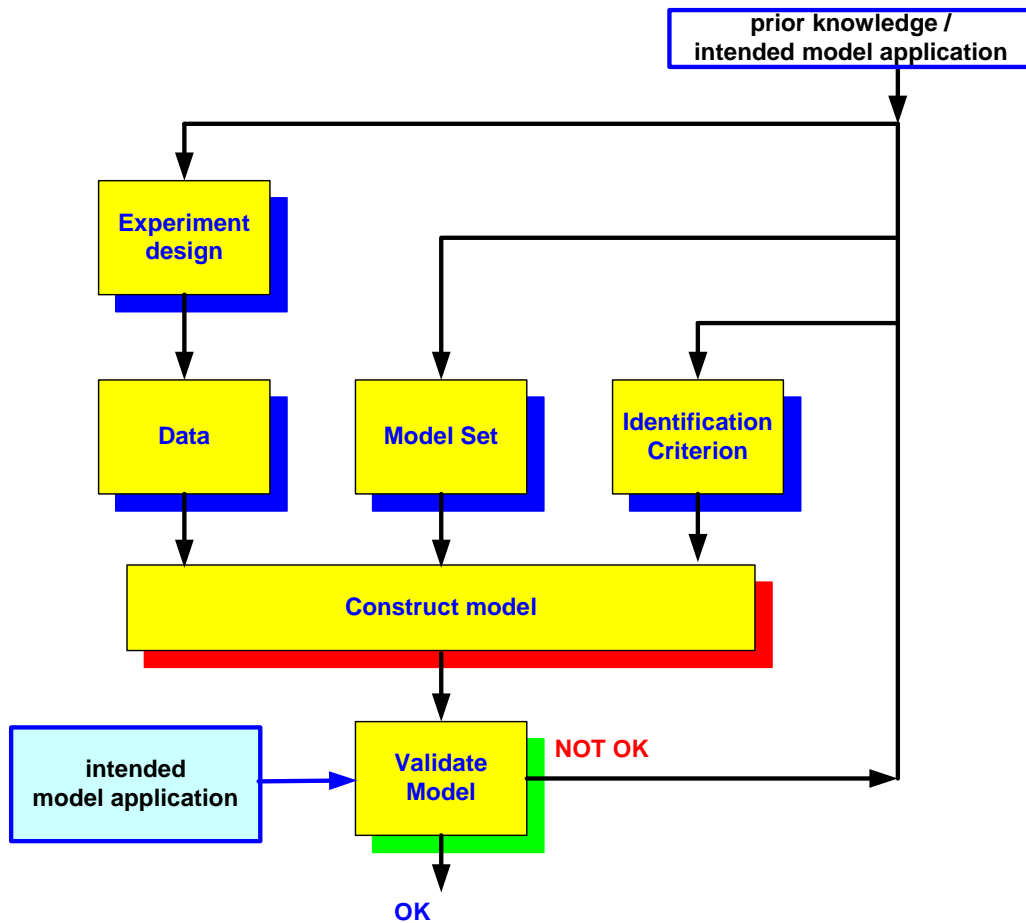
Figure 1.9: The identification procedure

The three basic ingredients of an identification procedure are

Data. Data might be available from normal operating records, but it may as well be possible to design tailor-made experiments to perform on the process in order to

obtain specific information, as e.g. step responses, sinus responses etcetera.

Model Set. It has to be specified beforehand within which set of models one is going to evaluate the most accurate model for the process at hand. In the model set several basic properties of the models have to be fixed, as e.g. linearity/nonlinearity, time-invariance, discrete/continuous-time, and other structural properties (as e.g. the order) of the models.

Identification criterion. Given measurement data and a model set, one has to specify in which way the optimal model from the model set is going to be determined. In applying the criterion, the models in the model set are going to be confronted with the measurement data.

In all three different aspects, a prior knowledge about the system to be identified can play an important role.

Given specific choices for the three phenomena described above, it is generally a matter of numerical optimization to construct an identified model.

Additionally the final question that has to be dealt with, is the question whether one is satisfied with the model obtained. This latter step in the procedure is indicated by the term *model validation*. The question whether one is satisfied with the result will in many situations be very much dependent on the question what the model is intended for. The ultimate answer to the validation question is then, that one is satisfied with the model if in the intended model application one is satisfied with the result. If the model is invalidated, then a redesign of the identification experiment or adjustment of model set and identification criterion may lead to an improved model.

The several aspects briefly indicated here, will be subject of further analysis in the several chapters to come.

1.4   Historical overview and present highlights

Many of the system identification methods that are nowadays available date back to the basic principles of least squares, as introduced in Gauss (1809), who was dealing with the question of modelling the movement of planets. System identification has received a growing interest over the last decades. The basic methods were developed in the sixties and seventies of the previous century starting from the introduction of computers for performing the often heavy calculations, see Åström and Bohlin (1965) and Åström and Eykhoff (1971). A number of books written in the seventies have recorded these developments, see e.g. Eykhoff (1974), Goodwin and Payne (1977). Being based on the theories of stochastic processes and statistical analysis, system identification at that time was specifically seen as a problem of parameter estimation. It was commonly assumed that one knew the correct model structure or order and the character of the noise disturbance on the data. The main underlying assumption in this approach appeared to be the assumption that the data generating system can be modelled exactly by a linear, time-invariant, finite-order model. Here the "system" refers not only to the input-output transfer function but also to the particular description of how noise affects the measurement data. This assumption was reflected by the situation that an *exact* parameter θ_0 was supposed to be present in the parameter set Θ.

In the 1980's, this basic assumption has been relaxed, giving more attention to the more realistic situation that system identification generally comes down to "approximate modelling" rather than "exact modelling". Issues of approximation have become popular, a development which was pulled mainly by the Swedish school of researchers in Lund, Linköping and Uppsala. See e.g. Ljung and Caines (1979), Ljung and Söderström (1983), Wahlberg and Ljung (1985). A good overview of this development, which turned "parameter estimation" into "system identification" is given in the works of Ljung (1999) whose book first appeared in 1987, and Söderström and Stoica (1989).

Interest in the issue of approximation made people move away from notions as consistency, and made them pay attention to the type of approximation that becomes involved. A related issue that comes into the picture is the issue of the intended application or goal of the model. As identifying a system no longer means finding an exact representation, but rather finding an approximation, then specific model goals might dictate which type of approximations are desirable. Or in other words: which aspects of the system dynamics will be incorporated in the model, and which aspects will be neglected. The intended model goal will have to point to the right way to go here.

Especially in the area of approximate modelling, the 1990's have shown an increasing interest in identifying approximate models that are suitable for serving as a basis for model-based control design. This means that, although one realizes that models obtained are only approximative, one would like to obtain models that are accurate descriptions of the system dynamics in those aspects of the system that are specifically important from a control-design point of view. Surveys of this development are given in Gevers (1993), Van den Hof and Schrama (1995), Albertos and Sala (2002), Hjalmarsson (2005) and Gevers (2005).

Another area of interest which is extremely relevant from an applications point of view, is the question concerning the accuracy of identified (approximate) models. Experimental data provides us with information concerning the dynamical system; besides the problem of extracting an appropriate model from the measured data, it is important to be able to make statements concerning the accuracy and reliability of this result. This area, sometimes denoted as model uncertainty estimation has been a part of the classical analysis in the form of providing confidence intervals for parameter estimates, however, always restricted to the situation in which consistent models were estimated. In an approximative setting of identification, this issue is still an important subject of research, being closely related to the question of model (in)validation, and to the goal-oriented design of experiments, see e.g. Bombois *et al.*(2006).

Whereas most identification techniques are developed and analyzed in the time domain, the frequency domain also offers a multitude of methods and tools, and sometimes particular advantages. In the course of years the difference between the two domains has become less, as been more been characterized as a difference between the used excitation signals, being periodic or not. An account of this development is given in Schoukens and Pintelon (1991) and Pintelon and Schoukens (2001).

As indicated before, several choices can be made for the identification criterion. In bounded error modelling, or set-membership identification, typically hard-bounded specifications are given for the residual signals in order to invalidate the accompanying models. Unlike the least-squares prediction error approaches, these methods do not lead to a single model estimate, but they principally deliver a set of (invalidated) models. In this sense they directly point to a model uncertainty quantification. More details on this area can be found in Milanese and Vicino (1991) and Milanese *et al.* (1996). A principal problem here

is the choice of the residual bounding; an inappropriate choice can easily lead to overly conservative model uncertainty bounds.

In so-called subspace identification the identification criterion is not expressed explicitly. This popular area which has emerged during the nineties (Van Overschee and De Moor, 1996; Verhaegen, 1994) connects with realization theory and essentially encompasses projections of signal spaces onto subspaces that represent limited-dimensional linear systems. A principal tool in these operations is the singular value decomposition. One of the advantages of the approach is that handling of multivariable systems is practically as simple as handling scalar systems.

Important challenges are present in the problem of identifying of models with nonlinear dynamics. Whereas is many applications it suffices to consider linear models of a linearized nonlinear plant, the challenge to express the nonlinear dynamical phenomena of the plant into a nonlinear model often enhances the capabilities of the model, e.g. when designing a control system that moves the plant through several operating regimes. For contributions in this area see Suykens and Vandewalle (1998), Nelles (2001), Tóth (2010), while an excellent survey paper highlighting the developments in identification of nonlinear models is provided in Schoukens and Ljung (2019). In this manuscript attention will mainly be focussed on linear models.

An important development in the period 2010-2020 has been the adoption of techniques and insights that originated from the domain of machine learning. While system identification techniques where basically developed on the basis of a maximum likelihood reasoning, implying that the objective is to have (asymptotically) unbiased models with minimum variance, the machine learning domain did adopt a Bayesian framework, aiming at a minimum mean squared error (MSE) of model estimates. By allowing a small bias newly introduced methods could actually reduce the variance and arrive at estimates with favourable MSE properties. This approach is then combined with a regularization mechanism to penalize models with a large number of parameters, thus providing a kind of automated selected of the model complexity when identifying the model dynamics, typically in the form of the system's pulse response. An account of this important development is provided in Pillonetto et al. (2914).

Motivated by developments in control, where distributed control methods and multi-agent systems have emerged, in the identification community the problem of data-driven modelling in structured dynamic networks has been introduced. This development can be considered as a third step in the sequence of open-loop experiments, closed-loop experiments and networked experiments. Systems are considered to be composed of multiple subsystems that are interconnected through series, parallel and feedback connections, like e.g. in an electronic circuit. Several identification-related problems can then be addressed on the basis of measured data that is taken at different locations in the network. Early publications introducing the considered identification problems are provided in Gonçalves and Warnick (2008), Materassi and Innocenti (2010), Chiuso and Pillonetto (2012) and Van den Hof et al. (2013).

Bibliography

P. Albertos and A. Sala (Eds.)(2002). *Iterative Identification and Control.* Springer Verlag, London, UK, ISBN 1-85233-509-2.

K.J. Åström and T. Bohlin (1965). Numerical identification of linear dynamic systems from normal operating records. *Proc. IFAC Symp. Selft-Adaptive Contr. Systems*, Teddington, England, pp. 96-110.

K.J. Åström and P. Eykhoff (1971). System identification - a survey. *Automatica*, vol. 7, pp. 123-162.

X. Bombois, G. Scorletti, M. Gevers, P.M.J. Van den Hof and R. Hildebrand (2006). Least costly identification experiment for control. *Automatica*, Vol. 42, no. 10, pp. 1651-1662.

A. Chiuso and G. Pillonetto (2012). A Bayesian approach to sparse dynamic network identification. *Automatica*, Vol. 48, no. 8, pp. 1553-1565.

P. Eykhoff (1974). *System Identification: Parameter and State Estimation*. Wiley & Sons, London.

K.F. Gauss (1809). *Theoria motus corporum celestium*. English translation: *Theory of the Motion of the Heavenly Bodies*. Dover, New York, 1963.

M. Gevers (1993). Towards a joint design of identification and control? In: H.L. Trentelman and J.C. Willems (Eds.), *Essays on Control: Perspectives in the Theory and its Applications*. Proc. 1993 European Control Conference, Groningen, The Netherlands, Birkhäuser, Boston, pp. 111-151.

M. Gevers (2005). Identification for control: from the early achievements to the revival of experiment design. *European J. Control*, Vol. 11, no. 4-5, pp. 335-352.

M. Gevers (2006). A personal view of the development of system identification. *IEEE Control Systems Magazine*, Vol. 26, no. 6, pp. 93-105.

J. Gonçalves and S. Warnick (2008). Necessary and sufficient conditions for dynamic structure reconstruction of LTI networks. *IEEE Trans. Autom. Control*, Vol. 53, no. 7, pp. 1670-1674.

G.C. Goodwin and R.L. Payne (1977). *Dynamic System Identification: Experiment Design and Data Analysis*. Academic Press, New York.

P.S.C. Heuberger, P.M.J. Van den Hof and B. Wahlberg (Eds.) (2005). *Modelling and Identification with Rational Orthogonal Basis Functions*. Springer Verlag, London, UK, 2005.

H. Hjalmarsson, N. Gevers, S. Gunnarsson, O. Lequin (1998). Iterative feedback tuning: theory and applications. *IEEE Control Systems Magazine*, Vol. 18, no. 4, pp. 26-41.

H. Hjalmarsson (2004). From experiment design to closed-loop control. *Automatica*, Vol. 41, no. 3, pp. 393-438.

R. Johansson (1993). *System Modelling and Identification*. Prentice-Hall, Englewood Cliffs, NJ.

L. Ljung (1987, 1999). *System Identification - Theory for the User*. Prentice-Hall, Englewood Cliffs, NJ, 1987. Second Edition, 1999.

L. Ljung and P.E. Caines (1979). Asymptotic normality of prediction error estimators for approximate system models. *Stochastics*, vol. 3, pp. 29-46.

L. Ljung and T. Söderström (1983). *Theory and Practice of Recursive Identification*. MIT Press, Cambridge, MA, USA.

D. Materassi and G. Innocenti (2010). Topological identification in networks of dynamical systems. *IEEE Trans. Autom. Control*, Vol. 55, no. 8, pp. 1860-1871.

M. Milanese and M. Vicino (1990). Optimal estimation theory for dynamic systems with set membership uncertainty: an overview. *Automatica*, vol. 27, pp. 997-1009.

M. Milanese, J. Norton, H. Piet-Lahanier and E. Walter (Eds.) (1996). *Bounding Approaches to System Identification*. Plenum Press, New York.

O. Nelles (2001). *Nonlinear System Identification - From Classical Approaches to Neural Networks and Fuzzy Models.* Springer Verlag, Inc., New York, ISBN 3-540-67369-5.

J.P. Norton (1986). *An Introduction to Identification.* Academic Press, London, UK.

G. Pillonetto, F. Dinuzzo, T. Chen G. De Nicolao and L. Ljung (2014). Kernel methods in system identification, machine learning and function estimation: a survey. *Automatica*, Vol. 50, pp. 657-682.

R. Pintelon and J. Schoukens (2001). *System Identification - A Frequency Domain Approach.* IEEE Press, Piscataway, NJ, USA, ISBN 0-7803-6000-1.

J. Schoukens and R. Pintelon (1991). *Identification of Linear Systems - A Practical Guide to Accurate Modeling.* Pergamon Press, Oxford, UK.

J. Schoukens and L. Ljung (2019). Nonlinear system identification - A user-oriented roadmap. *Control Systems Magazine*, December 2019, pp. 28-99.

T. Söderström and P. Stoica (1989). *System Identification.* Prentice-Hall, Hemel Hempstead, U.K.

J.A.K. Suykens and J.P.L. Vandewalle (Eds.) (1998). *Nonlinear Modelling - Advanced Black-Box Techniques.* Kluwer Academic Publ., Dordrecht, The Netherlands.

R. Tóth (2010). *Modeling and Identification of Linear Parameter-Varying Systems - An Orthornomal Basis Function Approach.* Springer Verlag, Berlin, Germany.

P.M.J. Van den Hof and R.J.P. Schrama (1995). Identification and control - closed loop issues. *Automatica*, vol. 31, pp. 1751-1770.

P.M.J. Van den Hof, A.G. Dankers, P.S.C. Heuberger and X. Bombois (2013). Identificaiton of dynamic models in complex networks with prediction error methods - basic methods for consistent module estimates. *Automatica*, Vol. 49, no. 10, pp. 2994-3006.

P. Van Overschee and B.L.R. de Moor (1996). *Subspace Identification for Linear Systems.* Kluwer Academic Publ., Dordrecht, The Netherlands.

M. Verhaegen (1994). Identification of the deterministic part of MIMO state space models given in innovations form from input-output data. *Automatica*, Vol. 30, no. 1, pp. 61-74.

M. Verhaegen and V. Verdult (2007). *Filtering and System Identification - a Least squares Approach.* Cambridge University Press, Cambridge, UK.

E. Walter and L. Pronzato (1997). *Identification of Parametric Models from Experimental Data.* Springer, Berlin, 1997.

B. Wahlberg and L. Ljung (1986). Design variables for bias distribution in transfer function estimation. *IEEE Trans. Automat. Control*, vol. AC-31, no. 2, pp. 134-144.

Y. Zhu (2001). *Multivariable System Identification for Process Control.* Elsevier Science Ltd., Oxford, UK, ISBN 0-08-043985-3.

Chapter 2

Deterministic and stochastic signals and systems

2.1 Introduction

System identification is dealing with signals and systems. Based on measured signals of a physical process the aim is to arrive at a model description of this process in the form of a dynamical system.

For building up the framework used for handling signals and systems, attention will be paid to several analysis tools. Basic information content of signals will be examined in terms of the frequency components that are present in a signal (Fourier series, Fourier transforms), and in the distribution of energy and/or power of signals over frequency.

First attention will be given to continuous-time systems and related signals. However, since all of signal processing performed by digital hardware has to be done in discrete-time (sampled signals), attention will be focused on sampling continuous-time signals and on the evaluation of relevant properties of discrete-time signals and systems.

The Discrete-Time Fourier Transform (DTFT) for infinite sequences as well as the Discrete Fourier Transform (DFT) for finite sequences will be summarized, and specific attention will be given to both deterministic signals and stochastic processes. For the analysis of identification methods in later chapters it will appear attractive to be able to also deal with signals that are composed of both deterministic and stochastic components. In view of this, the notion of quasi-stationary processes/signals is discussed.

The treatment of the material will be done in a summarizing style rather than on an introductory level. It is assumed that the reader has a basic knowledge of signals and systems theory.

2.2 Continuous-time systems analysis

A linear time-invariant finite-dimensional (LTIFD) dynamical system, operating on continuous-time signals is generally denoted by a (ordinary) differential equation which relates an input signal u and an output signal y. A common notation for this is given by

$$y(t) = G(p)u(t), \quad t \in \mathbb{R}$$

where p is the differential operator, $pu(t) := \frac{\partial u(t)}{\partial t}$, and $G(p)$ is a rational function in p, whose numerator and denominator constitute the mentioned differential equation.
For known input signal and initial conditions this description determines the response $y(t)$ of the system.

For analyzing the properties of this dynamical system, in terms of e.g. poles and zeros and its frequency response, the Laplace transform is used, leading to the relation

$$Y(s) = G(s)U(s),$$

where s is the Laplace variable, being a complex indeterminate, and $Y(s), U(s)$ the Laplace transforms of output and input respectively. The *transfer function* $G(s)$ is a complex function, and poles and zeros of $G(s)$ in the complex plain give insight in the dynamic properties of the system. Some relevant properties of the dynamical system G:

- *Linearity.* Linearity of the dynamical system is induced by the ordinary linear differential equation that governs the dynamical system.

- *Time-invariance.* Time-invariance of the dynamical system is induced by the fact that the differential equation has constant coefficients, implying that $G(s)$ is independent of the time t.

- *Causality.* The mechanism that $y(t)$ does not depend on $u(\tau)$ for $\tau > t$. This is reflected by the condition that $g(t) = 0$, $t < 0$. In terms of $G(s)$ this is reflected by the condition $\lim_{|s| \to \infty} G(s) < \infty$.

- *Stability.* A system is called bounded-input bounded-output (BIBO)-stable if it is analytic (has no poles) in the right half plane, $Re(s) \geq 0$.

The frequency response of $G(s)$ is given by $G(i\omega)$, $\omega \in \mathbb{R}$. It determines in which way sinusoidal input signals are processed by the system. For $u(t) = sin(\omega t)$ the stationary response of the system is

$$y(t) = |G(i\omega)| \cdot sin(\omega t + \phi)$$

with $\phi = \arg G(i\omega)$.
A direct relation between input and output signals can also be obtained by convolution:

$$y(t) = \int_0^\infty g(\tau)u(t - \tau)d\tau$$

where $g(\tau)$ is the inverse Laplace transform of $G(s)$, i.e. they are related by the Laplace transform relations

$$G(s) = \int_{-\infty}^\infty g(t)e^{-st}dt.$$

$$g(\tau) = \int_{\sigma-i\omega}^{\sigma+i\omega} G(s)e^{s\tau}ds.$$

The signal $\{g(\tau)\}$ is the impulse response of the system G.

2.3 Continuous-time signal analysis

2.3.1 Introduction

The analysis of signals will particularly address questions as: "what is the frequency content of a signal?", and "how is the energy or power of a signal distributed over frequency?". In this section these questions will be treated. A distinction will be made between deterministic signals and stochastic processes.

2.3.2 Deterministic signals

Deterministic signals appear in several different forms. As an illustration of this difference three different types of signals are depicted in Figure 2.1. In specifying relevant signal properties we denote the *energy* of the signal u by

$$\mathcal{E}_u := \int_{-\infty}^{\infty} u^2(t)dt$$

and the *power* of the signal by

$$\mathcal{P}_u := \frac{1}{T} \int_{-T/2}^{T/2} u^2(t)dt,$$

where T is allowed to tend to infinity in case one considers an infinite-time signal.

Signals that have finite energy are referred to as energy signals, while signals with finite power are called power signals. In this way it can be verified that the signal in Figure 2.1(a) is an energy-signal, while the signals in (b) and (c) are power-signals.

The basic tool for analyzing the frequency content of a signal is the Fourier analysis, i.e. the Fourier series and the Fourier transform. The Fourier series refers to periodic signals, showing that any periodic signal can be written as a summation of harmonic functions (sinusoids). The Fourier transform is a generalization that can also handle non-periodic signals.

Periodic signals - Fourier series

For a periodic signal with period T_0 that satisfies the Dirichlet conditions [1], the corresponding Fourier series is given by

$$u(t) \quad = \quad \sum_{k=-\infty}^{\infty} c_k e^{ik\omega_0 t} \tag{2.1}$$

$$c_k \quad = \quad \frac{1}{T_0} \int_{T_0} u(t)e^{-ik\omega_0 t}dt, \tag{2.2}$$

with $\omega_0 = 2\pi/T_0$. It describes the decomposition of a periodic signal in harmonic components. Periodic signals have unbounded energy, but their power satisfies

$$\mathcal{P}_u = \frac{1}{T_0} \int_0^{T_0} u^2(t)dt = \sum_{k=-\infty}^{\infty} |c_k|^2. \tag{2.3}$$

---

[1]The Dirichlet conditions are that the signal u: (a) has at most a finite number of discontinuities in one period, (b) has at most a finite number of maxima and minima in one period, and (c) is bounded in the sense that $\int_{T_0} |u(t)|dt < \infty$, See Phillips et al. (2008). If the right hand side of (2.1) is evaluated in a point t where u is discontinuous, then it equals $\frac{1}{2}[u(t^-) + u(t^+)]$, with $u(t^-) = \lim_{\tau \uparrow t} u(\tau)$ and $u(t^+) = \lim_{\tau \downarrow t} u(\tau)$.

The above result can simply be verified by substituting the Fourier series of u into the expression for the power of the signal. This shows that every exponential function in u has an independent contribution to the power of the signal.
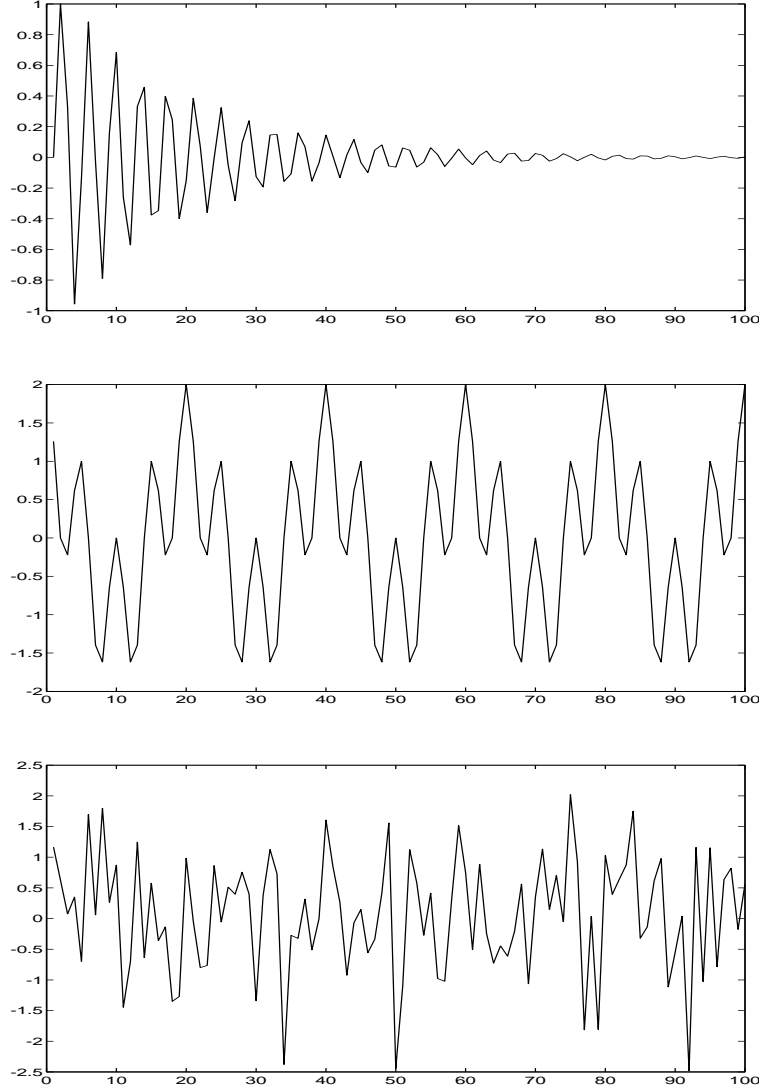
Figure 2.1: Three different types of signals: (a) finite-energy signal, (b) periodic finite-power signal, and (c) random-like signal (e.g. a realization of a stationary stochastic process.

If we assume that $u(t)$ is real-valued, the consequence is that the Fourier series coefficients will satisfy $c_{-k} = c_k^*$.

General signals - Fourier transform

The standard Fourier transform of an infinite-time signal is defined by the following trans-

form pair[2]:

$$U(\omega) \;\; = \;\; \int_{-\infty}^{\infty} u(t) e^{-i\omega t} dt \tag{2.4}$$

$$u(t) \;\; = \;\; \frac{1}{2\pi} \int_{-\infty}^{\infty} U(\omega) e^{i\omega t} d\omega. \tag{2.5}$$

The signal u has to satisfy certain conditions in order for the integral (2.4) to exist. The Fourier transform exists for signals that satisfy the Dirichlet conditions [3], being a set of sufficient conditions.

The Dirichlet conditions imply that the signals have to satisfy $\int_{-\infty}^{\infty} |u(t)| dt < \infty$. This signal class contains at least all energy-signals. Note that in order for a signal to have finite energy it is necessary that $|u(t)| \to 0$ for $t \to \infty$.

Additionally analytical power-signals, including periodic signals, can be transformed, provided that the mathematical framework for representing the transforms is extended to incorporate Dirac impulse functions, satisfying $\delta_c(t) = 0, t \neq 0$ and $\int_{-\infty}^{\infty} \delta_c(t) dt = 1$. With the notion "analytical signal" is meant that the signals are characterized by analytical expressions. The standard tables for Fourier transform and its basic properties can be applied. This includes all kinds of periodic signals, the step function, the sign function etcetera.

For the above classes of signals the Fourier transform can be applied. When transforming signals from the second category (finite power signals), the Fourier transform will generally be unbounded, i.e. it will contain Dirac impulses. This is caused by the fact that the energy content of these signals is unbounded.

The rules for calculating Fourier transforms of specific signals and the specific relations between transformed signals can be found in any book on Fourier analysis are all based on the transform pair (2.4),(2.5). Note that the Fourier transform is actually obtained from the Fourier series, by periodically extending a finite-time signal, obtaining its Fourier series coefficients and taking the limit with the period length tending to infinity.

For non-analytical signals, i.e. signals that can not be constructed easily by a mathematical expression, and having infinite energy, the Fourier transform will not exist. This happens e.g. for realizations of stochastic processes, like the signal depicted in Figure 2.1(c). These kind of signals will be discussed separately in section 2.3.3.

Finite-time signals
When considering continuous-time signals over a finite-time the corresponding Fourier transform is denoted by

$$U_T(\omega) := \int_0^T u(t) e^{-i\omega t} dt. \tag{2.6}$$

---

[2]In this work the argument ω is used in $U(\omega)$ for convenience; the connection with the Laplace transform $U(s)$ appears more natural in the notation $U(i\omega)$.

[3]The Dirichlet conditions for general (non-periodic) signals are that on any finite internal the signal u: (a) has at most a finite number of discontinuities, (b) has at most a finite number of maxima and minima, and (c) is bounded, and additionally u should be absolutely integrable, i.e. $\int_{-\infty}^{\infty} |u(t)| dt < \infty$, See Phillips et al. (2008). If the right hand side of (2.5) is evaluated in a point t where u is discontinuous, then it equals $\frac{1}{2}[u(t^-) + u(t^+)]$, with $u(t^-) = \lim_{\tau \uparrow t} u(\tau)$ and $u(t^+) = \lim_{\tau \downarrow t} u(\tau)$.

This concerns finite-time signals that are defined over the time-interval $[0, T]$. The transform comes down to the formal Fourier transform of an infinite-signal that is created by extending the finite-time signal to infinity with zeros padded on both sides of the time-interval.

Periodic signals
For a periodic signal with period T_0 the coefficients of the Fourier series can be directly related to a finite-time Fourier transform. Directly from (2.2) it follows that

$$c_k = \frac{1}{T_0} U_{T_0}(k\omega_0). \tag{2.7}$$

For periodic signals, the expressions for the Fourier transform can be shown to be directly related to the Fourier series coefficients. Equating the Fourier series (2.1) with the inverse Fourier transform (2.5) it follows that for this periodic signal u the Fourier transform satisfies

$$U(\omega) = 2\pi \sum_{k=-\infty}^{\infty} c_k \delta_c(\omega - k\omega_0). \tag{2.8}$$

This shows that in the Fourier transform of a periodic signal the integral expression in (2.4) reduces to a summation.

Example 2.3.1 (Fourier transform of sinusoidal signal)
Consider the sinusoidal signal:
$$u(t) = A \cdot cos(\omega_0 t)$$

Writing $u(t) = \frac{A}{2}[e^{i\omega_0 t} + e^{-i\omega_0 t}]$ it follows from (2.1) that $c_1 = c_{-1} = A/2$ and $c_k = 0$, $k \neq 1, -1$.
Applying (2.8) then leads to

$$U(\omega) = A\pi[\delta_c(\omega - \omega_0) + \delta_c(\omega + \omega_0)].$$

Power of a periodic signal
With the expression (2.7) for c_k the power of a periodic signal can be written as

$$\mathcal{P}_u = \sum_{k=-\infty}^{\infty} |c_k|^2 = \frac{1}{T_0^2} \sum_{k=-\infty}^{\infty} |U_{T_0}(k\omega_0)|^2, \tag{2.9}$$

showing that a discrete number of frequencies $k\omega_0$ contribute to the power of the signal.

Spectral densities of infinite-time energy and power signals:
The energy / power spectral density of a signal characterizes the distribution of the energy / power of a signal over the different frequency components. These spectral densities are naturally obtained by utilizing *Parseval's relation* for energy signals:

$$\int_{-\infty}^{\infty} u^2(t)dt = \frac{1}{2\pi} \int_{-\infty}^{\infty} |U(\omega)|^2 d\omega,$$

showing two equivalent expressions for the energy of a signal. This directly leads to the following notion (see e.g. Phillips et al., 2008).

Proposition 2.3.2 (Energy Spectral Density Function.) *Let $u(t)$ be a finite energy signal, i.e. $\int_{-\infty}^{\infty} u(t)^2 dt = \mathcal{E}_u < \infty$. Then*

$$\mathcal{E}_u = \frac{1}{2\pi} \int_{-\infty}^{\infty} \Psi_u(\omega) d\omega$$

where the Energy Spectral Density $\Psi_u(\omega)$ is given by

$$\Psi_u(\omega) = |U(\omega)|^2.$$

With the same line of reasoning a similar expression can be given for the situation of power signals[4].

Proposition 2.3.3 (Power Spectral Density Function.) *Let $u(t)$ be a finite power signal of length T, i.e. $\frac{1}{T} \int_{-T/2}^{T/2} |u(t)|^2 dt = \mathcal{P}_u < \infty$. Then*

$$\mathcal{P}_u = \frac{1}{2\pi} \int_{-\infty}^{\infty} \Phi_u(\omega) d\omega$$

where the Power Spectral Density $\Phi_u(\omega)$ is given by

$$\Phi_u(\omega) = \frac{1}{T} |U_T(\omega)|^2 \tag{2.10}$$

with $U_T(\omega)$ as defined in (2.6).

Note that for the particular situation of a periodic signal expression (2.10) is less suitable. In this case (2.9) directly shows that

$$\Phi_u(\omega) = 2\pi \sum_{k=-\infty}^{\infty} |c_k|^2 \delta_c(\omega - k\omega_0).$$

A simple example is given for illustration.

Example 2.3.4 (Power spectral density of sinusoidal signal)
Consider again the sinusoidal signal

$$u(t) = A \cdot cos(\omega_0 t).$$

Then $c_{-1} = c_1 = A/2$, and consequently

$$\Phi_u(\omega) = \frac{A^2 \pi}{2} [\delta_c(\omega - \omega_0) + \delta_c(\omega + \omega_0)].$$

$\square$

Signal properties processed by continuous-time systems.
Fourier transforms and energy and power spectral densities are transformed by dynamical systems in the following way. Consider a LTIFD system determined by $y(t) = G(p)u(t)$, with u and y infinite time signals. Then

$$Y(\omega) = G(i\omega)U(\omega)$$

$$\Psi_y(\omega) = |G(i\omega)|^2 \Psi_u(\omega)$$

$$\Phi_y(\omega) = |G(i\omega)|^2 \Phi_u(\omega).$$

---

[4]Simply take a signal u that is zero outside the interval $(-T/2, T/2)$ and use the Parseval's relation with a premultiplication of $1/T$.

2.3.3   Stochastic processes

When considering realizations of a stationary stochastic process we have two possibilities to analyze the properties of a realization $\{x(t)\}$, $t \in \mathbb{R}$.

(a) If we restrict attention to one single realization of the process, the signal $\{x(t)\}$, $t \in \mathbb{R}$, can be considered as a (deterministic) finite-power signal, and the analysis as presented in the previous part of this section applies.

(b) If we want to focus on the properties of the stochastic process, and not on one single (random) realization of the process, we have to analyze in which sense properties of the stochastic process can be recovered from discrete samples of the stochastic process.

In this subsection attention will be paid to the situation (b) described above. For situation (a) we refer to the previous sections.

In this section a stationary stochastic process x will be considered, i.e.

(a) For every $t \in \mathbb{R}$, $x(t)$ is a random variable with a fixed probability density function that governs the outcome of $x(t)$.

(b) $E(x(t))$ and $E(x(t)x(t - \tau))$ are independent of t for each value of $\tau \in \mathbb{R}$.

The considered notion of stationarity (limited to restrictions on the first two moments $E(x(t))$ and $E(x(t)x(t - \tau))$) is mostly referred to as *wide-sense stationarity*, in contrast with a more strict notion that is related to the time-invariance of the probability density functions.

Some useful notions related to stationary stochastic processes are:

- White noise process.
  A stationary stochastic process x is called a white noise process if x is a sequence of independent (and identically distributed) random variables.
  Identically distributed means that the probability density function (pdf) of $x(t)$ is independent of t, and independent means that the joint pdf of $(x(t_1), x(t_2))$ is the product of the two separate pdf's. As a direct result $Ex(t)x(t - \tau) = 0$ for all $\tau \neq 0$.

- Auto-correlation function $R_x(\tau) = E[x(t)x(t - \tau)]$.

- Cross-correlation function $R_{xy}(\tau) = E[x(t)y(t - \tau)]$.

- Power (auto)-spectral density function, or spectrum

$$\Phi_x(\omega) = \int_{-\infty}^{\infty} R_x(\tau)e^{-i\omega\tau}d\tau$$

- Power (cross)-spectral density function, or cross-spectrum

$$\Phi_{xy}(\omega) = \int_{-\infty}^{\infty} R_{xy}(\tau)e^{-i\omega\tau}d\tau$$

Consequences of these definitions are:

$$R_x(0) \;\; = \;\; Ex^2(t) = \frac{1}{2\pi} \int_{-\infty}^{\infty} \Phi_x(\omega)d\omega \tag{2.11}$$

$$R_{xy}(0) \;\; = \;\; E[x(t)y(t)] = \frac{1}{2\pi} \int_{-\infty}^{\infty} \Phi_{xy}(\omega)d\omega. \tag{2.12}$$

Note that the notions used here, are very similar to the corresponding notions for deterministic signals. For instance, $\Phi_x(\omega)$ here indicates the distribution of the average-power (over the ensemble) of the stochastic process over different frequencies.

Given a LTIFD system relating input and output signals according to $y(t) = G(p)u(t)$ with u, y zero-mean stationary stochastic processes, then the spectral densities satisfy:

$$\Phi_y(\omega) \;\; = \;\; |G(i\omega)|^2 \cdot \Phi_u(\omega) \tag{2.13}$$

$$\Phi_{yu}(\omega) \;\; = \;\; G(i\omega) \cdot \Phi_u(\omega). \tag{2.14}$$

2.4 Discrete-time signal analysis

2.4.1 Introduction

In almost all situations of applied signal analysis and signal processing one will be dealing with sampled signals. These signals are easily treated by modern microprocessor-based equipment. As a result a theory is required for handling and analyzing discrete-time signals, similar to the tools that are available for analyzing continuous-time signals. This refers to the decomposition of a signal into its basic harmonics, evaluating the frequency content of signals and evaluating the distribution of energy and/or power over frequency.

2.4.2 Deterministic signals

For discrete-time signals the notation $u_d(k) := u(kT_s)$ will be adopted. In this expression u is the continuous-time signal that possibly underlies the discrete-time signal, and T_s is the sampling period. k is the (discrete) time variable that is an integer running index: $k = 1, 2, \cdots$. The sample frequency ω_s is defined by $\omega_s = \frac{2\pi}{T_s}$. In terms of energy and power of signals, similar definitions are used as before:

$$\mathcal{E}_u := \sum_{k=-\infty}^{\infty} u_d^2(k)$$

and the *power* of the signal:

$$\mathcal{P}_u := \frac{1}{N} \sum_{k=0}^{N-1} u_d^2(k).$$

The basic tool for analyzing the frequency content of a discrete-time signal is the discrete-time Fourier analysis, i.e. the discrete-time Fourier series and the discrete-time Fourier transform. The Fourier series refers to periodic signals, showing that any periodic signal can be written as a summation of harmonic functions (sinusoids). The Fourier transform is a generalization that can also handle non-periodic signals.

Periodic signals - Discrete-Time Fourier Series

For a periodic signal with period N_0, which means that $u_d(k + N_0) = u_d(k)$ for all $k \in \mathbb{Z}$, the *Discrete-Time Fourier Series* of the signal u_d is given by[5]:

$$u_d(k) = \sum_{\ell=0}^{N_0-1} a_\ell e^{i\frac{2\pi}{N_0}\ell k} \tag{2.15}$$

where the Fourier coefficients are given by

$$a_\ell = \frac{1}{N_0} \sum_{k=0}^{N_0-1} u_d(k) e^{-i\frac{2\pi}{N_0}\ell k}. \tag{2.16}$$

The power of periodic signals can again be written directly as a function of the Fourier coefficients:

$$\mathcal{P}_u = \frac{1}{N_0} \sum_{k=0}^{N_0-1} u_d^2(k) = \sum_{\ell=0}^{N_0-1} |a_\ell|^2.$$

This shows that every exponential function in u has an independent contribution to the power of the signal, which is simply a summation of the contributions of each separate frequency. As the Fourier coefficients a_ℓ are periodic with period N_0, the sum on the right hand side can be taken over any N_0 consecutive values of ℓ.

Non-periodic signal - Discrete-Time Fourier Transform

We now move to signals that are non-periodic. The *Discrete-Time Fourier Transform* for sampled (discrete-time) signals is given by the transform pair:

$$U_s(\omega) \quad := \quad \sum_{k=-\infty}^{\infty} u_d(k) e^{-i\omega k T_s} \tag{2.17}$$

$$u_d(k) \quad = \quad \frac{T_s}{2\pi} \int_{2\pi/T_s} U_s(\omega) e^{i\omega k T_s} d\omega. \tag{2.18}$$

The DTFT leads to a bounded transform $|U_s(\omega)|$ for any discrete-time signal that satisfies

$$\sum_{k=-\infty}^{\infty} |u_d(k)| < \infty,$$

being the discrete-time equivalent of the Dirichlet conditions discussed in section 2.3. As a result the DTFT can be applied to any finite-time signal, as well as to infinite-time finite-energy signals.

Note that the discrete-time Fourier transform (DTFT) transforms a discrete sequence of time-domain samples, into a function $U_s(\omega)$ that takes its values continuously over ω's. By construction (since k is integer valued) the transform $U_s(\omega)$ is a periodic function with period $2\pi/T_s = \omega_s$. Corresponding to this, the integral in (2.18) is taken over any range of ω with length $2\pi/T_s$, being the period length of the integrand.

---

[5]The given expression for $u_d(k)$ actually has resulted from $u(kT_s) = \sum_{\ell=0}^{N_0-1} a_\ell e^{i\frac{\omega_s}{N_0}\cdot\ell\cdot k T_s}$, which shows that the effect of the sampling interval T_s is canceled out in the exponent.

Finite-time signals

When considering discrete time signals over a finite time, the corresponding Fourier transform is denoted by:

$$U_N(\omega) := \sum_{k=0}^{N-1} u_d(k) e^{-i\omega k T_s}, \tag{2.19}$$

and is known as the Discrete Fourier Transform (DFT), to be further discussed in more detail in section 2.4.4.

Periodic signals

Although the DTFT is formally not fit for dealing with periodic signals, as they are not finite energy signals, the transform can still be given some interpretation when allowing to include (unbounded) Dirac functions as possible terms in $U_s(\omega)$.

For a periodic signal with period N_0 the coefficients of the Fourier series can be directly related to a finite-time Fourier transform taken over one period of the periodic signal. Directly from (2.16) it follows that

$$a_\ell = \frac{1}{N_0} U_{N_0}(\ell \omega_0). \tag{2.20}$$

Additionally the expressions for the Fourier transform can be shown to be directly related to the Fourier series coefficients. Equating the Fourier series (2.15) with the inverse Fourier transform (2.18) it follows that for this periodic signal u the Fourier transform satisfies

$$U_s(\omega) = \frac{2\pi}{T_s} \sum_{k=-\infty}^{\infty} a_k \delta_c(\omega - k\omega_0) \tag{2.21}$$

with $\omega_0 = \frac{2\pi}{N_0 T_s}$. In this expression the δ-functions serve to replace the integral expression in (2.18).

Example 2.4.1 (Discrete-time Fourier transform of a sinusoid) *Consider the signal*

$$u(k) = A \cdot cos(\omega_0(k T_s))$$

with $\omega_0 = 2\pi/(N_0 T_s)$, i.e. there are N_0 samples in a single period of the signal. We consider N to be a multiple of N_0, $N = r N_0$, with $r \in \mathbb{N}$. Then

$$U_N(\omega) = \sum_{k=0}^{N-1} \frac{A}{2} \left[e^{i(\omega_0 - \omega)k T_s} + e^{-i(\omega_0 + \omega)k T_s} \right].$$

Using lemma 2A.1 it follows that

$$U_N(\omega) = \begin{cases} N \cdot \frac{A}{2} & for\ \omega = \pm\omega_0 = \pm\frac{2\pi}{N_0 T_s}, \\ 0 & for\ \omega = \frac{2\pi\ell}{N T_s},\quad \ell \in \mathbb{Z}, \ell \neq r. \end{cases} \tag{2.22}$$

$\square$

For a more extensive explanation see also example 2A.2.

Spectral densities of energy and power signals

Again, similar to the situation of continuous-time signals we can consider the distribution of energy and/or power of a signal over frequency.

Proposition 2.4.2 (Energy Spectral Density Function.) *Let $u_d(k)$ be a finite-energy sampled-data signal, sampled with a sampling interval T_s. Then*

$$\mathcal{E}_u = \frac{T_s}{2\pi} \int_{2\pi/T_s} \Psi_u(\omega) d\omega$$

where the Energy Spectral Density $\Psi_u(\omega)$ is given by

$$\Psi_u(\omega) = |U_s(\omega)|^2.$$

Proposition 2.4.3 (Power Spectral Density Function.) *Let $u_d(k)$ be a finite-power sampled-data signal, i.e. $\frac{1}{N}\sum_{k=0}^{N-1} |u_d(k)|^2 = \mathcal{P}_u < \infty$, sampled with a sampling interval T_s. Then*

$$\mathcal{P}_u = \frac{T_s}{2\pi} \int_{2\pi/T_s} \Phi_u(\omega) d\omega \tag{2.23}$$

where the Power Spectral Density $\Phi_u(\omega)$ is given by

$$\Phi_u(\omega) = \frac{1}{N}|U_N(\omega)|^2$$

The proof is added in the appendix.

As in the case of continuous-time signals, the (discrete-time) Fourier transform of sampled-data signals constitutes a way to characterize the distribution of energy and/or power of the corresponding signals over the different frequencies.

For finite power signals the quantity $\frac{1}{N}|U_N(\omega)|^2$ is referred to as the *periodogram* of the (finite-time) discrete-time signal. This periodogram determines the distribution of power over frequencies.

For periodic signals the power spectral density can again be computed directly on the basis of the discrete-time Fourier coefficients of the signals. Since in this case $\mathcal{P}_u = \sum_{\ell=0}^{N_0-1} |a_\ell|^2$ it follows from combination of (2.20) and (2.23) that

$$\Phi_u(\omega) = \frac{2\pi}{T_s} \sum_{k=-\infty}^{\infty} |a_k|^2 \delta_c(\omega - k\omega_0).$$

2.4.3   Sampling continuous-time signals

In this subsection the sampling and reconstruction theorem of Shannon will be recalled briefly. It considers the question under which condition a sampled signal can exactly represent a infinite-time continuous-time signal from which it is constructed. The operation of sampling a signal is schematically depicted in Figure 2.2.

The signal u is a continuous-time signal taking values for all $t \in \mathbb{R}$, while its sampled version $u_d(k) = u(kT_s)$ is a discrete sequence defined for integer values $k \in \mathbb{Z}$.
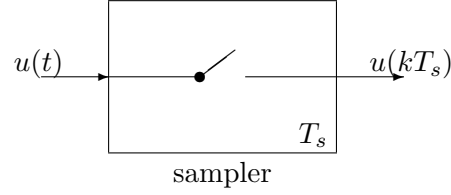
Figure 2.2: Sampling a continuous-time signal

As a first step the Fourier transforms of the continuous-time and discrete-time signals will be related to each other. Under the condition that $u_d(k) = u(kT_s)$ it follows from the Fourier transform expressions that

$$U_s(\omega) = \sum_{k=-\infty}^{\infty} u(kT_s)e^{-i\omega kT_s}. \tag{2.24}$$

By substituting the inverse Fourier transform relation (2.5) for $u(kT_s)$ it follows that

$$U_s(\omega) = \frac{1}{2\pi} \int_{-\pi}^{\pi} U(\xi) \sum_{k=-\infty}^{\infty} e^{i(\xi-\omega)kT_s} d\xi \tag{2.25}$$

$$= \frac{1}{2\pi} U(\omega) * \sum_{k=-\infty}^{\infty} e^{-i\omega kT_s} \tag{2.26}$$

where $*$ is the convolution operator, and $U(\omega)$ the Fourier transform of the underlying continuous-time signal.

Since $e^{-i\omega kT_s} = \mathcal{F}(\delta_c(t - kT_s))$[6], it follows from linearity of the Fourier Transform that $\sum_{k=-\infty}^{\infty} e^{-i\omega kT_s} = \mathcal{F}\left(\sum_{k=-\infty}^{\infty} \delta_c(t - kT_s)\right)$.

The summation of Dirac functions, being the so-called comb of Dirac,

$$p(t) := \sum_{k=-\infty}^{\infty} \delta_c(t - kT_s)$$

is written in its Fourier Series:

$$p(t) = \sum_{k=-\infty}^{\infty} c_k e^{ik\omega_s t}$$

with

$$c_k = \frac{1}{T_s} \int_{-T/2}^{T/2} p(t)e^{ik\omega_s t} dt = \frac{1}{T_s}.$$

Therefore $p(t) = \sum_{k=-\infty}^{\infty} \frac{1}{T_s} e^{ik\omega_s t}$ and since from (2.26) it follows that $U_s(\omega) = \mathcal{F}(u(t)\cdot p(t))$, the expression for $U_s(\omega)$ then becomes

$$U_s(\omega) = \int_{-\infty}^{\infty} u(t) \sum_{k=-\infty}^{\infty} \frac{1}{T_s} e^{ik\omega_s t} e^{-i\omega t} dt \tag{2.27}$$

$$= \frac{1}{T_s} \cdot \sum_{k=-\infty}^{\infty} U(\omega - k\omega_s). \tag{2.28}$$

---

[6] $\mathcal{F}$ is the Fourier transform.

Consequently, the Fourier transform U_s of the sampled signal is constructed as a shifted summation of the Fourier transform of the continuous-time signal u. Thus the Fourier transform U_s becomes periodic in the frequency domain with period $\omega_s = 2\pi/T_s$, being the (radial) sampling frequency. This mechanism is illustrated in Figure 2.3.
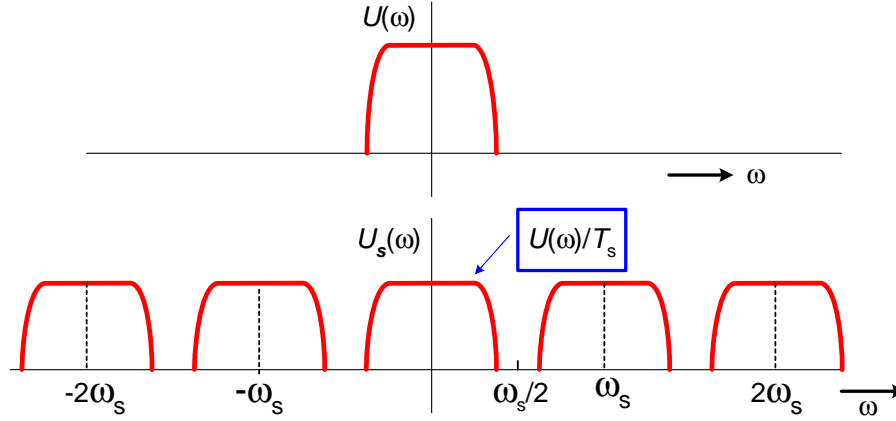
Figure 2.3: Fourier transform $U(\omega)$ of continuous-time signal and of its sampled version $U_s(\omega)$.

The fact that the Fourier transform of u becomes periodically repeated, directly points to the possibility for reconstructing the original signal $u(t)$ from its sampled version u_d. This is reflected in the theorem of Shannon which states that provided we have a continuous-time signal which satisfies:

$$U(\omega) = 0 \quad |\omega| > \omega_s/2, \tag{2.29}$$

we can exactly recover $U(\omega)$ from $U_s(\omega)$ by applying a low-pass filter that exactly extracts the frequency region $[-\omega_s/2, +\omega_s/2]$. The frequency $\omega_s/2$ is also denoted as the Nyquist-frequency ω_N.

When dealing with a signal $u(t)$ that is not band-limited, i.e. its Fourier transform does not satisfy (2.29), then the Fourier transform U_s is still constructed according to (2.28), but in that case the shifted versions of $U(\omega)$ will be folded on top of each other in $U_s(\omega)$. This effect is called *aliasing*. The main consequence of this is that low-pass filtering of u_s will not recover the original $U(\omega)$ anymore.

The basic consequence of the results in this section is that when sampling a continuous-time signal, one has to take care that the signal that is sampled does not contain any frequency components for frequencies higher than the Nyquist frequency $\omega_s/2$. Only in that case all information of the continuous-time signal can be recovered from the sampled signal. This leads to the standard use of -continuous-time- anti-aliasing filters before a sampling operation.

The exact reconstruction of a continuous-time signal from its sampled data, as referred to in the Shannon Theorem, can be done by using the inverse relation between U_s and U. Provided that the continuous-time signal is band-limited, as mentioned above, it follows that

$$U(\omega) = T_s \cdot U_s(\omega)H(\omega)$$

where $H(\omega)$ is the low-pass filter with cut-off frequency ω_N, determined by

$$H(\omega) = \begin{cases} 1 & -\omega_N \le \omega \le \omega_N \\ 0 & |\omega| > \omega_N \end{cases}$$

The standard Fourier transform-pair[7]

$$\frac{\omega_N}{\pi} \ sinc(\omega_N t) \quad \leftrightarrow \quad H(\omega) \tag{2.30}$$

can now be used to reconstruct the signal u according to [8]

$$u(t) = T_s \cdot \frac{\omega_N}{\pi} \ sinc(\omega_N t) * \mathcal{F}^{-1}\left(U_s(\omega)\right).$$

The inverse Fourier transform of $U_s(\omega)$, denoted by $u_s(t)$ needs to satisfy

$$U_s(\omega) = \int_{-\infty}^{\infty} u_s(t) e^{-i\omega t} dt$$

and with (2.24) it follows that

$$u_s(t) = \sum_{k=-\infty}^{\infty} u(t)\delta_c(t - kT_s).$$

Since $T_s \omega_N / \pi = 1$, $u(t)$ can be written as

$$u(t) = \int_{-\infty}^{\infty} sinc(\omega_N \tau) \cdot \sum_{k=-\infty}^{\infty} u(t-\tau)\delta_c(t - \tau - kT_s)d\tau \tag{2.31}$$

$$= \sum_{k=-\infty}^{\infty} u(kT_s) \cdot sinc(\omega_N(t - kT_s)). \tag{2.32}$$

This expression shows how the continuous-time signal u can be completely calculated by using only the sampled values $\{u(kT_s)\}_{k=-\infty,\cdots,\infty}$ of the original continuous-time signal. Note that it requires an infinite number of sampled data points to fully recover the underlying continuous-time signal, even if u takes values for only a finite time period. It also shows that the sinc-functions actually form a basis for the set of signals that are bandlimited in frequency.

Impulse sampling
The ideal sampling and reconstruction scheme discussed above is often referred to as impulse sampling and reconstruction. This is motivated by the fact that the Fourier transform U_s of the sampled signal can be interpreted as the (continuous-time) Fourier transform of the (continuous-time) signal

$$u_s(t) = \sum_{k=-\infty}^{\infty} u(t)\delta_c(t - kT_s).$$

This latter signal is related to the original continuous-time signal u through multiplication with a so-called comb of Dirac pulses. The related operations are schematically depicted in Figure 2.4.
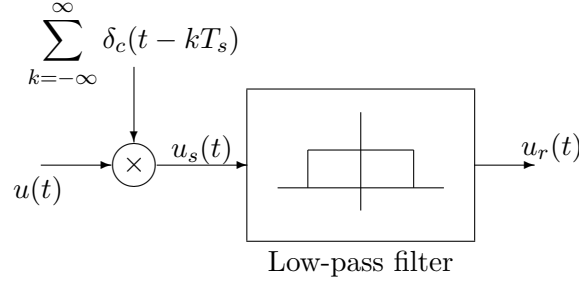
Figure 2.4: Impulse sampling and reconstruction

In this Figure the -artificial- signal $u_s(t)$ is a continuous-time signal that only takes values unequal to zero when $t = kT_s$ for integer values $k \in \mathbb{Z}$. At these values of t the signal becomes unbounded, being a δ-function with a weight that is equal to $u(kT_s)$.

Sampled-data signals and discrete-time signals
It is quite important to remark that discrete-time signals can be considered to be either originated from sampling continuous-time signals or simply as just a discrete-time sequence of numbers. In this section the first interpretation is followed, leading to the use of the sampling interval T_s in all expressions for Fourier transforms and the like. As a result, DTFT and spectral densities are formulated as functions of the continuous-time radial frequency ω. This allows a direct analysis of frequency properties of signals stated in terms that relate to their continuous-time equivalents.

However, in most situations of discrete-time signal analysis, the connection with a sampling mechanism is simply discarded, and indeed this is very well possible without loosing any information. When interpreting discrete-time signals just as discrete sequences of numbers, all results and notions introduced here still apply. This situation is best dealt with by introducing the variable transformation

$$\omega T_s \to \omega$$

which is actually equivalent to inserting $T_s = 1$.
Under this variable transformation all expressions for Fourier transforms and spectral densities are given in terms of the "discrete" radial frequency and the considered notions become periodic with a period length of 2π.

2.4.4 Discrete Fourier Transform

We now restrict attention for a moment to the situation of finite-time signals. For finite-time signals we have already mentioned the notation $U_N(\omega)$ as given in (2.19).
Actually this finite-time DTFT concerns the following transform pair:

$$U_N(\omega) = \sum_{k=0}^{N-1} u_d(k)e^{-i\omega kT_s}. \tag{2.33}$$

$$u_d(k) = \frac{1}{N}\sum_{\ell=0}^{N-1} U_N(\frac{\ell}{N}\omega_s)e^{i\frac{2\pi\ell}{N}k}. \tag{2.34}$$

---

[7] The *sinc* function is defined by $sinc(t) = \frac{sin(t)}{t}$ for $t \neq 0$, and $sinc(0) = 1$.
[8] $\mathcal{F}^{-1}$ is the inverse Fourier transform.

A verification of the validity of this transform pair is added in the appendix. Considering this transform pair, a few remarks have to be made.

- Note that while $U_N(\omega)$ takes its values on a continuous region of ω, only N discrete values of U_N are necessary for reconstructing the original signal u_d. These N discrete values are N points within one period of the periodic function $U_N(\omega)$.

- The DTFT is periodic with period $2\pi/T_s$.

- The sequence $\{U_N(\omega), \ \omega = \frac{\ell}{N}\omega_s, \ \ell = 0, \cdots N-1\}$ is defined as the *Discrete Fourier Transform* (DFT) of the signal $u_d(k), \ k = 0, \cdots N-1$. It is given by

$$U_N(\frac{\ell\omega_s}{N}) = \sum_{k=0}^{N-1} u_d(k)e^{-i\frac{2\pi\ell}{N}k}, \quad \ell = 0, \cdots N-1.$$

- The DFT constitutes a one-to-one mapping from an N-length sequence of time-domain samples to an N-length sequence of frequency-domain samples.

- The inverse DFT, defined by (2.34), also defines a time-domain sequence outside the interval $[0, N-1]$. Actually it induces a periodic extension of the original time-sequence $u_d(k)$, as the reconstructed signal (2.34) is periodic with period N.

- Because of reasons of symmetry, the DTFT satisfies

$$U_N(-\omega) = U_N(\omega)^*.$$

As a result the DTFT is completely determined by $U_N(\omega)$ for ω in the interval $\omega \in [0, \pi/T_s]$. This implies that the one-to-one mapping between time- and frequency domain actually takes place between N real-valued time-domain samples, and $N/2$ complex-valued frequency domain samples.

In very many situations discrete-time signals are being analyzed without taking account of the fact that they originate from sampled continuous-time signals. Similar to the situation of the previous section, this implies that in that case the expressions for the DTFT are used for $T_s = 1$:

$$U_N(\omega) \ = \ \sum_{k=0}^{N-1} u_d(k)e^{-i\omega k}. \tag{2.35}$$

$$u_d(k) \ = \ \frac{1}{N}\sum_{\ell=0}^{N-1} U_N(\frac{2\pi\ell}{N})e^{i\frac{2\pi\ell}{N}k}. \tag{2.36}$$

In many books on discrete-time signal processing this is the only situation that is considered. Discrete-time Fourier transforms, spectral densities, periodograms will then be considered generally over the frequency interval $\omega \in [0, \pi]$, being half of a single period of the corresponding periodic function in the frequency domain. Whenever we connect a sampling time to the discrete-time signal, then $\omega = \pi$ gets the interpretation of being equal to half of the (radial) sampling frequency.

Spectral properties of finite-time sampled signals

Similar to the situation of infinite-time signals, we can exploit Parseval's relation for quantifying the energy and power of finite-time (deterministic) sampled signals.

Consider the Discrete Fourier Transform as discussed above. Then

$$\sum_{k=0}^{N-1} u_d(k)^2 = \frac{1}{N} \sum_{k=0}^{N-1} |U_N(\frac{k\omega_s}{N})|^2 \tag{2.37}$$

$$\frac{1}{N} \sum_{k=0}^{N-1} u_d(k)^2 = \frac{1}{N} \sum_{k=0}^{N-1} |\frac{1}{\sqrt{N}} U_N(\frac{k\omega_s}{N})|^2. \tag{2.38}$$

It may be clear that the first expression is used for signals having the character of having finite energy, while the second expression is specially used for finite power signals. Note that over a finite time-interval this distinction is not really relevant as the operation of dividing by a finite N is just a matter of scaling. The main difference has to be found in the corresponding asymptotic analysis, when $N \to \infty$. Note that the expressions above actually are alternatives for the integral expressions for signal power as presented in Proposition 2.4.3. For finite time signals, there is no need to take the integral over the power spectral density as in (2.23); the power also results from summing the squared magnitude of the DFT over an equidistant frequency grid.

2.4.5   Stochastic processes

Completely in line with the sampling and reconstruction result for time-sequences the following result for stochastic processes can be formulated.

Sampling and reconstruction of stochastic processes

Consider a continuous-time stationary stochastic process $x(t)$, $t \in \mathbb{R}$, which is going to be sampled with a radial sampling frequency $\omega_s = \frac{2\pi}{T_s}$. As a result we obtain a stationary stochastic process $x(kT_s)$, $k \in \mathbb{Z}$.

Consider the sampling and reconstruction mechanism as illustrated in Figure 2.4 and defined in (2.32), given by

$$x_r(t) = \frac{\omega_N}{\pi} \sum_{k=-\infty}^{\infty} x(kT_s) sinc(\omega_N(t - kT_s)).$$

Note that x_r is again a stochastic process.

Let the power spectral density of $x(t)$ be given by $\Phi_x(\omega)$.

If

$$\Phi_x(\omega) = 0 \quad \text{for } |\omega| > \omega_s/2 \tag{2.39}$$

then the reconstructed process x_r satisfies:

$$E[x(t) - x_r(t)]^2 = 0.$$

For more details see e.g. Shanmugan and Breipohl (1988).

Next correlation functions and spectral densities will be considered, assuming the stochastic process to be zero-mean.

Correlation functions and spectral densities

Correlation functions of the discrete-time sampled stochastic process are related to the corresponding properties of the continuous-time process.

Consider the correlation function $R_x(\tau)$, $\tau \in \mathbb{R}$ of the continuous-time process. It can simply be verified that the correlation function of the discrete-time process,

$$R_{x_d}(k) := Ex(\ell T_s)x((\ell - k)T_s)$$

satisfies

$$R_{x_d}(k) = R_x(kT_s)$$

where R_x is the correlation function of the continuous-time process. The discrete-time correlation function is simply a sampled version of the continuous-time one.

The power spectral density of x_d is defined by the DTFT of R_{x_d} according to:

$$\Phi_{x_d}(\omega) = \sum_{k=-\infty}^{\infty} R_{x_d}(k)e^{-i\omega k T_s} \tag{2.40}$$

$$R_{x_d}(k) = \frac{T_s}{2\pi} \int_{2\pi/T_s} \Phi_{x_d}(\omega)e^{i\omega k T_s}d\omega. \tag{2.41}$$

As a consequence the mean power of the sampled signal, $Ex_d(k)^2 = Ex(kT_s)^2$ satisfies:

$$Ex_d(k)^2 = R_{x_d}(0) = \frac{T_s}{2\pi} \int_{2\pi/T_s} \Phi_{x_d}(\omega)d\omega. \tag{2.42}$$

As R_{x_d} is a sampled version of the continuous-time correlation function R_x, it follows directly from the analysis in the previous subsections that provided the condition (2.39) is satisfied, the spectral density $\Phi_{x_d}(\omega)$ is simply a periodic extension of the continuous-time spectral density $\Phi_x(\omega)$ with period length ω_s.

Similar to the situation of deterministic signals, discrete-time stochastic processes will very often be considered, regardless of the fact whether the random variables are obtained by sampling a continuous-time stochastic process or not. In that situation the sampling interval T_s does not play a role and the respective formulas for DTFT and its inverse are utilized with $T_s = 1$:

$$\Phi_{x_d}(\omega) = \sum_{k=-\infty}^{\infty} R_{x_d}(k)e^{-i\omega k} \tag{2.43}$$

$$R_{x_d}(k) = \frac{1}{2\pi} \int_{-\pi}^{\pi} \Phi_{x_d}(\omega)e^{i\omega k}d\omega. \tag{2.44}$$

$$Ex_d(k)^2 = \frac{1}{2\pi} \int_{-\pi}^{\pi} \Phi_{x_d}(\omega)d\omega. \tag{2.45}$$

There has already been discussed that we can analyze a realization of a stochastic process x in two different ways: either as a deterministic finite-power signal where its finite-time power spectrum is governed by the periodogram

$$\frac{1}{N}|X_N(\omega)|^2$$

which according to the proof of Proposition 2.4.3 leads to the expression

$$\Phi_x(\omega) = \sum_{\tau=-\infty}^{\infty} \hat{R}_x^N(\tau)e^{-i\omega\tau};$$

or as a realization of a stochastic process with a power spectrum induced by the characteristics of the stochastic process, i.e. with $\Phi_x(\omega)$ given by

$$\Phi_x(\omega) = \sum_{\tau=-\infty}^{\infty} R_x(\tau)e^{-i\omega\tau}.$$

In the former situation, it is not trivial that the spectral properties, i.c. the periodogram, converge for $N \to \infty$. However it can be verified that in this situation under minor conditions on the stochastic process,

$$\lim_{N\to\infty} E \frac{1}{N}|X_N(\omega)|^2 = \Phi_x(\omega). \tag{2.46}$$

For more details see Ljung (1999; 2D.3, p. 51).

2.5   Quasi-stationary processes

Until now we have analyzed signals that originate either from some kind of deterministic mechanism, or as a realization of a stochastic process. In practical engineering situations of analyzing and processing measurement signals we have to face the situation that we have to deal with both types of signals at the same time. For instance, consider the situation that we excite a process with a user-designed signal, like e.g. a sum of sinusoids, a step function etc., and we observe the output signal that is produced by the system as a response to this input signal.
The observation of the output signal will generally not by exact, i.e. the measured output signal will be contaminated by noise. The typical behaviour of a disturbance or noise signal is that it is (a) not measurable and (b) changes with different realizations, i.e. when the experiment is repeated a different disturbance signal will be present but probably with the same statistical properties.
As a consequence one will frequently have to deal with signals of the form

$$y(k) = w(k) + v(k) \quad k \in \mathbb{Z}$$

where $w(k)$ is some deterministic signal, being the result of a measurable signal that is processed through a (linear) system, and $v(k)$ being a realization of a zero-mean stationary stochastic process.

In order to analyze the signal $y(k)$, e.g. for determining its frequency content, or the distribution of its energy/power over frequency, we have to determine what its principal characteristics are.
If we consider $y(k)$ to be a stochastic process, then this process will generally be nonstationary. This can be understood by realizing that

$$Ey(k) = w(k),$$

caused by the fact that $w(k)$ is nonstochastic.
If we consider $y(k)$ to be a deterministic finite-power signal, we neglect the fact that we are only dealing with one single realization of a possible measurement, while a second realization may have different properties. If we can take account – to some extent – of the statistical
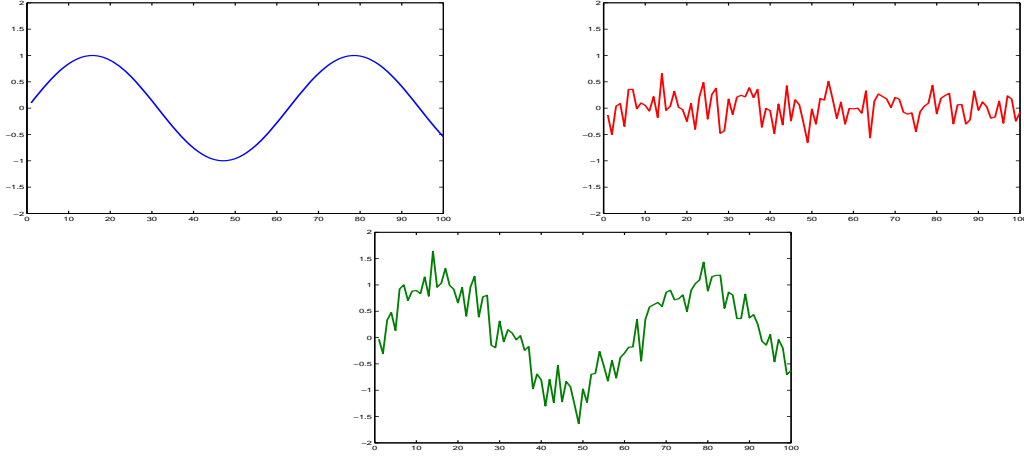
Figure 2.5: Example of a quasi-stationary process; deterministic sinusoid signal w (left upper); stochastic noise disturbance v (right upper); summation $w + v$ (lower).

properties of the signal we are able to draw conclusions on the on-average behaviour of signal processing and estimation methods.

For dealing with these types of signals in a way that facilitates its analysis, a generalized expectation operation is introduced, denoted by $\bar{E}$[9] being defined by

$$\bar{E}y(k) = \lim_{N \to \infty} \frac{1}{N} \sum_{k=0}^{N-1} Ey(k).$$

This generalized expectation operation combines a statistical expectation with a time-averaging. Note the two special cases:

- If $y(k)$ is a deterministic sequence then

$$\bar{E}y(k) = \lim_{N \to \infty} \frac{1}{N} \sum_{k=0}^{N-1} y(k);$$

- If $y(k)$ is a stationary stochastic process then

$$\bar{E}y(k) = Ey(k).$$

Using this generalized expectation operator, the following notion of quasi-stationarity is defined.

Definition 2.5.1 *A stochastic process or deterministic sequence $\{u(k)\}$ is called quasi-stationary if there exist $c_1, c_2 \in \mathbb{R}$ such that:*

(a) $|Eu(k)| < c_1$ for all k, and

(b) $R_u(\tau) := \bar{E}[u(k)u(k-\tau)]$ satisfies $|R_u(\tau)| < c_2$ for all τ.

---

[9]Note that the notation used can be slightly misleading. The expression $\bar{E}y(k)$ is not a function of k anymore, since an averaging over k is involved.

Note again that the expectation E is taken over the stochastic components in the signal, while the time-averaging is taken over the deterministic components. For a deterministic sequence to be quasi-stationary it has to be bounded, in the sense that the limit

$$\lim_{N\to\infty} \frac{1}{N} \sum_{k=0}^{N-1} u(k)u(k-\tau)$$

is finite for all τ.

For a zero-mean stationary stochastic process, the conditions as mentioned in the definition are automatically satisfied, as in that case $Eu(k) = 0$, and $R_u(\tau)$ is the auto-correlation function of the process.

Similar to the situation of stationary stochastic processes, two processes/signals y and u will be called *jointly quasi-stationary* if they are both quasi-stationary and if $R_{yu}(\tau) := \bar{E}[y(k)u(k-\tau)]$ exists and is finite for all τ.

With slight abuse of notation, the following terms will be used:

- *Correlation function*:
$$R_y(\tau) := \bar{E}[y(k)y(k-\tau)]$$

- *Cross-correlation function*:
$$R_{yu}(\tau) := \bar{E}[y(k)u(k-\tau)]$$

- *Power spectral density or power spectrum*:
$$\Phi_y(\omega) := \sum_{\tau=-\infty}^{\infty} R_y(\tau)e^{-i\omega\tau}$$

- *Power cross-spectral density or cross spectrum*:
$$\Phi_{yu}(\omega) := \sum_{\tau=-\infty}^{\infty} R_{yu}(\tau)e^{-i\omega\tau}$$

Using these respective terms, one has to realize that they are formally correct only in the case that we are dealing with a stationary stochastic process.

The generalized expectation operator also induces a generalized notion of power of a signal:

$$\mathcal{P}_y := \bar{E}[y^2(k)].$$

In the case of a stationary stochastic process this equals the ensemble-average power of the process, while for a deterministic sequence it reflects the time-average power of the signal. It follows directly from the above relations and the inverse DFT that

$$\bar{E}[y^2(k)] = \frac{1}{2\pi} \int_{-\pi}^{\pi} \Phi_y(\omega)d\omega,$$

and thus the power spectral density $\Phi_y(\omega)$ clearly reflects the distribution of the power of y over frequency.

Relating this notion of power of a quasi-stationary signal to the previously used notion of power of a deterministic finite-power signal (the latter being defined on the basis of the periodogram), it appears that for y being quasi-stationary:

$$E \; \frac{1}{N}|Y_N(\omega)|^2 \to_w \Phi_y(\omega) \quad \text{for } N \to \infty,$$

meaning that the convergence is weakly, i.e. it holds under some restrictive conditions. For more details on this see Ljung (1999, p.38,39).

Two quasi-stationary signals are called uncorrelated if their cross-correlation function equals zero.

Example 2.5.2 (Uncorrelated quasi-stationary signals) Consider the signal

$$y(k) = w(k) + v(k)$$

with $w(k)$ a quasi-stationary deterministic signal with spectrum $\Phi_w(\omega)$ and $v(k)$ a zero-mean stationary stochastic process with spectrum $\Phi_v(\omega)$. Then

(a) $\bar{E}[w(k)v(k-\tau)] = \lim_{N\to\infty} \frac{1}{N} \sum_{k=0}^{N-1} w(k)Ev(k-\tau) = 0$, as v is zero-mean. So by definition w and v are uncorrelated.

(b) As a direct result it follows that $\Phi_y(\omega) = \Phi_w(\omega) + \Phi_v(\omega)$.

Why quasi-stationary processes/signals
When taking signal measurements of physical quantities, one can argue if it really matters whether we consider the measured signals as general finite-power signals whose behaviour in time tells us everything about the underlying phenomenon, or whether we consider the measured signal as one realization of some underlying stochastic process. For evaluation of the frequency content of the measured signal, and for determining the distribution of its energy/power over frequency the framework of quasi-stationary signals is not really necessary.
The need for a notion as quasi-stationarity is much more motivated from a point of view that considers the *analysis* of estimation and signal processing algorithms. In terms of estimation problems, for instance, we would like to estimate underlying phenomena that generate or greatly influence the measured signals. From a dynamical system we would like to be able to identify the dynamic properties of the system from (noise-disturbed) measurements of the external input and output signals. The framework of quasi-stationary signals allows us to draw conclusions on the behaviour of identification methods, concerning biasedness, consistency etcetera (the on-average behaviour), while only one single measurement sequence of the data is available.

2.6 Discrete-time systems analysis

2.6.1 Sampling continuous-time systems

General band-limited signals
Suppose we have given a continuous-time system determined by the input/output relation

$$y(t) = G_c(p)u(t),$$

where $G_c(s)$ is a rational transfer function that specifies a linear, time-invariant, finite-dimensional system.

If the input and output signals related to this system are sampled with a radial sampling frequency ω_s, the first question to be answered is: Can we find a discrete-time systems relation between the sampled signals $u(kT_s)$ and $y(kT_s)$?

If the continuous-time signals u and y are band-limited, the sampling and reconstruction analysis as presented in section 2.4.3 can be used to analyze the above question. Under the condition that $U(\omega) = 0$ for $|\omega| > \omega_s/2$, the use of the reconstruction equation for u (2.32) leads to (see the Appendix for a detailed analysis)

$$y(kT_s) \quad = \quad \sum_{\ell=-\infty}^{\infty} g_d(\ell)u((k-\ell)T_s) \tag{2.47}$$

$$\text{with} \quad g_d(\ell) \quad = \quad \int_{-\infty}^{\infty} g(\ell T_s - \tau)sinc(\frac{\omega_s \tau}{2})d\tau. \tag{2.48}$$

This shows two important things. Firstly the equivalent discrete-time system will in general not be causal, i.e. $g_d(\ell) \neq 0$ for $\ell < 0$; secondly it will generally not have a finite-dimensional representation, which means that the discrete-time system $G_d(z) = \sum_{k=-\infty}^{\infty} g_d(k)z^{-k}$ can not simply be written as a rational transfer function

$$G_d(z) = \frac{b_0 z^{n_b} + \cdots b_{n_b}}{z^{n_a} + a_1 z^{n-1} + \cdots + a_{n_a}}. \tag{2.49}$$

The above two aspects show the shortcomings of this way of arriving at a discrete-time representation of the concerned system. One of the reasons for these difficulties is that the sampling and reconstruction result of section 2.4.3 for band-limited signals requires an infinite number of data for reconstruction of the continuous-time signal.

Zero-order hold equivalence between continuous-time and discrete-time systems
A practical alternative for the analysis given above can be found by realizing that in many computer control applications inputs of dynamical systems are generated by process computers, providing discrete-time input signals that through digital-to-analog (D/A) conversion are kept constant in between two sampling instants. This implies that we are dealing with continuous-time signals that are piecewise constant, i.e.

$$u(t) = u(kT_s) \ \text{ for } kT_s \leq t < (k+1)T_s.$$

Now one can again raise the question whether we can formulate a discrete-time system relation between the sampled-data inputs and outputs, given a continuous-time system $y(t) = G_c(p)u(t)$.
Writing

$$y(kT_s) \quad = \quad \int_{\tau=0}^{\infty} g_c(\tau)u(kT_s - \tau)d\tau \tag{2.50}$$

$$= \quad \sum_{\ell=1}^{\infty} \int_{\tau=(\ell-1)T_s}^{\ell T_s} g_c(\tau)u(kT_s - \tau)d\tau \tag{2.51}$$

$$= \quad \sum_{\ell=1}^{\infty} g_d(\ell)u_d(k-\ell) \tag{2.52}$$

with $u_d(k) = u(kT_s)$ and

$$g_d(\ell) = \int_{\tau=(\ell-1)T_s}^{\ell T_s} g_c(\tau)d\tau. \tag{2.53}$$

As a result we can write the equivalent discrete-time system as:

$$y_d(k) = \sum_{\ell=1}^{\infty} g_d(\ell)u_d(k-\ell). \tag{2.54}$$

This equivalent discrete-time system appears to be causal ($g_d(k) = 0$, $k < 0$), and it can also be shown to have a finite-dimensional representation. This latter phenomenon can be characterized easily when using state space representations of both continuous-time and discrete-time systems:

Given a continuous-time system $G(s)$ being represented by the state space representation:

$$\dot{x}(t) = A_c x(t) + B_c u(t) \tag{2.55}$$
$$y(t) = Cx(t) + Du(t). \tag{2.56}$$

Then the zero order hold equivalent discrete-time system for a sampling period T_s is given by

$$x_d(k+1) = A_d x_d(k) + B_d u_d(k) \tag{2.57}$$
$$y_d(k) = Cx_d(k) + Du_d(k) \tag{2.58}$$

with the usual notation for u_d, y_d and x_d, and

$$A_d = e^{A_c T_s} \tag{2.59}$$
$$B_d = \int_0^{T_s} e^{A_c \tau}d\tau \cdot B_c. \tag{2.60}$$

If the continuous-time system has state-space dimension n, then the equivalent discrete-time system has the same state-space dimension.

For more details see e.g. the textbook by Åström and Wittenmark (1984).

Frequency domain interpretation

A frequency domain formulation of the sampled system can be obtained by applying a DTFT to (2.54). For u being a deterministic signal and under the assumption of zero initial conditions (i.e. $u(t) = 0$ for $t < 0$)it follows that

$$Y(\omega) = G_d(e^{i\omega T_s})U(\omega)$$

with $G_d(e^{i\omega T_s}) = \sum_{k=-\infty}^{\infty} g_d(k)e^{-i\omega k T_s}$ the DTFT of g_d. The notation for the argument of G_d has been chosen different from the argument of U and Y; this is done to allow a simple relation with the z-transform of g_d, as indicated in the next subsection.

Similar to the situation of sampled-data signal spectra, the frequency response $G_d(e^{i\omega T_s})$ of the sampled-data system is periodic as a function of ω with period $2\pi/T_s = \omega_s$.

2.6.2   Discrete-time systems

General notation

For specifying discrete-time systems relations between input and output signals two shift operators will be used; the *forward shift operator q*:

$$qu_d(k) = u_d(k+1)$$

and the *backward shift operator* q^{-1}:

$$q^{-1}u_d(k) = u_d(k-1)$$

Using these operators it follows that

$$y_d(k) = \sum_{\ell=0}^{\infty} g(\ell)(q^{-\ell}u_d(k)) = G(q)u_d(k)$$

with

$$G(q) = \sum_{\ell=0}^{\infty} g(\ell)q^{-\ell}.$$

In the notation $g(k)$ the subscript d is discarded for simplicity of notation. The sequence $\{g(k)\}_{k=0,1,...}$ is the *pulse response* of the system. With slight abuse of notation, we will also refer to $G(q)$ as the *transfer function* of the system. Strictly speaking, however, the transfer function is defined by the function $G(z)$:

$$G(z) = \sum_{k=0}^{\infty} g(k)z^{-k} \tag{2.61}$$

where z is a complex indeterminate.

If an input signal with bounded amplitude is chosen, then an output with bounded amplitude results, provided that the system is (bounded input, bounded output) BIBO-stable. This property is reflected by the condition that

$$\sum_{k=0}^{\infty} |g(k)| < \infty. \tag{2.62}$$

This condition means that the series expansion (2.61) is convergent for $|z| \geq 1$, which implies that $G(z)$ is analytic (i.e. has no poles) in the region given by $|z| \geq 1$, i.e. on and outside the unit circle in the complex plain.

Additionaly a discrete-time system will be called *monic* if $g(0) = 1$.

Frequency response and Bode plots

Analogously to the situation of continuous-time system, the frequency response of a discrete-time system is determined by the output of the system when excited with a sinusoidal input signal.

Consider the signal:

$$u(k) = cos(\omega k) = Re\{e^{i\omega k}\}.$$

The output of the discrete-time system is given by

$$y(k) \quad = \quad \sum_{\ell=0}^{\infty} g(\ell)u(k-\ell) = Re\{e^{i\omega k}\sum_{\ell=0}^{\infty} g(\ell)e^{-i\omega\ell}\} \tag{2.63}$$

$$= \quad Re\{e^{i\omega k}G(e^{i\omega})\}. \tag{2.64}$$

Consequently

$$y(k) = |G(e^{i\omega})| \cdot cos(\omega k + \phi) \tag{2.65}$$

with $\phi = \arg[G(e^{i\omega})]$.

The complex-valued function $G(e^{i\omega})$ is referred to as the *frequency response* of the discrete-time system. It evaluates the transfer function in the complex plain over the unit circle $z = e^{i\omega}$. Note the difference with a continuous-time system, where the frequency response is reflected by the evaluation of $G(s)$ over the imaginary axis $s = i\omega$.
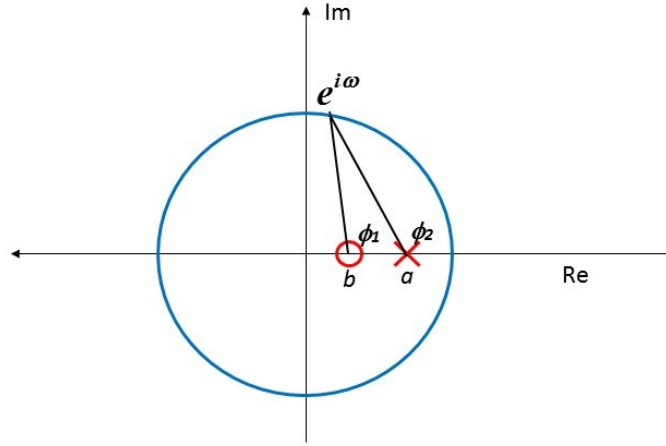
Figure 2.6: Zero/pole location and evaluation of frequency response of first order discrete-time system

For discrete-time systems with a real-valued pulse response (and thus real-valued coefficients) it holds that $G(e^{-i\omega}) = G(e^{i\omega})^*$ and so for reasons of symmetry, full information on the frequency response of the system is obtained by $G(e^{i\omega})$ for $\omega \in [0, \pi]$. In Figure 2.6 this is illustrated for a first order system, given by

$$G(z) = \frac{z-b}{z-a}. \tag{2.66}$$

By writing the expression

$$G(e^{i\omega}) = \frac{e^{i\omega}-b}{e^{i\omega}-a} \tag{2.67}$$

it follows that

$$|G(e^{i\omega})| \quad = \quad \frac{|e^{i\omega}-b|}{|e^{i\omega}-a|} \quad \text{and} \tag{2.68}$$

$$\arg G(e^{i\omega}) \quad = \quad \arg(e^{i\omega}-b) - \arg(e^{i\omega}-a). \tag{2.69}$$

The first equation generates the amplitude Bode plot, whereas the second defines the phase Bode plot. For the considered first order system these Bode plots are given in Figure 2.7, where the values $b = 0.3$ and $a = 0.8$ are chosen. Note that the frequency function is given for frequencies up to $\omega = \pi$.
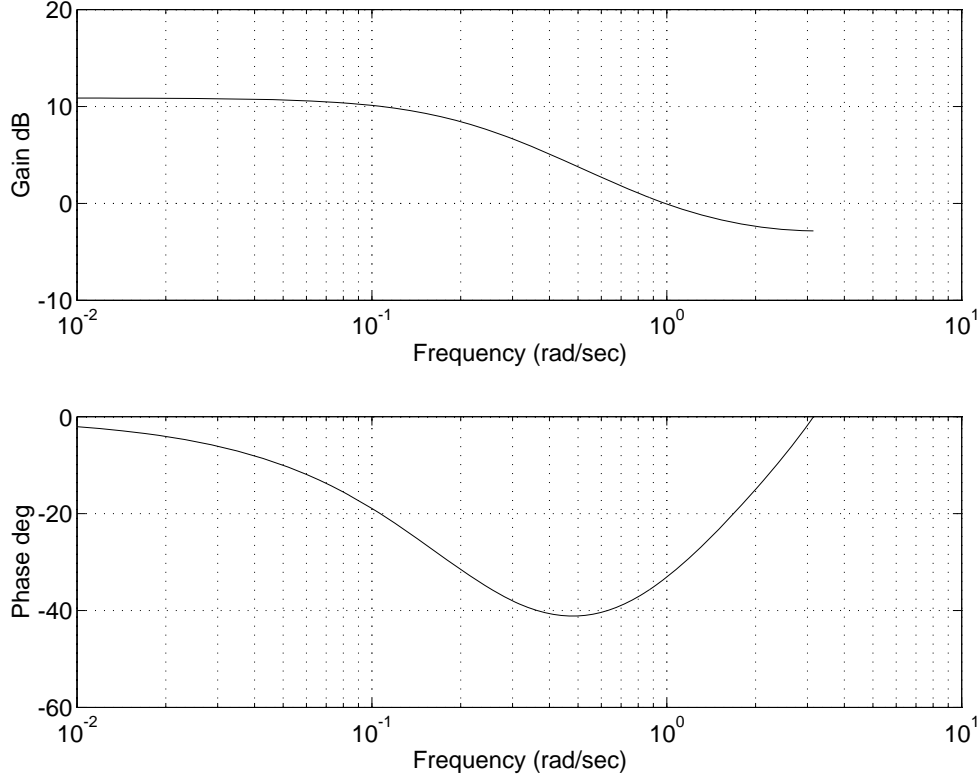
Figure 2.7: Bode-amplitude and Bode-phase plot of first order discrete-time system

In this discrete-time case, unlike the situation in the continuous-time case, there is no asymptotic point in frequency where ω tends to. Note that in the discrete-time case the phase contribution of every (real) zero varies between 0^0 and $+180^0$, while the contribution of each (real) pole varies between 0^0 and -180^0. For a complex conjugate pair and zeros/poles it can simply be verified that the contribution to the phase in $\omega = \pi$ is given by respectively $+360^0$ and -360^0.

Signal properties processed by discrete-time systems.
Similar to the situation of continuous-time systems, there exist simple relations between the correlation functions and the spectral densities of the input and output signals of a dynamical system.

Consider an input/output system $y(k) = G(q)u(k)$, and u and y quasi-stationary, then

$$R_{yu}(k) = G(q)R_u(k) \tag{2.70}$$

$$R_{yu}(k) = g(k) \star R_u(k). \tag{2.71}$$
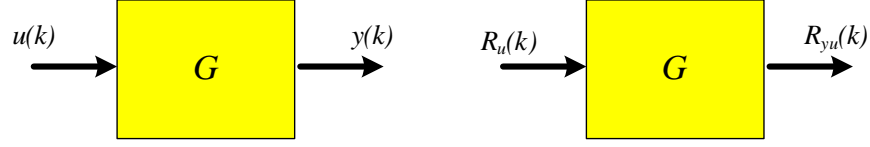
Figure 2.8: Cross-correlation function of two signals that are related through a dynamical system G.

The direct consequence for the cross-spectral density function is:

$$\Phi_{yu}(\omega) = G(e^{i\omega})\Phi_u(\omega). \tag{2.72}$$

For the cross-correlation $R_{uy}(k)$ it can be verified that

$$R_{uy}(k) = G^*(q)R_u(k) \tag{2.73}$$

$$R_{uy}(k) = g(-k) \star R_u(k). \tag{2.74}$$

and consequently

$$\Phi_{uy}(\omega) = G^*(e^{i\omega})\Phi_u(\omega) = G(e^{-i\omega})\Phi_u(\omega). \tag{2.75}$$
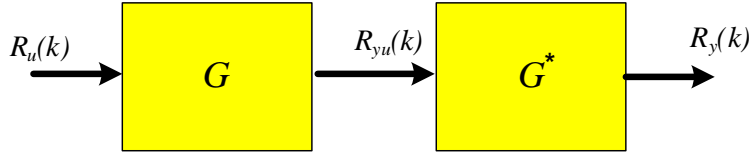
Figure 2.9: Auto-correlation function of two signals that are related through a dynamical system G.

The combination of the above results is shown in Figure 2.9, and lead to the expressions:

$$R_y(k) = g(-k) \star g(k) \star R_u(k) \tag{2.76}$$

$$\Phi_y(\omega) = G(e^{-i\omega})G(e^{i\omega})\Phi_u(\omega) = |G(e^{i\omega})|^2 \cdot \Phi_u(\omega). \tag{2.77}$$
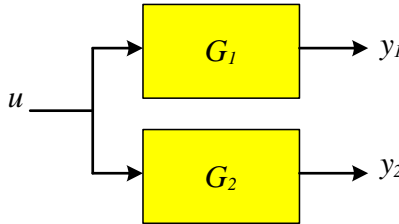
Figure 2.10: Two signals y_1, y_2 originating from the same source signal u.

If there are two dynamical systems G_1, G_2 as depicted in Figure 2.10, that generate y_1, y_2, then application of the formulas above lead to the results:

$$y_2 = G_2 G_1^{-1} y_1$$

and therefore

$$
\begin{align}
\Phi_{y_2 y_1} &= G_2 G_1^{-1} \Phi_{y_1} \tag{2.78} \\
&= G_2 G_1^{-1} |G_1|^2 \Phi_u = G_2 G_1^{-1} [G_1 G_1^*] \Phi_u \tag{2.79} \\
&= G_2 G_1^* \Phi_u \tag{2.80}
\end{align}
$$

so that

$$
\Phi_{y_2 y_1}(\omega) = G_2(e^{i\omega}) G_1(e^{-i\omega}) \Phi_u(\omega).
$$

If u is a deterministic sequence for which the DTFT exists, then additionally, under the assumption of zero initial conditions (i.e. $u(t) = 0$, $t < 0$):

- $Y(\omega) = G(e^{i\omega}) U(\omega)$.

2.7　Relevant MATLAB-commands

2.7.1　DFT and Inverse DFT

Discrete Fourier Transform and Inverse Discrete Fourier Transform are obtained by the MATLAB-commands `fft` and `ifft`.

```
y = fft(x)
```

A DFT is calculated for a discrete-time signal present in vector x with length N according to

$$
X_N(k) = \sum_{j=1}^{N} x(j) e^{-i \frac{2\pi}{N}(j-1)(k-1)} \tag{2.81}
$$

The result $\{X_N(k)\}_{k=1,\cdots,N}$ is stored in vector y.
The execution time of this instruction is fastest if N is a power of 2 because in that case a radix-2 Fast Fourier Transform algorithm is used.

```
x = ifft(y)
```

An inverse DFT is calculated for a discrete-frequency sequence present in vector y with length N according to

$$
x(k) = \frac{1}{N} \sum_{j=1}^{N} y(j) e^{i \frac{2\pi}{N}(j-1)(k-1)}. \tag{2.82}
$$

Here also holds that the execution time is fastest if N is a power of 2.

2.7.2 Conversion between continuous-time and discrete-time systems

There are several possibilities for converting continuous-time and discrete-time systems into one another.

```
[SYSD] = c2d(SYSC,$T_s$,Method)
```

Continuous-to-discrete conversion. Given a continuous-time system SYSC, and a sampling time T_s, an equivalent discrete-time system SYSD is constructed with any of the available methods; Method = 'ZOH' refers to the zero-order hold equivalent.

```
[SYSC] = d2c(SYSD,Method)
```

Discrete-to-continuous conversion. Given discrete-time system SYSD an equivalent continuous-time system SYSC is constructed. Method = 'ZOH' refers to the zero-order hold equivalent.

Besides the zero-order hold equivalence, there are more possibilities for converting continuous-time and discrete-time systems.

Frequency responses of discrete-time systems can be obtained by the commands `bode` and `freqresp`.

2.8   Overview of Fourier Transforms

	Transform	Inverse transform
CTFT	$U(\omega) = \displaystyle\int_{-\infty}^{\infty} u(t)e^{-i\omega t}dt$	$u(t) = \dfrac{1}{2\pi}\displaystyle\int_{-\infty}^{\infty} U(\omega)e^{i\omega t}d\omega$
DTFT	$U_s(\omega) := \displaystyle\sum_{k=-\infty}^{\infty} u_d(k)e^{-i\omega k T_s}$	$u_d(k) = \dfrac{T_s}{2\pi}\displaystyle\int_{2\pi/T_s} U_s(\omega)e^{i\omega k T_s}d\omega$
DTFT, $T_s = 1$	$U_s(\omega) := \displaystyle\sum_{k=-\infty}^{\infty} u_d(k)e^{-i\omega k}$	$u_d(k) = \dfrac{1}{2\pi}\displaystyle\int_{2\pi} U_s(\omega)e^{i\omega k}d\omega$
DFT	$U_N(\dfrac{\ell\omega_s}{N}) = \displaystyle\sum_{k=0}^{N-1} u_d(k)e^{-i\frac{2\pi\ell}{N}k}$	$u_d(k) = \dfrac{1}{N}\displaystyle\sum_{\ell=0}^{N-1} U_N(\dfrac{\ell\omega_s}{N})e^{i\frac{2\pi\ell}{N}k}$

Table 2.1: Summary of Fourier transforms; CTFT = Continuous-Time Fourier Transform; DTFT = Discrete-Time Fourier Transform; DFT = Discrete Fourier-Transform

2.9   Summary

In this section a brief review and summary of the basic concepts in signals and systems analysis has been presented and the appropriate notation has been set. In order to deal with signals that are composed of both a deterministic and a stochastic component (as will happen in many engineering applications of measured signals) the notion of quasi-stationary signals has been discussed. For a detailed treatment of the fundamentals the reader is referred to more specialized textbooks, as listed in the bibliography.

Appendix

Proof of (2.24); DTFT of periodic signal.
Combining the two expressions:

$$u_d(k) = \frac{T_s}{2\pi} \int_{\frac{2\pi}{T_s}} U_s(\omega) e^{i\omega k T_s} d\omega \tag{2A.1}$$

$$u_d(k) = \sum_{\ell=0}^{N_0-1} a_\ell e^{i\frac{2\pi}{N_0}\ell k}. \tag{2A.2}$$

As a result, in a single period of the ω-domain (of length $T_s/2\pi$):

$$\frac{T_s}{2\pi} \cdot U_s(\omega) = \sum_{\ell=0}^{N_0-1} a_\ell \delta_c(\omega T_s - \frac{2\pi\ell}{N_0})$$

showing that

$$U_s(\omega) = \frac{2\pi}{T_s} \cdot \sum_{\ell=0}^{N_0-1} a_\ell \delta_c(\omega - \omega_0 \ell).$$

Extending the above expression to the full domain of ω this leads to

$$U_s(\omega) = \frac{2\pi}{T_s} \cdot \sum_{\ell=-\infty}^{\infty} a_\ell \delta_c(\omega - \omega_0 \ell).$$

Proof of (2.48) - Sampling continuous-time systems
Starting from

$$y(t) = \int_{\infty}^{\infty} g_c(\tau) u(t - \tau) d\tau$$

and using the reconstruction formula (2.32) for $u(t)$ it follows that

$$y(t) = \int_{-\infty}^{\infty} g_c(\tau) \sum_{m=-\infty}^{\infty} u(mT_s) sinc(\omega_N(t - \tau - mT_s)) d\tau.$$

Evaluating this expression for $t = kT_s$ and replacing m by $m = k - \ell$ delivers:

$$y(kT_s) = \int_{-\infty}^{\infty} g_c(\tau) \sum_{\ell=-\infty}^{\infty} u((k - \ell)T_s) sinc(\omega_N(\ell T_s - \tau)) d\tau \tag{2A.3}$$

$$= \sum_{\ell=-\infty}^{\infty} g_d(\ell) u((k - \ell)T_s) \tag{2A.4}$$

with

$$g_d(\ell) = \int_{-\infty}^{\infty} g_c(\tau) sinc(\omega_N(\ell T_s - \tau)) d\tau \tag{2A.5}$$

$$= \int_{-\infty}^{\infty} g_c(\ell T_s - \tau) sinc(\omega_N \tau) d\tau \tag{2A.6}$$

where the latter equation follows from the fact that the integral expression is a convolution, which can be rewritten by change of variables $\tau \rightarrow \ell T_s - \tau$.

Lemma 2A.1 *Let $k \in \mathbb{Z}$ and $N \in \mathbb{N}$. Then*

$$\sum_{\ell=0}^{N-1} e^{i\frac{2\pi\ell}{N}k} = N \quad for\ k = 0,$$

$$= 0 \quad for\ k \neq 0.$$

Proof: The proof follows simply by applying the finite sum formula: $\sum_{\ell=0}^{N-1} a^\ell = \frac{1-a^N}{1-a}$ for $a \in \mathbb{C}$, $a \neq 1$. $\qquad\qquad\qquad\qquad\qquad\qquad\qquad\qquad\qquad\qquad\qquad\qquad\qquad \square$

Example 2A.2 (DTFT of a periodic signal) *Let $u(t)$ be a periodic signal with length $N = rN_0$ and basic period N_0. Then*

$$U_N(\omega) = \sum_{t=0}^{rN_0-1} u(t)e^{-i\omega t}$$

$$= \sum_{\ell=1}^{r} \sum_{m=0}^{N_0-1} u(m)e^{-i\omega[(\ell-1)N_0+m]}$$

$$= \sum_{\ell=1}^{r} e^{-i\omega(\ell-1)N_0} \sum_{m=0}^{N_0-1} u(m)e^{-i\omega m}. \tag{2A.7}$$

Since with Lemma 2A.1

$$\sum_{\ell=1}^{r} e^{-i\omega(\ell-1)N_0} = r \quad for\ \omega = \frac{2\pi k}{N_0},\ k = 1, \cdots N_0,$$

$$= 0 \quad for\ \omega = \frac{2\pi j}{N},\ j = 1, \cdots, N; j \neq r, 2r, \cdots N_0 r,$$

it follows that

$$U_N(\omega) = r \cdot U_{N_0}(\omega), \tag{2A.8}$$

for $\omega = \frac{2\pi k}{N_0}$, $k = 1, \cdots N_0$, where $U_{N_0}(\omega)$ is the DTFT of u over one period of the signal, and $U_N(\omega)$ will be 0 at frequencies outside this grid but being a member of the grid $\{\omega = \frac{2\pi k}{N}, k = 1, \cdots N\}$.
For $N \rightarrow \infty$ and N_0 finite, it follows that $U_N(\omega) = 0$ almost everywhere, except in the frequencies $\omega = \frac{2\pi k}{N_0}$ where the DTFT grows with r.

Proof of Proposition 2.4.3.

Starting from $\frac{1}{N} \sum_{k=0}^{N-1} u_d(k)^2 = \hat{R}_u^N(0)$ and using the result of Lemma 3.3.1 that $\frac{1}{N}|U_N(\omega)|^2$ is the DTFT of $\hat{R}_u^N(\tau)$, it follows that

$$\hat{R}_u^N(\tau) = \frac{T_s}{2\pi} \int_{-\pi/T_s}^{\pi/T_s} \frac{1}{N}|U_N(\omega)|^2 e^{i\omega\tau} d\omega$$

showing that

$$\hat{R}_u^N(0) = \frac{T_s}{2\pi} \int_{-\pi/T_s}^{\pi/T_s} \frac{1}{N}|U_N(\omega)|^2 d\omega.$$

Proof of the DFT-pair (2.33)**-**(2.34)**.**

Substituting the expression (2.33) into (2.34) shows that

$$u_d(k) = \frac{1}{N}\sum_{\ell=0}^{N-1}\sum_{m=0}^{N-1} u_d(m) e^{-i\frac{\ell\omega_s}{N}mT_s} e^{i\frac{2\pi\ell}{N}k} \tag{2A.9}$$

$$= \frac{1}{N}\sum_{m=0}^{N-1} u_d(m) \cdot \sum_{\ell=0}^{N-1} e^{i\frac{2\pi\ell}{N}(k-m)}. \tag{2A.10}$$

With Lemma 2A.1 the sum of exponentials will equal $N\delta(k-m)$ [10], which proves the validity of the transform pair.

Bibliography

K.J. Åström and B. Wittenmark (1984). *Computer Controlled Systems: Theory and Design.* Prentice Hall Inc., Englewood Cliffs, NJ.

R.L. Fante (1988). *Signal Analysis and Estimation - An Introduction.* John Wiley & Sons, Inc., New York.

G.M. Jenkins and D.G. Watts (1968). *Spectral Analysis and its Applications.* Holden-Day, Oakland, CA.

E.W. Kamen and B.S. Heck (2007). *Fundamentals of Signals and Systems Using the Web and Matlab.* Prentice Hall, Upper Saddle River, NJ, 3/e.

L. Ljung (1999). *System Identification - Theory for the User.* Prentice-Hall, Englewood Cliffs, NJ, 2/e.

L. Ljung and T. Glad (1994). *Modeling of Dynamic Systems.* Prentice Hall, Englewood Cliffs, NJ.

A.V. Oppenheim and R.W. Schafer (1989). *Discrete-Time Signal Processing.* Prentice Hall, Englewood Cliffs, NJ.

C.L. Phillips, J.M. Parr and E.A. Riskin (2008). *Signals, Systems and Transformations.* Prentice Hall, Englewood Cliffs, NJ, 4/e.

K.S. Shanmugan and A.M. Breipohl (1988). *Random Signals - Detection, Estimation and Data Analysis.* John Wiley & Sons, Inc., New York.

C.W. Therrien (1992). *Discrete Random Signals and Statistical Signal Processing.* Prentice Hall, Englewood Cliffs, NJ.

---

[10] $\delta(\cdot)$ is the discrete pulse function, i.e. $\delta(k) = 1$ for $k = 0$ and $\delta(k) = 0$ elsewhere.

Chapter 3

Identification of nonparametric models

3.1 Introduction

The identification of nonparametric system models is very often a first step in obtaining experimental information on the dynamic properties of a dynamical system. Most common examples of nonparametric system properties are:

- Frequency response in terms of the Bode amplitude and phase plot;

- Nyquist curve;

- Step and/or pulse response.

These phenomena are helpful in assessing the properties of a dynamical system, and or often used by "system engineers" for purposes of systems analysis and/or synthesis. They are referred to as "nonparametric models", whenever they are not constructed from a model representation with a limited number of coefficients, as e.g. a state space model with a limited state dimension. This despite of the fact that every frequency response or time signal is stored digitally in our computer memory by a finite number of coefficients.

In order to specify nonparametric models of dynamic systems on the basis of measurement data, attention has to be given to related nonparametric representations of signal properties, such as correlation functions and signal spectra. Therefore the estimation of correlation functions and spectra of signals is a necessary part of nonparametric identification.

In this chapter, we will consider a data generating system of the form

$$y(t) = G_0(q)u(t) + v(t) \tag{3.1}$$

where v is a zero-mean stationary stochastic process with spectral density $\Phi_v(\omega)$ and u is a quasi-stationary deterministic signal, being uncorrelated to v. All statistical properties of estimators will be based on the stochastic process v only, and not on realizations of input signals. The input signal u is considered to be a fixed measured data sequence; this still allows u to be *generated* as a realization of a stochastic process[1].

In the sequel of this chapter, several principles will be discussed to obtain information on G_0 from measurement samples of u and y.

---

[1]For the situation of stochastic input signals the reader is referred to e.g. Priestley (1981) and Broersen (1995).

3.2   Transient Analysis

In transient analysis, we determine the system's response to a particular signal (typically a pulse or a step signal), in order to extract the basic properties of the system from the measured response. By applying a pulse or step input signal to the system, the pulse or step response can be observed from the output. Generally this provides good insights into important properties of the system, as e.g. the presence and length of time delays, static gain and time constants. However the output measurement will very often be disturbed by noise. If the noise term is considerable, it will be hard to assess the real properties of the system by a single measurement.

Multiple experiments, and averaging the system response over the several experiments, is one way to achieve noise reduction; however, it only will improve on the estimates if the disturbance signals in separate experiments are independent of each other.

Another way to obtain the pulse response (and by integration the step response) of a system, is by estimation through correlation analysis, as discussed in the next section.

3.3   Correlation Analysis

3.3.1   Introduction

In correlation analysis, the fact that u and v are uncorrelated is exploited, by rewriting the relation of the data generating system (3.1). To this end equation (3.1) is premultiplied left and right by $u(t - \tau)$ while expectation is taken. This leads to

$$R_{yu}(\tau) = G_0(q)R_u(\tau), \tag{3.2}$$

or equivalently,

$$R_{yu}(\tau) = \sum_{k=0}^{\infty} g_0(k)R_u(\tau - k) \tag{3.3}$$

where $\{g_0(k)\}_{k=0,\cdots,\infty}$ is the pulse response sequence of G_0. Equation (3.3) is known as the Wiener-Hopf equation.

Note that by correlating the input and output signals of G_0 the disturbance signal v has been eliminated from the equations.

If the input signal is a white noise process, i.e. $R_u(\tau) = \sigma_u^2 \delta(\tau)$, then it follows straightforwardly that

$$R_{yu}(\tau) = g_0(\tau)\sigma_u^2, \quad \text{or} \tag{3.4}$$

$$g_0(\tau) = \frac{R_{yu}(\tau)}{\sigma_u^2} \tag{3.5}$$

and so estimating the cross-correlation function directly provides us with information on the pulse response of G_0.

In the situation of other input signals it is nontrivial how to solve equation (3.3) for $\{g_0(k)\}$. A simplification can be made if we may assume that the length of the system's pulse response is finite, i.e.

$$g_0(k) = 0, \quad k \geq n_g. \tag{3.6}$$

In this case the set of equations (3.3) can be written into a finite matrix equation:

$$
\begin{bmatrix}
R_{yu}(0) \\
R_{yu}(1) \\
\vdots \\
R_{yu}(n_g - 1)
\end{bmatrix}
=
\begin{bmatrix}
R_u(0) & R_u(1) & \cdots & R_u(n_g - 1) \\
R_u(1) & R_u(0) & \cdots & \vdots \\
\vdots & \ddots & \ddots & \vdots \\
R_u(n_g - 1) & \cdots & \cdots & R_u(0)
\end{bmatrix}
\begin{bmatrix}
g_0(0) \\
g_0(1) \\
\vdots \\
g_0(n_g - 1)
\end{bmatrix}
\tag{3.7}
$$

where use is made of the property that $R_u(\tau) = R_u(-\tau)$.

When estimates are available of the auto- and cross-correlation functions R_u and R_{yu} over the appropriate time horizon, and when the matrix on the right hand side is invertible, this results in an estimate of the (finite) pulse response of the system. This estimator is further analyzed in chapter 4, when discussing finite impulse response (FIR) models.

3.3.2 Estimation of auto-correlation functions

First we will consider the estimation of the auto-correlation function of a quasi-stationary signal. The situation of estimating cross-correlation functions will appear to be closely related.

When given a quasi-stationary signal u, its auto-correlation function has been defined to be

$$
R_u(\tau) := \bar{E}u(t)u(t - \tau) = \lim_{N \to \infty} \frac{1}{N} \sum_{t=0}^{N-1} Eu(t)u(t - \tau). \tag{3.8}
$$

If there are only N measurement samples of the signal available, the most straightforward estimate of the correlation function seems to be

$$
\hat{R}_u^N(\tau) := \frac{1}{N} \sum_{t=0}^{N-1} u(t)u(t - \tau), \qquad |\tau| \leq N - 1 \tag{3.9}
$$

known as the *sample correlation function*. Note that in the above expression for the sample correlation, the effective summation interval has length $N - \tau$, as we cannot use measurements of $u(t)$ for $t < 0$ or $t \geq N$. The following properties can be formulated for this estimate, provided that u is not deterministic.

(a) $E\hat{R}_u^N(\tau) = \dfrac{N - |\tau|}{N} R_u(\tau)$ and thus is the estimate biased for $\tau \neq 0$. However asymptotically, for $N \to \infty$ the bias will disappear, i.e. $\lim_{N \to \infty} E\hat{R}_u^N(\tau) = R_u(\tau)$.

(b) The alternative estimate

$$
\frac{1}{N - |\tau|} \sum_{t=0}^{N-1} u(t)u(t - \tau)
$$

is unbiased for all N and τ.

(c) $var(\hat{R}_u^N(\tau)) = O(1/N)$, meaning that for large enough N the variance becomes proportional to $1/N$, and thus the variance tends to zero for infinite number of data. The exact expressions for (co)variance of the estimates are rather complicated. Approximate expressions for large N are known for several specific situations, e.g. in

the situation where u is a zero-mean stochastic process with a Gaussian distribution, it follows that (see e.g. Priestley, 1981):

$$cov\{\hat{R}_u^N(\tau), \hat{R}_u^N(\tau + k)\} \sim$$

$$\sim \frac{1}{N} \sum_{m=-\infty}^{\infty} \{R_u(m)R_u(m+k) + R_u(m+\tau+k)R_u(m-\tau)\} \quad (3.10)$$

$$var\{\hat{R}_u^N(\tau)\} \sim \frac{1}{N} \sum_{m=-\infty}^{\infty} \{R_u^2(m) + R_u(m+\tau)R_u(m-\tau)\}. \quad (3.11)$$

More complex expressions are available for u being a filtered white noise process with bounded moments up to order 4 (see Söderström and Stoica, 1989, pp. 570).

If u is deterministic, then the above analysis does not apply, as in this case simply $R_u(\tau) = \lim_{N\to\infty} \hat{R}_u^N(\tau)$, being a non-stochastic variable, provided that the limit exists. Whereas the sample correlation estimate is not unbiased for finite N, it has an additional property that makes it attractive to use. This is formulated in the following lemma (see e.g. Oppenheim and Schafer (1989)).

Lemma 3.3.1 *Let u be quasi-stationary, defined on the time interval $[0, N-1]$. Consider the sample correlation,*

$$\hat{R}_u^N(\tau) := \frac{1}{N} \sum_{t=0}^{N-1} u(t)u(t-\tau), \quad |\tau| \leq N-1$$

$$:= 0 \quad\quad\quad\quad\quad\quad |\tau| \geq N. \quad (3.12)$$

Then the Discrete-Time Fourier Transform of this sample correlation satisfies:

$$\boxed{\sum_{\tau=-\infty}^{\infty} \hat{R}_u^N(\tau)e^{-i\omega\tau} = \frac{1}{N}|U_N(\omega)|^2} \quad\quad (3.13)$$

with $U_N(\omega)$ the DTFT of the signal, $U_N(\omega) = \sum_{t=0}^{N-1} u(t)e^{-i\omega t}$.

Proof: Substituting the definitions it follows that

$$\sum_{\tau=-\infty}^{\infty} \hat{R}_u^N(\tau)e^{-i\omega\tau} = \frac{1}{N} \sum_{t=-\infty}^{\infty} \sum_{\tau=-\infty}^{\infty} u(t)u(t-\tau)e^{-i\omega\tau}$$

with $u(t) := 0$ for $t < 0$ or $t \geq N$. By variable substitution $\ell = t - \tau$ we arrive at

$$\frac{1}{N} \sum_{t=-\infty}^{\infty} u(t)e^{-i\omega t} \cdot \sum_{\ell=-\infty}^{\infty} u(\ell)e^{i\omega\ell}$$

which equals $\frac{1}{N}U_N(\omega)U_N(\omega)^*$. $\square$

This lemma states that the sample correlation function through Fourier transform is related to the periodogram $\frac{1}{N}|U_N(\omega)|^2$ (see section 2.4). Since there exist efficient and fast computational methods for calculating Fourier transforms of signals (Fast Fourier Transform), it is not uncommon to calculate the sample correlation function of a signal by first determining $U_N(\omega)$, and subsequently inverse Fourier transforming the periodogram to obtain $\hat{R}_u^N(\tau)$.

3.3.3 Estimation of cross-correlation functions

The estimation of cross-correlation functions is very similar to the situation of the previous subsection. For y, u jointly quasi-stationary we consider the sample cross-correlation by

$$\hat{R}_{yu}^N(\tau) := \frac{1}{N} \sum_{t=0}^{N-1} y(t)u(t-\tau). \tag{3.14}$$

In line with the previous discussion this estimate is asymptotically unbiased, its variance decays with $1/N$ and for the situation of y, u being a multivariate zero-mean stationary stochastic process, the asymptotic covariance of the estimates satisfies

$$cov\{\hat{R}_{yu}^N(\tau_1), \hat{R}_{yu}^N(\tau_2)\} \sim \frac{1}{N} \sum_{m=-\infty}^{\infty} \{R_u(m)R_y(m+\tau_2-\tau_1)+R_{yu}(m+\tau_2)R_{uy}(m-\tau_1)\}. \tag{3.15}$$

In the situation that y and u are related through a dynamical system, according to (3.1) a more specific result holds true, as formulated next.

Proposition 3.3.2 *Let u and y be related according to (3.1) with v_0 a zero-mean stationary stochastic process with bounded fourth moment, and u a deterministic signal. Then*

$$\sqrt{N}(\hat{R}_{yu}^N(\tau) - ER_{yu}(\tau)) \in \mathcal{A}s\mathcal{N}(0, \Lambda) \tag{3.16}$$

with

$$\Lambda := \sum_{t=-\infty}^{\infty} R_{v_0}(t)R_u(t) \tag{3.17}$$

Proof: Substituting (3.1) into the expression for $\hat{R}_{yu}^N(\tau)$ it follows that

$$\hat{R}_{yu}^N(\tau) = \frac{1}{N} \sum_{t=0}^{N-1} G_0(q)u(t)u(t-\tau) + \frac{1}{N} \sum_{t=0}^{N-1} v(t)u(t-\tau).$$

As a result

$$\sqrt{N}(\hat{R}_{yu}^N(\tau) - ER_{yu}(\tau)) = \frac{1}{\sqrt{N}} \sum_{t=0}^{N-1} v(t)u(t-\tau).$$

The asymptotic properties of the right hand side expression are derived in Hakvoort and Van den Hof (1995), based on the work of Ljung (1987) and Hjalmarsson (1993). □

In other words, in the considered situation the sample cross-correlation function is asymptotically unbiased and its asymptotic variance is given by Λ/N. As the variance decays to zero for increasing N, the estimate is also consistent. Asymptotically the estimate has a Gaussian distribution.

With respect to the Fourier transform of the sample cross-correlation function, it can be verified that as a simple extension of Lemma 3.3.1:

$$\sum_{\tau=-\infty}^{\infty} \hat{R}_{yu}^N(\tau)e^{-i\omega\tau} = \frac{1}{N}Y_N(\omega)U_N(\omega)^*. \tag{3.18}$$

3.3.4   Summary

- For (jointly) quasi-stationary signals u and y, sample auto- and cross-correlation functions

$$\hat{R}_y^N(\tau) \ := \ \frac{1}{N} \sum_{t=0}^{N-1} y(t)y(t-\tau) \tag{3.19}$$

$$\hat{R}_{yu}^N(\tau) \ := \ \frac{1}{N} \sum_{t=0}^{N-1} y(t)u(t-\tau) \tag{3.20}$$

are, for any fixed value of τ,

  - asymptotic unbiased estimates of $R_y(\tau)$ and $R_{yu}(\tau)$,
  - with a variance decaying to 0 for $N \rightarrow \infty$.

- For dynamical systems with measured inputs (and therefore known R_u), the estimates of the cross-correlation function directly lead to an asymptotic unbiased and consistent estimate of the pulse response elements $g_0(k)$ of the underlying system, through equation (3.7).

3.4   Frequency Response Identification - ETFE

3.4.1   Sinewave testing

A very simple way to extract information on the frequency response of a dynamical system is to excite the system with a simple sinewave:

$$u(t) = c \cdot \cos(\omega t).$$

Given the system relation (3.1) the response of the system, after transient effects have disappeared, will be given by

$$y(t) = c\, a \cdot \cos(\omega t + \phi) + v(t). \tag{3.21}$$

with $a = |G_0(e^{i\omega})|$ and $\phi = arg(G_0(e^{i\omega}))$.

If one is able to extract the amplification factor and the phase shift (graphically) from the measurements, knowledge is obtained about the response of the system for one specific frequency. This experiment can be repeated for several frequencies, in order to construct a graphic representation of the system's frequency response.

It may be clear that the principal problem with this method is to extract the appropriate information a and ϕ from the signal y, as this output signal is contaminated by noise.

Frequency analysis by correlation

One method to overcome the difficulties of handling the noise term in the observed output signal, is by using correlation with sine and cosine functions of the given and known frequency. By correlating the output signal with these auxiliary signals, the effect of the noise can be canceled.

To this end one constructs (Ljung, 1999):

$$y_s(N) \quad = \quad \frac{1}{N} \sum_{t=0}^{N-1} y(t) \sin(\omega t) \tag{3.22}$$

$$y_c(N) \quad = \quad \frac{1}{N} \sum_{t=0}^{N-1} y(t) \cos(\omega t). \tag{3.23}$$

Substituting (3.21) then yields:

$$y_s(N) \quad = \quad \frac{1}{N} \sum_{t=0}^{N-1} ca \cdot \cos(\omega t + \phi) \sin(\omega t) + \frac{1}{N} \sum_{t=0}^{N-1} v(t) \sin(\omega t) \tag{3.24}$$

$$= \quad -\frac{ca}{2} \sin \, \phi + \frac{1}{N} \sum_{t=0}^{N-1} \frac{ca}{2} \sin(2\omega t + \phi) + \frac{1}{N} \sum_{t=0}^{N-1} v(t) \sin(\omega t), \tag{3.25}$$

and similarly

$$y_c(N) \quad = \quad \frac{1}{N} \sum_{t=0}^{N-1} ca \cdot \cos(\omega t + \phi) \cos(\omega t) + \frac{1}{N} \sum_{t=0}^{N-1} v(t) \cos(\omega t) \tag{3.26}$$

$$= \quad \frac{ca}{2} \cos \, \phi + \frac{1}{N} \sum_{t=0}^{N-1} \frac{ca}{2} \cos(2\omega t + \phi) + \frac{1}{N} \sum_{t=0}^{N-1} v(t) \cos(\omega t). \tag{3.27}$$

It can be verified that for $N \rightarrow \infty$ the second terms on the right hand side of (3.25) and (3.27) will tend to zero. This will also hold for the third terms in these expressions[2], provided that the noise signal v does not contain any pure sinusoids with frequency ω. In this situation we obtain:

$$y_s(N) \quad \sim \quad -\frac{ca}{2} \sin \phi \tag{3.28}$$

$$y_c(N) \quad \sim \quad \frac{ca}{2} \cos \phi \tag{3.29}$$

motivating the estimate:

$$\text{Re } \hat{G}(e^{i\omega}) \quad = \quad a \cos \phi = \frac{2}{c} y_c(N) \tag{3.30}$$

$$\text{Im } \hat{G}(e^{i\omega}) \quad = \quad a \sin \phi = -\frac{2}{c} y_s(N) \tag{3.31}$$

or similarly:

$$|\hat{G}(e^{i\omega})| = \hat{a} := \frac{2}{c} \sqrt{[y_s(N)^2 + y_c(N)^2]} \tag{3.32}$$

$$\arg(\hat{G}(e^{i\omega})) = \hat{\phi} := -\arctan \frac{y_s(N)}{y_c(N)}. \tag{3.33}$$

Note that by using the relation:

$$\frac{1}{N} Y_N(\omega) = y_c(N) - iy_s(N) \tag{3.34}$$

---

[2]The variance of the third terms decay with $1/N$ provided that $\sum_{\tau=0}^{\infty} \tau |R_v(\tau)| < \infty$ (Ljung, 1999).

it follows that

$$\hat{G}(e^{i\omega}) = \frac{Y_N(\omega)}{Nc/2}. \tag{3.35}$$

An estimate has been constructed for the frequency response at the particular frequency ω. Again, by repeating the experiment for several different values of ω, one can obtain insight into the frequency response of the system over a specified frequency region.

As we can observe from example 2.4.1, for the considered input signal, it follows that $U_N(\omega) = Nc/2$, showing that the constructed estimate for one frequency can also be written as

$$\hat{G}(e^{i\omega}) = \frac{Y_N(\omega)}{U_N(\omega)}. \tag{3.36}$$

The above estimate will be shown to have a close relationship with the estimate that can be obtained through Fourier analysis, as discussed next.

3.4.2   Fourier analysis - ETFE

While in the previous subsection an estimate has been constructed of the frequency response of a system for a single sinusoid excitation, the actual expression (3.36) for the estimate can equally well be applied to other excitation signals too. For general type of quasi-stationary deterministic input signals the expression:

$$\breve{G}_N(e^{i\omega}) := \frac{Y_N(\omega)}{U_N(\omega)} \tag{3.37}$$

is defined as the *Empirical Transfer Function Estimate* (ETFE), see Ljung (1987). This name refers to the fact that an estimate of the input/output transfer function is obtained by simply taking the quotient of the Fourier transforms of output and input signal, given a single data sequence of input and output signals. No assumptions on the underlying data generating system have been imposed, except for its linearity.

For analyzing the properties of this estimate, we first have to consider the following result (for the formal statement and proof see Theorem 3A.1).

If $y(t) = G(q)u(t)$, and u quasi-stationary, then

$$Y_N(\omega) = G(e^{i\omega})U_N(\omega) + R_N(\omega) \tag{3.38}$$

with

- $R_N(\omega) = 0$ for all $\omega = \frac{2\pi k}{N}$, $k \in \mathbb{Z}$ if u is a periodic signal with period N;

- $R_N(\omega) \leq c_1$ for all ω if u is a general quasi-stationary signal.

The term $R_N(\omega)$ reflects the contribution of data samples that are outside the measurement interval $[0, N-1]$. This contribution will be exactly zero (no leakage) whenever the signal u on the interval $[0, N-1]$ is periodically extended outside this interval.

A second result that we need for the analysis of the ETFE estimate is related to the noise contribution.

Let $v(t) = H(q)e(t)$, with H stable and e a zero-mean white noise process. Then

$$EV_N(\omega) = 0 \quad \text{for all } \omega = \frac{2\pi k}{N}, k \in \mathbb{Z}. \qquad (3.39)$$

$$E\frac{1}{N}|V_N(\omega)|^2 \to \Phi_v(\omega) \text{ for } N \to \infty. \qquad (3.40)$$

Again, the formal statement and proof are added in Theorem 3A.2.
Going back to the system's equation (3.1):

$$y(t) = G_0(q)u(t) + v(t)$$

it now follows that

$$Y_N(\omega) = G_0(e^{i\omega})U_N(\omega) + R_N(\omega) + V_N(\omega)$$

and therefore

$$\breve{G}_N(e^{i\omega}) := \frac{Y_N(\omega)}{U_N(\omega)} = G_0(e^{i\omega}) + \frac{V_N(\omega)}{U_N(\omega)} + \frac{R_N(\omega)}{U_N(\omega)} \qquad (3.41)$$

The stochastic component in $\breve{G}_N(e^{i\omega})$ is reflected in the second term on the right hand side, induced by the output noise disturbance signal v. By employing the statistical properties of $V_N(\omega)$, it follows that at those frequencies in the frequency grid $\Omega_N := \{\frac{2\pi k}{N}, k = 0, \cdots, N-1\}$ where the input signal has a nonzero power contribution, i.e. $\frac{1}{\sqrt{N}}U_N(\omega) \neq 0$, the term $E\frac{V_N(\omega)}{U_N(\omega)} = 0$ and so

$$E\breve{G}_N(e^{i\omega}) = G_0(e^{i\omega}) + \frac{R_N(\omega)}{U_N(\omega)}. \qquad (3.42)$$

Bias of ETFE-estimates
If during the experiment the input signal is taken as a signal in the interval $[0, N-1]$ that is continued periodically outside this interval, then $R_N(\omega) = 0$ for frequencies in the frequency grid Ω_N. Consequently

$$E\breve{G}_N(e^{i\omega}) = G_0(e^{i\omega})$$

and so the ETFE estimate is unbiased at those frequencies in the frequency grid Ω_N where $U_N(\omega) \neq 0$.

If knowledge about this periodic extension of the input signal is lacking, the ETFE estimate will incur a bias error, reflected by

$$|E\breve{G}_N(e^{i\omega}) - G_0(e^{i\omega})| = \left|\frac{R_N(\omega)}{U_N(\omega)}\right| \leq \frac{c_1/\sqrt{N}}{\left|\frac{1}{\sqrt{N}}U_N(\omega)\right|}.$$

The bias error will vanish asymptotically at those frequencies where $\frac{1}{\sqrt{N}}U_N(\omega) \neq 0$, i.e. those frequencies where $\Phi_u(\omega) \neq 0$.

Variance of ETFE-estimates
Since

$$E(|\breve{G}_N(e^{i\omega}) - E\breve{G}_N(e^{i\omega})|^2) = E\left(\left|\frac{V_N(\omega)}{U_N(\omega)}\right|^2\right)$$

and u is considered a deterministic sequence with power spectral density $\Phi_u(\omega) = \frac{1}{N}|U_N(\omega)|^2$, the statistical properties of $V_N(\omega)$, formulated in (3.40), then lead to the property that for all $\omega \in \Omega_N$:

$$\lim_{N \to \infty} var(\breve{G}_N(e^{i\omega})) = \frac{\Phi_v(\omega)}{\Phi_u(\omega)}.$$

ETFE-estimate from periodic input signals

If the input signal is periodic with period N_0, and the data length N contains an integer number of periods, i.e. $N = rN_0$, with r integer-valued, the asymptotic properties of $\breve{G}_N(e^{i\omega})$ can be considered for increasing values of r.

Since u is periodic with period N_0, it follows that $\frac{1}{N}|U_N(\omega)|^2 = \frac{r^2}{N} \cdot |U_{N_0}(\omega)|^2$ with r the number of periods in the input signal (see e.g. Example 2A.2). This shows that

$$\frac{1}{N}|U_N(\omega)|^2 = r \cdot \frac{1}{N_0}|U_{N_0}(\omega)|^2. \tag{3.43}$$

With increasing r, the periodogram $\frac{1}{N}|U_N(\omega)|^2$ will tend to zero at frequencies outside the frequency grid $\omega = \frac{2\pi k}{N_0}$, k integer, while for the frequencies within this grid the periodogram will increase like r. As a result, the variance of the ETFE in these frequency points will decay like $1/r$ and so tend to 0 for $N \to \infty$.

Stated differently, because of the periodic nature of the input signal, the asymptotic power spectral density function $\Phi_u(\omega)$ of u will only have nonzero contributions in the frequency grid Ω_{N_0}. In those frequencies where $\Phi_u(\omega) \neq 0$, it will contain Dirac pulses, and therefore the variance of the ETFE-estimate will tend to zero. In combination with the fact that the estimate is asymptotically unbiased, it follows that $\breve{G}_N(e^{i\omega})$ is consistent in this case.

ETFE-estimate from general quasi-stationary deterministic input signals

For general input signals the ETFE estimate remains (asymptotically) unbiased. For increasing values of N, the variance contribution approaches $\frac{\Phi_v(\omega)}{\Phi_u(\omega)}$ for all $\omega \in \Omega_N$. However now, for increasing N this expression is not guaranteed to converge to 0; it is equal to the noise-to-input signal ratio at the particular frequencies considered. The appealing result is thus that the variance of an ETFE-estimate at a particular frequency is determined by the noise-to-signal ratio at that frequency. For increasing N the frequency grid becomes more dense, i.e. an estimate is obtained at an increasing number of frequencies, but the variance of these estimates does not improve. Note that in this situation the frequency resolution is given by $2\pi/N$.

The difference between the two experimental situations discussed above is quite remarkable. An unbiased ETFE is obtained either at a fixed and limited number of frequencies with decaying variance, or at a growing number of frequencies[3], but with non-vanishing variance.

A possible bias problem induced by leakage can also be avoided by applying *tapering* , i.e. by taking care that the considered input signal is preceded with N_g zeros and ends also with N_g zeros where N_g is the length of the pulse response of the system (see Theorem 3A.1). An example of this situation is depicted in Figure 3.1 where a tapered input signal is sketched for $N = 200$ and $N_g = 50$.

---

[3]neglecting the frequencies at which a bias error occurs.
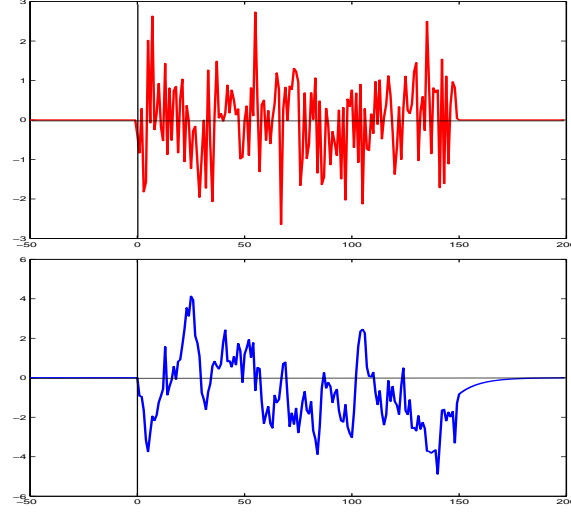
Figure 3.1: Tapered input signal (upper figure) and output signal (lower figure) for $N = 200$, $N_g = 50$.

Summary of results

The ETFE-estimate
$$\breve{G}_N(e^{i\omega}) = \frac{Y_N(\omega)}{U_N(\omega)}$$

has the following properties:

(a) The ETFE is asymptotically unbiased, $\lim_{N\to\infty} E\breve{G}_N(e^{i\omega}) = G_0(e^{i\omega})$, in those frequencies $\omega \in \Omega_N$ where $U_N(\omega) \neq 0$;

(b) Its variance asymptotically tends to $\frac{\Phi_v(\omega)}{\Phi_u(\omega)}$.

(c) The ETFE's at different frequencies are asymptotically uncorrelated.

If the input signal u is periodic with period $N_0 = N/r$, r integer, then for increasing values of r:

• The ETFE is consistent in all frequencies $\omega \in \Omega_{N_0}$ where $\Phi_u(\omega) \neq 0$

If the input signal u is a general quasi-stationary signal, the variance of the ETFE will not to tend to 0 for increasing values of N.

Example 3.4.1 The effect of choosing different input signals for obtaining an ETFE is illustrated by applying the estimator to simulation data obtained from the system

$$G_0(z) = \frac{b_1 z^{-1} + \cdots + b_5 z^{-5}}{1 + a_1 z^{-1} + \cdots + a_5 z^{-5}} \tag{3.44}$$

with $b_1 = 0.2530$, $b_2 = -0.9724$, $b_3 = 1.4283$, $b_4 = -0.9493$, $b_5 = 0.2410$; $a_1 = -4.15$, $a_2 = 6.8831$, $a_3 = -5.6871$, $a_4 = 2.3333$, $a_5 = -0.3787$.

An output noise is added to the simulated output, coloured by a second order noise filter

$$H_0(z) = \frac{1 - 1.38z^{-1} + 0.4z^{-2}}{1 - 1.9z^{-1} + 0.91z^{-2}}, \tag{3.45}$$

while the white noise signal e_0 has variance 0.0025, leading to a signal-to-noise ratio at the output of $11.6dB$, being equivalent to around 30% noise disturbance in amplitude on the noise-free output signal. As input signal we have chosen two different options:
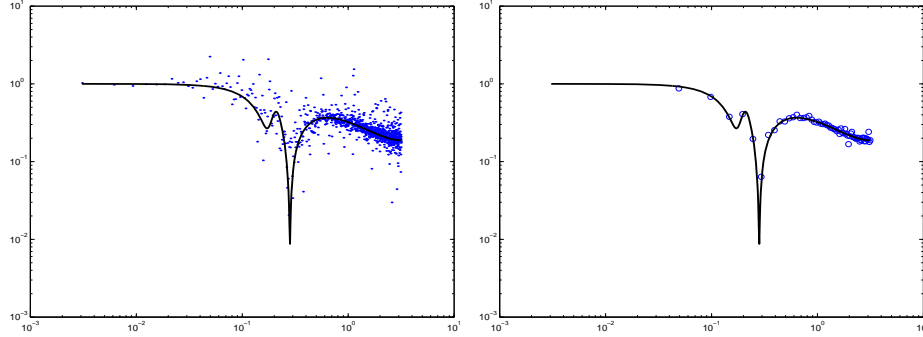
Figure 3.2: Left: Bode-amplitude plot of ETFE based on random input with length $N = 2048$ (dotted), and of data generating system G_0 (solid-line); Right: Bode-amplitude plot of ETFE based on periodic input with $N = 2048$ and period length $N_0 = 128$ (o), and of data generating system G_0 (solid-line).

(a) A zero mean unit variance white noise signal with length $N = 2048$;

(b) A zero mean unit variance white noise signal with length $N_0 = 128$, but repeated 16 times, arriving at an input signal with length $N = 2048$.

The results of the ETFE are sketched in Figure 3.2. It shows the ETFE obtained in situation (a) compared to the frequency response of G_0. Estimates are obtained for 1024 frequency points in the interval $[0, \pi]$. As is clearly illustrated by the result, the ETFE is very erratic. The result for situation (b) is given in the right plot, where estimates are obtained for (only) 64 frequencies in the interval $[0, \pi]$. However in this situation the reduced variance of the estimates is clearly shown.

3.4.3   Smoothing the ETFE

In the situation that there is no possibility for exciting the system with periodic inputs, there is an alternative for achieving a frequency response estimate that has a reduced variance, and thus is more smooth, in comparison with the rough ETFE as discussed in the previous subsection.

Based upon the assumption that the frequency response of the underlying data generating system is a smooth function of frequency, the very erratic behaviour of the ETFE can be processed into a smooth function, by a so-called smoothing operation. Based on the ETFE,

a frequency response estimate is constructed by averaging $\breve{G}(e^{i\omega})$ over several frequency points in the neighborhood of ω.

This can be formalized by writing:

$$\hat{G}(e^{i\omega}) = \frac{\displaystyle\int_{\omega-\Delta}^{\omega+\Delta} W(\xi - \omega)\breve{G}(e^{i\xi})d\xi}{\displaystyle\int_{\omega-\Delta}^{\omega+\Delta} W(\xi - \omega)d\xi}, \tag{3.46}$$

where $W(\xi)$ is a frequency-window, that performs an "averaging" operation of the ETFE over a specific frequency region around ω. In first instance there are two aspects around the role of W:

- (3.46) should achieve an averaging of $\breve{G}(e^{i\omega})$ over neighboring points, where the weight of $\breve{G}(e^{i\xi})$ should be (inversely) related to $|\xi - \omega|$; i.e. it should be maximum for $\xi = \omega$ and decrease for increasing $|\xi - \omega|$. This phenomenon is due to the fact that $\breve{G}(e^{i\xi})$ is a less reliable estimate of $\breve{G}(e^{i\omega})$ the further ξ is away from ω;

- In this averaging, the several measurement points $\breve{G}(e^{i\xi})$ should be weighted with a weight that is inversely proportional to their variance; i.e. ETFE-points that have a large variance are less reliable, and should contribute less to the final estimate. Note that the variance of $\breve{G}(e^{i\xi})$ asymptotically equals $\Phi_v(\xi)/[\frac{1}{N}|U_N(\xi)|^2]$.

Combining both arguments, and employing the assumption that $\Phi_v(\xi)$ can be considered constant over the frequency range $\omega - \Delta \leq \xi \leq \omega + \Delta$ where the window is active, we can write

$$
\begin{aligned}
\hat{G}_N(e^{i\omega}) &= \frac{\displaystyle\int_{-\pi}^{\pi} W_\gamma(\xi - \omega)|U_N(\xi)|^2\breve{G}_N(e^{i\xi})d\xi}{\displaystyle\int_{-\pi}^{\pi} W_\gamma(\xi - \omega)|U_N(\xi)|^2 d\xi}, \\
&= \frac{\displaystyle\int_{-\pi}^{\pi} W_\gamma(\xi - \omega)Y_N(\xi)U_N^*(\xi)d\xi}{\displaystyle\int_{-\pi}^{\pi} W_\gamma(\xi - \omega)|U_N(\xi)|^2 d\xi},
\end{aligned} \tag{3.47}
$$

where $W_\gamma(\xi)$ is a positive real-valued frequency function, which is maximum for $\xi = 0$ and whose width is characterized by the parameter γ. This γ-dependency of W_γ now takes over the role of the finite integration interval $\omega - \Delta \leq \xi \leq \omega + \Delta$ as considered in (3.46). An extensive discussion on the specific choice of window will be postponed until the next section, where spectral estimation will be considered.

Here we limit the discussion by stating that a narrow window will only achieve a limiting variance reduction, and thus will not lead to a smooth frequency function. A window that is too wide will result in a smooth estimate, but will introduce additional bias, as the averaging operation will be performed over a region of $\breve{G}_N(e^{i\xi})$ where the real frequency function of G_0 can not be considered to be constant. This shows that the choice of the frequency width embodies a bias/variance trade-off. Examples given in the next section will illustrate this trade-off.

In practice the ETFE will be available in a finite number of frequencies. This implies that in smoothing algorithms the integral expressions in (3.47) can not be calculated exactly; both numerator and denominator will have to be approximated by a discrete-time convolution on the frequency response samples of $Y_N(\xi)U_N^*(\xi)$ and $|U_N(\xi)|^2$.

3.5   Frequency Response Identification - Spectral Analysis

3.5.1   Introduction

Transfer function estimation by spectral analysis is based on the assumption concerning the data generating system:

$$y(t) = G_0(q)u(t) + v(t) \tag{3.48}$$

that signals u and v are uncorrelated. In that situation it follows from the way in which discrete spectra are transformed by linear systems, that

$$\Phi_{yu}(\omega) = G_0(e^{i\omega})\Phi_u(\omega) \tag{3.49}$$

and so

$$G_0(e^{i\omega}) = \frac{\Phi_{yu}(\omega)}{\Phi_u(\omega)} \tag{3.50}$$

for those frequencies where $\Phi_u(\omega) > 0$. This directly leads to a suggestion for an estimate of the frequency response through

$$\hat{G}(e^{i\omega}) = \frac{\hat{\Phi_{yu}}(\omega)}{\hat{\Phi_u}(\omega)}. \tag{3.51}$$

Thus by estimating the two spectral densities in the above expression, a direct frequency response estimate of the system results.

It will appear that this spectral estimate of a transfer function will have a close relationship to the (smoothed) ETFE presented in the previous section.

3.5.2   Estimating auto- and cross-spectral densities

The spectral density of a quasi-stationary signal u has been defined by

$$\Phi_u(\omega) = \sum_{\tau=-\infty}^{\infty} R_u(\tau)e^{-i\omega\tau}. \tag{3.52}$$

When basing an estimate on a finite number of data, a natural estimate becomes

$$\Phi_u^{\breve{N}}(\omega) \quad := \quad \sum_{\tau=-\infty}^{\infty} \hat{R}_u^N(\tau)e^{-i\omega\tau} \tag{3.53}$$

$$= \quad \frac{1}{N}|U_N(\omega)|^2. \tag{3.54}$$

The latter equality follows directly from Lemma 3.3.1, and shows that the periodogram is a natural estimate for the spectral density of a signal.

When discussing the properties of this periodogram estimate, results will follow that are closely related to the ones obtained for the properties of the ETFE in the previous section. If the signal u contains periodic components, then the periodogram (as well as the spectral density) will become unbounded for increasing N. This is illustrated in example 2A.2. As a result, sinusoidal components in a quasi-stationary signal will appear as clear-cut peaks in the periodogram.

For other situations the following result can be stated.

Theorem 3.5.1 *Let u be a quasi-stationary signal that additionally satisfies that*
$$\sum_{\tau=-\infty}^{\infty} |\tau R_u(\tau)| = c_u < \infty. \text{ Then}$$

(a) $\lim_{N\to\infty} E\Phi_u^{\breve{N}}(\omega) = \Phi_u(\omega)$;

(b) $\lim_{N\to\infty} E(\Phi_u^{\breve{N}}(\omega) - \Phi_u(\omega))^2 = (\Phi_u(\omega))^2$;

(c) $E[\breve{\Phi}_u^N(\omega_1) - \Phi_u(\omega_1)][\breve{\Phi}_u^N(\omega_2) - \Phi_u(\omega_2)] = R_N^{(1)}$, *and* $\lim_{N\to\infty} R_N^{(1)} = 0$ *for* $|\omega_1 - \omega_2| \geq \frac{2\pi}{N}$.

Proof: See Ljung and Glad (1994). □

The theorem shows that in the considered situation the periodogram estimate is an asymptotically unbiased estimate of the spectral density. However, its variance is equal to the square of the spectral density itself, and so it does not tend to zero. This situation is similar to the situation of ETFE's as discussed in the previous section, where actually the same mechanisms are present. Theorem 3.5.1 is closely related to Theorem 3A.2 which was formulated for stationary stochastic processes only. In case u is a deterministic sequence, the expectation operator in Theorem 3.5.1 can simply be discarded, as in that case the estimate is not a stochastic variable.

Generally, the periodogram estimate for a (non-periodic) measurement signal will be an erratic function over frequency, fluctuating heavily around its "correct" value.

The arguments and results that are given for estimating auto spectral densities hold equally well for estimating cross-spectral densities. In that case

$$\Phi_{yu}^{\breve{N}}(\omega) := \sum_{\tau=-\infty}^{\infty} \hat{R}_{yu}^N(\tau)e^{-i\omega\tau} = \frac{1}{N}Y_N(\omega)U_N^*(\omega). \tag{3.55}$$

3.5.3 Lag windows and frequency windows

For smoothing the periodogram estimate, we can follow the same line of reasoning as for the ETFE, arriving at a smoothing operation in the frequency domain, by applying a so-called frequency window. However we can also start by considering a smoothing operation in the time-domain, by operating on the correlation function estimate $\hat{R}_u^N(\tau)$. The essential reason why the spectral density will have a non-vanishing variance, is the fact that for increasing τ the number of measurement points on the basis of which $\hat{R}_u^N(\tau)$ can be constructed (see (3.9)) becomes smaller. However the decreasing reliability of $\hat{R}_u^N(\tau)$ with increasing τ is not accounted for in the Fourier transform (3.53).

We can incorporate this mechanism in the spectral estimate, by applying a so-called *lag window* to the correlation function estimate before applying the Fourier transform:

$$\hat{\Phi_u^N}(\omega) = \sum_{\tau=-\infty}^{\infty} w_\gamma(\tau) \cdot \hat{R}_u^N(\tau) e^{-i\omega\tau}. \qquad (3.56)$$

Here, $w_\gamma(\tau)$ is a positive real-valued window function satisfying

$$w_\gamma(\tau) = 0 \quad \tau > \gamma \qquad (3.57)$$

showing that $\gamma > 0$ is a variable that determines the width of the window. This lag window causes $w_\gamma(\tau)\hat{R}_u^N(\tau)$ to be regularized to zero. The smaller the value of γ, the bigger the part of the sample correlation estimate that is "smoothed out". The higher the value of γ, the less smoothing is taking place. A typical choice for a lag window is e.g. a rectangular form:

$$
\begin{aligned}
w_\gamma(\tau) &= 1 \quad 0 \le \tau \le \gamma & (3.58)\\
&= 0 \quad \tau > \gamma. & (3.59)
\end{aligned}
$$

However more general choices are also possible, having a more smooth decay of the window towards zero. Three popular choices of windows are sketched in Figure 3.3 and characterized in Table 3.1. For an extensive list of windows the reader is referred to Jenkins and Watts (1968), Brillinger (1981) and Priestley (1981).

The three lag-windows are also sketched in Figure 3.3.
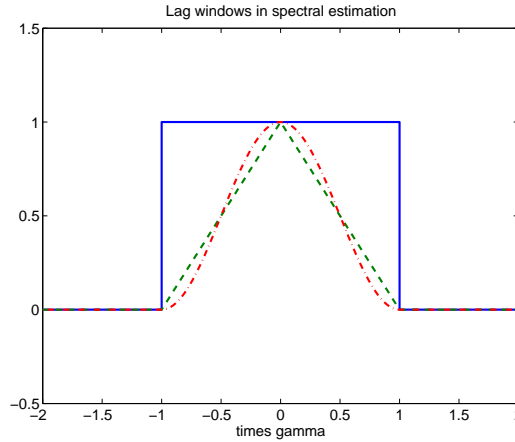
Figure 3.3: Lag-windows $w_\gamma(\tau)$; rectangular window (solid), Bartlett window (dashed), and Hamming window (dash-dotted).

Design rules for the choice of γ are:

- γ should be small compared to the number of data N, in order to guarantee enough smoothing operation;

- $|\hat{R}_u(\tau)| << \hat{R}_u(0)$ for $\tau \ge \gamma$ in order to guarantee that interesting dynamics is not smoothed out.

	$2\pi \cdot W_\gamma(\omega)$	$w_\gamma(\tau),\ 0 \leq |\tau| \leq \gamma$
Rectangular	$\frac{sin(\gamma+\frac{1}{2})\omega}{sin(\omega/2)}$	1
Bartlett	$\frac{1}{\gamma}\left(\frac{sin\ \gamma\omega/2}{sin\ \omega/2}\right)^2$	$1 - \frac{\tau}{\gamma}$
Hamming	$\frac{1}{2}D_\gamma(\omega) + \frac{1}{4}D_\gamma(\omega - \frac{\pi}{\gamma})$ $+\frac{1}{4}D_\gamma(\omega + \frac{\pi}{\gamma})$, where $D_\gamma(\omega) = \frac{sin(\gamma+\frac{1}{2})\omega}{sin(\omega/2)}$	$\frac{1}{2}(1 + cos\frac{\pi\tau}{\gamma})$

Table 3.1: Windows for spectral estimation.

The first point refers to a sufficient reduction of variance, whereas the second point refers to the avoidance of substantial bias.

The application of a lag window in the time domain, has a direct interpretation as a smoothing operation in the frequency domain. Using the fact that $\hat{R}_u^N(\tau)$ and $\hat{\Phi}_u^N(\omega)$ are related through Fourier transform, and using the fact that multiplication in the time-domain relates to convolution in the frequency domain, the following derivation becomes trivial

$$\hat{\Phi_u^N}(\omega) = \sum_{\tau=-\infty}^{\infty} w_\gamma(\tau) \cdot \hat{R}_u^N(\tau)e^{-i\omega\tau} \tag{3.60}$$

$$= \mathcal{F}\{w_\gamma(\tau) \cdot \hat{R}_u^N(\tau)\} \tag{3.61}$$

$$= W_\gamma(\omega) \star \frac{1}{N}|U_N(\omega)|^2 \tag{3.62}$$

$$= \frac{1}{2\pi}\int_{-\pi}^{\pi} W_\gamma(\xi - \omega)\frac{1}{N}|U_N(\xi)|^2 d\xi \tag{3.63}$$

where the *frequency window* $W_\gamma(\omega)$ is the Fourier transform of the lag window $w_\gamma(\tau)$, i.e.

$$w_\gamma(\tau) = \frac{1}{2\pi}\int_{-\pi}^{\pi} W_\gamma(\xi)e^{i\xi\tau}d\xi, \tag{3.64}$$

and where the $\star$ in (3.62) is the convolution operator.

The frequency-windows $W_\gamma(\omega)$, equivalent to the previously presented lag windows, are given in Table 3.1 also, and their characteristics are sketched in Figure 3.4. In this plot the frequency window for the rectangular lag-window has been scaled by 0.5 in order to give it a similar amplitude as the other two windows. It is clearly illustrated in these figures how the several frequency-windows perform their smoothing operation. The higher the value of γ the narrower the window, and the less smoothing operation is performed when applying the window to the periodogram estimate, as in (3.63). If γ is chosen small, then the spectrum estimate is a smoothed version of the periodogram, where a wide frequency region is averaged out. Finding a correct choice of γ is sometimes a difficult task. Choosing γ too small may result in a spectral estimate in which relatively sharp peaks in the real spectrum have been smoothed out, and choosing γ too big will result in an erratic spectral estimate, having too high variance.
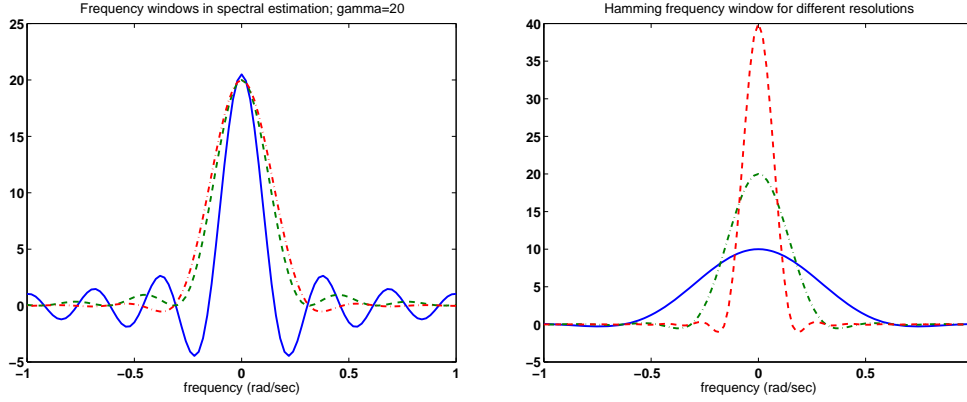
Figure 3.4: Frequency-windows in spectral estimation. Left: $W_\gamma(\xi)$, $\gamma = 20$ for rectangular window (solid), Bartlett window (dashed) and Hamming window (dash-dotted). Right: $W_\gamma(\xi)$ of Hamming window for $\gamma = 10$ (solid), $\gamma = 20$ (dash-dotted) and $\gamma = 40$ (dashed).

3.5.4 Periodogram averaging - Welch's method

Another approach to the estimation of signal spectra is by averaging periodogram estimates over several data segments. In this method one decomposes a signal of length N into r sequences of length N_0 and constructs a periodogram of each sequence:

$$\breve{\Phi}_{u,j}^N(\omega) = \frac{1}{N_0}|U_{N_0,j}(\omega)|^2 \tag{3.65}$$

where j denotes the different sequences, $j = 1, \cdots r$.
A spectral estimate of the signal u is then obtained by averaging over the several periodograms:

$$\hat{\Phi_u^N}(\omega) = \frac{1}{r}\sum_{j=1}^r \breve{\Phi}_{u,j}^N(\omega). \tag{3.66}$$

This idea refers to the classical way of reducing the variance of an estimate by taking averages of several independent estimates. Independence of the several estimates will only be possible when the several data segments do not overlap. In general the data segments will be chosen with a length N_0 that is a power of 2, in order to facilitate efficient calculation of the periodograms through Fast Fourier Transform.
Also in this method the conflicting aspects of reducing the variance and obtaining a high frequency resolution are present. Variance reduction is related to the number of averages r that is achieved, while the frequency resolution is related to the number of data samples in a data segment. In finding a satisfactory compromise between these choices, the use of overlapping data segments is also possible.
If u is a stochastic process, this method of periodogram averaging has some relationship with a windowing operation related to the windows discussed in section 3.5.3. This can be observed from the following derivation.
Let $u_j(t)$ denote the signal in the j-th data segment, then

$$\frac{1}{N_0}|U_{N_0,j}(\omega)|^2 = \sum_{\tau=-\infty}^{\infty} \hat{R}_{u_j}^{N_0}(\tau)e^{-i\omega\tau} = \frac{1}{N_0}\sum_{\tau=-\infty}^{\infty}\sum_{t=0}^{N_0-1} u_j(t)u_j(t-\tau)e^{-i\omega\tau}, \tag{3.67}$$

using the convention that $u_j(t) := 0$ outside the interval $[0, N_0 - 1]$.

As a result we can write

$$\frac{1}{r} \sum_{j=1}^{r} \frac{1}{N_0} |U_{N_0,j}(\omega)|^2 = \frac{1}{r} \sum_{j=1}^{r} \sum_{\tau=-N_0}^{N_0} \frac{1}{N_0} \sum_{t=0}^{N_0-1} u_j(t) u_j(t-\tau) e^{-i\omega\tau} \qquad (3.68)$$

which leads to

$$E\hat{\Phi_u^N}(\omega) = \sum_{\tau=-N_0}^{N_0} \frac{N_0 - |\tau|}{N_0} R_u(\tau) e^{-i\omega\tau}, \qquad (3.69)$$

where $R_u(\tau) := Eu(t)u(t-\tau) = Eu_j(t)u_j(t-\tau)$.

Through averaging of periodograms, apparently a lag-window is applied to the correlation function of the signal, being the same as the (triangular) Bartlett-window discussed in the previous section. Note the difference however that here the lag window is applied to the correlation function R_u, while in spectral estimation the lag window is applied to the sample correlation $\hat{R}_u^N(\tau)$. In the frequency domain the effect of the averaging of periodograms naturally relates to the application of the Bartlett frequency window, convoluted with the spectral density $\Phi_u(\omega)$.

For this reason, the procedure of periodogram averaging is also known as the Bartlett-procedure. When the averaging mechanism is combined with a data window it is referred to as the Welch-method, see also Therrien (1992).

3.5.5 Spectral estimate and ETFE

Returning to the frequency response estimate of a dynamical system, based on estimates of the auto- and cross-spectral densities, as given in section 3.5.1, the use of smoothed spectral estimates leads to:

$$\hat{G}_N(e^{i\omega}) = \frac{\dfrac{1}{2\pi} \displaystyle\int_{-\pi}^{\pi} W_\gamma(\xi - \omega) \dfrac{1}{N} Y_N(\xi) U_N^*(\xi) d\xi}{\dfrac{1}{2\pi} \displaystyle\int_{-\pi}^{\pi} W_\gamma(\xi - \omega) \dfrac{1}{N} |U_N(\xi)|^2 d\xi}. \qquad (3.70)$$

It appears that this estimate is equal to the ETFE estimate after smoothing, as shown in section 3.4.3, (3.47). As a result the two different philosophies for arriving at a frequency response estimate of a dynamical system, either by smoothing the ETFE or by spectral division based on smoothed spectral estimates, bring us to one and the same solution. The only difference between the two estimates is in the way the smoothing or windowing operation is performed:

- For smoothing the *ETFE* the smoothing operation has to be applied in the frequency domain. The required convolution in this (continuous) frequency domain has to be approximated by a convolution over discrete frequency samples.

- In spectral analysis the smoothing operation is applied to the sample auto-correlation $\hat{R}_u^N(\tau)$ and cross-correlation $\hat{R}_{yu}^N(\tau)$ in the time-domain. No approximation is required here.

When no smoothing is applied to the ETFE and the spectral estimate, both algorithms lead to one and the same estimated frequency response $\hat{G}_N(e^{i\omega})$.

Example 3.5.2 *Example 3.4.1 continued.*
The non-parametric estimation methods discussed in the previous sections are applied to
input/output data from the data generating system of Example 3.4.1, where the input is a
zero mean unit variance white noise signal, and the data has length $N = 2560$. Frequency
response estimates using Fourier analysis are depicted in Figure 3.5.
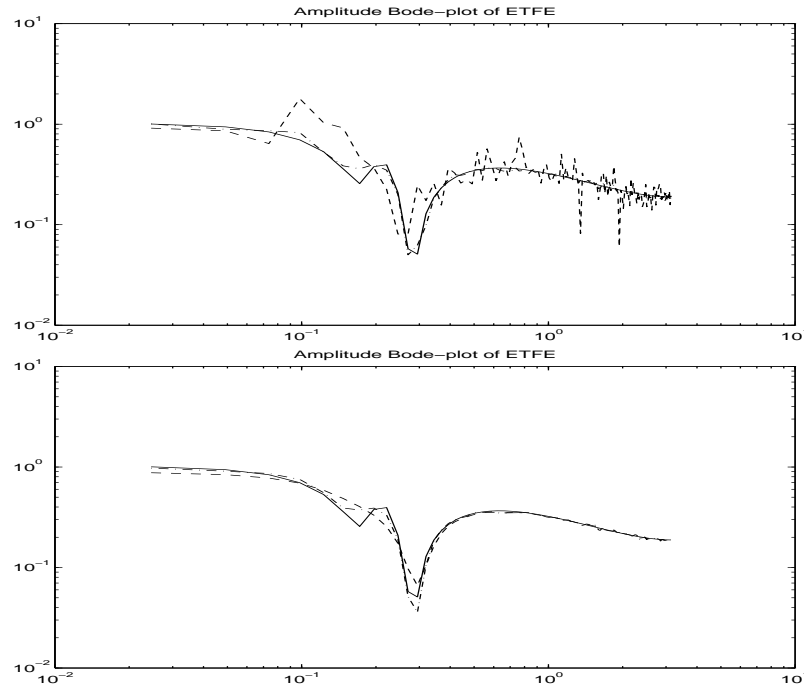
Figure 3.5: Frequency response estimates by (smoothed) ETFE. Upper: Bode amplitude
plot of G_0 (solid), ETFE (dashed) and smoothed ETFE with $\gamma = 200$ (dotted). Lower:
Bode amplitude plot of G_0 (solid), ETFE with $\gamma = 30$ (dashed) and ETFE with $\gamma = 70$
(dash-dotted).

Results are given for several values of the width of the Hamming window that is applied in
order to smooth the ETFE's. As is clear from the upper plot in Figure 3.5 the raw ETFE is
a very erratic function. Smoothing the ETFE with a very narrow frequency filter ($\gamma = 200$)
reduces the variance drastically.
The lower plot in Figure 3.5 shows that when using a wider frequency window (smaller
values of γ), the variance in the estimate is reduced, however at the cost of an increasing
bias. Especially for the given system G_0 which has rather sharp curves in its frequency
response, an appropriate choice of window is a rather difficult task.
Figure 3.6 shows similar results, now for frequency response estimates that are obtained
by spectral analysis, with a Hamming window being applied to the sample cross-variance
function. This sample cross-correlation function, together with the Hamming windows that
have been applied, are depicted in Figure 3.7. As is clearly illustrated in this latter figure,
the choice $\gamma = 10$ causes a substantial part of the system dynamics to be filtered out by the
window, leading to a substantial bias. The choice $\gamma = 30$ is the version that is the default
choice suggested by the appropriate `MATLAB`-routine.
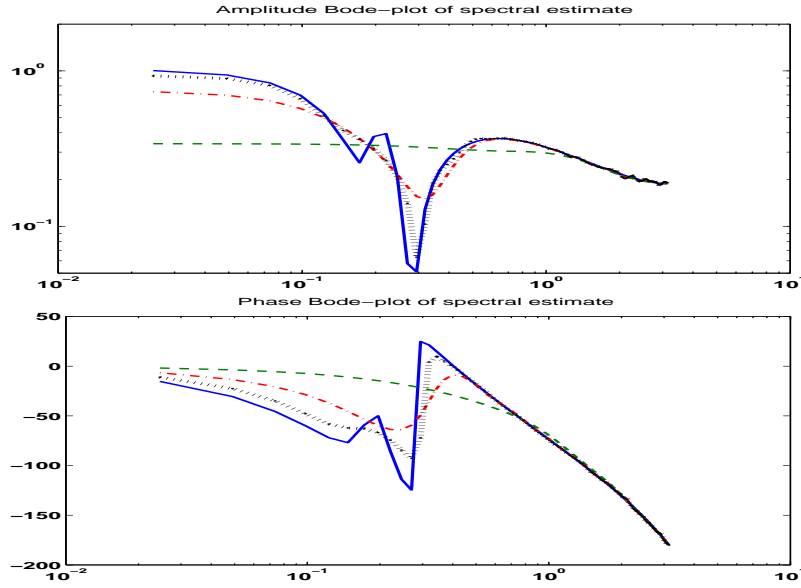
Figure 3.6: Frequency response estimates by (smoothed) spectral analysis using a Hamming window with lag width $\gamma = 10, 30, 70$. Bode amplitude (upper) and phase (lower) plot of G_0 (solid) and estimates with $\gamma = 10$ (dashed), $\gamma = 30$ (dash-dotted) and $\gamma = 70$ (dotted).

3.5.6 Extension to the multivariable case

The nonparametric estimation techniques are also fit for estimating the frequency response of multivariable systems having m inputs and p outputs. One of the important aspects that has to be taken into account then, is that the standard estimate of the input spectral density function:

$$\breve{\Phi}_u^N(\omega) = \frac{1}{N} U_N(\omega) U_N^*(\omega)$$

now becomes an $m \times m$ matrix which by construction has rank 1 since $U_N(\omega)$ is an length-m column vector. As a result this matrix will not be invertible. Typically one will need m different experiments with Fourier-transformed inputs $U_N^{(i)}(\omega)$, $i = 1, \cdots m$, to construct an estimate

$$\breve{\Phi}_u^N(\omega) = \frac{1}{m} \sum_{i=1}^{m} \frac{1}{N} U_N^{(i)}(\omega)(U_N^{(i)})^*(\omega)$$

that is invertible, and can be used in the expressions for estimating the multivariable frequency response.

If in each of the m experiments only one input is excited, e.g. in experiment i input number i is excited only, then matrix $\breve{\Phi}_u^N(\omega)$ becomes diagonal. Note however that separate excitation of the inputs is not necessary for obtaining an invertible matrix.

3.5.7 Coherency spectrum

Estimating the input/output dynamical system is only one of the interesting phenomena in revealing the underlying data generating system from observed input and output variables. Additionally it may be very illuminating to be able to make statements about the disturbance v and its spectral density $\Phi_v(\omega)$ that is contaminating our output measurements, as
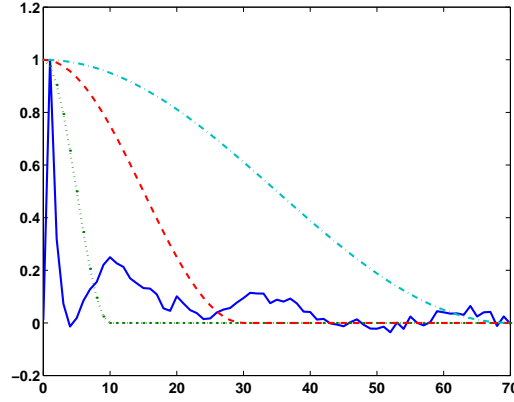
Figure 3.7: Sample cross-correlation function $\hat{R}_{yu}^N(\tau)$ (solid) together with the Hamming lag-windows applied in Figure 3.6, $w_{10}(\tau)$ (dotted), $w_{30}(\tau)$ (dashed) and $w_{70}(\tau)$ (dash-dotted).

specified in (3.1). As the signal v is not directly measurable estimates of $\Phi_v(\omega)$ will have to be based on input and output measurements also.

As

$$\Phi_{yu}(\omega) = G_0(e^{i\omega})\Phi_u(\omega) \quad \text{and} \tag{3.71}$$

$$\Phi_y(\omega) = |G_0(e^{i\omega})|^2\Phi_u(\omega) + \Phi_v(\omega) \tag{3.72}$$

substituting both equations into one another shows that

$$\Phi_v(\omega) = \Phi_y(\omega) - \frac{|\Phi_{yu}(\omega)|^2}{\Phi_u(\omega)}. \tag{3.73}$$

Thus a straightforward estimate of the disturbance spectrum is obtained by

$$\hat{\Phi_v^N}(\omega) = \hat{\Phi_y^N}(\omega) - \frac{|\hat{\Phi_{yu}^N}(\omega)|^2}{\hat{\Phi_u^N}(\omega)}. \tag{3.74}$$

The quantity

$$C_{yu}(\omega) := \sqrt{\frac{|\Phi_{yu}(\omega)|^2}{\Phi_y(\omega)\Phi_u(\omega)}} \tag{3.75}$$

is defined as the *coherency spectrum* between y and u. Taking positive real values between 0 and 1, it acts as a kind of frequency-dependent correlation coefficient between the input and output. It is closely related to the signal-to-noise ratio of the system, as it follows from simple calculations that

$$\Phi_v(\omega) = \Phi_y(\omega)[1 - C_{yu}(\omega)^2]. \tag{3.76}$$

For $C_{yu}(\omega) = 1$, the noise spectrum is zero at this frequency, and so the output of the system is completely determined by the noise free part $|G_0(e^{i\omega})|^2\Phi_u(\omega)$. For $C_{yu}(\omega) = 0$, the output spectrum equals the noise spectrum, $\Phi_y(\omega) = \Phi_v(\omega)$, and there is no contribution of the input signal in the output.
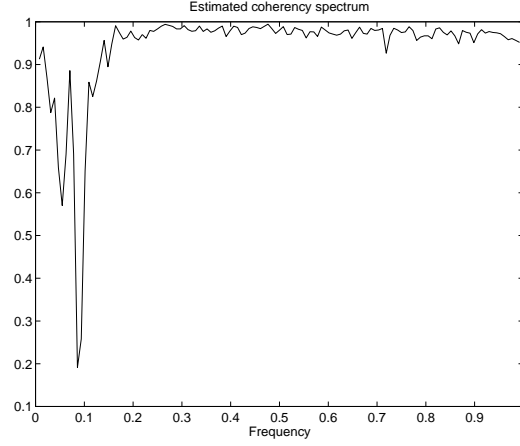
Figure 3.8: Estimated coherency spectrum for data in example 3.5.2. Estimates based on the Welch method of periodogram averaging with the data sequence divided into 10 segments of 256. The frequency axis is in $\pi rad/sec$.

An estimate of the coherency spectrum is obtained by

$$\hat{C}_{yu}^{N}(\omega) := \sqrt{\frac{|\hat{\Phi_{yu}^{N}}(\omega)|^2}{\hat{\Phi_y^{N}}(\omega)\hat{\Phi_u^{N}}(\omega)}}. \tag{3.77}$$

For the data as handled in example 3.5.2 the estimated coherence spectrum is given in Figure 3.8.

Note that in this example, the dips in the estimated coherence spectrum are not caused by an increasing power of the noise disturbance term at these frequencies, but rather by two zeros of G_0 that are located close to the unit circle, with frequencies $0.09\pi rad/sec$ and $0.055\pi rad/sec$.

For constructing an estimate of the coherency spectrum it is necessary that the auto- and cross-spectral densities are smoothed versions of the periodogram estimates. If no smoothing is applied, and consequently the (raw) periodograms are taken as spectral estimates, then substitution into (3.77) shows that

$$\hat{C}_{yu}^{N}(\omega) = \sqrt{\frac{[\frac{1}{N}Y_N(\omega)U_N^*(\omega)]^2}{\frac{1}{N}|Y_N(\omega)|^2 \cdot \frac{1}{N}|U_N(\omega)|^2}} = 1. \tag{3.78}$$

The estimate of the coherency spectrum will in this situation be fixed to 1, and it will not reveal any relevant information.

3.6 Relevant Matlab-commands

3.6.1 Correlation analysis

For correlation analysis the SYSTEM IDENTIFICATION TOOLBOX of MATLAB provides two different routines. One for the estimation of correlation functions, and one for the estimation of pulse responses.

Estimation of correlation functions

```
R = covf(z,M,maxsize)
R = covf(z,M)
```

For signals present in columns of `z`, `R` contains the sample cross-correlation functions of these signals, calculated at `M` time shifts. The estimate $\hat{R}_{z_j z_i}$ is returned in row number $i + (j-1) * nz$ of `R`, where nz is the number of signals in `z`.

Estimation of pulse responses

```
[ir,r,cl] = cra(z,M,NA,PLOT)
ir = cra(z)
```

For output and input data present in `z`, correlation analysis provides an estimate of the pulse response of the underlying system delivered in `ir`, having length `M` and starting with the direct feedthrough term.
The applied procedure is:

- Estimate an AR-model for the input signal u, i.e. $A(q)u(t) = \varepsilon(t)$ (see chapter 4).

- Construct the signals $u_F(t) = A(q)u(t)$ and $y_F(t) = A(q)y(t)$. $A(q)$ is a (prewhitening) filter constructed to make u_F as white as possible.

- Construct the sample cross-correlation function $\hat{R}_{y_F u_F}(\tau)$, and $\hat{R}_{u_F}(0)$.

- The estimated pulse response is determined by $g(\tau) = \hat{R}_{y_F u_F}(\tau)/\hat{R}_{u_F}(0)$.

`NA` is the order of the prewhitening filter, by default `NA = 10`.
`M` is the number of lags that is computed, by default `M = 20`.
`r` is a `M` $\times 4$ matrix containing as columns: τ, $\hat{R}_{y_F}(\tau)$, $\hat{R}_{u_F}(\tau)$ and $\hat{R}_{y_F u_F}(\tau)$.
`cl` is the 99% confidence level for the pulse response estimate.
The variable `PLOT` contains options for plotting the results.

3.6.2 Fourier Analysis

Frequency response estimation
For Fourier analysis there is one procedure in the SYSTEM IDENTIFICATION TOOLBOX of MATLAB that delivers a transfer function estimate on the basis of input and output signals.

```
[G] = etfe(DATA,M,N)
[G] = etfe(DATA,M)
[G] = etfe(DATA)
```

For output and input data present in `DATA`, in a `IDDATA`-object, a smoothed ETFE of the frequency response is provided in the `IDFRD`-object `G`, which is similar to a spectral analysis estimate by smoothing the raw spectral estimates with a Hamming window in the frequency domain. The Hamming window has a lag γ equal to `M`. The estimate `G` corresponds to

$$\hat{G}(e^{i\omega}) = \frac{W_\gamma(\omega) \star Y_N(\omega)U_N^*(\omega)}{W_\gamma(\omega) \star |U_N(\omega)|^2},$$

where the Hamming window $W_\gamma(\omega)$ is applied in the (discretized) frequency domain. The `IDDATA`- and `IDFRD`-objets are defined within Matlab's System Identification Tooolbox.
By default `M=[ ]` and no smoothing is applied; in this case `G` contains the ETFE of the process.
`N` is the number of frequency points; the frequency points are restricted to be linearly distributed over the interval $(0, \pi]$. `N` must be a power of 2. By default `N = 128`.

3.6.3   Spectral analysis

Estimation of frequency response and auto-spectral densities
Transfer function estimation by spectral analysis can be done in two different procedures. The SYSTEM IDENTIFICATION TOOLBOX of MATLAB provides the following method, based on the so-called Blackman-Tukey procedure of spectral estimation.

```
[G] = spa(DATA,M,w,maxsize)
[G] = spa(DATA)
[Gtf,Gnoi,Gio] = spa(DATA,...)
```

For output and input data present in the `IDDATA`-object `DATA`, a spectral estimate of the frequency response is provided in `IDFRD`-object `G`, using a spectral analysis estimates $\hat{\Phi_{yu}^N}(\omega)$ and $\hat{\Phi_u^N}(\omega)$, with a Hamming window with lag $\gamma = $ `M`. Additionally the noise spectrum is estimated in `Gnoi` and the spectrum of the joint input and output signals in `Gio`. The estimate `G` corresponds to

$$\hat{G}(e^{i\omega}) = \frac{\sum_{\tau=-\gamma}^{\gamma} w_\gamma(\tau)\hat{R}_{yu}(\tau)e^{i\omega\tau}}{\sum_{\tau=-\gamma}^{\gamma} w_\gamma(\tau)\hat{R}_u(\tau)e^{i\omega\tau}}.$$

When `z` is only one signal, `G` contains its auto-spectral density estimate.
The variable `w` is an (optional) user-provided set of frequencies at which the frequency response has to be estimated. Default, 128 frequency points are picked linearly distributed over the interval $(0, \pi]$.
The default value of M is chosen to be $M = min(30, length(z)/10)$. `maxsize` is a variable related to memory trade-off.

Estimation of frequency response, signal spectral and coherency spectrum
A second method for spectral analysis is present in the SIGNAL PROCESSING TOOLBOX of MATLAB; it is meant not only for transfer function estimation, but also delivers auto- and cross-spectral densities of signals, as well as a coherency spectrum estimate.

```
Pxx = pwelch(x)
[Pxx,w] = pwelch(x)
```

Given a time-signal in `x`, an estimate are provided for the spectral density of this signal, by applying the Welch method of periodogram averaging for spectral estimation. `w` contains the frequencies at which the spectral density is estimated.

```
Cxy = mscohere(x,y)
```

For time signals present in vectors `x` and `y`, `mscohere` provides the magnitude squared coherence estimate `Cxy`, using Welch's averaged periodogram method.

3.7   Summary

In this section basic methods have been discussed to estimate a non-parametric frequency response (sometimes called a FRF - frequency response function) directly from input and output data.

For periodic input signals and an integer number of periods, the Emperical Transfer Function Estimate (ETFE) leads to an unbiased estimate in a fixed number of frequencies with a variance tending to 0 for increasing data length. For general input signals (e.g. deterministic sequences generated by a random generator) the ETFE will generally be an erratic function of frequency, which requires a smoothing operation before it can be sensibly interpreted.

Appendix

Theorem 3A.1 (Transformation of DTFT's) *Let $G(q) = \sum_{k=0}^{\infty} g(k)q^{-k}$ be a dynamical system satisfying $\sum_{k=0}^{\infty} k|g(k)| < \infty$, relating the quasi-stationary signals $u(t)$, $y(t)$ through:*

$$y(t) = G(q)u(t)$$

while u satisfies $|u(t)| \leq \bar{u}$ for all t (including $t < 0$). Then

$$Y_N(\omega) = G(e^{i\omega}) \cdot U_N(e^{i\omega}) + R_N(\omega) \tag{3A.1}$$

with

(a) If u is periodic with period N, then $R_N(\omega) = 0$ for $\omega = \frac{2\pi k}{N}$.

(b) For general u, $|R_N(\omega)| \leq c_1$ and $c_1 = 2\bar{u} \sum_{k=0}^{\infty} k|g(k)|$.

(c) If G has a finite pulse response: $G(q) = \sum_{k=0}^{N_g} g(k)q^{-k}$ then $R_N(\omega) = 0$ if $u(t) = 0$ for $t \in [-N_g, -1] \cup [N - N_g, N - 1]$.

Proof:
Part (a).
By applying the definition of the DTFT it follows that

$$
\begin{aligned}
Y_N(\omega) &= \sum_{t=0}^{N-1} \sum_{k=0}^{\infty} g(k)u(t-k)e^{-i\omega t} \\
&= \sum_{t=0}^{N-1} \sum_{k=0}^{\infty} g(k)e^{-i\omega k}u(t-k)e^{-i\omega(t-k)}
\end{aligned}
$$

By change of variables: $t - k \to \tau$:

$$Y_N(\omega) = \sum_{k=0}^{\infty} g(k)e^{-i\omega k} \sum_{\tau=-k}^{N-1-k} u(\tau)e^{-i\omega\tau}.$$

The second term in this summation can be written as:

$$\sum_{\tau=-k}^{N-1-k} u(\tau)e^{-i\omega\tau} = \sum_{\tau=0}^{N-1} u(\tau)e^{-i\omega\tau} + \sum_{\tau=-k}^{-1} u(\tau)e^{-i\omega\tau} - \sum_{\tau=N-k}^{N-1} u(\tau)e^{-i\omega\tau}. \tag{3A.2}$$

If u is periodic with period N, then the second summation term satisfies

$$\sum_{\tau=-k}^{-1} u(\tau)e^{-i\omega\tau} = \sum_{\tau=N-k}^{N-1} u(\tau)e^{-i\omega(\tau-N)}$$

which for frequencies $\omega = \frac{2\pi k}{N}$ will satisfy

$$\sum_{\tau=N-k}^{N-1} u(\tau)e^{-i\frac{2\pi k}{N}(\tau-N)} = \sum_{\tau=N-k}^{N-1} u(\tau)e^{-i\frac{2\pi k}{N}(\tau)}$$

becoming equal to the third term in (3A.2). As a result for each value of k, $\sum_{\tau=-k}^{N-1-k} u(\tau)e^{-i\omega\tau} = \sum_{\tau=0}^{N-1} u(\tau)e^{-i\omega\tau} = U_N(\omega)$, showing that for $\omega = \frac{2\pi k}{N}$, $Y_N(\omega) = G(e^{i\omega})U_N(e^{i\omega})$.

The proof of part (b) can be found in Theorem 2.1 in Ljung (1999). The proof of (c) follows from a similar analysis and is left as an exercise.   □

Theorem 3A.2 *Let v be a stationary stochastic process, determined by*

$$v(t) = H(q)e(t)$$

with e a zero-mean white noise process with variance σ_e^2 and bounded moments of all orders, and H a stable proper transfer function. Let Ω_N denote the frequency grid determined by

$$\Omega_N := \{\frac{2\pi k}{N}, k = 0, \cdots, N-1\}.$$

Then for all $\omega \in \Omega_N$:

(a) $EV_N(\omega) = 0$ *for all N;*

(b) $\begin{pmatrix} Re\{\frac{1}{\sqrt{N}}V_N(\omega)\} \\ Im\{\frac{1}{\sqrt{N}}V_N(\omega)\} \end{pmatrix} \xrightarrow{d} \mathcal{N}(0, \Lambda),$ *for $N \to \infty$, with*

$$\Lambda = \begin{pmatrix} \frac{1}{2}\Phi_v(\omega) & 0 \\ 0 & \frac{1}{2}\Phi_v(\omega) \end{pmatrix} \quad \omega \neq 0, \pi \tag{3A.3}$$

$$= \begin{pmatrix} \Phi_v(\omega) & 0 \\ 0 & 0 \end{pmatrix} \quad \omega = 0, \pi. \tag{3A.4}$$

(c) DTFT's $V_N(\omega_1), V_N(\omega_2)$ for distinct frequencies ω_1, ω_2 are asymptotically independent.

Proof: The proof of Part (a) follows directly from considering that $v(t) = \sum_{k=0}^{\infty} h(k)e(t-k)$. Therefore $v(t)$ is a weighted sum of zero-mean independent random variables, implying that the result is also zero-mean. For the proofs of Parts (b) and (c) the reader is referred to Brillinger (1981).   □

Bibliography

D.R. Brillinger (1981). *Time Series - Data Analysis and Theory*. McGraw-Hill, New York, expanded edition.

P.M.T. Broersen (1995). A comparison of transfer function estimators. *IEEE Trans. Instrum. Measurem., 44*, pp. 657-661.

R.G. Hakvoort and P.M.J. Van den Hof (1995). Consistent parameter bounding identification for linearly parametrized model sets. *Automatica, 31*, pp. 957-969.

H. Hjalmarsson (1993). *Aspects on Incomplete Modelling in System Identification*. Dr. Dissertation, Dept. Electrical Engineering, Linköping University, Sweden.

G.M. Jenkins and D.G. Watts (1968). *Spectral Analysis and its Applications.* Holden-Day, Oakland, CA.

L. Ljung (1999). *System Identification - Theory for the User.* Prentice-Hall, Englewood Cliffs, NJ, Second edition.

L. Ljung and T. Glad (1994). *Modeling of Dynamic Systems.* Prentice Hall, Englewood Cliffs, NJ.

A.V. Oppenheim and R.W. Schafer (1989). *Discrete-time Signal Processing.* Prentice Hall, Englewood Cliffs, NJ.

R. Pintelon and J. Schoukens (2001). *System Identification - A Frequency Domain Approach.* IEEE Press, Piscataway, NJ, USA, ISBN 0-7803-6000-1.

M.B. Priestley (1981). *Spectral Analysis and Time Series.* Academic Press, London, UK.

T. Söderström and P. Stoica (1989). *System Identification.* Prentice-Hall, Hemel Hempstead, U.K.

C.W. Therrien (1992). *Discrete Random Signals and Statistical Signal Processing.* Prentice Hall, Englewood Cliffs, NJ.

Chapter 4

Prediction error identification methods

4.1 Introduction

Identification of parametric models is basically motivated by the fact that in many applications and in many situations that we need a representation of a dynamical system in terms of a model, nonparametric representations as e.g. Bode plots, Nyquist plots, step responses etc. are not sufficient. When considering several application areas in which models are used, as e.g.

- Process simulation

- Prediction of future behaviour

- Control design

it is apparent that nonparametric models can only be of limited use. As e.g. in process simulation it would be rather inefficient to simulate output signals on the basis of nonparametric system representations; in control design there are very efficient methods for designing controllers on the basis of (limited order) dynamical models. The capturing of the essential dynamics of a given dynamic system into a limited number of coefficients is the basic issue here.

This chapter deals with the identification of parametric linear dynamic models using so-called prediction error methods. Prediction error methods have become a wide-spread technique for system identification. Being developed in the last three decades, the stage has now been reached that there are (relatively) user-friendly software tools available for solving these prediction error identification problems. In the engineering community the *System Identification Toolbox* of *MATLAB*[1] has become the basic tool for dealing with these problems.

There are several books treating the class of prediction error methods. In this chapter we will give a brief overview of techniques, results, and interpretations, staying quite close to the material presented in Ljung (1987). In general we will restrict attention to the case of processes having scalar input and output signals. Despite problems of identifiability of

---

[1]Trademark of Mathworks, Inc.

parametrizations, most results and discussions will have straightforward extensions to the multivariable case.

4.2 Systems and disturbances

We will pay attention to dynamical systems of the form

$$y(t) = G(q)u(t) + v(t) \tag{4.1}$$

where $G(z)$ is a proper rational transfer function that is analytic (i.e. has no poles) in $|z| \geq 1$, which means that the dynamical system is stable. The system G thus has the property that it is LTIFD (linear time-invariant finite-dimensional). In (4.1) $\{y(t)\}$ is the (measured) output signal, $\{u(t)\}$ the (measured) input signal, and $v(t)$ is a nonmeasurable disturbance term.

The dynamical system representation in terms of the transfer function G is of course an abstraction from reality. Many systems that are subject of investigation will not satisfy the LTIFD property, but will exhibit (small) deviations from this framework. Additionally, measurements that are taken from a dynamical system will always be contaminated with disturbance signals. In order to deal with all these effects, the disturbance terms $v(t)$ is added to the system equations. This signal $v(t)$ may reflect:

- measurement noise, induced by measurement devices;

- process disturbances;

- effect of nonmeasurable input signals;

- effects of system linearization.

Actually the disturbance term $v(t)$ is supposed to reflect all deviations of the LTIFD framework that occur in the measurement data.

It has to be noted that the location of the disturbance term v on the output of the system is not a severe restriction, as long as we deal with linear systems. Because of the principle of superposition, both input, process and output disturbances can be characterized as an output disturbance.

The question how to model the disturbance signal $v(t)$ is quite an important one. It should be able to reflect all disturbance terms that one expects to be present in a given situation. Several disturbance "paradigms" are possible. In the area of so-called "bounded error models" the disturbance $v(t)$ is e.g. modelled as a signal that belongs to the class of signals characterized by

$$|v(t)| \leq \bar{v} \in \mathbb{R}, \tag{4.2}$$

formally denoted as $\|v\|_{\ell_\infty} \leq \bar{v}$. For an overview of these so-called bounded error models see e.g. Milanese et al. 1996.

In prediction error identification, as will be treated in this chapter, the disturbance v is modelled as a zero-mean stationary stochastic process with a (rational) spectral density $\Phi_v(\omega)$. This means that we can write

$$v(t) = H(q)e(t) \tag{4.3}$$
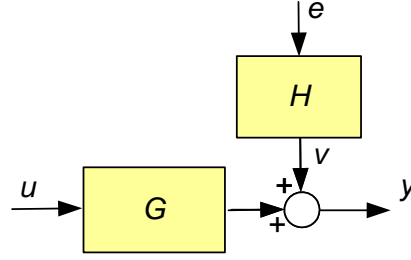
Figure 4.1: Data-generating system.

where $H(z)$ is a proper rational transfer functions that is stable, and $\{e(t)\}$ is a sequence of zero mean, identically distributed, independent random variables (white noise).

The transfer function $H(z)$ will be restricted to be monic, i.e. $H(z)$ has a Laurent expansion around $z = \infty$,

$$H(z) = 1 + \sum_{k=1}^{\infty} h_k z^{-k} \tag{4.4}$$

and $H(z)$ is minimum-phase, i.e. it has a stable inverse.

The assumption that $H(z)$ has a stable inverse is motivated by the fact that for every stochastic process w with a rational spectral density $\Phi_w(\omega)$, there exists a stable and stably invertible $H(z)$ such that $\Phi_w(\omega) = \Phi_v(\omega)$, with v defined by $v(t) = H(q)e(t)$. Suppose that we would have data that had been generated by a system (4.1) with H non-minimum-phase, then there exists a minimum-phase H_1 that generates output data that -as far as it concerns spectral properties of the signals- can not be distinguished from the original data.

$H(z)$ is restricted to be monic in order to guarantee a unique representation of (4.1). Since the disturbance signal e can not be measured its variance is not uniquely determined from (4.1). Note that this equation allows the level of the noise $v(t) = H(q)e(t)$ to be dependent on both the variance of e and the gain of H. By restricting H to be monic this freedom is removed from the representation, and thus for a given $\Phi_v(\omega)$ this results in a unique H and a variance σ_e^2 of e.

There has not been made a specification yet for the probability density function (pdf) of $e(t)$. It appears that when we limit attention to second order moments of v, i.e. its mean and its covariance function $R_v(\tau)$, these notions are independent of the pdf of e. Using

$$H(q) = \sum_{k=0}^{\infty} h(k) q^{-k} \tag{4.5}$$

one can construct the mean and covariance function of v by

$$Ev(t) = \sum_{k=0}^{\infty} h(k) Ee(t-k) = 0 \tag{4.6}$$

and

$$
\begin{aligned}
R_v(\tau) &:= Ev(t)v(t-\tau) \\
&= \sum_{k=0}^{\infty}\sum_{j=0}^{\infty} h(k)h(j)E[e(t-k)e(t-\tau-j)] \\
&= \sum_{k=0}^{\infty}\sum_{j=0}^{\infty} h(k)h(j)\sigma_e^2\delta(k-\tau-j) \\
&= \sigma_e^2 \sum_{k=0}^{\infty} h(k)h(k-\tau).
\end{aligned}
\tag{4.7}
$$

This supports the statement made above that the second order properties of v (and thus also of y) are dependent on H and σ_e^2.

4.3   Prediction

4.3.1   Introduction

The capability of a model to predict future values of signals will appear to be an important property when evaluating models as candidate representatives of systems to be modelled. In this section 4.3 we will analyze how general models of the form as presented in the previous section can serve as predictions. Here we will specifically direct attention to dynamical systems of the form (4.1).

4.3.2   One step ahead prediction of $y(t)$

Consider the situation
$$
y(t) = G(q)u(t) + v(t)
\tag{4.8}
$$
with $v(t) = H(q)e(t)$ as before.
We can formulate the following (one-step-ahead) prediction problem:

> Given the system (4.8), and given observations $\{(y(s), u(s)), s \le t-1\}$; what is the best prediction of $y(t)$?

In order to analyse this situation, the system equation can be rewritten:

$$
\begin{aligned}
y(t) &= G(q)u(t) + H(q)e(t) \\
&= G(q)u(t) + [H(q) - 1]e(t) + e(t).
\end{aligned}
$$

Note that the first two terms on the right hand side expression now contain signals that are available at time $t-1$, provided that $G(q)$ is strictly proper (i.e. it does not have a constant (direct feedthrough) term. By substituting $e(t) = H(q)^{-1}[y(t) - G(q)u(t)]$ into the second term of the latter equation equation, one obtains:

$$
y(t) = G(q)u(t) + [H(q) - 1]H^{-1}(q)[y(t) - G(q)u(t)] + e(t)
$$

and consequently

$$y(t) = H^{-1}(q)G(q)u(t) + [1 - H^{-1}(q)]y(t) + e(t). \tag{4.9}$$

The assumption that $H(z)$ proper, monic and has a stable inverse, implies that $H^{-1}(z)$ also is proper, monic and stable, i.e.

$$\frac{1}{H(z)} = 1 + d_1 z^{-1} + d_2 z^{-2} + \cdots$$

with $\{d_i\}$ a sequence which tends to 0. As a direct result of this, the expression

$$H^{-1}(q)G(q)u(t) + [1 - H^{-1}(q)]y(t)$$

is fully determined by $G(q)$, $H(q)$ and by past observations y^{t-1}, u^{t-1}. This expression will be referred to as the one-step-ahead predictor of $y(t)$, and denoted as

$$\hat{y}(t|t-1) = H^{-1}(q)G(q)u(t) + [1 - H^{-1}(q)]y(t) \tag{4.10}$$

As a result:

$$y(t) = \hat{y}(t|t-1) + e(t).$$

This equation represents a decomposition of $y(t)$ in a term $\hat{y}(t|t-1)$ that is available at time instant $t-1$, and a term $e(t)$ that is unavailable at that time.

The "best" prediction of $y(t)$ is not uniquely determined. There are several possibilities that can be chosen, dependent on the choice of what to be called as "best". Let the probability density function of $e(t)$ be denoted by $f_e(x)$. Then we can analyze the conditional probability density function of $y(t)$, given y^{t-1}, u^{t-1}. With $f_e(x)\Delta x \simeq P(x \leq e(t) \leq x + \Delta x)$ it follows that

$$\begin{aligned} P(x \leq y(t) \leq x + \Delta x \mid y^{t-1}, u^{t-1}) &= P(x \leq e(t) + \hat{y}(t|t-1) \leq x + \Delta x \mid y^{t-1}, u^{t-1}) \\ &= P(x - \hat{y}(t|t-1)) \leq e(t) \leq x - m(t-1) + \Delta x) \\ &= f_e(x - \hat{y}(t|t-1))\Delta x \end{aligned}$$

One possible choice is to pick that value of $y(t)$ for which $f_e(x - \hat{y}(t|t-1))$ has its maximum value. This is called the *maximum a posteriori (MAP) prediction*. Another predictor, that will be used throughout this chapter is the *conditional expectation* of $y(t)$, or $E(y(t)|y^{t-1}, u^{t-1})$. Because of the fact that $Ee(t) = 0$ for all t, it follows that

$$E(y(t)|y^{t-1}, u^{t-1}) = \hat{y}(t|t-1)$$

In other words, the one-step-ahead predictor (4.10) has the interpretation of being the best one-step-ahead predictor in the sense of the conditional expectation. And this holds irrespective of the probability density function of e, as long as $Ee(t) = 0$.

The conditional expectation of $y(t)$, as denoted above, has an additional property; it is the best one step ahead prediction of $y(t)$ if we consider a quadratic error criterion.
Let $\tilde{y}(t)$ be an arbitrary function of (y^{t-1}, u^{t-1}). Then

$$E[y(t) - \tilde{y}(t)]^2 \geq Ee(t)^2 \tag{4.11}$$

and equality is obtained for $\tilde{y}(t) = \hat{y}(t|t-1)$.

Remark 4.3.1 *If $G(z)$ is not strictly proper, i.e. if $G(z)$ has a constant (direct feedtrough) term, then $G(q)u(t)$ is not completely known at time instant $t-1$, as it also contains a term that is dependent on $u(t)$. In that situation, the one-step-ahead prediction $\hat{y}(t|t-1)$ is defined by $E(y(t)|y^{t-1}, u^t)$.*

The prediction result implies that one can predict the next sample of a zero-mean stochastic (noise) process given observations from the past. This is illustrated in the following example.

Example 4.3.2 Consider the stochastic process

$$v(t) = e(t) + ce(t-1) \tag{4.12}$$

with e a unit-variance white noise process. Then

$$H(q) = 1 + cq^{-1}$$
$$H(z) = 1 + cz^{-1}$$
$$H(z)^{-1} = \frac{z}{z+c}.$$

The latter function is stable for $|c| < 1$. In that case

$$H^{-1}(z) = \frac{1}{1+cz^{-1}} = \sum_{k=0}^{\infty}(-cz^{-1})^k = \sum_{k=0}^{\infty}(-c)^k z^{-k}$$

The expression for the one-step-ahead predictor now follows from (4.10) with $G(q) = 0$ and $y = v$, leading to

$$
\begin{aligned}
\hat{v}(t|t-1) &= [1 - \sum_{k=0}^{\infty}(-c)^k q^{-k}]v(t) \\
&= \frac{cq^{-1}}{1+cq^{-1}}v(t) = \frac{c}{1+cq^{-1}}v(t-1)
\end{aligned}
$$

leading to

$$\hat{v}(t|t-1) = cv(t-1) - c\hat{v}(t-1|t-2). \tag{4.13}$$

As a result the one step ahead predictor can be constructed through a recursive relation based on $\{v(t)\}$.   □

The one-step-ahead predictor has been derived for the situation that the datagenerating mechanism that generates $y(t)$ is described by a model $G(q), H(q)$ that is known. If y satisfies this condition, then apparently

$$y(t) - \hat{y}(t|t-1) = e(t)$$

which is a direct result of the derivation of (4.10).
For general $y(t)$ however, one can now denote the one-step-ahead prediction error as:

$$\varepsilon(t) := y(t) - \hat{y}(t|t-1) \tag{4.14}$$

This prediction error can only be calculated a posteriori, when the measurement $y(t)$ has become available. Substituting equation (4.10) for the one-step-ahead prediction, the prediction error reads:

$$\varepsilon(t) = H^{-1}(q)[y(t) - G(q)u(t)] \qquad (4.15)$$

This prediction error $\varepsilon(t)$ is exactly that component of $y(t)$ that could not have been predicted at time instant $t - 1$. For this reason it is also called the *innovation* at time t. When we substitute the system relation (4.8) into (4.15) it is immediate that $\varepsilon(t) = e(t)$, but this of course only holds if the datagenerating system indeed is equal to $(G(q), H(q))$.

Remark 4.3.3 *With a similar line of reasoning an expression can be derived for the k-step-ahead ($k > 1$) prediction of $y(t)$, i.e. $E(y(t)|y^{t-k}, u^t)$. In that case in expression (4.10) for the one-step-ahead prediction, $H^{-1}(q)$ has to be replaced by $\bar{H}_k(q)H^{-1}(q)$ with*

$$\bar{H}_k(q) = \sum_{\ell=0}^{k-1} h(\ell)q^{-\ell} \qquad (4.16)$$

The one-step-ahead prediction of $y(t)$ can be calculated when past data y^{t-1}, u^t is available. However it has to be noted that this implies the assumption that an infinitely long data sequence is available. In general the two expressions $H^{-1}(q)G(q)$ and $[1 - H^{-1}(q)]$ in (4.10) will reflect series expansions in q^{-1} of infinite length. If we have data available from a certain time moment on, e.g. for $t \geq 0$, then (4.10) still can provide a prediction of $y(t)$, by assuming that $u^{-1}, y^{-1} = 0$. However this will only be an approximation of the optimal predictor, assuming zero initial conditions. The exact predictor, based on conditional expectation, can be calculated with the Kalman filter, incorporating a possibly nonzero initial state. Nevertheless we will deal with the predictor (4.10) in the sequel of this chapter, thereby implicitly assuming that the initial conditions are 0.

Remark 4.3.4 *As an alternative for the expression of the one-step-ahead prediction $\hat{y}(t|t-1)$ (4.10), we will also use the notation,*

$$\hat{y}(t|t-1) = W(q) \begin{bmatrix} u(t) \\ y(t) \end{bmatrix} \qquad (4.17)$$

with $W(q)$ the predictor function:

$$\begin{aligned} W(q) & := & [W_u(q) \ \ W_y(q)] \\ & = & [H^{-1}(q)G(q) \ \ \ 1 - H^{-1}(q)] \end{aligned}$$

4.3.3 Predictor models

A linear model, as it is used in this chapter, is determined by the relation

$$y(t) = G(q)u(t) + H(q)e(t) \qquad (4.18)$$

and possibly with the probability density function $f_e(\cdot)$ of e.
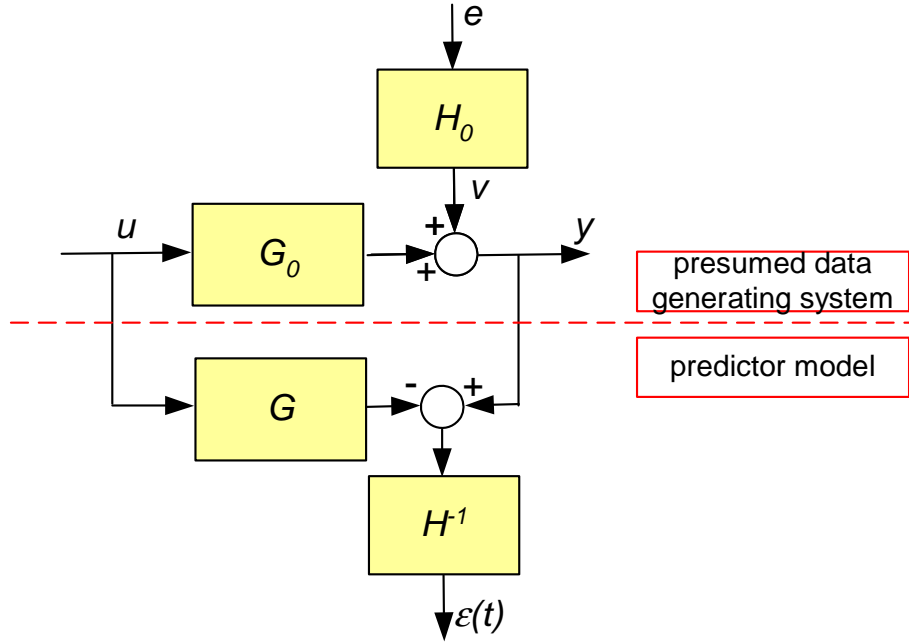
Figure 4.2: Data-generating system G_0, H_0 and predictor model G, H.

A particular model thus corresponds to the specification of $G(q), H(q)$ and $f_e(\cdot)$. For this model we can compute the one-step-ahead prediction $\hat{y}(t|t-1)$. Since this prediction is not dependent on $f_e(\cdot)$, the prediction properties of the model are only determined by $G(q), H(q)$. Models that are specified by only these two rational functions will be called *predictor models.*

How can we employ these models in the context of an identification problem?

Predictor models provide a (one-step-ahead) prediction of the output $y(t)$, given data from the past. The prediction error that is made can serve as a signal that indicates how well a model is able to describe the dynamics that underlies a measured data sequence. This can be visualized in the following block diagram in Figure 4.2, in which equations (4.3), (4.8) and (4.15) are combined.

In this respect the predictor model can be considered as a mapping from data u, y to a prediction error ε. If the data generating system G_0, H_0 is equal to the model G, H, then $\varepsilon = e$. However, also in the situation that the model differs from the data generating system, the model pertains its role as a predictor, and provides a predicted output signal and a prediction error.

4.4   Black box model structures and model sets

A predictor model is determined by a collection of two rational functions, $(G(z), H(z))$. For the purpose of system identification we need a set of models that can be considered as candidate models for the process to be modelled, and within which an optimal model is going to be determined, according to a specific criterion. In this respect a model set $\mathcal{M}$ is

defined as any collection of predictor models:

$$\mathcal{M} := \{(G(q,\theta), H(q,\theta)) \mid \theta \in \Theta \subset \mathbb{R}^d\} \qquad (4.19)$$

where a real valued parameter θ ranges over a subset of $\mathbb{R}^d$. It is assumed that this model set is composed of predictor models that exhibit the same properties as assumed in the foregoing part of this chapter, such as properness and stability of $G(z)$, $H(z)$ and stable invertibility and monicity of $H(z)$.

Underlying the set of models, there is a parametrization that determines the specific relation between a parameter $\theta \in \Theta$ and a model M within $\mathcal{M}$.
The *parametrization* of $\mathcal{M}$ is defined as a surjective mapping:

$$\tilde{M} \; : \; \Theta \to \mathcal{M} \qquad (4.20)$$

with Θ denoting the parameter set. There are many different ways of parametrizing sets of models as meant above. In prediction error identification methods a very popular way of parametrization is by parametrizing $G(q,\theta)$ and $H(q,\theta)$ in terms of fractions of polynomials in q^{-1}. As an example we will first discuss the -so called- *ARX* model set.

Definition 4.4.1 *ARX model set.*
An ARX model set is determined by two polynomials:

$$
\begin{aligned}
A(q^{-1},\theta) &= 1 + a_1 q^{-1} + a_2 q^{-2} + \cdots + a_{n_a} q^{-n_a} \\
B(q^{-1},\theta) &= b_0 + b_1 q^{-1} + b_2 q^{-2} + \cdots + b_{n_b-1} q^{-n_b+1}
\end{aligned}
$$

with

$$\theta := [a_1 \; a_2 \; \cdots \; a_{n_a} \; b_0 \; b_1 \; \cdots \; b_{n_b-1}]^T$$

such that

$$
\begin{aligned}
\mathcal{M} = \; & \{(G(q,\theta), H(q,\theta)) \mid \\
& G(q,\theta) = \frac{B(q^{-1},\theta)}{A(q^{-1},\theta)}, \; H(q,\theta) = \frac{1}{A(q^{-1},\theta)}, \; \theta \in \Theta \subset \mathbb{R}^{n_a+n_b}\}.
\end{aligned}
$$

$\square$

The acronym ARX can be explained when writing a corresponding model in its equation form:

$$y(t) = \frac{B(q^{-1},\theta)}{A(q^{-1},\theta)} u(t) + \frac{1}{A(q^{-1},\theta)} e(t)$$

or equivalently

$$A(q^{-1},\theta)y(t) = B(q^{-1},\theta)u(t) + e(t)$$

AR refers to the *Auto*Regressive part $A(q^{-1},\theta)y(t)$ in the model, while X refers to an e*X*ogenous term $B(q^{-1},\theta)u(t)$.
The model set is completely determined once the integers n_a, n_b and the parameter set Θ have been specified.

Note that an important aspect of the parametrization $\tilde{M}$ is, that it determines whether and in which way for every model in the set the two rational functions $G(z,\theta)$ and $H(z,\theta)$

ARX	$A(q^{-1})y(t) = B(q^{-1})u(t) + e(t)$
ARMAX	$A(q^{-1})y(t) = B(q^{-1})u(t) + C(q^{-1})e(t)$
OE, Output error	$y(t) = \dfrac{B(q^{-1})}{F(q^{-1})}u(t) + e(t)$
FIR, Finite impulse response	$y(t) = B(q^{-1})u(t) + e(t)$
BJ, Box-Jenkins	$y(t) = \dfrac{B(q^{-1})}{F(q^{-1})}u(t) + \dfrac{C(q^{-1})}{D(q^{-1})}e(t)$

Table 4.1: Model structures in equation form

are related to each other. The choice for an ARX model set implies that all models in the set have a common denominator in $G(z, \theta)$ and $H(z, \theta)$. Since this can be considered a structural property of the model set concerned, we will also refer to this model set as having an ARX *model structure*. This type of structural property of a model set will appear to have important consequences, as will be shown in the sequel of this chapter.

Apart from the ARX model structure, there exists a number of other model structures, that are frequently applied in identification problems. The most important ones are listed in Table 4.1, in which each model structure is denoted in an equation form and denoted with an appropriate name.

Note that in Table 4.1, the polynomials $A(q^{-1})$, $B(q^{-1})$, $C(q^{-1})$, $D(q^{-1})$ and $F(q^{-1})$ are polynomials in q^{-1} with respective degrees n_a, $n_b - 1$, n_c, n_d, n_f, and that $A(q^{-1})$, $C(q^{-1})$, $D(q^{-1})$ and $F(q^{-1})$ are monic [2]. The coefficients of the polynomials are collected in a parameter vector θ, which - for brevity - has not been denoted in the table.

The choice for applying a specific model structure in an identification problem can be a very important issue. Choosing the wrong structure, may lead to identified models that are "bad". The choice for a specific model structure can be based on a priori information on the process to be modelled (knowledge about how and where disturbance signals enter our process); however it can also appear during the identification and validation procedure (e.g. residual tests indicate that a specific extension of the model structure is required). The choice may also be dictated by other arguments dealing with specific properties of the

---

[2] The degree for polynomial B has been chosen $n_b - 1$ rather than n_b in order to comply with the use of this variable in the System Identification Matlab Toolbox. In this way all integer variables n_a - n_f reflect the number of unknown parameters in the respective polynomials.

Model structure	$G(q,\theta)$	$H(q,\theta)$
ARX	$\dfrac{B(q^{-1},\theta)}{A(q^{-1},\theta)}$	$\dfrac{1}{A(q^{-1},\theta)}$
ARMAX	$\dfrac{B(q^{-1},\theta)}{A(q^{-1},\theta)}$	$\dfrac{C(q^{-1},\theta)}{A(q^{-1},\theta)}$
OE	$\dfrac{B(q^{-1},\theta)}{F(q^{-1},\theta)}$	1
FIR	$B(q^{-1},\theta)$	1
BJ	$\dfrac{B(q^{-1},\theta)}{F(q^{-1},\theta)}$	$\dfrac{C(q^{-1},\theta)}{D(q^{-1},\theta)}$

Table 4.2: Model structures in transfer functions form

model structure. Concerning this latter situation, we have to mention two properties of model structures that will appear to be important.

Linearity-in-the-parameters.
The model structures ARX and FIR have the property that the one-step-ahead prediction $\hat{y}(t|t-1)$, (4.10), is a linear function of the polynomial coefficients that constitute the parameter vector. For an *ARX* model structure the prediction becomes

$$\hat{y}(t|t-1) = B(q^{-1})u(t) + (1 - A(q^{-1}))y(t) \tag{4.21}$$

In the right hand side of this expression, it appears that all terms are simple products of one data sample and one polynomial coefficient. This implies that $\hat{y}(t|t-1)$ is an expression that is linear in the unknown θ.
A consequence of this linearity is that a least squares identification criterion defined on the prediction errors $\varepsilon(t)$ is a quadratic function in θ. As a result, there will be an analytical expression for the optimal parameter $\hat{\theta}$ that minimizes the quadratic criterion. The identification problem is a so-called linear regression problem, and is very attractive from a computational point of view. This situation will be given further attention in section 4.6. Note that for a FIR model structure the same situation holds, however now limited to the special case of $A(q^{-1}) = 1$. Actually the FIR model structure is simply a special case of an ARX model structure.

Independent parametrization of $G(q,\theta)$ and $H(q,\theta)$.
The model structures OE, FIR and BJ have the property that the two transfer functions $G(q,\theta)$ and $H(q,\theta)$ are parametrized independently in the corresponding model sets. This is shown by the fact that for these model structures there do not appear any polynomials that appear as common factors in G and H. More formally, for model sets of this structure there exists a decomposition of the parameter vector $\theta = \begin{pmatrix} \rho \\ \eta \end{pmatrix}$ such that

$$\mathcal{M} = \{(G(q,\rho), H(q,\eta)) \mid \rho \in \Gamma \subset \mathbb{R}^{d_1},\ \eta \in \Delta \subset \mathbb{R}^{d_2}\}.$$

Use of a model structure with this property has the advantage that in some specific situations the transfer functions $G(q,\rho)$ and $H(q,\eta)$ can be estimated independently from each other. More attention will be paid to this phenomenon in section 4.9.3.

In the analysis of asymptotic properties of the estimated models, we will have to impose some regularity and stability conditions on the model sets that we can handle. This is formalized in the following notion of a uniformly stable model set.

Definition 4.4.2 *A parametrized model set $\mathcal{M}$ with parameter set Θ is uniformly stable if*

- Θ *is a connected open subset of $\mathbb{R}^d$;*

- μ *is a differentiable mapping, and*

- *the family of transfer functions $\{W(z, \theta), \frac{\partial}{\partial \theta} W(z, \theta), \theta \in \Theta\}$ is uniformly stable, with W the predictor filters as defined in Remark 4.3.4.*   □

Without going into detail we make the statement that parametrized model sets having a model structure as discussed in this section will be uniformly stable if the parameter set is confined to a region such that the polynomials $A(z^{-1}, \theta)$, $F(z^{-1}, \theta)$, $C(z^{-1}, \theta)$, and $D(z^{-1}, \theta)$ have no zeros for $|z| \geq 1$.

The parametrizations of models that are discussed so far are limited to fractions of polynomials. However other parametrizations are also possible, as e.g. a parametrization in terms of state space representations like

$$
\begin{aligned}
x(t+1) &= A(\theta)x(t) + B(\theta)u(t) + K(\theta)e(t) \\
y(t) &= C(\theta)x(t) + D(\theta)u(t) + e(t)
\end{aligned}
$$

where a model is determined by the collection of matrices $\{A, B, C, D, K\}$ which are parametrized by some parameter vector θ. In the situation sketched it follows that

$$
\begin{aligned}
G(z, \theta) &= D(\theta) + C(\theta)[zI - A(\theta)]^{-1}B(\theta) \\
H(z, \theta) &= 1 + C(\theta)[zI - A(\theta)]^{-1}K(\theta).
\end{aligned}
$$

The optimal one-step ahead predictor for this model (under zero initial state conditions) can be calculated in the same way as before by using (4.10).

Another parametrization that will appear to be attractive from an identification point of view is a parametrization that generalizes the FIR model structure, by using a more general expansion than the one that is used in the FIR structure:

$$
y(t) = \sum_{k=0}^{n_g} c_k F_k(q)u(t) + e(t). \tag{4.22}
$$

In this expression $\{F_k(z)\}_{k=1,\dots}$ is chosen to be an (orthonormal) basis for the Hilbert space of all stable systems, and the expansion coefficients c_k are collected in the parameter vector θ. This parametrization is referred to as ORTFIR and is further discussed in chapter 5.

4.5 Identification criterion

As discussed before an identification procedure has three basic ingredients:

- experimental data $Z^N = \{y(1), u(1), y(2), u(2), \cdots, y(N), u(N)\}$;

- a model set $\mathcal{M}$, specifying the class of candidate models among which (an) optimal model(s) will be selected; and

- an identification criterion (sometimes called identification method), that - given Z^N and $\mathcal{M}$ - determines which model(s) to select from $\mathcal{M}$.

In prediction error identification methods, the model set $\mathcal{M}$ is a specified set of predictor models and the identification criterion is based on prediction errors.

Consider the situation that there is given a data sequence

$$Z^N := \{y(1), u(1), y(2), u(2), \cdots, y(N), u(N)\}$$

and a parametrized model set $\mathcal{M}$, induced by the parametrization $\tilde{M}$ with parameter set Θ.

Now every model $\tilde{M}(\theta)$, $\theta \in \Theta$, in the model set $\mathcal{M}$ can predict the output $y(t)$ based on y^{t-1}, u^t, and for every time instant $t = 1, 2, \cdots, N$ the actual prediction error can be determined by comparing prediction and actual measurement $y(t)$.

As a result, every parameter $\theta \in \Theta$ gives rise to a prediction error

$$\varepsilon(t, \theta) = y(t) - \hat{y}(t|t-1; \theta) \qquad t = 1, \cdots, N \tag{4.23}$$

An accurate model generates "small" prediction errors.

There are a number of methods for the identification of models, i.c. the estimation of parameters, on the basis of these prediction errors.

a. minimization of a scalar-valued function of $\varepsilon(t, \theta)$ over $\theta \in \Theta$;

b. employing the complete (assumed) probability density function of $\varepsilon(t, \theta)$ to maximize its a posterior probability; this leads to the *maximum likelihood (ML) method*;

c. correlating $\varepsilon(t, \theta)$ with specific signals and aiming at non-correlation; this leads to *instrumental variable (IV) methods*.

In this chapter we will mainly deal with an identification criterion that reflects a function minimization, as mentioned in (a). In section 4.6.5 brief attention will be given to an instrumental variable method for ARX models. For motivation of a particular criterion function consider the following Proposition.

Proposition 4.5.1 *Consider the cost function $V(\theta) = \bar{E}\varepsilon^2(t, \theta)$ with*

$$\varepsilon(t, \theta) \;=\; H(q, \theta)^{-1}[y(t) - G(q, \theta)u(t)] \quad and$$
$$y(t) \;=\; G_0(q)u(t) + H_0(q)e(t)$$

and $\{e\}$ a white noise process with variance σ_e^2.
Then $V(\theta) \geq \sigma_e^2$ for all θ, with equality for $\hat{\theta}$ if

$$\begin{cases} G(q, \hat{\theta}) = G_0(q) \\ H(q, \hat{\theta}) = H_0(q) \end{cases}$$

Proof: Substitution of the equations gives

$$\varepsilon(t, \theta) = \frac{G_0(q) - G(q, \theta)}{H(q, \theta)} u(t) + \frac{H_0(q)}{H(q, \theta)} e(t)$$

Since u and e are uncorrelated they both have an independent contribution to the power $V(\theta)$ of $\varepsilon(t, \theta)$. If $G(q, \hat{\theta}) = G_0(q)$ the power contribution from u is zero, and thus minimal. Since H_0 and $H(q, \theta)$ are both monic, it follows that

$$\frac{H_0(q)}{H(q, \theta)} e(t) = [1 + \gamma_1(\theta)q^{-1} + \gamma_2(\theta)q^{-2} + \cdots]e(t)$$

and since $\{e\}$ is a white noise process this term has a variance contribution of

$$[1 + \gamma_1(\theta)^2 + \gamma_2(\theta)^2 \cdots]\sigma_e^2.$$

Its minimum value of σ_e^2 is obtained if $\gamma_i = 0$ for all i, which is achieved by $H(q, \hat{\theta}) = H_0(q)$.
$\square$

Minimization of the power if the prediction error signal delivers correct estimates of the plant and noise dynamics, if possible. This observation is a motivation for applying an identification criterion based on this prediction error power.

The criterion considered above is based on an infinite number of data, and on an ensemble averaging. If there is only one finite data sequence available, an alternative has to be sought for. The most simple and most frequently applied criterion function in identification, is a quadratic function on $\varepsilon(t, \theta)$, denoted as

$$V_N(\theta, Z^N) = \frac{1}{N} \sum_{t=1}^{N} \varepsilon(t, \theta)^2 \tag{4.24}$$

where the relation between $\varepsilon(t, \theta)$ and the data Z^N is determined by the chosen parametrized model set.

The estimated parameter $\hat{\theta}_N$ is defined as

$$\hat{\theta}_N = \arg \min_{\theta \in \Theta} V_N(\theta, Z^N) \tag{4.25}$$

which means that $\hat{\theta}_N$ is the value for θ that minimizes $V_N(\theta, Z^N)$. This criterion is known as the *least squares criterion*. Sometimes it will implicitly be assumed that this minimizing argument of $V_N(\theta, Z^N)$ is unique. If this is not the case, arg min is considered to be the set of minimizing arguments.

The choice of a quadratic criterion function actually dates back to Gauss' work in the 18th century. It is a function that generally leads to satisfactory results. Besides it is very attractive from a computational point of view. In the case that a model set is chosen that has a model structure which is linear-in-the-parameters, the quadratic criterion function (4.24) leads to a quadratic optimization problem, which generally has a unique solution that can be calculated analytically (linear regression problem).

Remark 4.5.2 *One disadvantage of the quadratic criterion function is its relatively high sensitivity to outliers in the data, i.e. data samples that have extreme high amplitudes. This lack of robustness against "bad data" has been a motivation for studying alternative criterion functions that are robust with respect to unknown variations in the probability density function, see e.g. Huber (1981).* $\square$

Remark 4.5.3 *There are several generalizations possible of a quadratic criterion function. In a general form one can write:*

$$V_N(\theta, Z^N) = \frac{1}{N} \sum_{t=1}^{N} \ell(\varepsilon(t,\theta), \theta, t) \tag{4.26}$$

where $\ell(\cdot)$ is a specific norm on $\mathbb{R}$. This norm can be parametrized itself by θ too, as well as being time-variant, e.g. for dealing with measurement data that are considered to be of varying reliability over the length of the time interval. The latter situation is specifically applied in time-recursive identification methods, see e.g. Ljung and Söderström (1983). □

Remark 4.5.4 *In the multivariable case, and particularly in the case of multiple output signals, the prediction error ε will be vector valued. The multivariable analogon of the quadratic criterion function can then be written as*

$$V_N(\theta, Z^N) = \frac{1}{N} \sum_{t=1}^{N} \varepsilon^T(t,\theta) \Lambda \varepsilon(t,\theta) \tag{4.27}$$

with Λ a prespecified symmetric, positive semi-definite $p \times p$-matrix - with p the output dimension of the model - that weighs the relative importance of the different components of $\varepsilon(t,\theta)$. □

Finally we would like to pay attention to one additional freedom that is available in prediction error identification methods.
In stead of having the criterion function (4.24) directly operating on the prediction error $\varepsilon(t,\theta)$, there is the possibility of first letting the prediction error be filtered through a stable linear filter $L(q)$, leading to

$$\varepsilon_F(t,\theta) = L(q)\varepsilon(t,\theta) \tag{4.28}$$

Similar to the situation discussed before, the quadratic (or any alternative) criterion function can now be applied to the filtered prediction error $\varepsilon_F(t,\theta)$, leading to

$$V_N(\theta, Z^N) = \frac{1}{N} \sum_{t=1}^{N} \varepsilon_F(t,\theta)^2 \tag{4.29}$$

With a proper choice of L, one can influence the criterion function (and consequently also the identified model) in a specific way. Here we like to mention that through the choice of L one is able to enhance or suppress the relative importance of specific frequency regions in the criterion function.
By choosing a filter L that enhances the low frequency components in ε and suppresses high frequency components, minimization of (4.29) will lead to an identified model that will be accurate in the particular low frequency region enhanced by L and less accurate in high frequency region suppressed by L. By suppressing high frequency components in ε, model inaccuracies in this frequency region will not play a major role in the criterion (4.29).

Employing the expression (4.15) for the prediction error in the function (4.29) we can write:

$$\varepsilon_F(t,\theta) = L(q)H^{-1}(q)(y(t) - G(q,\theta)u(t)) \tag{4.30}$$

which brings us to two observations:

1. The effect of prefiltering the prediction error in the criterion function (4.29) is identical to changing the noise model of the models in the model set from $H(q,\theta)$ to $H(q,\theta)L(q)^{-1}$.

2. If $G(z,\theta)$ and $H(z,\theta)$ are scalar transfer functions, then the effect of prefiltering the prediction error is identical to prefiltering the input and output data, i.e.

$$\varepsilon_F(t,\theta) = [H(q,\theta)]^{-1}[y_F(t) - G(q,\theta)u_F(t)] \tag{4.31}$$

with

$$y_F(t) \quad = \quad L(q)y(t) \tag{4.32}$$

$$u_F(t) \quad = \quad L(q)u(t) \tag{4.33}$$

The situation is depicted in figure 4.3 showing the two equivalent diagrams.
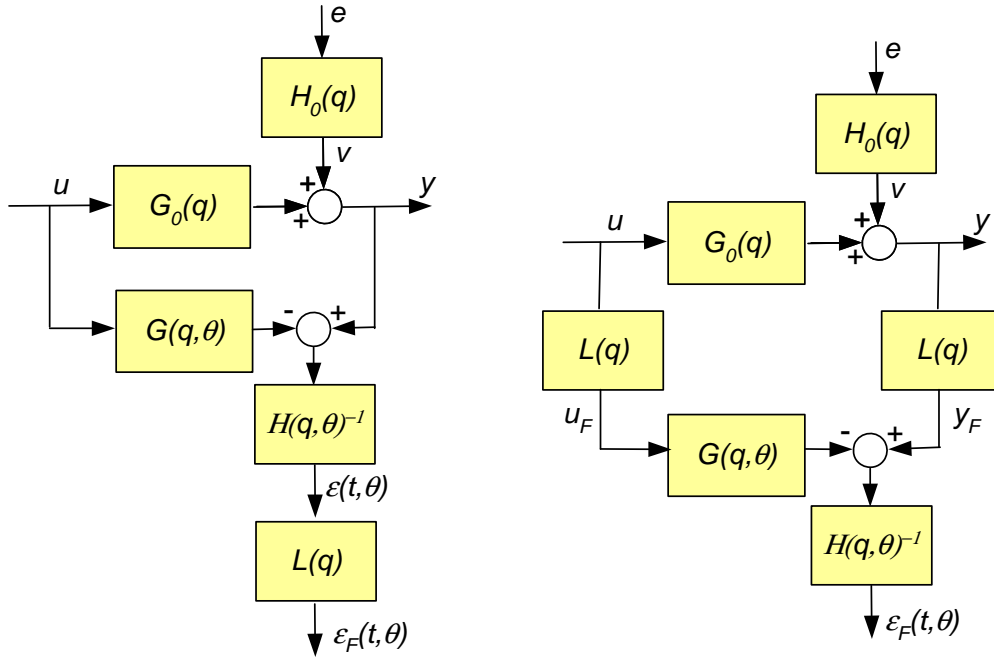
Figure 4.3: Predictor models with filtered prediction error.

As mentioned above, through a proper choice of L one can enhance or suppress specific aspects in the measured data. In the next chapter more attention will be paid to the design aspects of choosing the filter L.

4.6 Linear regression

4.6.1 Introduction

In case the model structure that is chosen has the property of having a one step ahead predictor that is linear in the unknown parameter, this appears to have important implications for the resulting identification problem. For the model structures discussed in this

chapter, this refers to the structures FIR and ARX. In these cases the specific property of linearity-in-the-parameters can be exploited in solving the least squares identification problem. In this section it will be shown how a linear least squares regression problem is solved. Some properties of the identification method are discussed and also brief attention is given to a closely related instrumental variable identification method.

4.6.2 The least squares problem for linear regression models

In section 4.4 it was shown that for an ARX model structure the one step ahead prediction of the output is given by

$$\hat{y}(t|t-1;\theta) = B(q^{-1},\theta)u(t) + [1 - A(q^{-1},\theta)]y(t). \tag{4.34}$$

This prediction can be written in the alternative form

$$\hat{y}(t|t-1) = \varphi^T(t)\theta \tag{4.35}$$

with $\varphi(t)$ the regression vector and θ the parameter vector, which in the ARX case satisfies

$$\varphi^T(t) \;=\; [-y(t-1) \;\; -y(t-2) \;\cdots\; -y(t-n_a) \; u(t) \; u(t-1) \;\cdots u(t-n_b+1)] \tag{4.36}$$

$$\text{and } \;\theta^T \;=\; [a_1 \;\; a_2 \cdots \; a_{n_a} \; b_0 \;\; b_1 \;\cdots b_{n_b-1}] \tag{4.37}$$

The quadratic criterion function of prediction errors can now be written as

$$V_N(\theta, Z^N) = \frac{1}{N} \sum_{t=1}^{N} [y(t) - \varphi^T(t)\theta]^2 \tag{4.38}$$

where

$$y(t) - \varphi^T(t)\theta = \varepsilon(t,\theta),$$

the prediction error.

The criterion function (or loss-function) (4.38) now is a function that is not only quadratic in $\varepsilon(t)$, but also in θ. This last property implies that the problem of minimizing (4.38) as a function of θ becomes a quadratic optimization problem, that in general will have a unique solution that can be obtained analytically. For a scalar valued θ this is schematically depicted in Figure 4.4.

The construction of this solution can simply be done through setting the first derivative of the quadratic function to zero and calculating the parameter value that corresponds with this zero first derivative. This solution strategy will be shown next,

$$\frac{\partial V_N(\theta, Z^N)}{\partial \theta} \;=\; \frac{2}{N} \sum_{t=1}^{N} [y(t) - \varphi^T(t)\theta] \cdot \left[-\frac{\partial \varphi^T(t)\theta}{\partial \theta} \right] \tag{4.39}$$

$$=\; -\frac{2}{N} \sum_{t=1}^{N} [y(t) - \varphi^T(t)\theta] \cdot \varphi(t). \tag{4.40}$$

As a result

$$\frac{\partial V_N(\theta, Z^N)}{\partial \theta}\bigg|_{\theta=\hat{\theta}_N} = 0 \Leftrightarrow \frac{1}{N} \sum_{t=1}^{N} \varphi(t)y(t) = \frac{1}{N} \sum_{t=1}^{N} \varphi(t)\varphi^T(t)\hat{\theta}_N. \tag{4.41}$$
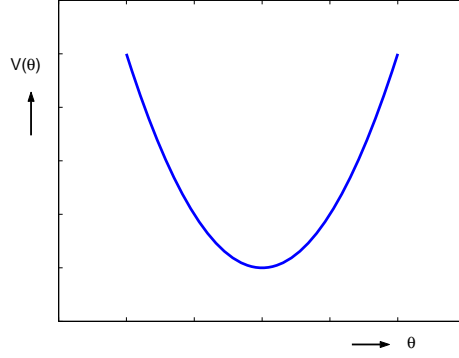
Figure 4.4: The criterion function is a quadratic function in θ.

If the respective matrix inverse exists then

$$\hat{\theta}_N = \arg\min_{\theta} V_N(\theta, Z^N) = \left[\frac{1}{N}\sum_{t=1}^{N}\varphi(t)\varphi^T(t)\right]^{-1}\left[\frac{1}{N}\sum_{t=1}^{N}\varphi(t)y(t)\right]. \qquad (4.42)$$

In the sequel we will also frequently use the notation

$$R(N) \quad := \quad \frac{1}{N}\sum_{t=1}^{N}\varphi(t)\varphi^T(t) \qquad ((n_a+n_b)\times(n_a+n_b)\text{ matrix}) \qquad (4.43)$$

$$f(N) \quad := \quad \frac{1}{N}\sum_{t=1}^{N}\varphi(t)y(t) \qquad ((n_a+n_b)\times 1\text{ vector}) \qquad (4.44)$$

leading to

$$\hat{\theta}_N = R(N)^{-1}f(N).$$

Note that in the ARX situation, $\varphi(t)$ contains delayed input and output samples, and as a consequence $R(N)$ and $f(N)$ are sample covariance functions of $\{y(t)\}$ and $\{u(t)\}$, where

$$R(N) \quad = \quad \left[\begin{array}{cc} R_{yy}^N & R_{yu}^N \\ R_{uy}^N & R_{uu}^N \end{array}\right] \qquad (4.45)$$

$$\text{and}\ \ f(N) \quad = \quad \left[\begin{array}{c} f_{yy}^N \\ f_{yu}^N \end{array}\right]. \qquad (4.46)$$

Remark 4.6.1 *Note that the notion of linearity-in-the-parameters is not related to a notion of linearity/nonlinearity of the models that are identified. All models that are considered in this chapter so far have linear dynamics. The notion of linearity-in-the-parameters only reflects a property of a parametrization / model structure.*

Remark 4.6.2 *The linear regression problem can also directly be used for identifying models with nonlinear dynamics, provided that the structure of the nonlinearity is specified on beforehand. Consider for instance the following model parametrization:*

$$y(t) = a_1 y(t-1)u(t-1) + b_1 u^2(t) + b_2 u(t-1)u(t-2) + e(t). \qquad (4.47)$$

which clearly involves nonlinear dynamics. By writing

$$y(t) = \varphi^T(t)\theta + e(t) \tag{4.48}$$

with $\varphi^T(t) = [y(t-1)u(t-1) \quad u^2(t) \quad u(t-1)u(t-2)]$ and $\theta = [a_1 \quad b_1 \quad b_2]^T$, and "defining" $\varphi^T(t)\theta$ as the predictor, a least squares solution can be obtained along exactly the same lines as sketched above.

Remark 4.6.3 *The linear regression representation $\hat{y}(t|t-1;\theta) = \varphi^T(t)\theta$ only applies to model structures that are linear-in-the-parameters. For other model structures, as e.g. ARMAX or OE, an attempt to write the prediction in this form will lead to an expression of the form*

$$\hat{y}(t|t-1;\theta) = \varphi^T(t,\theta)\theta. \tag{4.49}$$

In this expression the linearity property is lost as φ has become a function of θ.

4.6.3   The LS-estimator in matrix notation

An alternative formulation of the least squares problem for linear regression models is often simpler, using a matrix notation of the problem.
Employing the notation

$$\mathsf{Y}_N = \begin{bmatrix} y(1) \\ y(2) \\ \vdots \\ y(N) \end{bmatrix} \qquad\qquad \Phi_N = \begin{bmatrix} \varphi^T(1) \\ \varphi^T(2) \\ \vdots \\ \varphi^T(N) \end{bmatrix} \tag{4.50}$$

it follows that:

$$V_N(\theta, Z^N) = \frac{1}{N}|\mathsf{Y}_N - \Phi_N\theta|^2 \tag{4.51}$$

$$\text{and } \hat{\theta}_N = \left[\Phi_N^T\Phi_N\right]^{-1}\Phi_N^T\mathsf{Y}_N \tag{4.52}$$

In order to retain expressions that are computationally feasible for quasi-stationary input signals, it is preferable to use the expression

$$\hat{\theta}_N = \left[\frac{1}{N}\Phi_N^T\Phi_N\right]^{-1}\frac{1}{N}\Phi_N^T\mathsf{Y}_N. \tag{4.53}$$

In this way the two separate components of the right hand side expression remain bounded for increasing values of N.
$\hat{\theta}_N$ is the least squares solution of an overdetermined set of equations:

$$\mathsf{Y}_N = \Phi_N\theta. \tag{4.54}$$

By way of minimizing the quadratic errors on this matrix equation, an orthogonal projection $\hat{\mathsf{Y}}_N = \Phi_N\hat{\theta}_N$ is determined which maps Y_N into the space that is determined by the columns of Φ_N. This situation is schematically depicted in figure Fig. 4.5, for $N = 3$ and 2 parameters $\theta^{(1)}$, $\theta^{(2)}$.
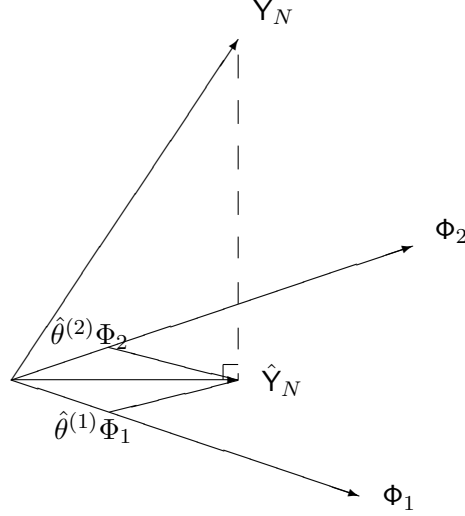
Figure 4.5:   Least squares problem as a projection, with $\Phi_N = [\Phi_1 \Phi_2]$.

Note that

$$V_N(\theta, Z^N) \;=\; \frac{1}{N} \, |\mathsf{Y}_N - \Phi_N \theta|^2 \tag{4.55}$$

$$\;=\; \frac{1}{N} \, [\mathsf{Y}_N - \Phi_N \theta]^T \, [\mathsf{Y}_N - \Phi_N \theta] \tag{4.56}$$

with $\Phi_N \theta = \hat{\mathsf{Y}}_N$.

4.6.4   Properties of the least squares estimator

Some of the basic properties of the linear regression least squares estimator will be indicated here. A thorough analysis will be postponed until sections 4.8-4.10. Here the issues of consistency and of asymptotic variance of the linear regression estimator will be shown.

Consistency

Suppose there is data available from a data generating system

$$y(t) = \frac{B_0(q^{-1})}{A_0(q^{-1})} u(t) + \frac{1}{A_0(q^{-1})} w_0(t). \tag{4.57}$$

This can be written in the form

$$y(t) = \varphi^T(t)\theta_0 + w_0(t) \tag{4.58}$$

where θ_0 denotes the coefficient vector of the system. Note that if w_0 is a white noise process, then the data generating system has an ARX structure.
When identifying a model through an ARX model structure with the same regression vector, this implies that

$$\hat{y}(t|t-1;\theta) = \varphi^T(t)\theta \tag{4.59}$$

and the least-squares parameter estimate is obtained by (4.42). When substituting the system output (4.58) into the parameter estimator (4.42) it follows that

$$
\begin{aligned}
\hat{\theta}_N &= R(N)^{-1} \cdot \frac{1}{N} \sum_{t=1}^{N} \varphi(t)y(t) \\
&= \theta_0 + R(N)^{-1} \cdot \frac{1}{N} \sum_{t=1}^{N} \varphi(t)w_0(t).
\end{aligned}
\tag{4.60}
$$

Consistency of the estimator follows if $\text{plim}_{N\to\infty} = \theta_0$. In order to achieve this two conditions have to be satisfied:

(a) $R^* := \underset{N\to\infty}{\text{plim}}\, R(N)$ should exist and be nonsingular;

(b) $h^* := \underset{N\to\infty}{\text{plim}}\, \dfrac{1}{N} \sum_{t=1}^{N} \varphi(t)w_0(t)$ should be 0.

Under mild conditions it can be shown that

$$
\begin{aligned}
R^* &= \bar{E}\varphi(t)\varphi^T(t) \\
h^* &= \bar{E}\varphi(t)w_0(t).
\end{aligned}
$$

The first condition on R^* will appear to be satisfied if the input signal u is sufficiently exciting the process (such that all process dynamics indeed exhibit themselves in the measurement data), and the model is not overparametrized (there are no pole-zero cancellations introduced in the step from (4.57) to (4.58)).
The second condition on h^* shows that

$$
\bar{E}
\begin{bmatrix}
-y(t-1) \\
\vdots \\
-y(t-n_a) \\
u(t) \\
\vdots \\
u(t-n_b+1)
\end{bmatrix}
w_0(t) = 0.
\tag{4.61}
$$

If the data generating process indeed has an ARX structure, i.e. the noise w_0 is a white noise process, then the above condition is satisfied.
Note that $y(t-i)$, $i > 0$ is correlated with $w_0(t-j)$, $j \geq i$; however if w_0 is a white noise process, $y(t-i)$ is not correlated with $w_0(t)$ and so the above condition is satisfied. In this case $\text{plim}_{N\to\infty} \hat{\theta}_N = \theta_0$, which implies that

$$
\lim_{N\to\infty} E(\hat{\theta}_N) = \theta_0.
$$

If the data generating process has a FIR structure (and so does the model), then condition (b) on h^* is given by

$$
\bar{E}
\begin{bmatrix}
u(t) \\
\vdots \\
u(t-n_b+1)
\end{bmatrix}
w_0(t) = 0.
\tag{4.62}
$$

In this situation a sufficient condition for consistency of $G(q, \hat{\theta}_N)$ is that the noise process w_0 is uncorrelated with the input signal components in the regression vector. This condition allows w_0 to be non-white.

This shows that an ARX model estimator is consistent provided that the data generating system also has an ARX structure. If the noise enters the data in a different way (if w_0 is non-white) then an ARX estimator will be biased. This bias is caused by the fact that the noise term is correlated with some of the components of the regression vector.

Asymptotic variance

The variance of an estimator is a measure for the variation that occurs in the estimate as a function of taking different different realizations of the noise process e. The variance of the least squares parameter estimator can be written as

$$cov(\hat{\theta}_N) = E(\hat{\theta}_N - \theta_0)(\hat{\theta}_N - \theta_0)^T \tag{4.63}$$

using the fact that $E\hat{\theta}_N = \theta_0$. When considering the matrix notation of the data generating process:

$$\mathsf{Y}_N = \Phi_N \theta_0 + \mathsf{W}_N \tag{4.64}$$

with $\mathsf{W}_N = [e(1)\ e(2)\ \cdots\ e(N)]^T$ and using (4.53) it follows that

$$cov(\hat{\theta}_N) = E[\frac{1}{N}\Phi_N^T\Phi_N]^{-1}\frac{1}{N}\Phi_N^T\mathsf{W}_N\mathsf{W}_N^T\Phi_N\frac{1}{N}[\frac{1}{N}\Phi_N^T\Phi_N]^{-1} \tag{4.65}$$

while the bias expression becomes:

$$E\hat{\theta}_N = \theta_0 + E\{(\frac{1}{N}\Phi_N^T\Phi_N)^{-1}\frac{1}{N}\Phi_N^T\mathsf{W}_N\}. \tag{4.66}$$

Using the fact that for e a white noise process, under weak conditions

$$\plim_{N\to\infty} \mathsf{W}_N\mathsf{W}_N^T = \sigma_e^2 I \tag{4.67}$$

which together with $\plim_{N\to\infty} \frac{1}{N}\Phi_N^T\Phi_N = R^*$ shows that for $N \to \infty$:

$$cov(\hat{\theta}_N) \simeq \frac{\sigma_e^2}{N}(R^*)^{-1}. \tag{4.68}$$

Note that the parameter variance tends to zero for $N \to \infty$. This is a direct consequence of the consistency property of the estimator. In expression (4.68) the variance of the estimator can be reduced by way of obtaining a matrix R^* that is well conditioned (i.e. its inverse does not grow rapidly). The choice of an appropriate input signal could be directed towards this goal. Equation (4.68) also shows the three basic elements that influence the variance of the estimator:

- Noise power σ_e^2; the more noise present on the data, the larger the parameter variance;

- Length of measurement interval; the more data points are measured the smaller the parameter variance;

- Input signal and input power; the higher the power of the input signal, the "larger" R^* will become, and thus the smaller the parameter variance.

If $\mathcal{S} \notin \mathcal{M}$ or $G_0 \notin \mathcal{G}$, the analysis of bias and variance becomes much more complicated.

Non-asymptotic properties

In the ARX situation of a stochastic regressor, the bias and variance of the estimator follow from (4.65) and (4.66). These expressions for bias and variance hold under the assumption that $\mathcal{S} \in \mathcal{M}$ and for finite values values of N.

If the regressor $\varphi(t)$ is deterministic, as is the case with FIR models with a deterministic input signal, the statistical analysis of the estimator (4.65) shows some particular simplifications. Denoting $y_o(t) := G_0(q)u(t)$, *i.e.* the noise free output signal, while $y(t) = y_o(t) + v(t)$, it follows from the earlier expressions that

$$E\hat{\theta}_N \;\; = \;\; (\frac{1}{N}\Phi_N^T\Phi_N)^{-1}\frac{1}{N}\sum_{t=1}^{N}\varphi(t)\cdot y_o(t) \tag{4.69}$$

$$\text{Cov}(\hat{\theta}_N) \;\; = \;\; (\frac{1}{N}\Phi_N^T\Phi_N)^{-1}\frac{1}{N}\Phi_N^T\cdot E\mathsf{V}_N\mathsf{V}_N^T\cdot\Phi_N\frac{1}{N}(\frac{1}{N}\Phi_N^T\Phi_N)^{-1} \tag{4.70}$$

with the output noise signal vector $\mathsf{V}_N^T := [v(1)\ v(2)\ \cdots\ v(N)]$. Note that these expressions are valid for finite N and irrespective of conditions like $G_0 \in \mathcal{G}$ or $\mathcal{S} \in \mathcal{M}$; they even hold true in the situation $G_0 \notin \mathcal{G}$. However if $G_0 \in \mathcal{G}$, then there exists a θ_0 such that $y_o(t) = \varphi^T(t)\theta_0$, thus leading to $E\hat{\theta}_N = \theta_0$. As a result, in this case the estimator is unbiased also for finite values of N. If the noise signal v is a stationary white noise process with variance σ_v^2, the covariance expression reduces to

$$\text{Cov}(\hat{\theta}_N) = \frac{\sigma_v^2}{N}\cdot(\frac{1}{N}\Phi_N^T\Phi_N)^{-1}. \tag{4.71}$$

This latter expression is closely related to the asymptotic parameter covariance matrix (4.68), that was presented for the general case in the situation $\mathcal{S} \in \mathcal{M}$.

4.6.5 Instrumental variable method

The instrumental variable (IV) method of system identification is closely related to the least squares linear regression method considered in this section. However, in spite minimizing a quadratic criterion function, the IV estimator is constructed by correlation with a vector of auxiliary (instrumental) signals.

We consider an ARX model set, written in a linear regression form

$$\varepsilon(t,\theta) = y(t) - \varphi^T(t)\theta \tag{4.72}$$

with $\varphi(t)$ the regression vector (vector with explanatory variables), given by

$$\varphi(t) = [-y(t-1)\ \cdots\ -y(t-n_a)\ u(t)\ \cdots u(t-n_b+1)]^T \tag{4.73}$$

and $\theta = [a_1\ a_2\ \cdots a_{n_a}\ b_0\ \cdots b_{n_b-1}]^T$, with $d = dim(\theta)$.

Now a vector valued signal $\{\zeta(t)\}$ is chosen with $\zeta(t) \in \mathbb{R}^d$, denoted as the instrumental variable, and the IV-estimator of the unknown parameter θ, denoted by $\hat{\theta}_N^{IV}$ is determined as the solution to the set of equations:

$$\frac{1}{N}\sum_{t=1}^{N}\zeta(t)\varepsilon(t,\hat{\theta}_N^{IV}) = 0 \tag{4.74}$$

This solution can be written as:

$$\hat{\theta}_N^{IV} = \left[\frac{1}{N} \sum_{t=1}^{N} \zeta(t)\varphi^T(t) \right]^{-1} \left[\frac{1}{N} \sum_{t=1}^{N} \zeta(t)y(t) \right] \tag{4.75}$$

provided the matrix to be inverted indeed is nonsingular.

Note that in the case of a least-squares linear regression estimator, the estimate $\hat{\theta}_N$ is obtained as the solution to the set of equations

$$\frac{1}{N} \sum_{t=1}^{N} \varphi(t)\varepsilon(t, \hat{\theta}_N) = 0 \tag{4.76}$$

Comparing this with (4.74) this shows the close relation between the construction of the two estimates. When choosing $\zeta(t)$ equal to $\varphi(t)$, for all t, the same estimates result.

Appropriate choices of instrumental variables are indicated by the related consistency analysis. This consistency analysis is very similar to the analysis for least squares estimators provided in section 4.6.4.

Assuming a data generating system, represented by

$$y(t) = \varphi^T(t)\theta_0 + w_0(t) \tag{4.77}$$

or equivalently

$$y(t) = \frac{B_0(q^{-1})}{A_0(q^{-1})}u(t) + \frac{1}{A_0(q^{-1})}w_0(t) \tag{4.78}$$

with $B_0(q^{-1})/A_0(q^{-1}) = G_0(q)$, and $\{w_0(t)\}$ any stationary stochastic process with rational spectral density, then substitution of the expression for $y(t)$ into the instrumental variables estimator $\hat{\theta}_N^{IV}$ (4.75), one obtains

$$\hat{\theta}_N^{IV} = \left[\frac{1}{N} \sum_{t=1}^{N} \zeta(t)\varphi^T(t) \right]^{-1} \left[\frac{1}{N} \sum_{t=1}^{N} \zeta(t)[\varphi^T(t)\theta_0 + w_0(t)] \right] \tag{4.79}$$

$$= \theta_0 + \left[\frac{1}{N} \sum_{t=1}^{N} \zeta(t)\varphi^T(t) \right]^{-1} \left[\frac{1}{N} \sum_{t=1}^{N} \zeta(t)w_0(t) \right] \tag{4.80}$$

Similar to the situation of the ARX least squares estimator, the instrumental variable estimator provides a consistent parameter estimator, $\text{plim}_{N\to\infty} \hat{\theta}_N^{IV} = \theta_0$, under the following two conditions:

(a) $\bar{E}\zeta(t)\varphi^T(t)$ is nonsingular;

(b) $\bar{E}\zeta(t)w_0(t) = 0$.

Condition (a) implies that the instruments should be correlated with the variables in the regression vector $\varphi(t)$;

Condition (b) implies that the instruments should be uncorrelated with the noise disturbance term $w_0(t)$.

Note that in the situation that w_0 is a white noise process (ARX data generating system) the choice $\zeta(t) = \varphi(t)$ satisfies these conditions. However if w_0 is not a white noise process

then the output-dependent entries of the regression vector $\varphi(t)$ have to be replaced by other (instrumental) signals that are not correlated with the disturbance terms. A straightforward choice for these instruments, is the addition of additional delayed input samples:

$$
\zeta(t) = \begin{bmatrix} u(t) \\ u(t-1) \\ \vdots \\ u(t-n_b+1) \\ u(t-n_b) \\ \vdots \\ u(t-n_b-n_a+1) \end{bmatrix}. \tag{4.81}
$$

Provided that the input signal is sufficiently exciting (see section 4.7.3) this choice of $\zeta(t)$ generally satisfies the above two conditions for consistency. This choice of $\zeta(t)$ is generally denoted as the basic IV method.

Under the given conditions the IV estimator will provide a consistent estimator of the ARX model parameters, even if the data generating system has a noise disturbance that does not satisfy the ARX structure.

For a more extensive discussion of IV estimation methods, the reader is referred to Söderström and Stoica (1983) and Ljung (1987).

4.7 Conditions on experimental data

4.7.1 Introduction

In the next few sections of this chapter we will analyze the asymptotic properties of the prediction error estimators. This means that we will analyze the convergence properties of the estimated model (what can we say about $\hat{\theta}_N$ for $N \to \infty$?); we will investigate under which conditions a consistent estimator can be obtained, and we will pay attention to the situation that the model set is not complex or flexible enough to contain the data generating system (approximate modelling). In this analysis we regularly have to make assumptions about the available data sequence(s). This refers to

(a) assumptions on the system that has generated the data, and

(b) assumptions on the excitation (input signal) that is present in the available data.

In this section 4.7 we will first pay attention to these assumptions.

In our analysis we will only deal with the asymptotic situation ($N \to \infty$), which implies that we will consider a data sequence of infinite length, denoted as

$$
Z^\infty := \{u(1), y(1), u(2), y(2), \cdots \}
$$

In this chapter the attention that is given to experimental situations will be directed towards the analysis of the identification methods. Issues of experiment setup and design are postponed until chapter 8.
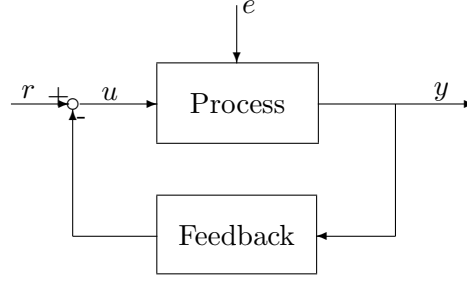
Figure 4.6: Block diagram of data generating mechanism, according to Assumption 4.7.1.

4.7.2   The data generating system

We will assume that the data sequence Z^∞ is generated by a system configuration as depicted in the block diagram in Figure 4.6. In this diagram, r is a deterministic external signal, and e is a white noise process. Linearity of the data generating mechanism is the most important restriction here.
We formalize the assumption as:

Assumption 4.7.1 *The data sequence Z^∞ satisfies:*

$$y(t) \;=\; \sum_{k=0}^{\infty} d^{(1)}(k)r(t-k) + \sum_{k=0}^{\infty} d^{(2)}(k)e(t-k) \tag{4.82}$$

$$u(t) \;=\; \sum_{k=0}^{\infty} d^{(3)}(k)r(t-k) + \sum_{k=0}^{\infty} d^{(4)}(k)e(t-k) \tag{4.83}$$

where

 (a) *$\{r(t)\}$ is a bounded deterministic sequence;*

 (b) *$\{e(t)\}$ is a sequence of independent random variables with zero mean and the property that $E[e(t)]^4 < C_e < \infty$;*

 (c) *the family of transfer functions $\sum_{k=0}^{\infty} d^{(i)}(k)z^{-k}$, $i = 1,..,4$, is uniformly stable, i.e. $max_i \|d^{(i)}(k)\| \le \bar{d}(k)$, $\sum_{k=0}^{\infty} \bar{d}(k) = C_d < \infty$;*

 (d) *$\{y(t)\}$, $\{u(t)\}$ are jointly quasi-stationary.*   □

The fact that $\{r(t)\}$ is assumed to be deterministic means that we consider $\{r(t)\}$ as a given - measurable - data sequence that can be reproduced if we want to repeat the experiment. It does not exclude that the particular sequence $\{r(t)\}$ is generated as a realization of a stochastic process. However, when dealing with probabilistic properties as e.g. expected values, we will consider e as the only probabilistic source.

When discussing properties as consistency, we need the concept and formulation of a "true system", in order to be able to relate an estimated model with the "true" model. To this end we formalize the following assumption.

Assumption 4.7.2 *There exist rational transfer functions $G_0(z)$, $H_0(z)$ with $H_0(z)$ monic, stable and stably invertible, such that the data sequence Z^∞ satisfies:*

$$y(t) = G_0(q)u(t) + H_0(q)e(t) \tag{4.84}$$

with e a white noise process with zero mean, variance σ_e^2, and satisfying the condition (b) of assumption 4.7.1.
This true system, determined by $(G_0(q), H_0(q))$ is denoted by $\mathcal{S}$. □

Note that in this assumption nothing is said about the order or McMillan degree of G_0, H_0. Finite dimensionality and linearity of the data generating system are the basic restrictions here.

Once we have given a model set $\mathcal{M}$ it will be important to distinguish whether the data generating system $\mathcal{S}$ can be represented exactly by an element of $\mathcal{M}$.
Let $\mathcal{M}$ be induced by a parametrization with parameter set Θ.
We introduce the following notation:

$$\Theta_T(\mathcal{S}, \mathcal{M}) := \{\theta \in \Theta \mid G(e^{i\omega}, \theta) = G_0(e^{i\omega}); \; H(e^{i\omega}, \theta) = H_0(e^{i\omega}); \; -\pi \le \omega \le \pi\}.$$

Whenever this set is nonempty, an exact representation of the system $\mathcal{S}$ is present in the model set $\mathcal{M}$. Consequently this situation will be referred to as:

$$\mathcal{S} \in \mathcal{M}$$

In the asymptotic analysis of prediction error identification methods we will pay attention to both situations $\mathcal{S} \in \mathcal{M}$ and $\mathcal{S} \notin \mathcal{M}$. One might argue whether it is of practical interest/relevance to consider the situation $\mathcal{S} \in \mathcal{M}$. Many processes that appear in nature will not be linear, time-invariant and finite dimensional, and consequently the models that we build for these processes - within the framework discussed here - will most of the time be abstractions from reality. However, even if this is the case, we may require from identification procedures, that *when* we are in a situation of $\mathcal{S} \in \mathcal{M}$, the real system (at least asymptotically) can be identified from data.

4.7.3 Persistence of excitation

In order to be able to extract sufficient information from data concerning the dynamics of the underlying data generating system, we have to impose conditions on the character of the input signal that is applied during the experiments. It is straightforward to understand that the character of the input signal highly determines the amount of relevant information that is present in the data. E.g. if we apply a constant input signal, $u(t) = c$, $t \in \mathbb{Z}$, we can not expect that the output signal contains any information on the dynamics of the system. Only static behaviour can be uniquely determined then.

Definition 4.7.3 *Let $\{u(t)\}$ be a quasi-stationary signal, and let the $n \times n$ matrix $\bar{R}_n$ be defined as the symmetric Toeplitz matrix:*

$$\bar{R}_n = \begin{bmatrix} R_u(0) & R_u(1) & \cdots & R_u(n-1) \\ R_u(1) & R_u(0) & \cdots & R_u(n-2) \\ \vdots & \ddots & \ddots & \vdots \\ R_u(n-1) & \cdots & R_u(1) & R_u(0) \end{bmatrix} \tag{4.85}$$

with $R_u(i) := \bar{E}u(t)u(t-i)$, *then $\{u(t)\}$ is "persistently exciting" of order n if $\bar{R}_n$ is nonsingular.*   □

This property of persistence of excitation of order n is a property concerning the "variation" that is present in the signal $\{u(t)\}$. Note that a sequence of zero mean independent random variables (white noise) is persistently exciting of any finite order, since for these signals $\bar{R}_n = I_n$ for all $1 \le n \in \mathbb{N}$.
The definition can be illustrated by considering a least squares identification criterion applied to a model set with FIR model structure.

Example 4.7.4 Consider a set of models having a FIR model structure, leading to a prediction error

$$\varepsilon(t, \theta) = y(t) - \sum_{k=1}^{n_b} b_k u(t-k) \tag{4.86}$$

with $\theta = [b_1 \ b_2 \ \cdots \ b_{n_b}]^T$, and $\theta \in \Theta$.
The sequence $\{b_k\}_{k=1,..,n_b}$ represents the finite impulse response of the transfer function between input and output of the model.
Consider the parameter

$$\theta^* = \arg\min_{\theta \in \Theta} \bar{V}(\theta) \tag{4.87}$$

with $\bar{V}(\theta) := \bar{E}\varepsilon(t, \theta)^2$, then through analysis of the linear regression scheme, it follows that θ^* is determined as the solution to the equation:

$$\begin{bmatrix} R_u(0) & R_u(1) & \cdots & R_u(n_b-1) \\ R_u(1) & \ddots & \cdots & R_u(n_b-2) \\ \vdots & \ddots & \ddots & \vdots \\ R_u(n_b-1) & \cdots & R_u(1) & R_u(0) \end{bmatrix} \begin{bmatrix} b_1^* \\ b_2^* \\ \vdots \\ b_{n_b}^* \end{bmatrix} = \begin{bmatrix} R_{yu}(1) \\ R_{yu}(2) \\ \vdots \\ R_{yu}(n_b) \end{bmatrix} \tag{4.88}$$

Note that uniqueness of the estimated parameter occurs if and only if the symmetric Toeplitz matrix has full rank. Alternatively we could state that the order of persistence of excitation of the input signal is equal to the number of FIR-coefficients that can be identified uniquely with the identification criterion (4.87).   □

An equivalent formulation of this concept is given in the following proposition:

Proposition 4.7.5 *A quasi-stationary signal $\{u(t)\}$, with spectrum $\Phi_u(\omega)$, is persistently exciting of order n if and only if for all filters of the form:*

$$M_n(q) = b_1 q^{-1} + b_2 q^{-2} + \cdots + b_n q^{-n} \tag{4.89}$$

the relation

$$|M_n(e^{i\omega})|^2 \Phi_u(\omega) = 0 \qquad \text{for all } \omega \tag{4.90}$$

implies that $M_n(e^{i\omega}) = 0$ for all ω.

Proof: Construct the vector $b = [b_1 \ b_2 \ \cdots b_n]^T$ and consider $\bar{R}_n$ as in definition 4.7.3. $\bar{R}_n$ is nonsingular if and only if the following implication holds true:

$$b^T \bar{R}_n b = 0 \ \Rightarrow \ b = 0 \tag{4.91}$$

One can verify that

$$b^T \bar{R}_n b = \bar{E}[M_n(q)u(t)]^2$$

with M_n as defined above, and using Parsseval's relation this equals

$$\frac{1}{2\pi} \int_{-\pi}^{\pi} |M_n(e^{i\omega})|^2 \Phi_u(\omega) d\omega$$

Consequently (4.91) can be rephrased to

$$|M_n(e^{i\omega}|^2 \Phi_u(\omega) = 0 \text{ for all } \omega \ \Rightarrow \ M_n(e^{i\omega}) = 0 \text{ for all } \omega.$$

$\square$

The interpretation of this result is, that if u is persistently exciting of order n, there does not exist an n-th order moving average filter that reduces the signal u to zero.
As a consequence of this proposition it can be verified that persistence of excitation of order n is guaranteed if the spectrum $\Phi_u(\omega)$ is unequal to zero in at least n points in the interval $-\pi < \omega \leq \pi$.

Example 4.7.6 Consider the signal

$$u(t) = sin(\omega_0 t). \tag{4.92}$$

Then in chapter 2 it has been shown that

$$\Phi_u(\omega) = \frac{\pi}{2}[\delta_c(\omega - \omega_0) + \delta_c(\omega + \omega_0)]. \tag{4.93}$$

showing that the power spectrum is unequal to zero in 2 frequencies, $\omega = \pm\omega_0$.
Any filter M that satisfies (4.90) will necessarily have zeros in $z = e^{i\omega_0}$ and in $z = e^{-i\omega_0}$. In order to create a filter with 2 zeros, one needs at least $n = 3$ in (4.89). And for $n = 3$ it is indeed possible to construct a filter given by

$$
\begin{aligned}
M_3(q) &= q^{-1} - 2cos(\omega_0)q^{-2} + 1 \\
&= q^{-1}[1 - e^{i\omega_0}q^{-1}][1 - e^{-i\omega_0}q^{-1}]
\end{aligned}
$$

that is not identically 0, and that satisfies (4.90).
This illustrates the fact that a sinusoid is persistently exciting of order 2. $\square$

The result of the example is appealing. A sinusoid principally exhibits two degrees of freedom: an amplitude and a phase, and by exciting a dynamical system with one sinusoid we can identify two system parameters.
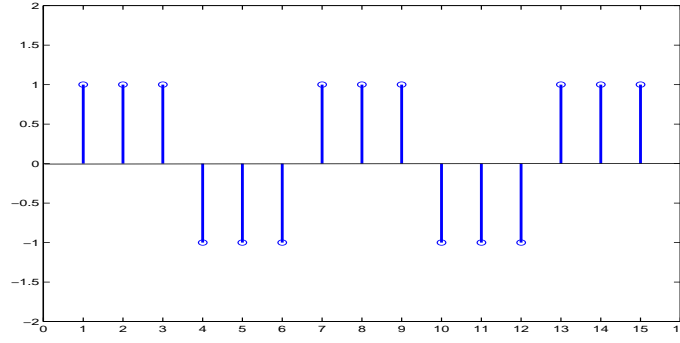
Figure 4.7: Block signal

Example 4.7.7 Consider the block signal $u(t)$ depicted in Figure 4.7.
The signal is periodic with a period of 6 time steps.
It can easily be verified that

$$
\begin{array}{llll}
R_u(0) = 1 & R_u(1) = \frac{1}{3} & R_u(2) = -\frac{1}{3} & R_u(3) = -1 \\
R_u(4) = -\frac{1}{3} & R_u(5) = \frac{1}{3} & R_u(6) = 1 & \text{etcetera}
\end{array}
$$

According to definition 4.7.3 the Toeplitz matrix

$$
\bar{R}_4 = \begin{bmatrix}
1 & \frac{1}{3} & -\frac{1}{3} & -1 \\
\frac{1}{3} & 1 & \frac{1}{3} & -\frac{1}{3} \\
-\frac{1}{3} & \frac{1}{3} & 1 & \frac{1}{3} \\
-1 & -\frac{1}{3} & \frac{1}{3} & 1
\end{bmatrix}
\tag{4.94}
$$

Since $\bar{R}_3$ is regular and $\bar{R}_4$ is singular, it follows that u is persistently exciting of order 3.

The concept of the order of "persistence of excitation" as discussed here is specifically directed towards quasi-stationary (finite power) signals. When applying this concept to transient signals like steps or pulses, it appears that these transient signals are persistently exciting of order 0. This may seem to indicate that these signals can not be used for identification at all. Note however that - as will be shown in chapter 9 - also transient excitation of a system can reveal the full dynamics of the process. This is also apparent from the fact that pulse responses and step responses completely characterize linear system dynamics (modulo initial conditions). It is the framework presented here that is not suitable for application of transient signals.

4.8 Asymptotic properties - Convergence

In analyzing the asymptotic properties of the identified models, determined by

$$
\hat{\theta}_N = \arg \min_{\theta \in \Theta} V_N(\theta, Z^N)
\tag{4.95}
$$

with $V_N(\theta, Z^N)$ the quadratic function (4.24), one of the questions that has to be raised deals with the limit properties of the criterion function $V_N(\theta, Z^N)$ as $N \to \infty$. In this respect the following convergence result can be shown to hold.

Proposition 4.8.1 *Let $\mathcal{M}$ be a model set, with parameter set Θ, that is uniformly stable, and let Z^∞ be a data sequence that is subject to Assumption 4.7.1.*
Then

$$\sup_{\theta \in \Theta} |V_N(\theta, Z^N) - \bar{V}(\theta)| \to 0 \quad \text{with probability } 1 \quad \text{as } N \to \infty \tag{4.96}$$

where

$$\bar{V}(\theta) = \bar{E}\varepsilon(t, \theta)^2 \tag{4.97}$$

□

The proof of this proposition is somewhat outside the scope of this course, see eg. Ljung (1987), Davis and Vinter (1985) for a thorough analysis.

The result states that the criterion function, defined as an averaging over time, converges to a criterion function that averages over an ensemble. Asymptotically the criterion function thus becomes independent of the specific realization of the noise sequence $\{v(t)\}$ that has affected the data sequence Z^∞.

Since the convergence result is uniform in θ, it also implies that the minimizing arguments of both criterion functions converge:

Proposition 4.8.2 *Consider the situation of Proposition 4.8.1, and let $\hat{\theta}_N$ be defined by* (4.95). *Then*

$$\hat{\theta}_N \to \theta^* := \arg\min_{\theta \in \Theta} \bar{V}(\theta) \quad \text{with probability } 1 \quad \text{as } N \to \infty \tag{4.98}$$

□

Since $\arg\min_{\theta \in \Theta} \bar{V}(\theta)$ is not necessarily a single element, the convergence (4.98) can be a convergence into the set Θ_c of minimizing arguments of $\bar{V}(\theta)$. This has to be interpreted as

$$\inf_{\bar{\theta} \in \Theta_c} |\hat{\theta}_N - \bar{\theta}| \to 0 \ \text{ as } N \to \infty \qquad \text{with } \Theta_c = \arg\min_{\theta \in \Theta} \bar{V}(\theta)$$

Note that for this convergence result it is not required that the "real" data generating system $\mathcal{S}$ is a minimizing argument of $\bar{V}(\theta)$. Consequently the estimate $\hat{\theta}_N$ converges to the best possible approximation of $\mathcal{S}$ that is possible within the model set chosen. The "quality" of the approximation is taken in the sense of the criterion $\bar{V}(\theta)$.

This is illustrated in the following example.

Example 4.8.3 *(Ljung, 1987).* Consider a data generating system $\mathcal{S}$ defined by

$$G_0(q) = \frac{b_0 q^{-1}}{1 + a_0 q^{-1}} \quad H_0(q) = \frac{1 + c_0 q^{-1}}{1 + a_0 q^{-1}} \tag{4.99}$$

leading to

$$y(t) + a_0 y(t-1) = b_0 u(t-1) + e(t) + c_0 e(t-1) \tag{4.100}$$

with $\{u(t)\}$ and $\{e(t)\}$ independent unit variance white noise sequences.
We consider a model set with an ARX model structure, determined by

$$G(q, \theta) = \frac{b q^{-1}}{1 + a q^{-1}} \quad H(q, \theta) = \frac{1}{1 + a q^{-1}} \quad \text{and } \theta = \begin{pmatrix} a \\ b \end{pmatrix} \in \Theta \subset \mathbb{R}^2 \tag{4.101}$$

leading to the following prediction error:

$$\varepsilon(t,\theta) = y(t) + ay(t-1) - bu(t-1) \tag{4.102}$$

and consequently

$$\bar{V}(\theta) = \bar{E}[y(t) + ay(t-1) - bu(t-1)]^2 \tag{4.103}$$

which can be written as

$$\bar{V}(\theta) = (1+a^2)R_y(0) + 2aR_y(1) + b^2 - 2bR_{yu}(1) - 2abR_{yu}(0) \tag{4.104}$$

As in this simulation example the real data generating process is known, expressions can be found for the values of the auto- and cross covariance functions in (4.104), by postmultiplying (4.100) with respectively $u(t), u(t-1), e(t), y(t-1)$ and taking expectations. This leads to the set of equations:

$$R_{yu}(0) + a_0 R_{yu}(-1) = b_0 R_u(1)$$
$$R_{yu}(1) + a_0 R_{yu}(0) = b_0 R_u(0)$$
$$R_{ye}(0) + a_0 R_{ye}(-1) = R_e(0) + c_0 R_e(1)$$
$$R_y(1) + a_0 R_y(0) = b_0 R_{yu}(0) + c_0 R_{ye}(0).$$

Using $R_{yu}(-1) = R_u(1) = 0$, this shows that $R_{yu}(0) = 0$, $R_{yu}(1) = b_0$, $R_{ye}(0) = 1$ and $R_y(1) = c_0 - a_0 R_y(0)$.
Denoting $r_0 = R_y(0)$, it follows that

$$\bar{V}(\theta) = (1 + a^2 - 2aa_0)r_0 + 2ac_0 + b^2 - 2bb_0 \tag{4.105}$$

Minimizing this expression with respect to the parameters a and b can be done by fixing the respective partial derivatives to 0.

$$\left.\frac{\partial \bar{V}(\theta)}{\partial a}\right|_{a=a^*} = 0 \quad \Leftrightarrow \quad 2(a^* - a_0)r_0 + 2c_0 = 0 \tag{4.106}$$

$$\left.\frac{\partial \bar{V}(\theta)}{\partial b}\right|_{b=b^*} = 0 \quad \Leftrightarrow \quad 2(b^* - b_0) = 0 \tag{4.107}$$

leading to $b^* = b_0$ and $a^* = a_0 - c_0/r_0$.
As a result

$$\bar{V}(\theta^*) = 1 + c_0^2 - \frac{c_0^2}{r_0} \tag{4.108}$$

while if we substitute $\theta_0 = [a_0 \ b_0]^T$, we obtain $\bar{V}(\theta_0) = 1 + c_0^2$ which will be larger than the previous expression.
The estimates a^*, b^* are the asymptotic estimates that are obtained by the prediction error method. Apparently this estimator is biased, but the bias is beneficial for the prediction performance of the model. It gives a strictly better predictor for $\hat{a} = a^*$ than for $\hat{a} = a_0$. $\square$

In the example a data generating system with an ARMAX structure has been modelled by an ARX model. This is the reason for the asymptotic parameter estimators to be biased. In this situation the asymptotic ARX model that is identified becomes dependent on the specific experimental conditions that underlie the data that is taken from the system. The input signal now plays an important role in the estimation of the model. This is typical for situations in which model structure and structure of the data generating system do not match.

4.9 Asymptotic properties - Consistency

4.9.1 Introduction

In this section we will consider the property of consistency of identified models, i.e. the property that asymptotically - with probability 1 - the correct data generating system is identified. In order to make a statement about the consistency, it is straightforward that we have to adopt some assumptions about the data generating system. With respect to this we will consider two different situations. First we will treat the situation that the data generating system and model set satisfy $\mathcal{S} \in \mathcal{M}$. As mentioned before this refers to both transfer functions $G_0(z)$, $H_0(z)$ that can be modelled exactly. Secondly we will pay attention to the important situation of consistency of the input/output transfer function $G(z, \hat{\theta}_N)$, irrespective of the fact whether the model set is "large" enough to contain a correct description for $H(z, \hat{\theta}_N)$.

When dealing with consistency, we will basically discuss consistency of the estimated transfer functions $(G(z, \hat{\theta}_N), H(z, \hat{\theta}_N))$. Consistency of the parameters $\hat{\theta}_N$ will be given only brief attention.

4.9.2 Consistency in the situation $\mathcal{S} \in \mathcal{M}$

Although the assumption that the system is present in the model set ($\mathcal{S} \in \mathcal{M}$) does not seem to be very realistic in view of real-life applications, the analysis of this situation shows useful insight into properties of identified models. We may expect that whenever a system *can* be modelled exactly within the model set chosen, the identification method should be able to identify the corresponding exact model. However, on the other hand, we have to keep in mind that the assumption is rather severe, and that consequently the required property of consistency is not the ultimate goal when evaluating identification methods. First we will give the formal result.

Proposition 4.9.1 *Let $\mathcal{S}$ be a data generating system and let Z^∞ be a data sequence corresponding to Assumptions 4.7.1, 4.7.2. Let $\mathcal{M}$ be a model set that is uniformly stable with parameter set Θ such that*

$$G(q, \theta) = q^{-n_k} \frac{b_0 + b_1 q^{-1} + \cdots + b_{n_b-1} q^{-n_b+1}}{1 + f_1 q^{-1} + \cdots + f_{n_f} q^{-n_f}} \tag{4.109}$$

with $(b_i, i = 0, \cdots, n_b - 1)$, $(f_j, j = 1, \cdots, n_f)$ being elements of the parameter vector θ. If $\{u(t)\}$ and $\{e(t)\}$ are uncorrelated (open-loop experiment), and if the input signal $\{u(t)\}$ is sufficiently exciting of an order $\geq n_b + n_f$ then

$$\theta^* \quad \text{satisfies} \quad \begin{cases} G(e^{i\omega}, \theta^*) = G_0(e^{i\omega}) \\ H(e^{i\omega}, \theta^*) = H_0(e^{i\omega}) \end{cases} \quad \text{for } -\pi \leq \omega \leq \pi. \tag{4.110}$$

$\square$

Together with the convergence result that is shown in the previous section, this leads to the observation that in the given situation for all ω:

$$
\begin{aligned}
G(e^{i\omega}, \hat{\theta}_N) &\rightarrow G_0(e^{i\omega}) \\
\text{and} \quad H(e^{i\omega}, \hat{\theta}_N) &\rightarrow H_0(e^{i\omega}) \qquad\qquad \text{with probability 1 as } N \to \infty.
\end{aligned}
$$

The consistency result of this prediction error method shows that consistency is obtained under conditions that are rather appealing: the model set should be able to describe the system exactly, and the input signal has to be sufficiently exciting in order to be able to extract all of the dynamics of the system from the external signals.

Note that the order of sufficient excitation of the input $(n_b + n_f)$ is equal to the number of real-valued parameters that is to be estimated. This order, mentioned in the proposition, is a sufficient condition; in specific situations lower orders may also lead to consistency.

For consistency of the estimated *parameter*, we need the additional condition that the parametrization $\mu : \Theta \to \mathcal{M}$ is an injective mapping, i.e. $\mu(\theta_1) = \mu(\theta_2)$ with $\theta_1, \theta_2 \in \Theta$ implies that $\theta_1 = \theta_2$. Under this condition the solution set $\Theta_T(\mathcal{S}, \mathcal{M})$ will only contain one element, being the "real" system parameter vector θ_0.

A proof of proposition 4.9.1 is given in the Appendix.

4.9.3   Consistency in the situation $G_0 \in \mathcal{G}$

In a number of situations it is much more important to obtain a good estimate of the input-output transfer function $G_0(q)$ than of the noise-output transfer function $H_0(q)$. When given a model set $\mathcal{M}$ with corresponding parameter set Θ, the corresponding set of input/output transfer functions is denoted by:

$$\mathcal{G} := \{G(z, \theta), \theta \in \Theta\} \qquad (4.111)$$

and additionally for a data generating system $\mathcal{S}$ we denote:

$$\Theta_G(\mathcal{S}, \mathcal{G}) := \{\theta \in \Theta \mid G(e^{i\omega}, \theta) = G_0(e^{i\omega}); \ -\pi \le \omega \le \pi\}.$$

We can now formalize the situation that the input/output transfer function $G_0(z)$ of the data generating system can be modelled exactly within the model set, irrespective of the fact whether the same holds for the noise transfer function $H_0(z)$. We denote:

$$G_0 \in \mathcal{G} \qquad (4.112)$$

being a situation that is equivalent to non-emptiness of $\Theta_G(\mathcal{S}, \mathcal{G})$.
Note that in example 4.8.3 we had the situation that $G_0 \in \mathcal{G}$ and $\mathcal{S} \notin \mathcal{M}$.
Now the following consistency result can be shown to hold:

Proposition 4.9.2 *Let $\mathcal{S}$ be a data generating system and let Z^∞ be a data sequence corresponding to Assumptions 4.7.1, 4.7.2. Let $\mathcal{M}$ be a model set with G and H parametrized independently, i.e.*

$$\mathcal{M} = \{(G(z, \rho), H(z, \eta)), \ \theta = \begin{pmatrix} \rho \\ \eta \end{pmatrix} \in \Theta\} \qquad (4.113)$$

and let $G(z, \rho)$ be structured according to (4.109).
If $\{u(t)\}$ and $\{e(t)\}$ are uncorrelated (open-loop experiment), and if the input signal $\{u(t)\}$ is sufficiently exciting of an order $\ge n_b + n_f$ then

$$\rho^* = \arg_\rho \min_{\theta \in \Theta} \bar{V}(\theta) \ \ satisfies \ \ G(e^{i\omega}, \rho^*) = G_0(e^{i\omega}) \quad for \ -\pi \le \omega \le \pi. \qquad (4.114)$$

$$\square$$

This result implies that for all ω

$$G(e^{i\omega}, \hat{\rho}_N) \rightarrow G_0(e^{i\omega}) \text{ with probability 1 as } N \to \infty.$$

Proof: Consider $\bar{V}(\theta) = \bar{E}\varepsilon(t, \theta)^2$.

$$
\begin{aligned}
\varepsilon(t, \theta) &= H^{-1}(q, \eta)[y(t) - G(q, \rho)u(t)] \\
&= \tilde{u}(t, \eta, \rho) + \tilde{e}(t, \eta), \\
\text{with } \tilde{u}(t, \eta, \rho) &= H^{-1}(q, \eta)[G_0(q) - G(q, \rho)]u(t) \\
\text{and } \tilde{e}(t, \eta) &= H^{-1}(q, \eta)H_0(q)e(t)
\end{aligned}
$$

Since $\{u(t)\}$ and $\{e(t)\}$ are uncorrelated, it follows that

$$\bar{V}(\theta) = \bar{V}(\rho, \eta) = \bar{E}\tilde{u}^2(t, \eta, \rho) + \bar{E}\tilde{e}^2(t, \eta)$$

With a similar reasoning as in the proof of Proposition 4.9.1 the first term is 0 if and only if $\rho \in \Theta_G(\mathcal{S}, \mathcal{G})$ provided that $\{u(t)\}$ is persistently exciting of sufficient order. As the second term is independent of ρ, this proves the result. □

In the situation discussed, there exists a consistency result for the input/output transfer function G irrespective of the modelling of the noise transfer function H. An important condition is that within the model set $\mathcal{M}$ the two transfer functions G and H are parametrized independently, through different parts of the parameter vector. This condition refers to properties of the model structures. Note that for model sets having an ARX structure, this condition is *not* satisfied, because of the common denominator in the two transfer functions. As discussed already in section 4.4 there are three model structures that do have this property of independent parametrization: OE, FIR and BJ.

4.10 Asymptotic distribution

4.10.1 Introduction

In addition to the problems of convergence and consistency related to asymptotic properties of parameter estimators, the question can be raised how "fast" these asymptotic properties can be reached. Complete knowledge of the random variable $\hat{\theta}_N$ is present in its probability density function (p.d.f.). However for finite values of N it is practically impossible to find explicit expressions for this p.d.f. In stead we have to deal with expressions for the asymptotic p.d.f. of the random variable $\hat{\theta}_N - \theta^*$, with θ^* the limiting estimator, i.e. $\theta^* = \arg\min \bar{V}(\theta)$.

Knowing this asymptotic distribution we can draw conclusions on the accuracy of the parameter estimator, at least for (very) large values of N. These results can be employed in two different ways. On the one hand with an asymptotic covariance matrix (and p.d.f.) we can specify confidence intervals concerning the estimated parameter, relating it to the "real" parameter. On the other hand, covariance matrices can be used as a qualitative measure of accuracy for the identification method. The expression can then be used in analytical or simulation studies concerning the question how different design variables as e.g. input signal, data pre-filter, and/or model set, influence the asymptotic variance of the estimator.

In this section we will discuss some general results on asymptotic normality of the parameter estimators without giving the corresponding proofs in full detail. The interested reader is referred to Ljung and Caines (1979), Davis and Vinter (1985) and Ljung (1987).

4.10.2   General expression for asymptotic normality

We will first present a formal result of which a sketch of proof is added in the appendix.

Proposition 4.10.1 *Let $\mathcal{M}$ be a model set that is uniformly stable with parameter set Θ, and let Z^∞ be a data sequence that is subject to Assumption 4.7.1.*
Consider the parameter estimator

$$\hat{\theta}_N = \arg \min_{\theta \in \Theta} V_N(\theta, Z^N)$$

with

$$V_N(\theta, Z^N) = \frac{1}{N} \sum_{t=1}^{N} \varepsilon(t, \theta)^2.$$

Denote

$$\bar{V}(\theta) = \bar{E} \varepsilon(t, \theta)^2\}$$

and let θ^* be a unique value satisfying $\theta^* \in \arg \min_{\theta \in \Theta} \bar{V}(\theta)$, $\bar{V}''(\theta^*) > 0$.
Then, under weak conditions[3],

$$\sqrt{N}(\hat{\theta}_N - \theta^*) \in As \; \mathcal{N}(0, P_\theta) \tag{4.115}$$

i.e. the random variable $\sqrt{N}(\hat{\theta}_N - \theta^*)$ converges in distribution to a Gaussian p.d.f. with zero mean and covariance matrix P_θ,
where

$$P_\theta = [\bar{V}''(\theta^*)]^{-1} Q [\bar{V}''(\theta^*)]^{-1} \tag{4.116}$$

$$Q = \lim_{N \to \infty} N \cdot E\{[V_N'(\theta^*, Z^N)][V_N'(\theta^*, Z^N)]^T\} \tag{4.117}$$

while $(\cdot)'$, $(\cdot)''$ respectively denote first and second derivative with respect to θ.

Moreover,

$$Cov(\sqrt{N}\hat{\theta}_N) \to P_\theta \quad as \; N \to \infty \tag{4.118}$$

□

The given expression for the covariance matrix P_θ in the general setting of Proposition 4.10.1 is quite complicated. Interpretations of this P_θ in specific situations will be considered in the next subsections.

The importance of the asymptotic normality result and the availabiltiy of a related covariance matrix is, that they can provide expressions for the confidence interval of the parameter estimator related to a specified probability. For a normal distribution a standard confidence interval is chosen by the 3σ-level (i.e. $\theta^{(i)} = \hat{\theta}_N^{(i)} \pm 3 \sqrt{\frac{1}{N P_\theta^{(ii)}}}$) corresponding to a probability level of 99%. In this expression $P_\theta^{(ii)}$ is the (i, i) matrix element of P_θ.

---

[3]The weak conditions refer to the situation that $\sqrt{N} D_N \to 0$ as $N \to \infty$, where $D_N = E \left[\frac{1}{N} \sum_{t=1}^{N} [\psi(t, \theta^*) \varepsilon(t, \theta^*) - \bar{E} \psi(t, \theta^*) \varepsilon(t, \theta^*)] \right]$ and $\psi(t, \theta^*) = -\frac{d}{d\theta} \varepsilon(t, \theta)|_{\theta = \theta^*}$.

4.10.3   Asymptotic variance in the situation $\mathcal{S} \in \mathcal{M}$

When data sequence and data generating system satisfy the conditions as formulated in Assumptions 4.7.1, 4.7.2, and when according to Proposition 4.9.1 a consistent estimator can be obtained, the prediction error $\varepsilon(t, \theta^*)$ will satisfy

$$\varepsilon(t, \theta^*) = e(t)$$

being a sequence of independent, identically distributed random variables with zero mean and variance σ_e^2.
In this situation the expressions for the asymptotic covariance matrix (4.116), (4.117) can be simplified.

Proposition 4.10.2 *In the situation $\mathcal{S} \in \mathcal{M}$ as described above, leading to a consistent parameter estimator $\theta^* = \theta_0$, the asymptotic covariance matrix becomes:*

$$P_\theta = \sigma_e^2 [\bar{E}\psi(t, \theta_0)(\psi(t, \theta_0))^T]^{-1} \tag{4.119}$$

with

$$\psi(t, \theta_0) := -\frac{\partial}{\partial \theta}\varepsilon(t, \theta)\Big|_{\theta=\theta_0}. \tag{4.120}$$

Proof: See appendix. □

The result of the Proposition has a natural interpretation. Note that $\psi(t, \theta)$ is the gradient of $\hat{y}(t|t-1; \theta) = y(t) - \varepsilon(t, \theta)$. Consequently the "larger" this gradient, the "smaller" the asymptotic covariance matrix. In other words, the more sensitive the predictor is with respect to the parameter, the more accurate the parameter can be estimated. A small variation of a parameter value then will lead to a large effect on the predictor and thus on the prediction error.

It is also possible to estimate the expression (4.119) from data. In that case, one may want to use as an estimate of P_θ:

$$\hat{P}_N = \hat{\lambda}_N [\frac{1}{N}\sum_{t=1}^{N} \psi(t, \hat{\theta}_N)\psi^T(t, \hat{\theta}_N)]^{-1} \tag{4.121}$$

$$\hat{\lambda}_N = \frac{1}{N}\sum_{t=1}^{N} \varepsilon^2(t, \hat{\theta}_N) \tag{4.122}$$

We will now present an example of the analytic calculation of the asymptotic covariance of a single parameter.

Example 4.10.3 Consider the data generating system $\mathcal{S}$ determined by:

$$y(t) + a_0 y(t-1) = b_0 u(t-1) + e(t) \tag{4.123}$$

The input signal $\{u(t)\}$ is a white noise process with variance σ_u^2 being uncorrelated with the white noise process $\{e(t)\}$ having a variance σ_e^2.

We use a model set $\mathcal{M}$ determined by

$$G(z, \theta) = \frac{bz^{-1}}{1 + az^{-1}} \quad H(z, \theta) = \frac{1}{1 + az^{-1}}$$

with $\theta = [a\ b]^T$ ranging over an appropriate parameter set Θ. The corresponding one-step-ahead predictor is

$$\hat{y}(t|t-1; \theta) = -ay(t-1) + bu(t-1)$$

and its gradient:

$$\psi(t, \theta) = \left[\begin{array}{c} -y(t-1) \\ u(t-1) \end{array} \right]$$

As a result the asymptotic covariance matrix can be written as

$$P_\theta = \sigma_e^2 \left[\begin{array}{cc} R_y(0) & R_{yu}(0) \\ R_{yu}(0) & R_u(0) \end{array} \right]^{-1}$$

We can compute the corresponding samples of the covariance functions that are present in this expression by squaring the left and right hand sides of (4.123) and taking expectations:

$$R_y(0) + a_0^2 R_y(0) + 2a_0 R_y(1) = b_0^2 \sigma_u^2 + \sigma_e^2$$

Additionally we multiply (4.123) with $y(t-1)$ and take expectations:

$$R_y(1) + a_0 R_y(0) = R_{yu}(0) = 0$$

Combining the two latter equations shows that

$$R_y(0) = \frac{b_0^2 \sigma_u^2 + \sigma_e^2}{1 - a_0^2}$$

As a result, the covariance matrix P_θ satisfies:

$$P_\theta = \sigma_e^2 \left[\begin{array}{cc} \dfrac{b_0^2 \sigma_u^2 + \sigma_e^2}{1 - a_0^2} & 0 \\ 0 & \sigma_u^2 \end{array} \right]^{-1}$$

leading to

$$Cov\ \hat{a}_N \quad \sim \quad \frac{\sigma_e^2}{N} \frac{1 - a_0^2}{b_0^2 \sigma_u^2 + \sigma_e^2} = \frac{1 - a_0^2}{N} \frac{\frac{\sigma_e^2}{\sigma_u^2}}{b_0^2 + \frac{\sigma_e^2}{\sigma_u^2}} \tag{4.124}$$

$$Cov\ \hat{b}_N \quad \sim \quad \frac{1}{N} \frac{\sigma_e^2}{\sigma_u^2} \tag{4.125}$$

Note that the covariance of $\hat{b}_N$ increases linearly with the ratio of the noise and input variance, whereas the covariance of $\hat{a}_N$ reaches an asymptotic value for increasing ratio of noise to input variance. This is due to the fact the parameter b is present in the input/output transfer function G only, whereas the parameter a is also present in the noise/output transfer function H. □

The result of proposition 4.10.2 also holds for linear regression models; for these models the prediction error gradient $\psi(t,\theta_0)$ can simply be calculated by

$$
\begin{aligned}
\psi(t,\theta_0) &= \left. -\frac{\partial}{\partial\theta}\varepsilon(t,\theta)\right|_{\theta=\theta_0} \\
&= -\frac{\partial}{\partial\theta}[y(t)-\varphi^T(t)\theta]_{\theta=\theta_0} \\
&= \varphi(t).
\end{aligned}
$$

As a result (4.119) simplifies to

$$
P_\theta = \sigma_e^2[\bar{E}\varphi(t,\theta_0)\varphi^T(t,\theta_0)]^{-1} \tag{4.126}
$$

which is in agreement with the asymptotic variance expression for linear regression models that was given in (4.68).

The expression (4.119) for the asymptotic covariance matrix can also be interpreted in a frequency domain context. To this end we exploit the predictor gradient $\psi(t,\theta_0)$ that appears in (4.119).
Note that

$$
\psi(t,\theta) := \frac{\partial}{\partial\theta}\hat{y}(t|t-1;\theta) = -\frac{\partial}{\partial\theta}(H(q,\theta)^{-1}[y(t)-G(q,\theta)u(t)]) \tag{4.127}
$$

leading to

$$
\begin{aligned}
\psi(t,\theta) &= \frac{1}{(H(q,\theta))^2}\cdot\frac{\partial H(q,\theta)}{\partial\theta}\cdot(y(t)-G(q,\theta)u(t))+ & (4.128) \\
&\quad +\frac{1}{H(q,\theta)}\cdot\frac{\partial G(q,\theta)}{\partial\theta}u(t) & (4.129) \\
&= \frac{1}{(H(q,\theta))^2}\cdot\left[\begin{array}{cc}\frac{\partial G(q,\theta)}{\partial\theta} & \frac{\partial H(q,\theta)}{\partial\theta}\end{array}\right]\left[\begin{array}{cc}H(q,\theta) & 0 \\ -G(q,\theta) & 1\end{array}\right]\left[\begin{array}{c}u(t) \\ y(t)\end{array}\right] & (4.130)
\end{aligned}
$$

Using $y(t)=G(q,\theta_0)u(t)+H(q,\theta_0)e(t)$, and denoting $T_\theta'(q,\theta_0)=\left[\begin{array}{cc}\frac{\partial G(q,\theta)}{\partial\theta} & \frac{\partial H(q,\theta)}{\partial\theta}\end{array}\right]_{\theta=\theta_0}$, it follows that

$$
\psi(t,\theta_0) = \frac{1}{H(q,\theta_0)}\cdot T_\theta'(q,\theta_0)\left[\begin{array}{c}u(t) \\ e(t)\end{array}\right] \tag{4.131}
$$

Applying Parsseval's relation now shows that (4.119) can be rewritten as

$$
P_\theta = \sigma_e^2\left[\frac{1}{2\pi}\int_{-\pi}^{\pi}\frac{1}{|H(e^{i\omega},\theta_0)|^2}T_\theta'(e^{i\omega},\theta_0)\Phi_\chi(\omega)T_\theta'(e^{-i\omega},\theta_0)^T d\omega\right]^{-1} \tag{4.132}
$$

with $\chi(t)=[u(t)\ e(t)]^T$.
Note that in open loop experimental conditions, with $\{u(t)\}$ and $\{e(t)\}$ being uncorrelated, the matrix-valued spectrum $\Phi_\chi(\omega)$ only has diagonal entries unequal to 0, i.e.

$$
\Phi_\chi(\omega) = \left[\begin{array}{cc}\Phi_u(\omega) & 0 \\ 0 & \sigma_e^2\end{array}\right] \tag{4.133}
$$

4.10.4   Asymptotic variance in the situation $G_0 \in \mathcal{G}$

For the situation $G_0 \in \mathcal{G}$ we will only sketch the main result, without proof.
We consider the situation as in the consistency result for $\mathcal{G}_0 \in \mathcal{G}$ ($\mathcal{S} \notin \mathcal{M}$), as presented in section 4.9.3, having a model set

$$\mathcal{M} = \{(G(q, \rho), H(q, \eta)), \ \theta = \begin{pmatrix} \rho \\ \eta \end{pmatrix} \in \Theta\} \tag{4.134}$$

i.e. G and H are parametrized independently, and we additionally assume that there is a unique θ^* such that

$$\theta^* = \arg \min_{\theta \in \Theta} \bar{V}(\theta) \ \text{ with } \theta^* = \begin{pmatrix} \rho_0 \\ \eta^* \end{pmatrix}. \tag{4.135}$$

and

$$F(z) := \frac{H_0(z)}{H(z, \eta^*)} = \sum_{i=0}^{\infty} f_i z^{-i} \tag{4.136}$$

Then it can be derived that

$$\sqrt{N}(\hat{\rho}_N - \rho_0) \in As \ \mathcal{N}(0, P_\rho) \tag{4.137}$$

with

$$P_\rho \ = \ \sigma_e^2 [\bar{E} \psi_\rho(t) \psi_\rho^T(t)]^{-1} [\bar{E} \tilde{\psi}(t) \tilde{\psi}^T(t)] [\bar{E} \psi_\rho(t) \psi_\rho^T(t)]^{-1} \tag{4.138}$$

$$\psi_\rho(t) \ = \ H^{-1}(q, \eta^*) \frac{\partial}{\partial \rho} G(q, \rho) \Big|_{\rho=\rho_0} u(t) \tag{4.139}$$

$$\tilde{\psi}(t) \ = \ \sum_{i=0}^{\infty} f_i \psi_\rho(t+i) \tag{4.140}$$

and the estimators $\hat{\rho}_N$ and $\hat{\eta}_N$ are asymptotically uncorrelated.

This result provides an expression for the asymptotic variance of parameter estimators for the case that model sets are applied that are not able to describe the noise/output transfer function H_0 accurately. This typically happens in the case of a model set having an output error (OE) model structure.

4.10.5   Parameter confidence intervals

If $\hat{\theta}_N$ has a Gaussian probability density function, the covariance matrix can be used to plot the contour lines of the density function, defined by the relation:

$$f_\theta(\theta) = constant.$$

In the case of a Gaussian distribution $\mathcal{N}(\theta_0, P_\theta)$, these contour lines are defined by the relation

$$(\hat{\theta}_N - \theta_0)^T P_\theta^{-1} (\hat{\theta}_N - \theta_0) = c \tag{4.141}$$

with $c \in \mathbb{R}$, and $c \geq 0$.

Since P_θ is positive semi-definite and symmetric all its eigenvalues will be real-valued and ≥ 0. Additionally the eigenvalue decomposition of P_θ can be written as

$$P_\theta = W \Lambda W^T$$

where W is a unitary matrix of eigenvectors w_i:

$$W = \begin{bmatrix} | & | & & | \\ w_1 & w_2 & \cdots & w_n \\ | & | & & | \end{bmatrix} \tag{4.142}$$

and Λ is a diagonal matrix with positive (≥ 0) eigenvalues λ_i:

$$\Lambda = \begin{bmatrix} \lambda_1 & & & 0 \\ & \lambda_2 & & \\ & & \ddots & \\ 0 & & & \lambda_n \end{bmatrix}. \tag{4.143}$$

Since W is unitary, its columns are orthonormal vectors, i.e. $W^T W = I_n$.
It can simply be verified now that the transformed estimator $\hat{\eta}_N = W^T \hat{\theta}_N$ is also normally distributed with mean value $W^T \theta_0$ and covariance matrix Λ.
The contour lines defined by (4.141) can now alternatively be written as

$$(\hat{\theta}_N - \theta_0)^T P_\theta^{-1} (\hat{\theta}_N - \theta_0) = (\hat{\eta}_N - \eta_0)^T \Lambda^{-1} (\hat{\eta}_N - \eta_0) = c \tag{4.144}$$

or equivalently

$$\sum_{i=1}^{n} \frac{|\hat{\eta}_N^{(i)} - \eta_0^{(i)}|^2}{\lambda_i} = c \tag{4.145}$$

with $(\cdot)^{(i)}$ denoting the i-th component of the vector considered. Equation (4.145) is the characterization of an ellipsoid in the orthogonal basis spanned by the components of $\hat{\eta}_N$, with the center point η_0. The orthogonal basis is determined by the relation

$$\hat{\eta}_N = W^T \hat{\theta}_N = \begin{pmatrix} w_1^T \\ w_2^T \\ \vdots \\ w_n^T \end{pmatrix} \hat{\theta}_N$$

The first basis vector is determined by

$$\begin{pmatrix} 1 \\ 0 \\ \vdots \\ 0 \end{pmatrix} = \begin{pmatrix} w_1^T \\ w_2^T \\ \vdots \\ w_n^T \end{pmatrix} \hat{\theta}_N$$

leading to $\hat{\theta}_N = w_1$, etcetera. Therefore the principal axes of the ellipsoid are aligned with the orthogonal eigenvectors $w_1, w_2, \cdots$ of P_θ. The principal axes of the ellipsoid are determined in size by $2\sqrt{c\lambda_i}$, $i = 1, \cdots n$. This is illustrated in figure 4.8 for a 2-dimensional example.
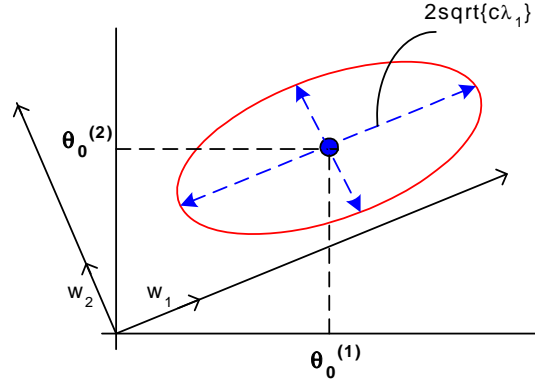
Figure 4.8: Ellipsoid indicating levels of equal probability density function for a normally distributed estimator $\hat{\theta}_N$ with covariance matrix P_θ having eigenvalues λ_1, λ_2 and eigenvectors w_1, w_2.

The constructed ellipsoidal areas generate parameter confidence intervals:

$$\mathcal{D}_{\theta_0} = \{\theta \mid (\theta - \theta_0)^T P_\theta^{-1} (\theta - \theta_0) < \frac{c_\chi(\alpha, n)}{N}\}$$

where $c_\chi(\alpha, n)$ is the α-probability level for a χ_n^2-distributed random variable, having n degrees of freedom, *i.e.* $Pr\{\chi_n^2 < c_\chi(\alpha, n)\} = \alpha$. If the distribution function of the parameter estimator is indeed correctly represented and Gaussian, the following probabilistic expression can be made:

$$\hat{\theta}_N \in \mathcal{D}_{\theta_0} \text{ with probability } \alpha.$$

Reversely, this statement can be rephrased in a statement on the value of the unknwon coefficient θ_0:

$$\theta_0 \in \mathcal{D}_\theta \text{ with probability } \alpha,$$

with

$$\mathcal{D}_\theta = \{\theta \mid (\theta - \hat{\theta}_N)^T P_\theta^{-1} (\theta - \hat{\theta}_N) < \frac{c_\chi(\alpha, n)}{N}\}.$$

4.10.6   Variance of estimated transfer functions

In many situations one will probably be more interested in the covariance of the estimated transfer functions $G(q, \hat{\theta}_N)$, $H(q, \hat{\theta}_N)$ rather than in the covariance of the parameter estimators themselves. So the question is raised, how we can derive an asymptotic covariance matrix of the estimated transfer function, given the asymptotic covariance matrix of the estimated parameters. We will restrict attention to the situation that $\mathcal{S} \in \mathcal{M}$.

We will denote

$$T(q, \theta) := \begin{bmatrix} G(q, \theta) & H(q, \theta) \end{bmatrix} \tag{4.146}$$

and

$$Cov\ T := E\{(\bar{T} - E\bar{T})^T (T - ET)\} \tag{4.147}$$

with $(\bar{\cdot})$ denoting complex conjugate.

This definition implies that in *Cov T* there is no information on the separate real and imaginary parts of *T*, but only information on its magnitude.

Denoting $T^*(q) = T(q, \theta^*)$, and $\hat{T}_N(q) = T(q, \hat{\theta}_N)$ a Taylor's expansion shows that

$$\hat{T}_N(e^{i\omega}) - T^*(e^{i\omega}) \simeq T'_\theta(e^{i\omega}, \theta^*)(\hat{\theta}_N - \theta^*). \tag{4.148}$$

with T'_θ the partial derivative of *T* with respect to θ. Using this relation it follows from (4.115),(4.119) that

$$\sqrt{N}(\hat{T}_N(e^{i\omega}) - T^*(e^{i\omega})) \in As \; \mathcal{N}(0, P(\omega)) \tag{4.149}$$

with

$$P(\omega) = T'_\theta(e^{i\omega}, \theta^*) P_\theta T'_\theta(e^{-i\omega}, \theta^*)^T \tag{4.150}$$

which formalizes the result for the asymptotic covariance matrix of $\hat{T}_N(e^{i\omega})$.

The above result can be used to characterize uncertainty bounds on the frequency responses of estimated models. The expression for $P(\omega)$ shows how the parameter covariance P_θ induces a frequency response covariance.

In a specific asymptotic situation, where not only the number of data but also the model order tends to infinity, the asymptotic covariance expression will be shown to simplify to an extremely simple - and appealing - expression.

Proposition 4.10.4 *Consider the situation of Proposition 4.10.1 with $\mathcal{S} \in \mathcal{M}$. Let $\mathcal{M}$ be such that each of the transfer functions $G(q, \theta)$, $H(q, \theta)$ for a model within $\mathcal{M}$ has McMillan degree n.*
If $n \to \infty$, $N \to \infty$ and $n << N$, then

$$Cov \; (\hat{T}_N(e^{i\omega})) \sim \frac{n}{N} \Phi_v(\omega)[\Phi_\chi(\omega)]^{-1} \tag{4.151}$$

Note that this is a result which is asymptotic in the model order. It has been shown for *FIR* models in Ljung and Yuan (1985) and for general model structures in Ljung (1985). It can be made plausible heuristically by parametrizing the two transfer functions $G(q, \theta)$, $H(q, \theta)$ directly in the frequency domain, by constructing a parameter vector containing $G(e^{i\omega_k})$, $H(e^{i\omega_k})$ for a large number of frequencies ω_k. Actually the transfer functions are parametrized as piecewise constant functions. Combining (4.118) and (4.132) and letting the number of frequency points go to infinity, then yields the result.

The interpretation of (4.151) is that asymptotically the covariance of the estimated transfer functions is determined by the noise-to-signal-ratio $\Phi_v(\omega)[\Phi_\chi(\omega)]^{-1}$.

If the system operates under open loop experimental conditions, then $\Phi_\chi(\omega)$ simplifies to a diagonal matrix, and consequently

$$Cov \; (\hat{G}_N(e^{i\omega})) \quad \sim \quad \frac{n}{N} \frac{\Phi_v(\omega)}{\Phi_u(\omega)} \tag{4.152}$$

$$Cov \; (\hat{H}_N(e^{i\omega})) \quad \sim \quad \frac{n}{N} \frac{\Phi_v(\omega)}{\sigma_e^2} = \frac{n}{N} |H_0(e^{i\omega})|^2 \tag{4.153}$$

where additionally $\hat{G}_N(e^{i\omega})$ and $\hat{H}_N(e^{i\omega})$ are uncorrelated.

Remark 4.10.5 *The results discussed in this section can readily be extended to the multivariable situation, as shown in Zhu (1989).*

4.11   Maximum likelihood interpretation of prediction error estimators

The prediction error identification approach has a predictor model as a starting point which -as pointed out in section 4.3- is independent of the probability density function (pdf) of the (white) noise that drives the noise model.

When following a statistical parameter estimation approach, the joint probability density function of the measured data is a starting point of the estimation procedure.

In the data generating system

$$y(t) = G_0(q)u(t) + H_0(q)e(t)$$

the pdf of a sequence of observations $\{y(1) \cdots y(N)\}$ is determined by the pdf of $\{e\}$; in this situation the input signal u is again considered as a given - deterministic- sequence. In the case of an exact parameter θ_0 reflecting the transfer functions G_0 and H_0, one can write also

$$y(t) = \hat{y}(t|t-1;\theta_0) + e(t)$$

The model of our observations is given by

$$y(t) = \hat{y}(t|t-1;\theta) + \varepsilon(t,\theta)$$

If $e(t)$ has a pdf $f_e(x,t)$, with $\{e\}$ a sequence of independent random variables, as is the case with white noise, then it can be shown that the joint probability density function for $y^N = (y(1) \cdots y(N))$ conditioned on the given input sequence u^N is given by

$$f_y(\theta, x^N) = \prod_{t=1}^{N} f_e(x(t) - \hat{x}(t|t-1;\theta)).$$

When substituting a measured sequence of input and output data, one obtains the - a posterior - likelihood of this measured data sequence:

$$L_y(\theta; y^N) = \prod_{t=1}^{N} f_e(y(t) - \hat{y}(t|t-1;\theta)) \tag{4.154}$$

which now has become a deterministic function of the unknown parameter θ. The maximum likelihood (ML) estimator is defined by that value of θ that maximizes the likelihood function (4.154). In other words: it selects that parameter value for which the observed data would have been most likely to occur.

If f_e is a Gaussian pdf, i.e.

$$f_e(x,t) = \frac{1}{\sqrt{2\pi}\sigma_e} e^{-\frac{x^2}{2\sigma_e^2}}$$

then

$$-\log L_y(\theta; y^N) = constant + N \cdot \log \sigma_e + \frac{1}{2} \sum_{t=1}^{N} \frac{\varepsilon(t,\theta)^2}{\sigma_e^2}. \tag{4.155}$$

Maximization of the likelihood function is obtained by minimization of its minus log likelihood, according to

$$
\begin{aligned}
\hat{\theta}_N^{ML} &= \arg\min_{\theta\in\Theta} N \cdot \log\sigma_e + \frac{1}{2}\sum_{t=1}^{N}\frac{\varepsilon(t,\theta)^2}{\sigma_e^2} && (4.156)\\
&= \arg\min_{\theta\in\Theta}\sum_{t=1}^{N}\varepsilon(t,\theta)^2 && (4.157)
\end{aligned}
$$

provided that either σ_e is known, or is an unknown parameter but not contained in θ.
It appears that in the considered (Gaussian) situation, the maximum likelihood estimator coincides with the simple least squares estimator considered before.
Maximum likelihood estimators have a number of attractive properties.

- For the situation of independent observations (e white noise) the ML estimator is consistent;

- Under some regularity conditions it tends to a normal distribution for $N \to \infty$, where the variance of the normal distribution is given by J_N^{-1} with J_N the Fisher Information Matrix :

$$
J_N = E\left[\frac{d}{d\theta}\log L_y(\theta; y^N)\right]\left[\frac{d}{d\theta}\log L_y(\theta; y^N)\right]^T\Bigg|_{\theta=\theta_0}
$$

- The Cramer-Rao bound :

$$
E(\hat{\theta}_N - \theta_0)(\hat{\theta}_N - \theta_0)^T \geq J_N^{-1}
$$

   shows that the mean square error of any unbiased estimator is lower bounded by a particular minimum value, specified by the Fisher information matrix. As a consequence, there is no other unbiased estimator which gives a smaller variance than the ML estimator, which makes the estimator asymptotically efficient.

For a Gaussian pdf f_e the Fisher information matrix can be shown to satisfy

$$
J_N = \frac{1}{\sigma_e^2}\sum_{t=1}^{N}E\psi(t,\theta_0)\psi^T(t,\theta_0)
$$

with $\psi(t,\theta_0) := \frac{\partial}{\partial\theta}\hat{y}(t|t-1;\theta)$. This shows the close resemblance with the expression for the asymptotic variance of prediction error estimators as formulated in Proposition 4.10.2. In the current context it holds that for any unbiased estimator $\hat{\theta}_N$:

$$
\text{cov}\,(\hat{\theta}_N) \geq J_N^{-1}
$$

for any value of N.
For a more detailed analysis see e.g. Ljung (1999) and Åström (1980).

4.12   Approximate modelling

4.12.1   Introduction

So far in this chapter we have been dealing with asymptotic properties of prediction error models in the cases that $\mathcal{S} \in \mathcal{M}$ or $\mathcal{G}_0 \in \mathcal{G}$. Now the question is raised whether we can derive any asymptotic properties of the estimated model in a general situation that $\mathcal{S} \notin \mathcal{M}$. In that situation we know that we cannot arrive at some "true" parameter, and thus the resulting model necessarily is an approximation of the "real" system.

The convergence results of section 4.8 are valid irrespective of the specification of any "true" system. In that section it is shown that the estimated model converges to the limit model that is specified as the minimizing argument of the criterion function $\bar{V}(\theta)$.

In this section we will take a closer look at this criterion function and we will show that it can help us in a characterization of the misfit between the limiting model and the data generating system.

We will again adopt Assumptions 4.7.1, 4.7.2 concerning the data generating system, which implies that there is a data generating system $\mathcal{S}$ such that any data sequence from this system is described by:

$$y(t) = G_0(q)u(t) + H_0(q)e(t) \tag{4.158}$$

with $\{e(t)\}$ a sequence of independent, identically distributed random random variables with variance σ_e^2.

For ease of notation we will also write

$$v(t) = H_0(q)e(t) \tag{4.159}$$

First attention will be given to an important result in which the asymptotic model is characterized in terms of properties formulated in the frequency domain. This result originates from Wahlberg and Ljung (1986). Secondly a less general result in terms of time-domain properties will be shown, due to Mullis and Roberts (1976).

4.12.2   Frequency domain characterization of asymptotic model

Having a model set $\mathcal{M}$ with predictor models $(G(q, \theta), H(q, \theta))$, the prediction error (4.15) satisfies

$$
\begin{align}
\varepsilon(t, \theta) &= H^{-1}(q, \theta)[y(t) - G(q, \theta)u(t)] \tag{4.160} \\
&= H^{-1}(q, \theta)[(G_0(q) - G(q, \theta))u(t) + v(t)] \tag{4.161}
\end{align}
$$

and as a result its spectral density satisfies:

$$\Phi_\varepsilon(\omega, \theta) = \frac{|G_0(e^{i\omega}) - G(e^{i\omega}, \theta)|^2 \Phi_u(\omega) + \Phi_v(\omega)}{|H(e^{i\omega}, \theta)|^2} \tag{4.162}$$

provided that $\{u(t)\}$ and $\{v(t)\}$ are uncorrelated.

By applying Parsseval's relation, it follows that

$$\bar{V}(\theta) = \bar{E}\varepsilon(t, \theta)^2 = \frac{1}{2\pi} \int_{-\pi}^{\pi} \Phi_\varepsilon(\omega, \theta)d\omega \tag{4.163}$$

and consequently

$$\bar{V}(\theta) = \frac{1}{2\pi} \int_{-\pi}^{\pi} \frac{|G_0(e^{i\omega}) - G(e^{i\omega}, \theta)|^2 \Phi_u(\omega) + \Phi_v(\omega)}{|H(e^{i\omega}, \theta)|^2} d\omega \qquad (4.164)$$

where

$$\Phi_v = \sigma_e^2 |H_0(e^{i\omega})|^2.$$

Since $\theta^* = \arg\min_{\theta \in \Theta} \bar{V}(\theta)$ is the value (or set of values) to which the parameter estimator $\hat{\theta}_N$ converges with probability 1, we now have a characterization of this limit estimate in the frequency domain. This limit estimate is that value of θ that minimizes the expression (4.164). The very important and illustrative formula (4.164) has become well known as "formula (8.66)", pointing to the corresponding equation in the book Ljung (1987).

For interpretation of this criterion formulated as a frequency domain expression, it is however more attractive to consider a slightly modified expression. Starting from (4.161), one can write:

$$\begin{aligned}
\varepsilon(t, \theta) &= H^{-1}(q, \theta)[(G_0(q) - G(q, \theta))u(t) + H_0(q)e(t)] - e(t) + e(t) \\
&= H^{-1}(q, \theta)\left[[G_0(q) - G(q, \theta)]u(t) + [H_0(q) - H(q, \theta)]e(t)\right] + e(t) \quad (4.165)
\end{aligned}$$

Now, because of the fact that $H_0(q)$ and $H(q, \theta)$ are monic for all θ, the second term on the right hand side is dependent on $e(t-1), e(t-2), \cdots$ but not on $e(t)$. And since $\{e(t)\}$ is a white noise process this implies that the second and the third term on the right hand side are uncorrelated. As a result, $E\varepsilon(t, \theta)$ can be written as a summation of three terms, originating from the three separate terms on the right hand side of the above equation. Since the third term is independent of θ, it follows that

$$\boxed{\theta^* = \arg\min_{\theta \in \Theta} \frac{1}{2\pi} \int_{-\pi}^{\pi} \frac{|G_0(e^{i\omega}) - G(e^{i\omega}, \theta)|^2 \Phi_u(\omega) + |H_0(e^{i\omega}) - H(e^{i\omega}, \theta)|^2 \sigma_e^2}{|H(e^{i\omega}, \theta)|^2} d\omega.}$$

$$(4.166)$$

This very nicely structured expression shows that the limiting estimate θ^* is obtained by minimizing additive errors on G_0 and H_0, where the two error terms in the numerator are weighted by the spectral density of their related signal (input u versus noise e). Additionally there is a weighting with the inverse of the noise model. A couple of simple special cases will be considered.

Fixed noise model
Let us consider the situation of a model set where the noise model $H(q, \theta)$ is fixed, i.e. $H(q, \theta) = H_*(q)$. Substituting this into (4.166) and removing the θ-independent terms from the expression (as they do not contribute to the minimization with respect to θ), it follows

$$\theta^* = \arg\min_{\theta \in \Theta} \frac{1}{2\pi} \int_{-\pi}^{\pi} |G_0(e^{i\omega}) - G(e^{i\omega}, \theta)|^2 \frac{\Phi_u(\omega)}{|H_*(e^{i\omega})|^2} d\omega \qquad (4.167)$$

It is clear now that the limiting estimate is obtained as that value of θ that makes $G(e^{i\omega}, \theta)$ the best mean square approximation of $G_0(e^{i\omega})$ with a frequency weighting $\Phi_u(\omega)/|H_*(e^{i\omega})|^2$.

This frequency weighting function determines how the errors in the different frequency regions are weighted with respect to each other. For those values where $\Phi_u(\omega)/|H_*(e^{i\omega})|^2$ is large, the relative importance of error terms $|G_0(e^{i\omega}) - G(e^{i\omega}, \theta)|^2$ in the total misfit is large, and consequently the estimated parameter will strive for a small error contribution $|G_0(e^{i\omega}) - G(e^{i\omega}, \theta)|^2$ at that frequency. By choosing the fixed noise model and the input spectrum, this weighting function can be influenced. In the next chapter we will pay more attention to this phenomenon.

Independent parametrizations for G and H
If $G(q, \rho)$ and $H(q, \eta)$ are parametrized independently, as e.g. in an OE or a BJ model structure, then substituting this into (4.166) leads to

$$\rho^* = \arg \min_{\theta \in \Theta} \frac{1}{2\pi} \int_{-\pi}^{\pi} |G_0(e^{i\omega}) - G(e^{i\omega}, \rho)|^2 \frac{\Phi_u(\omega)}{|H(e^{i\omega}, \eta^*)|^2} d\omega. \tag{4.168}$$

Note that this situation is similar to the case of a fixed noise mode, with the difference that in this latter case, the noise model $H(q, \eta^*)$ is not known a priori.

Prefiltering data
In section 4.5 we already discussed the possibility of prefiltering the prediction error, before applying the sum-of-squares criterion function. This leads to a filtered prediction error

$$\varepsilon_F(t, \theta) = L(q)\varepsilon(t, \theta) \tag{4.169}$$

and the corresponding limiting estimate Θ_C is determined as the set of minimizing arguments of the function

$$\bar{V}_F(\theta) = \bar{E}\varepsilon_F(t, \theta)^2 \tag{4.170}$$

Using similar arguments as before, this leads to the situation that

$$\theta^* = \arg \min_{\theta \in \Theta} \frac{1}{2\pi} \int_{-\pi}^{\pi} \{|G_0(e^{i\omega}) - G(e^{i\omega}, \theta)|^2 \Phi_u(\omega) + |H_0(e^{i\omega}) - H(e^{i\omega}, \theta)|^2 \sigma_e^2\} \frac{|L(e^{i\omega})|^2}{|H(e^{i\omega}, \theta)|^2} d\omega \tag{4.171}$$

and for the situation of a fixed noise model:

$$\theta^* = \arg \min_{\theta \in \Theta} \frac{1}{2\pi} \int_{-\pi}^{\pi} |G_0(e^{i\omega}) - G(e^{i\omega}, \theta)|^2 \frac{\Phi_u(\omega)|L(e^{i\omega})|^2}{|H_*(e^{i\omega})|^2} d\omega \tag{4.172}$$

Again, as also discussed in section 4.5, the influence of the prefilter L is that it redirects the noise model H to $L^{-1}H$. The prefiler L can also be considered as a design variable, that is available to the user for "shaping" the integral function to a desired form.

The situation of a fixed noise model especially refers to the case of model sets having a so-called Output Error (OE) structure. In that case the fixed noise model satisfies $H_*(q) = 1$.

Now the question is whether we can say anything about the asymptotic criterion optimization in the situation that the noise model is also parametrized. Taking a closer look at (4.166) it shows that the integrand essentially contains two terms that are both θ-dependent, and the result is that the interpretation of the system approximation that is involved becomes implicit.

Within the integrand of (4.164) the error term

$$|G_0(e^{i\omega}) - G(e^{i\omega}, \theta)|^2 \frac{\Phi_u(\omega)}{|H(e^{i\omega}, \theta)|^2}$$

shows an additive error term between the real and model frequency function that is weighted with a frequency weighting that is dependent on the (a priori unknown) noise model $H(e^{i\omega}, \theta)$. However there is also a second term in the integrand that is θ-dependent and that thus influences the finally obtained estimate.

In general terms one could say that the resulting estimate θ^* is obtained as a compromise between

- minimizing the additive error $|G_0(e^{i\omega}) - G(e^{i\omega}, \theta)|^2$ with a frequency weighting

$$\Phi_u(\omega)/|H(e^{i\omega}, \theta^*)|^2,$$

  and

- minimizing the noise spectrum error $|H_0(e^{i\omega}) - H(e^{i\omega}, \theta)|^2$ with the frequency weighting $\sigma_e^2/|H(e^{i\omega}, \theta)|^2$

We will illustrate the frequency domain expression (4.166) in the following example, that is taken from Ljung (1987).

Example 4.12.1 Consider a data generating system, determined by

$$y(t) = G_0(q)u(t)$$

with

$$G_0(q) = \frac{0.001q^{-2}(10 + 7.4q^{-1} + 0.924q^{-2} + 0.1764q^{-3})}{1 - 2.14q^{-1} + 1.553q^{-2} - 0.4387q^{-3} + 0.042q^{-4}}$$

No disturbances act on the system. The input is a PRBS (see chapter 8) with a clock period of one sample, which yields $\Phi_u(\omega) \approx 1$ for all ω.

On the basis of available input and output data, this system was identified with the prediction error method using a quadratic criterion function and prefilter $L(q) = 1$, with a model set having an Output Error (OE) structure:

$$\hat{y}(t|t-1; \theta) = \frac{b_1 q^{-1} + b_2 q^{-2}}{1 + f_1 q^{-1} + f_2 q^{-2}} u(t) \tag{4.173}$$

Note that both G_0 and the model set are strictly proper, i.e. $b_0 = 0$.

Bode plots of the true system and of the resulting model are given in Figure 4.9, reflecting $G_0(e^{i\omega})$ and $G(e^{i\omega}, \hat{\theta}_N)$ as functions of ω. We see that the model gives a good description of the low-frequency properties but is less accurate at high frequencies. According to (4.164), the limiting model is characterized by

$$\theta^* = \arg\min \frac{1}{2\pi} \int_{-\pi}^{\pi} |G_0(e^{i\omega}) - G(e^{i\omega}, \theta)|^2 d\omega \tag{4.174}$$

since $H_*(q) = 1$ and $\Phi_u(\omega) \equiv 1$. Since the amplitude of the true system falls off by a factor of 10^{-2} to 10^{-3} for $\omega > 1$, it is clear that errors at higher frequencies contribute only marginally to the criterion (4.174); the good low-frequency fit is the result.
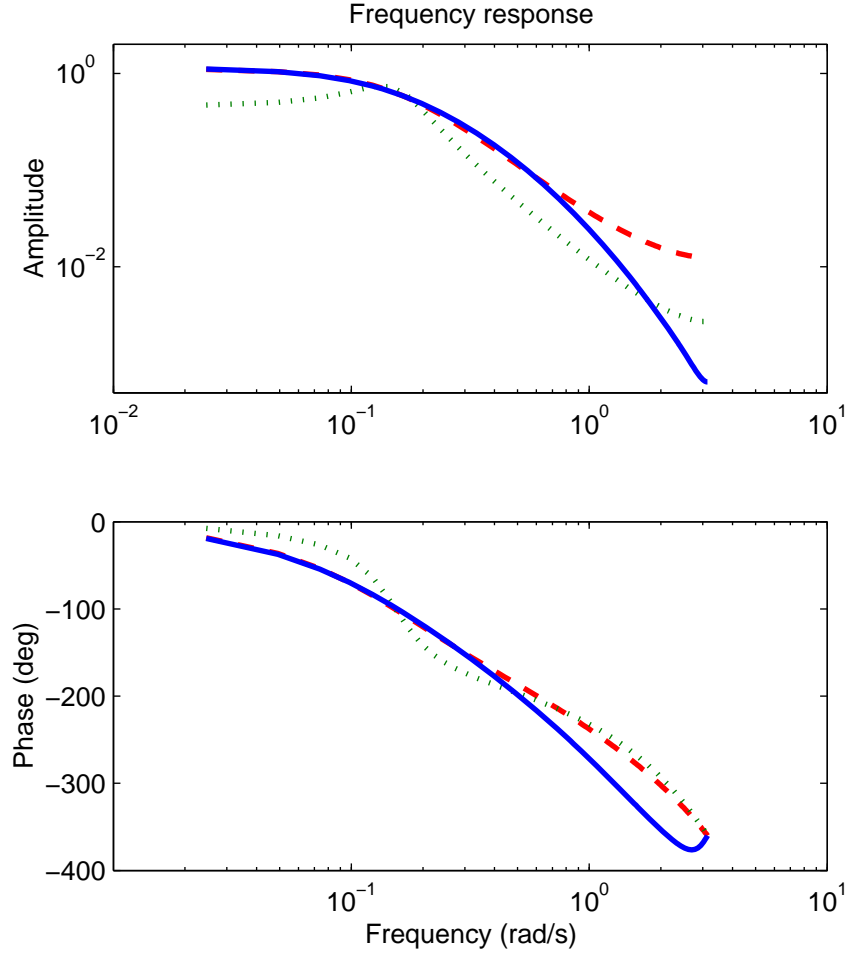
Figure 4.9: Amplitude and phase Bode plots of true system G_0 (solid line), second order OE model (dashed line), and second order ARX model (dotted line).

As an alternative, we consider a model set with an *ARX* model structure, according to

$$G(q, \theta) = \frac{b_1 q^{-1} + b_2 q^{-2}}{1 + a_1 q^{-1} + a_2 q^{-2}} \quad \text{and} \quad H(q, \theta) = \frac{1}{1 + a_1 q^{-1} + a_2 q^{-2}}$$

and corresponding to the linear regression predictor:

$$\hat{y}(t|t-1; \theta) = -a_1 y(t-1) - a_2 t(t-2) + b_1 u(t-1) + b_2 u(t-2) \tag{4.175}$$

When applied to the same data, this model structure gives an estimated model of which the Bode plots are also given in Figure 4.9, showing a considerably worse low-frequency fit. According to our discussion in this section, this limit model is obtained by minimizing

$$\frac{1}{2\pi} \int_{-\pi}^{\pi} |G_0(e^{i\omega}) - G(e^{i\omega}, \theta)|^2 \cdot |1 + a_1 e^{i\omega} + a_2 e^{2i\omega}|^2 d\omega$$

The limiting estimate $|A^*(e^{i\omega})|^2$ is plotted in Figure 4.10. It assumes values at high frequencies that are 10^4 times those at low frequencies. Hence, compared to (4.174) the latter
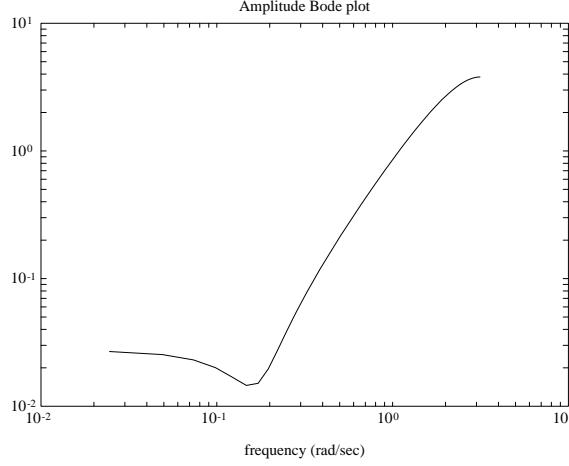
Figure 4.10: Weighting function $|A^*(e^{i\omega})|$ in ARX identification.

criterion penalizes high-frequency misfit much more. As a result the model improves at higher frequencies at the cost of a worse low-frequency behaviour. □

The mechanism that is illustrated in the example is particularly directed towards the frequency weighting of the additive error in the estimated input/output transfer function. The compromise that is made between minimization of this term and a fitting of the noise spectrum to the error spectrum, as mentioned before, will be of increasing influence on the final estimate, the higher the level of the noise disturbance on the data.

4.12.3   A time-domain result for asymptotic linear regression models

In this subsection one specific time-domain result will be shown that holds for linear regression models in the case of approximate modelling, i.e. $\mathcal{S} \notin \mathcal{M}$ and $G_0 \notin \mathcal{G}$. Starting from the same data generating system mentioned in section 4.12.1 and an ARX model set:

$$\varepsilon(t, \theta) = A(q^{-1}, \theta)y(t) - B(q^{-1}, \theta)u(t) \tag{4.176}$$

with the polynomial A having degree n_a and B being parametrized as before (see e.g. (4.109)), the asymptotic parameter estimate $\theta^* = \arg \min \bar{V}(\theta)$ is considered.

Proposition 4.12.2 *If in the considered situation the input signal satisfies $R_u(\tau) = 0$ for $\tau \neq 0$, then*

(a) $G(q, \theta^*)$ is stable;

(b) $g^*(k) = g_0(k)$ for $k = 0, 1, \cdots, n_b - 1$
    where

$$G_0(q) = \sum_{k=0}^{\infty} g_0(k)q^{-k} \tag{4.177}$$

$$G(q, \theta^*) = \sum_{k=0}^{\infty} g^*(k)q^{-k}. \tag{4.178}$$

The proof of part (b) is added in the appendix.

Especially this result (b) may seem remarkable. Despite the fact that the data generating system may not be present in the model set (both $\mathcal{S} \notin \mathcal{M}$ and $G_0 \notin \mathcal{G}$), the first n_b samples of the system's pulse response are exactly reproduced in the model, irrespective of the noise process H_0. The length of the interval over which this exact fit occurs, is determined by the order of the B-polynomial in the model set. By increasing this order, the interval of fit can be extended.

The consequence of this proposition will be illustrated with a couple of examples, in which ARX estimators will be compared with OE estimators. Therefore the character of an output error estimator will first be analysed in the given situation.

It can directly be verified that in the given situation with an OE model structure:

$$\bar{V}(\theta) = \bar{E}\{[G_0(q) - G(q\theta)]u(t)\}^2. \tag{4.179}$$

Writing $G(q, \theta) = \sum_{k=0}^{\infty} g(k, \theta)q^{-k}$ and using the (whiteness) property of $\{u(t)\}$ with $R_u(0) = \sigma_u^2$ it follows that

$$\bar{V}(\theta) = \sum_{k=0}^{\infty} [g_0(k) - g(k, \theta)]^2 \sigma_u^2. \tag{4.180}$$

Apparently, in the OE situation, the asymptotic parameter estimate is obtained by minimizing the quadratic deviations between the system's and the model's pulse response.

Example 4.12.3 Consider a noise free data generating system

$$\mathcal{S}: \ y(t) = G_0(q)u(t)$$

with

$$G_0(q) = \frac{0.9q^{-1}}{1 - 1.8q^{-1} + 0.8108q^{-2}}.$$

The system has order 2, having poles in $z = 0.9 \pm 0.028i$ and a zero in $z = 0$. In figure 4.11 the pulse responses of the system G_0 is shown, together with the pulse responses of the asymptotic first order ARX and OE estimates, using model sets determined by

$$
\begin{aligned}
\varepsilon_{ARX}(t) &= y(t) + a_1 y(t-1) - b_0 u(t) + b_1 u(t-1) \\
\varepsilon_{OE}(t) &= y(t) - \frac{b_0 + b_1 q^{-1}}{1 + a_1 q^{-1}} u(t).
\end{aligned}
$$

The input signal was chosen to be a unit variance white noise process.

Note that in both model sets considered, the number of parameters equals 3.

In the OE-model the 3 model parameters are used to arrive at a well-balanced approximation of the system's pulse response. In the ARX model two parameters are used to fit $g_0(0)$ and $g_0(1)$ exactly, while only one parameter remains for approximating the tail of the response.
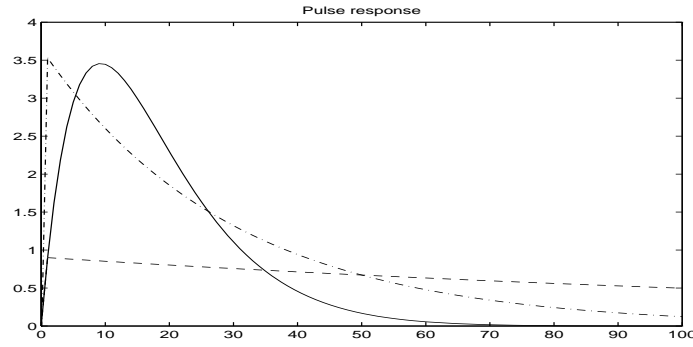
Figure 4.11: Pulse response of second order data generating system $G_0(q)$ of example 4.12.3 (solid) and asymptotic first order ARX (dashed) and OE models (dash-dotted).

Example 4.12.4 A situation is considered that is similar to the previous example, however now with a data generating system satisfying:

$$G_0(q) = \frac{1 - 0.9q^{-1}}{1 - 1.8q^{-1} + 0.8108q^{-2}}.$$

Again this system has order two, having poles in $z = 0.9 \pm 0.028i$ and zeros in $z = 0.9$ and $z = 0$.

In figure 4.12 again the pulse responses are sketched of the data generating system and of asymptotic first order OE and ARX models.
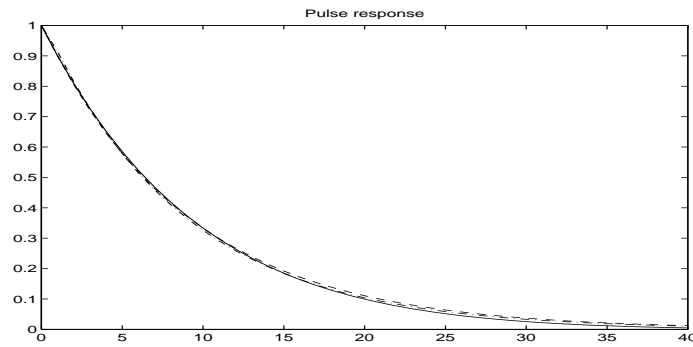
Figure 4.12: Pulse response of second order data generating system $G_0(q)$ of example 4.12.4 (solid) and asymptotic first order ARX (dahsed) and OE models (dash-dotted).

In contrast to the situation of example 4.12.3 the three responses now are ver close. Apparently the second process can much more accurate be approximated by a first order model. This can be explained by the fact that the location of the zero in $z = 0.9$ is very near to the two complex poles of the system. In the ARX model the exact fit of $g_0(0)$ and $g_0(1)$ is now not as dramatic as in 4.12.3.

Example 4.12.5 In the third example an experimentally obtained pulse reponse is used as a data generating system. 85 pulse response samples are obtained from measurements on (part of) the retina system. This pulse response is used for generating input/output data,
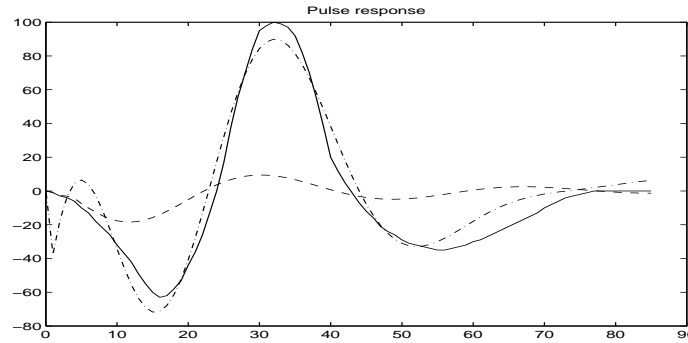
Figure 4.13: Pulse response of data generating (retina) system of example 4.12.5 (solid) and of asymptotic 5th order ARX- (dashed) and OE-model (dash-dotted) with $N = 3000$.

and 5th order ARX and OE-models are estimated under white input noise conditions. The results are depicted in figure 4.13. The consequences of the exact fit of $\{g_0(k)\}_{k=0,\cdots5}$ for the ARX model are considerably. $\square$

The results of this section support the more general frequency-domain results of section 4.12.2. As indicated there an ARX model structure will generally lead to an estimate that emphasizes the high-frequent behaviour of the model and achieves a less accurate low frequent behaviour. This same phenomenon is exhibited in the presented time-domain result.
Note that the difference between ARX and OE estimates will be larger the slower the "start" of the pulse response of G_0. In the case when G_0 contains a number of time-delays, the ARX estimate will particularly identify these delays, at the cost of an accurate description of the dynamics in the tail of the response.

The result of proposition 4.12.2 might suggest that it is a good strategy to drasticaly increase the degree of the polynomial $B(q, \theta)$. The exact fit of the pulse response will then take place over a larger interval. However this strategy can not be followed without care, as with an increasing number of parameters to be estimated, the variance of the estimators will increase.

4.13   Computational aspects

The basic computational aspect in dealing with prediction error identification methods is the aspect of the optimization algorithm that is involved. Considering a least squares identification criterion, the estimation of parameters boils down to a problem of optimizing a quadratic criterion function in $\varepsilon(t, \theta)$ with respect to an unknown parameter θ. In terms of computational aspects we have to distinguish between two situations:

(a) If $\hat{y}(t|t-1; \theta)$ depends linearly on θ then the criterion function $V_N(\theta, Z^N)$ becomes a quadratic function in θ, which generally will have an analytic solution. In this situation of linear regression, a parameter estimate can be found easily through linear algebraic relations. This situation applies to the model structures that have the property of linearity-in-the-parameters: *FIR*, *ARX*.

(b) If $\hat{y}(t|t-1;\theta)$ is not linearly dependent on θ, optimization of $V_N(\theta, Z^N)$ will generally be a nonlinear optimization problem, for which a solution can only be obtained through methods of iterative search (numerical optimization). This situation applies to all other model structures: *OE, ARMAX, BJ,* etc.

A commonly used method for iterative search is the *Newton-Raphson* algorithm:

$$\hat{\theta}_N^{(k+1)} = \hat{\theta}_N^{(k)} - \alpha_k [V_N''(\hat{\theta}_N^{(k)})]^{-1} V_N'(\hat{\theta}_N^{(k)}) \tag{4.181}$$

that employs both first and second derivative of the criterion function with respect to the unknown parameter. Here $\hat{\theta}_N^{(k)}$ denotes the parameter estimate in the k-th iterative step of the algorithm, and α_k is the step size. This step size can also be optimized by choosing:

$$\alpha_k = \arg\min_{\alpha} V_N(\hat{\theta}_N^{(k)} - \alpha [V_N''(\hat{\theta}_N^{(k)})]^{-1} V_N'(\hat{\theta}_N^{(k)})) \tag{4.182}$$

i.e. that value of α that minimizes $V_N(\hat{\theta}_N^{(k+1)})$.
This algorithm is designed to give a one-step convergence for quadratic functions. The local convergence of the Newton-Raphson algorithm is quadratic, i.e. when $\hat{\theta}_N^{(k)}$ is close to the optimum point $\hat{\theta}_N$ then $\|\hat{\theta}_N^{(k+1)} - \hat{\theta}_N\|$ is of the same magnitude as $\|\hat{\theta}_N^{(k)} - \hat{\theta}_N\|^2$.

The Gauss-Newton or quasi-Newton method uses an approximation of the second derivative $V_N''(\hat{\theta}_N^{(k)})$.
Note that $V_N'(\theta) = -\frac{2}{N} \sum_{t=1}^{N} \psi(t,\theta)\varepsilon(t,\theta)$ and

$$V_N''(\theta) = \frac{2}{N} \sum_{t=1}^{N} \psi(t,\theta)\psi^T(t,\theta) - \frac{2}{N} \sum_{t=1}^{N} \frac{\partial}{\partial\theta}(\psi^T(t,\theta))\varepsilon(t,\theta). \tag{4.183}$$

If $\theta = \theta_0$ then $\varepsilon(t,\theta)$ will asymptotically become a white noise signal, and the second term in this equation will vanish. The approximation $V_N''(\theta) \simeq \frac{2}{N} \sum_{t=1}^{N} \psi(t,\theta)\psi^T(t,\theta)$ is then used in the iterative search algorithm.
The Gauss-Newton algorithm generally exhibits a linear convergence.
For a general overview of iterative search algorithms, see Dennis and Schnabel (1983).
The gradient of the prediction, $\psi(t,\theta)$, has to be available in order to apply the iterative search methods as sketched above. Generally - for common model sets - this gradient can be obtained by filtering the data, as is illustrated in the next example considering an ARMAX model set.

Example 4.13.1 *Gradient calculation of ARMAX-predictor.*
For an ARMAX model set, the one-step-ahead prediction of the output is given by

$$\hat{y}(t|t-1;\theta) = H(q)^{-1}G(q)u(t) + (1 - H(q)^{-1})y(t), \quad \text{or} \tag{4.184}$$

$$C(q^{-1})\hat{y}(t|t-1;\theta) = B(q^{-1})u(t) + [C(q^{-1}) - A(q^{-1})]y(t) \tag{4.185}$$

Differentiation with respect to a_i, $i = 1, \cdots, n_a$ gives

$$C(q^{-1})\frac{\partial}{\partial a_i}\hat{y}(t|t-1;\theta) = -y(t-i) \tag{4.186}$$

and similarly for $j = 1, \cdots, n_b$

$$C(q^{-1})\frac{\partial}{\partial b_j}\hat{y}(t|t-1;\theta) = -u(t-j) \tag{4.187}$$

For differentiation with respect to c_k, $k = 1, \cdots, n_c$, it follows that

$$C(q^{-1})\frac{\partial}{\partial c_k}\hat{y}(t|t-1;\theta) + q^{-k}\hat{y}(t|t-1;\theta) = y(t-k) \tag{4.188}$$

Consequently, with

$$\phi(t,\theta) = [-y(t-1) \ \cdots - y(t-n_a) \ u(t-1) \ \cdots u(t-n_a) \ \varepsilon(t-1,\theta) \ \cdots \varepsilon(t-n_c,\theta)]^T$$

it follows that

$$\psi(t,\theta) = C(q^{-1})^{-1}\phi(t,\theta) \tag{4.189}$$

It may be apparent that from a computational point of view linear regression schemes are much more attractive than iterative search methods. In the latter situation one generally has the problem that only convergence to a local minimum can be achieved, whereas it is of course of interest to obtain the global minimum of the criterion function. This basic problem in nonlinear optimization problems can only be dealt with by starting the iterative search in several points of the parameter space, and thus by scanning this space for convergence to the global minimum. Finding an appropriate initial parameter value can be an important task that may contribute considerably to the ultimate result. If we start the iterative search at a "good" estimate, then the optimization procedure will only improve the result. For constructing initial model estimates, several methods are available and commonly applied.

- High order *FIR* modelling and consecutively model reduction by approximate realization techniques, as discussed in chapter 9.

- High order *ARX* modelling and model reduction, choosing among the wide class of model reduction techniques, as e.g. a model reduction based on (truncated) balanced realizations.

- Subspace identification techniques, directed towards an approximate (reduced-order) state space model, directly obtained from input and output measurement data.

- Pseudo-linear regression schemes, that approximate the nonlinear optimization problem by an iterative procedure of linear regression problems.

  A well known example of this class of methods is the method of Steiglitz and McBride (1965).

  In the $k-$th iteration, this method identifies the parameter $\hat{\theta}_N^{(k)}$ in an *ARX* model set, according to

  $$\varepsilon(t,\theta) = A(q^{-1},\theta)y^{(k-1)}(t) - B(q^{-1},\theta)u^{(k-1)}(t) \tag{4.190}$$

  with $y^{(k-1)}(t) = A(q^{-1},\hat{\theta}_N^{(k-1)})^{-1}y(t)$ and $u^{(k-1)}(t) = A(q^{-1},\hat{\theta}_N^{(k-1)})^{-1}u(t)$. These signals are filtered through the inverse of the denominator polynomial of the input/output model obtained in the previous step of the iteration.
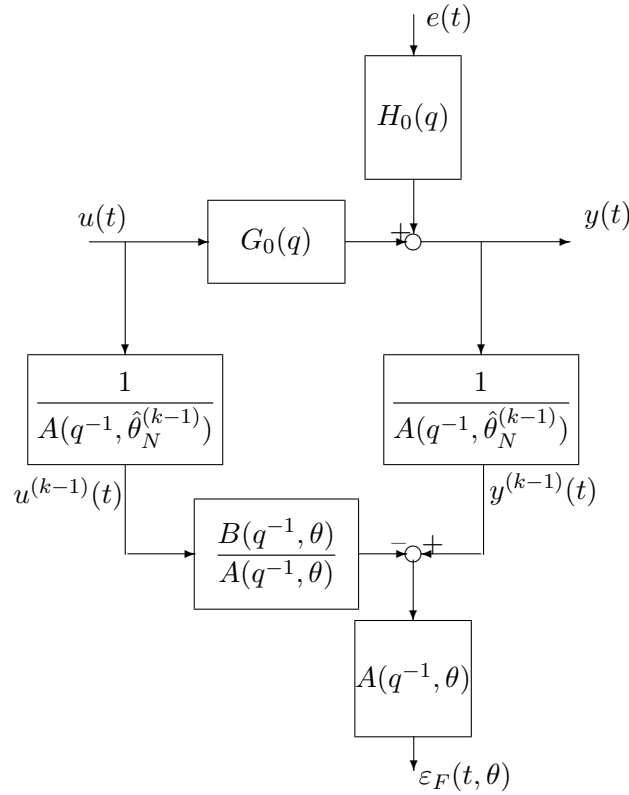
Figure 4.14: Pseudo-linear regression by the method of Steiglitz and McBride.

The mechanism is depicted in figure 4.14

If this procedure converges then it follows that the resulting prediction error is an output error. However this does not necessarily make the algorithm equivalent to an output error identification algorithm, as this output error is not necessarily minimized by the iterative approach. It has been shown by Stoica and Söderström (1981) that local convergence (and sometimes global convergence) to the true parameter vector can be obtained under the condition that the data generating system has an output error structure with white additive noise on the output. However note that in a situation of approximate modelling, the result of this iterative algorithm will generally be different from a (real) output error estimate.

Convergence and accuracy aspects of general pseudo-linear methods are analysed in Stoica *et al.* (1984, 1985).

The prediction error identification methods discussed in this and the previous chapter can also be implemented in a recursive way. This implies that models are estimated on-line while gathering the measurement data. The parameter estimate $\hat{\theta}_N$ obtained after N-datapoints, is updated to $\hat{\theta}_{N+1}$ when -at the next time instant- additional data is obtained. We will not discuss these methods further here, but will refer to the standard references Ljung (1987), Söderström and Stoica (1989), and specifially to Ljung and Söderström (1983).

4.14   Relevant MATLAB-commands

Parametric models are identified with a least-squares identification criterion, through MATLAB-commands that reflect the names of the model structures that are being used.

```
M = arx(DATA,NN)
M = oe(DATA,NN)
M = bj(DATA,NN)
M = armax(DATA,NN)
M = pem(DATA,NN)
```

In the respective m-files, parameters are estimated on the basis of output and input data present in IDDATA-object `DATA`, according to a model structure determined by the name of the routine, and with number of parameters per polynomial indicated in

$$\texttt{NN} = [n_a \ n_b \ n_c \ n_d \ n_f \ n_k]$$

referring to the general form

$$A(q,\theta)y(t) = q^{-n_k}\frac{B(q,\theta)}{F(q,\theta)}u(t) + \frac{C(q,\theta)}{D(q,\theta)}\varepsilon(t).$$

The structure vector `NN` in the above routines, only requires those integers that are relevant for the particular model structure. The PEM command refers to the use of the general structure including all five polynomials.

The output `M` is an estimated model in the IDPOLY-format as utilized in the System Identification Toolbox; it includes a nominal estimate, together with an estimated parameter variance.

Parameter estimates can be made visible by the following commands.

```
present(M)              for the numerical values, and
ffplot(M)               for a Bode plot of the frequency response.
```

4.15   Summary

In this chapter we have discussed the basic aspects and results that are involved in identification of linear dynamic models by prediction error identification methods. We have restricted attention to the so-called least squares criterion function, and to single input single output (SISO) models.

Key ingredients to an identification procedure are

- the data $\{u(1) \ y(1) \ \cdots \ u(N) \ y(N)\}$

- the model set $\mathcal{M} = \{(G(q,\theta), H(q,\theta))\}$ determined by a choice of structure (ARX, FIR, OE, BJ etcetera) and by appropriate degrees of the different polynomials;

- the identification criterion $\frac{1}{N}\sum_{t=1}^{N}\varepsilon^2(t,\theta)$

where the one-step-ahead prediction error ε is given by

$$\varepsilon(t,\theta) = H(q,\theta)^{-1}[y(t) - G(q,\theta)u(t)]$$

as indicated in Figure 4.2.

If the real data generating system $\mathcal{S} := (G_0, H_0)$ is contained in the model set $\mathcal{M}$, then this system will be consistently esimated provided that the input signal u is persistently exciting of a sufficient high order.

If only the real data generating input/output system G_0 is modelled correctly within $\mathcal{M}$ (situation $G_0 \in \mathcal{G}$), then G_0 will be estimated consistently under the same conditions on the input signal, provided that additionally the transfer functions $G(q,\theta)$ and $H(q,\theta)$ are parametrized independently within the model set $\mathcal{M}$. This additional condition is satisfied for the model structures FIR, OE, and BJ.

In its general form, minimization of the identification criterion will require non-linear (non-convex) optimization routines, usually being based on gradient type of iterative search routines. Here there is a risk of getting stuck in local minima. If the one-step-ahead predictor is linear-in-the-parameters (situation of ARX and FIR model structures) the identification criterion becomes quadratic in θ, and consequently the unique global minimum can be obtained analytically, without the burden of iterative search routines.

In the situation that a consistent estimator can not be obtained because of the fact that the model sets chosen are not able to describe all dynamical properties of the real data generating system, an interpretation of the asymptotic parameter estimator is obtained as the minizing argument of the identification (approximation) criterion, which is most easily interpreted in the frequency domain by

$$\theta^* = \arg\min_{\theta \in \Theta} \frac{1}{2\pi} \int_{-\pi}^{\pi} \frac{|G_0(e^{i\omega}) - G(e^{i\omega},\theta)|^2 \Phi_u(\omega) + |H_0(e^{i\omega}) - H(e^{i\omega},\theta)|^2 \sigma_e^2}{|H(e^{i\omega},\theta)|^2} d\omega$$

The basic reference for the material presented in this chapter is Ljung (1987, 1999). In Söderström and Stoica (1989) much of this material is also present as well as extensions to the multivariable situation.

Appendix

Proof of Proposition 4.9.1.

For any $\theta \in \Theta$ there holds:

$$
\begin{aligned}
\bar{V}(\theta) - \bar{V}(\theta_0) &= \bar{E}\varepsilon^2(t,\theta) - \bar{E}\varepsilon^2(t,\theta_0) &\text{(4A.1)}\\
&= -\bar{E}[\varepsilon(t,\theta_0) - \varepsilon(t,\theta)]\varepsilon(t,\theta_0) + \bar{E}[\varepsilon(t,\theta) - \varepsilon(t,\theta_0)]^2 &\text{(4A.2)}
\end{aligned}
$$

Since $\theta_0 \in \Theta_T(\mathcal{S},\mathcal{M})$, $\varepsilon(t,\theta_0) = -H_0^{-1}(q)G_0(q)u(t) + H_0^{-1}(q)y(t) = e(t)$.
Moreover

$$
\begin{aligned}
\varepsilon(t,\theta) - \varepsilon(t,\theta_0) &= y(t) - \hat{y}(t|t-1;\theta) - (y(t) - \hat{y}(t|t-1;\theta_0))\\
&= \hat{y}(t|t-1;\theta_0) - \hat{y}(t|t-1;\theta) &\text{(4A.3)}
\end{aligned}
$$

being an expression that is dependent on y^{t-1}, u^t, and independent of $\{e(t)\}$. Consequently

$$
\bar{E}[\varepsilon(t,\theta) - \varepsilon(t,\theta_0)]e(t) = \bar{E}[\hat{y}(t|t-1;\theta_0) - \hat{y}(t|t-1;\theta)]e(t) = 0 \qquad \text{(4A.4)}
$$

Equation (4A.2) now becomes:

$$
\bar{V}(\theta) - \bar{V}(\theta_0) = \bar{E}[\varepsilon(t,\theta) - \varepsilon(t,\theta_0)]^2 \qquad \text{(4A.5)}
$$

Now we have to analyze whether $\bar{V}(\theta) = \bar{V}(\theta_0)$ implies that $[G(q,\theta)\ H(q,\theta)] = [G_0(q)\ H_0(q)]$.
Denote $\tilde{G}(q) = G_0(q) - G(q,\theta)$, and $\tilde{H}(q) = H_0(q) - H(q,\theta)$. Then

$$
\begin{aligned}
\varepsilon(t,\theta) - \varepsilon(t,\theta_0) &= H^{-1}(q,\theta)[y(t) - G(q,\theta)u(t)] - e(t) &\text{(4A.6)}\\
&= H^{-1}(q,\theta)[G_0(q)u(t) + H_0(q)e(t) - G(q,\theta)u(t)] - e(t) &\text{(4A.7)}\\
&= H^{-1}(q,\theta)[\tilde{G}(q)u(t) + \tilde{H}(q)e(t)] &\text{(4A.8)}
\end{aligned}
$$

Since $\{u(t)\}$ and $\{e(t)\}$ are uncorrelated it follows that:

$$
\bar{V}(\theta) - \bar{V}(\theta_0) = 0 \Rightarrow \left\{ \begin{array}{l} \bar{E}[\tilde{G}(q)u(t)]^2 = 0 \\ \bar{E}[\tilde{H}(q)e(t)]^2 = 0 \end{array} \right. \qquad \text{(4A.9)}
$$

Because $\{e(t)\}$ is a white noise process, $\bar{E}[\tilde{H}(q)e(t)]^2 = 0$ implies that $\tilde{H}(q) = 0$, leading to
$H(q,\theta) = H_0(q)$.
In order to arrive at the implication

$$
\bar{V}(\theta) - \bar{V}(\theta_0) = 0 \Rightarrow \left\{ \begin{array}{l} G(q,\theta) = G_0(q) \\ H(q,\theta) = H_0(q) \end{array} \right. \qquad \text{(4A.10)}
$$

it is sufficient to require that the relation $\bar{E}[\tilde{G}(q)u(t)]^2 = 0$ implies $G(q,\theta) = G_0(q)$.
Writing $G_0(q) = q^{-n_k}\dfrac{B_0(q)}{F_0(q)}$ and $G(q,\theta) = q^{-n_k}\dfrac{B(q,\theta)}{F(q,\theta)}$ with $degr(B_0) = degr(B) = n_b - 1$,
$degr(F_0) = degr(F) = n_f$, then

$$
\tilde{G}(q) = q^{-n_k}\left[\frac{B_0(q)F(q,\theta) - B(q,\theta)F_0(q)}{F_0(q)F(q,\theta)}\right] \qquad \text{(4A.11)}
$$

having a numerator polynomial with a maximum number of $n_b + n_f$ coefficients.

If $\{u(t)\}$ is persistently exciting of an order $\geq n_b + n_f$ then - using Proposition 4.7.5 - it follows that $\bar{E}[\tilde{G}(q)u(t)]^2 = 0 \Rightarrow \tilde{G}(q) = 0$, showing the validity of (4A.10). $\qquad\square$

Sketch of Proof of Proposition 4.10.1.

Suppose that $\arg\min_{\theta \in \Theta} \bar{V}(\theta)$ consists of only one point θ^*.

Consider

$$V'_N(\hat{\theta}_N, Z^N) := \frac{\partial}{\partial \theta}(V'_N(\theta, Z^N))\Big|_{\theta = \hat{\theta}_N}.$$

By definition this derivative equals 0.

Expanding this expression in a Taylor series around θ^* gives, when neglecting higher order terms:

$$0 = V'_N(\theta^*, Z^N) + V''_N(\zeta_N, Z^N)(\hat{\theta}_N - \theta^*) \tag{4A.12}$$

with $\zeta_N = \lambda\hat{\theta}_N + (1 - \lambda)\theta^*$ for some real λ, $0 \leq \lambda \leq 1$.

Using a similar reasoning as for the convergence result (Proposition 4.8.1) it can be shown that

$$\sup_{\theta \in \Theta} |V''_N(\theta, Z^N) - \bar{V}''(\theta^*)| \to 0 \ \text{ with probability 1 as } N \to \infty$$

Then $V''_N(\zeta_N, Z^N) \to \bar{V}''(\theta^*)$ with probability 1 as $N \to \infty$.

This suggests that for large N we can write

$$\hat{\theta}_N - \theta^* = -\bar{V}''(\theta^*)^{-1}V'_N(\theta^*, Z^N)$$

provided the inverse exists.

Using $\psi(t, \theta^*) = -\frac{\partial}{\partial \theta}\varepsilon(t, \theta)\Big|_{\theta = \theta^*}$ we can write

$$V'_N(\theta^*, Z^N) = 2 \cdot \frac{1}{N}\sum_{t=1}^{N} \psi(t, \theta^*)\varepsilon(t, \theta^*). \tag{4A.13}$$

By definition $\bar{V}'(\theta^*) = -\bar{E}\psi(t, \theta^*)\varepsilon(t, \theta^*) = 0$, and so (4A.13) refers to a sum of zero mean random variables $\psi(t, \theta^*)\varepsilon(t, \theta^*)$.

If these terms would be independent we could directly apply the central limit theorem to show that $V'_N(\theta^*, Z^N)$ converges to a Gaussian distribution:

$$\frac{1}{\sqrt{N}}\sum_{t=1}^{N} \psi(t, \theta^*)\varepsilon(t, \theta^*) \in As\ \mathcal{N}(0, Q)$$

with

$$Q = \lim_{N \to \infty} N \cdot E\{[V'_N(\theta^*, Z^N)][V'_N(\theta^*, Z^N)]^T\}$$

The different terms of V_N' are not independent, but due to the uniform stability of the model set, the dependence between distant terms will decrease, and a similar result can still be shown to hold. We will not discuss the additional step of (4.118). $\square$

Proof of proposition 4.10.2.

Substituting $V_N'(\theta_0, Z^N) = 2\frac{1}{N}\sum_{t=1}^{N} \psi(t, \theta_0)e(t)$ into (4.117), shows that

$$Q = \lim_{N\to\infty} 4\frac{1}{N}\sum_{t=1}^{N}\sum_{s=1}^{N} E\psi(t, \theta_0)e(t)e(s)\psi^T(s, \theta_0).$$

Since $\{e(t)\}$ is a white noise sequence, and $\psi(t, \theta_0)$ is uncorrelated with $e(s)$ for $s < t$, it follows that

$$Q = \lim_{N\to\infty} 4\sigma_e^2 \bar{E}[\psi(t, \theta_0)(\psi(t, \theta_0))^T].$$

From $\bar{V}'(\theta) = -2\bar{E}\psi(t, \theta^*)\varepsilon(t, \theta)$ it follows that

$$\bar{V}''(\theta_0) = 2\bar{E}\psi(t, \theta_0)(\psi(t, \theta_0))^T - 2\bar{E}\psi'(t, \theta_0)\varepsilon(t, \theta_0)$$

while the second term on the right hand side equals 0, since $\psi(t, \theta_0)$ is uncorrelated with $e(t)$.

Substituting the above expressions in (4.116) shows the result. $\square$

Proof of proposition 4.12.2 (b).

Without loss of generality we take $R_u(0) = 1$.

From the analysis of ARX estimators, it follows that the asymptotic ARX model satisfies

$$\bar{E}\varepsilon(t, \theta^*)u(t-k) = 0 \qquad\qquad 0 \le k \le n_b - 1. \qquad (4A.14)$$

Further we denote $y^*(t) := \frac{B(q^{-1}, \theta^*)}{A(q^{-1}, \theta^*)}u(t)$ leading to

$$A(q^{-1}, \theta^*)y^*(t) = B(q^{-1}, \theta^*)u(t); \qquad (4A.15)$$

consequently

$$R_{y^*u}(\tau) = g^*(\tau). \qquad (4A.16)$$

Substitution of $\varepsilon(t, \theta^*)$ into (4A.14) then leads to

$$A(q^{-1}, \theta^*)g_0(k) = B(q^{-1}, \theta^*)\delta(k) \qquad\qquad 0 \le k \le n_b - 1 \qquad (4A.17)$$

while correlation of (4A.15) with $u(k)$ leads to

$$A(q^{-1}, \theta^*)g^*(k) = B(q^{-1}, \theta^*)\delta(k) \qquad\qquad \forall k. \qquad (4A.18)$$

As $g_0(k) = 0$ for $k < 0$ it follows directly that (4A.17) can be extended to the interval $-\infty < k \le n_b - 1$. Then the two (recursive) equations (4A.17), (4A.18) are identical over the interval $-\infty < k \le n_b - 1$, which proves the result. $\square$

Bibliography

K.J. Åström (1980). Maximum likelihood and prediction error methods. *Automatica, 16*, pp. 551-574.

M.H.A. Davis and R.B. Vinter (1985). *Stochastic Modelling and Control.* Chapman and Hall, London.

J.E. Dennis and R.E. Schnabel (1983). *Numerical Methods for Unconstrained Optimization and Nonlinear Equations.* Prentice-Hall, Englewood Cliffs, NJ.

P.J. Huber (1981). *Robust Statistics.* Wiley, New York.

L. Ljung and P.E. Caines (1979). Asymptotic normality of prediction error estimation for approximate system models. *Stochastics, 3*, pp. 29-46.

L. Ljung and T. Söderström (1983). *Theory and Practice of Recursive Identification.* MIT-Press, Cambridge, Mass.

L. Ljung and Z.D. Yuan (1985). Asymptotic properties of black-box identification of transfer functions. *IEEE Trans. Automat. Contr., AC-30*, pp. 514-530.

L. Ljung (1985). Asymptotic variance expressions for identified black box transfer function models. *IEEE Trans. Automat. Contr., AC-30*, pp. 834-844.

L. Ljung (1987). *System Identification - Theory for the User.* Prentice-Hall, Englewood Cliffs, NJ. Second edition, 1999.

M. Milanese, J. Norton, H. Piet-Lahanier and E. Walter (Eds.) (1996). *Bounding Approaches to System Identification.* Plenum Press, New York.

C.T. Mullis and R.A. Roberts (1976). The use of second order information in the approximation of discrete time linear systems. *IEEE Trans. Acoust., Speech, Signal Processing*, vol. ASSP-24, 226-238.

T. Söderström and P. Stoica (1983). *Instrumental Variable Methods for System Identification.* Lecture Notes in Control and Information Sciences, Springer-Verlag, New York.

T. Söderström and P. Stoica (1989). *System Identification.* Prentice-Hall, Hemel Hempstead, U.K.

K. Steiglitz and L.E. McBride (1965). A technique for the identification of linear systems. *IEEE Trans. Automat. Control, AC-10*, pp. 461-464.

P. Stoica and T. Söderström (1981). The Steiglitz-McBride identification algorithm revisited - convergence analysis and accuracy aspects. *IEEE Trans. Automat. Control, AC-26*, no. 3, pp. 712-717.

P. Stoica, T. Söderström, A. Ahlén and G. Solbrand (1984). On the asymptotic accuracy of pseudo-linear regression algorithms. *Int. J. Control*, vol. 39, no. 1, pp. 115-126.

P. Stoica, T. Söderström, A. Ahlén and G. Solbrand (1984). On the convergence of pseudo-linear regression algorithms. *Int. J. Control*, vol. 41, no. 6, pp. 1429-1444.

B. Wahlberg and L. Ljung (1986). Design variables for bias distribution in transfer function estimation. *IEEE Trans. Automat. Contr., AC-31*, pp. 134-144.

Y.C. Zhu (1989). Black-box identification of MIMO transfer functions: asymptotic properties of prediction error models. *Int. J. Adaptive Control and Sign. Processing*, vol. 3, pp. 357-373.

Chapter 5

System identification with generalized orthonormal basis functions

Abstract[1]

A least squares identification method is studied that estimates a finite number of expansion coefficients in the series expansion of a transfer function, where the expansion is in terms of recently introduced generalized basis functions. The basis functions are orthogonal in $\mathcal{H}_2$ and generalize the pulse, Laguerre and Kautz bases. One of their important properties is that when chosen properly they can substantially increase the speed of convergence of the series expansion. This leads to accurate approximate models with only few coefficients to be estimated. Explicit bounds are derived for the bias and variance errors that occur in the parameter estimates as well as in the resulting transfer function estimates.

5.1 Introduction

The use of orthogonal basis functions for the Hilbert space $\mathcal{H}_2$ of stable systems has a long history in modelling and identification of dynamical systems. The main part of this work dates back to the classical work of Lee (1933) and Wiener (1946), as also summarized in Lee (1960).

In the past decades orthogonal basis functions, as e.g. the Laguerre functions, have been employed for the purpose of system identification by e.g. King and Paraskevopoulos (1979), Nurges and Yaaksoo (1981), Nurges (1987). In these works the input and output signals of a dynamical system are transformed to a (Laguerre) transform domain, being induced by the orthogonal basis for the signal space. Consecutively, more or less standard identification techniques are applied to the signals in this transform domain. The main motivation for this approach has been directed towards data reduction, as the representation of the measurement data in the transform domain becomes much more efficient once an appropriate

---

[1]This chapter is a reprint from P.M.J. Van den Hof, P.S.C. Heuberger and J. Bokor (1995). System identification with generalized orthonormal basis functions. *Automatica*, Vol. 31, pp. 1821-1834. As a result notation may be slightly different from the notation in the other chapters. For a more compact treatment see also Heuberger et al. (2005).

basis is chosen.

In Wahlberg (1990, 1991, 1994a) orthogonal functions are applied for the identification of a finite sequence of expansion coefficients. Given the fact that every stable system has a unique series expansion in terms of a prechosen basis, a model representation in terms of a finite length series expansion can serve as an approximate model, where the coefficients of the series expansion can be estimated from input-output data.

Consider a stable system $G(z) \in \mathcal{H}_2$, written as

$$G(z) = \sum_{k=0}^{\infty} G_k z^{-k} \tag{5.1}$$

with $\{G_k\}_{k=0,1,2,\cdots}$ the sequence of Markov parameters. Let $\{f_k(z)\}_{k=0,1,2,\cdots}$ be an orthonormal basis for the set of systems $\mathcal{H}_2$. Then there exists a unique series expansion:

$$G(z) = \sum_{k=0}^{\infty} L_k f_k(z) \tag{5.2}$$

with $\{L_k\}_{k=0,1,2,\cdots}$ the (real-valued) expansion coefficients.

The orthonormality of the basis is reflected by the property that

$$\frac{1}{2\pi} \int_{-\pi}^{\pi} f_k(e^{i\omega}) f_l(e^{-i\omega}) d\omega = \left\{ \begin{array}{ll} 1 & k = l \\ 0 & k \neq l \end{array} \right. . \tag{5.3}$$

Note that $f_k(z) = z^{-k}$ is one of the possibilities for choosing such a basis. If a model of the system G is represented by a finite length series expansion:

$$\hat{G}(z) = \sum_{k=0}^{n-1} \hat{L}_k f_k(z). \tag{5.4}$$

then it is easily understandable that the accuracy of the model, in terms of the minimal possible deviation between system and model (in any prechosen norm), will be essentially dependent on the choice of basis functions $f_k(z)$. Note that the choice $f_k(z) = z^{-k}$ corresponds to the use of so-called FIR (finite impulse response) models (Ljung, 1987).

As the accuracy of the models is limited by the basis functions, the development of appropriate basis functions is a topic that has gained considerable interest. The issue here is that it is profitable to design basis functions that reflect the dominant dynamics of the process to be modelled.

Laguerre functions are determined by

$$f_k(z) = \sqrt{1 - a^2} z \frac{(1 - az)^k}{(z - a)^{k+1}}, \qquad |a| < 1. \tag{5.5}$$

see e.g. Gottlieb (1938) and Szegö (1975), and they exhibit the choice of a scalar design variable a that has to be chosen in a range that matches the dominating (first order) dynamics of the process to be modelled. Considerations for optimal choices of a are discussed e.g. in Clowes (1965) and Fu and Dumont (1993). For moderately damped systems, Kautz functions have been employed, which actually are second order generalizations of the Laguerre functions, see Kautz (1954), Wahlberg (1990, 1994a, 1994b).

Recently a generalized set of orthonormal basis functions has been developed that is generated by inner (all pass) transfer functions of any prechosen order, Heuberger and Bosgra (1990), Heuberger (1991), Heuberger *et al.* (1992, 1993). This type of basis functions generalizes the Laguerre and Kautz-type bases, which appear as special cases when choosing first order and second order inner functions. Given any inner transfer function (with any set of eigenvalues), an orthonormal basis for the space of stable systems $\mathcal{H}_2$ (and similarly for the signal space ℓ_2) can be constructed.

Using generalized basis functions that contain dynamics can have important advantages in identification and approximation problems. It has been shown in Heuberger *et al.* (1992, 1993), that if the dynamics of the basis generating system and the dynamics of the system to be modelled approach each other, the convergence rate of a series expansion of the system becomes very fast. Needless to say that the identification of expansion coefficients in a series expansion benefits very much from a fast convergence rate; the number of coefficients to be determined to accurately model the system becomes smaller. This concerns a reduction of both bias and variance contributions in the estimated models.

In this paper, we will focus on the properties of the identification scheme that estimates expansion coefficients in such series expansions, by using simple (least squares) linear regression algorithms. To this end we will consider the following problem set-up, compatible with the standard framework for identification as presented in Ljung (1987).

Consider a linear, time-invariant, discrete-time data generating system:

$$y(t) = G_0(q)u(t) + H_0(q)e_0(t) \tag{5.6}$$

with $G_0(z) = \sum_{k=0}^{\infty} g_k^{(0)} z^{-k}$ a scalar stable transfer function, i.e. bounded for $|z| \geq 1$; $y(t)$ and $u(t)$ scalar-valued output and input signals; q^{-1} the delay operator; H_0 a stable rational and monic transfer function, and e_0 a unit variance, zero mean white noise process. We will also denote $v(t) = H_0(q)e_0(t)$.

A linear model structure will be employed, determined by

$$\hat{y}(t, \theta) = \sum_{k=0}^{n-1} L_k(\theta) f_k(q) u(t), \tag{5.7}$$

with θ varying over an appropriate parameter space $\Theta \subset \mathbb{R}^d$.

Given data $\{u(t), y(t)\}_{t=1,\cdots,N}$ that is taken from experiments on this system, the corresponding one-step-ahead prediction error is given by

$$\varepsilon(t, \theta) = y(t) - \sum_{k=0}^{n-1} L_k(\theta) f_k(q) u(t). \tag{5.8}$$

The least-squares parameter estimate is determined by

$$\hat{\theta}_N(n) = \arg\min_{\theta \in \Theta} \frac{1}{N} \sum_{t=1}^{N} \varepsilon(t, \theta)^2, \tag{5.9}$$

and the corresponding estimated transfer function by

$$G(z, \hat{\theta}_N) = \sum_{k=0}^{n-1} L_k(\hat{\theta}_N) f_k(z). \tag{5.10}$$

This identification method has some favorable properties. Firstly it is a linear regression scheme, which leads to a simple analytical solution; secondly it is of the type of *output-error-method*, which has the advantage that the input/output system $G_0(z)$ can be estimated consistently whenever the unknown noise disturbance $v(t)$ is uncorrelated with the input signal (Ljung, 1987).

However, it is well known that for moderately damped systems, and/or in situations of high sampling rates, it may take a large value of n, the number of coefficients to be estimated, in order to capture the essential dynamics of the system G into its model. If we are able to improve the basis functions in such a way that an accurate description of the model to be estimated can be achieved by a small number of coefficients in a series expansion, then this is beneficial from both aspects of bias and variance of the model estimate.

In this paper we will analyse bias and variance errors for the asymptotic parameter and transfer function estimates, for the general class of orthogonal basis functions as recently introduced in Heuberger and Bosgra (1990), Heuberger (1991), Heuberger *et al.* (1992, 1993). The results presented generalize corresponding results as provided by Wahlberg (1991, 1994a) for the Laguerre and Kautz bases.

In section 5.2 we will first present the general class of orthogonal basis functions, and the least squares identification will be formulated in section 5.3. Then in sections 5.4 and 5.5 we will introduce and analyse the Hambo transform of signals and systems, induced by the generalized orthogonal basis. This transform plays an important role in the statistical analysis of the asymptotic parameter estimates. This asymptotic analysis is completed in section 5.6. A simulation example in section 5.7 illustrates the identification method, and the paper is concluded with some summarizing remarks.

We will use the following notation.

$(\cdot)^T$	Transpose of a matrix.
$\mathbb{R}^{p \times m}$	set of real-valued matrices with dimension $p \times m$.
$\mathbf{C}$	Set of complex numbers.
$\mathbb{Z}_+$	Set of nonnegative integers.
$\ell_2[0, \infty)$	Space of squared summable sequences on the time interval $\mathbb{Z}_+$.
$\ell_2^{p \times m}[0, \infty)$	Space of matrix sequences $\{F_k \in \mathbb{R}^{p \times m}\}_{k=0,1,2,\cdots}$ such that $\sum_{k=0}^{\infty} tr(F_k^T F_k)$ is finite.
$\mathcal{H}_2^{p \times m}$	Set of real $p \times m$ matrix functions that are squared integrable on the unit circle.
$\| \cdot \|_2$	ℓ_2-norm of a vector; induced ℓ_2-norm or spectral norm of a constant matrix, i.e. its maximum singular value.
$\| \cdot \|_1$	ℓ_1-norm of a vector; induced ℓ_1-norm of a matrix operator.
$\| \cdot \|_\infty$	ℓ_∞-norm of a vector; induced ℓ_∞-norm of a matrix operator.
$\| \cdot \|_{\mathcal{H}_2}$	$\mathcal{H}_2$-norm of a stable transfer function.
$\bar{E}$	$\lim_{N \to \infty} \frac{1}{N} \sum_{t=1}^{N} E$
$\otimes$	Kronecker matrix product.
e_i	i-th Euclidean basis vector in $\mathbb{R}^n$.
I_n	$n \times n$ Identity matrix.
$\delta(t)$	Kronecker delta function, i.e. $\delta(t) = 1$, $t = 0$; $\delta(t) = 0$, $t \neq 0$.
:=	"is defined by".

The scalar transfer function $G(z)$ has an n_b-dimensional state space realization (A, B, C, D), with $A \in \mathbb{R}^{n_b \times n_b}$, and B, C, D of appropriate dimensions, if $G(z) = C(zI -$

$A)^{-1}B + D$. A realization is minimal if it has minimal dimension. The controllability Gramian P and observability Gramian Q are defined as the solutions to the Lyapunov equations $APA^T + BB^T = P$ and $A^TQA + C^TC = Q$ respectively, and the realization is called (internally) balanced if $P = Q = \Sigma$, with $\Sigma = diag(\sigma_1, \cdots, \sigma_{n_b})$, $\sigma_1 \geq \cdots \geq \sigma_{n_b}$. A system $G \in \mathcal{H}_2$ is called inner if it is stable and it satisfies $G(z^{-1})G(z) = 1$.

5.2 Generalized orthonormal basis functions

We will consider the generalized orthogonal basis functions that were introduced in Heuberger *et al.* (1992), based on the preliminary work of Heuberger and Bosgra (1990) and Heuberger (1991). The main result of concern is reflected in the following theorem.

Theorem 5.2.1 *Let $G_b(z)$ be a scalar inner function with McMillan degree $n_b > 0$, having a minimal balanced realization (A, B, C, D). Denote*

$$V_k(z) := z(zI - A)^{-1}BG_b^k(z) \tag{5.11}$$

Then the sequence of scalar rational functions $\{e_i^T V_k(e^{i\omega})\}_{i=1,\cdots,n_b;k=0,\cdots\infty}$ forms an orthonormal basis for the Hilbert space $\mathcal{H}_2$. □

Note that these basis functions exhibit the property that they can incorporate systems dynamics in a very general way. One can construct an inner function G_b from any given set of poles, and thus the resulting basis can incorporate dynamics of any complexity, combining e.g. both fast and slow dynamics in damped and resonant modes. A direct result is that for any specifically chosen $V_k(z)$, any strictly proper transfer function $G(z) \in \mathcal{H}_2$ has a unique series expansion

$$G(z) = z^{-1}\sum_{k=0}^{\infty} L_k V_k(z) \quad \text{with } L_k \in \ell^{1 \times n_b}[0, \infty). \tag{5.12}$$

For specific choices of $G_b(z)$ well known classical basis functions can be generated.

a. With $G_b(z) = z^{-1}$, having minimal balanced realization $(0, 1, 1, 0)$, the standard pulse basis $V_k(z) = z^{-k}$ results.

b. Choosing a first order inner function $G_b(z) = \dfrac{1 - az}{z - a}$, with some real-valued a, $|a| < 1$, and balanced realization

$$(A, B, C, D) = (a, \sqrt{1 - a^2}, \sqrt{1 - a^2}, -a) \tag{5.13}$$

the Laguerre basis results:

$$V_k(z) = \sqrt{1 - a^2} z \frac{(1 - az)^k}{(z - a)^{k+1}}. \tag{5.14}$$

c. Similarly the Kautz functions (Kautz, 1954; Wahlberg, 1990,1994a), originate from the choice of a second order inner function

$$G_b(z) = \frac{-cz^2 + b(c - 1)z + 1}{z^2 + b(c - 1)z - c} \tag{5.15}$$

with some real-valued b, c satisfying $|c|, |b| < 1$. A balanced realization of $G_b(z)$ can be found to be given by

$$
A \;=\; \begin{bmatrix} b & \sqrt{(1-b^2)} \\ c\sqrt{(1-b^2)} & -bc \end{bmatrix} \tag{5.16}
$$

$$
B \;=\; \begin{bmatrix} 0 \\ \sqrt{(1-c^2)} \end{bmatrix} \tag{5.17}
$$

$$
C \;=\; \begin{bmatrix} \gamma_2 & \gamma_1 \end{bmatrix} \quad D = -c \tag{5.18}
$$

with $\gamma_1 = -b\sqrt{(1-c^2)}$ and $\gamma_2 = \sqrt{(1-c^2)(1-b^2)}$, see also Heuberger *et al.* (1992, 1993).

The generalized orthonormal basis for $\mathcal{H}_2$ also induces a similar basis for the signal space $\ell_2[0, \infty)$ of squared summable sequences, through inverse z-transformation to the signal-domain. Denoting

$$
V_k(z) = \sum_{\ell=0}^{\infty} \phi_k(\ell) z^{-\ell}, \tag{5.19}
$$

it follows that $\{e_i^T \phi_k(\ell)\}_{i=1,\cdots,n_b;k=0,\cdots,\infty}$ is an orthonormal basis for the signal space $\ell_2[0, \infty)$. These ℓ_2 basis functions can also be constructed directly from G_b and its balanced realization (A, B, C, D), see Heuberger *et al.* (1992).

5.3   Identification of expansion coefficients

In this section we will consider and denote the least squares identification method in more detail.

The prediction error that results from applying the appropriate model structure conformable to (5.12) can be written as

$$
\varepsilon(t, \theta) = y(t) - \sum_{k=0}^{n-1} L_k V_k(q) u(t-1), \tag{5.20}
$$

with the unknown parameter θ is written as:

$$
\theta := [L_0 \cdots L_{n-1}]^T \quad \in \mathbb{R}^{n_b \cdot n}. \tag{5.21}
$$

We will assume that the input signal $\{u(t)\}$ is a quasi-stationary signal (Ljung, 1987) having a spectral density $\Phi_u(\omega)$, with a stable spectral factor $H_u(e^{i\omega})$, i.e. $\Phi_u(\omega) = H_u(e^{i\omega}) H_u(e^{-i\omega})$.

We will further denote

$$
x_k(t) \;:=\; V_k(q) u(t-1) \tag{5.22}
$$

$$
\psi(t) \;:=\; \begin{bmatrix} x_0(t) \\ x_1(t) \\ \vdots \\ x_{n-1}(t) \end{bmatrix} \tag{5.23}
$$

and consequently

$$\varepsilon(t, \theta) = y(t) - \psi^T(t)\theta. \tag{5.24}$$

Following Ljung (1987), under weak conditions the parameter estimate $\hat{\theta}_N(n)$ given by (5.9) will converge with probability 1 to the asymptotic estimate

$$\theta^*(n) = R(n)^{-1}F(n) \tag{5.25}$$

with

$$R(n) = \bar{E}\psi(t)\psi^T(t) \qquad F(n) = \bar{E}\psi(t)y(t). \tag{5.26}$$

For the analysis of bias and variance errors of this identification scheme, we will further use the following notation:

$$
\begin{aligned}
G_0(z) &= z^{-1}\sum_{k=0}^{\infty} L_k^{(0)} V_k(z) \\
\theta_0 &= [L_0^{(0)} \cdots L_{n-1}^{(0)}]^T \\
\theta_e &= [L_n^{(0)} \ L_{n+1}^{(0)} \cdots]^T \\
\psi_e(t) &= [x_n^T(t) \ x_{n+1}^T(t) \cdots]^T \\
\Omega_n(e^{i\omega}) &:= e^{-i\omega}[V_0^T(e^{i\omega}) \ V_1^T(e^{i\omega}) \ \cdots V_{n-1}^T(e^{i\omega})]^T \\
\Omega_e(e^{i\omega}) &:= e^{-i\omega}[V_n^T(e^{i\omega}) \ V_{n+1}^T(e^{i\omega}) \ \cdots]^T
\end{aligned}
$$

leading to the following alternative description of the data generating system:

$$
\begin{aligned}
y(t) &= \psi^T(t)\theta_0 + \psi_e^T(t)\theta_e + v(t), & (5.27) \\
G_0(e^{i\omega}) &= \Omega_n^T(e^{i\omega})\theta_0 + \Omega_e^T(e^{i\omega})\theta_e. & (5.28)
\end{aligned}
$$

In the analysis of the asymptotic parameter estimate $\theta^*(n)$ the block-Toeplitz structured matrix $R(n)$ will play an important role. Note that this matrix has a block-Toeplitz structure with the (j, ℓ) block-element given by $\bar{E}x_j(t)x_\ell^T(t)$. For the analysis of the properties of this block-Toeplitz matrix, we will employ a signal and system transformation that is induced by the generalized basis. This transformation is presented and discussed in the next two sections.

Remark 5.3.1 *In this paper we consider the identification of strictly proper systems by strictly proper models. All results will appear to hold similarly true for the case of proper systems and corresponding proper models, by only adapting the notation in this section.*

5.4 The Hambo transform of signals and systems

The presented generalized orthonormal basis for $\mathcal{H}_2/\ell_2$ induces a transformation of signals and systems to a transform domain. Next to the intrinsic importance of signal and systems analysis in this transform-domain (for some of these results see Heuberger (1991)), we can fruitfully use these transformations in the analysis of statistical properties of the identified models, as well as in the derivation of bias and variance error bounds.

Let $\{V_k(z)\}_{k=0,\cdots\infty}$ be an orthonormal basis, as defined in section 5.2, and let $\{\phi_k(t)\}_{k=0,\cdots\infty}$ be as defined in (5.19). Then for any signal $x(t) \in \ell_2^m$ there exists a unique transformation

$$\mathcal{X}(k) := \sum_{t=0}^{\infty} \phi_k(t)x^T(t) \tag{5.29}$$

and we denote the corresponding λ-transform of $\mathcal{X}(k)$ as:

$$\tilde{x}(\lambda) := \sum_{k=0}^{\infty} \mathcal{X}(k)\lambda^{-k} \tag{5.30}$$

We will refer to $\tilde{x}(\lambda)$ as the *Hambo*-transform of the signal $x(t)$. Note that $x \in \ell_2^m$, and $\tilde{x}(\lambda) \in \mathcal{H}_2^{n_b \times m}$.

Now consider a scalar system $y(t) = G(q)u(t)$ with $G \in \mathcal{H}_2$ with u, y signals in ℓ_2. Then there exists a Hambo-transformed system $\tilde{G}(\lambda) \in \mathcal{H}_2^{n_b \times n_b}$ such that

$$\tilde{y}(\lambda) = \tilde{G}(\lambda)\tilde{u}(\lambda). \tag{5.31}$$

In terms of the sequence of expansion coefficients, this can also be written as

$$\mathcal{Y}(k) = \tilde{G}(q)\mathcal{U}(k) \quad \text{for all } k \tag{5.32}$$

where the shift operator q operates on the sequence index k. The construction of this transformed system is given in the following proposition.

Proposition 5.4.1 *Consider a scalar system $G \in \mathcal{H}_2$ relating input and output signals according to $y(t) = G(q)u(t)$ with $u, y \in \ell_2$, with $G(z) = \sum_{k=0}^{\infty} g_k z^{-k}$.*
Consider an orthonormal basis $\{V_k(z)\}_{k=0,\cdots\infty}$ as defined in section 5.2, generated by a scalar inner transfer function $G_b(z)$ with balanced realization (A, B, C, D). Denote the rational function:

$$N(\lambda) := A + B(\lambda I - D)^{-1}C. \tag{5.33}$$

Then

$$\tilde{y}(\lambda) = \tilde{G}(\lambda)\tilde{u}(\lambda) \tag{5.34}$$

with

$$\tilde{G}(\lambda) := \sum_{k=0}^{\infty} g_k N(\lambda)^k. \tag{5.35}$$

Proof: See Appendix.   □

The interpretation of this proposition is that the Hambo-transform of any system G can be obtained by a simple variable-transformation on the original transfer function, where the variable transformation concerned is given by $z^{-1} = N(\lambda)$.

Note that this result generalizes the situation of a corresponding Laguerre transformation, where it concerns the variable-transformation $z = \dfrac{\lambda + a}{1 + a\lambda}$ (see also Wahlberg, 1991). However due to the fact that in our case the McMillan degree of the inner function that generates the basis is $n_b \geq 1$, the Hambo-transformed system $\tilde{G}$ increases in input/output-dimension to $\tilde{G} \in \mathcal{H}_2^{n_b \times n_b}$. Note that, as G is scalar, $N(\lambda)$ is an $n_b \times n_b$ rational transfer function

matrix of McMillan degree 1 (since D is scalar).

Note also the appealing symmetric structure of this result. Whereas G_b has a balanced realization (A, B, C, D), the variable-transformation function $N(\lambda)$ has a realization (D, C, B, A) which can also be shown to be balanced.

The previous Proposition considers scalar ℓ_2 signals and scalar systems. In the sequel of this paper we will also have to deal with specific situations of multivariable signals, for which there exist straightforward extensions of this result.

Proposition 5.4.2 *Consider a scalar transfer function $G \in \mathcal{H}_2$ relating m-dimensional input and output signals $u, y \in \ell_2^m$, according to* [2]

$$y(t) = [G(z)I_m]u(t) \tag{5.36}$$

Then

$$\tilde{y}(\lambda) = \tilde{G}(\lambda)\tilde{u}(\lambda) \tag{5.37}$$

with $\tilde{G}(\lambda)$ as defined in (5.35). □

Proof: For $m = 1$ the result is shown in Proposition 5.4.1. If we write the relation between y and u componentwise, i.e. $y_i(t) = G(z)u_i(t)$ it follows from the mentioned Proposition that $\tilde{y}_i(\lambda) = \tilde{G}(\lambda)\tilde{u}_i(\lambda)$, where $\tilde{y}_i, \tilde{u}_i \in \mathbb{R}^{n_b \times 1}(\lambda)$. It follows directly that $\tilde{y}(\lambda) = [\tilde{y}_1(\lambda) \quad \cdots \quad \tilde{y}_m(\lambda)] = \tilde{G}(\lambda)[\tilde{u}_1(\lambda) \quad \cdots \quad \tilde{u}_m(\lambda)] = \tilde{G}(\lambda)\tilde{u}(\lambda).$ □

One of the results that we will need in the analysis of least squares related block Toeplitz matrices is formulated in the following Proposition.

Proposition 5.4.3 *Consider a scalar inner transfer function $G_b(z)$ generating an orthogonal basis as discussed before. Then*

$$\tilde{G}_b(\lambda) = \lambda^{-1}I_{n_b}. \tag{5.38}$$

Proof: It can simply be verified that for all k, $G_b(q)\phi_k(t) = \phi_{k+1}(t)$. With Proposition 5.4.2 it follows that $\tilde{\phi}_{k+1}(\lambda) = \tilde{G}_b(\lambda)\tilde{\phi}_k(\lambda)$.

Since for each k, $\tilde{\phi}_k(\lambda) = \sum_{t=0}^{\infty} I_{n_b}\delta(t-k)\lambda^{-t}$, it follows that for all k,

$$I_{n_b}\lambda^{-k-1} = \tilde{G}_b(\lambda)I_{n_b}\lambda^{-k}. \tag{5.39}$$

Since this holds for all k it proves the result. □

The basis generating inner function transforms to a simple shift in the Hambo-domain. Next we will consider a result that reflects some properties of the back-transformation of Hambo-transformed systems to the original domain, i.e. the inverse Hambo transform.

Proposition 5.4.4 *Consider a scalar inner transfer function G_b generating an orthogonal basis as discussed before, and let G_b induce a corresponding Hambo-transform. Let $H \in \mathcal{H}_2$ be a scalar transfer function with Hambo-transform $\tilde{H}$. Then*

$$\tilde{H}(G_b(z))V_0(z) = V_0(z)H(z^{-1}). \tag{5.40}$$

---

[2]Since $G(z)$ is scalar we allow the notation $G(z)I_m$, which more formally should be denoted as $G(z) \otimes I_m$.

Proof: See appendix. □

The following lemma relates quadratic signal properties to properties of the transformed signals.

Lemma 5.4.5 *Let $x_j, x_\ell \in \ell_2^m$ and consider a Hambo-transform induced by an orthonormal basis $V_k(z)$ generated by an inner function $G_b(z)$ with McMillan degree $n_b \geq 1$. Then*

$$\sum_{t=0}^{\infty} x_j(t)x_\ell^T(t) = \sum_{k=0}^{\infty} \mathcal{X}_j^T(k)\mathcal{X}_\ell(k) = \frac{1}{2\pi}\int_{-\pi}^{\pi}\tilde{x}_j^T(e^{-i\omega})\tilde{x}_\ell(e^{i\omega})d\omega. \tag{5.41}$$

Proof: This Lemma is a direct consequence of the fact that due to the fact that the basis is orthonormal, it induces a transformation that is an isomorphism. □

The transformation that is discussed in this section refers to ℓ_2-signals and the corresponding transformation of systems actually concerns the transformation of the ℓ_2-behaviour or graph of a dynamical system. However, this same orthogonal basis for ℓ_2 can also be employed to induce a transformation of (quasi-)stationary stochastic processes to the transform domain, as briefly considered in the next section.

5.5 Hambo transformation of stochastic processes

Let v be a scalar valued stochastic process or quasi-stationary signal (Ljung, 1987), having a rational spectral density $\Phi_v(\omega)$. Let $H_v(e^{i\omega})$ be a stable spectral factor of $\Phi_v(\omega)$, and let $h_v(k)$ be its ℓ_2 impulse response, satisfying $H_v(z) = \sum_{k=0}^{\infty} h_v(k)z^{-k}$. Then

$$h_v(t) = H_v(q)\delta(t) \tag{5.42}$$

and consequently with Proposition 5.4.1

$$\tilde{h}_v = \tilde{H}_v\tilde{\delta}. \tag{5.43}$$

The Hambo-transform of the spectral density $\Phi_v(\omega)$ will be defined as

$$\tilde{\Phi}_v(\omega) := \tilde{H}_v^T(e^{-i\omega})\tilde{H}_v(e^{i\omega}). \tag{5.44}$$

Let $w(t) = P_{wv}(q)v(t)$ with P_{wv} a stable scalar transfer function. Then

$$\tilde{h}_w = \tilde{P}_{wv}\tilde{h}_v \tag{5.45}$$

with $h_w, h_v \in \ell_2$, the impulse responses of stable spectral factors of $\Phi_w(\omega)$, $\Phi_v(\omega)$, respectively. Similarly to Lemma 5.4.5 we can now formulate some properties of stochastic processes.

Lemma 5.5.1 *Let w, z be m-dimensional stationary stochastic processes, satisfying $w(t) = \sum_{k=0}^{\infty} h_w(k)e(t-k)$ and $z(t) = \sum_{k=0}^{\infty} h_z(k)e(t-k)$, with $\{e(t)\}$ a scalar-valued unit variance white noise process. Then*

$$\bar{E}[w(t)z^T(t)] = \frac{1}{2\pi}\int_{-\pi}^{\pi}\tilde{h}_w^T(e^{-i\omega})\tilde{h}_z(e^{i\omega})d\omega. \tag{5.46}$$

Lemma 5.5.2 *Let w, z, and v be m-dimensional stationary stochastic processes, satisfying*

$$w(t) = P_{wv}(q)I_m v(t) \tag{5.47}$$

$$z(t) = P_{zv}(q)I_m v(t), \tag{5.48}$$

with $P_{wv}, P_{zv} \in \mathcal{H}_2$, and $v(t) = \sum_{k=0}^{\infty} h_v(k)e(t-k)$, with $\{e(t)\}$ a scalar-valued unit variance white noise process. Then

$$\bar{E}w(t)z^T(t) = \frac{1}{2\pi}\int_{-\pi}^{\pi} \tilde{h}_v^T(e^{-i\omega})\tilde{P}_{wv}^T(e^{-i\omega})\tilde{P}_{wv}(e^{i\omega})\tilde{h}_v(e^{i\omega})d\omega.$$

The previous lemma's can simply be shown to hold also in the case of quasi-stationary signals. To this end we already used the operator $\bar{E} := \lim_{N\to\infty}\frac{1}{N}\sum_{t=0}^{N-1}E$, where E stands for expectation.

5.6 Asymptotic analysis of bias and variance

5.6.1 Analysis of the least squares problem

As mentioned in section 5.3, the main properties of the asymptotic parameter estimate, hinges on the characteristics of the matrix $R(n)$, as defined by (5.26), (5.23). We will first analyse this matrix in terms of its structural properties and of its eigenvalues.

The Hambo-transform is very efficiently employed in the following result.

Theorem 5.6.1 *The matrix $R(n)$ defined in (5.26) is a block-Toeplitz matrix, being the covariance matrix related to the spectral density function $\tilde{\Phi}_u(\omega)$.*

Proof: The (j,ℓ) block-element of matrix $R(n)$ is given by $\bar{E}x_j(t)x_\ell^T(t)$. Since $x_j(t) = G_b^j(q)I_{n_b} \cdot x_0(t)$ it follows with Lemma 5.5.2 that

$$\bar{E}x_j(t)x_\ell^T(t) = \frac{1}{2\pi}\int_{-\pi}^{\pi}\tilde{h}_{x_0}^T(e^{-i\omega})[\tilde{G}_b^T(e^{-i\omega})]^j[\tilde{G}_b(e^{i\omega})]^\ell\tilde{h}_{x_0}(e^{i\omega})d\omega.$$

With Proposition 5.4.3 it follows that

$$\bar{E}x_j(t)x_\ell^T(t) = \frac{1}{2\pi}\int_{-\pi}^{\pi}e^{i\omega(j-\ell)}\tilde{h}_{x_0}^T(e^{-i\omega})\tilde{h}_{x_0}(e^{i\omega})d\omega. \tag{5.49}$$

Since $x_0(t) = q^{-1}V_0(q)u(t)$ we can write $h_{x_0}(t) = q^{-1}V_0(q)H_u(q)\delta(t)$. Since H_u is scalar, we can write $h_{x_0}(t) = H_u(q)q^{-1}V_0(q)\delta(t) = H_u(q)h_{v_0}(t)$, with $h_{v_0}(t)$ the impulse response of the transfer function $q^{-1}V_0(q)$.

Applying Proposition 5.4.1 now shows $\tilde{h}_{x_0} = \tilde{H}_u\tilde{h}_{v_0} = \tilde{H}_u$. The latter equality follows from $\tilde{h}_{v_0} = I_{n_b}$, as the impulse response of $q^{-1}V_0(q)$ exactly matches the first n_b basis functions in the Hambo-domain. Consequently

$$\bar{E}x_j(t)x_\ell^T(t) = \frac{1}{2\pi}\int_{-\pi}^{\pi}e^{i\omega(j-\ell)}\tilde{H}_u^T(e^{-i\omega})\tilde{H}_u(e^{i\omega})d\omega = \frac{1}{2\pi}\int_{-\pi}^{\pi}e^{i\omega(j-\ell)}\tilde{\Phi}_u(\omega)d\omega$$

which proves the result. $\square$

Remark 5.6.2 *In Wahlberg (1991), treating the (first order) Laguerre case, the corresponding Toeplitz matrix is the covariance matrix related to the spectral density*

$$\Phi_u(\frac{e^{i\omega} + a}{1 + ae^{i\omega}}). \tag{5.50}$$

This implies that in that case a variable transformation

$$e^{i\omega} \to \frac{e^{i\omega} + a}{1 + ae^{i\omega}} \tag{5.51}$$

is involved, or equivalently

$$e^{-i\omega} \to \frac{1 + ae^{i\omega}}{e^{i\omega} + a}. \tag{5.52}$$

Using the balanced realization of a first order inner function, (5.13), this implies that in the setting of this paper, the variable transformation involved is given by $e^{-i\omega} \to N(e^{i\omega})$, while N has a minimal balanced realization

$$(A, B, C, D) = (-a, \sqrt{1 - a^2}, \sqrt{1 - a^2}, a).$$

This directly leads to the variable transformation (5.52).

The following Proposition bounds the eigenvalues of the block-Toeplitz matrix $R(n)$.

Proposition 5.6.3 *Let the block-Toeplitz matrix $R(n)$ defined in (5.26) have eigenvalues $\lambda_j(R(n))$. Then*

(a) For all n, the eigenvalues of $R(n)$ are bounded by

$$ess \inf_{\omega} \Phi_u(\omega) \leq \lambda_j(R(n)) \leq ess \sup_{\omega} \Phi_u(\omega);$$

(b) $\lim_{n\to\infty} \max_j \lambda_j(R(n)) = ess \sup_{\omega} \Phi_u(\omega)$.

Proof: See Appendix. □

In the sequel of this paper we will assume that the input spectrum is bounded away from zero, i.e. $ess \inf_{\omega} \Phi_u(\omega) \geq c > 0$.

5.6.2   Asymptotic bias error

The previous results on $R(n)$ can be employed in the derivation of upper bounds for the asymptotic bias errors both in estimated parameters and in the resulting transfer function estimate. Combining equations (5.25),(5.26) and (5.27), it follows that

$$\theta^* - \theta_0 = R(n)^{-1}\bar{E}[\psi(t)\psi_e^T(t)\theta_e]. \tag{5.53}$$

Consequently

$$\|\theta^* - \theta_0\|_2 \leq \|R(n)^{-1}\|_2 \cdot \|\bar{E}[\psi(t)\psi_e^T(t)]\|_2 \cdot \|\theta_e\|_2, \tag{5.54}$$

where for a (matrix) operator T, $\|T\|_2$ refers to the induced operator 2-norm. For simplicity of notation we have skipped the dependence of θ^* (and θ_0) on n.

We can now formulate the following upper bound on the bias error.

Proposition 5.6.4 *Consider the identification set-up as discussed in section 5.3. Then*

$$\|\theta^* - \theta_0\|_2 \leq \frac{ess \sup_\omega \Phi_u(\omega)}{ess \inf_\omega \Phi_u(\omega)} \cdot \|\theta_e\|_2, \tag{5.55}$$

where $\|\theta_e\|_2 = \sqrt{\sum_{k=n}^\infty L_k^{(0)} L_k^{(0)T}}.$ □

The Proof of the Proposition is added in the Appendix.

In this result, as in the sequel of this paper, we have employed an upper bound for $\|R(n)^{-1}\|_2$ as provided by Proposition 5.6.3. In many situations the input signal and its statistical properties will be known, and $\|R(n)^{-1}\|_2$ can be exactly calculated. In that case we can replace $(ess \inf_\omega \Phi_u(\omega))^{-1}$ in (5.55) by $\|R(n)^{-1}\|_2$.

For the bias in the transfer function estimate the result corresponding to Proposition 5.6.4 is as follows.

Proposition 5.6.5 *Consider the identification set-up as discussed in section 5.3. Then*

(a) For all $\omega_1 \in [-\pi, \pi]$,

$$\begin{aligned}
|G(e^{i\omega_1}, \theta^*) - G_0(e^{i\omega_1})| &\leq \|V_0(e^{i\omega_1})\|_\infty [\|\theta_0 - \theta^*\|_1 + \|\theta_e\|_1] \\
&\leq \|V_0(e^{i\omega_1})\|_\infty \cdot \{\sqrt{n_b n} \frac{ess \sup_\omega \Phi_u(\omega)}{ess \inf_\omega \Phi_u(\omega)} \|\theta_e\|_2 + \|\theta_e\|_1\},
\end{aligned}$$

where $\|V_0(e^{i\omega_1})\|_\infty$ *is the* ℓ_∞-*induced operator norm of the matrix* $V_0(e^{i\omega_1}) \in \mathbf{C}^{n_b \times 1}$, *i.e. the maximum absolute value over the elements in* $V_0(e^{i\omega_1})$.

(b) The $\mathcal{H}_2$-*norm of the model error is bounded by:*

$$\|G(z, \theta^*) - G_0(z)\|_{\mathcal{H}_2} \leq \sqrt{\|\theta_0 - \theta^*\|_2^2 + \|\theta_e\|_2^2} \leq \{1 + \frac{ess \sup_\omega \Phi_u(\omega)}{ess \inf_\omega \Phi_u(\omega)}\} \|\theta_e\|_2. \tag{5.56}$$

Proof: See Appendix. □

Note that this latter bound on the bias in the transfer function estimate as well as the previously derived bound, are dependent on the basis functions chosen. The factor $\|\theta_e\|_2^2$ is determined by the convergence rate of the series expansion of G_0 in the generalized basis. The closer the dynamics of the system G_0 will be to the dynamics of the inner transfer function G_b, the faster the convergence rate will be. An upper bound for this convergence rate is derived in the following Proposition, based on the results in Heuberger et al. (1992).

Proposition 5.6.6 *Let* $G_0(z)$ *have poles* μ_i, $i = 1, \cdots, n_s$, *and let* $G_b(z)$ *have poles* ρ_j, $j = 1, \cdots n_b$.
Denote

$$\lambda := \max_i \prod_{j=1}^{n_b} \left| \frac{\mu_i - \rho_j}{1 - \mu_i \rho_j} \right|. \tag{5.57}$$

Then there exists a constant $c \in \mathbb{R}$ *such that for all* $\eta > \lambda$

$$\|\theta_e\|_2 \leq c \cdot \frac{\eta^{n+1}}{\sqrt{1 - \eta^2}}. \tag{5.58}$$

Proof: A sketch of proof is given in the Appendix. For a detailed proof the reader is referred to Heuberger (1991) and Heuberger and Van den Hof (1996).   □

Note that when the two sets of poles converge to each other, λ will tend to 0, the upper bound on $\|\theta_e\|_2$ will decrease drastically, and the bias error will reduce accordingly. The above result clearly shows the important contribution that an appropriately chosen set of basis functions can have in achieving a reduction of the bias in estimated transfer functions.

The results in (5.55), (5.56) show that we achieve consistency of the parameter and transfer function estimates as $n \to \infty$ provided that the input spectrum is bounded away from 0 and $\|\theta_e\|_2 \to 0$ for $n \to \infty$. The latter condition is guaranteed if $G_0 \in \mathcal{H}_2$.

For the FIR case, corresponding with $G_b(z) = z^{-1}$, we know that under specific experimental conditions the finite number of expansion coefficients can also be estimated consistently, irrespective of the tail. This situation can also be formulated for the generalized case.

Corollary 5.6.7 *Consider the identification setup as discussed in section 5.3. If $\tilde{H}_u$ is an inner transfer function, then for all $n \geq 1$ it follows that $\theta^* = \theta_0$ and the transfer function error bounds become*

(a) $|G(e^{i\omega_1}, \theta^*) - G_0(e^{i\omega_1})| \leq \|V_0(e^{i\omega_1})\|_\infty \|\theta_e\|_1$, *for each ω_1;*

(b) $\|G(z, \theta^*) - G_0(z)\|_{\mathcal{H}_2} \leq \|\theta_e\|_2$.

Proof: Under the given condition it can simply be verified that $\tilde{\Phi}_u(\omega) = I_{n_b}$. This implies that the block-Toeplitz matrix $R(n) = I$, and that for all $n \geq 1$, $R_{12}(n) = 0$. Employing this relation in the proofs of Propositions 5.6.4, 5.6.5 shows the results.   □

Note that a special case of the situation of an inner $\tilde{H}_u$ is obtained if the input signal u is uncorrelated (white noise). In that situation $H_u = 1$ and consequently $\tilde{H}_u = I_{n_b}$, being inner.

5.6.3 Asymptotic variance

For an analysis of the asymptotic variance of the estimated transfer function, we can generalize the results obtained for the case of Laguerre functions in Wahlberg (1991). From classical analysis of prediction error identification methods, Ljung (1987), we know that under fairly weak conditions

$$\sqrt{N}(\hat{\theta}_N(n) - \theta^*) \to \mathcal{N}(0, Q_n) \quad \text{as } N \to \infty, \tag{5.59}$$

where $\mathcal{N}(0, Q_n)$ denotes a Gaussian distribution with zero mean and covariance matrix Q_n. For output error identification schemes, as applied in this paper, the asymptotic covariance matrix satisfies:

$$Q_n = [\bar{E}\psi(t)\psi^T(t)]^{-1}[\bar{E}\bar{\psi}(t)\bar{\psi}^T(t)][\bar{E}\psi(t)\psi^T(t)]^{-1} \tag{5.60}$$

with $\bar{\psi}(t) = \sum_{i=0}^{\infty} h_0(i)\psi(t+i)$, and $h_0(i)$ the impulse response of the corresponding transfer function H_0.

We know that, according to Theorem 5.6.1, the block-Toeplitz matrix $R(n) = \bar{E}\psi(t)\psi^T(t)$ is related to the spectral density function $\tilde{\Phi}_u(\omega)$. For the block-Toeplitz matrix $P(n) = \bar{E}\bar{\psi}(t)\bar{\psi}^T(t)$ we can formulate a similar result.

Lemma 5.6.8 *The block-Toeplitz matrix $P(n) = \bar{E}\bar{\psi}(t)\bar{\psi}^T(t)$ is the covariance matrix related to the spectral density function $\tilde{\Phi}_u(\omega) \cdot \tilde{\Phi}_v(\omega)$.* □

Proof: The proof follows along similar lines as followed in the proof of Theorem 5.6.1. □

From the asymptotic covariance of the parameter estimate, we can derive the expression for the transfer function estimate:

$$\frac{N}{n \cdot n_b} cov(\hat{G}(e^{i\omega_1}), \hat{G}(e^{i\omega_2})) \to \frac{1}{n \cdot n_b}\Omega_n^T(e^{i\omega_1})Q_n\Omega_n(e^{-i\omega_2}) \tag{5.61}$$

as $N \to \infty$, while $cov(\cdot, \cdot)$ refers to the cross-covariance matrix in the joint asymptotic distribution of

$$[G(e^{i\omega_1}, \hat{\theta}_N) - G(e^{i\omega_1}, \theta^*), G(e^{i\omega_2}, \hat{\theta}_N) - G(e^{i\omega_2}, \theta^*)].$$

In (5.61) the term $n \cdot n_b$ refers to the number of scalar parameters that is estimated.
Now we have the ingredients for formulating an expression for the asymptotic covariance $(n \to \infty, N \to \infty)$ of the estimated transfer functions.

Theorem 5.6.9 *Assume the spectral density $\Phi_u(\omega)$ to be bounded away from zero and sufficiently smooth. Then for $N, n \to \infty$, $n^2/N \to 0$:*

$$\frac{N}{n \cdot n_b} cov(G(e^{i\omega_1}, \hat{\theta}_N), G(e^{i\omega_2}, \hat{\theta}_N)) \to$$

$$\begin{cases} 0 & for\ G_b(e^{i\omega_1}) \neq G_b(e^{i\omega_2}), \\ \frac{1}{n_b}V_0^T(e^{i\omega_1})V_0(e^{-i\omega_1}) \cdot \frac{\Phi_v(\omega_1)}{\Phi_u(\omega_1)} & for\ \omega_1 = \omega_2. \end{cases}$$

The proof is added in the Appendix.
Theorem 5.6.9 gives a closed form expression for the asymptotic covariance. Note that it implies that the variance of the transfer function estimate for a specific ω_1 is given by

$$\frac{n}{N}V_0^T(e^{i\omega_1})V_0(e^{-i\omega_1}) \cdot \frac{\Phi_v(\omega_1)}{\Phi_u(\omega_1)} \tag{5.62}$$

which is the noise to input signal ratio weighted with an additional weighting factor that is determined by the basis functions. This additional weighting, which is not present in the case of FIR estimation, again generalizes the weighting that is also present in the case of Laguerre basis functions, see Wahlberg (1991). Since the frequency function $V_0(e^{i\omega})$ has a low pass character, it ensures that the variance will have a roll-off at high frequencies. This is unlike the case of FIR estimation, where the absolute variance generally increases with increasing frequency.
The role of V_0 in this variance expression clearly shows that there is a design variable involved that can be chosen also from a point of view of variance reduction. In that case V_0 has to be chosen in such a way that it reduces the effect of the noise ($\Phi_v(\omega)$) in those frequency regions where the noise is dominating.
The result of the theorem also shows that - for $n_b = 1$ - the transfer function estimates will be asymptotically uncorrelated. In that case it can simply be shown that $G_b(e^{i\omega_1}) \neq G_b(e^{i\omega_2})$ implies $\omega_1 \neq \omega_2$ for $\omega_1, \omega_2 \in [0, \pi]$. In the case $n_b > 1$ this latter situation is not guaranteed.
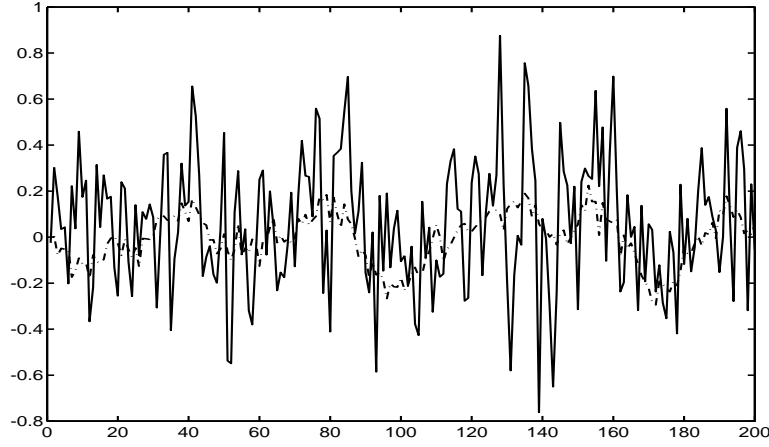
Figure 5.1: Simulated noise disturbed output signal $y(t)$ (solid) and noise signal $v(t)$ (dashed) on time interval $t = 1, .., 200$.

5.7   Simulation example

In order to illustrate the identification method considered in this paper, we will show the results of an example where an identification is performed on the basis of simulation data. The simulated system is determined by:

$$G_0(z) = \frac{b_1 z^{-1} + \cdots + b_5 z^{-5}}{1 + a_1 z^{-1} + \cdots + a_5 z^{-5}} \tag{5.63}$$

with $b_1 = 0.2530$, $b_2 = -0.9724$, $b_3 = 1.4283$, $b_4 = -0.9493$, $b_5 = 0.2410$; $a_1 = -4.15$, $a_2 = 6.8831$, $a_3 = -5.6871$, $a_4 = 2.3333$, $a_5 = -0.3787$. The system has poles in $0.95 \pm 0.2i$, $0.85 \pm 0.09i$ and 0.55. The static gain of the system is 1.

An output noise is added to the simulated output, coloured by a second order noise filter

$$H_0(z) = \frac{1 - 1.38 z^{-1} + 0.4 z^{-2}}{1 - 1.9 z^{-1} + 0.91 z^{-2}}. \tag{5.64}$$

As input signal is chosen a zero mean unit variance white noise signal, while the input to the noise filter is also a white noise signal with variance 0.0025, leading to a signal-to-noise ratio at the output of $11.6dB$, being equivalent to around 30% noise disturbance in amplitude on the noise-free output signal.

Orthogonal basis functions have been chosen generated by a fourth order inner function, having poles: $0.9 \pm 0.3i$ and $0.7 \pm 0.2i$. As the choice of basis functions can highly influence the accuracy of the identified model, we have chosen these basis functions, having poles that are only slightly in the direction of the system dynamics. They are not really accurate representations of the system poles, thus avoiding the use of knowledge that is generally not available in an identification situation.

We have used a data set of input and output signals with length $N = 1200$, and have estimated 5 coefficients of the series expansion.

The output signal and its noise contribution are depicted in Figure 5.1. In Figure 5.2 the Bode amplitude plot of G_0 is sketched together with the amplitude plots of each of the four
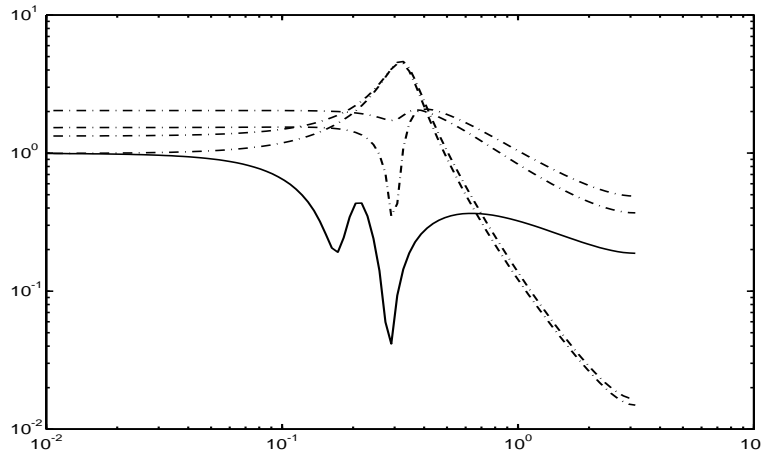
Figure 5.2: Bode amplitude plot of simulated system G_0 (solid) and of basis functions V_0 (four-dimensional) (dashed).

components of V_0, i.e. the first four basis functions. Note that all other basis functions will show the same Bode amplitude plot, as they only differ in multiplication by a scalar inner function, which does not change its amplitude. We have used 5 different realizations of 1200 data points to estimate 5 different models. Their Bode amplitude plots are given in Figure 5.3 and the corresponding step responses in Figure 5.4.

Figure 5.5 shows the relevant expressions in the asymptotic variance expression (5.62). This refers to the plots of $V_0^T V_0$ and of the noise spectrum $\Phi_v(\omega)$ as well as their product. Since $\Phi_u(\omega) = 1$, this latter product determines the asymptotic variance of the estimated transfer function.

To illustrate the power of the identification method, we have made a comparison with the identification of 5th order (least squares) output error models, dealing with a parametrized prediction error

$$\varepsilon(t, \theta) = y(t) - \frac{b_1 q^{-1} + b_2 q^{-2} + \cdots + b_5 q^{-5}}{1 + a_1 q^{-1} + \cdots + a_5 q^{-5}} u(t). \tag{5.65}$$

Note that G_0 is also a 5th-order system.

In Figures 5.6 and 5.7 the results of the estimated 5th order output error models are sketched. Here also five different realizations of the input/output data are used. It can be observed that the models based on the generalized orthogonal basis functions have a good ability to identify the resonant behaviour of the system in the frequency range from 0.15 to 0.5 rad/sec, while the output error models clearly have less performance here. The variance of both types of identification methods seem to be comparable. Note that the OE algorithm requires a nonlinear optimization whereas the identification of expansion coefficients is a convex optimization problem. Providing the output error algorithm with an initial parameter estimate based on the poles of the basis functions, did not influence the obtained results essentially.

Figure 5.3: Bode amplitude plot of simulated system G_0 (solid) and of five estimated models with $n = 5$, $N = 1200$ using five different realizations of the input/output data (dashed).

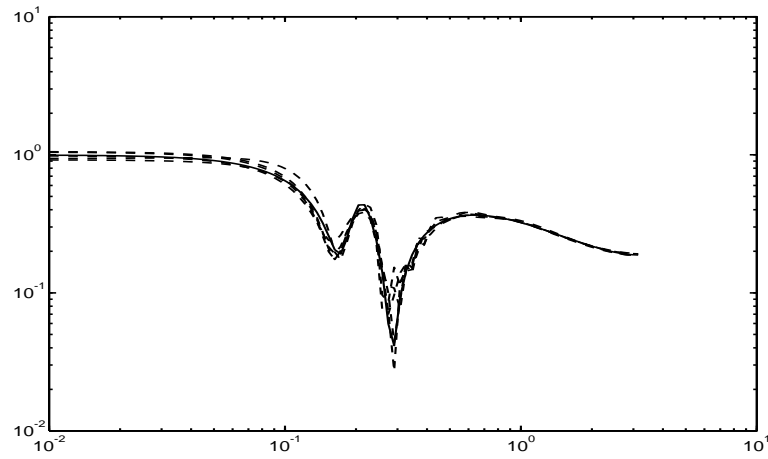Figure 5.4: Step response of simulated system G_0 (solid) and of five estimated models with $n = 5$, $N = 1200$ using five different realizations of the input/output data (dashed).

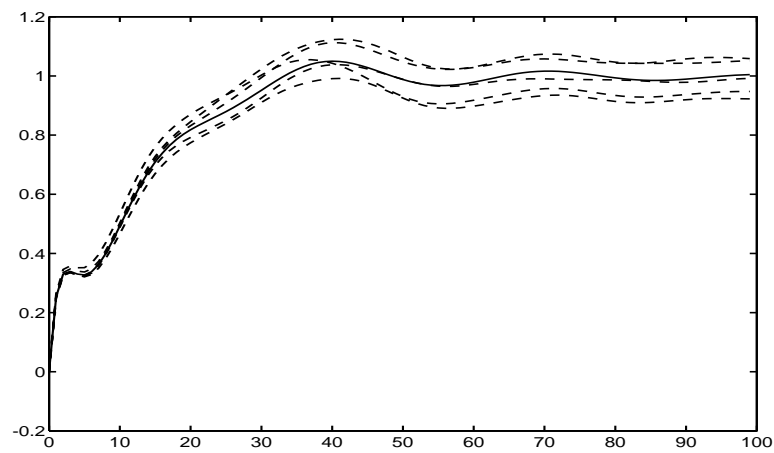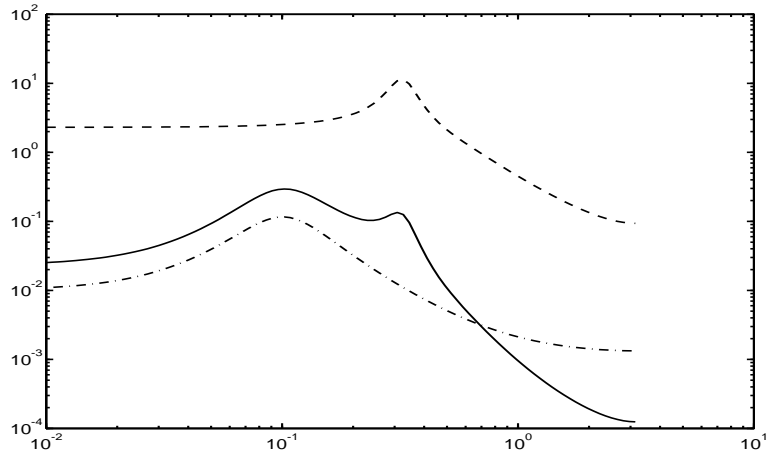Figure 5.5: Bode amplitude plot of $\dfrac{1}{n_b}V_0^T V_0$ (dashed), spectrum $\Phi_v(\omega)$ (dash-dotted) and their product (solid).
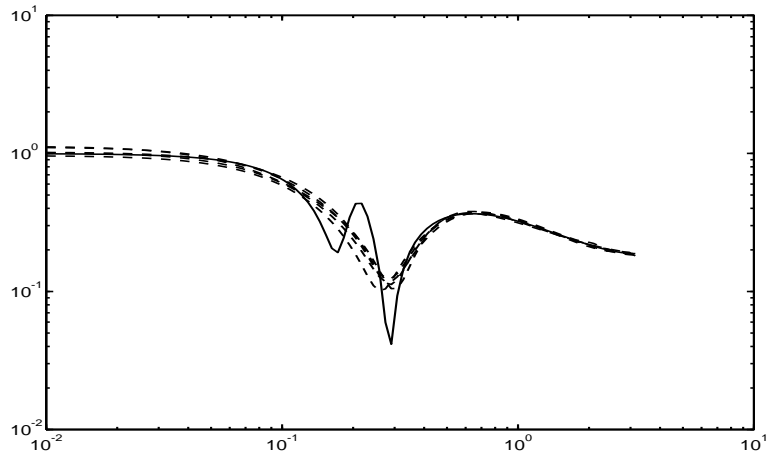
Figure 5.6: Bode amplitude plot of G_0 (solid) and five 5-th order OE models (dashed).
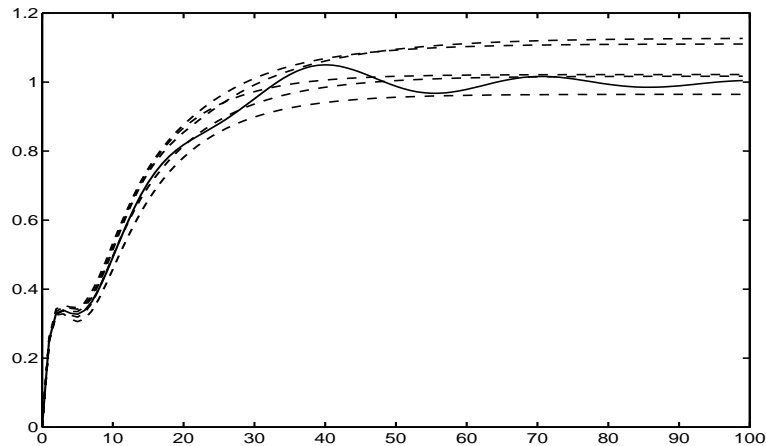
Figure 5.7: Step response of G_0 (solid) and five 5-th order OE models (dashed).

5.8   Discussion

In this paper we have analyzed some asymptotic properties of linear estimation schemes that identify a finite number of expansion coefficients in a series expansion of a linear stable transfer function, employing recently developed generalized orthogonal basis functions. These basis functions generalize the well known pulse, Laguerre and Kautz basis functions and are shown to provide flexible design variables, that when properly chosen provide fast convergence of the series expansion. In an identification context this implies that only few coefficients have to be estimated to obtain accurate estimates, while simple linear regression schemes can be used. Both bias and variance errors are analyzed and error bounds are established.

As the accuracy of the chosen basis functions can substantially improve the identification results in both bias and variance, the introduced method points to the use of iterative procedures, where the basis functions are updated iteratively. Previously estimated models can then be used to dictate the poles of the basis. Such iterative methods already have been applied successfully in practical experiments, see e.g. De Callafon *et al.*(1993).

The flexibility of the introduced basis functions provides a means to introduce uncertain a priori knowledge into the identification procedure. In contrast with other identification techniques, where a priori knowledge definitely has to be certain, this a priori knowledge (i.e. the system poles), is allowed to be approximate. The only consequence is that the accuracy of the identified models will be higher, the "better" the a priori knowledge is.

Apart from the identification of nominal models, the basis functions introduced here, have also been applied in the identification of model error bounds, see De Vries (1994) and Hakvoort and Van den Hof (1994).

Appendix

Proof of Proposition 5.4.1.
Let us consider the situation for $G(z) = z^{-1}$. In this situation $y(t) = u(t-1)$. Consequently $\mathcal{Y}(k) := \sum_{t=0}^{\infty} \phi_k(t) y(t) = \sum_{t=0}^{\infty} \phi_k(t) u(t-1)$. From Heuberger *et al.* (1992), we know that for each $k \in \mathbb{Z}$:

$$\begin{bmatrix} \phi_0(t) \\ \phi_1(t) \\ \vdots \\ \phi_k(t) \end{bmatrix} = A_{k+1} \begin{bmatrix} \phi_0(t-1) \\ \phi_1(t-1) \\ \vdots \\ \phi_k(t-1) \end{bmatrix}$$

with the matrix $A_k \in \mathbb{R}^{kn_b \times kn_b}$ given by

$$A_k = \begin{bmatrix} A & 0 & \cdots & \cdot & 0 \\ BC & A & 0 & \cdot & 0 \\ BDC & BC & \cdot & \cdot & 0 \\ \vdots & \vdots & \cdot & \ddots & 0 \\ BD^{k-2}C & BD^{k-3}C & \cdots & BC & A \end{bmatrix}.$$

Using this in the expression for $\mathcal{Y}(k)$ shows that

$$\begin{aligned} \mathcal{Y}(k) &= \sum_{t=0}^{\infty} \phi_k(t) u(t-1) \\ &= [0\ 0\ \cdots\ I_{n_b}] A_{k+1} \sum_{t=0}^{\infty} \begin{bmatrix} \phi_0(t-1) \\ \phi_1(t-1) \\ \vdots \\ \phi_k(t-1) \end{bmatrix} u(t-1) = [0\ 0\ \cdots\ I_{n_b}] A_{k+1} \begin{bmatrix} \mathcal{U}(0) \\ \mathcal{U}(1) \\ \vdots \\ \mathcal{U}(k) \end{bmatrix}. \end{aligned}$$

As a result, for each k,

$$\mathcal{Y}(k) = A\mathcal{U}(k) + BC\mathcal{U}(k-1) + BDC\mathcal{U}(k-2) + \cdots + BD^{k-1}C\mathcal{U}(0).$$

This immediately shows that

$$\tilde{y}(\lambda) = [A + B(\lambda - D)^{-1}C]\tilde{u}(\lambda), \tag{5A.1}$$

leading to $\tilde{G}(\lambda) = [A + B(\lambda - D)^{-1}C]$.
Putting several time delay transfer functions in cascade, it follows straightforwardly that $G(z) = z^{-k}$ leads to $\tilde{G}(\lambda) = N(\lambda)^k$, which proves the result. $\square$

Lemma 5A.1 *Consider a scalar inner transfer function G_b generating an orthogonal basis as discussed in section 5.2, with V_0 and N as defined by (5.11) and (5.33) respectively. Then*

$$V_0(z)z = N(G_b(z))V_0(z) \tag{5A.2}$$

Proof:

$$\begin{aligned} N(G_b(z))V_0(z)z^{-1} &= \left(A + B(G_b(z) - D)^{-1}C\right)(zI - A)^{-1}B = \\ &= A(zI - A)^{-1}B + B(G_b(z) - D)^{-1}C(zI - A)^{-1}B = \\ &= A(zI - A)^{-1}B + B(C(zI - A)^{-1}B)^{-1}C(zI - A)^{-1}B = \\ &= A(zI - A)^{-1}B + B = zI(zI - A)^{-1}B = V_0(z). \end{aligned}$$

$\square$

Proof of Proposition 5.4.4.
Write H in its Laurent expansion: $H(z) = \sum_{i=0}^{\infty} h_i z^{-i}$, then $V_0(z)H(z^{-1}) = \sum_{i=0}^{\infty} h_i V_0(z)z^i$. Using Lemma 5A.1 it follows that this equals $\sum_{i=0}^{\infty} h_i N^i(G_b(z))V_0(z)$. Using equation (5.35) now shows that this is equivalent to $\tilde{H}(G_b(z))V_0(z)$. $\square$

Proof of Proposition 5.6.3.
Part (a).
Denote the vector $\mu(n) := [\mu_0^T \; \mu_1^T \; \cdots \; \mu_{n-1}^T]^T$, $\mu_i \in \mathbb{R}^{n_b}$. Then

$$\mu(n)^T R(n)\mu(n) = \sum_{k=0}^{n-1} \sum_{\ell=0}^{n-1} \mu_k^T c_{k\ell} \mu_\ell \tag{5A.3}$$

with

$$c_{k\ell} = \frac{1}{2\pi} \int_{-\pi}^{\pi} V_k(e^{i\omega}) V_\ell^T(e^{-i\omega}) \Phi_u(\omega) d\omega. \tag{5A.4}$$

Denoting $\eta(e^{i\omega}) := \sum_{k=0}^{n-1} \mu_k^T V_k(e^{i\omega})$, it follows that

$$\mu(n)^T R(n)\mu(n) = \frac{1}{2\pi} \int_{-\pi}^{\pi} \eta(e^{i\omega}) \Phi_u(\omega) \eta(e^{-i\omega}) d\omega, \tag{5A.5}$$

while the orthonormality of the basis functions implies that

$$\frac{1}{2\pi} \int_{-\pi}^{\pi} |\eta(e^{i\omega})|^2 d\omega = \mu(n)^T \mu(n). \tag{5A.6}$$

Since $ess\inf_\omega \Phi_u(\omega) \cdot \mu(n)^T \mu(n) \le \mu(n)^T R(n)\mu(n) \le ess\sup_\omega \Phi_u(\omega) \cdot \mu(n)^T \mu(n)$, it follows that

$$ess\inf_\omega \Phi_u(\omega) \le \|R(n)\|_2 \le ess\sup_\omega \Phi_u(\omega). \tag{5A.7}$$

The latter equation can be verified by realizing that, since $R(n)$ is symmetric, there exists $Q(n)$ satisfying $R(n) = Q(n)Q(n)^T$ leading to

$$ess\inf_\omega \Phi_u(\omega) \le \|Q(n)\|_2^2 \le ess\sup_\omega \Phi_u(\omega).$$

Part (b).
The Hermitian form $T_n := \mu^T(n)R(n)\mu(n)$ can be written as

$$T_n = \nu^T(n) diag\{\lambda_1^{(n)}, \cdots, \lambda_{n_b n}^{(n)}\} \nu(n)$$

through unitary transformation preserving the norm, i.e. $\nu^T(n)\nu(n) = \mu^T(n)\mu(n)$. Consequently

$$\frac{\mu(n)^T R(n)\mu(n)}{\mu^T(n)\mu(n)} \le \max_i \lambda_i^{(n)}, \tag{5A.8}$$

which is known to be bounded by $ess\sup_\omega \Phi_u(\omega)$.
Since the Hermitian form T_n is related to the Toeplitz form (5A.5), Theorem 5.2.1 in Grenander and Szegö (1958) directly leads to the result that

$$\lim_{n\to\infty} \max_i \lambda_i^{(n)} = ess\sup_\omega \Phi_u(\omega).$$

Proof of Proposition 5.6.4. With Proposition 5.6.3(a) it follows that $\|R(n)^{-1}\|_2 \le (ess\inf_\omega \Phi_u(\omega))^{-1}$. For constructing a bound on the second term on the right hand side of (5.54), we first consider the following notation.

Denote $R_{12}(n) := \bar{E}[\psi(t)\psi_e^T(t)]$; then we can write

$$R := \bar{E}\begin{bmatrix} \psi(t) \\ \psi_e(t) \end{bmatrix} \begin{bmatrix} \psi^T(t) & \psi_e^T(t) \end{bmatrix}] = \begin{bmatrix} R(n) & R_{12}(n) \\ R_{21}(n) & R_{22}(n) \end{bmatrix},$$

which is an infinite block-Toeplitz matrix, of which $R(n)$ is a finite part.

As $R_{12}(n) = \begin{bmatrix} I_{n_b n} & 0 \end{bmatrix} R \begin{bmatrix} 0_{n_b n \times \infty} \\ I \end{bmatrix}$ it follows that

$$\|R_{12}(n)\|_2 \le \|\begin{bmatrix} I_{n_b n} & 0 \end{bmatrix}\|_2 \|R\|_2 \| \begin{bmatrix} 0_{n_b n \times \infty} \\ I \end{bmatrix} \|_2 \le \|R\|_2.$$

As a result

$$\|R_{12}(n)\|_2 \le \lim_{n \to \infty} \max_j \lambda_j(R(n)),$$

which by Proposition 5.6.3(b) is equal to $ess\sup_\omega \Phi_u(\omega)$. This proves the result. $\square$

Proof of Proposition 5.6.5. Writing

$$G(e^{i\omega}, \theta^*) - G_0(e^{i\omega}) = [\Omega^T(e^{i\omega}) \ \Omega_e^T(e^{i\omega})] \begin{bmatrix} \theta^* - \theta_0 \\ \theta_e \end{bmatrix}$$

it follows that for each ω_1:

$$|G(e^{i\omega_1}, \theta^*) - G_0(e^{i\omega_1})| \le \| \begin{bmatrix} \Omega^T(e^{i\omega_1}) & \Omega_e^T(e^{i\omega_1}) \end{bmatrix} \|_1 \cdot \| \begin{bmatrix} \theta^* - \theta_0 \\ \theta_e \end{bmatrix} \|_1,$$

where $\| \cdot \|_1$ refers to the induced ℓ_1 matrix norm and the ℓ_1-norm, respectively. It follows from the fact that G_b is inner that

$$|G(e^{i\omega_1}, \theta^*) - G_0(e^{i\omega_1})| \le \|V_0^T(e^{i\omega_1})\|_1 \cdot \| \begin{bmatrix} \theta^* - \theta_0 \\ \theta_e \end{bmatrix} \|_1 =$$

$$= \|V_0^T(e^{i\omega_1})\|_1 \cdot [\|\theta^* - \theta_0\|_1 + \|\theta_e\|_1] = \|V_0(e^{i\omega_1})\|_\infty \cdot [\|\theta^* - \theta_0\|_1 + \|\theta_e\|_1].$$

Part (a) of the Proposition now follows by substituting the error bound obtained in Proposition 5.6.4, and using the inequality $\|\theta^* - \theta_0\|_1 \le \sqrt{n_b n}\|\theta^* - \theta_0\|_2$.

Because of the orthonormality of the basis functions on the unit circle, it follows that

$$\|G(z, \theta^*) - G_0(z)\|_{\mathcal{H}_2} = \| \begin{bmatrix} \theta^* - \theta_0 \\ \theta_e \end{bmatrix} \|_2,$$

which together with Proposition 5.6.4 proves the result of (b). $\square$

Proof of Theorem 5.6.6.

We will only give a sketch of proof of this result. For a full proof the reader is referred to Heuberger (1991) and Heuberger and Van den Hof (1996). The proof is constructed along the following line of reasoning:

(a) Let $x_0(t)$ be the impulse response of $zG_0(z) = \sum_{k=0}^{\infty} L_k V_k(z)$.
Then $\tilde{x}_0^T(\lambda) = \sum_{k=0}^{\infty} L_k \lambda^{-k}$.

This follows straightforwardly by applying the definitions of the Hambo transforma-
tions. Consequently the poles of $\tilde{x}_0(\lambda)$ will determine (a lower bound for the) the
speed of convergence of the series expansion of G_0.

(b) $\tilde{x}_0(\lambda) = \tilde{G}_0(\lambda)C^T \dfrac{\lambda}{\lambda - D}$.

This follows from applying the Hambo transform to the relation: $x_0(t) = G_0(z)\delta(t+1)$
with $\delta(t)$ the unit pulse.

(c) Let $\{\mu_i\}_{i=1,\cdots,n_s}$ denote the poles of G_0. Then the poles of $\tilde{G}_0$ are given by $\lambda_i = \{G_b^{-1}(\mu_i)\}_{i=1,\cdots,n_s}$ leading to $|\lambda_i| = \prod_{j=1}^{n_b} \left| \frac{\mu_i - \rho_j}{1 - \mu_i \rho_j} \right|$.

The first statement is proven in Van den Hof *et al.* (1994), and the latter implication
follows directly by substituting the appropriate expressions.

(d) The poles of $\tilde{x}_0(\lambda)$ are the poles of $\tilde{G}_0(\lambda)$ possibly minus poles in $\lambda = 0$.

This follows from careful analysis of the expression under (b).

(e) Since λ in (5.57) is the maximum amplitude of poles of $\sum_{k=0}^{\infty} L_k \lambda^{-k}$, it follows that
there exist $\alpha_i \in \mathbb{R}$ such that for all $\eta > \lambda$, $|L_{k,i}| \leq \alpha_i \eta^{k+1}$, with $L_{k,i}$ the ith-element
of L_k. As $\|\theta_e\|_2^2 = \sum_{k=n}^{\infty} \sum_{i=1}^{n_b} L_{k,i}^2$, the result follows by substitution.

Lemma 5A.2 *Let v be a scalar-valued stationary stochastic process with rational spectral
density $\Phi_v(\omega)$. Let $e^{-i\bar{\omega}} = G_b(e^{i\omega})$. Then*

$$V_0^T(e^{i\omega})\tilde{\Phi}_v(\bar{\omega})V_0(e^{-i\omega}) = V_0^T(e^{i\omega})\Phi_v(\omega)V_0(e^{-i\omega}). \qquad (5A.9)$$

Proof: Let H_v be a stable spectral factor of Φ_v, satisfying $\Phi_v(\omega) = H_v(e^{-i\omega})H_v(e^{i\omega})$.
Then $\tilde{\Phi}_v(\omega) = \tilde{H}_v^T(e^{-i\omega})\tilde{H}_v(e^{i\omega})$ and it follows that
$V_0^T(e^{i\omega})\tilde{\Phi}_v(\bar{\omega})V_0(e^{-i\omega}) = V_0^T(e^{i\omega})\tilde{H}_v^T(G_b(e^{i\omega}))\tilde{H}_v(G_b(e^{-i\omega}))V_0(e^{-i\omega})$. Using Proposition
5.4.4, this latter expression is equal to $H_v(e^{-i\omega})V_0^T(e^{i\omega})V_0(e^{-i\omega})H_v(e^{i\omega})$. Since H_v is scalar
this proves the lemma. $\square$

Proof of Theorem 5.6.9. Using (5.61), and substituting $\Omega_n(e^{i\omega})$ shows that

$$\frac{1}{n_b n}\Omega_n^T(e^{i\omega_1})Q_n\Omega_n(e^{-i\omega_2}) =$$

$$\frac{1}{n_b n}[V_0^T(e^{i\omega_1})\ V_1^T(e^{i\omega_1})\ \cdots V_{n-1}^T(e^{i\omega_1})] \cdot Q_n \cdot [V_0^T(e^{-i\omega_2})\ V_1^T(e^{-i\omega_2})\ \cdots V_{n-1}^T(e^{-i\omega_2})]^T.$$

Note that this latter expression can be written as

$$\frac{1}{n_b n}V_0^T(e^{i\omega_1})[I\ \ G_b(e^{i\omega_1})I\ \ \cdots\ \ G_b^{n-1}(e^{i\omega_1})I] \cdot Q_n \cdot$$

$$[I\ \ G_b(e^{-i\omega_2})I\ \ \cdots\ \ G_b^{n-1}(e^{-i\omega_2})I]^T V_0(e^{-i\omega_2})).$$

$$(5A.10)$$

Now we evaluate the following expression:

$$\frac{1}{n}[I \ \ G_b(e^{i\omega_1})I \ \ \cdots \ \ G_b^{n-1}(e^{i\omega_1})I] \cdot Q_n \cdot [I \ \ G_b(e^{-i\omega_2})I \ \ \cdots \ \ G_b^{n-1}(e^{-i\omega_2})I]^T. \qquad (5A.11)$$

Since G_b is an inner function we can consider the variable transformation

$$e^{-i\bar{\omega}} := G_b(e^{i\omega}). \qquad (5A.12)$$

Employing this transformation in the expression (5A.11), this latter expression is equivalent to:

$$\frac{1}{n}[I \ \ e^{-i\bar{\omega}_1}I \ \ \cdots \ \ e^{-i\bar{\omega}_1(n-1)}I] \cdot Q_n \cdot [I \ \ e^{i\bar{\omega}_2}I \ \ \cdots \ \ e^{i\bar{\omega}_2(n-1)}I]^T.$$

The convergence result of Hannan and Wahlberg (1989) and Ljung and Yuan (1985) now show that for $n \to \infty$, this expression converges to

$$\begin{array}{ll} 0 & \text{if } \bar{\omega}_1 \neq \bar{\omega}_2 \\ Q(\bar{\omega}_1), & \text{if } \bar{\omega}_1 = \bar{\omega}_2, \end{array} \qquad (5A.13)$$

where $Q(\omega)$ is the spectral density related to the Toeplitz matrix Q_n in the limit as $n \to \infty$. Employing Lemma 5A.2, together with (5.60), it follows that for $n \to \infty$ the spectrum related to the Toeplitz matrix Q_n is given by $\tilde{\Phi}_v(\omega)\tilde{\Phi}_u(\omega)^{-1}$. This is due to the fact that the symbol (spectrum) of a Toeplitz matrix which is the product of several Toeplitz matrices, asymptotically ($n \to \infty$) equals the product of the symbols (spectra) of the separate Toeplitz matrices, see Grenander and Szegö (1958).
Combining this with (5A.10) now shows that, for $n \to \infty$,

$$\frac{1}{n_b n}\Omega_n^T(e^{i\omega_1})Q_n\Omega_n(e^{-i\omega_2}) \ = \ \frac{1}{n_b}V_0^T(e^{i\omega_1})Q(\bar{\omega})V_0(e^{-i\omega_2}) =$$

$$= \ \begin{cases} 0 & \text{if } \bar{\omega}_1 \neq \bar{\omega}_2, \\ \dfrac{1}{n_b}V_0^T(e^{i\omega_1})\tilde{\Phi}_v(\bar{\omega}_1)\tilde{\Phi}_u(\bar{\omega}_1)^{-1}V_0(e^{-i\omega_1}) & \text{if } \bar{\omega}_1 = \bar{\omega}_2. \end{cases}$$

$$(5A.14)$$

Employing Lemma 5A.2 now shows that the resulting expression in (5A.14) becomes:

$$\frac{1}{n_b}V_0^T(e^{i\omega_1})\Phi_v(\omega_1)\Phi_u(\omega_1)^{-1}V_0(e^{-i\omega_1}).$$

In using Lemma 5A.2 it has to be realized that there always will exist a scalar-valued stationary stochastic process z with rational spectrum Φ_z such that $\tilde{\Phi}_z = \tilde{\Phi}_v\tilde{\Phi}_u^{-1}$. $\qquad \square$

Bibliography

G.J. Clowes (1965). Choice of the time scaling factor for linear system approximations using orthonormal Laguerre functions. *IEEE Trans. Autom. Contr.*, **AC-10**, 487–489.

R.A. de Callafon, P.M.J. Van den Hof and M. Steinbuch (1993). Control relevant identification of a compact disc pick-up mechanism. *Proc. 32nd IEEE Conf. Decision and Control*, San Antonio, TX, USA, pp. 2050-2055.

D.K. de Vries (1994). *Identification of Model Uncertainty for Control Design.* Dr. Dissertation, Mechanical Engineering Systems and Control Group, Delft Univ. Technology, September 1994.

Y. Fu and G.A. Dumont (1993). An optimum time scale for discrete Laguerre network. *IEEE Trans. Autom. Control*, **AC-38**, 934–938.

G.C. Goodwin, M. Gevers and D.Q. Mayne (1991). Bias and variance distribution in transfer function estimation. *Preprints 9th IFAC/IFORS Symp. Identification and Syst. Param. Estim.*, July 1991, Budapest, Hungary, pp. 952-957.

M.J. Gottlieb (1938). Concerning some polynomials orthogonal on finite or enumerable set of points. *Amer. J. Math.*, **60**, 453–458.

U. Grenander and G. Szegö (1958). *Toeplitz Forms and Their Applications.* Univ. California Press, Berkeley, 1958.

R.G. Hakvoort and P.M.J. Van den Hof (1994). An instrumental variable procedure for identification of probabilistic frequency response uncertainty regions. *Proc. 33rd IEEE Conf. Decision and Control*, Lake Buena Vista, FL, pp. 3596-3601.

E.J. Hannan and B. Wahlberg (1989). Convergence rates for inverse Toeplitz matrix forms. *J. Multiv. Analysis*, **31**, no. 1, 127–135.

P.S.C. Heuberger and O.H. Bosgra (1990). Approximate system identification using system based orthonormal functions. *Proc. 29th IEEE Conf. Decision and Control*, Honolulu, HI, pp. 1086-1092.

P.S.C. Heuberger (1991). *On Approximate System Identification with System Based Orthonormal Functions.* Dr. Dissertation, Delft University of Technology, The Netherlands, 1991.

P.S.C. Heuberger, P.M.J. Van den Hof and O.H. Bosgra (1993). A generalized orthonormal basis for linear dynamical systems. *Proc. 32nd IEEE Conf. Decision and Control*, San Antonio, TX, pp. 2850-2855.

P.S.C. Heuberger, P.M.J. Van den Hof and O.H. Bosgra (1995). A generalized orthonormal basis for linear dynamical systems. *IEEE Trans. Autom. Control*, Vol. AC-40, pp. 451-465.

P.S.C. Heuberger and P.M.J. Van den Hof (1996). The Hambo transform: a transformation of signals and systems induced by generalized orthonormal basis functions. *Proc. 13th IFAC World Congress*, San Francisco, CA, July 1996, Vol. I, pp. 103-108.

P.S.C. Heuberger, P.M.J. Van den Hof and B. Wahlberg (Eds.) (2005). *Modelling and Identification with Rational Orthogonal Basis Functions.* Springer Verlag.

W.H. Kautz (1954). Transient synthesis in the time domain. *IRE Trans. Circ. Theory*, **CT-1**, 29-39.

R.E. King and P.N. Paraskevopoulos (1979). Parametric identification of discrete time SISO systems. *It. J. Control*, **30**, 1023–1029.

Y.W. Lee (1933). Synthesis of electrical networks by means of the Fourier transforms of Laguerre functions. *J. Mathem. Physics*, **11**, 83–113.

Y.W. Lee (1960). *Statistical Theory of Communication.* John Wiley & Sons, Inc., New York, NY.

L. Ljung and Z.D. Yuan (1985). Asymptotic properties of black-box identification of transfer functions. *IEEE Trans. Autom. Control*, **AC-30**, 514–530.

L. Ljung (1987). *System Identification - Theory for the User.* Prentice Hall, Englewood Cliffs, NJ.

Y. Nurges (1987). Laguerre models in problems of approximation and identification of discrete systems. *Autom. and Remote Contr.*, **48**, 346–352.

Y. Nurges and Y. Yaaksoo (1981). Laguerre state equations for a multivariable discrete system. *Autom. and Remote Contr.*, **42**, 1601–1603.

G. Szegö (1975). *Orthogonal Polynomials.* Fourth Edition. American Mathematical Society, Providence, RI,USA.

P.M.J. Van den Hof, P.S.C. Heuberger and J. Bokor (1994). System identification with generalized orthonormal basis functions. *Proc. 33rd IEEE Conf. Decision and Control*, Lake Buena Vista, FL, pp. 3382-3387.

B. Wahlberg (1990). *On the Use of Orthogonalized Exponentials in System Identification.* Report LiTH-ISY-1099, Dept. Electr. Eng., Linköping University, Sweden.

B. Wahlberg (1991). System identification using Laguerre models. *IEEE Trans. Automat. Contr.*, **AC-36**, 551–562.

B. Wahlberg (1994a). System identification using Kautz models. *IEEE Trans. Autom. Control*, **AC-39**, 1276-1282.

B. Wahlberg (1994b). Laguerre and Kautz models. *Prepr. 10th IFAC Symp. System Identification*, Copenhagen, Denmark, Vol. 3, pp. 1-12.

N. Wiener (1949). *Extrapolation, Interpolation and Smoothing of Stationary Time Series.* MIT Press, Cambridge, MA.

Chapter 6

Model set selection and model validation

6.1 Introduction

Considering the general identification procedure as sketched in figure 1.9 there are two issues that have yet to be discussed. In chapter 4 it has been discussed extensively what different model structures can be applied. However the design choice of a particular model set in a given situation has not been addressed yet. This will be the topic of section 6.2. Additionally in section 6.3 the issue of model validation will be addressed. These issues are collected in one chapter as they exhibit many relationships.

6.2 Model set selection

The choice of an appropriate model set is a very basic and important choice when performing system identification. Actually the choice of a model set comes down to the specification of three different phenomena:

- *Choice of model structure.* This refers to the choice of structure that is present in the transfer functions

$$[G(q, \theta), H(q, \theta)]$$

  and their relationships, leading to characterizations as ARX, OE, ARMAX, FIR etcetera, as discussed in chapter 4.

- *Choice of model complexity.* This refers to the choice of the orders of the two transfer functions. Considerations in terms of this problem are related to an ordering of model sets:

$$\mathcal{M}_1 \subset \mathcal{M}_2 \subset \mathcal{M}_3 \cdots$$

  where steps are made to larger model sets, and criteria have to be made available that assist in deciding which model set (which order of models) is most appropriate. In the approach of chapter 4 the complexity of the models is represented by the integer-valued numbers n_a, n_b, n_c, n_d, n_f.

- *Model parametrization.* This refers to the choice in which way the model sets are represented by parameter vectors that actually are used in the identification criteria,

and on which the identification algorithms are based. In this course we have almost exclusively addressed a parametrization of $\{[G(q,\theta) \ H(q,\theta)]\}$ in terms of fractions of polynomials.

The ultimate goal of the user of identification methods, will be to find a *good model* at a *low price*. These notions of quality and price can provide criteria on the basis of which appropriate choices for a model set can be made.

When is a model good?
Despite of the fact that the acceptance of a given model will be dependent on its ultimate use, a general expression on the quality of a model can be given by stating that one aims at a model with *small bias* and *small variance*. Now this expression in itself again reflects conflicting requirements. The wish to achieve a small bias motivates the use of large, flexible model sets (high order models), such that the "undermodelling" error is small. Aiming for a small variance, on the other hand, motivates the use of only a limited number of unknown parameters. This latter statement originates from the property that the variance of estimated parameters generally will increase with an increasing number of parameters. One could say that the total amount of information that is present in a data sequence is fixed; when this information has to be divided over a larger set of estimated parameters the information-per-parameter is reduced leading to a larger parameter variance.

When is a model expensive?
Considering the price of a model one can distinguish two different phenomena.

- The price associated with identification of the model.
  Apparently model structures that are linear-in-the-parameters, like FIR, ARX and ORTFIR (chapter 5) deliver estimated models much more fast and with considerably less computational effort than model structures that require non-linear optimization methods to iteratively identify the parameters. The occurrence of local-minima in the criterion function also plays a role in this respect.

- The price associated with application of the model.
  Dependent on the intended use of the model there may be clear restrictions on the complexity of the model that can be handled in the application situation. For instance models that are intended to be used in the design of real-time controllers for processes with high bandwidth (consider e.g. the CD-mechanism mentioned in chapter 1), are limited in model order through the computational speed and capacity of the real-time controller hard- and software.

In the trade-off that has to be made between quality and price, several aspects have been treated in the foregoing chapters play a role here, the two most important ones of which are:

- The issue of the computational complexity of nonlinear optimization methods, and the advantage of using linear regression schemes.

- The ability to model the input/output transfer function $G(q,\theta)$ independently of the modelling of the noise contribution through $H(q,\theta)$.

Ljung (1987) distinguishes four different sources of information, c.q. types of considerations, when discussing the problem of model set selection.

A priori considerations.

Based on physical insight in the process that is going to be modelled, there might be clear information on the (minimal) model order that may be required for modelling the system accurately. When on physical grounds something can be said about the character of the noise disturbance on the data, one may also be able to find arguments for choosing a particular model structure. For instance, when there is reason to believe that the noise disturbance on the measured data actually enters the process at a location such that it contains the process dynamics in its colouring, there is a good argument for choosing an ARMAX model structure.

Additionally before any data is processed in an identification algorithm one can make a statement concerning the relation between the number of parameters to be estimated (N_θ) and the number of data points (N) that is available. It it apparent that when estimating 50 parameters on the basis of 50 data points, the criterion function will take a very small value, but the estimated parameters will be very unreliable. In this situation no data reduction has been achieved. Generally there has to hold that $N >> N_\theta$. A more specific rule-of-thumb that is often used is

$$N > 10 N_\theta \tag{6.1}$$

but this relation has to be used with care, as the resulting variance is of course dependent on the signal-to-noise ratio in the measured data sequences.

Preliminary data analysis

Information concerning model order can also be obtained from preliminary data analysis, nonparametric identification (chapter 3) and approximate realization methods on the basis of transient responses (chapter 9). Examining non-parametrically identified frequency responses can provide information on the number of resonance peaks, and phase shift, and can be a good basis for an initial model order estimate. The same holds for the approximate realization methods, that, mainly through an SVD-based rank evaluation of a Hankel matrix, provide information on appropriate model orders.

A more specific method to estimate the model order (particularly of G) is by rank evaluation of the Toeplitz matrix, with elements of sample correlation functions, that appears in a least squares linear regression parameter estimate.

This approach is based on the following mechanism.

Suppose that the data generating system satisfies:

$$y(t) = \frac{b_0 + b_1 q^{-1} + \cdots + b_n q^{-n}}{1 + a_1 q^{-1} + \cdots + a_n q^{-n}} u(t) = \varphi_n^T(t) \theta_0, \tag{6.2}$$

with

$$\varphi_n(t) = [-y(t-1) \quad -y(t-2) \quad \cdots \quad -y(t-n) \quad u(t) \quad u(t-1) \quad \cdots \quad u(t-n)]^T. \tag{6.3}$$

Then $R_{(n)} := \bar{E}\varphi(t)\varphi^T(t)$ is a Toeplitz-structured matrix that is nonsingular provided that the input signal is sufficiently exciting; see also the analysis in section 4.6. However when considering $R_{(n+1)}$ it follows directly from (6.2) that this latter matrix will be singular, as one element is added to $\varphi(t)$ that is linearly dependent on the other elements.

So in general terms we can formulate an order test, by evaluating the rank of $R_{(i)}$ for increasing values of i, and once the matrix becomes (almost) singular (say for $i = j$) this indicates that the system order should be $j - 1$.

In practice the Toeplitz matrix will be composed of elements of the sample correlation functions, i.e.

$$\hat{R}_{(n)} = \frac{1}{N} \sum_{t=1}^{N} \varphi_n(t) \varphi_n^T(t). \tag{6.4}$$

The rank test is performed through several different characteristics, as e.g.

$$det\hat{R}_{(n)} \quad \text{or} \quad \frac{\sigma_{min}\hat{R}_{(n)}}{\sigma_{max}\hat{R}_{(n)}}$$

where σ_{min} and σ_{max} denote respectively the minimum and maximum singular value of the corresponding matrix.

It has to be stressed that this model order test is principally based on the availability of noise free data, which of course is rather unpractical. When there is noise present on the data an exact rank drop will hardly occur, but when the noise contribution is only small one may expect that the test is still valid and the Toeplitz matrix becomes "almost" singular in the case of overestimating the model order. In the situation of noise disturbed data the model order test becomes a test that has close connections to the ARX model structure. Model order estimates that are obtained in this way can therefore be quite different from model order estimates that are obtained with other model structures.

Comparing identified models from different model sets

Another possibility to determine model structure and model orders after identification of one or several models in different model sets. For a given model structure the most straight-forward approach to determine the orders of the respective polynomials is to evaluate the value of the criterion function

$$V_N(\hat{\theta}_N, Z^N) \tag{6.5}$$

for the different parameters $\hat{\theta}_N$ that are estimated for several choices of model orders. In figure 6.1(left) this is shown for an ARX structure, where on the X-axis the several ARX model sets are sketched indicated by their number of parameters. For a given number of parameters $(n_a + n_b + 1)$, several different model sets are possible, dependent on the separate values of n_a and n_b. The minimal value of the loss function $V_N(\hat{\theta}_N, Z^N)$ is plotted for all the different model sets.

The reasoning here is that one may expect a substantially decreasing value of $V_N(\hat{\theta}_N, Z^N)$ until the "correct" model set is reached. By choosing a model set that is too large (too high polynomial orders), the reduction in $V_N(\hat{\theta}_N, Z^N)$ will only be moderate. As a result one is looking for the "knee" in the characteristic plot.

It has to be noted here that in this type of plot the value of $V_N(\hat{\theta}_N, Z^N)$ will always decrease with increasing number of parameters, simply because of the fact that within a larger model set one necessarily finds a lower minimum of the criterion function. When a model orders are chosen that are too large (related to the real system), the additional freedom in the model will be used to "tune" the model to the specific realization of the noise disturbance. This mechanism is called *overfit*.

As the indicated plot of $V_N(\hat{\theta}_N, Z^N)$ may incorporate this mechanism of overfit, an alternative can be used, based on a separation of the data into two different sets: one part of the data that is used for identification of $\hat{\theta}_N$, and another part of the data for calculation

of the criterion function. This means:

$$Z^N = Z^{(1)} \ Z^{(2)}$$

$$\hat{\theta}_N^{(1)} = \arg\min_{\theta \in \Theta} V_N(\theta, Z^{(1)})$$

$$V_N(\hat{\theta}_N^{(1)}, Z^{(2)}) = \frac{1}{N^{(2)}} \sum_{t=1}^{N^{(2)}} \varepsilon(t, \hat{\theta}_N^{(1)})^2.$$

When in this case the model order in $\hat{\theta}_N^{(1)}$ has been chosen too high, this will result in an increase of the $V_N(\hat{\theta}_N^{(1)}, Z^{(2)})$. The fit that has been made on the specific noise realization that was present in the first part of the data, will now lead to an increase of the criterion function when evaluated over the second part of the data. This mechanism which is referred to as *cross-validation*, is sketched in figure 6.1(b) where a slight increase of the function value can be observed for $N_\theta > 5$.
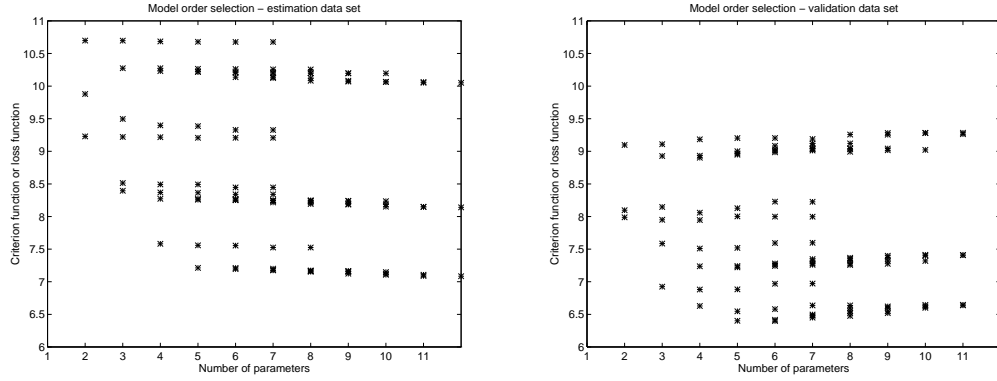
Figure 6.1: Model order test for an ARX model structure; system has an ARX structure with $n_a = 2$, $n_b = 3$. Left plot: criterion function evaluated on estimation data; right plot: criterion function evaluated on validation data for models based on estimation data.

The principle that is used in this test, is that, when determining the most suitable set of models, actually a "penalty" should be added to the criterion function for increasing complexity (higher order) of the model sets, in order to cope with this risk of overfitting. Formally spoken, we would like to evaluate $\bar{E}V_N(\hat{\theta}_N, Z^N)$ rather than $V_N(\hat{\theta}_N, Z^N)$. Analysis of this problem has led to several so-called *information criteria* suited for model order selection, the most important ones of which are

Akaike's Information Criterion (AIC).
This criterion states that the model set should be chosen that achieves the minimum value for the expression:

$$\frac{1}{2} log V_N(\hat{\theta}_N, Z^N) + \frac{N_\theta}{N} \tag{6.6}$$

with N_θ the number of parameters in the model set.
This criterion is based on maximum likelihood-considerations and assuming a Gaussian pdf of the noise disturbance.

Akaike's Final Prediction Error Criterion (FPE).

This criterion proposes to choose the model set that achieves a minimum value for the expression:

$$\frac{1 + N_\theta/N}{1 - N_\theta/N} V_N(\hat{\theta}_N, Z^N), \tag{6.7}$$

which is an estimate of the prediction error variance that is obtained when the identified model is applied to another data set than the one that is used for the identification.

Model validation

The ultimate method of verifying whether model structure and model orders have been chosen appropriately, is by validating the identified model. If in the end the identified model is considered to be acceptable, then apparently an appropriate choice of model set was made. This is a clear "a posteriori" approach. If the identified model is not acceptable, then a different choice of either the model structure and/or the model orders has to be made. This approach, which already was indicated when discussing the basic identification scheme in chapter 1, has some flavour of "trial and error". Since there is no universally applicable algorithm for model set selection, this effect is -to some extent- unavoidable. Further methods for model validation are discussed in the next subsection.

6.3   Model validation

The goal of model validation is to arrive at an answer to the question: "Is one satisfied with the identified model or not?". When a model is identified with a specific application in mind, the ultimate validation actually is obtained by showing that the model has a good performance in the intended application. However despite of these application-dependent considerations, there is a need for application-independent tools that are able to verify whether the identification procedure has been performed satisfactorily.

Model validation procedures should reveal whether one can have confidence in the models that are delivered. To this end identified models should be confronted with as much information that one has about the process, in order to find out whether there are clear inconsistencies. In this way, one would rather speak of *model invalidation*.

First of all inconsistencies should be checked by confronting the identified model with prior knowledge that is available from the process (e.g. based on physical considerations; steady state values that are known, knowledge about time constants etc.).

Next there are a number of generally applicable data-dependent tools that are available for model validation, and they will be discussed briefly.

- **Input/output behaviour in accordance with previous results?.** One can check whether the identified models match previously obtained characterizations of the process, as e.g. nonparametric models. A nonparametric model can be considered as a very high order representation of the system, having no unmodelled dynamics (within the linear time-invariant framework). A comparison with nonparametrically obtained models can thus reveal whether specific dynamics has been modelled erroneously. However care has to be take concerning the fact that also a nonparametric estimate is an estimated model, which could be inaccurate due to e.g. a wrongly chosen windowing operation. Comparison of modelled and measured step responses or other transient signals can also be used for validation.

- **Model reduction**. This can be an appropriate tool for verifying whether an estimated transfer function (either G or H) can be accurately approximated by a lower order representation. When (almost) pole/zero cancellations occur in a pole/zero plot this is an indication of a model order that has been chosen too high.

- **Parameter confidence intervals**. When the parameter confidence intervals are large, this points to a large variance in the estimate, and it can indicate that model orders have been chosen too large. Another indication of course can be that the number of data points is too small.

- **Simulation of the model**. A comparison of the output signal that is actually measured with the output signal that is simulated by the identified models can clearly reveal a lot of information of the model. This refers to evaluation of the *simulation error*

$$e_{sim}(t) = y(t) - G(q, \hat{\theta}_N)u(t), \qquad (6.8)$$

where u is the input signal that also excites the system.

Note that a high-quality model does not necessarily make this simulation error small. The "optimal" model $G(e, \hat{\theta}_N) = G_0(q)$ will lead to

$$e_{sim}(t) = v(t) = H_0(q)e(t). \qquad (6.9)$$

So, in a situation that there is a considerable amount of noise present in the data, $e_{sim}(t)$ does not reveal very much information concerning $G(q, \hat{\theta}_N)$.

Note that the simulation error can not be made smaller by adding an (artificial) noise term to the model output. This is due to the fact that the actual realization of $v(t)$ is unknown. As a result a simulation test can only provide information on the accuracy of the input/output transfer function $G(q, \hat{\theta}_N)$, and not of $H(q, \hat{\theta}_N)$.

In this simulation test, there is also a risk that an "overfit" of the model $G(q, \hat{\theta}_N)$ leads to a small simulation error, while this does not have to imply that the model is accurate. Also here a cross-validation is advisable so that the simulation test is performed on a data interval that has not been used for identification.

- **Residual tests**. The residual signal $\varepsilon(t, \hat{\theta}_N)$ can exhibit important information on the validation/invalidation of the identified model.

In a situation of a consistent model estimate, the residual (prediction error) $\varepsilon(t, \hat{\theta}_N)$ asymptotically becomes a white noise signal. Besides in the situation $G_0 \in \mathcal{G}$, a consistent estimation of the i/o transfer function $G(z, \hat{\theta}_N)$ will imply that the residual $\varepsilon(t, \hat{\theta}_N)$ asymptotically becomes uncorrelated with past input samples. Corresponding to these two situations we can formulate the following two model assumptions or, in statistical terms, the null hypotheses:

  (a) $\varepsilon(t, \hat{\theta}_N)$ is a realization of a zero mean white noise process;
  (b) $\varepsilon(t, \hat{\theta}_N)$ is a realization of a stochastic process, satisfying $\bar{E}\varepsilon(t)u(s) = 0$, $t > s$.

We will briefly discuss two tests on auto/cross-correlation functions that reflect the two hypotheses mentioned above.

Test on residual auto-correlation function.

Under model assumption (a) it follows that $R_\varepsilon(\tau) = \sigma_e^2 \delta(\tau)$. Denoting $\varepsilon(t) = \varepsilon(t, \hat\theta_N)$, we write

$$\hat{R}_\varepsilon^N(\tau) = \frac{1}{N} \sum_{t=1}^{N-\tau} \varepsilon(t+\tau)\varepsilon(t) \quad \tau > 0 \tag{6.10}$$

We may expect that $\dfrac{\hat{R}_\varepsilon^N(\tau)}{\hat{R}_\varepsilon^N(0)}$ is small for $\tau \geq 0$ and large N, provided that $\varepsilon(t)$ is a realization of a white noise process. The question is, how small should we expect this quotient to be?

Define for some $m \geq 1$:

$$\hat{r}_m = \begin{bmatrix} \hat{R}_\varepsilon^N(1) \\ \vdots \\ \hat{R}_\varepsilon^N(m) \end{bmatrix} \tag{6.11}$$

As a result of the central limit theorem it can be shown that $\sqrt{N}\hat{r}_m \in As\ \mathcal{N}(0, \sigma_e^4 I)$, which implies that all components of $\hat{r}_m$ are asymptotically independent. As a result,

$$\sqrt{N}\frac{\hat{R}_\varepsilon^N(\tau)}{\hat{R}_\varepsilon^N(0)} \in As\ \mathcal{N}(0,1) \tag{6.12}$$

Expressions (6.12) leads to a hypothesis test, based on

$$Pr(|\hat{R}_\varepsilon^N(\tau)|/\hat{R}_\varepsilon^N(0) \leq N_\alpha/\sqrt{N}) = \alpha \tag{6.13}$$

with N_α the α-level of the $\mathcal{N}(0,1)$-distribution, e.g. $N_{0.95} = 1.96$ (95% reliability interval). The null hypothesis can be accepted if

$$|\hat{R}_\varepsilon^N(\tau)|/\hat{R}_\varepsilon^N(0) \leq N_\alpha/\sqrt{N} \tag{6.14}$$

and otherwise rejected.

Test on cross-correlation between residual and past input.

Following a similar line of reasoning as in the previous test, we consider the sample correlation

$$\hat{R}_{\varepsilon u}^N(\tau) = \frac{1}{N} \sum_{t=1}^{N-\tau} \varepsilon(t+\tau)u(t) \tag{6.15}$$

If $\{\varepsilon(t)\}$ and $\{u(t)\}$ are independent, then application of the central limit theorem provides

$$\sqrt{N}\hat{R}_{\varepsilon u}^N(\tau) \in As\ \mathcal{N}(0, P) \tag{6.16}$$

where P can be shown (Ljung, 1987) to satisfy:

$$P = \sum_{k=-\infty}^{\infty} R_\varepsilon(k)R_u(k) \tag{6.17}$$

with the standard notation $R_\varepsilon(k) = \bar{E}\varepsilon(t)\varepsilon(t-k)$, $R_u(k) = \bar{E}u(t)u(t-k)$. Using similar notation as before, we can check whether

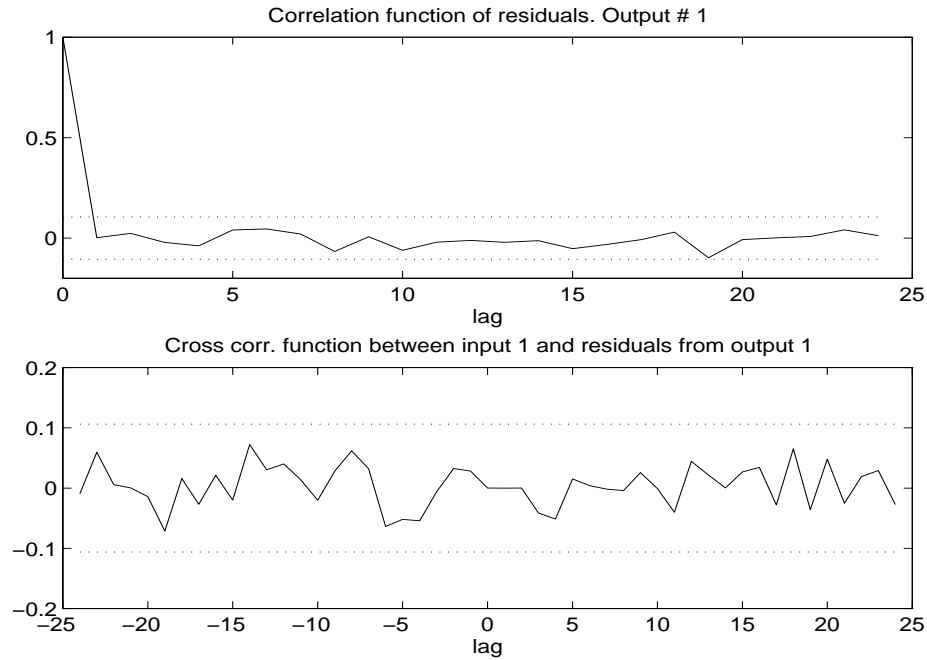$$|\hat{R}_{\varepsilon u}^N(\tau)| \leq \sqrt{P/N}N_\alpha$$

Figure 6.2: Hypothesis test on residual signal; upper: auto-correlation function $\hat{R}_\varepsilon(\tau)$ of $\varepsilon(\hat{\theta}_N)$ together with 99% confidence bounds; lower: cross-correlation function $\hat{R}_{\varepsilon u}(\tau)$ together with 99% confidence bounds.

and accept the null-hypothesis if this is satisfied. Since P is unknown the test will have to be based on $\hat{P}^N = \sum_{k=-\infty}^{\infty} \hat{R}_\varepsilon^N(k) R_u^N(k)$.

In the Matlab command RESID, both tests (6.12) and (6.16) have been implemented using a 3σ-level of probability, corresponding to $\sim N_{0.99}$. An example is shown in figure 6.2. The residual is taken from a third order ARX model that is estimated on the basis of 600 data points that were taken from a third order system that also had an ARX structure.

The test on the cross-correlation function allows a check on the accuracy of the plant model $G(q, \hat{\theta}_N)$. If this test is passed, then the test on the auto-correlation function can be used to validate the noise model $H(q, \hat{\theta}_N)$. Note that the latter test is more severe as it requires both G_0 and H_0 to be modelled accurately.

Correlation between $\varepsilon(t)$ and $u(t - \tau)$ for small values of τ can indicate that the presumed time-delay in the model is chosen too high.

Correlation between $\varepsilon(t)$ and $u(t - \tau)$ for negative values of τ (the residual signal is correlated with future values of u) can indicate the presence of a feedback loop in the data. However in the situation that the input signal has a spectrum which is not flat (signal is non-white), it can also point to inaccurate modelling of the first elements of the pulse response of G_0 (see Problem 8.1). This latter situation may occur if the time-delay in the model is chosen too high.

As may be clear from the list of tools given above, there is not one single (and optimal)

root to the ultimate model validation. It is mostly a matter of building up confidence in the models that have been identified, and to some extent it will be an engineering activity, incorporating -to some extent- an approach of trial and error.

In this procedure it is important to build up the model structures starting from the most simple ones to more complex structures. A linear regression estimate (ARX) is generally the most simple model to start with, particularly because of its computational simplicity. If there are reasons not to be satisfied with the result, then one can move to more general structures.

In the end line of a model validation procedure, one should always be aware of the fact that the ultimate model validation rests within the (intended) application of the model.

Example 6.3.1 In order to illustrate the role of the correlation tests, we consider a data generating system $\mathcal{S}$, that we excite with a step signal. The input signal together with the observed output signal are depicted in Figure 6.3.
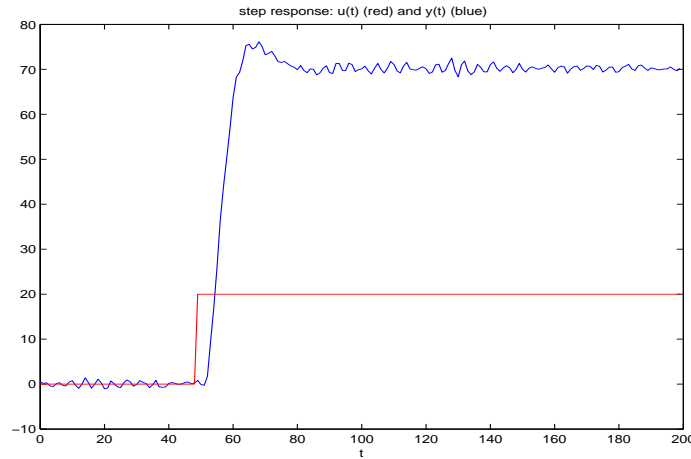
Figure 6.3: Step input and measured step response.

From the observed response we carefully conclude that the system G_0 has a limited order and a time delay of around $n_k = 3$.

Next a data set is generated on the basis of $N = 5000$ data points, using a random white noise as input signal. As a first model structure we evaluate an Output Error model structure with $n_b = n_f = 2$, $n_k = 3$.

For this estimated Output Error model, the results of the correlation tests are given in Figure 6.4(left).

Since both tests peak out of there confidence bounds, both models $G(\hat{\theta}_N)$ and $H(\hat{\theta}_N)$ are invalidated.

Next the order of the Output Error model set is increased to 3, according to $n_b = n_f = 3$; $n_k = 3$. The results of the corresponding correlation tests are given in Figure 6.4(right).

It now appears that $G(\hat{\theta}_N)$ is validated, but $H(\hat{\theta}_N)$ is not.

In the next step a noise model is introduced, through the choice of a Box Jenkins Model structure, with $n_b = n_f = 3; n_c = n_d = 3; n_k = 3$. The corresponding results in Figure 6.5(left) show that the order of the noise model is still not large enough. Increasing the order of the noise model to 4, leading to BJ with $n_b = n_f = 3; n_c = n_d = 4; n_k = 3$, leads to an identified model for which both $G(\hat{\theta}_N)$ and $H(\hat{\theta}_N)$ are validated (see Figure 6.5(right)).
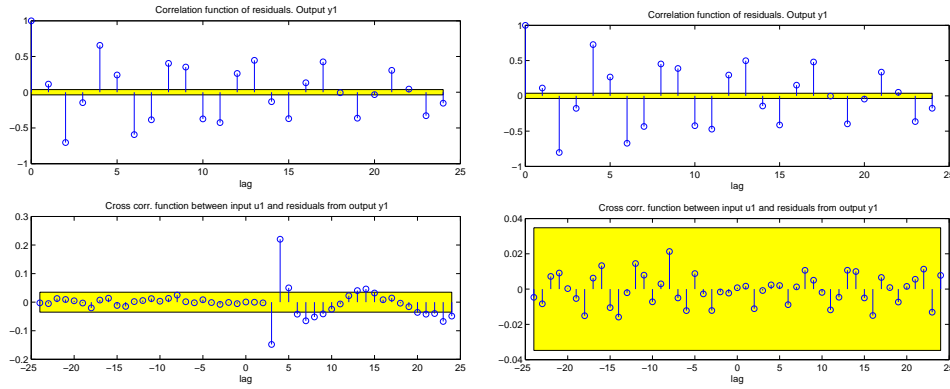
Figure 6.4: Auto- (upper figure) and cross-correlation (lower figure) tests for OE-model [2 2 3] (left) and OE-model [3 3 3] (right).
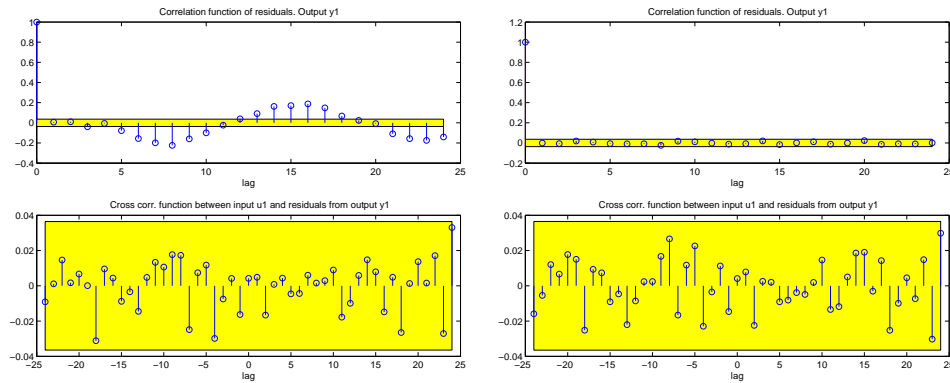
Figure 6.5: Auto- (upper figure) and cross-correlation (lower figure) tests for BJ-model [3 3 3 3 3] (left) and OE-model [3 4 4 3 3] (right).

6.4 A typical identification problem

In very brief format a typical identification procedure will be sketched that can be applicable to "standard" situations.

Step 1
After preparatory experiments in which the basic phenomena of the system have been learnt and the appropriate experimental setup has been configured, obtain a non-parametric estimate of the system by spectral estimation. Choose an appropriate window function in case the input signal is non-periodic. Try several windows and be careful that through the window smoothing there is not an introduction of severe bias. Use high sampling rates for this stage unless there are storage limitations.

Step 2
On the basis of the nonparametric model (and possibly on transient responses) decide for the appropriate sample interval for parametric modelling.

Step 3
Identify a parametric model by using a model structure that is linear-in-the-parameters (ARX, FIR). The order of this model can be chosen on the basis of an order test (ARXSTRUC)

where a cross-validation is used for validation purposes. However be sure that the order is chosen sufficiently high (in particular in the ARX case) such that the model for G_0 is at least accurate. This can be checked by inspection of the cross-correlation function $\hat{R}_{\varepsilon u}(\tau)$, preferably applied to a validation data set. A correct model for G_0 may require a model order that seems much too high, but this is often due to the fact that in an ARX model the high order is needed to provide an accurate estimate of H_0. This step is particularly directed towards achieving an estimate of G_0.

Step 4
Evalute the pole-zero plot of the estimate of G_0 from the previous step, and determine the order of the model. Use this order to identify an Output Error model, and validate this model with the appropriate tests.

Step 5
If a validated model for G_0 has been obtained, extend the model structure with a noise model, e.g. through a Box Jenkins model structure, and include an appropraite model for H_0. Validate the end result, e.g. by inspection of the auto-correlation test on the residual.

6.5   Relevant Matlab commands

Model order selection

```
[v] = arxstruc (z,zv,nn)
[nn] = selstruc (v,c)
```

The command `arxstruc` computes the loss function (identification criterion) values for families of ARX models, whose polynomial orders are specified in `nn`. The ARX models are identified on the basis of the identification data set `z`, while the loss function values are calculated over the validation data set `zv`.
`selstruc` performs an order estimation on the basis of the results of `arxstruc` by applying one of several criteria.

Model evaluation

```
[y]  = idsim (ue,IDMODEL)
[e]  = pe (IDMODEL,DATA)
[e]  = resid (IDMODEL,DATA)
[yh] = compare (DATA,IDMODEL,M)
[yp] = predict (IDMODEL,DATA,M)
```

`idsim` simulates model output of estimated models; `pe` allows to calculate the prediction error (residual) signal; `resid` performs the residual autocorrelation and cross-correlation tests; `compare` allows to compare predicted and simulated outputs with the measured data; `predict` generates the M-step forward prediction of the output.

Appendix

Problem 8.1
Show that for a non-white input signal u, the occurrence of a nonzero cross-correlation function $\hat{R}_{\varepsilon u}(\tau)$ for negative values of τ can be caused by a too high chosen time-delay in the model.

Solution
Consider the residual signal

$$\varepsilon(t, \hat{\theta}) = \hat{H}^{-1}(q) \left\{ [G_0(q) - \hat{G}(q)]u(t) + v(t) \right\} \tag{6A.1}$$

$$= \hat{H}^{-1}(q) \left\{ [\Delta G(q)]H_u(q)e_u(t) + v(t) \right\} \tag{6A.2}$$

with H_u the stable causal spectral factor of $\Phi_u(\omega)$, and e_u having a flat spectrum. Then

$$R_{\varepsilon u}(\tau) = \bar{E}[F_1(q)e_u(t) \cdot F_2(q)e_u(t)]$$

with

$$F_1 = \hat{H}^{-1}(q)\Delta G(q)H_u(q) \tag{6A.3}$$

$$F_2 = q^{-\tau}H_u(q) \tag{6A.4}$$

while

$$R_{\varepsilon u}(\tau) = \sigma_{e_u}^2 \cdot \sum_{k=-\infty}^{\infty} f_1(k)f_2(k)$$

with $\{f_i(k)\}_{k=0,\dots}$ the pulse response of filter F_i.

Filter F_1 is causal for all values of τ. For negative values of τ F_2 is anti-causal if $H_u = 1$, i.e. for input signals with a flat spectrum. However when H_u contains dynamics, then F_2 can get a causal part also for negative values of τ.

$\hat{R}_{\varepsilon u}(\tau)$ will have a nonzero contribution for negative values of τ if the pulse response sequences of F_1 and F_2 overlap. This will particularly occur if for negative τ, $f_2(k)$ has a contribution for those (small) values of $k \geq 0$ where the pulse response of $\Delta G(q)$ is nonzero. If u has a flat spectrum, i.e. $H_u = 1$, then F_2 will be anti-causal for negative values of τ and consequently $\hat{R}_{\varepsilon u}(\tau) = 0$.

Chapter 7

Frequency domain identification

7.1 Introduction

[1] So far the identification methods have been based on identification criterion that were formulated in the time-domain, employing the one-step-ahead predictor of the parametrized model. However since all our considerations are based on time-sequences of signals, any time-domain signal can be mapped with Fourier Transform to the frequency domain, allowing to interpret the obtained frequency domain data to be considered as the data, and allowing the identification criterion to be formulated in the frequency domain. This particular approach can have several advantages, like:

- Data compression; a very long time sequence can often be accurately represented by a finite number of frequency components, in particular if the time domain signal is periodic;

- Prefiltering of data amounts to a simple multiplication in the frequency domain;

- Data sequences of different experiments and different sampling frequencies can relatively easily be combined;

- The identification of continuous-time models can be realized along the same lines as for the discrete-time case.

Besides, many of the analysis results and methods and tools that are available for time-domain methods can directly be converted to the frequency domain. This has created a particular area denoted as "frequency domain identification" which is extensively developed and advocated in Pintelon and Schoukens (2012).

In several situations the "measurement data" is actually represented in the frequency domain:

- Sinusoidal or periodic excitation of the system provides hugely sized data records that can be effectively represented by its Fourier transforms $(Y_N(\omega), U_N(\omega))$;

- In particular in mechanical engineering (vibration/modal analysis) and electrical engineering (circuits), a frequency-domain treatment of signals is widespread and insightful.

---

[1]This chapter is still under construction, and therefore its text is still preliminary and rather fragmentary.

There exists a one-to-one relation between signals in the time domain and their Fourier representations in the frequency domain, through the (discrete) Fourier Transform[2]:

$$U_N(\omega) = \sum_{t=0}^{N-1} u(t) e^{-i\omega t}$$

$$u(t) = \frac{1}{N} \sum_{\ell=0}^{N-1} U_N \left(\frac{2\pi\ell}{N} \right) e^{i\frac{2\pi\ell}{N}t}$$

which maps a sequence of N real-valued time samples, into a sequence of N complex valued samples in the frequency domain, while the f-domain samples in positive and negative frequencies are complex conjugate versions of each other: $U_N(\omega) = U_N(2\pi - \omega)^\star$. The relationship between the time- and frequency samples is unique (one-to-one) and therefore the information content in both versions is the same.

Parallel to the situation in the time-domain, we can therefore formulate the identification problem (i.c. the identification criterion) in the frequency domain. Attractive properties of this frequency domain approach will typically appear when either

- Experimental data is obtained in the frequency domain, e.g. after sine sweep tests, where a finite set of frequency domain samples is obtained from measurements, or

- Experimental data is obtained on the basis of periodic input excitation in the time domain.

In the situation of periodic input excitation, with period length N_0, and considering an integer number of periods in the data, it is known that the Fourier transform of the periodic input signal will, asymptotically in N, only take values on a finite grid: $\omega = \frac{2\pi k}{N_0}$ with $k = 1, \cdots, N_0$. This implies that, in contrast with general time-domain data, we only have to consider N_0 points in the frequency domain, irrespective of the actual length of the time domain data set. Additional advantages of this data-reduction step will be addressed later.

7.2 Identification criteria in the frequency domain

7.2.1 Introduction

Starting from the time-domain (prediction error) approach, according to Chapter 4, we recall that the identification criterion is typically chosen as:

$$\hat{\theta}_N = \arg\min_\theta \frac{1}{N} \sum_{t=0}^{N-1} \varepsilon^2(t, \theta)$$

where the one-step ahead prediction error is specified by

$$\varepsilon(t, \theta) = H(q, \theta)^{-1} \left[y(t) - G(q, \theta) u(t) \right]. \tag{7.1}$$

---

[2]Note that in some literature the factor $1/N$ in $u(t)$ is replaced by a factor $1/\sqrt{N}$ in both expressions for $u(t)$ and $U_N(\omega)$.

Rewriting these expressions in the frequency domain, and utilizing Parseval's relation (2.38), we arrive at

$$\frac{1}{N} \sum_{t=0}^{N-1} \varepsilon^2(t, \theta) = \frac{1}{N} \sum_{k=0}^{N-1} \left| \mathcal{E}_N \left(\frac{2\pi k}{N}, \theta \right) \right|^2 \tag{7.2}$$

where the Fourier Transform of the prediction error signal can be written as:

$$\mathcal{E}_N(\omega, \theta) = H(e^{i\omega}, \theta)^{-1} \left[Y_N(\omega) - G(e^{i\omega}, \theta) U_N(\omega) \right] + R_N(\omega, \theta)$$

and where R_N reflects the transients of both H^{-1} and $H^{-1}G$.

There are two different approaches for how to consider frequency response data:

- We can consider the Fourier transformed i/o data: $Y_N(\omega), U_N(\omega)$ over a finite grid in the frequency domain, or

- We can consider a "measured" frequency response function (FRF) $\breve{G}(e^{i\omega})$ over a finite grid in the frequency domain, either directly measured or estimated through e.g. an ETFE estimate.

Identification criterion for f-domain data $Y_N(\omega_k), U_N(\omega_k)$

The typical identification criterion for given f-domain data $Y_N(\omega), U_N(\omega)$ then becomes, on the basis of (7.2)[3]:

$$\hat{\theta}_N := \arg \min_\theta \frac{1}{N} \sum_{k=0}^{N/2} \frac{|Y_N(\omega_k) - G(e^{i\omega_k}, \theta) U_N(\omega_k)|^2}{|H(e^{i\omega_k}, \theta)|^2} \tag{7.3}$$

with ω_k a frequency that runs over the Fourier grid: $\omega_k = \frac{2\pi k}{N}, \ k = 1, \cdots N$.

Identification criterion for FRF data $\breve{G}(e^{i\omega_k})$

If the frequency response function (FRF) $\breve{G}(e^{i\omega_k})$ is measured or estimated a priori, e.g. through ETFE, i.e.

$$\breve{G}(e^{i\omega_k}) = \frac{Y_N(\omega_k)}{U_N(\omega_k)},$$

then the criterion (7.3) transforms to

$$\hat{\theta}_N = \arg \min_\theta \frac{1}{N} \sum_{k=0}^{N/2} \left| \breve{G}(e^{i\omega_k}) - G(e^{i\omega_k}, \theta) \right|^2 \cdot \frac{|U_N(\omega_k)|^2}{|H(e^{i\omega_k}, \theta)|^2}. \tag{7.4}$$

Since $U_N(\omega_k)$ is typically not available when $\breve{G}$ is "measured", this criterion is often replaced by a simplified version for FRF data:

$$\hat{\theta}_N = \arg \min_\theta \frac{1}{N} \sum_{k=0}^{N-1} \left| \breve{G}(e^{i\omega_k}) - G(e^{i\omega_k}, \theta) \right|^2 \cdot W_k$$

where W_k is some predefined and fixed positive weighting function.

The set of frequencies ω_k over which the criterion is calculated, can be chosen by the user, and actually reflects a special choice of W_k. The weighting function can particularly be used to emphasize or de-emphasize particular frequency ranges, e.g. to select the frequency range over which an accurate model is desired.

---

[3]Neglecting the effect of initial conditions in the term R_N

7.2.2   Noise model in the frequency domain

While in the time-domain, then noise model $H(q,\theta)$ needs to be available as a parametric transfer function in order to calculate the prediction error $\varepsilon(t,\theta)$ (7.1), in the frequency domain it suffices to have $|H(e^{i\omega_k},\theta)|^2$ available in a finite number of frequency points, for calculation of the criterion (7.4). Consequently we can do without a rational representation of $H(q,\theta)$ and can also handle a non-parametric representation, or, in other words, just a sequence of real values $|H(e^{i\omega_k},\theta)|^2$, $k = 1, \cdots N$. This will facilitate the estimation of noise models, as will be illustrated later.

Modeling noise in the frequency domain
In order to characterize the properties of noise in the frequency domain, we will use the following properties of Fourier transformed noise:

Proposition 7.2.1 *Consider a white noise process $e(t)$ with $e \sim \mathcal{N}(0,\sigma_e^2)$. Then the Fourier transform $E_N(\omega_k)$ satisfies the following properties:*

- *The random variables $E_N(\omega_k)$, for $\omega_k = 2\pi\frac{k}{N}$, $k = 1, \cdots N$ have zero mean and are mutually independent.*

- *$E_N(\omega_k)$ is circular complex normally distributed, i.e. $E_N(\omega_k)$ has a pdf given by*

$$p(z) = \frac{1}{2\pi}e^{-z^*\Gamma^{-1}z},$$

satisfying the following properties:

$$\mathbb{E}\left[E_N(\omega_k)\right] = 0, \quad \mathbb{E}\left[E_N^2(\omega_k)\right] = 0, \quad \mathbb{E}\left[|E_N(\omega_k)|^2\right] = \sigma_E^2.$$

For colored noise we have the following result:

Proposition 7.2.2 *Consider a colored noise $v(t) = H(q)e(t)$. Then the Fourier transform $V_N(\omega_k)$ satisfies the following properties:*

- *For $N \to \infty$, the random variables $V_N(\omega_k)$, for $\omega_k = 2\pi\frac{k}{N}$, $k = 1, \cdots N$ have zero mean and are mutually independent.*

- *$V_N(\omega_k)$ is circular complex normally distributed,*

- *$V_N(\omega_k) \to H(\omega_k)E_N(\omega_k)$ for $N \to \infty$, and*

$$\mathbb{E}\left[V_N(\omega_k)\right] = 0, \quad \mathbb{E}\left[V_N^2(\omega_k)\right] = 0, \quad \mathbb{E}\left[|V_N(\omega_k)|^2\right] := \sigma_V^2(\omega_k) = |H(\omega_k)|^2\sigma_E^2$$

.

The identification criterion for given f-domain data $Y_N(\omega), U_N(\omega)$ (7.3) can then equivalently be written as:

$$\hat{\theta}_N := \arg\min_\theta \frac{1}{N} \sum_{k=0}^{N/2} \frac{|Y_N(\omega_k) - G(e^{i\omega_k},\theta)U_N(\omega_k)|^2}{\sigma_V^2(\omega_k)} \tag{7.5}$$

with ω_k on the Fourier grid: $\omega_k = \frac{2\pi k}{N}$, and stressing that $\sigma_V^2(\omega_k)$ just acts as a pointwise frequency weighting of the criterion. Note however that this weighting is typically unknown; it needs to be estimated from data too.

This criterion provides the *maximum likelihood estimator* for the situation that we have

- periodic input u and e Gaussian, or

- $N \to \infty$.

In general, $\sigma_V^2(\omega_k)$ will need to be estimated but not necessarily through a finite-dimensional LTI filter, but just as a sequence of points, resulting in the -so-called- *sample maximum likelihood estimator*.

7.3   Model structures

Model parametrizations for $G(e^{i\omega_k}, \theta)$ and $H(e^{i\omega_k}, \theta)$ are completely similar to the time domain model structures, and are simply obtained by replacing q by $e^{i\omega_k}$:

- Output error model structure

$$G(e^{i\omega_k}, \theta) \;=\; \frac{B(e^{-i\omega_k}, \theta)}{F(e^{-i\omega_k}, \theta)} = \frac{b_0 + b_1 e^{-i\omega_k} + b_2 e^{-2i\omega_k}}{1 + f_1 e^{-i\omega_k} + f_2 e^{-2i\omega_k}}$$

$$H(e^{i\omega_k}, \theta) \;=\; 1$$

- ARX model structure

$$G(e^{i\omega_k}, \theta) \;=\; \frac{B(e^{-i\omega_k}, \theta)}{A(e^{-i\omega_k}, \theta)} = \frac{b_0 + b_1 e^{-i\omega_k} + b_2 e^{-2i\omega_k}}{1 + a_1 e^{-i\omega_k} + a_2 e^{-2i\omega_k}}$$

$$H(e^{i\omega_k}, \theta) \;=\; \frac{1}{A(e^{-i\omega_k}, \theta)}.$$

The typical non-convex optimization problems that result for general model structures in the time domain, remain non-convex optimization problems in the frequency domain, when considering the identification criteria (7.2) and (7.3. Like in the time-domain case there are two structures that are linear-in-the-parameters:

- FIR (OE with $F = 1$; ARX with $A = 1$)

- ARX

that lead to convex optimization problems, and to an analytical solutions for $\hat{\theta}_N$.
When a nonlinear-in-the-parameters model structure is used, a nonconvex optimization problem needs to be solved. This can be done by gradient type of search methods, like Gauss-Newton-based methods, or by sequential least squares type of methods, see Section 7.5.

7.4   Linear regression in the f-domain

An ARX model applied to FRF data while using the criterion (7.3) with $U_N(\omega_k)$ is 1 for all frequencies, leads to the expression

$$V_N(\theta) = \frac{1}{N} \sum_{k=1}^{N} \left| \breve{G}(e^{i\omega_k}) A(e^{-i\omega_k}, \theta) - B(e^{-i\omega_k}, \theta) \right|^2$$

to be minimized over θ. For ease of notation we do not include any weighting function in the criterion now.

With

$$
\begin{aligned}
A(e^{-i\omega_k}, \theta) &= 1 + a_1 e^{-i\omega_k} + \cdots a_{n_a} e^{-n_a i\omega_k} \\
B(e^{-i\omega_k}, \theta) &= b_1 e^{-i\omega_k} + \cdots b_{n_b} e^{-n_b i\omega_k} \\
\theta^T &= [a_1 \ a_2 \cdots a_{n_a} \ b_1 \cdots b_{n_b}]
\end{aligned}
$$

this can be written as in a linear regression form, as follows.

With

$$
\begin{aligned}
\breve{G}(e^{i\omega_k})A(e^{-i\omega_k}, \theta) - B(e^{-i\omega_k}, \theta) = \\
\breve{G}(e^{i\omega_k})[1 + a_1 e^{-i\omega_k} + \cdots a_{n_a} e^{-n_a i\omega_k}] - [b_1 e^{-i\omega_k} + \cdots b_{n_b} e^{-n_b i\omega_k}]
\end{aligned}
$$

and denoting

$$
\Omega^T(e^{i\omega_k}) := [-e^{-i\omega_k}\breve{G}(e^{i\omega_k}) \cdots - e^{-n_a i\omega_k}\breve{G}(e^{i\omega_k}) \ e^{-i\omega_k} \cdots e^{-n_b i\omega_k}]
$$

it follows that

$$
V_N(\theta) = \frac{1}{N} \sum_{k=1}^{N} \left| \breve{G}(e^{i\omega_k}) - \Omega^T(e^{i\omega_k})\theta \right|^2. \tag{7.6}
$$

For comparison with the time domain mechanism, see Section 4.6.

In comparison with the time domain situation, there is one difference though, due to the fact that $\breve{G}(e^{i\omega_k})$ and $\Omega(e^{i\omega_k})$ are complex-valued variables now. In order to deal with this we denote

$$
\bar{G} := \begin{bmatrix} \Re\{\breve{G}(e^{i\omega_1})\} \\ \Im\{\breve{G}(e^{i\omega_1})\} \\ \vdots \\ \Re\{\breve{G}(e^{i\omega_N})\} \\ \Im\{\breve{G}(e^{i\omega_N})\} \end{bmatrix} \qquad \bar{\Omega} := \begin{bmatrix} \Re\{\Omega^T(e^{i\omega_1})\} \\ \Im\{\Omega^T(e^{i\omega_1})\} \\ \vdots \\ \Re\{\Omega^T(e^{i\omega_N})\} \\ \Im\{\Omega^T(e^{i\omega_N})\} \end{bmatrix}
$$

with $\Re$ and $\Im$ referring to the real and imaginary part.

The cost function (7.6) can now be written as

$$
V_N(\theta) = \frac{1}{N}(\bar{G} - \bar{\Omega}\theta)^T(\bar{G} - \bar{\Omega}\theta) \tag{7.7}
$$

where all terms are real-valued. Minimizing this cost function over θ will lead to the solution

$$
\hat{\theta}_N = (\bar{\Omega}^T\bar{\Omega})^{-1}\bar{\Omega}^T\bar{G},
$$

which again has close relationship with the time-domain expression (4.52).

Note that, like in the time-domain situation, the criterion actually has a high-frequency (ARX) weighting:

$$
\begin{aligned}
V_N(\theta) &= \frac{1}{N} \sum_{k=1}^{N} \left| \breve{G}(e^{i\omega_k})A(e^{-i\omega_k}, \theta) - B(e^{-i\omega_k}, \theta) \right|^2 \tag{7.8} \\
&= \frac{1}{N} \sum_{k=1}^{N} \left| \breve{G}(e^{i\omega_k}) - \frac{B(e^{-i\omega_k}, \theta)}{A(e^{-i\omega_k}, \theta)} \right|^2 \cdot |A(e^{-i\omega_k}, \theta)|^2 \tag{7.9}
\end{aligned}
$$

For a further interpretation of this weighting with the factor $|A(e^{-i\omega_k}, \theta)|^2$ see also Section 4.12.2.

7.5 Computational methods

In terms of computational methods for arriving at the frequency domain parameter estimate, all the aspects that are discussed in 4.13 are still relevant.

In particular, there is a frequency domain equivalent of the sequential least squares method of Steiglitz and McBride (1965), where subsequent steps of linear regression and data filtering are used to compensate for the effect of the typical ARX weighting of the identification criterion, like being present in (7.9).

In order to counteract the presumed negative effect of the weighting, a criterion with a fixed weight is applied:

$$V_N(\theta) = \frac{1}{N} \sum_{k=1}^{N} \left| \breve{G}(e^{i\omega_k}) A(e^{-i\omega_k}, \theta) - B(e^{-i\omega_k}, \theta) \right|^2 W_k$$

with W_k determined by the denominator polynomial from a previous estimate:

$$W_k = \frac{1}{|A(e^{-i\omega_k}, \hat{\theta}_{prev})|^2}$$

leading to an iterative algorithm and consecutive linear regression estimation steps. In this frequency domain identification setting, this approach is known as the method of Sanathanan and Koerner (1963).

Without a linear-in-the-parameters model structure, the optimization problem of minimizing the cost function will be a general non-convex optimization problem, that typically is solved by gradient-based methods such as Gauss-Newton methods.

7.6 Properties and Topics

In this section we list a set of properties and aspects that are related to the use of frequency domain identification methods, typically in relation to the time domain methods presented earlier.

1. Advantages of periodic excitation signals in identification

Periodic excitation (and taking a full number of periods into account) implies that

$$U_N(\omega)$$

takes values $\neq 0$ only in a finite frequency grid, being a subset of $\omega = 2\pi k/N_0$, $k = 1, .., N_0$, and N_0 the period length, see Figure 7.1.

- The consequence of this, is that when evaluating $Y_N(\omega)$, any component that is outside of the excited discrete frequency grid, can be assigned to noise. This is basically a very simple tool for removing noise from data.

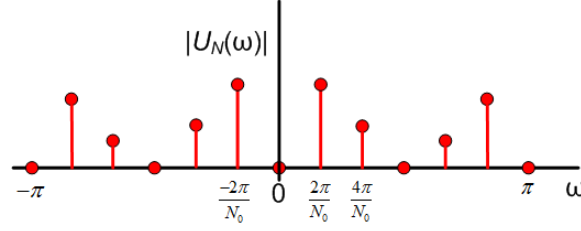Other consequences of using periodic input signals are that

Figure 7.1: Periodic input signals generate a Fourier transform that takes values only on a discrete frequency grid.

- Information on the system to be modelled will be obtained only in limited number of frequency points. However, in these frequency points, the information will be accurate, since noise that occurs outside of the excited frequency grid is not disturbing the estimates. There is a mechanism of experiment repetition involved when applying periodic signals, that is very effective for noise reduction.

- If input signals are non-periodic, transient effects (non-stationary initial conditions) have an influence on model accuracy and can/should be estimated too.

2. Non-parametric noise models from periodic inputs

Consider the data generating system:

$$y(t) = y_u + v(t), \quad \text{with } y_u(t) = G_0(q)u(t)$$

If u is periodic with period N_0, then y_u will also be periodic, after the decay of a possible transient. Consequently an improved estimate of y_u is obtained by averaging over K periods:

$$\bar{y}(t) = \frac{1}{K} \sum_{k=0}^{K-1} y(t + kN_0) \quad t = 0, \cdots N_0 - 1$$

leading to an improved estimate of the noise

$$\hat{v}(t) = y(t) - \bar{y}(t) \quad \text{with } \bar{y}(t) \text{ periodically extended.}$$
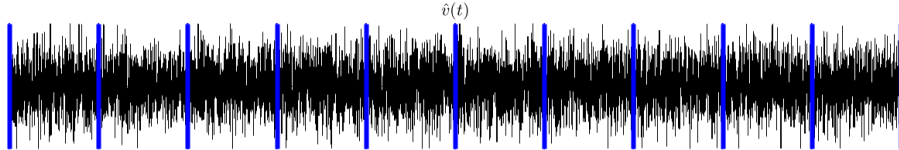
Given noise $\hat{v}(t)$

Figure 7.2: A noise signal $\hat{v}(t)$ decomposed over the different periods of the input signal. Fourier transform over each period leads to a sequence of DFT's $\hat{V}_{N_0}^{[1]}(\omega_k)$, $\hat{V}_{N_0}^{[2]}(\omega_k)$, $\ldots \hat{V}_{N_0}^{[K]}(\omega_k)$

The unbiased estimate of $\sigma_V^2(k)$ can be obtained according to

$$\hat{\sigma}_V^2(k) := \frac{1}{K-1} \sum_{i=1}^{K} \left| \hat{V}_{N_0}^{[i]}(\omega_k) \right|^2.$$

This we can substitute as an appropriate weighting in the (maximum-likelihood) estimator (7.5), leading to:

$$\hat{\theta}_N := \arg\min_\theta \frac{1}{N} \sum_{k=0}^{N/2} \frac{|Y_N(\omega_k) - G(e^{i\omega_k}, \theta)U_N(\omega_k)|^2}{\hat{\sigma}_V^2(\omega_k)}$$

thus avoiding the identification of a parametric noise model. The estimated sequence $\hat{\sigma}_V^2(k)$ acts as a nonparametric noise model.

3. Prefiltering

In the freqency domain prefiltering of signals becomes very simple, as it concerns a simple multiplication of Fourier transforms of filters and signals. Prefiltering in order to influence the approximation properties of estimated models comes down to adding a simple weighting term in the identification criterion:

$$\hat{\theta}_N = \arg\min_\theta \frac{1}{N} \sum_{k=0}^{N-1} \left| \breve{G}(e^{i\omega_k}) - G(e^{i\omega_k}, \theta) \right|^2 \cdot W_k.$$

This can be handled very easily in the respective optimization algorithms.

4. Continuous-time experimental setups

Experimental setups for identification typically are either:

- ZOH: The input to the system is a discrete-time signal, processed through a zero-order-hold (ZOH), to deliver an input to the (continuous-time) physical setup;
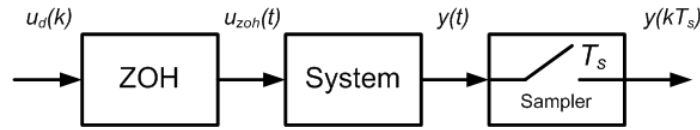
Figure 7.3: Zero-order hold equivalent of continuous-time system.

- BL: Input and output signals of the system are sampled versions of band-limited signals, e.g. after applying anti-aliasing filters.

- In the ZOH-setup, the equivalent discrete time system that keeps the output invariant at the sample moments, is given by

$$G(z) = (1 - z^{-1})\mathcal{Z}\left\{ \frac{G(s)}{s} \right\}$$

where $\mathcal{Z}\left\{ \frac{G(s)}{s} \right\}$ refers to the Z-transform of the sampled version of the time signal that results from the inverse Laplace transform of $G(s)/s$.
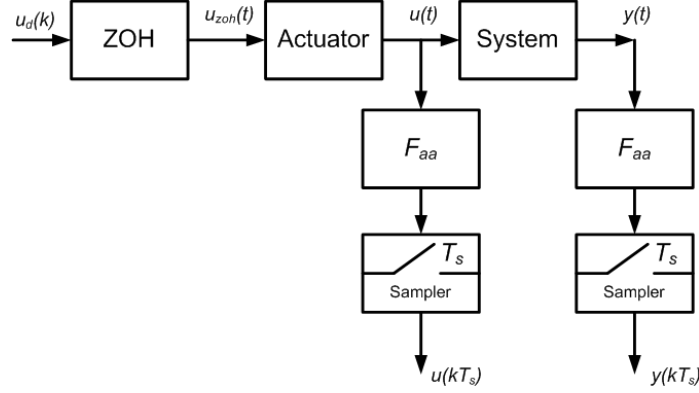
Figure 7.4: Equivalent discrete-time system of continuous system under band-limited assumptions.

- In the BL-setup, the continuous-time frequency response can be obtained directly from the DTFT, provided that the conditions of the Nyquist sampling theorem is obeyed i.e.
  CT frequency response = DT frequency response, for frequencies up to $\omega_s/2$.

$$G(i\omega) = G(e^{i\omega}), \qquad |\omega| < \omega_s/2.$$

The consequence of this is that under bandlimited assumptions on the measurement signals, a continuous-time (CT) model, can be estimated directly from $\breve{G}(e^{i\omega})$.
The only thing that needs to be changed for this is the model parametrization. In stead of a discrete- time representation, as used in section 7.3, we can now represent our models directly in the continuous-time, as

$$G(i\omega_k, \theta) \quad = \quad \frac{B(i\omega_k, \theta)}{A(i\omega_k, \theta)} = \frac{b_0(i\omega_k)^n + b_1(i\omega_k)^{n-1} + \cdots + b_n}{(i\omega_k)^n + a_1(i\omega_k)^{n-1} + a_n}$$

Estimating a transfer function model is a curve fitting problem in the frequency domain. It does not matter whether rational functions in $z = e^{i\omega_k}$ or $s = i\omega_k$ are used.

5. Additional properties of f-domain identification

- Condensing large (time domain) data sets, to a limited number of points in the f-domain. A data reduction mechanism can be in place, which can be very attractive from a computational perspective.

- Combining data from different experiments. Different experiments, focussing at different frequency ranges, can simply be combined in one data set.

- There is a flexible choice of the frequency region of interest for our models. The frequency domain is typically a very attractive domain for indicating in which aspects the user values high accuracy models. Frequency weighting of the cost functions, is then a very appealing and effective tool as a design variable in the identification methods.

7.7   Identification example

We consider a data generating systems G_0 with 4 poles and 2 zeros. The systems has two resonance peaks, of which one is well observed and the second one is dominated by noise. As input signal we apply two repetitions of a white noise sequence, of which the second is used for identification. The length of this data sequence is $N = 10,000$. As a first step we obtain an ETFE estimate of the underlying system, depicted in Figure 7.5 (right).
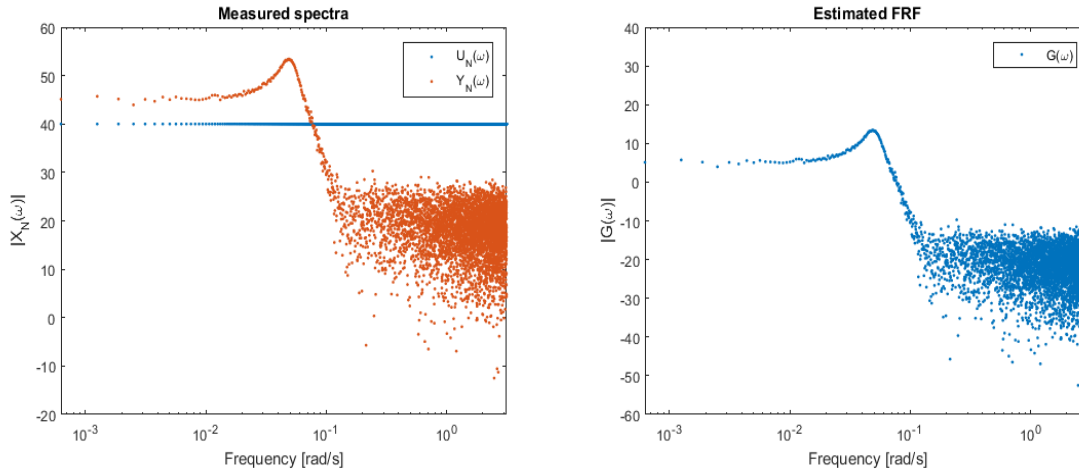
Figure 7.5: Left: Amplitude Fourier transform of input (blue) and output (red), based on $N = 10,000$ data points; right: ETFE estimate of the frequency response of G.

Next we estimate ARX and OE models having two poles and two zeros, and we limit the frequency domain criterion with a weighting function, to focus only the first 100 or 250 points in the frequency grid.
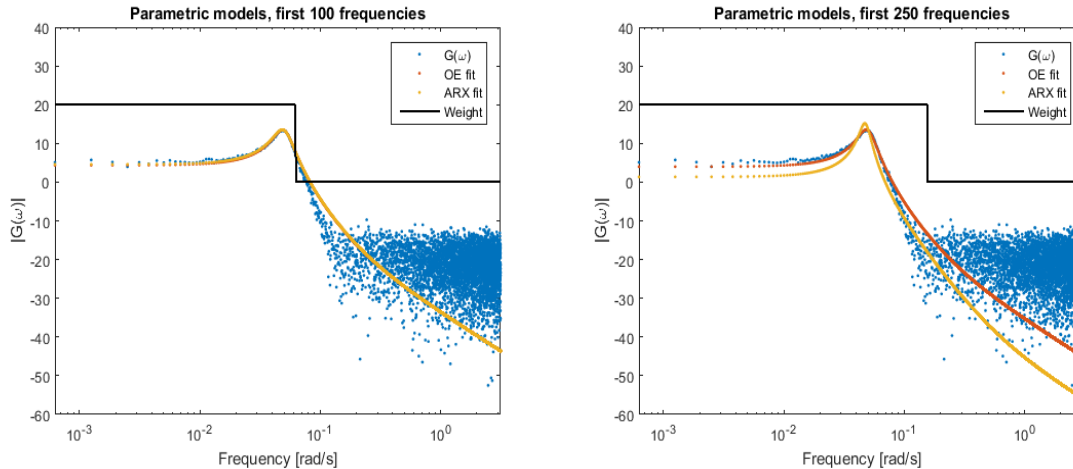
Figure 7.6: Identified second order OE (red) and second order ARX (yellow) models, and the applied frequency weighting (black) selecting only the first 100 frequencies (left) and the first 250 frequencies (right).

We observe that when considering a larger frequency range over which the data is taken

into account, the estimated ARX and OE models are going to divert from each other. This difference is becoming even more apparent when the frequency weighting is changed to include a wider band, as shown in Figure 7.7. The ARX includes an additional weighting factor of $|A(e^{i\omega_k}, \theta)|^2$ on the additive error between FRF and the model's frequency response, which puts an emphasis on fitting the high frequency components. Since these are extremely noisy, the estimated ARX model is diverting from the system's response and from the estimated OE model, which does not suffer from this weighting.
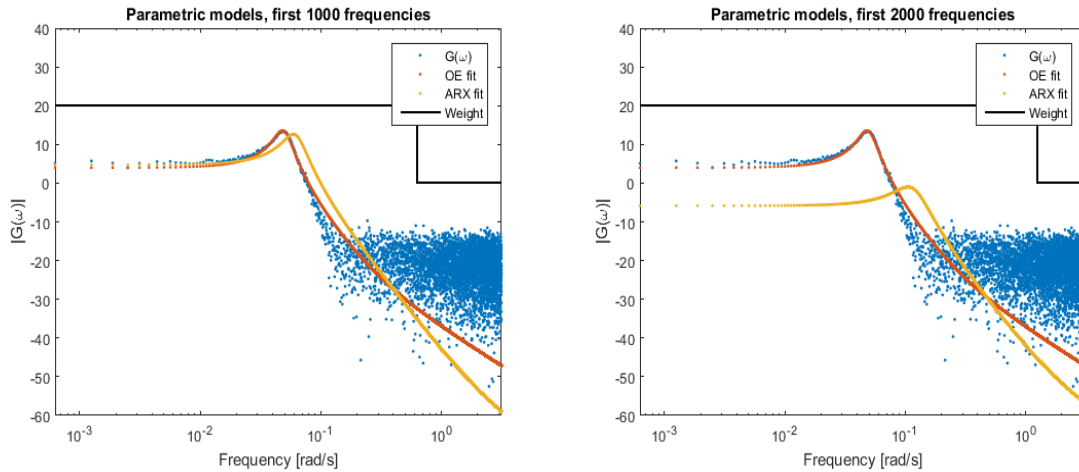
Figure 7.7: Same situation as in Figure 7.6, but now with frequency window (black) selecting the first 1000 frequencies (left) and the first 2000 frequencies (right).

These results should be interpreted in the same way as was done in the approximate modelling results of section 4.12.2.

7.8   Summary

- Freqquency domain identification is to a large extent dual/similar to time domain identification.

- It allows two approaches, based on either DFT of i/o data, or on measured/estimated frequency response functions.

- Periodic excitation is naturally connected to the frequency domain identification, and has several advantages.

- For periodic excitation there is less need for parametric noise models and also non-parametric noise models can be used.

- A bandlimited setup allows direct identification of continuous-time models.

- Theoretical principles and results are largely similar to the time-domain results.

Bibliography

R. Pintelon, P. Guillaume, Y. Rolain, J. Schoukens and H. Van hamme (1994). Parametric identification of transfer functions in the frequency domain - a survey. *IEEE Trans. Automatic Control, Vol. 39*, no. 11, pp. 2245-2260.

R. Pintelon and J. Schoukens (2012). *System Identification - A Frequency Domain Approach*. IEEE Press, Piscataway, NJ, USA, second edition.

C.K. Sanathanan and J. Koerner (1963). Transfer function synthesis as a ratio of two complex polynomials. *IEEE Trans. Autom. Control, AC-8*, pp. 56-58.

K. Steiglitz and L.E. McBride (1965). A technique for the identification of linear systems. *IEEE Trans. Automat. Control, AC-10*, pp. 461-464.

Chapter 8

Identification design

8.1 Introduction

The identification methods presented in the previous chapter show a number of user's choices that - to the experimenter - act as design variables, that can essentially influence the models that are finally identified. Take for instance the following choices that have to be made:

- Choice of model set and model structure;

- Choice of data-prefilter L, as discussed in section 5.5;

- Choice of experimental conditions; number of data, sampling interval, input spectrum etc.

Apparently, to some extent the experimenter is able to "tune" the identification result. In order to formalize this situation, we have to deal with the question how these choices affect the identified models, and conversely how to make these choices in order to obtain desirable properties of the identified models.
However any discussion on these topics will have to start by considering the question

> What do we want from our models?

If we want consistency of the model estimates, then the situation is relatively clear. Some validation tests concerning this situation are discussed in section 6.3. Of course, consistency requires a correct choice of the model set and the model structure, as discussed in the previous chapter; additionally some weak conditions on the experimental situation have to be satisfied, as persistence of excitation of the input signal. However note that as an ultimate objective in system's modelling, consistency is probably not a very realistic goal to pursue. We definitely have to require from our identification methods that they obtain consistent estimates in the - artificial - situation that this is indeed possible. However we surely have to deal with the question, what to require from our models in the situation that consistency cannot be achieved, e.g. caused by the fact that our models simply are not able to capture all of the (possibly nonlinear, infinite dimensional, time-varying) process dynamics.

If consistency is out of the question, probably a realistic and relevant answer to the question formulated above is

> We want our model to perform well in terms of the application for which the model is intentionally designed.

This implies that we should evaluate the "quality" of our estimated models in relation to the model application. Applications can e.g. be:

- Simulation

- Prediction

- Diagnosis

- Control design

and many others.

Taking control design as a model application, it would be fair to let the "quality" of an estimated model be determined by some performance measure of the process, while controlled by a controller that is designed on the basis of the estimated model. A relevant "identification design"-problem is then to choose the design variables in such a way that this performance measure is optimized. For control design as a model application this approach has been followed by a number of authors to arrive at -what is called- "control-relevant identification". See e.g. Schrama (1992), Gevers (1993), and Van den Hof and Schrama (1995). A specific treatment of these aspects is postponed to a later chapter. In section 8.2 we will first discuss how design variables in identification influence the identified models in terms of their frequency response fit.

Next, attention will be given to the aspects of experiment design in a general (and not application-specific) setting, by addressing issues as input design and related items like the choice of sampling frequency and data (pre)processing.

8.2   Design variables in transfer function approximation

In this section we will reconsider the frequency domain expression for the asymptotic parameter estimate (the limit model) as discussed previously in section 4.12. We will - mainly heuristically - discuss how we can influence the bias distribution of this limit model by appropriate choice of design variables. As mentioned in section 4.12, in the case of open-loop experimental conditions the asymptotic parameter estimate is obtained by

$$\theta_{\mathcal{D}}^* = \arg\min_{\theta \in \Theta} \frac{1}{2\pi} \int_{-\pi}^{\pi} \frac{|G_0(e^{i\omega}) - G(e^{i\omega}, \theta)|^2 \Phi_u(\omega) + \Phi_v(\omega)}{|H(e^{i\omega}, \theta)|^2} |L(e^{i\omega})|^2 d\omega \qquad (8.1)$$

where $\mathcal{D}$ reflects all design variables that affect the identified model, as model set $\mathcal{M}$, prefilter L, input spectrum Φ_u.

Heuristically, the bias expression can be interpreted as finding a compromise between two minimizations, the first one being,

$$\theta_{\mathcal{D}}^* \quad \approx \quad \arg \min_{\theta \in \Theta} \frac{1}{2\pi} \int_{-\pi}^{\pi} |G_0(e^{i\omega}) - G(e^{i\omega}, \theta)|^2 Q(\omega, \theta^*) d\omega \tag{8.2}$$

$$Q(\omega, \theta) \quad = \quad \Phi_u(\omega)|L(e^{i\omega})|^2 / |H(e^{i\omega}, \theta)|^2 \tag{8.3}$$

and the second being the fitting of $|H(e^{i\omega}, \theta)|^2$ to the error spectrum, i.e. the numerator spectrum in (8.1). In many of the situations we will apply system identification techniques in order to obtain an accurate estimate of the input-output transfer function $G_0(e^{i\omega})$. Therefore we will give a closer look at the bias distribution $G(e^{i\omega}, \theta^*) - G_0(e^{i\omega})$.

Visual inspection of Bode plots.
One often prefers to represent the transfer function in a Bode plot, where the amplitude Bode plot shows *log* $|G|$ and the phase Bode plot shows *arg* G both as functions of *log* ω. This has some physical significance in that relative errors are displayed rather than absolute ones. To focus on the relative error, we may rewrite $\theta_{\mathcal{D}}^*$ as:

$$\theta_{\mathcal{D}}^* = \arg \min_{\theta \in \Theta} \int_{-\pi}^{\pi} |\frac{G(e^{i\omega}, \theta) - G_0(e^{i\omega})}{G_0(e^{i\omega})}|^2 \cdot |G_0(e^{i\omega})|^2 Q(\omega, \theta^*) d\omega \tag{8.4}$$

which shows that in order to obtain a small relative error in G where $|G_0|$ is small, it requires a weighting function $Q(\omega, \theta^*)$ that is much larger at those frequencies.
Note that in this heuristic analysis, the frequency scale is linear, which means that the decade between say 1 and 10 rad/sec represents a 10 times larger weight than the decade between 0.1 and 1 rad/sec. To reflect a logarithmic frequency scale, one should compensate for ω in the weighting function:

$$|G_0(e^{i\omega})|^2 Q(\omega, \theta^*) d\omega = \omega |G_0(e^{i\omega})|^2 Q(\omega, \theta^*) d(log \ \omega) \tag{8.5}$$

To secure a good fit at low frequencies, $|G_0|^2 Q$ must be much larger than ω there.

Manipulating the weighting function.
It is true that the weighting function Q will not be known a priori in many cases, since in general it depends on θ^*. One should also note that as some design variables are changed (in order to change θ^*, i.e. the bias distribution), the noise model will also change. The exact effect on $Q(\omega, \theta^*)$ of e.g. introducing a prefilter may therefore be somewhat difficult to predict. However, Q is always available a posteriori, and so one can reconstruct which weighting function has produced the current estimate. Manipulating Q in the heuristic criterion (8.2) by changing design variables as

- Input spectrum $\Phi_u(\omega)$

- Noise model set $\{H(e^{i\omega}, \theta), \ \theta \in \Theta\}$

- Prefilter $L(q)$

is therefore quite straightforward, but may involve some trial and error.
The effect of the sampling interval on Q will be discussed in section 8.3.
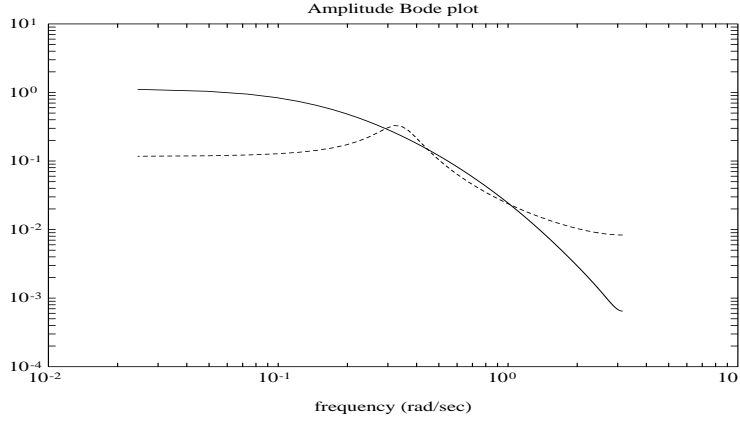
Illustration.

Figure 8.1: Bode plot of true system G_0 (solid line) and second order OE-model (dashed line) obtained by applying a high-pass (HP) prefilter $L_1(q)$.

Even though heuristic, (8.2) is a quite useful tool to understand and manipulate the bias distribution. This is illustrated in a continuation of example 4.12.1, also taken from Ljung (1987).

Example 8.2.1 *(Example 4.12.1 continued).* We consider again the data generating system as in example 4.12.1. The resulting model in the OE-structure (4.173) gave the Bode plot of figure 4.9. This corresponds to $Q(\omega) \equiv 1$ (θ-independent).

Comparing with (8.5) and (8.4), we see that high frequencies play very little role in the Bode plot fit, due to the rapid roll-off of $|G_0(e^{i\omega})|$.

To enhance the high-frequency fit, we filter the prediction errors through a fifth-order high-pass (HP) Butterworth filter $L_1(q)$ with cut-off frequency of 0.5 rad/sec. This is equivalent to introducing a fixed noise model $H(q) = 1/L_1(q)$, and changes the weighting function $Q(\omega)$ to this HP-filter. The Bode amplitude plot of the resulting estimate is given in figure 8.1. Comparing it with figure 4.9 the fit has become slightly better around $\omega = 1rad/s$. However the model has become worse for the lower frequencies, while the second-order model has problems to describe the fourth-order roll-off for $\omega > 1rad/s$.

Consider now the estimate obtained by the least-squares method in the ARX model structure. This was depicted in figure 4.9. If we want a better low-frequency fit, it seems reasonable to counteract the HP weighting function $Q(\omega, \theta^*)$ in figure 4.10 by low-pass (LP) filtering of the prediction errors. We thus construct $L_2(q)$ as a fifth order LP Butterworth filter with cut-off frequency 0.1 rad/sec. The ARX model structure is then applied to the input-output data filtered through $L_2(q)$. Equivalently, we could say that the prediction error method is used for the model structure

$$y(t) = \frac{b_1 q^{-1} + b_2 q^{-2}}{1 + a_1 q^{-1} + a_2 q^{-2}} u(t) + \frac{1}{L_2(q)(1 + a_1 q^{-1} + a_2 q^{-2})} e(t) \qquad (8.6)$$

The resulting estimate is shown in figure 8.2 and the corresponding weighting function $Q(\omega, \theta^*)$ in figure 8.3. Clearly we have now achieved a much better low-frequency fit in the frequency range $\omega \leq 0.4rad/s$. We may note that the estimates of figure 8.2 (filtered ARX) and figure 4.9 (unfiltered OE) are quite similar. One should then realize that the filtered
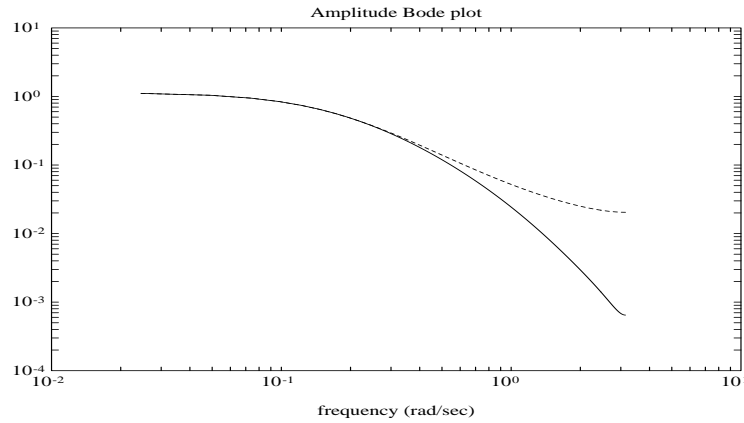
Figure 8.2: Bode plot of true system G_0 (solid line) and second order ARX-model (dashed line) obtained by applying a low-pass (LP) prefilter $L_2(q)$.
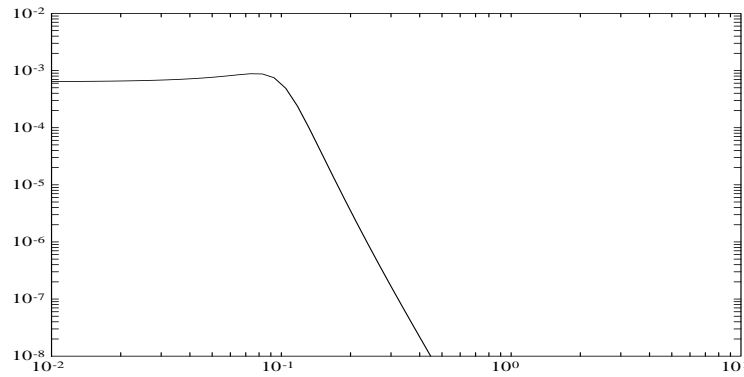
Figure 8.3: Weighting function $Q(\omega, \theta^*) = |L_2(e^{i\omega})|^2 \cdot |1 + a_1^* e^{-i\omega} + a_2^* e^{-2i\omega}|^2$ corresponding to the estimate in figure 8.2.

ARX estimate of figure 8.2 is much easier to obtain than the output error estimate of figure 4.9, which requires iterative search algorithms.

Note that the Steiglitz and McBride procedure as discussed in section 4.13 is an attempt to choose the filter L such that an output error minimization results. The point remains that for a real output error minimization L should be chosen parameter dependent.

8.3 Experiment design

8.3.1 Preparatory experiments

Every task of modelling that is related to a physical process, will generally have to be preceded by a preliminary phase in which a first process analysis is made. Even before the first experiments are performed on the process, one will have to consider aspects as

- What are the signals that possibly can act as inputs/outputs?

- Do we have an indication of the frequency range over which the process will exhibit its essential dynamics?

- Do we have an indication of normal and extreme signal amplitudes?

- Which instrumentation is most appropriate for data-acquisition and what has to be the location and type of measurement instruments?

Preparatory experiments are not specifically directed to a parametric identification of the process at hand, but are made to obtain that information from the process that enables the proper design of an identification experiment later on. Basic knowledge about the process is gathered. In this experimental phase we can distinguish a number of goals.

- Measurement of output signals while the input signal is kept constant (free run experiments). With these measurements it is determined to which extent noise is contaminating the output signals. The disturbance characteristics are determined both with respect to the amplitude (signal-to-noise ratio) and with respect to the frequency range where disturbances are present. If disturbances are present in a frequency range in which the process itself has hardly any dynamic contribution, then the noise signal can simply be filtered out of the measurement signals.

- Measurements with an exciting input signal meant for transient analysis. Typical signals here are steps and/or pulses. Typical information to be extracted from the data is e.g. the largest and smallest relevant frequencies and the static gain of the process, i.e. $G(z)|_{z=1}$, determining the response of the system to a constant input signal. Moreover one can use these experiments in order to finally decide which input and output signals are going to be considered. If the resulting model is going to be used for control design, it is desirable that the input signals that are going to be used as control inputs are able to reduce the effect of disturbances on the outputs, both with respect to amplitude and frequency range. This will guide the choice for appropriate control input signals.

  Additionally it can be verified whether and to which extent (amplitude) the process dynamics can be considered to be linear. Apart from possible physical restrictions one generally will be in favour of applying an input signal with a maximum achievable power, in order to increase the signal-to-noise ratio at the output. Considering a possible excitation of non-linear dynamics, the amplitude of the input signal may have to be restricted, as mentioned before.

  A possible test signal that can be used for determination of static nonlinearities is the so-called staircase-signal, as depicted in figure 8.4. The length of every step in the signal is chosen in such a way that the process response has more or less reached its static value. Next to indications on relevant frequencies and static gain, this experiment can provide an estimate of a static nonlinearity. To this end the static responses $\{(u_1, y_1), (u_2, y_2), \cdots\}$ are used to estimate a polynomial-fit on these characteristics.

- Measurements with an exciting input signal meant for correlation and frequency analysis. Typical input signals are sinus, white noise, PRBS (discussed later). These experiments can be performed to obtain a more accurate indication of the process dynamics and the frequency range of interest. They can also be used to determine
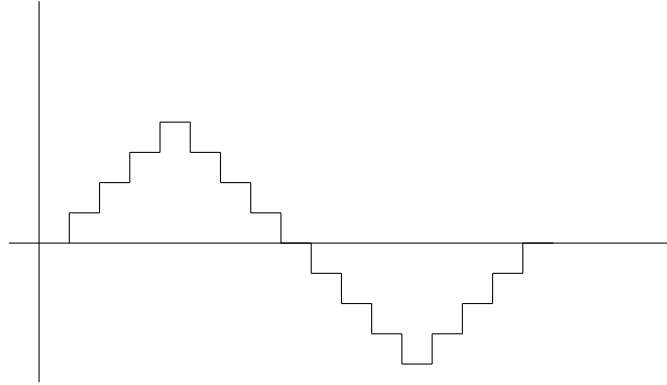
Figure 8.4: Staircase input signal.

the design variables for the final (parametric) identification experiment, as e.g. the length of the experiment, the type of signal chosen, the sample frequency etc., and to determine possible time-delays in the process.

The question whether all the experiments mentioned can indeed be performed is strongly determined by the type of process and the costs that are related to experimentation. When modelling mechanical servo systems as e.g. robots and optical drives, we generally observe compact set-ups, fast (high-frequency) dynamics, and generally it will be easily possible to extensively experiment with the process. Experiments will generally be "cheap". However looking at processes in the (chemical) process industry, the situation is completely different. Industrial production processes often have time-constants of the order of hours/days, which requires extremely long experiments in order to obtain a data set that is sufficiently long for accurate identification. Moreover these experiments will generally be rather expensive, e.g. due to loss of production capacity. In those situations it may be necessary to reduce the number of experiments to a minimum and to compress a number of steps discussed above.

8.3.2 Input design

In identification experiments generally use is made of input signals that are broad-banded, i.e. that have a spectrum that covers a wide frequency range. This generally guarantees that the signals are sufficiently exciting, and that the measured data contains information on the system to be modelled over a sufficiently wide frequency range. Besides discrete-time white noise, having a flat frequency spectrum, there are a few alternatives having comparable properties and even a number of additional advantages.

Random binary signal (RBS)
Let $\{w(t)\}$ be a stochastic white noise process, then

$$u(t) = c \cdot \text{sign}[w(t)]$$

is a binary signal that satisfies

$$R_u(\tau) \;=\; c^2 \quad \tau = 0 \tag{8.7}$$
$$\;=\; 0 \quad \tau \neq 0 \tag{8.8}$$

and consequently

$$\Phi_u(\omega) = c^2 \qquad -\pi < \omega < \pi.$$

Therefore the signal u has the spectral properties of white noise, but at the same time it is a binary signal assuming values $\pm c$. There are two additional attractive properties of this signal:

- u is bounded in amplitude. This is a very favorable property in view of the possible excitation of nonlinear dynamics in the process. If the process is assumed to be operating in an operational condition around which a linearization can be made under the restriction of an amplitude-bound, this amplitude-bound can be used as a constraint on the input signal. Moreover the amplitude of physical actuators may be restricted by the physical configuration (e.g. a valve can open only between fixed limits).

- u is binary, and therefore it has maximum signal power under an amplitude bound constraint. This is advantageous as one may expect that the accuracy of the model estimates will improve when the input power is increased, thus creating a higher signal-to-noise ratio at the output.

The first point mentioned is of course also shared by a uniform distributed white noise process (and not by a Gaussian white noise!). However the second property is typical for a binary signal. A typical such RBS signal is sketched in Figure 8.5(a).
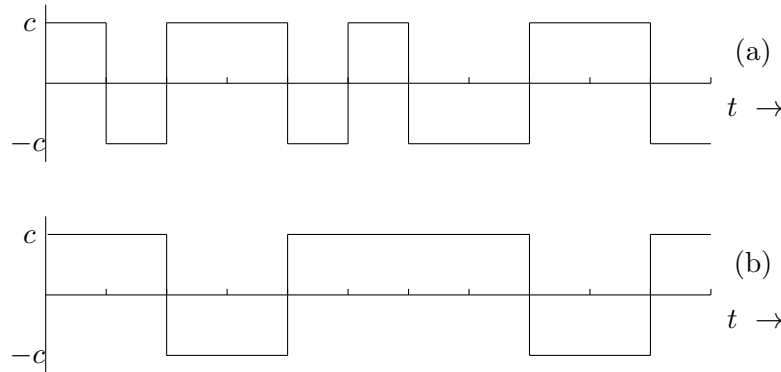
Figure 8.5: (a) Typical RBS with clock period equal to sampling interval ($N_c = 1$); (b) RBS with increased clock period $N_c = 2$.

Spectrum shaping by increase of clock-period
The RBS signal u will always have a flat spectrum. If one wishes to influence this spectrum, e.g. by amplifying particular frequency components, then a general linear filter can be applied. However in this way both the binary character and the amplitude bound of the signal are lost. An alternative for influencing the frequency content of the signal, while retaining these properties is by changing the clock-period of the signal. Instead of allowing the input signal to change sign every sample time, the input signal can be kept constant for $N_c > 1$ multiples of the sample interval. This is formalized by

$$u(int(t/N_c)) \qquad t = 0, 1, \cdots$$

where $int(t/N_c)$ is the largest integer that is smaller than or equal to t/N_c. An example of a RBS with $N_c = 2$ is given in Figure 8.5(b).
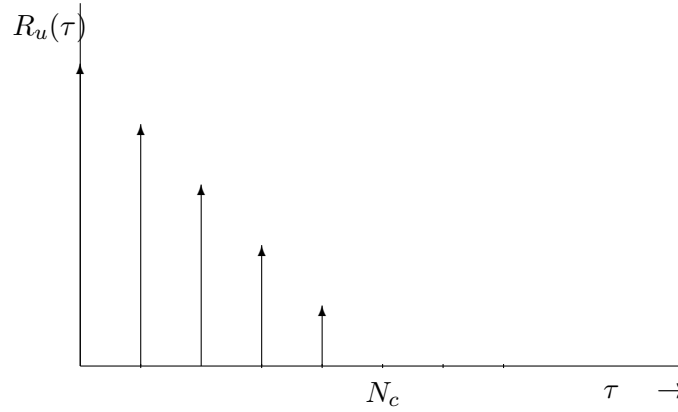
Figure 8.6: Covariance function of $u(t)$ as defined in (8.9), having a basic clock period of N_c sampling intervals.

The increase of the clock-period has a particular influence on the spectral properties of the signal, as formulated in the next Proposition, a proof of which is added in the appendix.

Proposition 8.3.1 *The RBS signal*

$$u(t) = c \cdot sign[w(int(t/N_c))] \tag{8.9}$$

with $\{w\}$ a white noise process, satisfies

$$
\begin{aligned}
R_u(\tau) &= \frac{N_c - \tau}{N_c}, \quad 0 \leq \tau \leq N_c \\
&= 0 \qquad\qquad \tau \geq N_c
\end{aligned}
\tag{8.10}
$$

and

$$\Phi_u(\omega) = \frac{1}{N_c} \frac{1 - cos(\omega N_c)}{1 - cos\omega}. \tag{8.11}$$

The covariance function of the signal $u(t)$ in this proposition is sketched in figure 8.6.

The expression for the spectrum $\Phi_u(\omega)$ is obtained by realizing that the covariance function $R_u(\tau)$ can equivalently be obtained by filtering a white noise process by the linear filter

$$F(q) = \frac{1}{\sqrt{N_c}}(1 + q^{-1} + q^{-2} + \cdots + q^{-N_c}) = \frac{1}{\sqrt{N_c}} \frac{1 - q^{-N_c}}{1 - q^{-1}} \tag{8.12}$$

In figure 8.7 the spectrum $\Phi_u(\omega)$ is sketched for a number of different values of N_c. It can clearly be verified that for increasing N_c there is a shift of signal power to the low-frequent part. From a flat signal spectrum for $N_c = 1$ (white noise property) a shift is made to a low frequent signal for $N_c > 1$, resulting in a signal for $N_c = 10$ that has negligible power in the higher frequencies.

Remark 8.3.2 *Note that $\Phi_u(\omega) = 0$ for $\omega = \frac{2\pi k}{N_c}$, $k = 1, .., int(N_c/2)$. This means that the spectrum has an increasing number of zero-crossings with increasing value of N_c. It is straightforward that one has to be careful with spectrum inversion at those frequency points, e.g. when using nonparametric (or very high order) identification.*
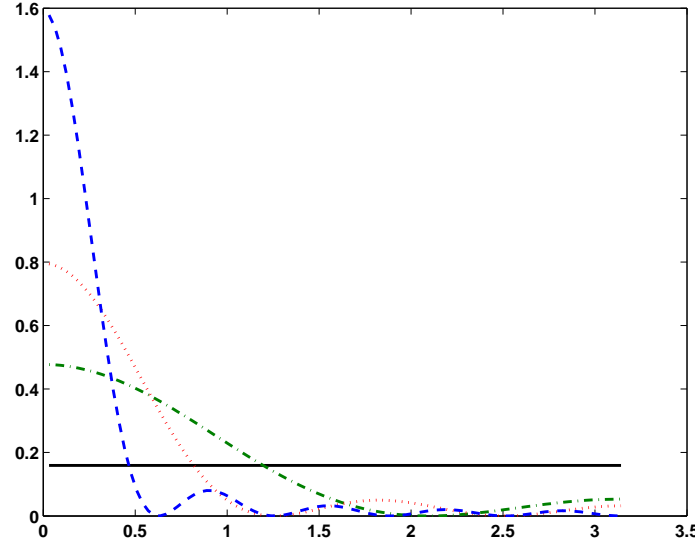
Figure 8.7: Spectrum $\frac{1}{2\pi}\Phi_u(\omega)$ of RBS with basic clock period $N_c = 1$ (solid), $N_c = 3$ (dash-dotted), $N_c = 5$ (dotted), and $N_c = 10$ (dashed).

Remark 8.3.3 *The effect on the spectral density that is obtained by changing the clock period of the RBS to a multiple of the sampling interval can of course also be obtained by filtering the RBS through a linear low-pass filter. However, a particular advantage of using the clock period mechanism here is that the resulting signal remains to be amplitude bounded. As mentioned before this has advantages both from a viewpoint of avoiding the excitation of nonlinear system dynamics and from a viewpoint of avoiding actuator wearing.*

As an alternative to the sign-function that is essentially used in the construction of the random binary signals considered here, there is also an option for constructing the binary signal through a deterministic mechanism of shift-registers leading to so-called pseudo-random binary signals (PRBS). This mechanism is explained in the appendix.

Besides the option of influencing the signal spectrum with a change of clock-period there are also some other alternatives:

1. Consider the random binary signal

$$u(t) = c \operatorname{sign}[R(q)w(t)] \tag{8.13}$$

   where $\{w(t)\}$ a stochastic white noise process, and $R(q)$ a stable linear filter that can be used by the experimenter to influence the spectral density of $\{u(t)\}$. The choice $R(q) = 1$ is equivalent to the situation considered before.

2. Consider the random binary signal $u(t)$ with values $\pm c$, determined by $Pr(u(t) = u(t-1)) = p$, and $Pr(u(t) = -u(t-1)) = 1 - p$, with p the non-switching probability, $(0 < p < 1)$. With $p = 1/2$ this signal has comparable properties as the previously mentioned RBS with $R(q) \equiv 0$. Choosing $p \neq 1/2$ gives the possibility to influence the spectral density of the signal. This RBS is analyzed in Tulleken (1990), where it is shown that

- $R_u(\tau) = c^2(2p-1)^\tau;$ and

- $\Phi_u(\omega) = \dfrac{1-q^2}{1+q^2-2q\cos(\omega)};$ with $q = 2p-1.$

A sketch of the spectral density of $u(t)$ for several values of p is given in figure 8.8.

Note that these spectra do not have the zero crossings as are present in an (P)RBS with extended clock period. This is considered an advantage of this probabilistic way of influencing the signal spectrum. Note that for non-switching probabilities > 0.5, the low-frequent behaviour of the signals is emphasized; for $p < 0.5$ it also possible to construct spectral densities with high-frequency emphasis.
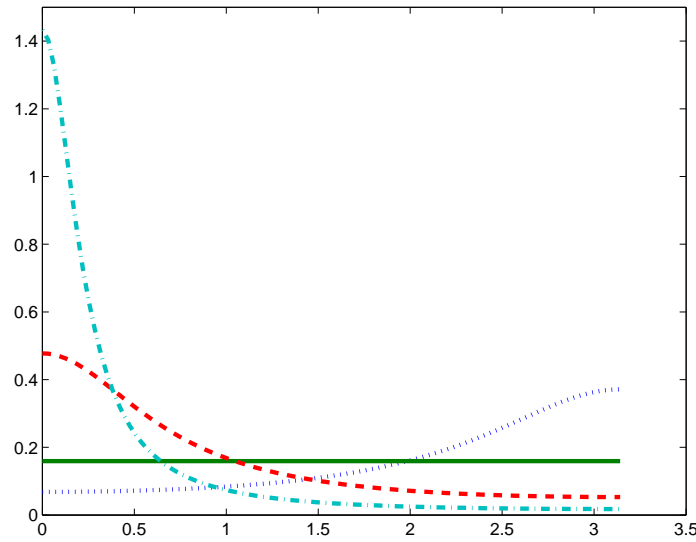
Figure 8.8: Spectrum $\frac{1}{2\pi}\Phi_u(\omega)$ for RBS with non-switching probabilities $p = 0.5$ (solid),$p = 0.75$ (dashed), $p = 0.90$ (dash-dotted) and $p = 0.3$ (dotted).

Periodic excitation - multisinusoidal input
In stead of distributing the input power over a relatively wide range of frequencies, one can also choose to concentrate it in a relatively small number of frequency points. This can be done by using a periodic input, e.g. in the form of a multisinusoidal input signal:

$$u(t) = \sum_{k=1}^{r} \alpha_k sin(\omega_k t + \phi_k)$$

with $\{\omega_k\}_{k=1,\cdots r}$ a user-chosen set of frequencies in the interval $[0, \pi)$.
This kind of periodic excitation is beneficial in e.g. nonparametric model identification as discussed in chapter 3, and in situations that accurate knowledge of the plant is required in a limited number of frequencies. It goes without saying that with this excitation no information is obtained of plant behaviour outside the frequencies that are contained in the input signal.
The choice of phase components $\{\phi_k\}_{k=1,\cdots r}$ can be made so as to minimize the time-domain amplitude of the input signal. This construction of signals is known as Schroeder-phased

sinusoids. However also a construction with randomly phased sinusoidal components is often applied. Multisines can also be constructed with minimum crest-factor, defined by

$$\mathrm{CF}(u) = \frac{\|u\|_\infty}{\|u\|_2}$$

i.e. the ratio of infinity-norm and 2-norm of the signal. For more information on general input design the reader is referred to Pintelon and Schoukens (2001) and Godfrey (1993). The random binary signal (8.13) is studied in Schoukens et a. (1995).

In case we consider consistency of the identified models as an achievable goal, that can be reached by choosing the correct model structure, the input signal can be chosen as to minimize some measure on the variance of the parameter estimates. This is the problem of optimal input, or experiment, design, and has been given wide attention in the literature, see e.g. Goodwin and Payne (1977). However in many practical situations the user can hardly assume that the true process is linear and of finite order. Identification must then be considered as a method of model approximation, in which the identified model will be dependent on the experimental conditions. A general advice then is to let the input have its major energy in the frequency band that is of interest for the intended application of the model.

8.3.3 Sampling frequency

The procedure of sampling the data that are produced by the system is inherent in computer-based data-acquisition systems. It is unavoidable that sampling as such leads to information losses, and it is important to select the sampling instances so that these losses are insignificant. In this section we shall assume that the sampling is carried out with equidistant sampling instants, and we shall discuss the choice of the sampling frequency ω_s or equivalently the sampling interval $T_s = \frac{2\pi}{\omega_s}$.

Discussing the problem of how to choose the sampling frequency, we have to distinguish two different situations:

(a) The sampling frequency during data-acquisition, and

(b) The sampling frequency that is used in the identification procedure, being equal to the sampling frequency for which the discrete-time model is built.

During data-acquisition the principal problem is to gather as much information as possible from the basically continuous-time signals into the discrete-time - sampled - signals. If the total time of experimentation ($T_N = N \cdot T_s$) is fixed, and there is no limitation on the number of data samples that can be processed, it is favorable to choose the sampling interval T_s as small as possible, i.e. to gather as much information as possible into the sampled signals. The higher the sampling frequency (the smaller the sampling interval), the less information is lost during the sampling-procedure.
If the number of data points N that one can collect is fixed, the choice for a specific sampling interval is coupled with the choice of the total experimentation time T_N. In this situation choosing a very small T_s will imply a very short period of experimentation, and will limit the information content in the signals. Due to the restricted experimentation time, disturbances will have a relatively large influence and information on the low-frequency dynamics in the

process will hardly be contained in the data set. A value of T_s that is larger than the essential time-constants of the process (corresponding to a sampling frequency ω_s that is smaller than the smallest relevant frequency), would lead to sampled signals that can not contain appropriate information on the relevant dynamics in the process. In this case an appropriate choice of T_s will have to be a trade-off between disturbance reduction and the incorporation of information on the relevant process dynamics. A general rule-of-thumb for the lower bound on the total experimentation time T_N is given by $5 - 10$-times the largest relevant time-constant in the process, where this time-constant is determined as $1/\omega$ with ω the smallest frequency of interest.

The question whether -for a given sampling interval- information on specific process dynamics is present in the sampled signals can be answered by employing the Theorem of Shannon. This states that a sampled signal with sampling frequency ω_s can exactly reproduce a continuous-time signal provided that the continuous-time signal is band-limited, i.e. it has no frequency content for frequencies $\omega \geq \omega_s/2$. This is visualized in the expression for the Fourier transform of $u_d(k) := u(kT_s)$:

$$U_d(\omega) = \frac{1}{T_s} \sum_{k=-\infty}^{\infty} U_c(\omega - \frac{2\pi k}{T_s}) \tag{8.14}$$

where U_c is the Fourier transform of the underlying continuous-time signal. If the continuous-time signal does not satisfy the restriction that $U_c(\omega) = 0$ for $\omega \geq \omega_s/2 = \frac{\pi}{T_s}$, then reproducing the signal $u_c(t)$ from its sampled version $u_d(k)$ leads to a distortion where the frequency components in the original continuous time signal with frequencies $\omega > \omega_s/2$ appear as low-frequent contributions in the reconstructed signal. This effect which is called frequency-folding or *aliasing* has to be prevented by taking care of the fact that all continuous signals that are being sampled are first band-limited through an operation of linear filtering through a (continuous-time) anti-aliasing filter. This anti-aliasing filter has to remove all frequency components in the continuous-time signal with frequencies $\omega \geq \omega_s/2$. In order to reduce this effect of aliasing, a rule-of thumb for the upper bound of the sampling interval is often given by:

$$\omega_s \geq 10 \cdot \omega_b \tag{8.15}$$

with ω_b the bandwidth[1] of the process. For a first-order system having $\omega_b = 1/\tau$ this rule of thumb can also be rewritten as

$$T_s \leq \frac{\tau_{set,95}}{5} \tag{8.16}$$

with $\tau_{set,95}$ the 95%-settling time of the step response of the process ($\tau_{set,95} \sim 3\tau$ for a first order process).

When we are going to construct discrete-time models additional arguments play a role when choosing for a specific sampling interval. The first one is the aspect of numerical accuracy and sensitivity. Consider a continuous-time system having a state-space description with state matrix A_c. If we apply a continuous-time signal that is piecewise constant between the sampling instants, we can formulate a discrete-time system relation leading to sampled output signals at the sampling instants. It can simply be verified that the (discrete-time) system that produces the correct sampled output signal, has a discrete-time state-space

---

[1]The bandwidth is defined as the maximum frequency ω for which the magnitude of the frequency function reaches the level of $1/\sqrt{2}$ times its static value.

description with state matrix $A_d = e^{A_c T_s}$. If T_s approaches 0 then A_d will approach the identity matrix, and consequently all poles of the discrete-time system will cluster around the point 1. This causes numerical difficulties. The difference equations related to the models now describe relations between sample values that are so close that they hardly vary within the range of the order of the difference equation.

Another implication of choosing a small sampling interval is related to the principle of the prediction error identification methods that we have discussed. The error criterion that is involved is determined by the one-step-ahead prediction error of models. As the sampling interval decreases, this one-step-ahead interval becomes smaller. The result is that the model fit may be concentrated to the high-frequency range. This can be illustrated by considering the asymptotic bias expression:

$$\theta^* \;=\; \arg\min_{\theta \in \Theta} \int_{-\pi/T_s}^{\pi/T_s} |G_0(e^{i\omega T_s}) - G(e^{i\omega T_s}, \theta)|^2 Q(\omega, \theta) d\omega \qquad (8.17)$$

$$Q(\omega, \theta) \;=\; \Phi_u(\omega)/|H(e^{i\omega T_s}, \theta)|^2 \qquad (8.18)$$

where we have incorporated the T_s-dependence. As T_s tends to zero, the frequency range over which the integral is taken increases. Generally the contribution of the difference $|G_0(e^{i\omega T_s}) - G(e^{i\omega T_s}, \theta)|$ will become smaller as ω increases, due to a roll-off in the transfer functions. However in situations where the noise model is coupled to the dynamics in $G(e^{i\omega T_s}, \theta)$, as is the case for an ARX model structure, then the product

$$\frac{|G_0(e^{i\omega T_s}) - G(e^{i\omega T_s}, \theta)|^2}{|H(e^{i\omega T_s}, \theta)|^2}$$

does not tend to zero as ω increases. Consequently the model fit is pushed into very high frequency bands as T_s decreases. Examples of this effect are given in Wahlberg and Ljung (1986).

The sampling interval for which we build the model should be the same as for the application in which the model will be used. Åström and Wittenmark (1984) have shown that a fast sampled model will often be non-minimum phase, and a system with dead time may be modelled with delay of many sampling periods. Such effects may cause problems if the models are going to be used for control design, and therefore will have to influence the choice of T_s.

A rule of thumb for limiting the sample frequency used in identification and model applications is sometimes given by:

$$\omega_s \leq 30 \cdot \omega_b \qquad (8.19)$$

With similar notation as before this is equivalent with

$$T_s \geq \frac{\tau_{set,95}}{15}. \qquad (8.20)$$

Note however that the rules-of-thumb (8.16) and (8.20) have to be applied with care, as they are principally based on the assumption of first order dynamics. For higher order systems they have to be used with great care.

The fact that there are different arguments for choosing sampling frequencies for data-acquisition and for identification and model application motivates the strategy that during

data-acquisition one uses a sample frequency that is as high as possible. All kinds of data processing operations can then be performed on this highly sampled signal. Before the data is really used for identification of parametric models one then reduces the sample frequency by digitally prefiltering and decimation to a level that is motivated from a point of view of model application. This strategy is suggested e.g. in Ljung (1987) and Backx and Damen (1989).

8.3.4 Processing of data

In this section we will briefly discuss a number of data-processing operations that have to be considered when preparing measured data sequences for use in identification algorithms. For a more extensive discussion the reader is referred to Söderström and Stoica (1989), Backx and Damen (1989) and Ljung (1987), while similar aspects are also discussed in Zhu and Backx (1993).

Anti-aliasing filters
It has been mentioned already in the previous subsection 8.3.3 that continuous-time signals have to be filtered to become band-limited, in order to achieve that the resulting sampled signals uniquely represent the continuous-time signal, and in order to avoid that the discrete-time signal is distorted in the low frequency region by high frequency components of the original continuous-time signal.
Output signals always need to be anti-aliasing-filtered by an analog (continuous-time) filter. The bandwidth of this filter is limited by the Nyquist frequency $\omega_s/2$. The result of this filter has to be that in the pass-band ($\omega < \omega_s/2$), the signals are not distorted in both amplitude and phase. For high frequencies the amplification has to show a fast roll-off. Apart from preventing aliasing, also a noise filtering is performed for high-frequency disturbances. This can improve the resulting signal-to-noise ratio.
The answer to the question whether also input signals have to be filtered through an anti-aliasing filter, is dependent on the specific situation. If data is obtained from the process under normal operating conditions, the (continuous-time) input signal to the process will generally not be piecewise constant between the sampling instants. If this input signal is not band-limited, it will have to be filtered to avoid aliasing. If the input signal is piecewise constant between sampling instants, the sampled signal will be determined by these (piecewise) constant values of the signal. The continuous-time signal will be uniquely determined by the sampled signal. In that case the input signal will generally not be filtered. Note that there still exist high-frequency components in this signal. By choosing the sampling frequency high enough in relation to the bandwidth of the process, the effect of these high-frequency components can generally be neglected.

Outliers / spikes
Extreme values of signals that have occurred during the experiments have to be removed from the data sequences. In practice such outliers or spikes are often caused by sensor errors, or other external disturbances. Because of the fact that these outliers show large amplitudes, they can have a huge influence on the identification algorithms. Note that when using quadratic error criteria these outliers influence the identification criterion through their quadratic value. Outliers are generally determined by visual inspection of the data, and possibly also of the prediction error signal. They are removed "by hand" and the missing signal values are reconstructed by interpolation from the neighboring samples through a linear interpolation filter.

Nonzero means and drifts in disturbances

Measured signals often show low-frequent drifts or nonzero (sample) means. They typically stem from external sources that we may or may not prefer to include in the modelling. In many situations it is impossible to circumvent these effects during open-loop experiments and are these phenomena that will be controlled by a controller to be designed. However drift or nonzero-mean in data may have a bad effect on identification results if they are not specifically accounted for. Note that these low-frequent contributions will not be averaged out and consequently they can not be modelled as uncorrelated noise on the output.

There are several ways to deal with these effects:

- Removing the effects by pretreatment of the data; or

- Explicitly estimating the effects.

Nonzero means and drifts can be removed from the data by filter operations. Removing of nonzero means can be done by correcting the signals by subtracting the present static values or an estimate thereof, in the sense of their sample means $\bar{u} = \frac{1}{N}\sum_{t=1}^{N} u(t)$, $\bar{y} = \frac{1}{N}\sum_{t=1}^{N} y(t)$. Standard identification methods are then applied to the corrected data $(u(t) - \bar{u}, y(t) - \bar{y})$. Similarly slowly varying disturbances can be removed from the data by high-pass filtering of the signals. In order to avoid the introduction of phase-shifts during this filtering, use can be made of symmetrical non-causal filters that operate off-line on the data sequence.

There are several ways of estimating trends in data and of incorporating these effects in the models to be estimated, as e.g. using noise models with integration which is equivalent with differencing the data. For more details the reader is referred to Ljung (1987) and Söderström and Stoica (1989).

Scaling of signals

Input and output signals of physical processes will generally have numerical values that are expressed in different units and different ranges, dependent on the fact whether we deal with *mbar*'s, *cm*'s, *sec*'s etc. In order to arrive at normalized transfer functions, signals are scaled in such a way that they exhibit an equal power with respect to their numerical values. For multivariable systems this scaling problem becomes even more pronounced, as different signal amplitudes then automatically lead to a different weighting of the signals in the prediction error criterion. In other words: signals with larger numerical values will then dominate over signals with smaller numerical values.

Compensation of time-delays

Information from previous experiments concerning possible time-delays present in the process, can now be used to compensate the data for these time-delays by shifting input and output signals with respect to each other. As a result the time-delays do not have to be parametrized in the identification procedure. Note that in multivariable systems with m inputs and p outputs generically $m + p - 1$ time delays can be corrected for in this way, while the maximum number of time delays present is equal to the number of scalar transfers, i.e. $p \times m$. Only for $m = 1$ or $p = 1$ all possible occurring time-delays can be corrected by shifting the signals.

Decimation

In addition to the discussion concerning the choice of sampling frequency, post-processing of the signals may contain a step of further reduction of the sampling frequency, called

decimation. In this final step the sampling frequency is realized that is desired from a viewpoint of discrete-time model description and model application. This reduction of sampling frequency or enlargement of the sampling interval again has to be preceded by an anti-aliasing filter which in this case is a discrete-time filter. Note that properties of input signals that are of importance from an identification point of view (see sections 8.2, 8.3) are formulated for a sampling frequency as is obtained after this decimation step. If a PRBS is used as input signal, and in view of the identification procedure one requires a constant input spectrum, then the clock period of the PRBS will have to be chosen equal to the sampling interval *after* decimation.

8.4 The use of prior knowledge in parameter estimation

8.4.1 Introduction

The identification procedures discussed so far only deal with black-box type of model sets, in which all parameters are allowed to vary freely over some parameter set. However in particular situations there may be more specific information available on the dynamical system that is to be identified. E.g. in physical processes it may be known on beforehand that the static gain of the process has some -known- value, which can be based on knowledge of first principle relations of the process, or based on previous experiments. In the identification of a linear model, and particularly if this identification is approximative, it can be very relevant to force the static gain of the identified model to this a priori known value. In nonlinear optimization procedures these kind of constraints can always be incorporated, however generally leading to ad-hoc tailor-made type of optimization algorithms only directed towards one particular situation. In the next subsection a solution for this problem is shown to exist in quite a simple form for the specific class of model structures that are linear-in-the-parameters.

8.4.2 Linear model structures with linear constraints

When applying a least squares identification criterion to a model structure that is linear-in-the-parameters as shown in section 4.6, the parameter estimate $\hat{\theta}_N$ is obtained by solving the following equation for the derivative of the criterion function:

$$\left.\frac{\partial V_N(\theta, Z^N)}{\partial \theta}\right|_{\theta=\hat{\theta}_N} = 0 \tag{8.21}$$

where the derivative is given by

$$\frac{\partial V_N(\theta, Z^N)}{\partial \theta} = f_N - R_N \theta \tag{8.22}$$

with the appropriate notation as defined in (4.43),(4.44).
When minimizing the least-squares identification criterion under an additional linear constraint, this can simply be incorporated into the algorithm by using the technique of Lagrange.

Imposing a priori knowledge on static gain.

When the input-output model $G(q, \theta)$ is parametrized according to

$$G(q, \theta) = \frac{b_0 + b_1 q^{-1} + \cdots + b_{n_b} q^{-n_b}}{1 + a_1 q^{-1} + \cdots + a_{n_a} q^{-n_a}} \qquad (8.23)$$

and one would like to impose the static gain $s_\infty := G(z)|_{z=1}$ of this model, this can be done by incorporating the restriction

$$\frac{b_0 + b_1 + \cdots + b_{n_b}}{1 + a_1 + \cdots + a_{n_a}} = s_\infty \qquad (8.24)$$

or equivalently:

$$w(\theta) = 0 \qquad (8.25)$$

with

$$\begin{aligned}
w(\theta) &= b_0 + b_1 + \cdots + b_{n_b} - s_\infty[1 + a_1 + \cdots + a_{n_a}] & (8.26) \\
&= \gamma^T \cdot \theta - s_\infty & (8.27)
\end{aligned}$$

where $\gamma^T = [-s_\infty \ -s_\infty \cdots -s_\infty \mid 1\ 1 \cdots\ 1]$.

Minimization of $V_N(\theta, Z^N)$ under the constraint $w(\theta) = 0$ is now obtained by:

$$\hat{\theta}_N = \arg_\theta \min_{\theta, \lambda}[V_N(\theta, Z^N) + \lambda w(\theta)]. \qquad (8.28)$$

Setting the derivative of the extended criterion to 0 then provides:

$$\begin{aligned}
\frac{\partial V_N(\theta, Z^N)}{\partial \theta} + \lambda\gamma &= 0 & (8.29) \\
w(\theta) &= 0 & (8.30)
\end{aligned}$$

which two equations have to be satisfied by $\hat{\theta}_N$ and $\hat{\lambda}$. This shows that the parameter estimate is obtained by solving

$$\begin{bmatrix} R_N & \gamma \\ \gamma^T & 0 \end{bmatrix} \begin{bmatrix} \hat{\theta}_N \\ \hat{\lambda} \end{bmatrix} = \begin{bmatrix} f_N \\ s_\infty \end{bmatrix}. \qquad (8.31)$$

By applying the matrix inversion lemma (Appendix B) it follows that

$$\begin{aligned}
\hat{\theta}_N &= R_N^{-1}\left\{I - \gamma[\gamma^T R_N^{-1}\gamma]^{-1}\gamma^T R_N^{-1}\right\} f_N + \\
&\quad + R_N^{-1}\left\{\gamma[\gamma^T R_N^{-1}\gamma]^{-1} s_\infty\right\} \\
&= R_N^{-1} f_N + R_N^{-1}\gamma[\gamma^T R_N^{-1}\gamma]^{-1}[s_\infty - \gamma^T R_N^{-1} f_N]. \qquad (8.32)
\end{aligned}$$

The parameter estimate for the constrained problem, can directly be calculated, without requiring a complex optimization procedure. This is induced by the fact that the constraint - as also the model structure - is linear in the parameters.

Note that in the above expression for $\hat{\theta}_N$, the unconstrained least-squares estimate $R_N^{-1} f_N$ appears explicitly in the right hand side of the expression.

For well-definedness of the constrained least-squares problem, it is necessary that the set of equations (8.31) remains uniquely solvable. This is guaranteed by requiring that $\gamma^T R_N^{-1}\gamma \neq 0$.

Constrained least-squares identification by restricting the static gain of the model has been discussed also in Inouye and Kojima (1990).

Imposing a priori knowledge on the frequency response.

The same mechanism as applied above can be used for imposing restrictions on the frequency response of the model in any user-chosen set of frequencies. Restricting the static gain refers to the specific situation of choosing frequency $\omega = 0$.
One can also force a set of r constraints:

$$\begin{bmatrix} G(e^{i\omega_1}, \hat{\theta}_N) \\ \vdots \\ G(e^{i\omega_r}, \hat{\theta}_N) \end{bmatrix} = \begin{bmatrix} g_1 \\ \vdots \\ g_r \end{bmatrix} =: g. \tag{8.33}$$

Then by following the same analysis as before, the constrained least-squares estimate will be determined by

$$\begin{bmatrix} R_N & \gamma \\ \gamma^T & 0 \end{bmatrix} \begin{bmatrix} \hat{\theta}_N \\ \hat{\lambda} \end{bmatrix} = \begin{bmatrix} f_N \\ g \end{bmatrix}, \tag{8.34}$$

where λ now is an r-vector of Lagrange multipliers, and γ a $(n_a + n_b + 1) \times r$ matrix given by

$$\gamma = \begin{bmatrix} -g_1 e^{-i\omega_1} & \cdots & -g_r e^{-i\omega_r} \\ \vdots & \vdots & \vdots \\ -g_1 e^{-in_a\omega_1} & \cdots & -g_r e^{-in_a\omega_r} \\ 1 & \cdots & 1 \\ e^{-i\omega_1} & \cdots & e^{-i\omega_r} \\ \vdots & \vdots & \vdots \\ e^{-in_b\omega_1} & \cdots & e^{-in_b\omega_r} \end{bmatrix} \tag{8.35}$$

The parameter estimate is given by

$$\hat{\theta}_N = R_N^{-1} f_N + R_N^{-1} \gamma [\gamma^T R_N^{-1} \gamma]^{-1} [g - \gamma^T R_N^{-1} f_N]. \tag{8.36}$$

Well-definedness of this parameter estimate is again restricted to the situation that the matrix $\gamma^T R_N^{-1} \gamma$ is nonsingular. The dimension of this square matrix is equal to the number of constraints r that has been imposed. It is intuitively clear that whenever the number of constraints becomes too large, they can not be met anymore by the restricted complexity model. Singularity of the matrix will definitely occur whenever the number of constraints r exceeds the number of parameters to be estimated. In that situation γ becomes a "fatt" matrix, and singularity of $\gamma^T R_N^{-1} \gamma$ is obvious.

8.5   Relevant Matlab commands

Input signal construction

```
[u] = IDINPUT (N,TYPE,BAND,LEVELS)
```
The command `idinput` generates an input signal as a random Gaussian signal, a random binary signal, a pseudo-random binary signal (PRBS) or a sum of sinusoids.

Data preprocessing

```
[ZD] = DETREND (Z)
```

removes means and/or linear trends from a data set.

```
[ZF] = IDFILT (Z,N,Wn)
```

allows to filter a data set low-pass, high-pass or band-pass filters.

```
[ZD] = IDRESAMP (Z,R)
[ZD] = DECIMATE (Z,R)
```

allow to resample a data set by decimation and interpolation.

Appendix

PRBS signals

Definition 8A.1 *PRBS.*
Let x be a binary state vector, $x(t) \in \{0,1\}^n$ for $t \in \mathbb{Z}_+$, $n > 1$, with a given initial value $x(0) \neq 0$, and let $a \in \{0,1\}^n$. Consider the binary signal $s(t)$ defined by the following algorithm:

$$s(t) = x_n(t) \tag{8A.1}$$

$$x_i(t+1) = x_{i-1}(t), \quad 2 \leq i \leq n \tag{8A.2}$$

$$x_1(t+1) = a_1 x_1(t) \oplus a_2 x_2(t) \oplus \cdots \oplus a_n x_n(t) \tag{8A.3}$$

with $\oplus$ modulo-2 addition; then $s(t)$ is called a pseudo-random binary signal (PRBS). □

Note that the modulo-2 addition satisfies: $0 \oplus 0 = 1 \oplus 1 = 0$, and $0 \oplus 1 = 1 \oplus 0 = 1$.
A PRBS is a binary signal that can be generated by a shift register of order n and a feedback loop, as indicated in figure 8.9. The register states $x_1 \cdots x_n$ are initiated on 0 or 1. Every initial state $x(0)$ is allowed except for $x = 0$. With the appearance of a clock-pulse, the value of state x_k is copied into state x_{k+1}, and a new value for the state x_1 is constructed via the feedback loop. The coefficients $a_1, \cdots a_n$ are also binary. This signal can be generated through a simple algorithm.
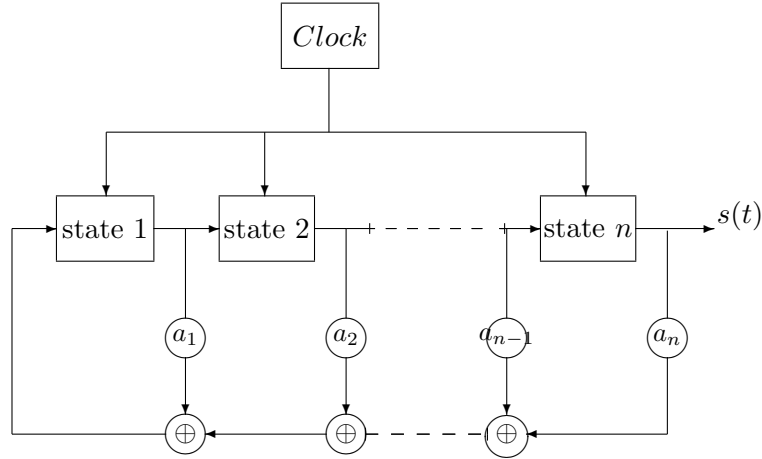
Figure 8.9: Shift register with modulo-2 feedback loop.

The shift register will generate a binary signal. This is a deterministic sequence: given the initial state and the coefficient vector a, all future states are completely determined.
It can simply be understood that such a PRBS is a periodic signal. The shift register has a finite number of states, and each state uniquely determines all future states. The period-length of the signal is an important property of the PRBS. This leads to the definition of a special classes of PRBSs.

Definition 8A.2 *Maximum length PRBS.*
Consider a pseudo-random binary signal constructed with a shift register of n states. Then the signal is called a maximum length PRBS if it is periodic with period $M = 2^n - 1$. □

The period length $M = 2^n - 1$ is the maximum period that is possible for such a signal. Note that the term -1 is caused by the fact that the $0 - state$ ($x = 0$) should be circumvented, since this state forces all future states to be equal to 0.

It will be discussed later on that a maximum length PRBS has properties that resemble the properties of a white noise signal. First we briefly consider the question under which conditions a PRBS becomes a maximum length PRBS. Apparently the properties of a PRBS are completely determined by the dimension n of the state (register) vector, and by the coefficient vector a that determines the feedback path.

Now let us denote

$$A(q^{-1}) = 1 \oplus a_1 q^{-1} \oplus a_2 q^{-2} \oplus \cdots \oplus a_n q^{-n} \tag{8A.4}$$

The PRBS $s(t)$ generated as in definition 8A.1 obeys the following homogeneous equation:

$$A(q^{-1})s(t) = 0 \tag{8A.5}$$

This can be understood by realizing that $s(t) = x_n(t) = x_{n-j}(t - j)$ for $j = 1, \cdots, (n - 1)$. As a result

$$
\begin{aligned}
A(q^{-1})s(t) &= x_n(t) \oplus a_1 x_n(t - 1) \oplus \cdots \oplus a_n x_n(t - n) & (8A.6) \\
&= x_1(t - n + 1) \oplus a_1 x_1(t - n) \oplus \cdots \oplus a_n x(t - n) & (8A.7) \\
&= 0 & (8A.8)
\end{aligned}
$$

where the latter equality follows from the fact that $x_1(t - n + 1)$ equals $a_1 x_1(t - n) \oplus \cdots \oplus a_n x(t - n)$ by definition. The problem to study now is the choice of the feedback coefficients a_i such that the equation (8A.5) has no solution $s(t)$ with period smaller than $2^n - 1$. A necessary and sufficient condition on $A(q^{-1})$ for this property to hold is provided in the following proposition.

Proposition 8A.3 *The homogeneous recursive relation* (8A.5) *has only solutions of period* $2^n - 1$ *(i.e. the corresponding PRBS is a maximum length PRBS) if and only if the following two conditions are satisfied:*

- *The binary polynomial $A(q^{-1})$ is irreducible, i.e. there do not exist any two polynomials $A_1(q^{-1})$ and $A_2(q^{-1})$ with binary coefficients such that $A(q^{-1}) = A_1(q^{-1})A_2(q^{-1})$ and $A_1, A_2 \neq A$;*

- *$A(q^{-1})$ is a factor of $1 \oplus q^{-M}$ but is not a factor of $1 \oplus q^{-p}$ for any $p < M = 2^n - 1$.*

For the proof of this proposition the reader is referred to Davies (1970) or Söderström and Stoica (1989). This result has led to the construction of tables of polynomials satisfying the conditions of the proposition. Examples are: for $n = 3 : a_1 = 1$, $a_3 = 1$; for $n = 6 : a_1 = 1$, $a_6 = 1$; for $n = 10 : a_3 = 1$, $a_{10} = 1$. Here all coefficients that are not mentioned should be chosen 0.

A maximum length PRBS has properties that are similar to the properties of a discrete-time white noise sequence. This will be formulated in the next proposition. However since we are generally interested in signals that vary around 0, rather than signals that vary between 0 and 1, we can simply transform the PRBS to

$$u(t) = c[-1 + 2s(t)] \tag{8A.9}$$

with $s(t)$ a maximum length PRBS as discussed before. The binary signal $u(t)$ will vary between the two values $-c$ and $+c$.

Proposition 8A.4 *(Davies, 1970). Let $u(t)$ be a maximum length PRBS according to* (8A.9) *and definition 8A.2, with period M. Then*

$$\bar{E}u(t) = \frac{c}{M} \tag{8A.10}$$

$$R_u(0) = (1 - \frac{1}{M^2})c^2 \tag{8A.11}$$

$$R_u(\tau) = -\frac{c^2}{M}(1 + \frac{1}{M}), \quad \tau = 1, \cdots, M-1 \tag{8A.12}$$

$\square$

The covariance function of a PRBS is sketched in figure 8.10.
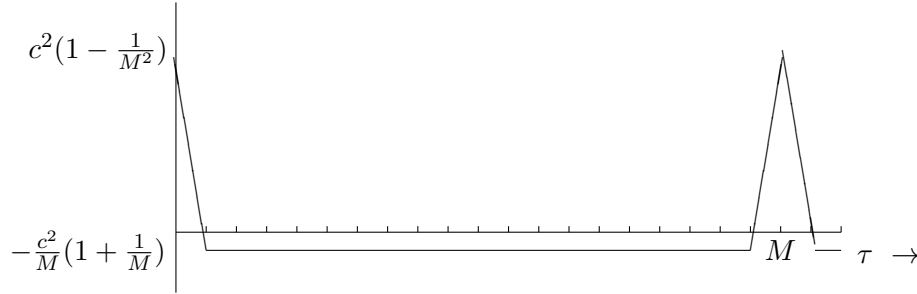
Figure 8.10: Covariance function of a maximum length PRBS.

Note that for $M \to \infty$ the covariance function of $u(t)$ resembles that of white noise with variance c^2. Due to their easy generation and their convenient properties the maximum length PRBSs have been used widely in system identification. The PRBS resembles white noise as far as the spectral properties are concerned. Influecing the signal spectrum by changing the clock-period, as described for RBS signals, can similarly be applied to the PRBS signals.

Proof of Proposition 8.3.1
Denote the white noise process: $e(t) := sign(w(t))$. Then $u(t) = e(int(t/N_c))$.
Since $\{e(t)\}$ is a white process it follows that $R_u(\tau) = 0$, $\tau \geq N_c$.
We now restrict attention to $0 \leq \tau \leq N_c - 1$.

$$R_u(\tau) = \bar{E}u(t+\tau)u(t) = \lim_{N \to \infty} \frac{1}{N} \sum_{t=0}^{N-1} E\ u(t+\tau)u(t). \tag{8A.13}$$

Suppose $N = N_c p$, then we can write

$$R_u(\tau) = \lim_{p \to \infty} \frac{1}{N_c p} \sum_{t=0}^{N_c p - 1} E\ u(t+\tau)u(t) \tag{8A.14}$$

With $t = N_c s + m$, m and s integer, this yields:

$$
\begin{aligned}
R_u(\tau) &= \lim_{p\to\infty} \frac{1}{N_c p} \sum_{s=0}^{p-1} \sum_{m=0}^{N_c-1} E\, u(N_c s + m + \tau)u(N_c s + m) \\
&= \frac{1}{N_c} \sum_{m=0}^{N_c-1} \lim_{p\to\infty} \frac{1}{p} \sum_{s=0}^{p-1} E\, e(s + int(\frac{m+\tau}{N_c}))e(s + int(\frac{m}{N_c})) \\
&= \frac{1}{N_c} \sum_{m=0}^{N_c-1} \lim_{p\to\infty} \frac{1}{p} \sum_{s=0}^{p-1} E\, e(s + int(\frac{m+\tau}{N_c}))e(s) \\
&= \frac{1}{N_c} \sum_{m=0}^{N_c-1} \bar{E}\, e(s + int(\frac{m+\tau}{N_c}))e(s) \\
&= \frac{1}{N_c} \sum_{m=0}^{N_c-\tau-1} Ee(s)^2 + \frac{1}{N_c} \sum_{m=N_c-\tau}^{N_c-1} \bar{E}e(s+1)e(s) \\
&= \frac{1}{N_c}\,(N_c - \tau) = \frac{N_c - \tau}{N_c}.
\end{aligned}
$$

A signal with the same covariance function can be obtained by filtering a white noise process $\{e(t)\}$ through a linear filter:

$$w(t) = F(q)e(t) \tag{8A.15}$$

with

$$F(q) = \frac{1}{\sqrt{N_c}}(1 + q^{-1} + q^{-2} + \cdots + q^{-N_c}) = \frac{1}{\sqrt{N_c}}\frac{1 - q^{-N_c}}{1 - q^{-1}}. \tag{8A.16}$$

Note that $R_w(\tau) = \bar{E}\sum_{j=0}^{\infty} f(j)e(t-j)\sum_{k=0}^{\infty} f(k)e(t-k)$ with $f(j) = 1/\sqrt{N_c}$ for $0 \le j \le N_c - 1$ and 0 elsewhere. Consequently $R_w(\tau) = \sum_{j=0}^{\infty} f(j)f(j-\tau) = \sum_{j=\tau}^{N_c} f(j)f(j-\tau)$ which can simple be shown to coincide with $R_u(\tau)$. As a result $\Phi_u(\omega) = F(e^{i\omega})F(e^{-i\omega})$ which equals

$$\frac{1}{N_c}\frac{(1 - e^{-i\omega N_c})(1 - e^{i\omega N_c})}{(1 - e^{-i\omega})(1 - e^{i\omega})} \tag{8A.17}$$

which is equivalent to the expression in the proposition.

Bibliography

K.J. Åström and B. Wittenmark (1984). *Computer Controlled Systems*. Prentice-Hall, Englewood Cliffs, NJ.

A.C.P.M. Backx and A.A.H. Damen (1989). Identification of industrial MIMO processes for fixed controllers. *Journal A, vol. 30*, no. 1, pp. 3-12.

W.D.T. Davies (1970). *System Identification for Self-Adaptive Control*. Wiley-Interscience, New York.

M. Gevers (1993). Towards a joint design of identification and control? In: H.L. Trentelman and J.C. Willems (Eds.), *Essays on Control: Perspectives in the Theory and its Applications*. Proc. 1993 European Control Conference, Groningen, The Netherlands, Birkhäuser, Boston, pp. 111-151.

K. Godfrey (Ed.) (1993). *Perturbation Signals for System Identification*. Prentice Hall, Hemel Hempstead, UK.

G.C. Goodwin and R.L. Payne (1977). *Dynamic System Identification - Experiment Design and Data Analysis*. Academic Press, New York.

Y. Inouye and T. Kojima (1990). Approximation of linear systems under the constraint of steady state values of the step responses. In: M.A. Kaashoek *et al.* (Eds.), *Realization and Modelling in System Theory*. Proc. Intern. Symposium MTNS-89, Volume 1, pp. 395-402. Birkhäuser Boston Inc., Boston.

L. Ljung (1987). *System Identification - Theory for the User*. Prentice-Hall, Englewood Cliffs, NJ.

R. Pintelon and J. Schoukens (2001). *System Identification - A Frequency Domain Approach*. IEEE Press, Piscataway, NJ, USA, ISBN 0-7803-6000-1.

J. Schoukens, P. Guillaume and R. Pintelon (1995). Generating piecewise-constant excitations with an arbitrary power spectrum. *IEE Proc. Control Theory Appl.*, Vol. 142, no. 3, pp. 241-252.

R.J.P. Schrama (1992). *Approximate Identification and Control Design*. Dr. Dissertation, Delft Univ. Technology.

H.J.A.F. Tulleken (1990). Generalized binary noise test-signal concept for improved identification experiment design. *Automatica*, vol. 26, no. 1, pp. 37-49.

P.M.J. Van den Hof and R.J.P. Schrama (1995). Identification and control - closed loop issues. *Automatica*, vol. 31, pp. 1751-1770.

B. Wahlberg and L. Ljung (1986). Design variables for bias distribution in transfer function estimation. *IEEE Trans. Automat. Contr., AC-31*, pp. 134-144.

Y. Zhu and T. Backx (1993). *Identification of Multivariable Industrial Processes*, Springer Verlag, Berlin.

Chapter 9

Realization theory and subspace identification method

9.1 Introduction

In the problem of identifying dynamical models on the basis of experimental data, there has been made a historic distinction between two different approaches. Initially this distinction was completely based on the type of experimental signals that were assumed available:

- measured pulse responses (transients), or

- general input/output measurements

of a dynamical system.

The most general (second) situation has led to the development of the class of prediction error identification methods, which has been extensively treated in Chapter 4.

The situation of availability of transient signals, like pulse responses, of a dynamical process has been handled classically by a different approach, called minimal or approximate realization. In this approach a state space model is obtained directly from the measured signals. Moreover, this estimate is obtained with techniques that result from realization theory and that rely on numerical linear algebra operations, rather than on criterion optimization techniques.

In a later extension, approximate realization techniques have also been generalized to handle general input/output types of signals, rather than only transient signals like pulse responses. This approach, called *subspace identification* is attracting an increasing attention, not in the least because of the relative simplicity of handling multivariable (multi-input, multi-output) identification problems.

In this chapter, we will first discuss the construction of models on the basis of transient signals. To this end the (exact) realization algorithm will be presented in Section 9.2.1. This algorithm underlies the methods that apply to noise disturbed data, leading to the approximate realization algorithm, discussed in Section 9.3.

Subspace identification will be discussed in Section 9.4.

9.2   Minimal realization of Markov parameters

9.2.1   The Ho/Kalman algorithm for infinite length sequences

The problem that is addressed in this section is: given the pulse response

$$\{g(t)\}_{t=0,\cdots,\infty} \tag{9.1}$$

of a finite-dimensional linear time-invariant discrete-time dynamical system $G(z)$, construct a minimal state space model of the system, in the form

$$
\begin{aligned}
x(t+1) &= Ax(t) + Bu(t); \quad x(0); \tag{9.2}\\
y(t) &= Cx(t) + Du(t). \tag{9.3}
\end{aligned}
$$

This problem actually is not an identification type of problem. It represents the transformation of one model (pulse response) into another model (state-space form), where the two models are required to be equivalent, in the sense that they reflect the same transfer function $G(z)$.

As the methods to be discussed are not not limited to scalar systems, we will directly handle the multivariable situation of m inputs and p outputs, so that $u(t) \in \mathbb{R}^m$, $y(t) \in \mathbb{R}^p$, $g(t) \in \mathbb{R}^{p\times m}$, $G \in \mathbb{R}^{p\times m}(z)$, and the state space matrices: $A \in \mathbb{R}^{n\times n}$, $B \in \mathbb{R}^{n\times m}$, $C \in \mathbb{R}^{p\times n}$ and $D \in \mathbb{R}^{p\times m}$, where n is the *state dimension*.

In this multivariable situation the sequence $\{g(t)\}$ can actually not be thought of as the output of the system to one single excitation signal. Column number j in $g(t)$ reflects the response of p output signals, to a pulse signal applied to input number j at time $t=0$. So actually m experiments have to be performed in order to construct the sequence $\{g(t)\}_{t=0,\cdots\infty}$. This sequence is denoted as the sequence of *Markov parameters* of the multivariable system $G(z)$.

The two representations (9.1) and (9.2),(9.3) relate to the corresponding transfer function according to:

$$G(z) = \sum_{t=0}^{\infty} g(t)z^{-t} \tag{9.4}$$

and

$$G(z) = D + C(zI - A)^{-1}B, \tag{9.5}$$

and by applying pulse input signals to (9.2) it follows that the sequence of Markov parameters satisfies

$$g(t) = \begin{cases} CA^{t-1}B & t \geq 1 \\ D & t = 0 \end{cases} \tag{9.6}$$

A state space model (A, B, C, D) is called a *realization* of $G(z)$ if it satisfies (9.5), and it is called *minimal* if it additionally has a minimal state dimension n.

Definition 9.2.1 (McMillan degree) *The McMillan degree of the dynamical system $G(z)$ is defined as the state dimension of any minimal realization of $G(z)$.*

When equating the two representations (9.4) and (9.5) two statements can be made directly:

- The initial state $x(0)$ (9.2) does not play any role in the problem. This is caused by the fact that model equivalence in considered in terms of transfer functions, and a transfer function only reflects the dynamic system response of systems that are initially at rest $(x(0) = 0)$.

- Equating (9.4) and (9.6) shows that the relation

$$D = g(0)$$

is immediate, and so the problem of constructing the matrix D can be separated from the construction of (A, B, C).

The procedure to construct a minimal state space model from a sequence of Markov parameters is due to Ho and Kalman (1966), and is based on operations on the matrix

$$\mathsf{H}_{n_r, n_c}(G) = \begin{bmatrix} g(1) & g(2) & \cdots & \cdots & g(n_c) \\ g(2) & g(3) & g(4) & \cdots & \vdots \\ g(3) & g(4) & g(5) & \cdots & \vdots \\ \vdots & \vdots & \vdots & \vdots & \vdots \\ g(n_r) & \cdots & \cdots & \cdots & g(n_r + n_c - 1) \end{bmatrix}, \tag{9.7}$$

which is referred as the (block) Hankel matrix of pulse response samples. A Hankel matrix is characterized by the property that elements on the skew diagonals are the same.
The Hankel matrix (9.7) exhibits two important properties:

1. If $G(z)$ has a realization (A, B, C, D), then

$$\mathsf{H}_{n_r, n_c}(G) = \Gamma_{o,n_r}(C, A) \cdot \Gamma_{c,n_c}(A, B) \tag{9.8}$$

   with

$$\Gamma_{o,n_r}(C, A) = \begin{bmatrix} C \\ CA \\ \vdots \\ CA^{n_r-1} \end{bmatrix}, \tag{9.9}$$

$$\Gamma_{c,n_c}(A, B) = \begin{bmatrix} B & AB & \cdots & A^{n_c-1}B \end{bmatrix}. \tag{9.10}$$

   Note that if A has dimension $n \times n$, then the matrix $\Gamma_{o,n}(C, A)$ is known as the observability matrix and $\Gamma_{c,n}(A, B)$ as the controllability[1] matrix of the state space model (A, B, C, D).

   Equation (9.8) directly follows from substituting (9.6) into the Hankel matrix (9.7).

2. For sufficiently large n_r, n_c the rank of the Hankel matrix satisfies

$$rank\ \mathsf{H}_{n_r, n_c}(G) = n \tag{9.11}$$

   where n is the McMillan degree of $G(z)$.

---

[1] In stead of controllability matrix, this matrix is often referred to as the reachability matrix, see e.g. Kailath (1980).

This property can be verified by noting that if (A, B, C, D) is a minimal realization of $G(z)$ with dimension n, then the corresponding observability and controllability matrices will have rank n. Sylvester's inequality (B.1) then shows that the Hankel matrix, being the product of these two matrices, will have the same rank, i.e. rank $\mathsf{H}_{n,n}(G) = n$. If this Hankel matrix is increased in row and column dimension, its rank will not increase, due to the fact that for any n-dimensional state space model there exist scalar constants $\{a_1, \cdots, a_n\}$ such that for any $j \geq 0$:

$$CA^{n+j}B = -a_1 CA^{n-1+j}B - a_2 CA^{n-2+j}B - \cdots - a_n CA^j B. \qquad (9.12)$$

This last property follows from the Cayley-Hamilton theorem C.2. It shows that from the $n+1$-st block row and block column of H, every block row (or column) can be written as a linear combination of the previous n block rows (or columns). Thus the rank of H will not increase with increasing dimensions.

In order to construct a minimal state space realization on the basis of a sequence of Markov parameters, one can now proceed as follows.

Suppose we have given a Hankel matrix of sufficiently large dimensions such that (9.11) holds true. Then for any (full rank) matrix decomposition

$$\mathsf{H}_{n_r,n_c}(G) = H_1 \cdot H_2 \qquad (9.13)$$

with $H_1 \in \mathbb{R}^{n_r p \times n}$ and $H_2 \in \mathbb{R}^{n \times n_c m}$ satisfying

$$rank\ H_1 = rank\ H_2 = rank\ \mathsf{H}_{n_r,n_c}(G) = n \qquad (9.14)$$

there exist matrices A, B, C from an n-dimensional state space model, such that

$$\begin{aligned} H_1 &= \Gamma_{o,n_r}(C, A) \quad \text{and} \qquad &(9.15) \\ H_2 &= \Gamma_{c,n_c}(A, B). \qquad &(9.16) \end{aligned}$$

These matrices (A, B, C) can be constructed as follows:

- When given $H_1 = \Gamma_{o,n_r}(C, A)$, i.e.

$$H_1 = \begin{bmatrix} C \\ CA \\ \vdots \\ CA^{n_r - 1} \end{bmatrix}, \qquad (9.17)$$

  the matrix C can be extracted by taking the first p rows of the matrix;

- When given $H_2 = \Gamma_{o,n_r}(C, A)$, i.e.

$$H_2 = \begin{bmatrix} B\ AB\ \cdots\ A^{n_c - 1}B \end{bmatrix}, \qquad (9.18)$$

  the matrix B can be extracted by taking the first m columns of the matrix.

- The matrix A can be isolated by using the shifted Hankel matrix:

$$
\overleftarrow{\mathsf{H}}_{n_r,n_c}(G) := \begin{bmatrix} g(2) & g(3) & \cdots & \cdots & g(n_c+1) \\ g(3) & g(4) & g(5) & \cdots & \vdots \\ g(4) & g(5) & g(6) & \cdots & \vdots \\ \vdots & \vdots & \vdots & \vdots & \vdots \\ g(n_r+1) & \cdots & \cdots & \cdots & g(n_r+n_c) \end{bmatrix}, \tag{9.19}
$$

which is simply obtained from the original Hankel matrix, by shifting the matrix one block column to the left, or equivalently one block row upwards.

Using the expression (9.6) for $g(t)$, it can directly be verified that with H_1 and H_2 satisfying (9.17) and (9.18), the shifted Hankel matrix can be written as:

$$
\overleftarrow{\mathsf{H}} = H_1 \cdot A \cdot H_2 \tag{9.20}
$$

where we have dropped subscripts and arguments to simplify notation. Note that this shifted Hankel matrix also can be constructed simply on the basis of available Markov parameters $\{g(2)\cdots g(n_r+n_c)\}$.

Because H_1 and H_2 have full column (resp. row-) rank, it follows that there exist matrices H_1^+, H_2^+ such that

$$
H_1^+ H_1 = H_2 H_2^+ = I_n. \tag{9.21}
$$

H_1^+ is referred to as the left pseudo-inverse of H_1, and H_2^+ as the right pseudo-inverse of H_2, and I_n the $n \times n$ identity matrix. Note that H_1 and H_2 do not have any (regular) inverses because they are not square matrices. The pseudo-inverses are determined as:

$$
\begin{aligned}
H_1^+ &= (H_1^T H_1)^{-1} H_1^T \quad \text{and} \tag{9.22} \\
H_2^+ &= H_2^T (H_2 H_2^T)^{-1} \tag{9.23}
\end{aligned}
$$

which can be verified to satisfy (9.21).

As a consequence the matrix A can be found by appropriate pre- and postmultiplication of (9.20), leading to

$$
H_1^+ \cdot \overleftarrow{\mathsf{H}} \cdot H_2^+ = A. \tag{9.24}
$$

Summarizing, the matrices B and C follow directly from a full rank decomposition of the Hankel matrix. The matrix A is constructed on the basis of a shifted Hankel matrix.
A reliable numerical procedure for either the full rank decomposition of H and for the construction of the pseudo-inverses H_1^+ and H_2^+ is the *singular value decomposition* (see Definition B.1). An SVD provides a decomposition

$$
\mathsf{H} = U_n \Sigma_n V_n^T \tag{9.25}
$$

where U_n and V_n are unitary matrices, i.e. $U_n^T U_n = I_n$ and $V_n^T V_n = I_n$, and Σ_n is a diagonal matrix with positive entries $\sigma_1 \geq \cdots \geq \sigma_s$, referred to as the singular values.

The choice

$$H_1 = U_n \Sigma_n^{\frac{1}{2}} \tag{9.26}$$

$$H_2 = \Sigma_n^{\frac{1}{2}} V_n^T \tag{9.27}$$

directly leads to:

$$H_1^+ = \Sigma_n^{-\frac{1}{2}} U_n^T \tag{9.28}$$

$$H_2^+ = V_n \Sigma_n^{-\frac{1}{2}} \tag{9.29}$$

and these matrices apparently satisfy the relations in (9.21).

Prior to the full rank decomposition of the Hankel matrix, the singular value decomposition also provides basic information concerning the rank of the matrix, and consequently reveals the required state space dimension of any minimal state space model. This is reflected by the fact that the rank of H is equal the rank of Σ_n which is equal to the number of singular values > 0.

The algorithm, known as Ho-Kalman algorithm, now reads as follows:

1. Construct a "large" Hankel matrix with row and column dimensions higher than the McMillan degree that one expects to be required.

2. Apply an SVD to this Hankel matrix to determine n, and construct U_n, Σ_n and V_n satisfying (9.25).

3. Construct H_1, H_2 according to (9.26), (9.27) and set

$$\Gamma_{o,n_r}(C, A) = H_1 \tag{9.30}$$

$$\Gamma_{c,n_c}(A, B) = H_2 \tag{9.31}$$

4. Construct C as the matrix determined by the first p rows of (9.30).

5. Construct B as the matrix determined by the first m columns of (9.31).

6. Construct the shifted Hankel matrix $\overleftarrow{\mathsf{H}}$ and determine A by

$$A = \Sigma_n^{-\frac{1}{2}} U_n^T \cdot \overleftarrow{\mathsf{H}} \cdot V_n \Sigma_n^{-\frac{1}{2}}. \tag{9.32}$$

7. Set $D = g(0)$.

The use of the singular value decomposition for the decomposition of the Hankel matrix was introduced in Zeiger and McEwen (1974).

The state space model that is obtained through this minimal realization algorithm does not exhibit a specific structure; generally all four matrices (A, B, C, D) will be filled with estimated coefficients. As it is known from linear systems theory that an m input - p output system with McMillan degree n can be represented by maximally $n(p+m)+pm$ coefficients (see e.g. Guidorzi (1981)), this has motivated work on minimal realization algorithms that provide state space models with specific (canonical) structures, as developed in Ackermann (1971) and Bonivento and Guidorzi (1971).

As mentioned above, the state space model provided by the Ho/Kalman algorithm does not exhibit an explicitly specified structure. However when observing the relations (9.26) and (9.27) it follows that the obtained realization will satisfy

$$\Gamma_o^T \Gamma_o = \Gamma_c \Gamma_c^T = \Sigma. \tag{9.33}$$

Note that

$$\Gamma_o^T \Gamma_o = \sum_{k=0}^{n_r-1} (A^T)^k C^T C A^k \quad \text{and} \tag{9.34}$$

$$\Gamma_c \Gamma_c^T = \sum_{k=0}^{n_c-1} A^k B B^T (A^T)^k. \tag{9.35}$$

If the underlying dynamical system is stable, the sums on the right hand side converge for $n_r, n_c \to \infty$ to

$$\sum_{k=0}^{\infty} (A^T)^k C^T C A^k = Q \tag{9.36}$$

$$\sum_{k=0}^{\infty} A^k B B^T (A^T)^k = P \tag{9.37}$$

where P is known as the *controllability Gramian* and Q as the *observability Gramian* of the state space model. Both Gramians can also be obtained directly from the state space model as the solutions to the Lyapunov equations

$$A^T Q A + C^T C = Q \tag{9.38}$$

$$A P A^T + B B^T = P. \tag{9.39}$$

For the state space model obtained by the Ho/Kalman algorithm, relation (9.33) holds true, which shows that when the row and column dimension of the Hankel matrix tends to infinity, the observability and controllability Gramian of the state space model will satisfy

$$P = Q = \Sigma, \tag{9.40}$$

with Σ a diagonal matrix. A realization satisfying this condition is called a *balanced realization*, a notion which is essentially introduced in Mullis and Roberts (1976) and further exploited also for model reduction procedures in Moore (1981). In a balanced realization the states have been transformed to such a form that every state is "as controllable as it is observable". Consequently the states can be order in terms of their contribution to the input-output properties of the dynamical system. Since its introduction, the notion of balanced realizations has been explored extensively in several areas of systems and control theory. For a more extensive handling of balanced realizations see e.g. Skelton (1988).

Example 9.2.2 Consider a pulse response sequence $g(0), g(1) \cdots$ given by

$$0, 1, 0.5, 0.25, 0.125, 0.0625, 0.03125, \cdots$$

As can be easily checked this reflects the pulse response of a first order system with one pole in $z = 0.5$. An exact minimal realization follows from applying the Ho/Kalman algorithm described in this section.

First a Hankel matrix is constructed that is sufficiently large:

$$\mathsf{H}_{3,3} = \begin{bmatrix} 1 & 0.5 & 0.25 \\ 0.5 & 0.25 & 0.125 \\ 0.25 & 0.125 & 0.0625 \end{bmatrix}. \tag{9.41}$$

The rank of this Hankel matrix is 1, as the second and third row (column) are obtained by simply multiplication of the previous row (column) by 0.5. As a result the state space dimension of any minimal realization will be equal to 1.

A full rank decomposition of this matrix can directly be written down as:

$$\mathsf{H}_{3,3} = \begin{bmatrix} 1 \\ 0.5 \\ 0.25 \end{bmatrix} \cdot [1 \ \ 0.5 \ \ 0.25]. \tag{9.42}$$

The B and C matrix are set equal to the first elements of the matrices in the decomposition: $B = 1$, $C = 1$. For the construction of A we need the shifted Hankel matrix:

$$\overleftarrow{\mathsf{H}}_{3,3} = \begin{bmatrix} 0.5 & 0.25 & 0.125 \\ 0.25 & 0.125 & 0.0625 \\ 0.125 & 0.0625 & 0.03125 \end{bmatrix}, \tag{9.43}$$

and the solution of A is obtained by solving the equation:

$$\begin{bmatrix} 0.5 & 0.25 & 0.125 \\ 0.25 & 0.125 & 0.0625 \\ 0.125 & 0.0625 & 0.03125 \end{bmatrix} = \begin{bmatrix} 1 \\ 0.5 \\ 0.25 \end{bmatrix} \cdot A \cdot [1 \ \ 0.5 \ \ 0.25]. \tag{9.44}$$

When premultiplying left and right hand side with $[1 \ 0 \ 0]$ and postmultiplying with $[1 \ 0 \ 0]^T$, the result follows: $A = 0.5$. Setting $D = g(0) = 0$ this delivers the solution:

$$(A, B, C, D) = (0.5, 1, 1, 0). \tag{9.45}$$

Note that we have constructed the full rank decomposition of $\mathsf{H}_{3,3}$ (9.42) by writing it down directly. Such a full rank decomposition is by far nonunique. E.g. we can multiply the first factor in (9.42) by a constant and at the same time divide the second factor by the same constant. In that case the realization that is found will be different, but the input/output properties in terms of its Markov parameters and transfer function will be the same.

In more complex situations it is not trivial how to write down a full rank decomposition. The "automated" procedure through SVD would in this example lead to:

$$\mathsf{H}_{3,3} = U\Sigma V^T \tag{9.46}$$

$$= \begin{bmatrix} 0.8729 & 0.0000 & 0.4880 \\ 0.4364 & -0.4472 & -0.7807 \\ 0.2182 & 0.8944 & -0.3904 \end{bmatrix} \cdot \begin{bmatrix} 1.3125 & 0 & 0 \\ 0 & 0 & 0 \\ 0 & 0 & 0 \end{bmatrix} \cdot \begin{bmatrix} 0.8729 & 0 & -0.4880 \\ 0.4364 & -0.4472 & 0.7807 \\ 0.2182 & 0.8944 & 0.3904 \end{bmatrix}^T,$$

or equivalently

$$\mathsf{H}_{3,3} = \begin{bmatrix} 0.8729 \\ 0.4364 \\ 0.2182 \end{bmatrix} 1.3125 \begin{bmatrix} 0.8729 & 0.4364 & 0.2182 \end{bmatrix}. \tag{9.47}$$

With this decomposition, the B and C matrices will be constructed as

$$B = C = 0.8729\sqrt{1.3125} = 1,$$

while the matrix A will be unchanged, according to the construction (9.32):

$$A = 1.3125^{-\frac{1}{2}} \begin{bmatrix} 0.8729 & 0.4364 & 0.2182 \end{bmatrix} \begin{bmatrix} 0.5 & 0.25 & 0.125 \\ 0.25 & 0.125 & 0.0625 \\ 0.125 & 0.0625 & 0.03125 \end{bmatrix} \begin{bmatrix} 0.8729 \\ 0.4364 \\ 0.2182 \end{bmatrix} 1.3125^{-\frac{1}{2}}$$

which can be verified to lead to $A = 0.5$.

9.2.2   Minimal realization of finite length sequences

In the previous subsection it has been shown that when there is an infinite sequence of Markov parameters available from a dynamical system with McMillan degree n, then only information concerning a finite portion of this sequence is required in order to reconstruct the underlying dynamical system exactly. The finite part that is used, is specified by the Markov parameters that are present in the Hankel matrix (9.7) and its shifted version (9.19).

In this subsection it will be specified in more detail what is the portion of an infinite sequence of Markov parameters that is required for its unique reconstruction in terms of the underlying dynamical system.

The realization problem restricted to finite length sequences is generally referred to as the *partial realization problem*, and the basic results are formulated by Tether (1970).

Proposition 9.2.3 *Let* $\{g(t)\}_{t=0,\cdots N}$ *be a given sequence of Markov parameters of a finite-dimensional dynamical system. Then the following two statements are equivalent:*

(a) *There exists a unique extension* $\{g(t)\}_{t=N+1,\cdots,\infty}$ *within the class of all extensions having a minimal McMillan degree;*

(b) *There exists values of* n_r, n_c *satisfying* $n_r + n_c = N$ *such that*

$$rank\ \mathsf{H}_{n_r+1,n_c} = rank\ \mathsf{H}_{n_r,n_c+1} = rank\ \mathsf{H}_{n_r,n_c}. \tag{9.48}$$

In words, the proposition states that for a finite sequence of Markov parameters we can construct very many extensions to infinity, leading to many different dynamical systems. Among all these systems we only look at the systems with minimal McMillan degree. In this class of systems with minimal McMillan degree there is exactly one unique element under the condition as formulated in part (b). This latter condition (b) implies that there exists some kind of linear dependency among the Markov parameters in the given finite sequence, as a result of which the rank condition can be satisfied. Part (b) states that when we have given a Hankel matrix composed of Markov parameters $\{g(t)\}_{t=0,\cdots,N-1}$, then the rank of this Hankel matrix does not increase if we extend the matrix with either one block

row or one block column. This reflects the "dependency" among the Markov parameters as meant above.

In the situation as formulated in the Proposition, the minimal McMillan degree of the system that matches the finite sequence of Markov parameters is equal to

$$rank\ \mathsf{H}_{n_r,n_c}.$$

This result follows directly from the fact that in the given situation the Ho/Kalman algorithm will provide a minimal realization of the finite sequence of Markov parameters, having a minimal state dimension equal to this rank.

Example 9.2.4 (Continuation of Example 9.2.2) In evaluating the consequences of the results presented here for the previous example 9.2.2 we have to find the minimal number N for which the condition (b) of Proposition 9.2.3 is satisfied. It can directly be verified that for our sequence

$$rank\ \mathsf{H}_{1,1} = rank\ \mathsf{H}_{2,1} = rank\ \mathsf{H}_{1,2} = 1. \tag{9.49}$$

As a result it follows that we could have applied the minimal realization algorithm on the basis of only the Markov parameters $g(0)$, $g(1)$ and $g(2)$, employing the Hankel matrices

$$\mathsf{H}_{1,1} = 1 \qquad \overleftarrow{\mathsf{H}}_{1,1} = 0.5. \tag{9.50}$$

A full rank decomposition of $\mathsf{H}_{1,1}$ is of course $1 \cdot 1$, leading to $C = B = 1$ and $A = 1 \cdot \overleftarrow{\mathsf{H}}_{1,1}$ $\cdot 1 = 0.5$.
This result is intuitively clear, as it actually states that a first order system is uniquely characterized by three coefficients. This is in correspondence with the parametrization of first order systems in terms of fractions of polynomials:

$$G(z) = \frac{b_0 + b_1 z^{-1}}{1 + a_1 z^{-1}} \tag{9.51}$$

where three coefficients represent the first order system.

9.3   Approximate realization of pulse and step response data

9.3.1   Introduction

Different from the situation of available "exact" Markov parameters of a dynamical system, is the situation that we have collected measurements on the system. In this case a sequence of nonexact or noise disturbed Markov parameters are available for modelling purposes. Alternatively we might have a finite sequence of Markov parameters available from correlation analysis as discussed in section 3.3. The related question then becomes whether we can extract the dynamics of the underlying system from these noisy measurements or nonexact estimates.
In these latter situations the finite sequence:

$$\{g(t)\}_{t=0,\cdots N} \tag{9.52}$$

will generally not be exactly related to the low-order dynamical system that underlies the Markov parameters.

For instance, suppose that this finite sequence reflects the measurement of pulse responses of a dynamical system with McMillan degree n; then through all kinds of (small) measurement errors, $g(t)$ will not be exactly equal to the Markov parameters of this n-dimensional system. Consequently, when constructing a Hankel matrix as discussed in section 9.2.2, the rank of this Hankel matrix will generically be equal to the smallest row/column dimension of the matrix; the dependency that is required to hold among the Markov parameters will not be present. As a result of this phenomenon, it will not be possible to construct an n-dimensional system that exactly matches the given finite sequence (9.52).

Several algorithms have been developed to deal with this situation. First we will discuss an algorithm that can be applied to (noise disturbed) pulse response data. With some modifications the algorithm can also be applied to step response data, and this is shown in section 9.3.3.

9.3.2 Approximate realization of pulse response data

The situation of noise disturbed Markov parameters can be handled with a few methods the most important of which is assigned to Kung (1978). It is based on a basic fact in linear algebra that any matrix can be approximated by a matrix of lower rank using singular value decomposition (see proposition B.2).

Suppose we have composed a Hankel matrix

$$\mathsf{H}_{n_r,n_c}$$

on the basis of the available Markov parameters, such that $n_r + n_c = N$. What we should need is an approximating (Hankel) matrix that matches the given Hankel matrix as closely as possible, and that has a rank that is smaller than $min\ (n_r, n_c)$. If this situation would be reached, then we could apply the standard Ho/Kalman algorithm again to the approximating matrix, and construct our realization.

This basic reasoning has led to the following approximate realization algorithm.

Approximate realization algorithm of Kung.

1. Given the finite sequence $\{g(t)\}_{t=1,\cdots N}$ construct a Hankel matrix H_{n_r,n_c} such that $n_r + n_c = N$.

2. Apply an SVD:
$$\mathsf{H}_{n_r,n_c} = U\Sigma V^T \tag{9.53}$$
and evaluate the singular values $\sigma_1 \cdots \sigma_{min(n_r,n_c)}$. Evaluate how the singular values decrease with growing index, and decide for a number n of singular values that are significant, and the remaining number of singular values that will be neglected.

3. Construct an approximating rank n matrix according to
$$\mathsf{H}(n) = U_n \Sigma_n V_n^T$$
by only retaining the significant singular values. Here $U_n = U \begin{bmatrix} I_n \\ 0 \end{bmatrix}$, $V_n = V \begin{bmatrix} I_n \\ 0 \end{bmatrix}$ and $\Sigma_n = \begin{bmatrix} I_n & 0 \end{bmatrix} \Sigma \begin{bmatrix} I_n \\ 0 \end{bmatrix}$.

4. Apply the Ho/Kalman algorithm to this matrix of reduced rank, i.e. construct the realization:

- Construct C from the first p rows of $U_n \Sigma_n^{\frac{1}{2}}$;
- Construct B from the first m columns of $\Sigma_n^{\frac{1}{2}} V_n^T$;
- Construct A according to

$$A = \Sigma_n^{-\frac{1}{2}} U_n^T \cdot \overset{\leftarrow}{\mathsf{H}} \cdot V_n \Sigma_n^{-\frac{1}{2}}. \tag{9.54}$$

where $\overset{\leftarrow}{\mathsf{H}}$ is the shifted Hankel matrix with original Markov parameters.

Actually this algorithm is a small variation to the method of Kung (1978), as discussed in Damen and Hajdasinski (1982). In the original method of Kung the matrix A is constructed from solving an equation based on shifted versions of the (reduced rank) controllability/observability matrices, rather than using the original Hankel matrix in a shifted version. The practical differences however are moderate.

The approximate realization algorithm contains two steps of approximation. The most obvious step is step number 3, where a rank reduction of the Hankel matrix is achieved. A second approximate step is somehow hidden in step number 4 too. This is due to the fact that the rank reduced matrix $\mathsf{H}(n)$ does not necessarily have a (block) Hankel structure. As a result of this, the matrices constructed in step 4 will not generate *exactly* the same Markov parameters as the elements of $\mathsf{H}(n)$.

Example 9.3.1 For illustrating the algorithm discussed in this section, we have constructed the pulse response sequence of the dynamical system G_0 as described in Example 3.4.1, and we have added an additive white noise disturbance to this response. Both exact and noise disturbed pulse response sequences are depicted in the upper left plot in figure 9.1. Based on the perturbed sequence of length 70, a Hankel matrix has been constructed, of which the singular values are examined in order to determine an appropriate order of the model. The singular values are shown in the upper right plot of the figure. The consequence of the noise disturbance is that all singular values will be unequal to 0. One has to make a decision now on what singular values are considered to be originating from the dynamical system, and which should be considered to be caused by the noise. From the singular value plot it seems appropriate to choose $n = 3$ as the principal underlying rank of the Hankel matrix, as the first three singular values are (much) larger than the following ones. As a result $n = 3$ is chosen for the order of the model to be constructed. The two lower plots in figure 9.1 show the pulse and step response of the third order model together with the responses of the system G_0.

The results show that a third order model is reasonably well able to capture the dynamics of the underlying system. However, it is of course not exact as it has a lower complexity (lower order) than the original system. The two modes of the system that have not been modelled, were more or less hidden in the noise disturbance on the pulse response.

9.3.3   Approximate realization of step response data

In a situation that measured step responses
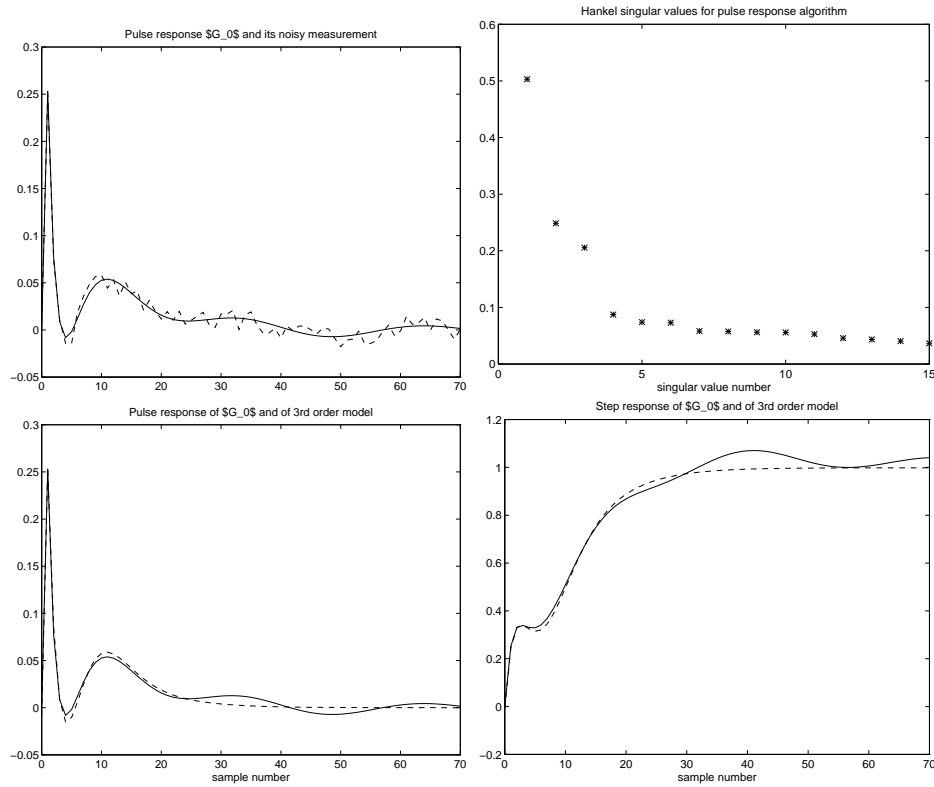
$$\{s(t)\}_{t=0,\cdots N} \tag{9.55}$$

Figure 9.1: Upper: left: Exact (solid) and noise disturbed (dashed) pulse response of G_0; right: Hankel singular values of $H_{35,35}$. Lower: left: pulse response of G_0 (solid) and of 3rd order model (dashed); right: step response of G_0 and of 3rd order model (dashed).

are available from a dynamical system (and this situation is practically very relevant e.g. in the situation of industrial production processes) it is advantageous to have the ability to construct an approximate model directly on the basis of these data.

A straightforward method could be to difference the step response data in order to arrive at pulse response data:

$$g(t) = s(t) - s(t-1), \tag{9.56}$$

and subsequently apply the realization methods from the previous section. However this is not attractive since the differencing operation (characterized by a transfer operation $(z-1)/z$) will introduce an amplification of high frequent noise on the measurement data.

As an alternative it is possible to directly use the step response data in an approximate realization method that this a slightly modified version of the methods discussed previously. This modification is due to Van Helmont *et al.* (1990).

As a starting point is taken that the basic ingredient of the Ho/Kalman algorithm is a full rank decomposition of the Hankel matrix (9.7) as shown in (9.13). If the original Hankel

matrix H_{n_r,n_c} is postmultiplied with a nonsingular $n_c m \times n_c m$ matrix T_{n_c} being given by

$$T_{n_c} = \begin{bmatrix} I_m & \cdots & \cdots & I_m \\ 0 & \ddots & & \vdots \\ \vdots & \ddots & \ddots & \vdots \\ 0 & \cdots & 0 & I_m \end{bmatrix} \tag{9.57}$$

then it follows that

$$R_{n_r,n_c} \;:=\; H_{n_r,n_c} T_{n_c} \tag{9.58}$$

$$= \begin{bmatrix} \sum\limits_{i=1}^{1} g(i) & \sum\limits_{i=1}^{2} g(i) & \cdots & \sum\limits_{i=1}^{n_c} g(i) \\ \sum\limits_{i=2}^{2} g(i) & \sum\limits_{i=2}^{3} g(i) & \cdots & \sum\limits_{i=2}^{n_c+1} g(i) \\ \sum\limits_{i=3}^{3} g(i) & \sum\limits_{i=3}^{4} g(i) & \cdots & \sum\limits_{i=3}^{n_c+2} g(i) \\ \vdots & \vdots & \vdots & \vdots \\ \sum\limits_{i=n_r}^{n_r} g(i) & \sum\limits_{i=n_r}^{n_r+1} g(i) & \cdots & \sum\limits_{i=n_r}^{n_r+n_c-1} g(i) \end{bmatrix} \tag{9.59}$$

$$= \begin{bmatrix} s(1)-s(0) & s(2)-s(0) & \cdots & \cdots & s(n_c)-s(0) \\ s(2)-s(1) & s(3)-s(1) & \cdots & \cdots & \vdots \\ s(3)-s(2) & s(4)-s(2) & \cdots & \cdots & \vdots \\ \vdots & \vdots & \vdots & \vdots & \vdots \\ s(n_r)-s(n_r-1) & \cdots & \cdots & \cdots & s(n_r+n_c-1)-s(n_r-1) \end{bmatrix} \tag{9.60}$$

and this latter matrix appears to be equal to

$$\begin{bmatrix} s(1) & s(2) & \cdots & s(n_c) \\ s(2) & s(3) & \cdots & \vdots \\ s(3) & s(4) & \cdots & \vdots \\ \vdots & \vdots & \vdots & \vdots \\ s(n_r) & \cdots & \cdots & s(n_r+n_c-1) \end{bmatrix} - \begin{bmatrix} s(0) & \cdots & s(0) \\ s(1) & \cdots & s(1) \\ \vdots & \vdots & \vdots \\ s(n_r-1) & \cdots & s(n_r-1) \end{bmatrix}. \tag{9.61}$$

Since R_{n_r,n_c} is obtained from H_{n_r,n_c} by postmultiplication of a (square) nonsingular matrix, it follows that both matrices share a lot of properties, as e.g. their rank. Moreover, because of the special structure of T_{n_c} it can also easily be verified that if we shift R_{n_r,n_c} over one block row upwards, dual to $\overleftarrow{H}_{n_r,n_c}$ in (9.19), then this shifted matrix satisfies:

$$R^{\uparrow}_{n_r,n_c} = \overleftarrow{H}_{n_r,n_c} \, T_{n_c}. \tag{9.62}$$

We can now make the following observation:

For any full rank matrix decomposition

$$\mathsf{R}_{n_r,n_c} = R_1 \cdot R_2 \tag{9.63}$$

the related decomposition of H_{n_r,n_c} is

$$\mathsf{H}_{n_r,n_c} = R_1 \cdot R_2 T^{-1}. \tag{9.64}$$

With (9.20) it follows that

$$\overleftarrow{\mathsf{H}}_{n_r,n_c} = R_1 \cdot A \cdot R_2 T^{-1} \tag{9.65}$$

or equivalently with (9.62)

$$\mathsf{R}^{\uparrow}_{n_r,n_c} = R_1 \cdot A \cdot R_2. \tag{9.66}$$

This implies that the basic properties that are owned by the Hankel matrix for the construction of a realization on the basis of pulse response data, are also owned by the matrix R for the construction of a realization on the basis of the matrix elements of R, being simple expressions of step response samples of the dynamical system.

We can now formulate the following (approximate) realization algorithm:

1. Given the finite sequence $\{s(t)\}_{t=1,\cdots N}$ construct the matrix R_{n_r,n_c} such that $n_r + n_c = N$.

2. Apply an SVD:
$$\mathsf{R}_{n_r,n_c} = U\Sigma V^T \tag{9.67}$$

   and evaluate the singular values $\sigma_1 \cdots \sigma_{min(n_r,n_c)}$. Evaluate how the singular values decrease with growing index, and decide for a number n of singular values that are significant, and the remaining number of singular values that will be neglected.

3. Construct an approximating rank n matrix according to

$$\mathsf{R}(n) = U_n \Sigma_n V_n^T$$

   by only retaining the significant singular values.

4. Construct the realization according to Ho/Kalman:

   - Construct C from the first p rows of $U\Sigma_n^{\frac{1}{2}}$;
   - Construct B from the first m columns of $\Sigma_n^{\frac{1}{2}}V^T$;
   - Construct A according to

$$A = \Sigma_n^{-\frac{1}{2}} U^T \cdot \mathsf{R}^{\uparrow} \cdot V\Sigma_n^{-\frac{1}{2}}. \tag{9.68}$$

Similar to the algorithm in the previous section, this algorithm also shows two approximation steps, both in step 3 and step 4.

The type of approximation that is performed here, can be quite different from the approximation in the pulse response approximate realization algorithm. This means that when constructing reduced order models, the pulse response realization may lead to models with different dynamics, than the models obtained by the step response realization algorithm. This difference is illustrated in example 9.3.2.

Example 9.3.2 In order to illustrate the difference in results between the pulse response based and the step response based algorithm, the two algorithms are applied to noise free pulse and step responses of the data generating system G_0 as also chosen in the previous example 9.3.1. Pulse and step response sequences were generated with a length of 70 samples. Figure 9.2 shows the singular values of $H_{35,35}$ and of $R_{35,35}$ in both linear and logarithmic scale.
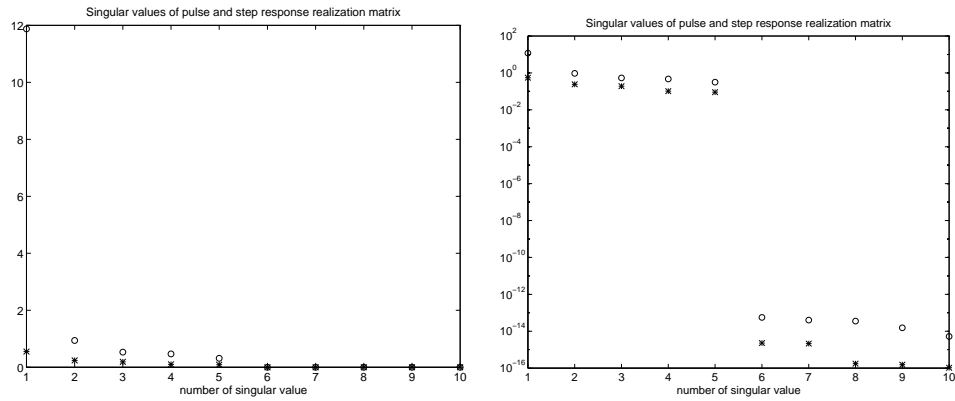

Figure 9.2: Singular values of pulse realization (Hankel) matrix $H_{35,35}$ ($*$) and of step realization matrix $R_{35,35}$ (o) in linear scale (left figure) and logarithmic scale (right figure).

As the system has order 5, only 5 singular values are essentially contributing. However it appears that the relation in magnitude among the first 5 singular values is quite different for the two different matrices.

In order to illustrate the approximation properties of the two different algorithms, figure 9.3 shows pulse responses and step responses of first and third order approximate models obtained by either of the two algorithms.

The results of the third order models (lower plot in figure 9.3 show that the pulse response algorithm leads to far better results than the step response algorithm. This is particularly due to the fact that the high-frequent response of the system is present more dominant in the pulse response than in the step response of the system. The results for the first order models (upper plots) show that the low frequent behaviour is better retained by the step response algorithm. A similar observation can be made here: the low frequent behaviour of the system is present more dominant in the step response of the system than in its (finite time) pulse response.
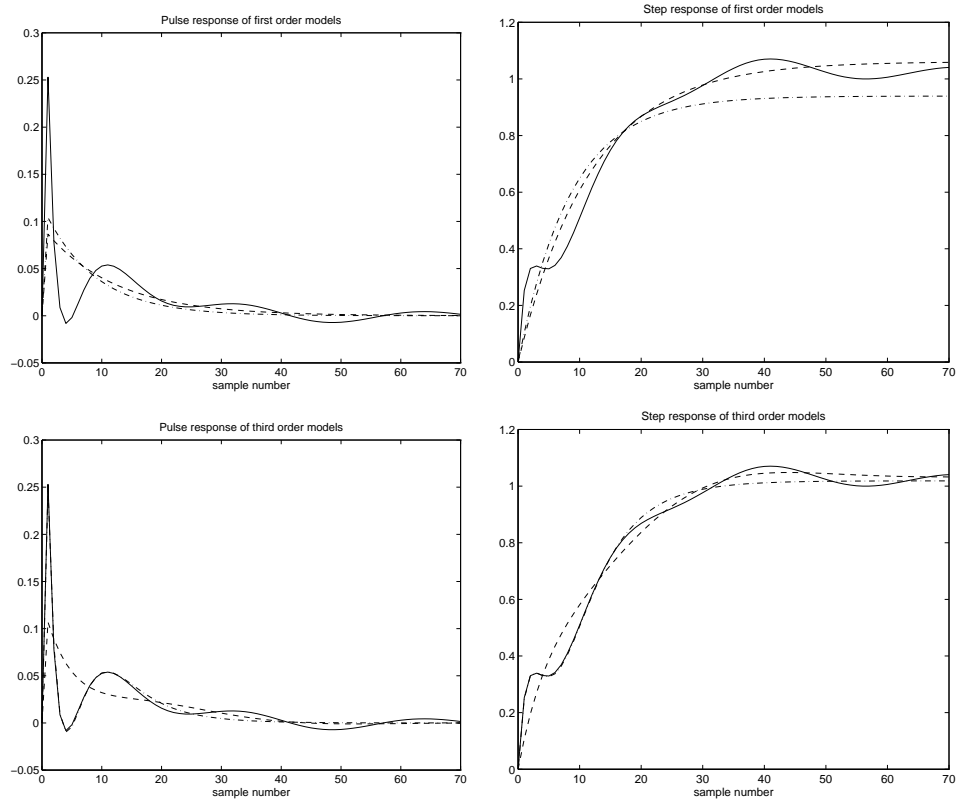
Figure 9.3: Upper: Pulse response (left) and step response (right) of G_0 (solid), and of first order models obtained by pulse response approximate realization (dash-dotted) and by step response approximate realization (dashed). Lower: ditto for third order models.

9.4 Subspace identification

(The text of this section still needs to be detailed and completed.)

9.4.1 Introduction

The realization theory presented in the previous part of this Chapter have been extended to be able to deal with general input and output data. Subspace identification methods have been developed to estimate state-space models from data. They are well suited for multivariable identification problems, and have many attractive features. Rather than analysis-driven, this class of identification methods is strongly algorithm-driven, relying on numerically robust algorithms and exploiting linear algebra tools as the singular value decomposition (SVD).

In this section only a very brief account of subspace methods will be given. The presentation is focussed on the main line of reasoning to arrive at an effective identification algorithm. The presentation follows the reasoning in section 10.6 of Ljung (1999).

9.4.2 State space models with disturbances

Starting from our data generating system

$$y(t) = G_0(q)u(t) + v(t) \tag{9.69}$$

we can write an equivalent state space model

$$
\begin{aligned}
x(t+1) &= A_0 x(t) + B_0 u(t) \\
y(t) &= C_0 x(t) + D_0 u(t) + v(t)
\end{aligned}
\tag{9.70}
$$

where $G_0(z) = C_0(zI - A_0)^{-1}B_0 + D_0$, and where $v(t)$ reflects the output noise disturbance on the output $y(t)$.

The state space model is not unique: for any nonsingular square matrix T, and $\bar{x}(t) := Tx(t)$ it follows that

$$
\begin{aligned}
\bar{x}(t+1) &= \bar{A}_0 \bar{x}(t) + \bar{B}_0 u(t) \\
y(t) &= \bar{C}_0 \bar{x}(t) + D_0 u(t) + v(t)
\end{aligned}
\tag{9.71}
$$

with $\bar{A}_0 = TA_0T^{-1}$, $\bar{B}_0 = TB_0$, $\bar{C}_0 = C_0T^{-1}$, represents the same system (9.69).

If v is colored noise, i.e. $v(t) = H_0(q)e(t)$ then the generation of $v(t)$ from white noise $e(t)$ will require additional states in the system, representing the dynamics of the noise process. This can be represented in the state-space model by

$$
\begin{aligned}
\xi(t+1) &= A_0 \xi(t) + B_0 u(t) + K_0 e(t) \\
y(t) &= C_0 \xi(t) + D_0 u(t) + e(t)
\end{aligned}
\tag{9.72}
$$

with e the white noise input of the noise process with covariance matrix Λ_e, and with

$$
\begin{aligned}
G_0 &= C_0(zI - A_0^{-1}B_0 + D_0 \tag{9.73} \\
H_0 &= C_0(zI - A_0)^{-1}K_0 + I. \tag{9.74}
\end{aligned}
$$

The representation (9.72) is referred to as the *innovation form* of the system. The motivation for this term is found in the fact that the signal $e(t)$ is the innovation signal that remains when $y(t)$ is predicted on the basis of past values y^{t-1} and u^t, in accordance with the prediction theory in Chapter 4.

For Output Error (OE) model structures the output noise will be white, and correspondingly $K_0 = 0$.

In the sequel of this Chapter we will use the general form:

$$
\begin{aligned}
x(t+1) &= A_0 x(t) + B_0 u(t) + w(t) \\
y(t) &= C_0 x(t) + D_0 u(t) + \nu(t)
\end{aligned}
\tag{9.75}
$$

with w, ν white noise processes, with $\mathrm{E}[\nu(t)\nu(t)^T] = R$, $\mathrm{E}[w(t)w(t)^T] = Q$, $\mathrm{E}[w(t)\nu(t)^T] = S$. In this form the state x represents the dynamic properties of both the input-output transfer and the noise process.

9.4.3 Identification problem

For formulating our identification we consider the data generating system:

$$
\begin{aligned}
x(t+1) &= A_o x(t) + B_o u(t) + w(t) \\
y(t) &= C_o x(t) + D_o u(t) + \nu(t)
\end{aligned}
\tag{9.76}
$$

with

$$
\mathrm{E}\left[\begin{pmatrix} w \\ \nu \end{pmatrix} \begin{pmatrix} w^T & \nu^T \end{pmatrix}\right] = \begin{pmatrix} Q & S \\ S^T & R \end{pmatrix}.
\tag{9.77}
$$

The full state-space model identification problem now amounts to determining, on the basis of $\{u(t), y(t)\}_{t=1,\ldots,N}$:

- The order n (dimension of x) of the system;

- Matrices $[A, B, C, D]$, modulo a similarity transformation T;

- The covariance matrices $[Q, R, S]$ (optional)

There are different algorithms that provide estimates of the objects listed above. In the next subsection we will follow one of the primal approaches, that is separated in two steps:

1. Estimate the observability matrix

$$
O_r = \begin{bmatrix} C \\ CA \\ \vdots \\ CA^{r-1} \end{bmatrix}
$$

   that is determined by (C, A) and extract matrices C and A from this; with this step the basis of the state space, that is employed in the state space model, is determined;

2. For a given C and A, estimate the matrices B and D with a simple least-squares algorithm.

The procedure based on these two steps is further explained in the next subsection. It is referred to as subspace identification through observability matrix estimation.

9.4.4 Subspace identification through observability matrix estimation

For simplicity we start with step 2 of the procedure.

Step 2 - Estimating (B, D) when (C, A) are given.

Use the predictor:

$$
\hat{y}(t|t-1;\theta) := [C(qI - A)^{-1}B(\theta) + D(\theta)]u(t)
$$

with entries of B and D parametrized, and C and A being fixed.
This predictor is linear-in-the-parameters, and so can be written as

$$
\hat{y}(t|t-1;\theta) = \varphi^T(t)\theta
$$

where vector θ is composed of the entries of B and D:

- θ is a $(n+p)m \times 1$ vector.

- $\varphi^T(t)$ is a matrix of dimensions $p \times (n+p)m$,

- $\varphi(t)$ contains past (and present) values of $u(t)$ multiplied with known elements from A and C.

A least squares solution for θ can then simply be obtained:

$$\hat{\theta}_N = \arg\min_\theta \frac{1}{N} \sum_{t=1}^N [y(t) - \varphi^T(t)\theta]^T \Lambda^{-1} [y(t) - \varphi^T(t)\theta] \tag{9.78}$$

through a convex optimization problem, with an analytical result (for $\Lambda = I$):

$$\hat{\theta}_N = [\Phi^T \Phi]^{-1} \Phi^T Y$$

with

$$Y := \begin{bmatrix} y(1) \\ \vdots \\ y(N) \end{bmatrix} \quad \Phi := \begin{bmatrix} \varphi^T(1) \\ \vdots \\ \varphi^T(N) \end{bmatrix} \tag{9.79}$$

Step 1: Estimating C, A through estimating the observability matrix
We start with the output equation:

$$y(t) = Cx(t) + Du(t) + \nu(t). \tag{9.80}$$

Writing this down for $t+1$ (assuming for simplicity that $w(t) \equiv 0$), and utilizing the state equation $x(t+1) = Ax(t) + Bu(t)$, we obtain:

$$\begin{align} y(t+1) &= Cx(t+1) + Du(t+1) + \nu(t+1) \tag{9.81} \\ &= CAx(t) + Du(t+1) + CBu(t) + \nu(t+1) \tag{9.82} \end{align}$$

and for $t+2$:

$$\begin{align} y(t+2) &= CAx(t+1) + Du(t+2) + CBu(t+1) + \nu(t+2) \tag{9.83} \\ &= CA^2 x(t) + Du(t+2) + CBu(t+1) + CABu(t) + \nu(t+2) \tag{9.84} \end{align}$$

Continuing this, and denoting

$$Y_r(t) := \begin{bmatrix} y(t) \\ \vdots \\ y(t+r-1) \end{bmatrix}, \ U_r(t) := \begin{bmatrix} u(t) \\ \vdots \\ u(t+r-1) \end{bmatrix}, \ V(t) := \begin{bmatrix} \nu(t) \\ \vdots \\ \nu(t+r-1) \end{bmatrix} \tag{9.85}$$

leads to

$$Y_r(t) = O_r x(t) + S_r U_r(t) + V(t) \tag{9.86}$$

with extended observability matrix

$$O_r = \begin{bmatrix} C \\ CA \\ \vdots \\ CA^{r-1} \end{bmatrix} \quad \text{and} \quad S_r = \begin{bmatrix} D & 0 & 0 & \cdots & 0 \\ CB & D & 0 & \cdots & 0 \\ CAB & CB & \cdots & \cdots & 0 \\ \vdots & \ddots & \ddots & \ddots & 0 \\ CA^r B & \cdots & \cdots & \cdots & D \end{bmatrix} \tag{9.87}$$

With $\mathbf{Y} := [Y_r(1) \;\cdots\; Y_r(N)]$, and similar notation for x, U_r, V this becomes

$$\mathbf{Y} = O_r\mathbf{X} + S_r\mathbf{U} + \mathbf{V}. \qquad \mathbf{Y} \in \mathbb{R}^{r \times N}. \tag{9.88}$$

Estimation of O_r can now be done through projections/correlations. This means that are going to process the equation with right multiplications such that the terms with $\mathbf{U}$ and $\mathbf{V}$ disappear.

Removal of input-dependent term

$$\mathbf{Y} = O_r\mathbf{X} + S_r\mathbf{U} + \mathbf{V}. \tag{9.89}$$

Right multiplication with projector matrix $\mathbf{U}^{\perp} := I - \mathbf{U}^T(\mathbf{U}\mathbf{U}^T)^{-1}\mathbf{U}$ delivers

$$\mathbf{Y}\mathbf{U}^{\perp} = O_r\mathbf{X}\mathbf{U}^{\perp} + \mathbf{V}\mathbf{U}^{\perp} \tag{9.90}$$

since

$$\mathbf{U}\mathbf{U}^{\perp} = \mathbf{U}[I - \mathbf{U}^T(\mathbf{U}\mathbf{U}^T)^{-1}\mathbf{U}] = \mathbf{U} - \mathbf{U} = 0 \tag{9.91}$$

$\mathbf{U}^{\perp}$ provides a projection onto the space that is orthogonal to (the row space of) U.

Removal of noise-dependent term

$$\mathbf{Y}\mathbf{U}^{\perp} = O_r\mathbf{X}\mathbf{U}^{\perp} + \mathbf{V}\mathbf{U}^{\perp} \tag{9.92}$$

Design an instrument matrix

$$\mathbf{\Phi} = [\phi(1) \;\cdots\; \phi(N)] \;\; \text{with } \phi(t) \in \mathbb{R}^s, s \geq n \tag{9.93}$$

leading to

$$\frac{1}{N}\mathbf{Y}\mathbf{U}^{\perp}\mathbf{\Phi}^T = O_r\frac{1}{N}\mathbf{X}\mathbf{U}^{\perp}\mathbf{\Phi}^T + \frac{1}{N}\mathbf{V}\mathbf{U}^{\perp}\mathbf{\Phi}^T \tag{9.94}$$

such that

- $\lim\limits_{N\to\infty} \dfrac{1}{N}\mathbf{V}\mathbf{U}^{\perp}\mathbf{\Phi}^T = 0$, and

- $\lim\limits_{N\to\infty} \dfrac{1}{N}\mathbf{X}\mathbf{U}^{\perp}\mathbf{\Phi}^T = \tilde{T}$, having full row rank

Before it is explained how to exactly construct the instrument matrix $\mathbf{\Phi}$, we proceed with the algorithm, assuming that $\mathbf{\Phi}$ satisfies the conditions listed above, i.e. that in the folloiwing equaiton the second term on teh right hand side disappears (w.p. 1) for N tending to infinity.

$$\underbrace{\frac{1}{N}\mathbf{Y}\mathbf{U}^{\perp}\mathbf{\Phi}^T}_{G_N} = O_r \underbrace{\frac{1}{N}\mathbf{X}\mathbf{U}^{\perp}\mathbf{\Phi}^T}_{\tilde{\mathbf{T}}_{\mathbf{N}}} + \frac{1}{N}\mathbf{V}\mathbf{U}^{\perp}\mathbf{\Phi}^T \tag{9.95}$$

$$\Downarrow N \to \infty \tag{9.96}$$

$$G = O_r\tilde{\mathbf{T}} \tag{9.97}$$

Then G_N is a noisy estimate of $O_r\tilde{T}$, and for N sufficiently large, it holds that the column space of $G_N \equiv$ the column space of O_r

The column space of G_N can be determined through a singular value decomposition: $G_N = U\Sigma V^T$, and U has the same column space as G_N. By setting U equal to the observability matrix O_r, C and A can be determined.

As a result the sequence of steps becomes:

- Calculate G_N and determine $G_N = U\Sigma V^T$;

- Set $U = O_r$, i.e.

$$
U = \begin{bmatrix} C \\ CA \\ CA^2 \\ \cdots \\ CA^{r-1} \end{bmatrix} = O_r
$$

- Set C equal to the first p rows of O_r

- Construct O_{r-1} and construct its (block-)shifted version $O_{r-1}^\uparrow$

- Determine A on the basis of $O_{r-1}^\uparrow = O_{r-1}A$, i.e.

$$
A = O_{r-1}^+ O_{r-1}^\uparrow
$$

The resulting state space model will have a state dimension that is equal to rank $O_r = $ rank U. Therefore the SVD $G_N = U\Sigma V^T$ will determine the state dimension of the resulting state space model.
On the basis of the SVD:

$$
G_N = U\Sigma V^T
$$

an approximation

$$
G_N = U_n\Sigma_n V_n^T
$$

can be made, to limit the column space to dimension n, and therefore to limit the state dimension to n. In this way the SVD of G_N acts as a model order selection mechanism.

Construction of instrument matrix Φ
The two conditions:

- $\lim\limits_{N\to\infty} \dfrac{1}{N}\mathbf{V}\mathbf{U}^\perp\mathbf{\Phi}^T = 0$, and

- $\lim\limits_{N\to\infty} \dfrac{1}{N}\mathbf{X}\mathbf{U}^\perp\mathbf{\Phi}^T = \tilde{T}$, having full row rank

have to be satisfied.

With $\mathbf{U}^\perp = I - \mathbf{U}^T(\mathbf{U}\mathbf{U}^T)^{-1}\mathbf{U}$, and u being uncorrelated with ν (in open-loop case), the crucial condition to satisfy is

$$
\lim_{N\to\infty} \frac{1}{N}\mathbf{V}\mathbf{\Phi}^T = 0 \tag{9.98}
$$

$\lim\limits_{N\to\infty} \dfrac{1}{N}\mathbf{V}\mathbf{\Phi}^T = 0$ implies

$$
\lim_{N\to\infty} \frac{1}{N} \begin{bmatrix} \nu(1) & \cdots & \nu(N) \\ \nu(2) & \cdots & \nu(N+1) \\ \vdots & \vdots & \vdots \\ \nu(r) & \cdots & \nu(r+N-1) \end{bmatrix} \begin{bmatrix} \phi^T(1) \\ \phi^T(2) \\ \vdots \\ \phi^T(N) \end{bmatrix} = 0 \tag{9.99}
$$

which through the whiteness of $\nu(t)$ can be achieved (asymptotically) if

$$\phi(t) \text{ is uncorrelated with } \nu(t). \tag{9.100}$$

e.g. (in open loop when u and ν are independent):

$$\phi(t) = [y(t-1) \ \ldots \ y(t-s_1) \ u(t-1) \ \ldots \ u(t-s_2)]^T \tag{9.101}$$

Subspace ID through observability matrix estimation - algorithm
We can now summarize the full subspace identification algorithm as follows:

- Choose $r \geq n$ and instrument $\phi(t)$, and construct G_N

- Construct a low rank approximation

$$W_1 G_N W_2 = U\Sigma V^T \approx U_n \Sigma_n V_n^T \tag{9.102}$$

  with user-chosen weighting matrices W_1, W_2.

- Construct $\hat{O}_r = W_1^{-1} U_1 T$ with T any nonsingular matrix

- Determine C, A from $\hat{O}_r$

- With C, A given, determine B, D through an LS-algorithm.

Weighting matrices W_1, W_2 are chosen differently for different methods, as N4SID (Van Overschee et al.), MOESP (Verhaegen), CVA (Larimore), IVM (Viberg).

9.4.5 Summary

Subspace identification is an attractive identification procedure with several attractive featues

- It provides algorithms that rely on relatively simple and highly reliable tools from linear algebra, such as LS algorithms, convex optimization and approximations and projections through singular value decomposition. It does not require nonlinear (non-convex) optimization algorithms with uncertain.

- The methods are fit for application to MIMO identification problems without heavily introducing technical complexity.

- The methods are attractive to use, also as initial model for prediction error / maximum likelihood optimization.

- Thre are extensions available for dealing with closed-loop data.

One of the downsides of the method is that because of the multi-step character of the algorithms, approximation properties of the methods, i.e. what happens if $(\mathcal{S} \notin \mathcal{M})$ (see Chapter 4), are hard to analyze.

Bibliography

Realization Theory

J.E. Ackermann (1971). Canonical minimal realization of a matrix of impulse response sequences. *Information and Control*, Vol. 19, pp. 224-231.

C. Bonivento and R.P. Guidorzi (1971). Canonical input-output description of linear multivariable systems. *Richerche di Automatica*, Vol. 2, pp. 72-83.

A.A.H. Damen and A.K. Hajdasinski (1982). Practical tests with different approximate realizations based on the singular value decomposition of the Hankel matrix. In: G.A. Bekey and G.W. Saridis (Eds.), *Identification and System Parameter Estimation 1982*. Proc. 6th IFAC Symp. Identif. and Syst. Param. Estim., Washington DC, pp. 903-908.

G. Golub and C.I. Van Loan (1983). *Matrix Computations*. John Hopkins Univ. Press, Baltimore.

G. Golub and C. Reinsch (1970). Singular value decomposition and least squares solutions. *Num. Math.*, Vol. 14, pp. 403-420. Repr. in J.H. Wilkinson and C. Reinsch (Eds.), *Handbook for Automatic Computation*, vol. II, Linear Algebra. Springer Verlag, 1971, Contribution I/10, pp. 134-151.

R.P. Guidorzi (1981). Invariants and canonical forms for systems structural and parametric identification. *Automatica*, Vol. 17, pp. 117-133.

B.L. Ho and R.E. Kalman (1966). Effective construction of linear state-variable models from input-output functions. *Regelungstechnik*, Vol. 14, pp. 545-548.

T. Kailath (1980). *Linear Systems*. Prentice-Hall, Englewood Cliffs, NJ.

S. Kung (1978). A new identification and model reduction algorithm via singular value decompositions. *Proc. 12th Asilomar Conf. Circuits Syst. and Computers*, Pacific Grove, CA, Nov. 6-8, 1978, pp. 705-714.

B.C. Moore (1981). Principal component analysis in linear systems: controllability, observability and model reduction. *IEEE Trans. Automat. Contr.*, Vol. AC-26, pp. 17-32.

C.T. Mullis and R.A. Roberts (1976). Synthesis of minimum roundoff noise fixed point digital filters. *IEEE Trans. Circuits Syst.*, Col. CAS-23, pp. 551-562.

R.E. Skelton (1988). *Dynamic Systems Control - Linear systems analysis and synthesis*. Wiley & Sons, New York.

A.J. Tether (1970). Construction of minimal linear state-variable models from finite input-output data. *IEEE Trans. Automat. Contr.*, Vol. AC-15, pp. 427-436.

J.B. van Helmont, A.J.J. van der Weiden and H. Anneveld (1990). Design of optimal controller for a coal fired Benson boiler based on a modified approximate realization algorithm. In R. Whalley (Ed.), *Application of Multivariable System Techniques (AMST 90)*. Elsevier Publ. Comp., London, pp. 313-320.

H.P. Zeiger and J. McEwen (1974). Approximate linear realizations of given dimension via Ho's algorithm. *IEEE Trans. Automat. Contr.*, Vol. AC-19, p. 153.

Subspace Identification

W.E. Larimore (1990). Canonical variate analysis in identification, filtering and adaptive control. *Proc. 29th IEEE Conf. Decision and Control*, Honolulu, HI, pp. 596-604.

L. Ljung (1999). *System Identificaiton - Theory for the User*. Prentice-Hall, 1999.

P. Van Overschee and B. De Moor (1994). N4SID: Subspace algorithms for the identification of combined deterministic and stochastic systems. *Automatica*, Vol. 30, no. 1, pp. 75-93.

P. Van Overschee and B. De Moor (1996). *Subspace Identification for Linear Systems; Theory, Implementation,m Applications.* Kluwer Aced. Publ., Dordrecht.

M. Verhaegen and P. Dewilde (1992). Subspace model identification part 1. The output-error state-space model identification class of algorithms. *Int. J. Control*, Vol. 56, no. 5, pp. 1187-2010.

M. Verhaegen and V. Verdult (2007). *Filtering and System Identification - A Least Squares Approach.* Cambridge University Press, UK.

M. Viberg (1995). Subspace-based methods for the identification of linear time-invariant systems. *Automatica*, Vol. 31, no. 12, pp. 1835-1851.

Chapter 10

Identification on the basis of closed-loop experiments

10.1   Introduction

10.1.1   Closed loop configuration and problem setting

Many systems operate under feedback control. This can be due to required safety of operation or to unstable behaviour of the plant, as occurs in many industrial production processes like paper production, glass production, separation processes like crystallization, etcetera. But also mechanical servo systems like robots, positioning systems as wafer steppers (for the production of integrated circuits) and the servo system present in a compact disc player, are examples of processes that typically exhibit unstable dynamical behaviour in open loop. As a consequence experiments can only be performed under presence of a stabilizing controller. Even in situations where plants are stable, production restrictions can be strong reasons for not allowing experiments in open loop.

Many processes in non-technical areas as for example biological and economical systems operate only under closed-loop conditions and it is not even possible to remove the feedback loop.

There can be additional reasons for performing experiments in closed loop. Suppose that the plant under consideration is operating under control of a given controller, and that the objective of the identification is to design a better performing controller for the plant. Then the plant dynamics that exhibit themselves under presence of the old controller, might be much more relevant for designing an improved controller, than the open loop dynamics.

It is very important to know if and how the open loop system can be identified when it must operate under feedback control during the experiment. It will be shown that the feedback can cause difficulties but also that in some specific situations these difficulties may be circumvented.

The experimental situation to be discussed in this chapter is depicted in Fig. 10.1. The data generating system is assumed to be given by the relations

$$
\begin{aligned}
y(t) &= G_0(q)u(t) + H_0(q)e(t) & \text{(10.1)} \\
u(t) &= C(q)[r_2(t) - y(t)] + r_1(t) & \text{(10.2)}
\end{aligned}
$$

where $\{e(t)\}$ is a sequence of independent identically distributed random variables as before.

In contrast to the situation dealt with in open loop identification, the input $\{u(t)\}$ and noise $\{e(t)\}$ are not uncorrelated anymore, due to the presence of the feedback controller $C(q)$.
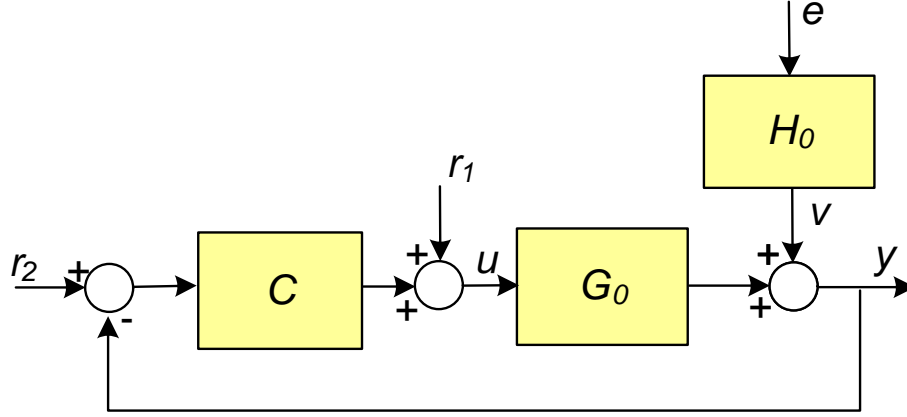

Figure 10.1: Configuration of system operating in closed loop.

In (10.2) the signal r_1 can be a reference value, a setpoint or a noise disturbance on the regulator output. Similarly, signal r_2 can be a setpoint or a measurement noise on the output signal. In situations that we are not interested in the separate effects of r_1 and r_2 we will deal with the signal r defined by:

$$r(t) := r_1(t) + C(q)r_2(t) \tag{10.3}$$

As a result the feedback law can be rewritten as:

$$u(t) = r(t) - C(q)y(t) \tag{10.4}$$

In most situations the goal of identification of the system above is the determination of an estimate of the transfer function $G_0(z)$ and possibly $H_0(z)$. Sometimes one may also wish to determine the controller $C(z)$ in the feedback path.

Referring to the system relations (10.1)-(10.4), the closed loop data generating system can be shown to be characterized by:

$$y(t) = (I + G_0(q)C(q))^{-1}[G_0(q)r(t) + H_0(q)e(t)] \tag{10.5}$$

$$u(t) = (I + C(q)G_0(q))^{-1}[r(t) - C(q)H_0(q)e(t)]. \tag{10.6}$$

In some parts of this chapter we will adopt an appropriate matrix notation of the transfer functions that allows a correct interpretation of the results also in the case of multivariable systems. To this end we distinguish between the input sensitivity and output sensitivity function, denoted as

$$S_0(z) = (I + C(z)G_0(z))^{-1} \quad \text{input sensitivity, and} \tag{10.7}$$

$$W_0(z) = (I + G_0(z)C(z))^{-1} \quad \text{output sensitivity.} \tag{10.8}$$

Using this notation and employing the fact that $W_0 G_0 = G_0 S_0$ and $C W_0 = S_0 C$, we can rewrite the systems equations into the form:

$$y(t) = G_0(q)S_0(q)r(t) + W_0(q)H_0(q)e(t) \tag{10.9}$$

$$u(t) = S_0(q)r(t) - C(q)W_0(q)H_0(q)e(t) \tag{10.10}$$

However, when it is not explicitly stated otherwise, we will consider the scalar situation, for which holds that $W_0 = S_0$.

Dealing with a system configuration as sketched in figure 10.1 we will assume that the closed loop system is internally stable, which is guaranteed by stability of the four transfer functions in (10.9)- (10.10), as formalized in the next definition.

Definition 10.1.1 *Closed loop stability.*
Consider a closed loop system configuration defined in (10.1),(10.2) *and depicted in Figure 10.1. Denote the rational transfer function*

$$T(G_0, C) := \begin{bmatrix} G_0 \\ I \end{bmatrix} (I + CG_0)^{-1} \begin{bmatrix} C & I \end{bmatrix} \tag{10.11}$$

representing the mapping from $col(r_2, r_1)$ *to* $col(y, u)$.
The controller C is said to stabilize the plant G_0 if $T(G_0, C)$ is stable, i.e. analytic for $|z| \geq 1$. □

Note that in our configuration the input-output transfer function G_0 does not necessarily have to be stable. However many identification methods discussed will be able to provide only stable estimates $G(q, \hat{\theta}_N)$, due to the requirement of a uniformly stable model set (see definition 4.4.2). We will assume that G_0 is stable unless this is specifically discussed in the text. Additionally it will be assumed that r is quasi-stationary. The considered experimental situation then is in accordance with Assumption 4.7.1 concerning the data generating mechanism.

10.1.2 Is there a closed loop identification problem?

In order to illustrate the problems that may occur in closed loop system identification, we will first show two simple examples, of applying standard open loop identification techniques to the situation of closed loop experimental conditions. A non-parametric (spectral) estimate of the i/o transfer function will be considered, as well as a parametric ARX prediction error identification method. The examples are taken, respectively, from Söderström and Stoica (1989) and Ljung (1999).

Example 10.1.2 (Application of spectral analysis.) *Consider a scalar system as depicted in Fig. 10.1, and assume that $r_2(t) \equiv 0$, $\{r_1\}$ and $\{e\}$ uncorrelated, and that y, u are available from measurements.*
From (10.9)-(10.10) *the following descriptions of the input and output signals are obtained:*

$$y(t) = S_0(q)[G_0(q)r_1(t) + v(t)] \tag{10.12}$$
$$u(t) = S_0(q)[r_1(t) - C(q)v(t)] \tag{10.13}$$

Hence

$$\Phi_u(\omega) = |S_0(e^{i\omega})|^2[\Phi_{r_1}(\omega) + |C(e^{i\omega})|^2\Phi_v(\omega)] \tag{10.14}$$
$$\Phi_{yu}(\omega) = |S_0(e^{i\omega})|^2[G_0(e^{i\omega})\Phi_{r_1}(\omega) - C^*(e^{i\omega})\Phi_v(\omega)] \tag{10.15}$$

Assuming that the spectral densities $\Phi_u(\omega)$ and $\Phi_{yu}(\omega)$ can be estimated exactly, which should be true at least asymptotically as the number of data points tends to infinity, it is found that the spectral analysis estimate of $G_0(e^{i\omega})$ is given by:

$$\hat{G}(e^{i\omega}) = \frac{\Phi_{yu}(\omega)}{\Phi_u(\omega)} = \frac{G_0(e^{i\omega})\Phi_{r_1}(\omega) - C^*(e^{i\omega})\Phi_v(\omega)}{\Phi_{r_1}(\omega) + |C(e^{i\omega})|^2\Phi_v(\omega)} \qquad (10.16)$$

If there are no disturbances e then $\Phi_v(\omega) = 0$ and (10.16) simplifies to

$$\hat{G}(e^{i\omega}) = G_0(e^{i\omega}) \qquad (10.17)$$

i.e. it is possible to identify the true system dynamics.
However in the other extreme case when there is no external signal r_1, $\Phi_{r_1}(\omega) = 0$ and (10.16) becomes

$$\hat{G}(e^{i\omega}) = \frac{-1}{C(e^{i\omega})} \qquad (10.18)$$

Here the result is the inverse of the regulator. If both disturbances e and external signal r_1 are present, the result will be a weighted combination of both extreme cases, with weighting factors dependent on the spectra $\Phi_{r_1}(\omega)$ and $\Phi_v(\omega)$.
For the special case $C(q) = 0$, referring to the open-loop case, equation (10.16) leads to $\hat{G} = G_0$, i.e. the system can be identified consistently, which is a known result.   □

The example shows that straightforward application of spectral analysis to input/output data of a system operating in closed loop, generally will lead to biased estimates. It is easy to understand the reason for the difficulties encountered when applying spectral analysis as in the example. The model (10.18) provided by the method gives a valid description of the relation between the signals $\{u(t)\}$ and $\{y(t)\}$. However this relation corresponds to the inverse of the feedback law. Note that:

- In the situation leading to (10.18) the feedback path is noise-free, while the relation of interest (10.1) corresponding to the forward path is corrupted by noise.

- The nonparametric model used by the spectral analysis method by its very definition has no structural restrictions (e.g. not even a restriction of causality). Hence it cannot eliminate certain true but uninteresting relationships between $\{u(t)\}$ and $\{y(t)\}$ (such as the inverse feedback law).

The situation should be different if a parametric model is used.
However in the next example we will first illustrate that direct application of parametric identification techniques also can lead to undesirable results.

Example 10.1.3 (Parametric identification under proportional feedback.) *We consider the situation $r_1 \equiv r_2 \equiv 0$, and suppose that a system is controlled by a proportional regulator during the experiment:*

$$u(t) = f\ y(t) \quad \text{with } f \in I\!R \qquad (10.19)$$

We consider a first-order ARX model set:

$$\varepsilon(t,\theta) = y(t) + a\ y(t-1) - b\ u(t-1), \qquad \theta = (a\ b)^T \qquad (10.20)$$

Inserting the feedback law (10.19) *into the model gives:*

$$\varepsilon(t,\theta) = y(t) + (a - bf)y(t-1) \tag{10.21}$$

which is the prediction error when we apply data that are obtained from closed loop experiments. From this we conclude that all models $(\hat{a}, \hat{b})$ subject to

$$
\begin{aligned}
\hat{a} &= a + \gamma f \\
\hat{b} &= b + \gamma
\end{aligned}
$$

with γ an arbitrary scalar (i.e. all models having $\hat{a} - \hat{b}f$ equal and fixed) generate the same prediction error (10.21) *under the feedback* (10.19). *Consequently there is no way to distinguish between these models as they induce the same prediction errors. Notice that it is of no help to know the regulator coefficient f. Apparently the experimental condition* (10.19) *is not informative enough with respect to the model set* (10.20). *It is true, though, that the input signal $\{u(t)\}$ is persistently exciting of sufficient order, since it consists of filtered white noise. Persistence of excitation is thus not a sufficient condition on the input in closed-loop experiments.*

If the model set (10.20) *is restricted, for example by constraining b to be 1:*

$$\varepsilon(t,\theta) = y(t) + a\ y(t-1) - u(t-1), \qquad \theta = a \tag{10.22}$$

then it is clear that the data are sufficiently informative to distinguish between different values of the a-parameter.   □

It has been illustrated that there do exist specific closed loop identification problems, both with respect to the consistency of the results and with respect to possible lack of uniqueness of estimates due to the experimental situation.

10.1.3   Subproblems and assessment criteria

The several closed-loop identification methods that will be discussed in this paper can be evaluated with respect to a number of different aspects/criteria. We will first present these assessment criteria.

(a) **Consistency of $(\hat{G}, \hat{H})$.** This is a basic requirement. Whenever our model set is rich enough to contain the data generating system ($\mathcal{S} \in \mathcal{M}$), the identification method should be able to consistently identify the plant, under additional conditions on excitation properties of the plant signals.

(b) **Consistency of $\hat{G}$.** The ability to identify G_0 consistently in the situation $G_0 \in \mathcal{G}$. This implies that the consistent modelling of G_0 is not dependent on possible under-modelling or misspecification of H_0. Particularly in situations where the disturbance process v contains complex dynamics, this property is favorable.

(c) **Tunable bias expression.** An explicit approximation criterion can be formulated that governs the asymptotic i/o model $G(q, \theta^*)$ in a way that is not dependent on Φ_v. This refers to an expression for the asymptotic bias distribution, as also formulated for open-loop experimental conditions in (4.164).

In the sequel of this chapter these problems will be referred to as Problems (a)-(c). By far most results on closed loop identification deal with the consistency problem (a). Standard references are Gustavsson, Ljung and Söderström (1977) and Anderson and Gevers (1982). For an overview of these results see also Söderström and Stoica (1989). *Approximate* identification under closed loop circumstances is an area that only recently is given attention in the literature.

Additional to the properties mentioned in the definition above, attention will be given to the following issues:

(d) **Fixed model order**. The ability of identification methods to consider model sets $\mathcal{G}$ of models with a fixed and prespecified model order. This property is important when the application of the identified model, e.g. in model-based control design, puts limitations on the acceptable complexity of the model.

(e) **Unstable plants**. The ability to (consistently) identify unstable plants.

(f) **Stabilized model** $(G(q, \theta^*), C)$. This refers to the situation that there is an a priori guarantee that the (asymptotically) identified model $G(q, \theta^*)$ is guaranteed to be stabilized by the present controller C. This property might be relevant when the identified model is going to be used as a basis for redesigning the controller.

(g) **Knowledge of controller** C. This concerns the question whether exact knowledge of the controller is required by the considered identification method.

(h) **Accuracy**. The (asymptotic) variance of the model estimates.

When starting to discuss the closed loop identification problems, we have to formalize what is the "plant data and a priori information" that is referred to in the problem definition. What do we consider to be available as plant data? Several situations have to be distinguished, and different methods to tackle the problems take different plant data as a starting point. Information on several levels and of several types can be available.

- measurements of plant input and output, u, y;

- knowledge about presence and excitation properties of r_1, r_2;

- measurements of r_1, r_2;

- knowledge of $C(q)$.

Most identification methods discussed in this chapter assume that measured values of y, u are available. However, on the other items the required information becomes dependent on the method used. When discussing each method, we will make a clear reference to the required plant data and a priori knowledge.

Apart from the regular assumptions on data and data generating system as also used in Chapter 4 we will regularly need one additional condition:

Assumption 10.1.4 *The data generating system $\mathcal{S}$ and the model set $\mathcal{M}$ satisfy the condition that $G_0(z)$ and $G(z, \theta)$ are strictly proper for all $\theta \in \Theta$, i.e. $G_0(\infty) = G(\infty, \theta) = 0$ for all θ.*

This assumption is weak and is introduced to avoid algebraic loops in the closed loop system. An algebraic loop occurs if neither $G_0(z)$ nor $C(z)$ contains a delay. Then $y(t)$ depends momentarily on $u(t)$, which in turn depends momentarily on $y(t)$. For some identification methods, as discussed later on, such a situation would make a consistent estimation impossible. To avoid this situation it is assumed that the system G_0 has at least one delay so that $y(t)$ depends only on past input values. For multivariable situations this restriction can be further relaxed, as discussed in Van den Hof *et al.* (1992).

10.1.4   Overview of contents

In this chapter we will discuss several closed loop identification methods. We will start by reviewing the "classical" methods that are mainly directed towards the construction of consistent estimates (Problems (a)-(b)). The corresponding techniques for Instrumental Variable methods (section 10.2), Direct Identification methods (section 10.3), Indirect Identification (section 10.4) and Joint Input/Output Identification (section 10.5) have been developed in the 1970's. The Instrumental Variable method that will be discussed is the only method that is not related to a quadratic prediction error identification criterion.
In sections 10.7-10.9 identification strategies will be discussed that only recently have been proposed. They are mainly directed to solving problems (b)-(c) and have emerged from a research area in which one is tempting to identify models that are specifically suited for consecutive (robust) control design.
In this chapter we will not discuss the connections with the control design problem, but restrict attention to the identification part of the matter. In an abbreviated format, the principal results as presented in this chapter can also be found in the survey paper Van den Hof (1998).

10.2   Instrumental variable (IV) method

For applying an instrumental variable (IV) method, we consider the situation that at least one of the signals r_1 or r_2 is measurable. We will denote this measurable signal by r, and we will assume that this signal is uncorrelated with the disturbance signal e.
Let us first consider the basic phenomena in an IV identification method.
We have an ARX model set, written in a linear regression form (compare section 4.6.5) as:

$$\varepsilon(t, \theta) = y(t) - \varphi^T(t)\theta \tag{10.23}$$

with $\varphi(t)$ the regression vector (vector with explanatory variables), given by

$$\varphi(t) = [-y(t-1) \ \cdots \ -y(t-n_a) \ u(t) \ \cdots u(t-n_b)]^T \tag{10.24}$$

and $\theta = [a_1 \ a_2 \ \cdots a_{n_a} \ b_0 \ \cdots b_{n_b}]^T$, with $d = dim(\theta)$.
Now consider a vector valued signal $\{\zeta(t)\}$ with $\zeta(t) \in \mathbb{R}^d$, denoted as the instrumental variable, then the IV-estimate of the unknown parameter θ, denoted by $\hat{\theta}_N^{IV}$ is determined by

$$\hat{\theta}_N^{IV} = \left[\frac{1}{N}\sum_{t=1}^{N}\zeta(t)\varphi^T(t)\right]^{-1}\left[\frac{1}{N}\sum_{t=1}^{N}\zeta(t)y(t)\right] \tag{10.25}$$

provided the matrix to be inverted indeed is nonsingular.

Assuming we have a data generating system, represented by

$$y(t) = \varphi^T(t)\theta_0 + w(t) \tag{10.26}$$

or equivalently

$$y(t) = \frac{B_0(q^{-1})}{A_0(q^{-1})}u(t) + \frac{1}{A_0(q^{-1})}w(t) \tag{10.27}$$

with $B_0(q^{-1})/A_0(q^{-1}) = G_0(q)$, and $\{w(t)\}$ any stationary stochastic process with rational spectral density, it follows that

$$\hat{\theta}_N^{IV} = \theta_0 + \left[\frac{1}{N}\sum_{t=1}^{N}\zeta(t)\varphi^T(t)\right]^{-1}\left[\frac{1}{N}\sum_{t=1}^{N}\zeta(t)w(t)\right]. \tag{10.28}$$

The IV estimator provides a consistent parameter estimate, $\text{plim}_{N\to\infty}\hat{\theta}_N^{IV} = \theta_0$, under the following two conditions:

$$\bullet \qquad \bar{E}\zeta(t)\varphi^T(t) \quad \text{is nonsingular} \tag{10.29}$$

$$\bullet \qquad \bar{E}\zeta(t)w(t) = 0 \tag{10.30}$$

Note that in this analysis the question whether experiments have been taken from the plant operating under either open loop or closed-loop experimental conditions, has not been raised yet. This aspect comes into the picture when analyzing the two conditions (10.29), (10.30).

In a closed loop situation, in general every element of the regression vector (4.73) will be correlated with the noise disturbance $w(t)$, and consequently a choice $\zeta(t) = \varphi(t)$ will definitely not satisfy condition (10.30). However when there is an external signal r available that is uncorrelated with the noise w, this gives the possibility to satisfy both conditions (10.29), (10.30).
Take for instance,

$$\zeta(t) = [r(t)\ r(t-1)\ \cdots\ r(t-d+1)]^T \tag{10.31}$$

it can simply be verified that $\zeta(t)$ is not correlated with the noise signals in the loop that originate from w, and moreover that it indeed is correlated with the input and output samples in the regression vector $\varphi(t)$, as required by (10.29).
This brings us to the following formal result:

Proposition 10.2.1 *Let $\mathcal{S}$ be a data generating system and let Z^∞ be a data sequence corresponding to Assumptions 4.7.1, 4.7.2, with r and e uncorrelated. Let $\mathcal{M}$ be an ARX model set that is uniformly stable with parameter set $\Theta \subset \mathbb{R}^d$ such that $\mathcal{S} \in \mathcal{M}$. Let $\{\zeta\}$ be an instrumental variable determined by (10.31), Then under weak conditions, as e.g. (10.29), the instrumental variable estimate (4.75) is consistent.*

Note that validity of the mentioned condition (10.29) will depend on the data generating system, and the experimental condition. It will be necessary that the instrumental variable signal r has - some unspecified - sufficient excitation properties.
In the discussion so far we have not required whiteness of the noise contribution w. This means that we can hold a similar reasoning as above, based on a data generating system similar as (4.78) but with w chosen as:

$$w(t) = \frac{H_0(q)}{A_0(q)}e(t) \tag{10.32}$$

	IV method
Consistency $(G(q, \hat{\theta}_N), H(q, \hat{\theta}_N))$	$+$
Consistency $G(q, \hat{\theta}_N)$	$+$
Tunable bias	$-$
Fixed model order	$+$
Unstable plants	$+$
$(G(q, \hat{\theta}_N), C)$ stable	$-$
C assumed known	no

Table 10.1: Properties of IV closed-loop identification method

with $\{e(t)\}$ a sequence of independent identically distributed random variables (white noise). Note that it no longer holds true that $\mathcal{S} \in \mathcal{M}$, since the noise contribution on the output signal is not modelled correctly with an ARX model set. However still the parameter θ (parametrizing the i/o transfer function) can be estimated consistently.

Proposition 10.2.2 *Consider the situation of Proposition 10.2.1 with an ARX model set satisfying $G_0 \in \mathcal{G}$ (and not necessarily $\mathcal{S} \in \mathcal{M}$). Then - under weak conditions - the same instrumental variable estimate provides a consistent estimate $G(q, \hat{\theta}_N^{IV})$, i.e. for all ω, $G(e^{i\omega}, \hat{\theta}_N^{IV}) \to G_0(e^{i\omega})$ w.p. 1 as $N \to \infty$.*

With this IV-method, problems (a) and (b) as mentioned in section 10.1.1 can be solved under fairly general conditions. Since the IV identification method does not have the form of a criterion optimization (as e.g. a least squares method), an approximation criterion for the case $G_0 \notin \mathcal{G}$, as is the topic in problem (c), can not be made as explicit as in the situation of open loop prediction error methods.

The several properties of the IV identification method in view of the aspects as mentioned in the beginning of the chapter are summarized in Table 10.1.
For IV estimates the model set that is considered has an ARX structure. Since this structure provides a uniformly stable model set, in terms of definition 4.4.2, even in situations that the roots of the polynomial $A(q, \theta)$ are outside the unit circle, the IV identification method has no problem with a consistent identification of unstable plants. This of course under the condition that experiments are performed under closed-loop conditions with a stabilizing controller.
IV methods for closed-loop system identification are further discussed in Söderström et al. (1987) and Gilson and Van den Hof (2003).

10.3 Direct identification

10.3.1 General approach

In the so-called direct identification approach a common open-loop identification method is applied to recorded data $\{u(t)\}$, $\{y(t)\}$ that is obtained while the process was operating under closed loop experimental conditions. Actually the presence of feedback is simply discarded; the data is treated as if there was no feedback at all. This is of course an attractive approach if it works, since one does not have to bother about the presence of feedback at all.

We will analyse the consistency properties of this approach for several types of experimental conditions, i.e. with and without the presence of an external excitation signal r. For the general approach as discussed in this and the next two subsections, knowledge of the controller is not assumed to be available.

Consider a data generating system, as in equations (10.1)-(10.4) where the signals $\{u(t)\}$, $\{y(t)\}$ are determined by (10.5)-(10.6).

Writing the standard one-step-ahead prediction error of a model $[G(q,\theta)\ H(q,\theta)]$ as derived in Chapter 4:

$$\varepsilon(t,\theta) = H(q,\theta)^{-1}(y(t) - G(q,\theta)u(t)) \tag{10.33}$$

and substituting the relations for $y(t)$ and $u(t)$, we obtain

$$\varepsilon(t,\theta) = T_{\varepsilon r}(q,\theta)r(t) + T_{\varepsilon e}(q,\theta)e(t) \tag{10.34}$$

with

$$T_{\varepsilon r}(q,\theta) = \frac{S_0(q)}{H(q,\theta)}[G_0(q) - G(q,\theta)] \tag{10.35}$$

$$\text{and} \quad T_{\varepsilon e}(q,\theta) = \frac{H_0(q)}{H(q,\theta)}\frac{S_0(q)}{S(q,\theta)} \tag{10.36}$$

where $S(q,\theta)$ is the sensitivity function of the model, i.e. $S(q,\theta) = [1 + C(q)G(q,\theta)]^{-1}$.

When $G_0(q)$ and $G(q,\theta)$ are strictly proper as assumed in Assumption 10.1.4, and $H_0(q)$ and $H(q,\theta)$ are proper and monic, it can simply be verified that $T_{\varepsilon e}(q,\theta)$ is proper and monic for all θ. Consequently this transfer function can be written as:

$$T_{\varepsilon e}(q,\theta) = 1 + T_{\varepsilon e}^{sp}(q,\theta) \tag{10.37}$$

with $T_{\varepsilon e}^{sp}(q,\theta)$ being the strictly proper part of $T_{\varepsilon e}(q,\theta)$.

In the direct identification method, the estimated model is obtained by

$$\hat{\theta}_N = \arg \min_{\theta \in \Theta} V_N(\theta, Z^N) \tag{10.38}$$

while according to the convergence result given in Chapter 4 the parameter estimate converges with probability 1 to its asymptotic value θ^* determined by

$$\theta^* = \arg \min_{\theta \in \Theta} \bar{V}(\theta) \tag{10.39}$$

Now let us consider this asymptotic identification criterion $\bar{V}(\theta)$

$$\bar{V}(\theta) = \bar{E}\varepsilon^2(t,\theta) \tag{10.40}$$

Considering this criterion in view of (10.34) and (10.37), and taking account of the fact that $\{e(t)\}$ is a white noise process that is uncorrelated with $\{r(t)\}$, we can directly achieve the following lower bound on $\bar{V}(\theta)$:

$$\bar{V}(\theta) = \bar{E}\ \varepsilon^2(t,\theta) \geq E\ e^2(t) \tag{10.41}$$

and as a result the global minimum satisfies the following result.

Proposition 10.3.1 *Let $\mathcal{S}$ be a data generating system and let Z^∞ be a data sequence corresponding to Assumptions 4.7.1, 4.7.2, with $\{r(t)\}$ being uncorrelated to $\{e(t)\}$. Let $\mathcal{M}$ be a uniformly stable model set with parameter set $\Theta \subset \mathbb{R}^d$ such that $\mathcal{S} \in \mathcal{M}$, and let Assumption 10.1.4 be satisfied for $\mathcal{S}$ and $\mathcal{M}$.*
If $\{r(t)\}$ is persistently exciting of a sufficiently high order, then $\theta^* \in \arg\min_{\theta \in \Theta} \bar{V}(\theta)$ if and only if

$$\begin{cases} T_{\varepsilon r}(e^{i\omega}, \theta^*) = 0, & and \\ T_{\varepsilon e}(e^{i\omega}, \theta^*) = 1 & for\ all\ \ \omega \in \mathbb{R} \end{cases} \tag{10.42}$$

The proposition specifies the convergence result from Chapter 4 for the closed loop situation. It follows directly from (10.41), taking into account that, since r and e are uncorrelated, the contribution of the two terms in (10.34) simply add up in the identification criterion. Since $G(q, \theta) = G_0(q)$, $H(q, \theta) = H_0(q)$ indeed satisfy the conditions (10.42) it follows that the lower bound in (10.41) indeed can be reached within $\mathcal{M}$.

In the proposition the asymptotically identified models are completely characterized. The question whether and in which situation we can arrive at consistent estimates $G(e^{i\omega}, \theta^*)$, $H(e^{i\omega}, \theta^*)$ now can be reformulated into the question whether (10.42) implies that $G(e^{i\omega}, \theta^*) = G_0(e^{i\omega})$ and $H(e^{i\omega}, \theta^*) = H_0(e^{i\omega})$ for all ω.
We will analyse this situation in two different experimental situations, to be briefly treated in the following two subsections.

10.3.2 Situation with external excitation

We consider the situation of a system operating under closed loop experimental conditions, where a persistently exciting external signal r is present.
When evaluating the asymptotic parameter estimates, characterized by (10.42), we see that by using (10.35),

$$T_{\varepsilon r}(e^{i\omega}, \theta^*) = 0 \ \Rightarrow \ G(e^{i\omega}, \theta^*) = G_0(e^{i\omega}) \ \text{ for all } \omega \tag{10.43}$$

This implies that $S(e^{i\omega}, \theta^*) = S_0(e^{i\omega})$ which shows the validity of the implication

$$T_{\varepsilon e}(e^{i\omega}, \theta^*) = 1 \ \Rightarrow \ H(e^{i\omega}, \theta^*) = H_0(e^{i\omega}) \ \text{ for all } \omega \tag{10.44}$$

and the following corollary follows.

Corollary 10.3.2 *Consider the situation as described in Proposition 10.3.1.*
If $\{r(t)\}$ is persistently exciting of a sufficiently high order, then the estimates $G(e^{i\omega}, \hat{\theta}_N)$, $H(e^{i\omega}, \hat{\theta}_N)$ are consistent for all ω.

As a result, a unique and consistent model is obtained despite the presence of feedback. Note also that we do not have to be able to measure the external signal $\{r(t)\}$. It is sufficient that this external (and persistently exciting) signal is present.

10.3.3 Situation without external excitation

In the situation without an external excitation signal r, it can simply be verified that the characterization of the asymptotic estimates in Proposition 10.3.1 by (10.42), simplifies to

$$T_{\varepsilon e}(e^{i\omega}, \theta^*) = 1 \quad \text{for all } \omega \tag{10.45}$$

and consistency is obtained if and only if this equation implies that $G(e^{i\omega}, \theta^*) = G_0(e^{i\omega})$ and $H(e^{i\omega}, \theta^*) = H_0(e^{i\omega})$ for all ω.

Using (10.36) we can rewrite (10.45) as

$$H_0(e^{i\omega})^{-1}(1 + G_0(e^{i\omega})C(e^{i\omega})) = H(e^{i\omega}, \theta^*)^{-1}(1 + G(e^{i\omega}, \theta^*)C(e^{i\omega})) \qquad (10.46)$$

for all ω. However without any additional conditions, this relation is not sufficient to conclude uniqueness of the solution. It depends on the system, the model set, and the controller whether or not this equation implies that $G(e^{i\omega}, \theta^*) = G_0(e^{i\omega})$ and $H(e^{i\omega}, \theta^*) = H_0(e^{i\omega})$.

As an illustration of the problem, consider the following heuristic reasoning. If the controller $C(q)$ has low order, then the transfer function $H(q, \theta^*)^{-1}(1 + G(q, \theta^*)C(q))$ may also be of low order and the identity above may then give too few restrictions to determine the estimated model uniquely.

On the other hand, if $C(q)$ has a sufficiently high order, then the identity above will lead to sufficient equations to determine the estimated model uniquely.

As an example we will illustrate this phenomenon for the case of an ARX model set, as a special case of the ARMAX situation considered in Söderström and Stoica (1989).

Example 10.3.3 (Closed loop ARX identification without external signal.) *Consider a data generating system determined by*

$$G_0(q) = \frac{B_0(q^{-1})}{A_0(q^{-1})}, \qquad H_0(q) = \frac{1}{A_0(q^{-1})} \qquad (10.47)$$

with $degr(B_0(q^{-1})) = degr(A_0(q^{-1})) = n_m$, and consider a corresponding ARX model set:

$$\varepsilon(t, \theta) = B(q^{-1}, \theta)u(t) - A(q^{-1}, \theta)y(t) \qquad (10.48)$$

with $degr(A) = degr(B) = n_m$.

The asymptotic solutions obtained by the direct identification method, without the presence of an external signal r, are characterized by (10.46):

$$A(q^{-1}, \theta^*) + B(q^{-1}, \theta^*)C(q) = A_0(q^{-1}) + B_0(q^{-1})C(q) \qquad (10.49)$$

Suppose $C(q) = \frac{R(q^{-1})}{P(q^{-1})}$ with $R(q^{-1})$ and $P(q^{-1})$ polynomials in q^{-1} of degree n_c. The whole set of solutions to (10.49) is now given by:

$$A(q^{-1}, \theta^*) = A_0(q^{-1}) + D(q^{-1})R(q^{-1}) \qquad (10.50)$$
$$B(q^{-1}, \theta^*) = B_0(q^{-1}) - D(q^{-1})P(q^{-1}) \qquad (10.51)$$

with $D(q^{-1})$ any polynomial.

However the additional terms in (10.50), (10.51) reflecting the polynomial $D(q^{-1})$ can only be present under the condition that $degr(D(q^{-1})R(q^{-1})) \leq n_m$ and $degr(D(q^{-1})P(q^{-1})) \leq n_m$. If these restrictions are not satisfied then (10.50), (10.51) refer to estimated parameter values that are outside the permitted parameter range, since the degrees of $A(q^{-1}, \theta^*)$ and $B(q^{-1}, \theta^*)$ are fixed to n_m. If $n_c < n_m$ then indeed there exists a whole set of solutions to (10.50), (10.51). If $n_c > n_m$ it follows that $D(q^{-1}) = 0$ and (10.50), (10.51) will generate a unique solution. If $n_c = n_m$ any zero^{th} order polynomial $D(q^{-1})$ (which means $D(q^{-1}) = d \in {\rm I\!R}$) could formally be applied, but since the polynomials $A(q^{-1}, \theta^*)$ and $A_0(q^{-1})$ both have to be monic, the only possible choice is $d = 0$, which also shows that a unique solution is obtained.

The conclusion that we can draw is formulated in the following corollary.

Corollary 10.3.4 *Consider the situation as described in Proposition 10.3.1. If there is no external excitation signal r present, then the estimates $G(e^{i\omega}, \hat{\theta}_N)$, $H(e^{i\omega}, \hat{\theta}_N)$ can be consistent for all ω, provided that the applied controller has a sufficiently high order.*

However note that the required order of the controller will generally depend on the data generating system. The generalization of the above Corollary from the ARMAX situation, treated in Söderström and Stoica (1989), to the situation of OE and BJ model structures, is considered in Bombois et al. (2006).

10.3.4 General excitation condition for consistency

The consistency result for prediction error model estimates as formulated in chapter 4 can directly be extended to the closed-loop situation. In the proof of Proposition 4.9.1 one has to take care of the fact that signals u and e now can no longer be considered to be uncorrelated. As a result an excitation condition needs to be formulated that slightly extends the notion of persistence of excitation, as was used in the open loop case.

Definition 10.3.5 (Ljung (1999)) *A quasi-stationary data sequence Z^∞ is informative enough with respect to model set $\mathcal{M}$ if for any two models (G_1, H_1), (G_2, H_2) in the model set, with predictor filters $W_i(q) = [H_i^{-1}(q)G_i(q) \quad 1 - H_i^{-1}(q)]$, $i = 1, 2$, it holds that*

$$E[(W_1(q) - W_2(q)) \begin{pmatrix} u(t) \\ y(t) \end{pmatrix}]^2 = 0 \tag{10.52}$$

implies that $W_1(e^{i\omega}) = W_2(e^{i\omega})$ for almost all ω.

As a direct generalization of Proposition 4.9.1 the following consistency result can now be formulated:

Proposition 10.3.6 *Let $\mathcal{S}$ be a data generating system and let Z^∞ be a data sequence corresponding to Assumptions 4.7.1, 4.7.2. Let $\mathcal{M}$ be a uniformly stable model set with parameter set $\Theta \subset \mathbb{R}^d$ such that $\mathcal{S} \in \mathcal{M}$, and let Assumption 10.1.4 be satisfied for $\mathcal{S}$ and $\mathcal{M}$.*
If Z^∞ is informative enough with respect to $\mathcal{M}$ then

$$\begin{array}{ll} G(e^{i\omega}, \theta^*) = G_0(e^{i\omega}) \\ H(e^{i\omega}, \theta^*) = H_0(e^{i\omega}) \end{array} \quad for \ -\pi \leq \omega \leq \pi. \tag{10.53}$$

and consequently the direct estimates of G_0 and H_0 are consistent.

The excitation condition formulated here is less easy to interpret and quantify, and therefore the excitation conditions as formulated in the previous two sections are more convenient in practice.
Note that if we do not apply any order restrictions to the model set $\mathcal{M}$, then the condition under which a data sequence Z^∞ will be informative enough (for all $\mathcal{M}$) can quite simply be derived from the frequency domain equivalent of (10.52). By rewriting this latter equation as

$$\frac{1}{2\pi} \int_{-\pi}^{\pi} \tilde{W}(e^{i\omega}) \Phi_z(\omega) \tilde{W}^T(e^{-i\omega}) d\omega = 0$$

with $\tilde{W}(q) = W_1(q) - W_2(q)$, and

$$\Phi_z(\omega) = \left[\begin{array}{cc} \Phi_u(\omega) & \Phi_{uy}(\omega) \\ \Phi_{yu}(\omega) & \Phi_y(\omega) \end{array} \right]$$

it follows that $\tilde{W}(e^{i\omega})$ is implied by the (sufficient) condition that $\Phi_z(\omega)$ is positive definite for almost all ω.

Note that an informative data sequence can also be generated by a closed-loop system with a nonlinear or a time-varying controller. This will allow the direct identification method to identify consistent estimates of the plant model. The situation of applying a sequence of different controllers during the identification experiment is further considered in Söderström *et al.* (1976).

10.3.5   A frequency domain expression for the limit model

Until now we have only discussed the way in which direct identification methods in closed loop can cope with problem (a) as stated in the introduction. This refers to the consistent estimation of a (complete) model $G(q, \theta)$, $H(q, \theta)$.

The other two problems (b)-(c) can generally not be solved with this direct identification methods, as will be illustrated by using a frequency domain expression for the asymptotic model estimates, similar to the results in section 4.12 for the open loop case.

Using the expressions for the prediction error (10.34)-(10.36) it follows directly that we can rewrite the asymptotic identification criterion $\bar{V}(\theta)$ as:

$$\bar{V}(\theta) = \frac{1}{2\pi} \int_{-\pi}^{\pi} \{ |G_0(e^{i\omega}) - G(e^{i\omega}, \theta)|^2 \frac{|S_0(e^{i\omega})|^2}{|H(e^{i\omega}, \theta)|^2} \Phi_r(\omega) + \frac{|H_0(e^{i\omega})|^2 |S_0(e^{i\omega})|^2}{|H(e^{i\omega}, \theta)|^2 |S(e^{i\omega}, \theta)|^2} \Phi_e(\omega) \} d\omega \quad (10.54)$$

where $S(e^{i\omega}, \theta)$ is the model sensitivity function, i.e. $S(e^{i\omega}, \theta) = (1 + C(e^{i\omega})G(e^{i\omega}, \theta))^{-1}$.

Note that in the integrand of this expression either of the two terms contain the parametrized transfer functions $G(q, \theta)$ and $H(q, \theta)$.

If we would be in a situation that $G_0 \in \mathcal{G}$ and $\mathcal{S} \notin \mathcal{M}$, it can not be concluded that consistency of G would result, not even if $G(q, \theta)$ and $H(q, \theta)$ are parametrized independently. This result that is valid in the open loop case can not be transferred to the closed loop situation. It can be verified by considering the situation of an Output Error (OE) model set. In this case $H(q, \theta) = 1$. The choice $G(q, \theta) = G_0(q)$ in (10.54) would make the first term in the integrand zero, however the second term also is dependent on $G(q, \theta)$ (through $S(q, \theta)$) and will not necessarily be minimal for $G(q, \theta) = G_0(q, \theta)$. Thus in general a solution $G(q, \theta^*) \neq G_0(q)$ will result, even if $G_0 \in \mathcal{G}$.

The expression (10.54) characterizes the asymptotic model estimate, however this characterization is rather implicit. As shown above, it can be deduced that a plant model will generally be biased whenever the noise model is not estimated consistently; the distribution of this bias over frequency can not be assessed from this expression. In order to provide a more explicit expression for the asymptotic bias, the following analysis is performed (Ljung, 1993):

By denoting

$$\begin{aligned} \Delta G(q, \theta) &= G_0(q) - G(q, \theta) \\ \Delta H(q, \theta) &= H_0(q) - H(q, \theta) \end{aligned}$$

it can be observed that

$$
\begin{aligned}
\varepsilon(t,\theta) &= \frac{1}{H(q,\theta)}[\Delta G(q,\theta)u(t) + H_0(q)e(t) - H(q,\theta)e(t)] + e(t) \\
&= \varepsilon_1(t,\theta) + e(t),
\end{aligned}
$$

with

$$
\varepsilon_1(t,\theta) = \frac{1}{H(q,\theta)}[\Delta G(q,\theta)u(t) + \Delta H(q,\theta)e(t)].
$$

If either G_0 and $G(q,\theta)$, or C are strictly proper, then $E(\varepsilon_1(t,\theta)e(t)) = 0$, and so

$$
\Phi_\varepsilon(\omega,\theta) = \Phi_{\varepsilon_1}(\omega,\theta) + \lambda_0.
$$

Now by writing (leaving away the arguments):

$$
\varepsilon_1(t,\theta) = \frac{1}{H}[\Delta G[S_0 r(t) - CS_0 H_0 e(t)] + \Delta H e(t)]
$$

we can write its spectrum as:

$$
\begin{aligned}
\Phi_{\varepsilon_1} &= \frac{1}{|H|^2}\left\{|\Delta G|^2 \Phi_u + |\Delta H|^2 \sigma_e^2 - 2\mathrm{Re}(\Delta G C S_0 H_0 \Delta H)\sigma_e^2\right\} \\
&= \frac{\Phi_u}{|H|^2}\left\{|\Delta G|^2 + \frac{|\Delta H|^2 \sigma_e^2}{\Phi_u} - 2\frac{\mathrm{Re}(\Delta G C S_0 H_0 \Delta H)\sigma_e^2}{\Phi_u}\right\} \\
&= \frac{\Phi_u}{|H|^2}\left\{|\Delta G - B|^2 + \frac{|\Delta H|^2 \sigma_e^2}{\Phi_u} - |B|^2\right\}
\end{aligned}
$$

where B is given by:

$$
B = \frac{CS_0 H_0 \Delta H \sigma_e^2}{\Phi_u}.
$$

As a result we can write for the situation of a fixed noise model H^*:

$$
G(e^{i\omega},\theta^*) = \arg\min_\theta \frac{1}{2\pi}\int_{-\pi}^{\pi}|G_0(e^{i\omega}) - B(e^{i\omega}) - G(e^{i\omega},\theta)|^2 \frac{\Phi_u(\omega)}{|H^*(e^{i\omega})|^2}d\omega. \qquad (10.55)
$$

If we restrict attention to the situation that both G_0 and $G(\theta)$ are causal and stable, and so ΔG will be causal and stable, then only the causal and stable part of B will contribute in the minimization of the integral expression. In this situation, we can write:

$$
B = M_+ \Delta H \sigma_e^2
$$

with M_+ obtained through the decomposition:

$$
\frac{CS_0 H_0}{\Phi_u} = M_+ + M_-
$$

where M_+ causal, stable and M_- anticausal.

The expression (10.55) shows that - for a fixed noise model H^* - the plant model will converge to a biased estimate $G_0 - B$, where the bias is determined by the noise level within the loop, the input signal power, and the accuracy of the noise model. This implies that the bias in the estimate of G_0 may be small in either of the following situations:

- The fixed noise model H^* is an accurate description of H_0;

- The signal to noise ratio at the input u is large;

10.3.6   Asymptotic variance

For the direct identification method, an expression for the asymptotic variance of the transfer function estimate can be given for the situation that $S \in \mathcal{M}$, and both plant model and noise are estimated. In this case the result that already has been formulated in Proposition 4.151 directly applies, provided that the non-zero cross-spectrum between input u and disturbance e is taken into account. This implies that the result of Proposition 4.151 generalizes to

$$cov\left(\begin{array}{c} \hat{G}(e^{i\omega}) \\ \hat{H}(e^{i\omega}) \end{array} \right) \sim \frac{n}{N} \Phi_v(\omega) \cdot \left[\begin{array}{cc} \Phi_u(\omega) & \Phi_{eu}(\omega) \\ \Phi_{ue}(\omega) & \sigma_e^2 \end{array} \right]^{-1}. \tag{10.56}$$

With the relation $\Phi_{ue} = -CS_0 H_0 \sigma_e^2$ and using the notation

$$\Phi_u(\omega) = \Phi_u^r(\omega) + \Phi_u^e(\omega) \tag{10.57}$$

with

$$\Phi_u^r(\omega) = |S_0(e^{i\omega})|^2 \Phi_r(\omega) \tag{10.58}$$

$$\Phi_u^e(\omega) = |C(e^{i\omega})S_0(e^{i\omega})H_0(e^{i\omega})|^2 \sigma_e^2 \tag{10.59}$$

and using the fact that $\Phi_u \sigma_e^2 - |\Phi_{ue}|^2 = \sigma_e^2 \Phi_u^r$ it follows that

$$cov\left(\begin{array}{c} \hat{G} \\ \hat{H} \end{array} \right) \sim \frac{n}{N} \frac{\Phi_v}{\Phi_u^r} \cdot \left[\begin{array}{cc} 1 & (CS_0 H_0)^* \\ CS_0 H_0 & \dfrac{\Phi_u}{\sigma_e^2} \end{array} \right]. \tag{10.60}$$

As a result the variance expressions for $\hat{G}$ and $\hat{H}$ become:

$$cov(\hat{G}) \quad \sim \quad \frac{n}{N} \frac{\Phi_v}{\Phi_u^r} = \frac{n}{N} \frac{\Phi_v}{\Phi_u} \left[1 + \frac{\Phi_u^e}{\Phi_u^r} \right] \tag{10.61}$$

$$cov(\hat{H}) \quad \sim \quad \frac{n}{N} \frac{\Phi_v}{\sigma_e^2} \frac{\Phi_u}{\Phi_u^r} = \frac{n}{N} \frac{\Phi_v}{\sigma_e^2} \left[1 + \frac{\Phi_u^e}{\Phi_u^r} \right]. \tag{10.62}$$

The case of an open-loop experimental situation now appears as a special situation in which $\Phi_u^e = 0$, $\Phi_u^r = \Phi_u$, and $C = 0$, and thus leading to the well known open-loop expressions as already given in (4.152),(4.153):

$$cov(\hat{G}) \sim \frac{n}{N} \frac{\Phi_v}{\Phi_u} \quad cov(\hat{H}) \sim \frac{n}{N} \frac{\Phi_v}{\sigma_e^2}. \tag{10.63}$$

The closed-loop expressions show that only the noisefree part u_r of the input signal contributes to variance reduction of the estimates. This implies that whenever the input signal of the process is limited in power, then only part of the input signal can be used to reduce the variance of a parameter estimate. If there is no input power limitation, one can of course always compensate for this "loss" of variance-reducing signal by adding a reference signal with an increased power.

The given variance expressions are restricted to the situation that $S \in \mathcal{M}$ and that both $G(\theta)$ and $H(\theta)$ are identified; they do not hold true for the situation $G_0 \in \mathcal{G}$, $S \notin \mathcal{M}$.

	Direct method
Consistency $(G(q, \hat{\theta}_N), H(q, \hat{\theta}_N))$	$+$
Consistency $G(q, \hat{\theta}_N)$	$-$
Tunable bias	$-$
Fixed model order	$+$
Unstable plants	$\square$
$(G(q, \hat{\theta}_N), C)$ stable	$-$
C assumed known	no

Table 10.2: Properties of direct method for closed-loop identification

Remark 10.3.7 *The situation of estimating a plant model in the situation $G_0 \in \mathcal{G}$ and having a fixed and correct noise model $H_* = H_0$ is considered in Ljung (1993). Using the fact that*

$$cov \; \hat{\theta}_N = \frac{\sigma_e^2}{N}[E\psi(t)\psi^T(t)]^{-1} \tag{10.64}$$

where $\psi(t)$ is the negative gradient of the prediction error (10.33), this leads to

$$cov(\hat{G}) \sim \frac{n}{N}\frac{\Phi_v}{\Phi_u} \tag{10.65}$$

as it is immaterial whether the input spectrum is a result of open loop or closed loop operation. Note that this expression gives a smaller variance than the situation in which both G and H are estimated, and that in this (unrealistic) case the total input power contributes to a reduction of the estimate variance.

Remark 10.3.8 *The asymptotic-in-order expression for the asymptotic variance of the estimated plant model G shows that only the reference part of the input signals is used for variance reduction, cf. the factor Φ_{u_r} in the denominator of (10.61). This is particularly due to the fact that also the order of the noise model is supposed to tend to infinity. In this situation all information in the process noise is employed for estimating the noise model. A reduced order noise model is crucial for utilizing the process noise signal also for reducing the variance of the G-estimate, as shown in Remark 10.3.7.*

Remark 10.3.9 *If no external reference signal is present, then $\Phi_{u_r}(\omega) = 0$, and expressions (10.61) and (10.62) show a zero denominator, leading to infinite covariance matrices. This seems to be in conflict with Corollary 10.3.4 where it was shown that also without external excitiaton the direct method is able to consistently identify the model. However the additional condition for this result is that the controller should have a sufficiently high order. Since the analysis leading to (10.61) and (10.62) is asymptotic-in-order, the controller can never satisfy this condition.*

10.3.7 Overview of properties

In Table 10.2 an overview is given of the properties of the direct identification approach in closed-loop identification.
Concerning the property of handling unstable plants, the limitation here is that model sets are restricted to be uniformly stable, as specified in definition 4.4.2. Because of their specific

structure, only ARX and ARMAX model sets can provide uniformly stable predictors while the models themselves are unstable. In order to verify this, note that for an ARMAX model set, the predictor filter is given by:

$$
\begin{aligned}
\hat{y}(t|t-1;\theta) &= H(q,\theta)^{-1}G(q,\theta)u(t) + (1 - H(q,\theta)^{-1})y(t) & (10.66) \\
&= \frac{B(q,\theta)}{C(q,\theta)}u(t) + (1 - A(q,\theta))y(t). & (10.67)
\end{aligned}
$$

This predictor filter (and its derivative) are uniformly stable for parametrizations where the roots of $C(z,\theta)$ are restricted to the interior of the unit circle, i.e. $|z| \leq 1$; no restriction has to be laid upon the roots of $A(z,\theta)$.

As a result consistent identification of unstable input/output plants G_0 is possible provided that one is dealing with both a data generating system and a parametrized model set in one and the same ARX or ARMAX form. This conditioned result is indicated in Table 10.2 by the symbol $\square$.

Note that the overview of properties refers to the general direct method only. For the specific approach based on the tailor-made parametrization, as presented in section 10.6 some of the properties are different.

10.4   Indirect identification

As an alternative to the direct identification approach, the method of indirect identification avoids to take measurement data from within the closed loop. This implies that it does not use measurement data of the input signal, but it bases its estimate on measurements of y and r only.

Again, we assume that (at least) one of the external signals r_1 or r_2 is measurable, leading to a measurable component r, as used before.

The general indirect method consists of two steps:

1. Identify the closed loop system using r as input and y as output, using a standard (open loop) model set;

2. Determine the open loop system parameters from the closed loop model obtained in step 1, using knowledge of the controller.

The first step of the procedure is a standard open-loop type of identification problem, as the reference signal r is assumed to be uncorrelated with the disturbance signal e.

Employing (10.5) for the data generating system, it follows that the system that is subject of identification in the first step is given by:

$$
y(t) = S_0(q)[G_0(q)r(t) + H_0(q)e(t)]. \tag{10.68}
$$

This system is going to be identified with a model set, determined by

$$
\mathcal{M}: \quad y(t) = G_c(q,\theta)r(t) + H_c(q,\theta)\varepsilon(t) \tag{10.69}
$$

with $\theta \in \Theta$, where G_c and H_c are simply parametrized in terms of polynomial fractions as is common in the open loop situation.

This implies that one is actually identifying the system transfers $S_0 G_0$ and $S_0 H_0$.

Under the usual conditions, a prediction error method can provide a consistent estimate, i.e. $G_c(e^{i\omega}, \theta^*) = S_0(e^{i\omega})G_0(e^{i\omega})$ and $H_c(e^{i\omega}, \theta^*) = S_0(e^{i\omega})H_0(e^{i\omega})$ provided that the model set is chosen appropriately and the input signal (r) is sufficiently exciting.

In the second step, in order to arrive at an estimate of $G_0(q)$ and $H_0(q)$ one has to solve the following equations:

$$\frac{G(q, \hat{\rho})}{1 + G(q, \hat{\rho})C(q)} = G_c(q, \hat{\theta}_N) \tag{10.70}$$

$$\frac{H(q, \hat{\rho})}{1 + G(q, \hat{\rho})C(q)} = H_c(q, \hat{\theta}_N) \tag{10.71}$$

with respect to the parameter vector ρ which parametrizes the open loop plant. The estimated model from (10.70),(10.71) can be written as

$$G(q, \hat{\rho}) = \frac{G_c(q, \hat{\theta}_N)}{1 - C(q)G_c(q, \hat{\theta}_N)} \tag{10.72}$$

$$H(g, \hat{\rho}) = \frac{H_c(q, \hat{\theta}_N)}{1 - C(q)G_c(q, \hat{\theta}_N)} \tag{10.73}$$

provided of course that the right-hand inverses exist.

Let us assume that the estimates of step 1 are the asymptotic (consistent) estimates, so that $G_c(q, \hat{\theta}_N) = S_0(q)G_0(q)$ and $H_c(q, \hat{\theta}_N) = S_0(q)H_0(q)$.

In that situation it can be verified that $G(q, \hat{\rho}) = G_0(q)$ and $H(q, \hat{\rho}) = H_0(q)$.

When comparing this method with the direct approach, conditions for arriving at a consistent estimate are rather similar. However this does not mean that both methods give the same results in the finite sample case or that they are equally easy to apply. An advantage of the direct approach is that only one step is required. For the indirect approach it is not obvious how the equations (10.70), (10.71) should be solved for models $G(q, \rho), H(q, \rho)$ of prespecified complexity (McMillan degree). Note that this second step is not an identification-type problem. In the finite sample case there may very well be no exact solution with respect to ρ within a specific desired model class. It is then an open question in what sense these "identities" should be "solved". Accuracy of the identified model can easily be lost if the identities are not solved exactly.

On the other hand, estimates for the open loop characteristics can directly be calculated by way of equations (10.72) and (10.73). In this situation the McMillan degree of the resulting models will increase; the McMillan degree of G will generally become equal to the sum of McMillan degrees of $G_c(q, \hat{\theta}_N)$ and $C(q)$, as can be verified from (10.72).

The indirect method can also deal with the situation $S \notin \mathcal{M}$, $G_0 \in \mathcal{G}$ (cf. problem (b)). This can be understood as follows. If in the first step we identify $G_c(q, \hat{\theta}_N)$ consistently, then (10.72) shows that we arrive at a consistent estimate of G_0. This is dependent on neither the closed-loop nor the open loop noise model.

Concerning the asymptotic bias expression, the first step of the indirect identification delivers an asymptotic criterion:

$$\theta^* = \arg\min_\theta \frac{1}{2\pi} \int_{-\pi}^{\pi} \left| \frac{G_0(e^{i\omega})}{1 + C(e^{i\omega})G_0(e^{i\omega})} - G_c(e^{i\omega}, \theta) \right|^2 \frac{|L(e^{i\omega})|^2 \Phi_r(\omega)}{|H_c(e^{i\omega}, \eta^*)|^2} d\omega \tag{10.74}$$

	Indirect method
Consistency $(G(q,\hat{\theta}_N), H(q,\hat{\theta}_N))$	$+$
Consistency $G(q,\hat{\theta}_N)$	$+$
Tunable bias	$+$
Fixed model order	$-$
Unstable plants	$+$
$(G(q,\hat{\theta}_N), C)$ stable	$\square$
C assumed known	yes

Table 10.3: Properties of indirect method for closed-loop identification

provided that an independent parametrization of G_c and H_c is applied, and L is the prediction error prefilter. If in the second step of the procedure one restricts to exact solutions to the equation (10.72), then the resulting (asymptotic) parameter estimate is characterized by

$$\rho^* = \arg\min_{\theta} \frac{1}{2\pi} \int_{-\pi}^{\pi} \left| \frac{G_0(e^{i\omega})}{1 + C(e^{i\omega})G_0(e^{i\omega})} - \frac{G(e^{i\omega}, \rho)}{1 + C(e^{i\omega})G(e^{i\omega}, \rho)} \right|^2 \frac{|L(e^{i\omega})|^2 \Phi_r(\omega)}{|H_c(e^{i\omega}, \eta^*)|^2} d\omega \tag{10.75}$$

showing that the bias expression becomes explicitly tunable.

The overview of properties of this indirect method is given in Table 10.3.

The indirect method has no problems in dealing with unstable plants. This is due to the fact that the closed-loop transfer functions G_c and H_c will be stable objects, even if G_0 is unstable.

It will be shown later in section 10.9 that if the controller C is stable, then the indirect method provides (approximate) plant estimates $G(q,\hat{\theta}_N)$ that are guaranteed to be stabilized by C. This explains the symbol $\square$ in the table of properties (Table 10.3).

Extension of the method to the multivariable case is considered in Van den Hof and De Callafon (1996), while in Codrons et al. (2002) particular attention is given to the situation of unstable and non-minimum phase controllers.

10.5 Joint input-output identification

10.5.1 General setting

In the so-called joint input-output identification method, the situation is considered that an external excitation signal r is present, but not measurable. Knowledge of the controller $C(q)$ is not assumed available.

Consider the situation of a data-generating system as characterized by (10.5), (10.6), where r is a stationary stochastic process, having a (innovations) representation

$$r(t) = K_0(q)w(t) \tag{10.76}$$

with $K_0(z)$ a rational transfer function, with $K_0(z)$ and $K_0(z)^{-1}$ monic, proper and stable, and $\{w(t)\}$ a sequence of independent, identically distributed, zero mean random variables (white noise).

In the joint i/o approach, as discussed e.g. in Ng *et al.* (1977), Anderson and Gevers (1982) and Söderström and Stoica (1989), the combined signal $(y(t)\ u(t))^T$ is considered as a multivariable time-series, having a rational spectral density, and as a result there has to exist a (innovations) representation, satisfying

$$\begin{bmatrix} u(t) \\ y(t) \end{bmatrix} = \Upsilon_0(q) \begin{bmatrix} e_1(t) \\ e_2(t) \end{bmatrix} \tag{10.77}$$

with $(e_1(t)\ e_2(t))^T$ a white noise process with covariance matrix Λ_0, and $\Upsilon_0(z)$ a rational transfer function matrix with $\Upsilon_0(z)$ as well as $\Upsilon_0(z)^{-1}$ monic, proper and stable.

Since y and u are available from measurements, a model for (10.77) can also be estimated, applying any prediction error identification method. This situation actually refers to the open loop identification of a model without a measurable input term, i.e. only the identification of a (multivariable) noise model $H(q, \theta)$.

Using an appropriate prediction error identification method, as in the open loop case, it is possible to construct a consistent estimate $\Upsilon(z, \hat{\theta}_N)$ of $\Upsilon_0(z)$.

In the second step of the procedure estimates of G_0, H_0, C_0, K_0 and Λ_0 are then derived from (the estimated) Υ_0, where C_0 refers to the controller present in the data generating system.

This joint i/o method not only estimates the system dynamics G_0 and H_0, but also delivers estimates of the controller C_0, the input-shaping filter K_0 and the input noise covariance Λ_0.

We will consecutively discuss the several steps in this procedure.

10.5.2   An innovations representation of the closed loop system

First we have to construct an innovations representation of the real data generating system, as represented in (10.77).

Manipulating the system's equations (10.5),(10.6), and (10.76), shows that (arguments are suppressed for brevity),

$$\begin{bmatrix} u(t) \\ y(t) \end{bmatrix} = \begin{bmatrix} S_0 K_0 & -S_0 C_0 H_0 \\ S_0 G_0 K_0 & S_0 H_0 \end{bmatrix} \begin{bmatrix} w(t) \\ e(t) \end{bmatrix} \tag{10.78}$$

Note that the transfer function in this expression does not satisfy the conditions of an innovations representation, as e.g. it is not necessarily monic. In order for the transfer function to be monic it should tend to the identity matrix I for $z \to \infty$. With Assumption 10.1.4 it follows that $G_0(\infty) = 0$ and consequently $S_0(\infty) = 1$. Moreover $H_0(\infty) = K_0(\infty) = 1$, which shows that in (10.78) the transfer function for $z \to \infty$ tends to

$$\begin{bmatrix} 1 & -C_0(\infty) \\ 0 & 1 \end{bmatrix}$$

If we rewrite the transfer function in (10.78) as

$$\begin{bmatrix} S_0 K_0 & -S_0 C_0 H_0 \\ S_0 G_0 K_0 & S_0 H_0 \end{bmatrix} \begin{bmatrix} 1 & -C_0(\infty) \\ 0 & 1 \end{bmatrix}^{-1} \begin{bmatrix} 1 & -C_0(\infty) \\ 0 & 1 \end{bmatrix} \tag{10.79}$$

we can write

$$\begin{bmatrix} u(t) \\ y(t) \end{bmatrix} = \Upsilon_0(q) \begin{bmatrix} w_1(t) \\ e(t) \end{bmatrix} \qquad \text{with} \tag{10.80}$$

$$\Upsilon_0(z) = \begin{bmatrix} S_0 K_0 & -C_0 H_0 S_0 \\ G_0 S_0 K_0 & H_0 S_0 \end{bmatrix} \begin{bmatrix} 1 & -C_0(\infty) \\ 0 & 1 \end{bmatrix}^{-1}$$

$$= \begin{bmatrix} S_0 K_0 & S_0 K_0 C_0(\infty) - S_0 C_0 H_0 \\ S_0 G_0 K_0 & S_0 H_0 + S_0 G_0 K_0 C_0(\infty) \end{bmatrix} \tag{10.81}$$

$$w_1(t) = w(t) - C_0(\infty) e(t) \tag{10.82}$$

By construction we have created the situation that $\Upsilon_0(\infty) = I$.
Moreover $(w_1(t)\ e(t))^T$ is a white noise process with covariance matrix

$$\Lambda_0 = \begin{bmatrix} \sigma_w^2 + C_0(\infty)^2 \sigma_e^2 & -C_0(\infty)\sigma_e^2 \\ -C_0(\infty)\sigma_e^2 & \sigma_e^2 \end{bmatrix} \tag{10.83}$$

The representation (10.81) is an innovations representation of $(u(t)\ y(t))^T$ under the additional condition that both $\Upsilon_0(z)$ and $\Upsilon_0(z)^{-1}$ are stable.
Stability of $\Upsilon_0(z)$ is assured if S_0, $S_0 C_0$ and $S_0 C_0 H_0$ are stable, which holds true because of the stability assumptions on the closed loop system.

With the matrix inversion lemma (see e.g. Kailath, 1980), we can construct the inverse of $\Upsilon_0(z)$ as,

$$\Upsilon_0(z)^{-1} = \begin{bmatrix} 1 & C_0(\infty) \\ 0 & 1 \end{bmatrix} \begin{bmatrix} K_0^{-1} & K_0^{-1} C_0 \\ -H_0^{-1} G_0 & H_0^{-1} \end{bmatrix} \tag{10.84}$$

Under additional stability assumptions on $H_0(z)^{-1} G_0(z)$ and $K_0(z)^{-1} C_0(z)$ this inverse is stable too, and consequently the representation (10.81) is the unique innovations representation of $(u(t)\ y(t))^T$.

10.5.3   Consistency result

As mentioned in section 10.5.1, it is possible by applying a standard (open loop) prediction error identification method, to identify a consistent estimate $\hat{\Upsilon}(z)$ of $\Upsilon_0(z)$ which also results in a consistent estimate $\hat{\Lambda}$ of Λ_0, the noise covariance matrix.
The question now is, under which conditions the available estimates $\hat{\Upsilon}(z)$, $\hat{\Lambda}$ induce unique and consistent estimates of the data generating system (G_0, H_0) in the second step of the procedure.

To this end let us parametrize $G(z,\theta)$, $H(z,\theta)$, $C(z,\theta)$, $\sigma_w(\theta)$ and $\sigma_e(\theta)$ with $\theta \in \Theta$ leading to a parametrized $\Upsilon(z,\theta)$ and $\Lambda(\theta)$ having a structure corresponding to (10.81), (10.83).
Suppose that there exists a $\theta_0 \in \Theta$ such that $\Upsilon(z,\theta_0) = \Upsilon_0(z)$ and $\Lambda(\theta_0) = \Lambda_0$.
If $\hat{\Upsilon}(z) = \Upsilon_0(z)$ and $\hat{\Lambda} = \Lambda_0$, then

$$\begin{rcases} \Upsilon(z,\theta^*) = \hat{\Upsilon}(z) \\ \Lambda(\theta^*) = \hat{\Lambda} \end{rcases} \Rightarrow \begin{cases} G(z,\theta^*) = G_0(z),\ H(z,\theta^*) = H_0(z),\ C(z,\theta^*) = C_0(z), \\ K(z,\theta^*) = K_0(z),\ \sigma_e(\theta^*) = \sigma_e,\ \sigma_w(\theta^*) = \sigma_w \end{cases}$$

$$\tag{10.85}$$

For the formal statement and proof of this result, the reader is referred to the literature mentioned before.

This result for the joint i/o method shows similar aspects as the indirect identification method. Once the first step in the procedure has provided a consistent estimate, it is possible to obtain a consistent estimate of the data generating system in the second step.

	Joint i/o method
Consistency $(G(q,\hat{\theta}_N), H(q,\hat{\theta}_N))$	$+$
Consistency $G(q,\hat{\theta}_N)$	$-$
Tunable bias	$-$
Fixed model order	$-$
Unstable plants	$+$
$(G(q,\hat{\theta}_N), C)$ stable	$-$
C assumed known	no

Table 10.4: Properties of joint i/o-method for closed-loop identification

However, note that whenever the first step has not provided an exact description, in this case of $\Upsilon_0(z)$ and Λ_0, then the second step in the procedure becomes an approximation, for which it is hard to draw any conclusions on the resulting estimates.

Note that this joint i/o method allows the identification of not only the data generating system (G_0, H_0) but also of the controller C_0.
Apparently this joint i/o method is able to deal with problem (a) of the problems formulated in section 10.1.3. Its properties are summarized in Table 10.4.

10.6   Method with tailor-made parametrization

Indirect identification requires two separate steps: (1) identification of the closed-loop system, and (2) recalculation of the open-loop plant model. The two steps can be combined into one, by using a tailor-made parametrization for the closed-loop system. This means that we employ knowledge of the closed-loop structure of the configuration, and knowledge of the controller into the parametrization of the closed-loop system.
Stated differently, the closed-loop system is identified by using parameters of the open-loop plant G_0.
Consider the situation that an external signal r is available and measurable, that is persistently exciting of a sufficiently high order, and suppose that we have knowledge about the controller $C(q)$.
An output error one-step-ahead predictor for the dynamical system having r as input and y as output, will have the form

$$\hat{y}(t|t-1;\theta) = M(q,\theta)r(t) \tag{10.86}$$

with $M(q,\theta)$ the parametrized transfer function between r and y. However since we know the structure of this transfer function, we can parametrize $M(q,\theta)$ in terms of the original parameters θ of the plant $G(q,\theta)$, by writing

$$M(q,\theta) = G(q,\theta)S(q,\theta) = \frac{G(q,\theta)}{1 + G(q,\theta)C(q)} \tag{10.87}$$

which leads to the identification problem $\hat{\theta}_N = \arg\min_{\theta \in \Theta} V_N(\theta, Z^N)$ with

$$\varepsilon(t,\theta) = y(t) - \frac{G(q,\theta)}{1 + G(q,\theta)C(q)}r(t) \tag{10.88}$$

We have applied a tailor-made parametrization of the model, actually using knowledge of the fact that the data is obtained from closed loop experiments, and using the knowledge of the controller $C(q)$.

The identification problem sketched above will also require a tailor-made optimization algorithm, as the model set is parametrized in a structure that is different from the standard (open-loop) model sets.

For this identification method, we can also provide again a frequency domain expression for the asymptotic identification criterion $\bar{V}(\theta)$. By substituting the expression (10.5) for $y(t)$ in (10.88) and determining the spectrum of ε, it follows that

$$\bar{V}(\theta) = \frac{1}{2\pi} \int_{-\pi}^{\pi} \{|S_0(e^{i\omega})G_0(e^{i\omega}) - S(e^{i\omega},\theta)G(e^{i\omega},\theta)|^2 \Phi_r(\omega) + |S_0(e^{i\omega})H_0(e^{i\omega})|^2 \Phi_e(\omega)\} d\omega \tag{10.89}$$

Since the second term in the integrand is parameter-independent this leads to

$$\theta^* = \arg\min_{\theta\in\Theta} \frac{1}{2\pi} \int_{-\pi}^{\pi} |S_0(e^{i\omega})G_0(e^{i\omega}) - S(e^{i\omega},\theta)G(e^{i\omega},\theta)|^2 \Phi_r(\omega) d\omega \tag{10.90}$$

By writing (arguments are suppressed for simplicity),

$$S_0 G_0 - SG = \frac{G_0}{1+G_0C} - \frac{G}{1+GC} = \frac{G_0(1+GC) - G(1+G_0C)}{(1+G_0C)(1+GC)} = \frac{G_0 - G}{(1+G_0C)(1+GC)}$$

it follows that

$$\theta^* = \arg\min_{\theta\in\Theta} \frac{1}{2\pi} \int_{-\pi}^{\pi} |S_0(e^{i\omega})[G_0(e^{i\omega}) - G(e^{i\omega},\theta)]S(e^{i\omega},\theta)|^2 \Phi_r(\omega) d\omega \tag{10.91}$$

It can be verified that whenever there exists a θ such that $G(q,\theta) = G_0(q)$ this choice will be a minimizing argument of the integral expression above, and moreover that, provided that r is persistently exciting of sufficient order, this solution will be unique. This leads to the following Proposition.

Proposition 10.6.1 *Let $\mathcal{S}$ be a data generating system and let Z^∞, consisting of signals r, u, y be a data sequence corresponding to Assumptions 4.7.1, 4.7.2, with $\{r(t)\}$ uncorrelated to $\{e(t)\}$. Let $\mathcal{M}$ be a uniformly stable model set, parametrized according to (10.88), and satisfying $G_0 \in \mathcal{G}$.*
If $\{r(t)\}$ is persistently exciting of a sufficiently high order, then

- *$G(e^{i\omega}, \hat{\theta}_N)$ is a consistent estimate of $G_0(e^{i\omega})$ for all ω, and*

- *there exists an explicit approximation criterion (10.91), characterizing $G(e^{i\omega}, \theta^*)$ being independent of $H_0(e^{i\omega})$.*

The proposition shows that this method can deal with problems (b)-(c) as formulated in the introduction section. However the price that has to be paid is that one has to deal with a complicated parametrized model structure (10.88), with its resulting computational burden.

An additional remark has to be made with respect to the requirement that the model set $\mathcal{M}$ should be uniformly stable. By definition 4.4.2 this requires that the considered

	Tailor-made
Consistency $(G(q,\hat{\theta}_N), H(q,\hat{\theta}_N))$	□
Consistency $G(q,\hat{\theta}_N)$	□
Tunable bias	+
Fixed model order	+
Unstable plants	+
$(G(q,\hat{\theta}_N), C)$ stable	+
C assumed known	yes

Table 10.5: Properties of closed-loop identification method with tailor-made parametrization. The indication □ points to the possible lack of connectedness of the parameter set.

parameter set Θ is connected. Now, in the given situation this is not trivially satisfied. When evaluating the model structure as given in (10.88) for the situation that $G(q,\theta)$ is parametrized as a common quotient of two polynomials with free coefficients, the region of θ for which the transfer function $\frac{G(q,\theta)}{1+C(q)G(q,\theta)}$ is stable can be composed of two (or more) disconnected regions. This implies that whenever a gradient method is started to optimize the identification criterion, from within one of the (disconnected) regions, one will never be able to arrive at a possible optimal estimate in one of the other regions.

An example illustrating this effect is given in figure 10.2, where the criterion function $V_N(\theta)$ is sketched for the situation of a constant plant $G_0 = 3.5$ controlled by a 7-th order controller, with white noise signals entering as reference signal and as disturbance. The plant is parametrized by one scalar parameter: $G(q,\theta) = \theta$.
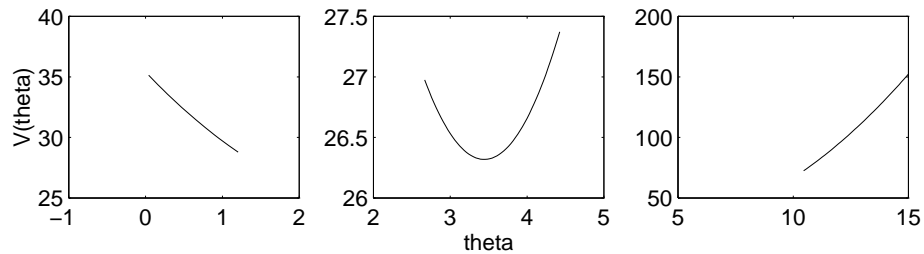
Figure 10.2: *Criterion function $V_N(\theta)$ for static model $G(q,\theta) = \theta$ for closed-loop identification with a tailor-made parametrization; $\theta_o = 3.5$.*

In this case there are three disconnected areas within $\Theta = \mathbb{R}$ that correspond to a stable closed-loop system. The parameter regions: $(-\infty, 0], [1.27, 2.64]$ and $[4.69, 9.98]$ lead to a unstable closed-loop system. If the nonlinear optimization is started in the region shown in the left figure or the right figure, the resulting parameter estimate will be on the boundary of stability, and will not correspond to the global minimum of the criterion function. The latter situation can only occur for the connected region shown in the middle figure.

The problem with possible lack of connectedness of the parameter region, can be avoided by identifying models that are of sufficiently high order. It is shown in Van Donkelaar and Van den Hof (2000), that a sufficient condition for connectedness of the parameter set is that the model order of $G(q,\theta)$ is at least as big as the order of the controller.

The tailor-made parametrization applied to an instrumental variable identification criterion is considered in Gilson and Van den Hof (2001).

10.7   Two-stage method

A two-stage identification method is introduced in an attempt to deal with all identification problems (a)-(c), while also handling model sets of models with a fixed and prespecified McMillan degree. This method avoids complicated parametrized model sets, as are required in the direct method discussed in section 10.3.5, and does not need a prior knowledge about the dynamics of the controller $C(q)$. It it composed of two consecutive identification steps that can be performed with standard (open loop) methods.
We consider the closed loop experimental situation as discussed before, and similar to (some of the) previous methods we assume that there is available a measurable and persistently exciting external signal r that is uncorrelated with the noise e.
The two-stage method is introduced in Van den Hof and Schrama (1993).

The system relation (10.6) in the closed loop case shows that the input signal satisfies:

$$u(t) = S_0(q)r(t) - S_0(q)C(q)H_0(q)e(t) \tag{10.92}$$

Since r and e are uncorrelated signals, and u and r are available from measurements, it follows that we can identify the sensitivity function S_0 in an open loop way.
To this end, consider a model set, determined by

$$u(t) = S(q,\beta)r(t) + R(q,\gamma)\varepsilon_u(t) \qquad \beta \in B \subset \mathbb{R}^{d_\beta}; \ \ \gamma \in \Gamma \subset \mathbb{R}^{d_\gamma} \tag{10.93}$$

where $\varepsilon_u(t)$ is the one step ahead prediction error of $u(t)$, and S and R are parametrized independently, and the estimate $S(q,\hat{\beta}_N)$ of $S_0(q)$ is determined by a least squares prediction error criterion based on $\varepsilon_u(t)$.
From the results on open loop identification, we know that we can identify $S_0(q)$ consistently irrespective of the noise term in (10.92). Consistency of $S(q,\hat{\beta}_N)$ can of course only be reached when $S_0 \in \mathcal{T} := \{S(q,\beta) \mid \beta \in B\}$.

In the second step of the procedure, we employ the other system relation (10.5),

$$y(t) = G_0(q)S_0(q)r(t) + S_0(q)H_0(q)e(t) \tag{10.94}$$

which we can rewrite as:

$$y(t) = G_0(q)u^r(t) + S_0(q)H_0(q)e(t) \tag{10.95}$$
$$u^r(t) := S_0(q)r(t) \tag{10.96}$$

Since u^r and e are uncorrelated, it follows from (10.95) that when u^r would be available from measurements, G_0 could be estimated in an open loop way, using the common open-loop techniques. In stead of knowing u^r, we have an estimate of this signal available through

$$\hat{u}_N^r(t) = S(q,\hat{\beta}_N)r(t) \tag{10.97}$$

Accordingly we rewrite (10.95) as

$$y(t) = G_0(q)\hat{u}_N^r(t) + S_0(q)H_0(q)e(t) + G_0(q)[S_0(q) - S(q,\hat{\beta}_N)]r(t) \tag{10.98}$$

The second step in the procedure consists of applying a standard prediction error identification method, to a model set

$$y(t) = G(q, \theta)\hat{u}_N^r(t) + W(q, \eta)\varepsilon_y(t) \tag{10.99}$$

with $G(q, \theta)$, $W(q, \eta)$ parametrized independently, $\theta \in \Theta \subset \mathbb{R}^{d_\theta}$, $\eta \in \Omega \subset \mathbb{R}^{d_\eta}$, and a least squares identification criterion determining

$$\left[\begin{array}{c} \hat{\theta}_N \\ \hat{\eta}_N \end{array} \right] = \arg\min_{\theta, \eta} \frac{1}{N} \sum_{t=1}^{N} \varepsilon_y(t)^2. \tag{10.100}$$

The resulting transfer function estimates are then obtained by

$$\begin{aligned} G(q, \hat{\theta}_N) \qquad &\text{and} \\ H(q, \hat{\eta}_N) \;\; &= \;\; W(q, \hat{\eta}_N)S(q, \hat{\beta}_N)^{-1} \end{aligned} \tag{10.101}$$

where the latter equation stems from the fact that the noise model $W(q)$ is a model for the disturbance filter $S_0 H_0$ rather than for H_0 only.

Note that when applying this prediction error identification with model set (10.99), we could obtain consistency of $G(q, \hat{\theta}_N)$ and $H(q, \hat{\eta}_N)$ if the data generating system (10.98) would be an open loop system. However due to the fact that in this system relation we now consider the noise term to consist of two terms, one dependent on e and one dependent on r, the data generating system is no longer an open loop system. However, the noise term that is correlated to r will vanish as the estimated sensitivity function in the first step approaches $S_0(q)$.

This leads to the following Proposition.

Proposition 10.7.1 *Let $\mathcal{S}$ be a data generating system and consider two independent data sequences containing signals r, u, y corresponding to Assumptions 4.7.1, 4.7.2, with $\{r(t)\}$ being uncorrelated with $\{e(t)\}$.*

Consider the two-stage identification procedure presented in this section with least squares identification criteria and uniformly stable model sets $\mathcal{T}$ (10.93) in the first step and $\mathcal{M}$ (10.99) in the second step, let $\{r(t)\}$ be persistently exciting of a sufficiently high order, and let the two steps of the procedure be applied to the two independent data sequences of the process.

If $S_0 \in \mathcal{T}$ and $G_0 \in \mathcal{G}$ then $G(e^{i\omega}, \hat{\theta}_N) \to G_0(e^{i\omega})$, for all ω, with probability 1 as $N \to \infty$.

Proof: The proof is given in Van den Hof and Schrama (1993). The two independent data sequences are taken in order to guarantee that the estimated sensitivity function in the first step - and thus the simulated noise-free input signal for the second step - is uncorrelated to the noise disturbance in the second step. □

As a result of this Proposition this method is able to deal with problem (b), the consistent identification of $G_0(q)$, irrespective of the modelling of the noise disturbance on the data. Note that for the identification of the sensitivity function in the first step of the procedure, we can simply apply a (very) high order model. We will only use the estimate $S(q, \hat{\beta}_N)$ to simulate $\hat{u}_N^r(t)$. Of course considerations of variance may restrict the model order to be used. A block diagram, indicating the recasting of the closed loop problem into two open loop problems, is sketched in Figure 10.3.
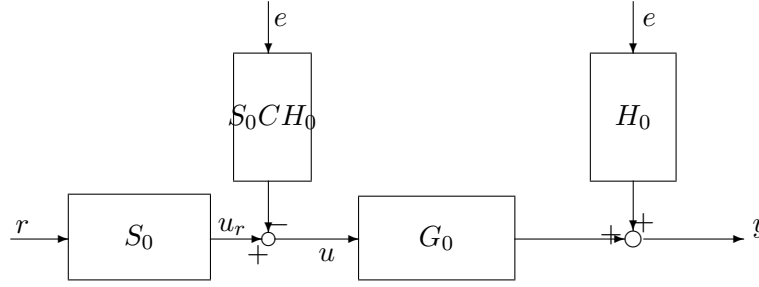
Figure 10.3: Block diagram of closed loop system, showing intermediate signal u_r

Additionally, this method also appears to be able to treat problem (c), the explicit characterization of the asymptotic model in the case that $G_0 \notin \mathcal{G}$. This will be clarified now.

The above Proposition can be extended to also include consistency of the noise model $H(q, \hat{\eta}_N)$.

In the case that we accept undermodelling in the second step of the procedure, $(G_0 \notin \mathcal{G})$, the bias distribution of the asymptotic model can be characterized. As the second step in this procedure is simply an open-loop type identification problem, the expression for the asymptotic bias distribution, as derived for the open loop situation, can simply be applied. This leads to the following result.

Proposition 10.7.2 *Consider the situation of Proposition 10.7.1.*
If $S_0 \in \mathcal{T}$, and if in step 2 of the identification procedure, determined by (10.99), (10.100), a fixed noise model is used, i.e. $W(q, \eta) = W_*(q)$, then $\hat{\theta}_N \to \theta^*$ with probability 1 as $N \to \infty$, with:

$$\theta^* = \arg \min_\theta \int_{-\pi}^{\pi} |G_0(e^{i\omega}) - G(e^{i\omega}, \theta)|^2 \frac{|S_0(e^{i\omega})|^2 \Phi_r(\omega)}{|W_*(e^{i\omega})|^2} \, d\omega \tag{10.102}$$

In this situation of approximate modelling of G_0, the asymptotic estimate can be characterized by the explicit approximation criterion (10.102). Note that in this expression the spectrum of the input signal now is represented by $\Phi_{u_r}(\omega) = |S_0(e^{i\omega})|^2 \Phi_r(\omega)$. It is remarkable, and at the same time quite appealing, that in this closed loop situation, the approximation of G_0 is obtained with an approximation criterion that has the sensitivity function S_0 of the closed loop system as a weighting function in the frequency domain expression (10.102). The fixed noise model $W_*(q)$ can be used as a design variable in order to "shape" the bias distribution (10.102) to a desired form.

An even more general result is formulated in the following proposition, dealing also with the situation that $S_0 \notin \mathcal{T}$.

Proposition 10.7.3 *Consider the situation of Proposition 10.7.1.*
If both in step 1 and step 2 of the identification procedure fixed noise models are used, i.e. $R(q, \gamma) = R_*(q)$ and $W(q, \eta) = W_*(q)$, then $\hat{\theta}_N \to \theta^*$ with probability 1 as $N \to \infty$, with:

$$\theta^* = \arg \min_\theta \int_{-\pi}^{\pi} |G_0(e^{i\omega}) S_0(e^{i\omega}) - G(e^{i\omega}, \theta) S(e^{i\omega}, \beta^*)|^2 \frac{\Phi_r(\omega)}{|W_*(e^{i\omega})|^2} \, d\omega \tag{10.103}$$
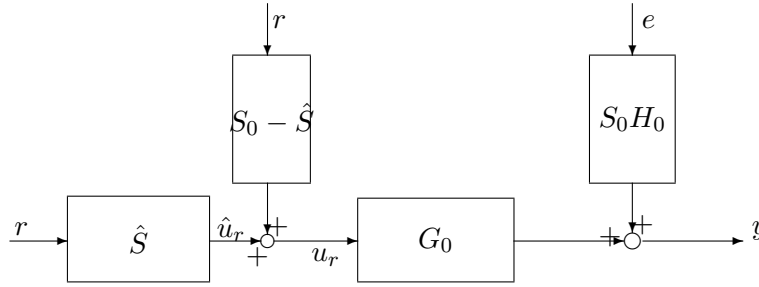
Figure 10.4: Identification problem in second step of the procedure

and

$$\beta^* = \arg \min_\beta \int_{-\pi}^{\pi} |S_0(e^{i\omega}) - S(e^{i\omega}, \beta)|^2 \frac{\Phi_r(\omega)}{|H_*(e^{i\omega})|^2} \, d\omega \qquad (10.104)$$

Proposition 10.7.3 shows that even if in both steps of the procedure non-consistent estimates are obtained, the bias distribution of $G(q, \theta^*)$ is characterized by a frequency domain expression which now becomes dependent on the identification result from the first step (cf. (10.104)), but that still is not dependent on noise disturbance terms.

Remark 10.7.4 *Note that in (10.103) the integrand expression can be rewritten, using the relation:*

$$G_0(e^{i\omega})S_0(e^{i\omega}) - G(e^{i\omega}, \theta)S(e^{i\omega}, \beta^*) =$$

$$= [G_0(e^{i\omega}) - G(e^{i\omega}, \theta)]S_0(e^{i\omega}) + G(e^{i\omega}, \theta)[S_0(e^{i\omega}) - S(e^{i\omega}, \beta^*)] \qquad (10.105)$$

which shows how an error made in the first step affects the estimation of G_0. If $S(q, \beta^*) = S_0(q)$ then (10.103) reduces to (10.102). If the error made in the first step is sufficiently small it will have a limited effect on the final estimate $G(q, \theta^*)$. This effect is also illustrated in the block diagram of Figure 10.4.

Note that the results presented in this section show that a consistent estimation of the sensitivity function S_0 is not even necessary to get a good approximate identification of the transfer function G_0. Equations (10.103) and (10.105) suggest that as long as the error in the estimated sensitivity function is sufficiently small, the i/o transfer function can be identified accurately. In this respect one could also think of applying an high order FIR (finite impulse response) model structure in the first step, having a sufficient polynomial degree in order to describe the essential dynamics of the sensitivity function. This model structure will be applied in the simulation example described later on.

Example 10.7.5 *Simulation example.*
We will now present a simulation example that illustrates this two-stage method.
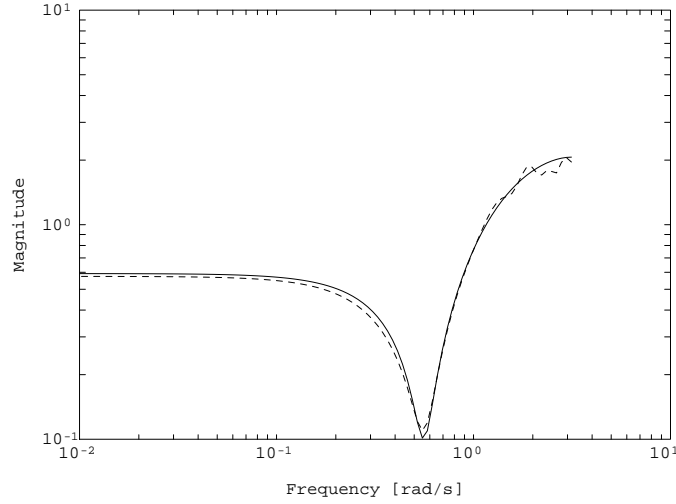
Figure 10.5: Bode amplitude plot of exact sensitivity function S_0 (solid line) and estimated sensitivity function $S(q, \hat{\beta}_N)$ (dashed line).

We consider a linear system operating in closed loop according to figure 10.1, with

$$G_0 \quad = \quad \frac{1}{1 - 1.6q^{-1} + 0.89q^{-2}} \tag{10.106}$$

$$C \quad = \quad q^{-1} - 0.8q^{-2} \tag{10.107}$$

$$H_0 \quad = \quad \frac{1 - 1.56q^{-1} + 1.045q^{-2} - 0.3338q^{-3}}{1 - 2.35q^{-1} + 2.09q^{-2} - 0.6675q^{-3}} \tag{10.108}$$

The noise signal e and the reference signal r are independent unit variance zero mean random signals. The controller is designed in such a way that the closed loop transfer function $G_0 S_0$ has a denominator polynomial $(z - 0.3)^2$.

The two-stage identification strategy is applied to a data set generated by this closed loop system, using data sequences of length $N = 2048$.

In the first step, the sensitivity function is estimated by applying an FIR output error model structure, estimating 15 impulse response $(b-)$parameters:

$$S(q, \beta) = \sum_{k=0}^{14} \beta(k) q^{-k} \; ; \qquad R(q, \gamma) = 1 \tag{10.109}$$

Note that the real sensitivity function S_0 is a rational transfer function of order 4. The magnitude Bode plot of the estimated sensitivity function is depicted in figure 10.5, together with the exact one.

The estimate $S(q, \hat{\beta}_N)$ is used to reconstruct a noise free input signal $\hat{u}_N^r$ according to (10.97). Figure 10.6 shows this reconstructed input signal, compared with the real input $u(t)$ and the optimally reconstructed input signal $u^r(t) = S_0(q)r(t)$.
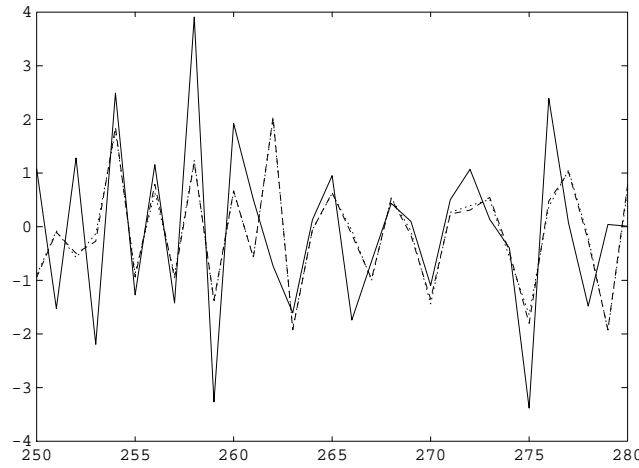
Figure 10.6: Simulated input signal u (solid line), non-measurable input signal u^r caused by r (dashed line) and reconstructed input signal $\hat{u}^r_N$ (dotted line)

Note that, despite of the severe noise contribution on the signal u caused by the feedback loop, the reconstruction of u^r by $\hat{u}^r_N$ is extremely accurate.

In the second step an output error model structure is applied such that $G_0 \in \mathcal{G}$, by taking

$$G(q, \theta) = \frac{b_0 + b_1 q^{-1} + b_2 q^{-2}}{1 + a_1 q^{-1} + a_2 q^{-2}} \quad and \ W(q, \eta) = 1 \tag{10.110}$$

Figure 10.7 shows the result of $G(q, \hat{\theta}_N)$. The magnitude Bode plot is compared with the second order model obtained from a one-step direct identification strategy in which an output error method is applied, using only the measurements of u and y. The results clearly show the degraded performance of the direct identification strategy, while the indirect method gives accurate results. This is also clearly illustrated in the Nyquist plot of the same transfer functions, as depicted in figure 10.8.

The degraded results of the direct identification method, here is caused by the fact that in this method the incorrect modelling of the noise (no noise model in the output error model structure) deteriorates the estimation of the i/o transfer function. The mechanism, which is (asymptotically) not present in the open-loop situation, becomes very apparent in the closed loop case. □

Remark 10.7.6 *Concerning the ability of the method to deal with unstable plants in the second step of the procedure, again uniform stability of the model set $\mathcal{M}$ will generally require $\mathcal{G}$ to be restricted to contain stable models only. Identification of unstable plants would be possible if the set of transfer functions $G_0, S_o H_0$ would share the same denominator, and thus could be modelled with an ARMAX model. Compare with figure 10.4 to see that this set of transfer functions describes the data generating system in the second step of the identification procedure. However for such a model structure used in the second step of the procedure, the tunability of the asymptotic bias expression would be lost. Incorporating restrictions on the input signal u_r might lead to appropriate conditions for handling unstable*
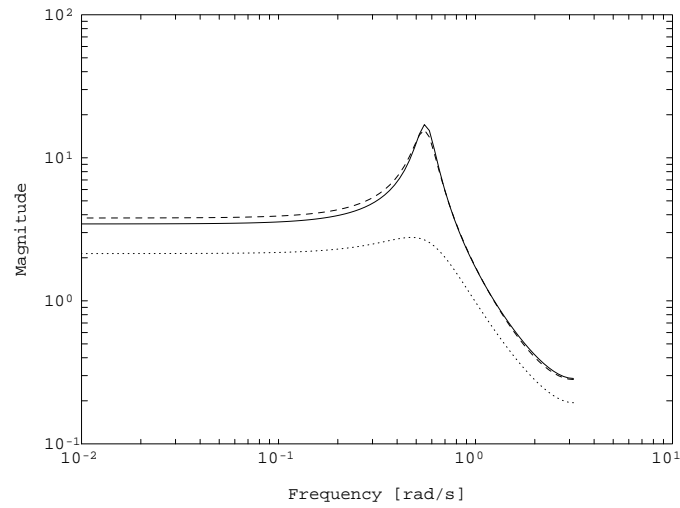
Figure 10.7: Bode amplitude plot of transfer function G_0 (solid line), output error estimate $G(q, \hat{\theta}_N)$ obtained from the two-stage method (dashed line), and output error estimate obtained from the direct method (dotted line). Order of the models is 2.
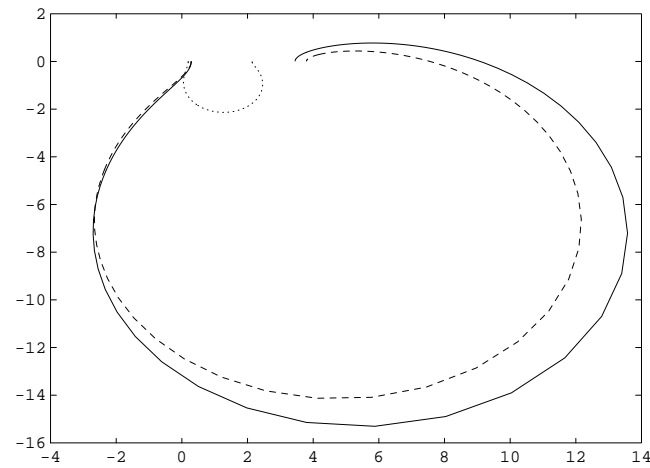

Figure 10.8: Nyquist curve of transfer function G_0 (solid line), output error estimate $G(q, \hat{\theta}_N)$ obtained from the two-stage method (dashed line), and output error estimate obtained from the direct method (dotted line). Order of the models is 2.

	Two-stage method
Consistency $(G(q, \hat{\theta}_N), H(q, \hat{\theta}_N))$	+
Consistency $G(q, \hat{\theta}_N)$	+
Tunable bias	+
Fixed model order	+
Unstable plants	−
$(G(q, \hat{\theta}_N), C)$ stable	−
C assumed known	no

Table 10.6: Properties of two-stage method for closed-loop identification

plants also. However this has not been shown yet. The asymptotic results of Propositions 10.7.2 and 10.7.3 remain valid also for unstable plants.

The properties of the two-stage method are summarized in Table 10.6.

One of the nice features of the two-stage method is that it does not require special purpose methods. The standard available methods and algorithms for open-loop identification can be used.

The method has been successfully applied to several industrial processes as a compact disc servo mechanism (De Callafon *et al.*, 1993), a sugar cane crushing plant (Partanen and Bitmead, 1993), and a crystallization plant (Eek *et al.*, 1996).

The two-stage method has been extended to deal also with nonlinear controllers. In the projection method (Forssell and Ljung, 2000) the first step in the procedure has been generalized to also include noncausal models.

10.8 Identification of coprime factorizations

10.8.1 General setting

Until now we have mainly considered the identification of stable plants controlled by (often) stable controllers. Application of the standard open loop identification tools forces us to consider model sets that are uniformly stable, in order to be able to arrive at the same asymptotic results (convergence, consistency) as in the open loop case. Thus, for application of standard open loop techniques to unstable (but controlled) systems the above mentioned asymptotic results can fail to provide consistent estimates.

However, especially in closed loop experimental conditions, it is a relevant question how to identify systems that are unstable. Besides, the restriction to stable controllers is also an unpleasant restriction, since many controllers in practice are unstable (e.g. PID-controllers, containing an integrator $(z - 1)^{-1}$).

In this section we will consider the problem of identifying an unstable system, which during the experiment is controlled by a possibly unstable controller.

First we recall the system relations (10.9),(10.10):

$$
\begin{align}
y(t) &= G_0(q)S_0(q)r(t) + W_0(q)H_0(q)e(t) \tag{10.111}\\
u(t) &= S_0(q)r(t) - C(q)W_0(q)H_0(q)e(t) \tag{10.112}
\end{align}
$$

Now the following strategy can be followed.

Based on relation (10.112), we can obtain an estimate $\hat{D}(q)$ of the transfer function S_0 between r and u, by applying standard open loop techniques and using measured signals r and u. If r is uncorrelated with e, this problem is an open-loop identification problem.

Based on relation (10.111), we can similarly obtain an estimate $\hat{N}(q)$ of the transfer function $G_0 S_0$ between r and y, by applying similar open loop methods and using measured signals r and y.

Note that the pair $(G_0 S_0, S_0)$ can be considered a factorization of G_0, since $G_0 S_0 (S_0)^{-1} = G_0$. Since the closed loop system is stable, the two separate factors composing this factorization are also stable, and moreover they can be identified from data measured in the closed loop.

As a result, we can arrive at an estimate $\hat{G}(z) = \hat{N}(z)\hat{D}(z)^{-1}$ of the open loop plant $G_0(z)$. If the estimates of both factors are obtained from independent data sequences, we may expect that the resulting estimate $\hat{G}(z)$ is consistent in the case that both estimators $\hat{D}(z)$ and $\hat{N}(z)$ are consistent.

When the external exciting signal r is not measurable, the method sketched above can not be followed directly. However, it appears to be that this lack of information can be completely compensated for, if we have knowledge about the controller $C(z)$.

Note that from system relations (10.1)-(10.4) it follows that

$$r(t) = r_1(t) + C(q)r_2(t) = u(t) + C(q)y(t) \tag{10.113}$$

Using knowledge of $C(q)$, together with measurements of u and y, we can simply "reconstruct" the reference signal r in the relations (10.112),(10.111) as used above. So in stead of a measurable signal r, we can equally well deal with the situation that y, u are measurable and C is known. Note that for arriving at consistent models, the basic requirement of persistence of excitation of r then is replaced by a similar condition on the signal $u + Cy$.

It appears to be true that the signal $\{u(t) + C(q)y(t)\}$ is uncorrelated with $\{e(t)\}$ provided that r_1, r_2 are uncorrelated with e. Additionally we can still use the relations (10.111), (10.112) even if r is not measurable. In that case we will consider $r(t)$ to be given by $r(t) = u(t) + C(q)y(t)$.

It has been discussed that $(G_0 S_0, S_0)$ is a specific stable factorization of G_0 of which the two factors can be identified from data measured in the closed loop. We can raise the question whether there exist more of these factorizations that can be identified from similar data. By introducing an artificial signal

$$x(t) = F(q)r(t) = F(q)[u(t) + C(q)y(t)] \tag{10.114}$$

with $F(z)$ any chosen and fixed stable rational transfer function, we can rewrite the system's relations as

$$y(t) = N_{0,F}(q)x(t) + W_0(q)H_0(q)e(t) \tag{10.115}$$

$$u(t) = D_{0,F}(q)x(t) - C(q)W_0(q)H_0(q)e(t) \tag{10.116}$$

where $N_{0,F} = G_0 S_0 F^{-1}$ and $D_{0,F} = S_0 F^{-1}$. Thus we have obtained another factorization of G_0 in terms of the factors $(N_{0,F}, D_{0,F})$. Since we can reconstruct the signal x from measurement data, these factors can also be identified from data, as in the situation considered

above, provided of course that the factors themselves are stable. This situation is sketched in figure 10.9.

We will now characterize the freedom that is available in choosing this fixed transfer function F. To this end we need the notion of a coprime factorization over $I\!R\mathcal{H}_\infty$.

Definition 10.8.1 *Coprime factorization over $I\!R\mathcal{H}_\infty$ (Vidyasagar, 1985).*
Let G_0 be a (possibly unstable), and let N, D be stable rational transfer functions in $I\!R\mathcal{H}_\infty$. Then the pair (N, D) is a (right) coprime factorization (rcf) of G_0 over $I\!R\mathcal{H}_\infty$, if

(a) $G_0 = ND^{-1}$, and

(b) there exist stable transfer functions $X, Y \in I\!R\mathcal{H}_\infty$ such that $XN + YD = I$ □

The equation in (b) above is generally denoted as the (right) Bezout identity.
There exists a dual definition for left coprime factorizations (lcf) $(\tilde{D}, \tilde{N})$ with $G_0 = \tilde{D}^{-1}\tilde{N}$, in which the condition in (b) has to be replaced by $\tilde{N}\tilde{X} + \tilde{D}\tilde{Y} = I$. For scalar transfer functions, right and left coprimeness are equivalent.
The interpretation of coprimeness of two stable factors over $I\!R\mathcal{H}_\infty$, is that they do not have any common unstable zeros, i.e. zeros in $|z| \geq 1$, that cancel in the quotient of the two factors.

Example 10.8.2 *Consider the transfer function*

$$G_0(z) = \frac{z - 0.5}{z - 0.7}. \tag{10.117}$$

Examples of coprime factorizations (over $I\!R\mathcal{H}_\infty$) N_0, D_0 of this function are:

- $N_0 = G_0$; $D_0 = 1$;
  note that $X = 0$, $Y = 1$ will satisfy the Bezout identity $XN_0 + YD_0 = 1$.

- $N_0 = \dfrac{z - 0.5}{z - 0.9}$; $D_0 = \dfrac{z - 0.7}{z - 0.9}$;
  here e.g. $X = 3.5(1 - 0.9z^{-1})$ and $Y = -2.5(1 - 0.9z^{-1})$ will satisfy the Bezout identity.

Note that a factorization $N_0 = \dfrac{z - 1.2}{z - 0.7}$, $D_0 = \dfrac{z - 1.2}{z - 0.5}$ is not coprime.

The notion of coprimeness of factorizations can be used to characterize the freedom that is present in the choice of the filter F.

Proposition 10.8.3 *Consider a data generating system according to (10.1),(10.2), such that the closed loop system is internally stable, and let $F(z)$ be a rational transfer function defining $x(t)$ as in (10.114). Let the controller C have a left coprime factorization $(\tilde{D}_c, \tilde{N}_c)$. Then the following two expressions are equivalent*

a. the mappings $col(y, u) \to x$ and $x \to (y, u)$ are stable;

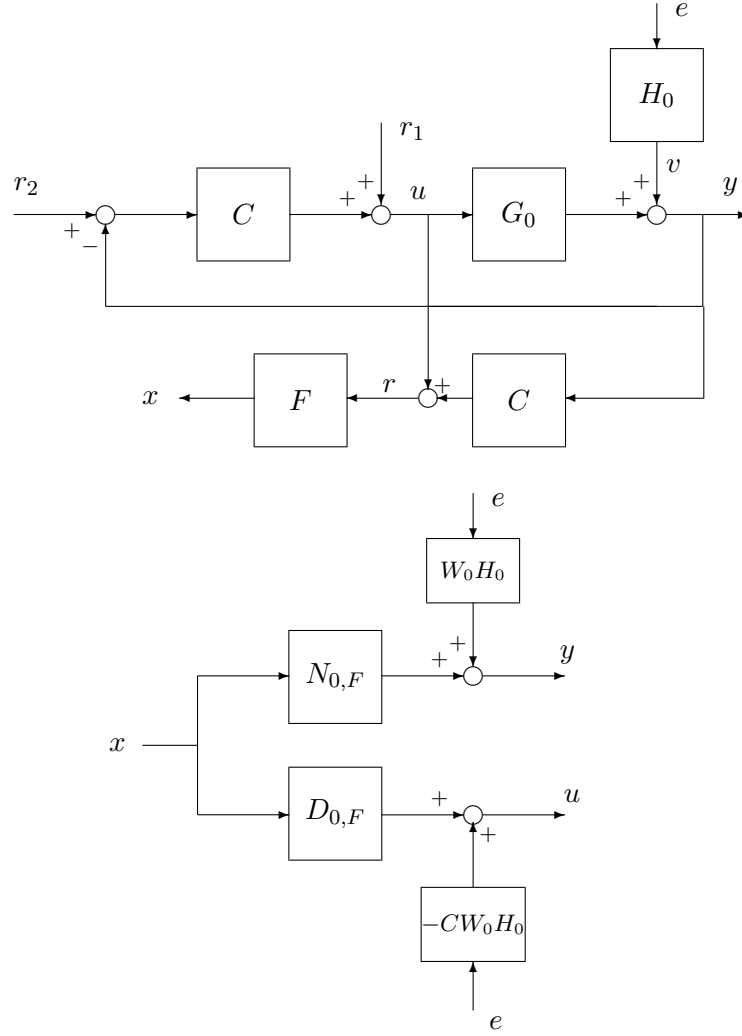*b. $F(z) = W\tilde{D}_c$ with W any stable and stably invertible rational transfer function.* □

Figure 10.9: Coprime factor identification from closed loop data.

The proof of this Proposition is added in the appendix.

The Proposition shows that there is a huge freedom in choosing F given the restriction that the mappings $col(y, u) \to x$ and $x \to col(y, u)$ are stable. Stability of these mappings is required by the fact that we want to have a bounded signal x as an input in our identification procedure, and that we want to estimate stable factors in order to be able to apply the standard (open-loop) prediction error methods and analysis thereof.

Note that all factorizations of G_0 that are induced by these different choices of F reflect factorizations of which the stable factors can be identified from input/output data, cf. equations (10.115),(10.116).

For any choice of F satisfying the conditions of Proposition 10.8.3 the induced factorization of G_0 can be shown to be right coprime. This is formulated in the following result.

Proposition 10.8.4 *Consider the situation of Proposition 10.8.3. For any choice of $F = W\tilde{D}_c$ with W stable and stably invertible, the induced factorization of G_0, given by $(G_0 S_0 F^{-1}, S_0 F^{-1})$ is right coprime.*   □

Proof: Let (X, Y) be right Bezout factors of (N, D), and denote $[X_1 \ Y_1] = W(\tilde{D}_c D + \tilde{N}_c N)[X \ Y]$. Then by employing (10A.1) it can simply be verified that X_1, Y_1 are stable and are right Bezout factors of $(G_0 S_0 F^{-1}, S_0 F^{-1})$. $\qquad\square$

The method of identification of (right) coprime factorizations of the plant, as presented in this section is introduced in Schrama (1990, 1991) and further developed in Schrama (1992) and Van den Hof *et al.* (1995), specifically directed towards the identification of models that are appropriate for subsequent control design. The coprime factor identification method is also discussed in Zhu and Stoorvogel (1992).

There exists an alternative formulation for the freedom that is present in the choice of filter F, as formulated in the following Proposition.

Proposition 10.8.5 *The filter F yields stable mappings $(y, u) \to x$ and $x \to (y, u)$ if and only if there exists an auxiliary system G_x with rcf (N_x, D_x), stabilized by C, such that $F = (D_x + CN_x)^{-1}$. For all such F the induced factorization $G_0 = N_{0,F} D_{0,F}^{-1}$ is right coprime.*

Proof: Consider the situation of Proposition 10.8.3. First we show that for any C with lcf $\tilde{D}_c^{-1} \tilde{N}_c$ and any stable and stably invertible W there always exists a system G_x with rcf $N_x D_x^{-1}$ such that $W = [\tilde{D}_c D_x + \tilde{N}_c N_x]^{-1}$.

Take a system G_a with rcf $N_a D_a^{-1}$ that is stabilized by C. With Lemma 10A.1 it follows that $\tilde{D}_c D_a + \tilde{N}_c N_a = \Lambda$ with Λ stable and stably invertible. Then choosing $D_x = D_a \Lambda^{-1} W^{-1}$ and $N_x = N_a \Lambda^{-1} W^{-1}$ delivers the desired rcf of a system G_x as mentioned above.

Since $F = W \tilde{D}_c$ and substituting $W = [\tilde{D}_c D_x + \tilde{N}_c N_x]^{-1}$ it follows that $F = [D_x + CN_x]^{-1}$. $\qquad\square$

We will comment upon this result in the next section, where we will discuss the dual Youla parametrization.

Employing this specific characterization of F, the coprime plant factors that can be identified from closed loop data satisfy

$$\begin{pmatrix} N_{0,F} \\ D_{0,F} \end{pmatrix} = \begin{pmatrix} G_0(I + CG_0)^{-1}(I + CG_x)D_x \\ (I + CG_0)^{-1}(I + CG_x)D_x \end{pmatrix}. \tag{10.118}$$

In terms of identifying a model of the plant dynamics, we are faced with the system relations (10.115),(10.116) as also sketched in figure 10.9. We can now formulate the prediction error for the 1-input 2-output dynamical system relating "input" $x(t)$ to "output" $col(y(t), u(t))$ by:

$$\varepsilon(t, \theta) = \begin{bmatrix} H_y(q, \theta)^{-1} & 0 \\ 0 & H_u(q, \theta)^{-1} \end{bmatrix} \begin{bmatrix} y(t) - N(q, \theta)x(t) \\ u(t) - D(q, \theta)x(t) \end{bmatrix} \tag{10.119}$$

where $H_y(q, \theta)$ and $H_u(q, \theta)$ are the noise models in the two transfer functions. If these noise models are fixed, i.e. $H_y(q, \theta) = H_{y*}(q)$ and $H_u(q, \theta) = H_{u*}(q)$, then a least squares identification criterion will yield the asymptotic estimate determined by[1]

$$\theta^* = \arg \min_{\theta} \frac{1}{2\pi} \int_{-\pi}^{\pi} \begin{bmatrix} N_{0,F} - N(\theta) \\ D_{0,F} - D(\theta) \end{bmatrix}^* \begin{bmatrix} |H_{y*}|^{-2} & 0 \\ 0 & |H_{u*}|^{-2} \end{bmatrix} \begin{bmatrix} N_{0,F} - N(\theta) \\ D_{0,F} - D(\theta) \end{bmatrix} \Phi_x d\omega. \tag{10.120}$$

---

[1] The arguments $e^{i\omega}$ have been suppressed for clarity.

However using the system's relations

$$
\begin{align}
y(t) &= N_{0,F}(q)x(t) + W_0(q)H_0(q)e(t) \tag{10.121} \\
u(t) &= D_{0,F}(q)x(t) - C(q)W_0(q)H_0(q)e(t) \tag{10.122}
\end{align}
$$

together with the relation $x(t) = F(q)r(t)$ (10.114) then the asymptotic parameter estimate can equivalently be characterized by

$$
\theta^* = \arg\min_\theta \frac{1}{2\pi} \int_{-\pi}^{\pi} \left\{ \frac{|G_0 S_0 - N(\theta)F|^2}{|H_{y*}|^2} + \frac{|S_0 - D(\theta)F|^2}{|H_{u*}|^2} \right\} \Phi_r d\omega. \tag{10.123}
$$

The integral expression now changes from a simple additive mismatch on the open loop plant dynamics (as in chapter 4), to a weighted mismatch on sensitivity functions and plant-times-sensitivity functions, clearly exhibiting the role of the controller also in this criterion. By choosing a model structure in which H_y and H_u are fixed (not parametrized), the asymptotic identification criterion becomes explicit, as meant in Problem (c) in the introduction. However the model parametrization appearing in this criterion is still in the form of parametrized factors $N(\theta), D(\theta)$ and not of its transfer function model $G(\theta)$.
In order to be able to characterize the asymptotic criterion in terms of $G_0(q)$ and $G(q, \theta)$, a restriction on the parametrization of $N(\theta)$ and $D(\theta)$ is required.
Requiring that

$$
\begin{align}
N(q,\theta)F &= G(q,\theta)S(q,\theta) \tag{10.124} \\
D(q,\theta)F &= S(q,\theta) \tag{10.125}
\end{align}
$$

with $S(q,\theta) = [1 + C(q)G(q,\theta)]^{-1}$ the sensitivity function of the parametrized model, would provide us with an asymptotic identification criterion that can be characterized in terms of $G_0(q)$, $S_0(q)$ and $G(q,\theta)$, $S(q,\theta)$. This parametrization restriction implies that

$$
D(q,\theta) + C(q)N(q,\theta) = F^{-1}, \tag{10.126}
$$

and actually connects the two separate coprime factors to each other. Note that the two plant factors $(N_{0,F}, D_{0,F})$ satisfy the (similar) relation

$$
D_{0,F}(q) + C(q)N_{0,F}(q) = F^{-1} \tag{10.127}
$$

by construction. It has to be remarked that the restriction on the parametrization (10.126) is nontrivial to incorporate in standard identification algorithms.
A second remark is that the dynamics that is present in the coprime factors $N_{0,F}, D_{0,F}$ strongly depends on the choice of the auxiliary system G_x leading to F. This also holds for the question whether the factors can be accurately modelled by restricted complexity models. If both factors exhibit (very) high order dynamics, then approximate identification of these factors may lead to an inaccurate plant model. This implies that somehow one has to remove the common dynamics in both factors. This problem will be treated in the next subsection.

Until now we have considered the identification of a plant model $G(q, \hat{\theta}_N)$ only. A disturbance model $H(q, \hat{\theta}_N)$ for the noise shaping filter $H_0(q)$ can be constructed using the separate estimates $H_y(q, \hat{\theta}_N)$ and $H_u(q, \hat{\theta}_N)$. On the basis of the system's equations (10.115) and (10.116), noticing that

	Coprime factor method
Consistency $(G(q,\hat{\theta}_N), H(q,\hat{\theta}_N))$	+
Consistency $G(q,\hat{\theta}_N)$	+
Tunable bias	+
Fixed model order	□
Unstable plants	+
$(G(q,\hat{\theta}_N), C)$ stable	−
C assumed known	no

Table 10.7: Properties of coprime factor identification method.

$H_y(q,\hat{\theta}_N)$ is a model of $W_0(q)H_0(q)$
$H_u(q,\hat{\theta}_N)$ is a model of $-C(q)W_0(q)H_0(q)$

it follows that an appropriate model for H_0 is given by

$$H(q,\hat{\theta}_N) = H_y(q,\hat{\theta}_N) - G(q,\hat{\theta}_N)H_u(q,\hat{\theta}_N). \tag{10.128}$$

This expression will lead to a monic transfer function $H(q,\hat{\theta}_N)$ provided that we have restricted the plant model $G(q,\hat{\theta}_N)$ to be strictly proper. If this is not the case, then more complex expressions have to be used for the construction of a (monic) noise model, similar to the situation of the joint input/output method from section 10.5. Generally speaking, this coprime factor identification approach can be considered to be a generalization of the joint i/o method.

For analyzing the results on consistency, the open-loop framework as presented in chapter 4 can fully be used. This is due to the fact that the closed-loop identification problem actually has been split in two open-loop type of identification problems. If the model sets for parametrizing $N(q,\theta), D(q,\theta)$ have been chosen properly, then consistent estimates of the plant factors can be achieved under the generally known conditions. This situation refers to Problems (a) and (b) as mentioned in the introduction of this chapter. An explicit approximation criterion as considered in Problem (c) can be formulated; this approximation criterion can be written in terms of the model transfer function $G(q,\theta)$ provided that a parametrization constraint is taken into account, as discussed in (10.126).
As a final note we remark that due to this coprime factor framework the identification method discussed does not meet any problems in handling unstable plants and/or unstable controllers, as both are represented by a quotient of two stable factors.
In table 10.7 a summary is given of the properties of this method. The coprime factor identification method is successfully applied to a X-Y positioning table (Schrama, 1992) and to a compact disc servo mechanism (Van den Hof *et al.*. 1995).

10.8.2 Identification of models with limited order

One of the problems in identification of coprime factor models is that the order of estimated models $G(q,\hat{\theta}_N) = N(q,\hat{\theta}_N)D(q,\hat{\theta}_N)^{-1}$ will generally not be directly under control. This is caused by the fact that the quotient of the two coprime factors will lead to a plant model with a McMillan degree that generally will be larger than the McMillan degree of the separate factors.

Stated from the other point of view: for a given plant G_0 with McMillan degree n, the McMillan degree of corresponding coprime factors $N_{0,F}$, $D_{0,F}$ will be dependent on G_0, C, G_x and D_x, as can be understood from (10.118).

A relevant question then appears to be: "Under what conditions on $F(q)$ will the coprime factorizations $N_{0,F}$, $D_{0,F}$ have a McMillan degree that is equal to the McMillan degree of G_0?" If one would restrict attention to coprime factorizations with this property, then one could control the McMillan degree of the plant model, by enforcing the model order of the coprime factors separately.

Next we will consider a specific class of coprime factorizations that has the property as mentioned above.

Definition 10.8.6 (Normalized coprime factorization) *A right coprime factorization* (N_0, D_0) *is called* normalized *if it satisfies*

$$N^T(e^{-i\omega})N(e^{i\omega}) + D^T(e^{-i\omega})D(e^{i\omega}) = I,$$

which for the scalar case reduces to $|N(e^{i\omega})|^2 + |D(e^{i\omega})|^2 = 1$.   □

Again, a dual definition exists for left coprime factorizations.

One of the properties of normalized coprime factorizations is that they form a decomposition of the system G_0 in minimal order (stable) factors. In other words, if G_0 has McMillan degree n, then normalized coprime factors of G_0 will also have McMillan degree n.[2]

Example 10.8.7 *Let a plant G_0 be given by*

$$G_0(z) = \frac{z - 0.5}{z - 0.7}.$$

Then a normalized coprime factorization (N_0, D_0) of G_0 is given by

$$N_0(z) = \frac{z - 0.5}{1.425z - 0.84} \qquad D_0(z) = \frac{z - 0.7}{1.425z - 0.84}.$$

The Bode plots of the several transfer functions in the example are presented in figure 10.10. It has to be noted that the normalization property of the factorization implies that $|N_0(e^{i\omega})| \leq 1$ and $D_0(e^{i\omega})| \leq 1$. This mechanism is clearly visualized in the Bode plots of Figure 10.10.

By using normalized coprime factorizations one can avoid the identification of dynamics that is redundantly present in both factors.

The principle scheme that can be followed now is composed of two steps:

1. Construct a data filter F such that the coprime factors $N_{0,F}$, $D_{0,F}$ that are accessible from closed-loop data become normalized;

2. Identify $N_{0,F}$ and $D_{0,F}$ using a parametrization in terms of polynomial fractions and with a common denominator:

$$N(q, \theta) = \frac{B(q^{-1}, \theta)}{D(q^{-1}, \theta)} \qquad D(q, \theta) = \frac{A(q^{-1}, \theta)}{D(q^{-1}, \theta)} \qquad (10.129)$$

---

[2]In the exceptional case that G_0 contains all-pass factors, (one of) the normalized coprime factors will have McMillan degree $< n$, see Tsai *et al.* (1992).
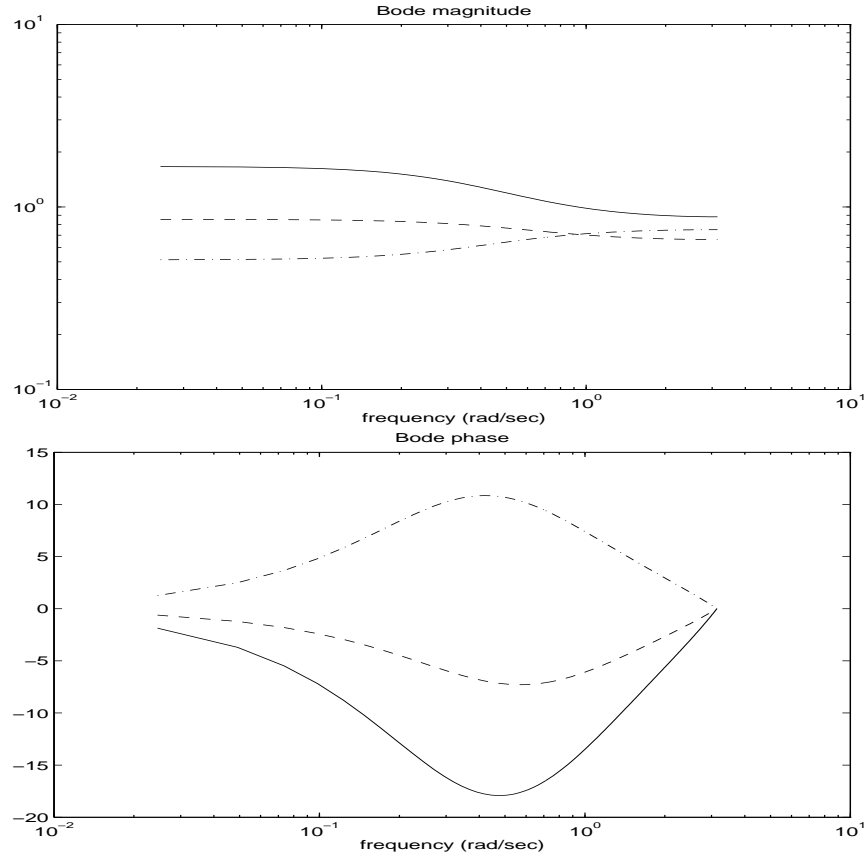
Figure 10.10: Bode magnitude (upper) and phase (lower) plot of G_0 (solid), N_0 (dashed) and D_0 (dash-dotted).

with A, B and D polynomials in q^{-1} with prespecified model orders n_a, n_b and n_d. The finally estimated plant model is then given by

$$G(q, \hat{\theta}_N) = \frac{B(q^{-1}, \hat{\theta}_N)}{A(q^{-1}, \hat{\theta}_N)}. \tag{10.130}$$

The normalization step 1 in this procedure is necessary in order to guarantee that one can indeed restrict attention to coprime factor models with a McMillan degree that is similar to the McMillan degree of the plant model. If there is no normalization, then $N_{0,F}$ and $D_{0,F}$ can be (very) high order factorizations, which require high order models for accurate modelling.

Step 1
The construction of $F(q)$ as mentioned above is guided by the following principle. If $G_x = G_0$ and (N_x, D_x) is a normalized right coprime factorization of G_x, then $N_{0,F} = N_x$ and $D_{0,F} = D_x$ being normalized also. This can be verified by considering the expression (10.118) for the factors $N_{0,F}$ and $D_{0,F}$. The resulting filter $F(q)$ is then given by

$$F(q) = [1 + C(q)G_x(q)]D_x(q). \tag{10.131}$$

There is of course no exact knowledge available of G_0 in order to construct G_x is this way. However, one can use a high-order accurate estimate of G_0 as a basis for constructing G_x, and determine a normalized coprime factorization (N_x, D_x) of G_x to construct the appropriate $F(q)$. If G_x is sufficiently accurate, then the resulting factors $N_{0,F}$, $D_{0,F}$ will be "close to normalized".

Step 2

Identification of a one-input, two-output system with a common denominator can now be performed with the standard procedures similar to the situation in section 10.8.1, leading to a plant model (10.130).

The algorithm presented here has been worked out in more detail in Van den Hof *et al.* (1995), where also the consequences are analyzed of inaccuracies that occur in the first step of the procedure, for the accuracy of the finally estimated plant models. One can observe that part of the mechanism is similar to the "two-stage" method of closed-loop identification. In a first step, actually exact plant information is required to prepare for the second step. In both methods, this first step is replaced by an high-order accurate estimate of this plant.

Whereas the general coprime factor identification does not require knowledge of the controller that is implemented in order to arrive at a plant model, the algorithm presented above does require this knowledge in order to optimally tune the filter F according to (10.131).

10.8.3   Application to a mechanical servo system

We will illustrate the proposed identification algorithm by applying it to data obtained from experiments on the radial servo mechanism in a CD (compact disc) player. The radial servo mechanism uses a radial actuator which consists of a permanent magnet/coil system mounted on the radial arm, in order to position the laser spot orthogonally to the tracks of the compact disc, see also Example 1.2.2. A simplified representation of the experimental set up of the radial control loop is depicted in Figure 10.11, where G_0 and C denote respectively the radial actuator and the known controller. The radial servo mechanism is marginally stable, due to the presence of a double integrator in the radial actuator G_0.
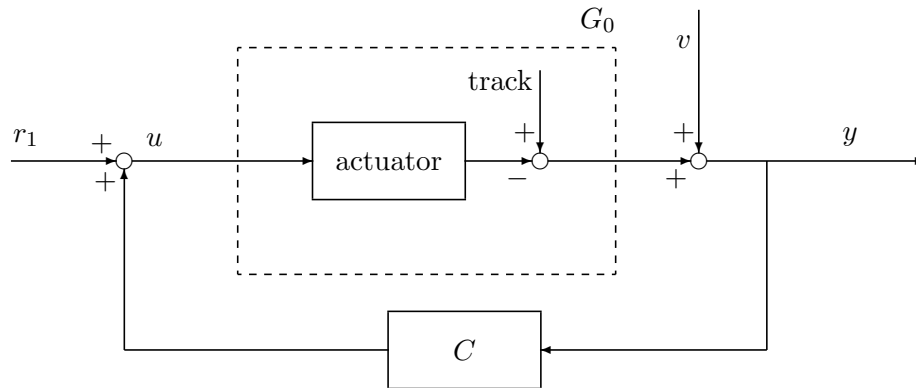

Figure 10.11: Block diagram of the radial control loop in a CD player.

This experimental set up is used to gather time sequences of 8192 points of the input $u(t)$ to the radial actuator G_0 and the disturbed track position error $y(t)$ in closed loop, while exciting the control loop by a bandlimited (100Hz–10kHz) white noise signal $r_1(t)$, added to the input $u(t)$.

The results of applying the two steps of the procedure presented in Section 10.8.2 are shown in a couple of figures. Recall from Section 10.8.2, that in the first step the aim is to find an auxiliary model G_x with a normalized *rcf* (N_x, D_x) used to construct the filter F, such that the factorization $(N_{0,F}, D_{0,F})$ of G_0 becomes (almost) normalized. The result of performing Step 1 is depicted in Figure 10.12. A high (32-nd) order model G_x has been estimated and a normalized factorization (N_x, D_x) has been obtained. Based on this factorization a filter F has been constructed according to (10.131), giving rise to a coprime factorization of G_0 in terms of $(N_{0,F}, D_{0,F})$.
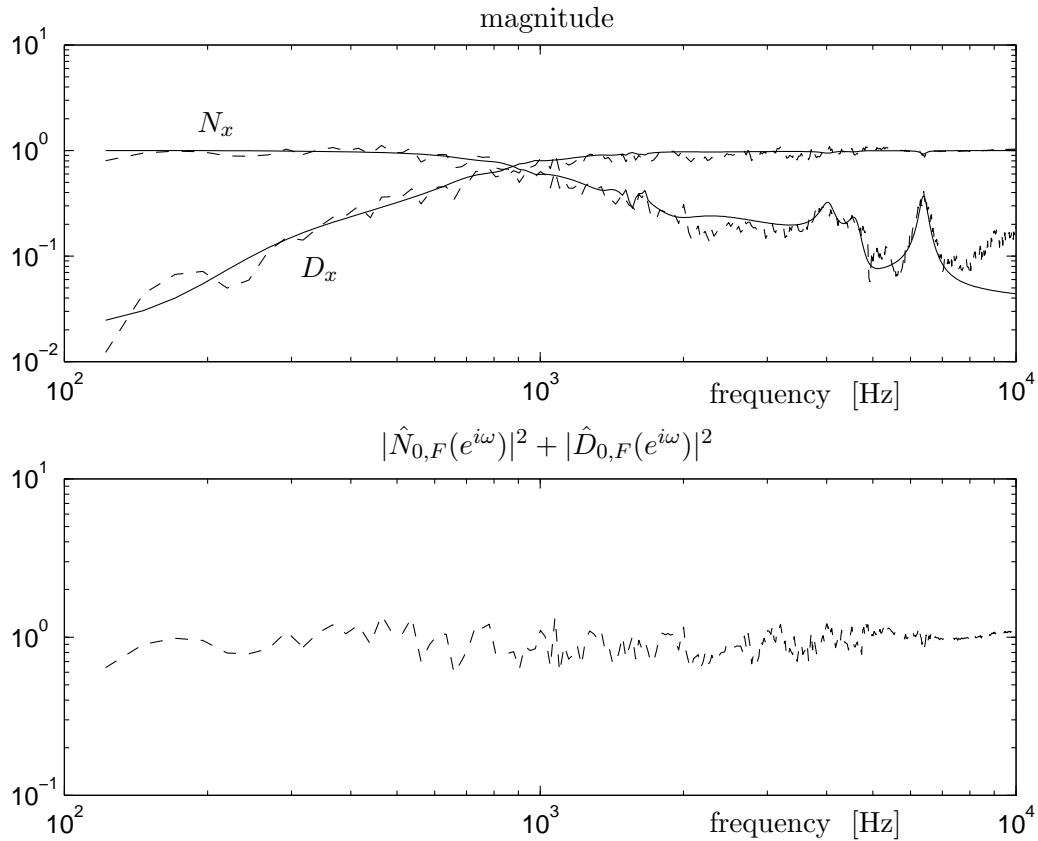
Figure 10.12: Results of Step 1 of the procedure. Upper figure: Bode magnitude plot of estimated 32nd order coprime plant factors (N_x, D_x) of auxiliary model G_x (solid) and spectral estimates of the factors $(N_{0,F}, D_{0,F})$ (dashed). Lower figure: Plot of $|\hat{N}_{0,F}(e^{i\omega})|^2 + |\hat{D}_{0,F}(e^{i\omega})|^2$ using the spectral estimates $\hat{N}_{0,F}$ and $\hat{D}_{0,F}$.

Figure 10.12(a) shows an amplitude Bode plot of a spectral estimate of the factors $N_{0,F}$ and $D_{0,F}$, respectively denoted by $\hat{N}_{0,F}$ and $\hat{D}_{0,F}$, along with the factorization N_x and D_x of the high order auxiliary model G_x. Additionally, it is verified whether the spectral estimates $(\hat{N}_{0,F}, \hat{D}_{0,F})$ are (almost) normalized. To this end the expression $|\hat{N}_{0,F}(e^{i\omega})|^2 + |\hat{D}_{0,F}(e^{i\omega})|^2$ is plotted in Figure 10.12(b). The fact that this expression is very close to unity shows that

the coprime factorization that is induced by the specific choice of F is (almost) normalized.
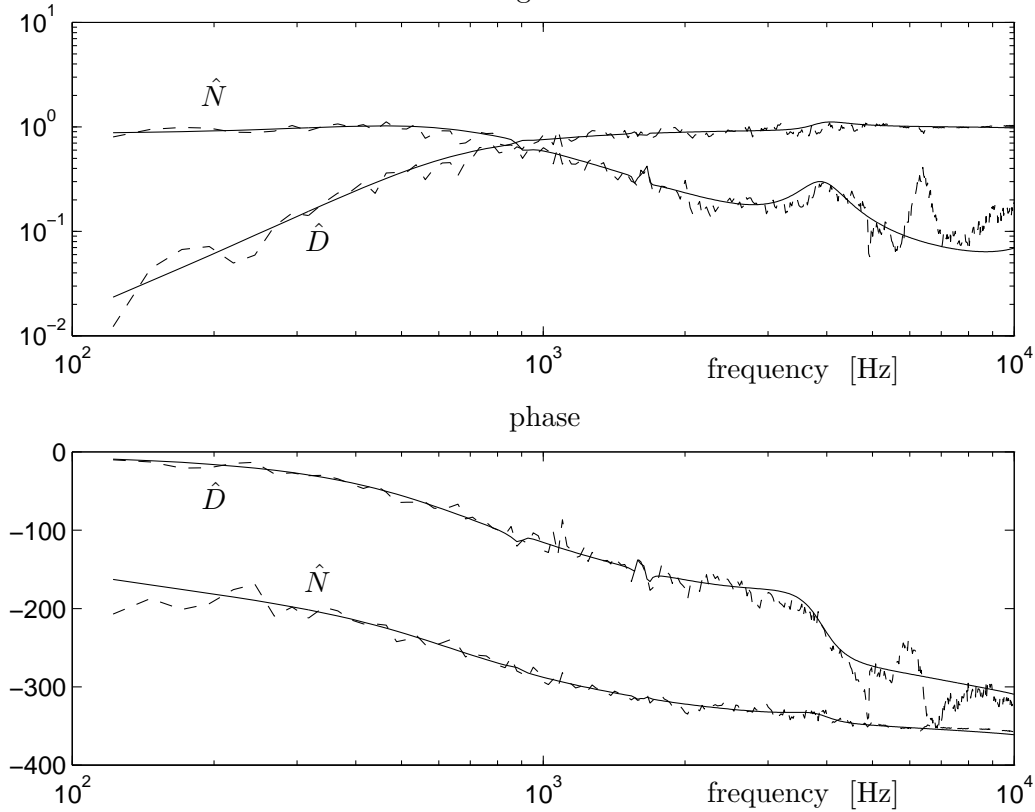

Figure 10.13: Bode plot of the results in Step 2 of the procedure: Identified 10th order coprime factors $(\hat{N}, \hat{D})$ (solid) and spectral estimates (dashed) of the factors $N_{0,F}$, $D_{0,F}$.

Figure 10.13 presents the result of a low (10th) order identified model of the factorization $(N_{0,F}, D_{0,F})$, which is obtained in the second step of the procedure outlined in section 10.8.2. The picture shows the amplitude and phase Bode plots, along with the previously obtained spectral estimates of the coprime factors.

Amplitude and phase Bode plots of the finally obtained 10th order model $G(q, \hat{\theta}_N)$ are depicted in Figure 10.14 along with the corresponding spectral estimate.

Scalar normalized coprime factorizations exhibit the property that their amplitude is bounded by 1. As a result, the integral action in the plant is necessarily represented by a small denominator factor $D_{0,F}$ for low frequencies, whereas a roll-off of G_0 for high frequencies will be represented by a roll-off of the numerator factor $N_{0,F}$. This is clearly visualized in the results.

This application shows the successful identification of an unstable plant, from closed-loop experimental data.

10.9   Identification with the dual Youla parametrization

In the previous section we have discussed the possibility of identifying models of an unstable system that is stabilized by a controller C, by identification of separate coprime factors of
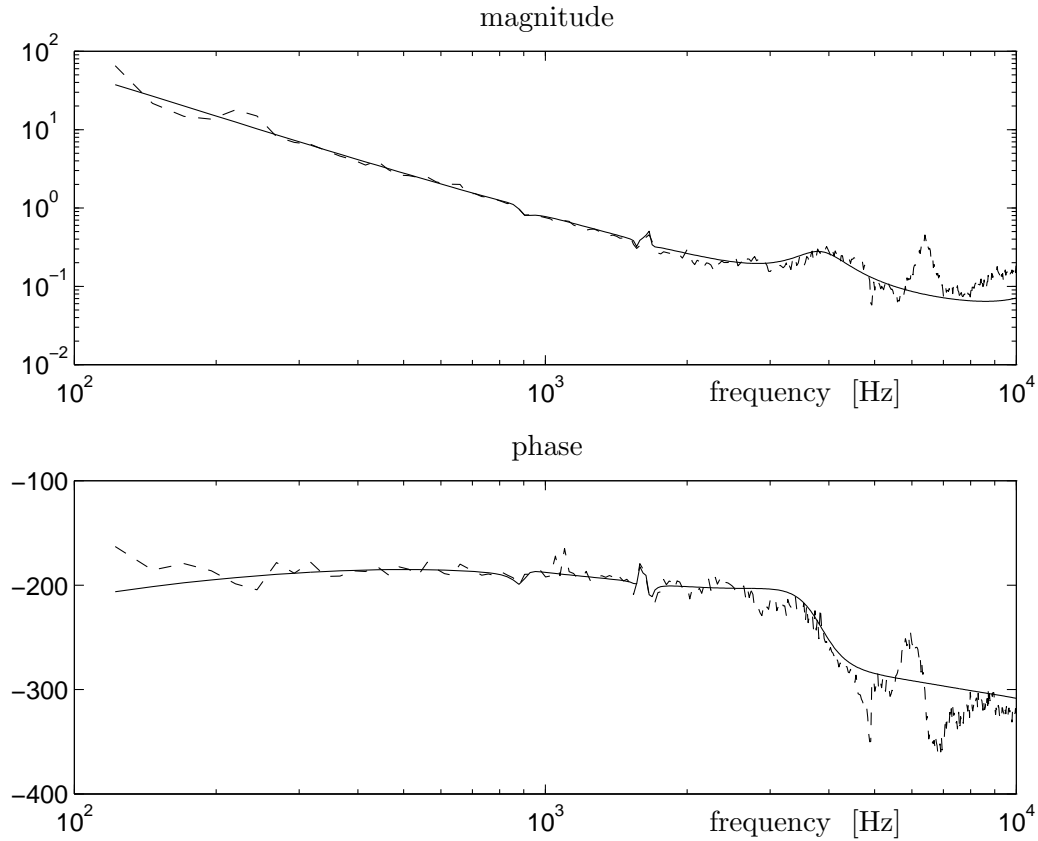
Figure 10.14: Bode plot of the results in Step 2 of the procedure: Identified 10th order model $\hat{G} = \hat{N}\hat{D}^{-1}$ (solid) and spectral estimate $\hat{N}_{0,F}\hat{D}_{0,F}^{-1}$ (dashed) of the plant G_0.

G_0. This leads to two identification problems corresponding to the mappings $x \rightarrow (y^T, u^T)^T$, while there is a structural relation between the two transfer functions to be estimated, i.e. $G_0 S_0 F^{-1}$ and $S_0 F^{-1}$.

In the final method to be discussed in this chapter, we will employ this structural relationship between the two transfer functions to be estimated, and we will reduce the problem to the identification of only one transfer function. At the same time, we will be able to construct a model set that contains only models that satisfy the additional property that they are stabilized by the given controller C. This latter situation implies that once we have estimated a model $\hat{G}$ of G_0 we have the guarantee that C stabilizes $\hat{G}$.

The method to be presented here, will appear to be a generalization of the indirect method of identification, as discussed in section 10.4.

The Youla parametrization, see e.g. Desoer *et al.* (1980), Vidyasagar (1985), gives a representation of all controllers that stabilize a given system G_0. In terms of an identification problem, we can use a dual form of this Youla-parametrization as suggested by Hanssen and Franklin (1988) and Schrama (1990), leading to a parametrization of the class of all systems G_0 that are stabilized by a given controller C. This is formulated in the following proposition.
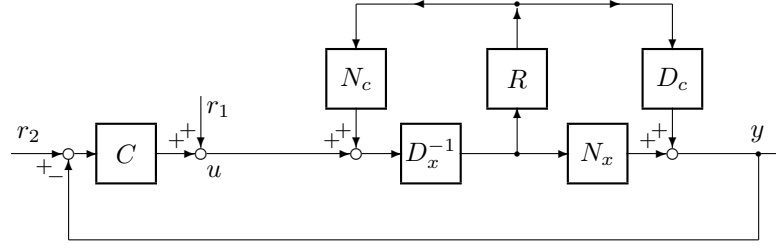
Figure 10.15: Dual-Youla parametrization for noise-free system

Proposition 10.9.1 ((Desoer *et al.* **, 1980))** *Let C be a controller with rcf (N_c, D_c), and let G_x with rcf (N_x, D_x) be any system that is stabilized by C. Then a plant G_0 is stabilized by C if and only if there exists an $R \in I\!R\mathcal{H}_\infty$ such that*

$$G_0 = (N_x + D_c R)(D_x - N_c R)^{-1}. \tag{10.132}$$

The above proposition determines a parametrization of the class of all linear, time-invariant, finite-dimensional systems that are stabilized by the given C. The parametrization is depicted in a block diagram in Figure 10.15.

Note that $N_x D_x^{-1}$ is just any (nominal, auxiliary) system that is stabilized by C. In the case of a stable controller C, a valid choice is given by $G_x = 0$, as the zero-transfer function is stabilized by any stable controller.

This also can be used to illustrate the relation of this method with the more classical indirect method in section 10.4.

For a stable controller C valid choices of the coprime factors are $N_c = C$, $D_c = 1$ and $N_x = 0$, $D_x = 1$. This particular choice of coprime factors leads to the representation:

$$G_0 = \frac{R}{1 - CR},$$

which directly corresponds to

$$R = \frac{G_0}{1 + CG_0}$$

being the closed-loop transfer function from r to y. So, in this particular situation the set of all plants that is stabilized by C is characterized by all stable closed-loop transfer functions.

Now we will focus on the more general situation, that is also valid for e.g. unstable controllers. The next Proposition shows that for any given system G_0, the corresponding stable R and the corresponding factorization (10.132) are uniquely determined.

Proposition 10.9.2 *Consider the situation of Proposition 10.9.1. Then for any plant G_0 that is stabilized by C holds*

(a) The stable transfer function R in (10.132) is uniquely determined by

$$R = R_0 := D_c^{-1}(I + G_0 C)^{-1}(G_0 - G_x)D_x. \tag{10.133}$$

(b) The coprime factorization in (10.132) is uniquely determined by

$$N_x + D_c R_0 = G_0(I + CG_0)^{-1}(I + CG_x)D_x \tag{10.134}$$

$$D_x - N_c R_0 = (I + CG_0)^{-1}(I + CG_x)D_x \tag{10.135}$$

Proof:
Part (a). With (10.132) it follows that $G_0[D_x - N_c R_0] = N_x + D_c R_0$. This is equivalent to $[D_c + G_0 N_c]R_0 = G_0 D_x - N_x$ which in turn is equivalent to $[I + G_0 C]D_c R_0 = [G_0 - G_x]D_x$ which proves the result.

Part (b). Simply substituting the expression (10.133) for R shows that

$$\begin{bmatrix} N_0 \\ D_0 \end{bmatrix} := \begin{bmatrix} N_x + D_c R \\ D_x - N_c R \end{bmatrix} = \begin{bmatrix} N_x + (I + G_0 C)^{-1}(G_0 - G_x)D_x \\ D_x - C(I + G_0 C)^{-1}(G_0 - G_x)D_x \end{bmatrix}$$

$$= \begin{bmatrix} G_x + (I + G_0 C)^{-1}(G_0 - G_x) \\ I - C(I + G_0 C)^{-1}(G_0 - G_x) \end{bmatrix} D_x \qquad (10.136)$$

which proves the result, employing the relations $C(I + G_0 C)^{-1} = (I + CG_0)^{-1}C$ and $(I + G_0 C)^{-1}G_0 = G_0(I + CG_0)^{-1}$. $\qquad\square$

This Proposition shows that the coprime factorization that is used in the Youla parametrization is exactly the same coprime factorization that we have constructed in the previous section, by exploiting the freedom in the prefilter F, see Proposition 10.8.5.

Now we face the interesting question whether we can exploit this Youla parametrization also in terms of system identification. To this end we first have to extend the corresponding system representation as sketched in figure 10.15 with the appropriate disturbance signal on the output. We do this in the standard way by adding a noise term to the output as depicted in Figure 10.16.
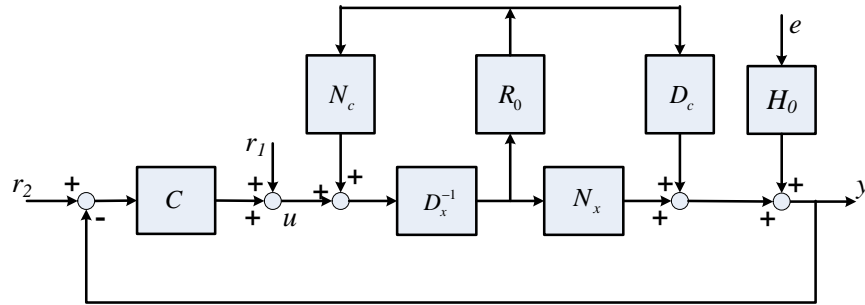

Figure 10.16: Dual Youla-representation of the data generating system with noise.

It appears that the effect of the noise term e on the measured signals u and y can be equivalently represented by adding am appropriately filtered noise term e at the output of the dual-Youla parameter R_0. This is depicted in Figure 10.17.

Proposition 10.9.3 *With respect to the measured signals u and y, the two schemes in Figures 10.16 and 10.17 and equivalent, provided that K_0 is chosen as*

$$K_0 = D_c^{-1} W_0 H_0.$$

Proof:
For the moment we consider the transfer of signals within the open-loop part of the scheme for the equation $y = G_0 u + H_0 e$. Equivalently we assume for the moment that the feedback loop is disconnected. The transfer function from e to z is then given by:

$$H_{ze} = \frac{K_0}{1 - R_0 N_c D_x^{-1}}$$

Figure 10.17: Dual Youla-representation of the data generating system with noise shifted to the dual-Youla parameter.

and the transfer from e to x by:

$$H_{xe} = \frac{N_c D_x^{-1} K_0}{1 - R_0 N_c D_x^{-1}}.$$

Consequently, the transfer from e to y is given by

$$H_{ye} = D_c H_{ze} + N_x H_{xe} = \frac{D_c K_0 + N_x N_c D_x^{-1} K_0}{1 - R_0 N_c D_x^{-1}}$$

and this transfer should be equal to H_0 (as in the open loop configuration). Rewriting the latter equation leads to

$$\frac{K_0(D_c + N_c G_x)}{1 - R_0 N_c D_x^{-1}} = H_0$$

or equivalently

$$K_0 = \frac{H_0(1 - R_0 N_c D_x^{-1})}{D_c + N_c G_x}.$$

Using the expression (10.133) for R_0 it follows that

$$K_0 = \frac{1 - \frac{D_c^{-1}(G_0 - G_x)}{1 + CG_0} N_c}{D_c + N_c G_x} H_0 \tag{10.137}$$

$$= \frac{1 + CG_0 - C(G_0 - G_x)}{(1 + CG_0)(1 + CG_x)D_c} H_0 \tag{10.138}$$

which shows that for $K_0 = D_c^{-1} W_0 H_0$ the effect of e on the output y is the same as in Figure 10.16. If the effect of e on y is the same, that this also necessarily holds for the effect of e on the input u in the closed-loop case. □

The scheme depicted in Figure 10.17 has a number of several nice properties, as formulated next.

Proposition 10.9.4 *In the block diagram as depicted in Figure 10.17, the following properties hold:*

- *The signals z and x satisfy*

$$z(t) = (D_c + G_x N_c)^{-1}(y(t) - G_x u(t)) \tag{10.139}$$

$$x(t) = (D_x + N_x C)^{-1}(u(t) + Cy(t)) \tag{10.140}$$

  and therefore can both be reconstructed on the basis of measured signals u, y, the (known) controller C, and the auxiliary model G_x;

- *The signal x is uncorrelated with the noise e.*

Proof:
We write the two system equations:

$$y = N_x x + D_c z \tag{10.141}$$

$$x = D_x^{-1}(u + N_c z). \tag{10.142}$$

Substituting (10.142) into (10.141) gives: $y = G_x(u + N_c z) + D_c z$ and equivalently $(D_c + N_c G_x)z = y - G_x u$, which directly shows the result for z.
Substituting (10.141) into (10.142) gives: $x = D_x^{-1}[u + N_c D_c^{-1}(y - N_x x)]$ or equivalently $(1 + G_x C)x = D_x^{-1}(u + Cy)$, which directly shows the result for x.
Since $u + Cy = r$ it follows that $x = (1 + G_x C)^{-1} D_x^{-1} r$ showing that x is a filtered version of r and therefore uncorrelated with e. □

As a result of these manipulations it follows that

$$z(t) = R_0(q)x(t) + K_0(q)e(t) \tag{10.143}$$

where it is noted that (a) $z(t)$ and $x(t)$ can simply be reconstructed from measured data and knowledge of the controller, and (b) $x(t)$ and $e(t)$ as in the previous section are uncorrelated to each other. As a result, (10.143) simply points to an open-loop type of identification problem, in which R_0 (and possibly K_0) can be identified by standard open-loop techniques, on the basis of available signals x and z.
The prediction error related to this identification problem can now be written as

$$\varepsilon(t, \theta) = K(q, \theta)^{-1}[z(t) - R(q, \theta)x(t)], \tag{10.144}$$

with $R(q, \theta)$ the parametrized model for the stable transfer function R_0 and $K(q, \theta)$ the parametrized noise model. A corresponding least squares identification criterion leads to the asymptotic estimate

$$\theta^* = \arg\min_{\theta \in \Theta} \frac{1}{2\pi} \int_{-\pi}^{\pi} \frac{|R_0(e^{i\omega}) - R(e^{i\omega}, \theta)|^2 \Phi_x(\omega) + |K_0(e^{i\omega})|^2 \sigma_e^2}{|K(e^{i\omega}, \theta)|^2} d\omega, \tag{10.145}$$

and the resulting model $G(\theta^*)$ is then calculated according to Proposition 10.9.1, by

$$G(q, \theta^*) = [N_x + D_c R(q, \theta^*)][D_x - N_c R(q, \theta^*)]^{-1}. \tag{10.146}$$

Similarly, by utilizing the expression $K_0 = D_c^{-1} W_0 H_0$, an estimated noise model is obtained through

$$H(q, \theta^*) = [I + G(q, \theta^*)C(q)]D_c(q)K(q, \theta^*). \tag{10.147}$$

If we assume that $G(z)C(z)$ is strictly proper (as in Assumption 10.1.4), and that $D_c(z)$ is monic, then $H(z, \theta^*)$ will be a monic transfer function.
The asymptotic identification criterion is worked out in the following proposition.

Proposition 10.9.5 *Consider the identification of the transfer function R_0 with the (scalar) model structure* (10.144) *using a fixed noise model $K(q,\theta) = K_*(q)$ and a least squares identification criterion. Then the asymptotic parameter estimate θ^* is characterized by*

$$\theta^* = \arg\min_{\theta \in \Theta} \frac{1}{2\pi} \int_{-\pi}^{\pi} \left| \frac{1}{D_c(1+G_0C)}[G_0 - G(\theta)]\frac{1}{(1+G(\theta)C)}\frac{1}{K_*} \right|^2 \Phi_r d\omega \quad (10.148)$$

$$= \arg\min_{\theta \in \Theta} \frac{1}{2\pi} \int_{-\pi}^{\pi} \left| \frac{1}{D_c}\left[\frac{G_0}{1+G_0C} - \frac{G(\theta)}{1+G(\theta)C} \right]\frac{1}{K_*} \right|^2 \Phi_r d\omega. \quad (10.149)$$

Proof: Substituting the expression (10.133) for R_0 and $R(\theta)$ it follows that

$$R_0 - R(\theta) = \frac{1}{D_c(1+G_0C)}(G_0 - G_x)D_x - \frac{1}{D_c(1+G(\theta)C)}(G(\theta) - G_x)D_x$$

$$= \frac{1}{D_c}\frac{G_0 - G(\theta)}{(1+G_0C)(1+G(\theta)C)}[1 + G_xC]D_x. \quad (10.150)$$

Using the fact that $[1 + G_xC]D_x = D_x + CN_x = F^{-1}$ this leads to the required result. $\quad\Box$

An interesting remark that has to be made, is that the stable transfer function R_0 to be estimated in this approach, is strongly dependent on the nominal system G_x that is chosen as a basis for the dual Youla-parametrization. If we choose $G_x = G_0$ (i.e. we have complete knowledge of the input/output system to be identified), then the resulting R_0 will be zero. Whenever G_x is "close" to G_0 then we may expect R_0 to be a "small" transfer function. In this way, R_0 represents the difference between "assumed knowledge" about the system and the actual system itself.

The presented procedure of identifying R_0 is introduced, analyzed and employed in Hanssen (1988), Schrama (1991, 1992) and Lee *et al.* (1992); see also Van den Hof and Schrama (1995).
The following remarks can be made with respect to this identification method.

- The identification method fruitfully uses knowledge of the controller that is implemented when experiments are performed. Knowledge of this controller is instrumental in the identification, similar to the situation of the indirect identification method in section 10.4.

- An estimated factor $R(\hat{\theta}_N)$ that is stable, will automatically yield a model $G(\hat{\theta}_N)$ that is guaranteed to be stabilized by C.

- Having identified the parameter θ^* and the corresponding transfer function $R(\theta^*)$ with a fixed McMillan degree n_r, the McMillan degree of $G(\theta^*)$ will generally be much larger. This is due to the required reparametrization as presented in (10.146). This implies that in the identification as discussed above, the complexity (McMillan degree) of the resulting model $G(\theta^*)$ is not simply tunable. Constructing an appropriate parameter space Θ in such a way that the corresponding set of models $\{G(\theta), \theta \in \Theta\}$ has a fixed McMillan degree, is a nontrivial parametrization problem, that has not been solved yet.

- The asymptotic identification criterion, as reflected by (10.148), is not dependent on the chosen auxiliary model G_x or its factorization.

	Dual-Youla method
Consistency $(G(q, \hat{\theta}_N), H(q, \hat{\theta}_N))$	$+$
Consistency $G(q, \hat{\theta}_N)$	$+$
Tunable bias	$+$
Fixed model order	$-$
Unstable plants	$+$
$(G(q, \hat{\theta}_N), C)$ stable	$+$
C assumed known	yes

Table 10.8: Properties of dual-Youla identification method.

Similar to the identification of coprime factorizations, the identification method discussed in this section has potentials to solve all three Problems (a)-(c) as stated in the introduction. Note that for arriving at consistent estimates it is always required that the "input signal" $x(t)$ is persistently exciting of a sufficiently high order; this requires the availability of a sufficiently exciting reference signal $r(t)$.

As indicated before, the dual-Youla identification can be interpreted as a generalization of the indirect identification method as discussed in section 10.4. If the controller C is stable, then the auxiliary system $G_x = 0$ is a valid choice, and appropriate choices of coprime factorizations can be: $N_c = C$, $D_c = I$, $N_x = 0$ and $D_x = I$.
These choices lead to the expressions:

$$R_0 = (I + G_0 C)^{-1} G_0 = G_0 S_0 \tag{10.151}$$

$$z(t) = (D_c + G_x N_c)^{-1}(y(t) - G_x u(t)) = y(t) \tag{10.152}$$

$$x(t) = (D_x + C N_x)^{-1} r(t) = r(t). \tag{10.153}$$

Apparently, in this situation the transfer function R_0 to be identified is equal to the plant-times-sensitivity, representing the transfer between the external signal r and the output signal y. The generalization that is involved in the dual-Youla method is thus particularly directed towards the situation of unstable controllers.
Since identified models in the dual-Youla method are guaranteed to be stabilized by the controller C, this same result also holds for the indirect identification method, as indicated already in Table 10.3.
In Table 10.8 the properties of the dual-Youla identification method are summarized.

10.10   Analysis of indirect methods

10.10.1   Key role of noise models

The typical choice that is being made for the noise models in indirect identification methods, is that they are chosen to be either fixed (non-parametrized) or parametrized with parameters that are independent of the parameters that are used for the plant model. This choice has been made in order to stress the approximation properties of the asymptotically estimated models. However the role of noise models is a key phenomenon in distinguishing the direct and and indirects methods in closed loop identification. Actually the difference between these two principle methods can be fully characterized by a difference in the structure of the noise models. This is reflected in the following proposition.

Proposition 10.10.1 (Forssell and Ljung (1999)) *Consider a predictor model with a closed-loop predictor, leading to a prediction error*

$$\varepsilon(t,\theta) = H_c(q,\theta)^{-1} \left[y(t) - \frac{G(q,\theta)}{1 + C(q)G(q,\theta)} r(t) \right], \qquad (10.154)$$

where $C(q)$ is considered to be known. If the chosen parametrized noise model $H_c(q,\theta)$ is chosen to be a structured (closed-loop) noise model:

$$H_c(q,\theta) = \frac{H(q,\theta)}{1 + C(q)G(q,\theta)} \qquad (10.155)$$

with $H(q,\theta)$ monic, stable and stably invertible. Then the prediction error $\varepsilon(t,\theta)$ can equivalently be written as

$$\varepsilon(t,\theta) = H(q,\theta)^{-1} \left[y(t) - G(q,\theta)u(t) \right], \qquad (10.156)$$

which is the expression of the prediction error of the direct method. *This shows that by an appropriate choice of parametrized noise model the indirect method becomes a direct method.*

This shows that the advantage of the indirect approaches is that consistent estimates of the plant model are obtained, without having to pay attention to a noise model. However if one would like to reach the same precision (i.e. minimum variance) of models as for the direct method, then a dedicated noise model needs to be estimated. The Proposition above is formulated in the setting of the Tailor-made parametrization approach of section 10.6. However it can also be positioned in the setting of the classical indirect method, where we consider a parametrized predictor model

$$\varepsilon(t,\theta) = H_c(q,\theta)^{-1} \left[y(t) - G_c(q,\theta)r(t) \right].$$

Equivalence with the direct method is now obtained if we choose a parametrized noise model according to

$$H_c(q,\theta) = H(q,\theta)(I - C(q)G_c(q,\theta)) \qquad (10.157)$$

with $H(q,\theta)$ a standard monic, stable and stably invertible. This is fully aligned with the expressions for the recalculation of plant and noise models from closed-loop estimated objects in the indirect method, as shown in (10.72)-(10.73).

10.10.2   Bias

The indirect methods presented in this chapter show expressions for the asymptotic bias distribution that are very much alike. When using fixed (non-parametrized) noise models during identification, consistent plant models of G_0 can be obtained, and the bias distribution has the form[3]

$$\theta^* = \arg\min_{\theta \in \Theta} \frac{1}{2\pi} \int_{-\pi}^{\pi} |S_0 G_0 - S(\theta)G(\theta)|^2 \frac{\Phi_{r_1}}{|K_*|^2} d\omega. \qquad (10.158)$$

By designing the (fixed) noise model K_* (or the signal spectrum Φ_{r_1}), this bias expression can explicitly be tuned to the designer's needs. However the expression is different from

---

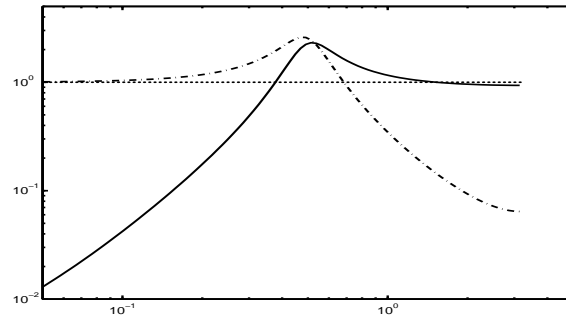[3]Details vary slightly over the several identification methods.

Figure 10.18: Typical curve for Bode magnitude plot of sensitivity function S_0 (solid) and related complementary sensitivity $G_0C/(1+CG_0)$ (dashed).

the related open-loop expression (4.164). Instead of a weighted additive error on G_0, the integrand contains an additive error on G_0S_0. Straightforward calculations show that

$$G_0S_0 - G(\theta)S(\theta) = S_0[G_0 - G(\theta)]S(\theta),$$

so that the asymptotic bias distribution can be characterized by

$$\theta^* = \arg\min \| \frac{[G_0 - G(\theta)]\Phi_{r_1}^{\frac{1}{2}}}{(1+CG_0)(1+CG(\theta))K_*} \|_2. \tag{10.159}$$

This implies that in the (indirect) closed-loop situation, the additive error on G_0 is always weighted with S_0. Thus emphasis will be given to an accurate model fit in the frequency region where S_0 is large and the identified model will be less accurate in the frequency region where S_0 is small. In Figure 10.18 a typical characteristic of S_0 and closed-loop transfer $G_0C/(1+CG_0)$ is sketched. This illustrates that emphasis will be given to an accurate model fit in the frequency region that particularly determines the bandwidth of the control system. In this area (where $|S_0| \geq 1$), the noise contribution of v in the output signal y is amplified by the controller. According to Bode's sensitivity integral (Sung and Hara, 1988) for a stable controller:

$$\int_0^{\pi} log \ |S(e^{i\omega})| \ d\omega = c \ \ (\text{constant})$$

with c determined by the unstable poles of the plant, and $c = 0$ for G_0 stable. This implies that the attenuation of signal power in the low frequency range, will always be "compensated" for by an amplification of signal power in the higher frequency range. The aspect that closed-loop identification stresses the closed-loop relevance of identified (approximate) models, has been given strong attention in the research on "identification for control". Whereas direct identification needs consistent estimation of noise models in order to consistently identify G_0, indirect methods can do without noise models. Incorporation of noise models in indirect methods is very well possible, but this will result in bias distributions that become dependent on the identified noise models as well as on (the unknown) Φ_v.

10.10.3 Variance

For analyzing the asymptotic variance of the transfer function estimates we consider again the prediction error framework (Ljung, 1999) that provides variance expressions that are

asymptotic in both n (model order) and N (number of data). For the direct identification approach, and in the situation that $\mathcal{S} \in \mathcal{M}$ this delivers:

$$cov\left(\begin{array}{c} \hat{G}(e^{i\omega}) \\ \hat{H}(e^{i\omega}) \end{array}\right) \sim \frac{n}{N}\Phi_v(\omega)\cdot\left[\begin{array}{cc} \Phi_u(\omega) & \Phi_{eu}(\omega) \\ \Phi_{ue}(\omega) & \lambda_0 \end{array}\right]^{-1}. \tag{10.160}$$

The following notation will be introduced:

$$u(t) = u^r(t) + u^e(t)$$

with $u^r := S_0(q)r_1$ and $u^e := -CS_0(q)v$ and the related spectra $\Phi_u^r = |S_0|^2\Phi_{r_1}$ and $\Phi_u^e = |CS_0|^2\Phi_v$. Using the expression $\Phi_{ue} = -CS_0H_0\lambda_0$, (5.62) leads to (Ljung, 1993; Gevers et al., 1997):

$$cov\left(\begin{array}{c} \hat{G} \\ \hat{H} \end{array}\right) \sim \frac{n}{N}\frac{\Phi_v}{\Phi_u^r} \cdot \left[\begin{array}{cc} 1 & (CS_0H_0)^* \\ CS_0H_0 & \dfrac{\Phi_u}{\lambda_0} \end{array}\right],$$

and consequently

$$cov(\hat{G}) \sim \frac{n}{N}\frac{\Phi_v}{\Phi_u^r} \qquad cov(\hat{H}) \sim \frac{n}{N}\frac{\Phi_v}{\lambda_0}\frac{\Phi_u}{\Phi_u^r}. \tag{10.161}$$

This shows that only the noise-free part u^r of the input signal u contributes to variance reduction of the transfer functions. Note that for $u^r = u$ the corresponding open-loop results appear.

The asymptotic expressions require some further explanation. The asymptotic variance results of the direct method require the model order of both plant model and noise model to go to infinity. In particular when the order of the noise model tends to infinity, a consequence is that all noise power is required to estimate the (infinite-dimensional) noise model, and noise in the closed-loop systems does not contribute to variance reduction. If the noise model is not estimated, but fixed to its correct value, then the variance expression for $\hat{G}$, asymptotic in the model order of G only, becomes

$$cov(\hat{G}) \sim \frac{n}{N}\frac{\Phi_v}{\Phi_u}$$

showing that now the full input power (including its noise part) is used for variance reduction. See Corollary 10 in Forssel and Ljung (1999) and Remark 1 in Gevers et al. (2001). As a result, a limited order of the noise model is a crucial element in obtaining reduced variance results for the plant model.

In Gevers et al. (2001) it is shown that for *all* indirect methods presented in this chapter, these expression (10.161) remain the same. However, again there is one point of difference between the direct and indirect approach. The indirect methods arrive at the expression for $cov(\hat{G})$ also without estimating a noise model (situation $G_0 \in \mathcal{G}$), whereas the direct method requires a consistent estimation of H_0 for the validity of (10.161).

The asymptotic variance analysis tool gives an appealing indication of the mechanisms that contribute to variance reduction. It also illustrates one of the basic mechanisms in closed-loop identification, i.e. that noise in the feedback loop does not contribute to variance reduction for indirect methods and for the direct method when the noise model increases in order. Particularly in the situation that the input power of the process is limited, it is relevant to take these mechanisms into account when designing experiments. This has led to the following results (Gevers and Ljung, 1986), motivated from a variance perspective:

- If the input power is constrained then minimum variance of the transfer function estimates is achieved by an open-loop experiment;

- If the output power is constrained then the optimal experiment is a closed-loop experiment.

Because of the "doubly asymptotic" nature of the results ($N, n \rightarrow \infty$), this asymptotic variance analysis tool is also quite crude and should be treated with case, as indicated above.

For finite model orders, the variance results will likely become different over the several methods. The direct method will reach the Cramer-Rao lower bound for the variance in the situation $\mathcal{S} \in \mathcal{M}$. Similar to the open-loop situation, the variance will typically increase when no noise models are estimated in the indirect methods. This will also be true for the situation that two - independent - identification steps are performed on one and the same data set, without taking account of the relation between the disturbance terms in the two steps. Without adjustment of the identification criteria, the two stage method and the coprime factor method are likely to exhibit an increased variance because of this.

For finite model orders and the situation $\mathcal{S} \in \mathcal{M}$, it is claimed in Gustavsson et al. (1977) that all methods (direct and indirect) lead to the same variance; however for indirect methods this result seems to hold true only for particular (ARMAX) model structures. A more extensive analysis of the finite order case is provided in Forssell and Ljung (1999).

10.11   Model validation in closed-loop

The issue of how to validate models that are identified on the basis of closed-loop data is very much dependent on the identification approach that is chosen. For all methods where the several identification steps are basically "open-loop" type of identifications (input and noise are uncorrelated), the model validation tools as discussed in chapter 6 are available, including the correlation tests based on $\hat{R}_\varepsilon^N(\tau)$ and $\hat{R}_{\varepsilon u}^N(\tau)$.

Special attention has to be given to the situation of the direct identification method in closed-loop. Considering the prediction error in this situation:

$$\varepsilon(t, \theta) = \frac{G_0 - G(\theta)}{H(\theta)(1 + CG_0)} r(t) + \frac{H_0(1 + CG(\theta))}{H(\theta)(1 + CG_0)} e(t) \tag{10.162}$$

it can be observed that if $\hat{G}$ and $\hat{H}$ are estimated consistently, $\varepsilon(t, \theta^*) = e(t)$ which can be verified by analyzing the autocovariance function $\hat{R}_\varepsilon^N(\tau)$. If $\hat{R}_\varepsilon^N(\tau)$ is a Dirac-function (taking account of the usual confidence bounds) this can be taken as an indication that $\hat{G}$ and $\hat{H}$ are estimated consistently, provided that the contribution to $\varepsilon(t, \theta)$ of the r-dependent term will generally not lead to a white noise term.

For checking the consistency of $\hat{G}$ one would normally perform a correlation test on $\hat{R}_{\varepsilon r}(\tau)$, to verify whether this covariance function is equal to 0 for all τ. However when doing direct identification the signal r is usually not taken into account, and the standard identification tools will provide a correlation test on $\hat{R}_{\varepsilon u}^N(\tau)$. The interpretation of this latter test asks for some extra attention when closed-loop data is involved.

Writing

$$\varepsilon(t, \theta) = H(\theta)^{-1}[(G_0 - G(\theta))u(t) + H_0 e(t)] \tag{10.163}$$

it follows that

$$R_{\varepsilon u}(\tau) = H(\theta)^{-1}[G_0 - G(\theta)]R_u(\tau) + H(\theta)^{-1}H_0 R_{eu}(\tau). \qquad (10.164)$$

Concerning the term $R_{eu}(\tau)$ one can make the following observations:

For $\tau > 0$, $R_{eu}(\tau) = 0$ since $e(t)$ is uncorrelated with past values of the input u.
For $\tau = 0$, $R_{eu}(\tau) = 0$ only if C contains a delay;
For $\tau < 0$, $R_{eu}(\tau)$ is the (time-)mirrored pulse response of $-H_0 S_0 C$.

The latter statements are implied by the fact that the e-dependent term in $u(t)$ is given by $-H_0 S_0 C e(t)$.
When $R_{eu}(\tau)$ is a time-signal with values unequal to zero for $\tau \leq 0$, it can easily be observed that whenever $H(\theta) \neq H_0$, there will be a nonzero contribution of the second term in (10.164) to the cross-covariance function $R_{\varepsilon u}(\tau)$. As a result it follows that $R_{\varepsilon u}(\tau) = 0$ *does not imply* that $G(\theta^*) = G_0$.
The implication of this result is that in a situation where the "classical" validation tests $\hat{R}_{\hat{\varepsilon}}^N(\tau)$ and $\hat{R}_{\varepsilon u}^N(\tau)$ fail, it is unclear whether the invalidation is due to an incorrect estimate $\hat{G}$ or $\hat{H}$. Unlike the open-loop case, there is no indication now so as whether to increase the model order for either $G(\theta)$ or $H(\theta)$ or both.

10.12   Evaluation

The assessment criteria as discussed in section 10.1.3 have been evaluated for the several identification methods, and the results are listed in Table 10.9.
The methods that are most simply applicable are the direct method and the two-stage method. When considerable bias is expected from correlation between u and e, then the two-stage method should be preferred. For the identification of unstable plants the coprime factor, dual-Youla/Kucera and tailor-made parametrization method are suitable, of which the latter one seems to be most complex from an optimization point of view. When approximate -limited complexity- models are required, the coprime factor method is attractive. When additionally the controller is not accurately known, the two-stage method has advantages.
All methods are presented in a one-input, one-output configuration. The basic ideas as well as the main properties are simply extendable to MIMO systems.
The basic choice between direct and indirect approaches should be found in the evaluation of the following questions:

(a) Is there confidence in the fact that (G_0, H_0) and e satisfy the basic linear, time-invariant and limited order assumptions in the prediction error framework?

(b) Is there confidence in the fact that C operates as a linear time-invariant controller?

The direct method takes an affirmative answer to (a) as a starting point. Its results are not dependent on controller linearity; however the method requires exact modelling in terms of question (a). The indirect methods are essentially dependent on an affirmative answer to (b), and might be more suitable to handle departures from aspect (a).

	IV	Direct	Tailor-m	Two-stage	Copr.fact.	Indir/Dual-Y.
Consistency $(\hat{G}, \hat{H})$	$+$	$+$	$\square^5$	$+$	$+$	$+$
Consistency $\hat{G}$	$+$	$-$	$\square^5$	$+$	$+$	$+$
Tunable bias	$-$	$-$	$+$	$+$	$+$	$+$
Fixed model order	$+$	$+$	$+$	$+$	$\square^3$	$-$
Unstable plants	$+$	$\square^1$	$+$	$-^2$	$+$	$+$
$(G(q, \hat{\theta}_N), C)$ stable	$-$	$-$	$+$	$-$	$-$	$\square/+^4$
C assumed known	no	no	yes	no	no	yes

Table 10.9: Main properties of the different closed-loop identification methods.

So far the experimental setup has been considered where a single external signal r_1 is available from measurements. In all methods the situation of an available signal r_2 (in stead of r_1) can be treated similarly without loss of generality. A choice of a more principal nature is reflected by the assumption that the controller output is measured disturbance free. This leads to the (exact) equality

$$r = u + C(q)y.$$

The above equality displays that whenever u and y are available from measurements, knowledge of r and C is completely interchangeable. I.e. when r is measured, this generates full knowledge of C, through a noise-free identification of C on the basis of a short data sequence r, u, y. Consequently, for the indirect methods that are listed in Table 10.9, the requirement of having exact knowledge of C is not a limitation.

This situation is different when considering an experimental setup where the controller output (like the plant output) is disturbed by noise. Such a configuration is depicted in Figure 10.19, where d is an additional (unmeasurable) disturbance signal, uncorrelated with the other external signals r and v.

The appropriate relation now becomes

$$r + d = u + C(q)y$$

and apparently now there does exist a principal difference between the information content in r and in knowledge of C. Two situations can be distinguished:

- r is available and C is unknown. In this case the indirect identification methods have no other option than to use the measured r as the external signal in the several methods. In this way the disturbance d will act as an additional disturbance signal in the loop that will lead to an increased variance of the model estimates.

- C is exactly known. In this case the signal $u + Cy$ can be exactly reconstructed and subsequently be used as the "external" signal in the several indirect methods. In

---

[1] Only in those situations where the real plant (G_0, H_0) has an ARX or ARMAX structure.

[2] Not possible to identify unstable plants if in the second step attention is restricted to independently parametrized G and K.

[3] An accurate (high order) estimate of G_0 as well as knowledge of C is required; this information can be obtained from data.

[4] For the indirect method, stability is guaranteed only if C is stable.

[5] Consistency holds when the parameter set is restricted to a connected subset containing the exact plant vector θ_0.
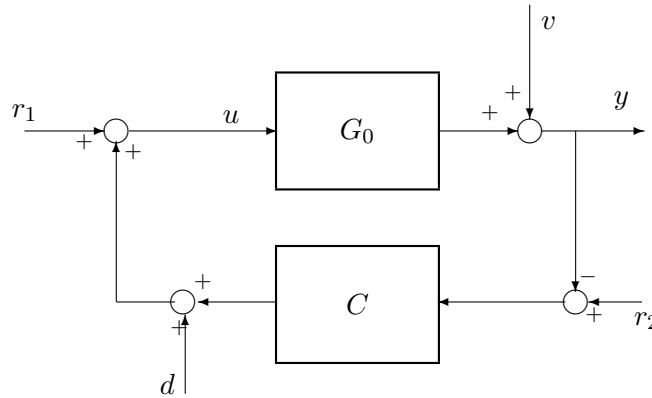
Figure 10.19: Closed-loop configuration with disturbance on controller output.

> this way the disturbance signal d is effectively used as an external input, leading to an improved signal to noise ratio in the estimation schemes, and thus to a reduced variance of the model estimates.

When measured signals u and y are given, one can argue what is the extra information content of having knowledge of r and/or C. From the comparative results of direct and indirect identification methods, one can conclude that this extra information allows the consistent identification of G_0, irrespective of the noise model H_0.

An additional aspect that may favour closed-loop experiments over open-loop ones, is the fact that a controller can have a linearizing effect on nonlinear plant dynamics; the presence of the controller can cause the plant to behave linearly in an appropriate working point.

For all identification methods discussed, the final estimation step comes down to the application of a standard (open-loop) prediction error algorithm. This implies that also the standard tools can be applied when it comes down to model validation (Ljung, 1999).

Appendix

Lemma 10A.1 *Schrama (1992). Consider rational transfer functions $G_0(z)$ with right coprime factorization (N, D) and $C(z)$ with left coprime factorization $(\tilde{D}_c, \tilde{N}_c)$.*
Then $T(G_0, C) := \begin{bmatrix} G_0 \\ I \end{bmatrix} (I + CG_0)^{-1} \begin{bmatrix} C & I \end{bmatrix}$ is stable if and only if $\tilde{D}_c D + \tilde{N}_c N$ is stable and stably invertible. $\square$

Proof: Denote $\Lambda = \tilde{D}_c D + \tilde{N}_c N$. Then $T(G_0, C) = \begin{bmatrix} N \\ D \end{bmatrix} \Lambda^{-1} \begin{bmatrix} \tilde{N}_c & \tilde{D}_c \end{bmatrix}$.

If Λ^{-1} is stable then $T(G_0, C)$ is stable, since all coprime factors are stable. This proves $(\Leftarrow)$.

Since (N, D) right coprime, it follows that there exist stable X, Y such that $XN + YD = I$. Similarly, since $(\tilde{D}_c, \tilde{N}_c)$ left coprime, there exist stable $\tilde{X}_c, \tilde{Y}_c$ such that $\tilde{N}_c \tilde{X}_c + \tilde{D}_c \tilde{Y}_c = I$.

Stability of $T(G_0, C)$ implies stability of $\begin{bmatrix} X & Y \end{bmatrix} T(G_0, C) \begin{bmatrix} \tilde{X}_c \\ \tilde{Y}_c \end{bmatrix}$ which implies stability of Λ^{-1}. $\square$

Proof of Proposition 10.8.3.

$(a) \Rightarrow (b)$. The mapping $x \to col(y, u)$ is characterized by the transfer function $\begin{bmatrix} G_0 S_0 F^{-1} \\ S_0 F^{-1} \end{bmatrix}$.

By writing $\begin{bmatrix} G_0 S_0 F^{-1} \\ S_0 F^{-1} \end{bmatrix} = \begin{bmatrix} G_0 \\ I \end{bmatrix} (I + CG_0)^{-1} F^{-1}$ and substituting a right coprime factorization (N, D) for G_0, and a left coprime factorization $(\tilde{D}_c, \tilde{N}_c)$ for C we get, after some manipulation, that

$$\begin{bmatrix} G_0 S_0 F^{-1} \\ S_0 F^{-1} \end{bmatrix} = \begin{bmatrix} N \\ D \end{bmatrix} (\tilde{D}_c D + \tilde{N}_c N)^{-1} \tilde{D}_c F^{-1}. \tag{10A.1}$$

Premultiplication of the latter expression with the stable transfer function $(\tilde{D}_c D + \tilde{N}_c N) \begin{bmatrix} X & Y \end{bmatrix}$ with (X, Y) right Bezout factors of (N, D) shows that $\tilde{D}_c F^{-1}$ is implied to be stable. As a result, $\tilde{D}_c F^{-1} = W$ with W any stable transfer function.

With respect to the mapping $col(y, u) \to x$, stability of F and FC implies stability of $W^{-1} \begin{bmatrix} \tilde{D}_c & \tilde{N}_c \end{bmatrix}$, which after postmultiplication with the left Bezout factors of $(\tilde{D}_c, \tilde{N}_c)$ implies that W^{-1} is stable.

This proves that $F = W^{-1} \tilde{D}_c$ with W a stable and stably invertible transfer function.

$(b) \Rightarrow (a)$. Stability of F and FC is straightforward. Stability of $S_0 F^{-1}$ and $G_0 S_0 F^{-1}$ follows from (10A.1), using the fact that $(\tilde{D}_c D + \tilde{N}_c N)^{-1}$ is stable (lemma 10A.1). $\square$

Proof of Proposition 10.10.1

The prediction error $\varepsilon(t, \theta)$ for the chosen parametrized noise model, becomes

$$\varepsilon(t, \theta) = \frac{1 + C(q)G(q, \theta)}{H(q, \theta)} \left[y(t) - \frac{G(q, \theta)}{1 + C(q)G(q, \theta)} r(t) \right]. \tag{10A.2}$$

When replacing $r(t)$ by $r(t) = u(t) + C(q)y(t)$ this delivers

$$\varepsilon(t, \theta) = \frac{1 + C(q)G(q, \theta)}{H(q, \theta)} \left[\frac{1}{C(q)G(q, \theta)} y(t) - \frac{G(q, \theta)}{1 + C(q)G(q, \theta)} u(t) \right] \tag{10A.3}$$

$$= H(q, \theta)^{-1} [y(t) - G(q, \theta)u(t)] \tag{10A.4}$$

being exactly the same expression as for the direct method.

Bibliography

B.D.O. Anderson and M.R. Gevers (1982). Identifiability of linear stochastic systems operating under linear feedback. *Automatica, 18*, no. 2, 195-213.

X. Bombois, G. Scorletti, M. Gevers, P.M.J. Van den Hof and R. Hildebrand (2006). Least costly identification experiment for control. *Automatica, 42*, pp. 1651-1662.

B. Codrons, B.D.O. Anderson and M. Gevers (2002). Closed-loop identification with an unstable or nonminimum phase controller. *Automatica, 38*, 2127-2137.

R.A. de Callafon, P.M.J. Van den Hof and M. Steinbuch (1993). Control-relevant identification of a compact disc pick-up mechanism. *Proc. 32nd IEEE Conf. Decision and Control*, San Antonio, TX, pp. 2050-2055.

C.A. Desoer, R.W. Liu, J. Murray and R. Saeks (1980). Feedback system design: the fractional representation approach to analysis and synthesis. *IEEE Trans. Automat. Contr., AC-25*, pp. 399-412.

R.A. Eek, J.A. Both and P.M.J. Van den Hof (1996). Closed-loop identification of a continuous crystallization process. *AIChE Journal, 42*, pp. 767-776.

U. Forssell and L. Ljung (1999). Closed-loop identification revisited. *Automatica, 35*, 1215–1241.

U. Forssell and L. Ljung (2000). A projection method for closed-loop identification. *IEEE Trans. Autom. Control, 45*, 2101-2106.

M. Gevers and L. Ljung (1986). Optimal experiment designs with respect to the intended model application. *Automatica*, **22**, 543-554.

M. Gevers, L. Ljung and P.M.J. Van den Hof (2001). Asymptotic variance expressions for closed-loop identification. *Automatica, 37*, 781-786, 2001.

M. Gilson and P.M.J. Van den Hof (2001). On the relation between a bias-eliminated least-squares (BELS) and an IV estimator in closed-loop identification. *Automatica, 37*, 1593-1600.

M. Gilson and P.M.J. Van den Hof (2003). IV methods for closed-loop system identification. Preprints *13th IFAC Symposium on System Identification*, August 27-29, 2003, Rotterdam, The Netherlands, pp. 537-542.

I. Gustavsson, L. Ljung and T. Söderström (1977). Identification of processes in closed loop - identifiability and accuracy aspects. *Automatica, 13*, 59-75.

F.R. Hansen and G.F. Franklin (1988). On a fractional representation approach to closed-loop experiment design. *Proc. American Control Conf.*, Atlanta, GA, USA, pp. 1319-1320.

T. Kailath (1980). *Linear Systems*. Prentice Hall, Englewood Cliffs, NJ.

W.S. Lee, B.D.O. Anderson, R.L. Kosut and I.M.Y. Mareels (1992). On adaptive robust control and control-relevant system identification. *Proc. 1992 American Control Conf.*, Chicago, IL, USA, pp. 2834-2841.

L. Ljung (1993). Information content in identification data from closed-loop operation. *Proc. 32nd IEEE Conf. Decision and Control*, San Antonio, TX, pp. 2248-2252.

L. Ljung (1999). *System Identification - Theory for the User*. Prentice-Hall, Englewood Cliffs, NJ, 2nd edition.

T.S. Ng, G.C. Goodwin and B.D.O. Anderson (1977). Identifiability of MIMO linear dynamic systems operating in closed loop. *Automatica, 13*, pp. 477-485.

A.G. Partanen and R.R. Bitmead (1993). Excitation versus control issues in closed loop identification of plant models for a sugar cane crushing mill. *Proc. 12th IFAC World*

Congress, Sydney, Australia, Vol. 9, pp. 49-56.

R.J.P. Schrama (1990). Open-loop identification of feedback controlled systems. In: O.H. Bosgra and P.M.J. Van den Hof (Eds.), *Selected Topics in Identification, Modelling and Control*. Delft University Press, Vol. 2, pp. 61-69.

R.J.P. Schrama (1991). An open-loop solution to the approximate closed loop identification problem. In: C. Banyasz & L. Keviczky (Eds.), *Identification and System Parameter Estimation 1991*. IFAC Symposia Series 1992, No. 3, pp. 761-766. Sel. Papers 9th IFAC/IFORS Symp., Budapest, July 8-12, 1991.

R.J.P. Schrama (1992). *Approximate Identification and Control Design - with Application to a Mechanical System*. Dr. Dissertation, Delft Univ. Technology, 1992.

T. Söderström, L. Ljung and I. Gustavsson (1976). Identifiability conditions for linear multivariable systems operating under feedback. *IEEE Trans. Automat. Contr., AC-21*, pp. 837-840.

T. Söderström and P. Stoica (1983). *Instrumental Variable Methods for System Identification*. Lecture Notes in Control and Information Sciences, Springer-Verlag, New York.

T. Söderström, P. Stoica and E. Trulsson (1987). Instrumental variable methods for closed-loop systems. In: *10th IFAC World Congress*. Munich - Germany. pp. 363–368.

T. Söderström and P. Stoica (1989). *System Identification*. Prentice-Hall, Hemel Hempstead, U.K.

H.K. Sung and S. Hara (1988). Properties of sensitivity and complementary sensitivity functions in single-input single-output digital control systems. *Int. J. Control, 48*, 2429-2439.

M.C. Tsai, E.J.M. Geddes and I. Postlethwaite (1992). Pole-zero cancellations and closed-loop properties of an $\mathcal{H}_\infty$-mixed sensitivity design problem. *Automatica, 28*, pp. 519-530.

P.M.J. Van den Hof, D.K. de Vries and P. Schoen (1992). Delay structure conditions for identifiability of closed-loop systems. *Automatica, 28*, no. 5, pp. 1047-1050.

P.M.J. Van den Hof and R.J.P. Schrama (1993). An indirect method for transfer function estimation from closed loop data. *Automatica, 29*, no. 6, pp. 1523-1527.

P.M.J. Van den Hof, R.J.P. Schrama, O.H. Bosgra and R.A. de Callafon (1995). Identification of normalized coprime plant factors from closed-loop experimental data. *European J. Control*, Vol. 1, pp. 62-74.

P.M.J. Van den Hof and R.J.P. Schrama (1995). Identification and control – closed-loop issues, *Automatica*, Vol. 31, pp. 1751-1770.

P.M.J. Van den Hof and R.A. de Callafon (1996). Multivariable closed-loop identification: from indirect identification to dual-Youla parametrization. *Proc. 35th IEEE Conference on Decision and Control*, Kobe, Japan, 11 - 13 December 1996, pp. 1397-1402.

P.M.J. Van den Hof (1998). Closed-loop issues in system identification. *Annual Reviews in Control*, Volume 22, pp. 173-186. Elsevier Science, Oxford, UK.

E.T. van Donkelaar and P.M.J. Van den Hof (2000). Analysis of closed-loop identification with a tailor-made parametrization. *European Journal of Control*, Vol. 6, no. 1, pp. 54-62.

M. Vidyasagar (1985). *Control System Synthesis - A Factorization Approach*. MIT Press, Cambridge, MA, USA.

Y.C. Zhu and A.A. Stoorvogel (1992). Closed loop identification of coprime factors. *Proc. 31st IEEE Conf. Decision and Control*, Tucson, AZ, pp. 453-454.

Appendix A

Statistical Notions

Variance and Covariance

For two scalar real-valued random variables x_1 and x_2, the covariance is defined as

$$cov(x_1, x_2) := E[x_1 - E(x_1)][x_2 - E(x_2)].$$

The variance of a single random variable is given by

$$var(x_1) := cov(x_1, x_1).$$

For a real-valued vector random variable θ, the covariance matrix is defined as

$$cov(\theta) := E[\theta - E(\theta)][\theta - E(\theta)]^T.$$

Estimation

Consider an estimate $\hat{\theta}_N$ of θ_0, based on N data points. The following properties are directed towards $\hat{\theta}_N$.

a *Unbiased.* $\hat{\theta}_N$ is unbiased if $E\hat{\theta}_N = \theta_0$.

b *Asymptotically unbiased.* $\hat{\theta}_N$ is asymptotically unbiased if $\lim_{N\to\infty} E\hat{\theta}_N = \theta_0$.

c *Consistent.*
  $\hat{\theta}_N$ is (weakly) consistent if for every $\delta > 0$,

$$\lim_{N\to\infty} Pr[|\hat{\theta}_N - \theta_0| > \delta] = 0$$

  also denoted as $\text{plim}_{N\to\infty} \hat{\theta}_N = \theta_0$.
  Weak consistency is also denoted as convergence in probability.
  $\hat{\theta}_N$ is strongly consistent if

$$Pr[\lim_{N\to\infty} \hat{\theta}_N = \theta_0] = 1$$

  implying that for almost all realizations $\hat{\theta}_N$, the limiting value $\lim_{N\to\infty} \hat{\theta}_N$ is equal to θ_0. This is also denoted as $\hat{\theta}_N \to \theta_0$ with probability (w.p.) 1 as $N \to \infty$.
  Strong consistency implies weak consistency.

d *Asymptotic efficient.* $\hat{\theta}_N$ is an asymptotic efficient estimate of θ_0 if

$$cov(\hat{\theta}_N) \leq cov(\bar{\theta}_N) \quad N \to \infty$$

for all consistent estimate $\bar{\theta}_N$. In this expression the inequality should be interpreted in a matrix-sense, being equivalent to the condition that $cov(\bar{\theta}_N) - cov(\hat{\theta}_N)$ is a positive semi-definite matrix.

e *Asymptotic normal.* $\hat{\theta}_N$ is asymptotic normally distributed if the random variable $\hat{\theta}_N$ converges to a normal distribution for $N \to \infty$. This is denoted as

$$\hat{\theta}_N \in As\mathcal{N}(\theta^*, P)$$

with θ^* the asymptotic mean, and P the covariance matrix of the asymptotic pdf. Since for consistent estimates P will be 0 the above expression will generally be written as

$$\frac{1}{\sqrt{N}}(\hat{\theta}_N - \theta^*) \in As\mathcal{N}(0, P_\theta)$$

with P_θ referred to as the asymptotic covariance matrix of $\hat{\theta}_N$.

Theorem of Slutsky
Let $x(N)$, $x_1(N)$, $x_2(N)$ be sequences of random variables for $N \in \mathbb{N}$.

(a) If $\text{plim}_{N\to\infty} x_1(N) = \hat{x}_1$ and $\text{plim}_{N\to\infty} x_2(N) = \hat{x}_2$, then $\text{plim}_{N\to\infty} x_1(N)x_2(N) = \hat{x}_1\hat{x}_2$.

(b) If $\text{plim}_{N\to\infty} x(N) = \hat{x}$ and h is a continuous function of $x(N)$, then $\text{plim}_{N\to\infty} h(x(N)) = h(\hat{x}_1)$.

χ^2-distribution
If $x_1, x_2, \cdots x_n$ are independent normally distributed random variables with mean 0 and variance 1, then $\sum_{i=1}^n x_i^2$ is a χ^2-distributed random variable with n degrees of freedom, denoted as

$$\sum_{i=1}^n x_i^2 \in \chi^2(n),$$

with the properties that its mean value is n and its variance is $2n$.

Appendix B

Matrix Theory

B.1 Rank conditions

Sylvester's inequality (Noble, 1969).
If A is an $p \times q$ matrix, and B a $q \times r$ matrix. Then

$$rank(A) + rank(B) - q \leq rank(AB) \leq min(rank(A), rank(B)). \qquad \text{(B.1)}$$

Block matrices
If a matrix A is nonsingular, then

$$\det \begin{bmatrix} A & B \\ C & D \end{bmatrix} = \det A \cdot \det(D - CA^{-1}B) \qquad \text{(B.2)}$$

and

$$\begin{bmatrix} A & B \\ C & D \end{bmatrix}^{-1} = \begin{bmatrix} A^{-1} + E\Delta^{-1}F & -E\Delta^{-1} \\ -\Delta^{-1}F & \Delta^{-1} \end{bmatrix} \qquad \text{(B.3)}$$

where $\Delta = D - CA^{-1}B$, $E = A^{-1}B$ and $F = CA^{-1}$. This latter result is known as the *matrix inversion lemma.*

B.2 Singular Value Decomposition

Definition B.1 (Singular Value Decomposition) *For every finite matrix $P \in I\!\!R^{q \times r}$ there exist unitary matrices $U \in I\!\!R^{q \times q}$, $V \in I\!\!R^{r \times r}$, i.e.*

$$\begin{aligned} U^T U &= I_q & \text{(B.4)} \\ V^T V &= I_r & \text{(B.5)} \end{aligned}$$

such that

$$P = U\Sigma V^T$$

with Σ a diagonal matrix with nonnegative diagonal entries

$$\sigma_1 \geq \sigma_2 \geq \cdots \geq \sigma_{min(q,r)} \geq 0.$$

Proposition B.2 *Let P be a $q \times r$ matrix with rank n, having a SVD $P = U\Sigma V^T$, and let $k < n$. Denote*

$$P_k := U\Sigma_k V^T, \qquad \Sigma_k = \begin{bmatrix} I_k & 0 \end{bmatrix} \Sigma \begin{bmatrix} I_k \\ 0 \end{bmatrix}. \tag{B.6}$$

Then P_k minimizes both

$$\|P - \widetilde{P}\|_2 \quad and \quad \|P - \widetilde{P}\|_F \tag{B.7}$$

over all matrices $\widetilde{P}$ of rank p.
Additionally

- $\|P - P_k\|_2 = \sigma_{k+1}$, *and*

- $\|P - P_k\|_F = \left(\sum_{i=k+1}^{min(q,r)} \sigma_i^2 \right)^{\frac{1}{2}}.$ $\square$

Let matrix P with rank n have an SVD

$$P = U\Sigma V^T = \begin{bmatrix} U_1 & U_2 \end{bmatrix} \begin{bmatrix} \Sigma_1 & 0 \\ 0 & 0 \end{bmatrix} \begin{bmatrix} V_1^T \\ V_2^T \end{bmatrix}. \tag{B.8}$$

Then:
The columns of U_1 constitute an orthonormal basis for the column space (range) of P;
The columns of V_1 constitute an orthonormal basis for the row space of P; and
the columns of V_2 constitute an orthonormal basis for the nullspace of P.

B.3   Projection operations

Let A be an $p \times r$ matrix, and B an $q \times r$ matrix. Then the orthogonal projection of the rows of A onto the row space of B is given by

$$AB^T(BB^T)^{-1}B = AVV^T \tag{B.9}$$

where V is taken from the singular value decomposition $B = U\Sigma V^T$.
Note that this property is related to the least-squares problem

$$\min_X \|A - XB\|_F \tag{B.10}$$

where $X \in \mathbb{R}^{p \times q}$ and $\| \cdot \|_F$ the Frobenius-norm defined by $\|Y\|_F = trace(Y^TY)$. The solution $\hat{X}$ to (B.10) is given by

$$\hat{X}^T = (BB^T)^{-1}BA^T \tag{B.11}$$

and the projection is thus given by $\hat{X}B = AB^T(BB^T)^{-1}B$.

Let A be an $p \times q$ matrix, and B an $p \times r$ matrix. Then the orthogonal projection of the columns of A onto the column space of B is given by

$$B(B^TB)^{-1}B^TA = UU^TA \tag{B.12}$$

where U is taken from the singular value decomposition $B = U\Sigma V^T$.

This property is related to the least-squares problem

$$\min_X \|A - BX\|_F \tag{B.13}$$

where $X \in \mathbb{R}^{r \times q}$. The solution $\hat{X}$ to (B.13) is given by

$$\hat{X} = (B^T B)^{-1} B^T A \tag{B.14}$$

and the projection is thus given by $B\hat{X} = B(B^T B)^{-1} B^T A$.

Bibliography

Noble, B. (1969). *Applied Linear Algebra.* Prentice-Hall, Englewood Cliffs, NJ.

Appendix C

Linear Systems Theory

C.1

Definition C.1 (Characteristic polynomial) *For any square $n \times n$ matrix A, the characteristic polynomial of A is defined as*

$$a(z) = det(zI - A) = z^n + a_1 z^{n-1} + a_2 z^{n-2} + \cdots + a_n$$

The equation $a(z) = 0$ is called the *characteristic equation* of A, and the n roots of this equation are called the *eigenvalues* of A.

Theorem C.2 (Cayley-Hamilton Theorem) *Any square $n \times n$ matrix A satisfies its own characteristic equation, i.e.*

$$a(A) = A^n + a_1 A^{n-1} + a_2 A^{n-2} + \cdots + a_n I = 0.$$

Index